

3rd Annual NASA SCL(E)* Workshop

1986

*Held at the
NASA Langley Research Center
Hampton, Virginia 23665
November 17-18, 1986*



National Aeronautics and
Space Administration

Langley Research Center
Hampton, Virginia 23665

Compiled by Larry Taylor

*Spacecraft Control Laboratory Experiment

3rd Annual SCOLE* Workshop

**SPONSORED BY NASA Langley Research Center &
UCLA Laboratory for Flight Systems Research**

**Monday, November 17, 1986 Building 1232, Rm 236
NASA Langley Research Center, Hampton, Virginia**

7:30 Breakfast at the NASA Cafeteria

8:00 Registration, Building 1232, Room 236

8:30 Introductory Remarks.....Larry Taylor

8:45 Panel Presentations Concerning the Modeling of SCOLE

Chairman, Jernan Juang

Peter Bainum

A. V. Balakrishnan

Suresh Joshi

Yogendra Kaked

Leonard Metirovitch

Larry Taylor

Dean Sparks

10:15 Panel Discussion Concerning the Modeling of SCOLE

Chairman, A. V. Balakrishnan

12:00 Lunch

1:00 SCOLE Laboratory Demonstration.....Jeff Williams

2:00 Panel Presentations Concerning the Control of SCOLE

Chairman, E. S. Armstrong

A. V. Balakrishnan

Emmanuel Collins

Mike Fisher

Howard Kaufman

Gene Lin

Leonard Metirovitch

R. K. Miller

4:00 Panel Discussion Concerning the Control of SCOLE
Chairman, A. V. Balakrishnan

6:00 Attitude Adjustment at the Chamberlin Hotel, Monitor Room

7:00 Banquet at the chamberlin Hotel, Monitor Room

Tuesday, November 18

- **The First NASA/DOD Control/Structures Interaction Conference Begins at the OMNI International Hotel, Norfolk, VA**
- **Those Wishing to Become Users of the SCOLE Laboratory Aparatus are Invited to the Spacecraft Control Lab in Bldg 1232 at 8:30am**

*** Spacecraft Control Laboratory Experiment**

OF

Table of Contents

	Page
Introductory Remarks..... Larry Taylor	1
Issues in Modeling and Controlling the SCOLE Configuration..... P. Bainum, A.S.S.R. Reddy, C. Diarra, F. Li	11
Optimal Torque Control for Slewing Maneuvers..... P. Bainum, F. Li	69
Mathematical Modeling of the SCOLE Configuration with Line-of-Sight Error as the Output..... S. M. Joshi	83
Slew Maneuver Dynamics of the Spacecraft Control Laboratory Experiment(SCOLE)..... Y. P. Kakad	93
Modeling and Identification of SCOLE..... L. Meirovitch, M. A. Norris	109
On Incorporating Damping and Gravity Effects in Models of Structural Dynamics of the SCOLE Configuration..... Larry Taylor, Terry Leary, Eric Stewart	121
Finite Element Model of SCOLE Laboratory Configuration..... Beth Lee, J. P. Williams, D. Sparks	149
Model Reference Control of Distributed Parameter Systems with Application to the SCOLE..... H. Kaufman, D. Minnick, M. Balas, A. Musalem	163
Proof-Mass Actuator Placement Strategies for Regulation of Flexure During the SCOLE Slew Maneuver..... Shalom Fisher	229

Active Damping of Vibrations in SCOLE Excited by Minimum-Time Rapid Slewing.....	261
Jiguan Gene Lin	
Control of SCOLE.....	313
L. Meirovitch, M. A. Norris	
Evaluation of On-Line Pulse Control for Vibration Suppression in Flexible Spacecraft.....	337
G. Bekey, S. Masri, R. Miller	
Active Stability Augmentation of Large Space Structures: A Stochastic Control Problem	
A.V. Balakrishnan.....	367
The SCOLE Design Challenge (Reprint).....	385
Larry Taylor, A.V. Balakrishnan	
Description of the Spacecraft Control Laboratory Experiment (SCOLE) Facility.....	413
Jeffrey P. Williams, Rosemary A. Rallo	
Workshop Attendees.....	459
"Awards".....	461
Summary of Panel Discussions.....	463

Introductory Remarks

by

**Larry Taylor
NASA Langley
Research Center**

SPACECRAFT CONTROL LABORATORY EXPERIMENT (SCOLE)

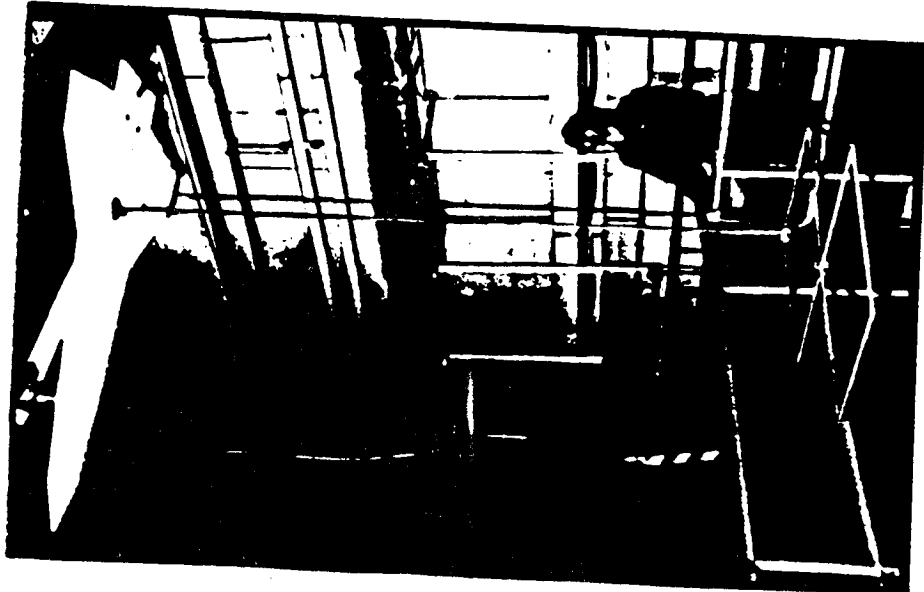
ORIGINAL PAGE IS
OF POOR QUALITY

Provides mathematical and experimental model for direct comparison of competing control schemes

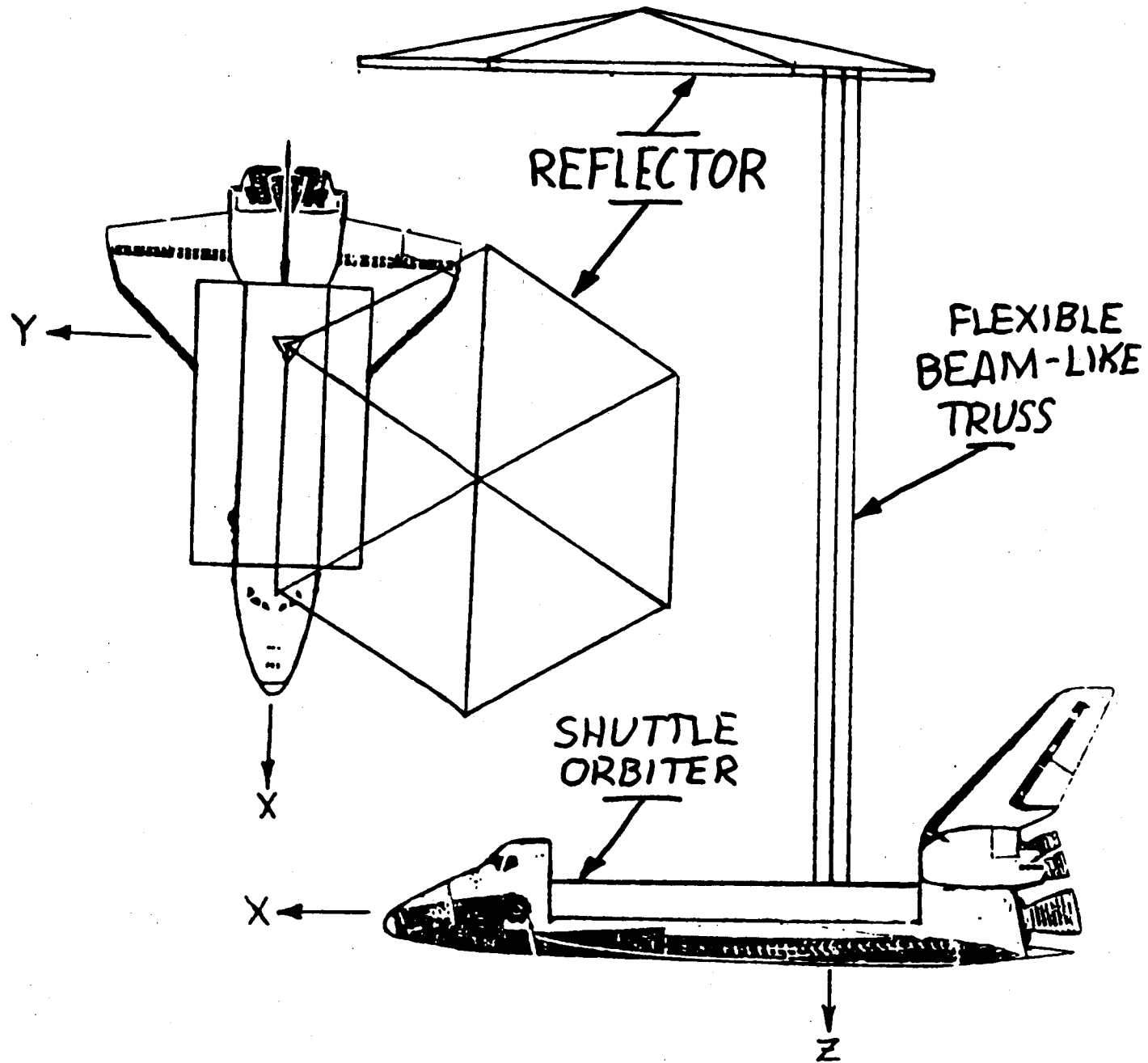
3-D Control problem

Flexible modes in control bandwidth

12 actuators
30 sensors
distributed computing



CONFIGURATION

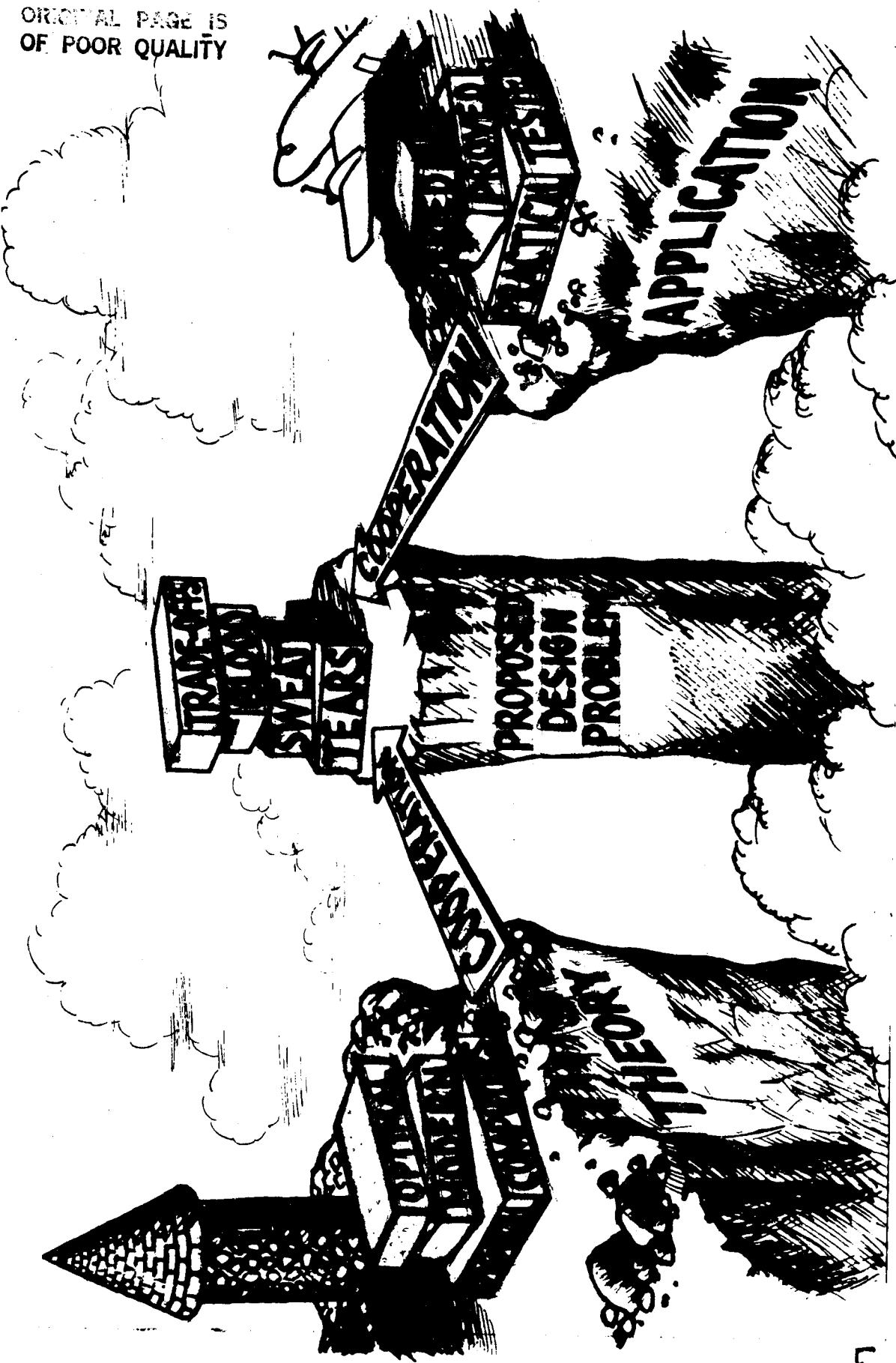


Benefits of the ~~Stall~~ologic Program

- o Comparison of Design Approaches
- o Novel Control Techniques
- o Validation of Design Methods
- o Precursor to Co-Investigators for Flight Experiments

SUGGESTED SOLUTION TO THE "GREAT CONTROL GAP"

ORIGINAL PAGE IS
OF POOR QUALITY



Results of the

SCOLE Program

- o NASA-IEEE Design Challenge
June '83
- o Eight Grants/Contracts Underway
Feb '84
- o SCOLE Workshop
Dec '84
- o Experimental Apparatus Ready
July '85

Timeliness of the

SCOTLAC Program

- o Ground Demonstrations on Two Dimensional Structures are Nearing Completion - A 3-Dimensional Problem is Needed to Advance Our Active Structural Control Capability
- o The Planned COFS Flight Tests Demand Development of Our Most Sophisticated Flexible Structure Control Capability - This Can Only be Accomplished by Ground Testing on Structures with 3-Dimensional Characteristics and Large Numbers of Inertial Sensors and Actuators

Equations of Motion

Shuttle (and Reflector) Body

$$\dot{\bar{w}}_1 = -\bar{I}_1^{-1} (\bar{w}_1 \bar{I}_1 \bar{w}_1 - M_1 - M_{1, \text{Beam}})$$

$$\dot{v}_1 = (F_1 + F_{1, \text{Beam}}) / m_1$$

$$\dot{T}_1^T = -\bar{w}_1 T_1^T$$

Roll (and Pitch) Beam Bending

$$p A_\phi \frac{d^2 u_\phi}{dt^2} - C I_\phi \frac{d^3 u_\phi}{ds^2 dt} + E I_\phi \frac{d^4 u_\phi}{ds^4} = \sum_{n=1}^4 [f_{\phi,n} \delta(s-s_n) + g_{\phi,n} \frac{d\delta}{ds}(s-s_n)]$$

Yaw Beam Torsion

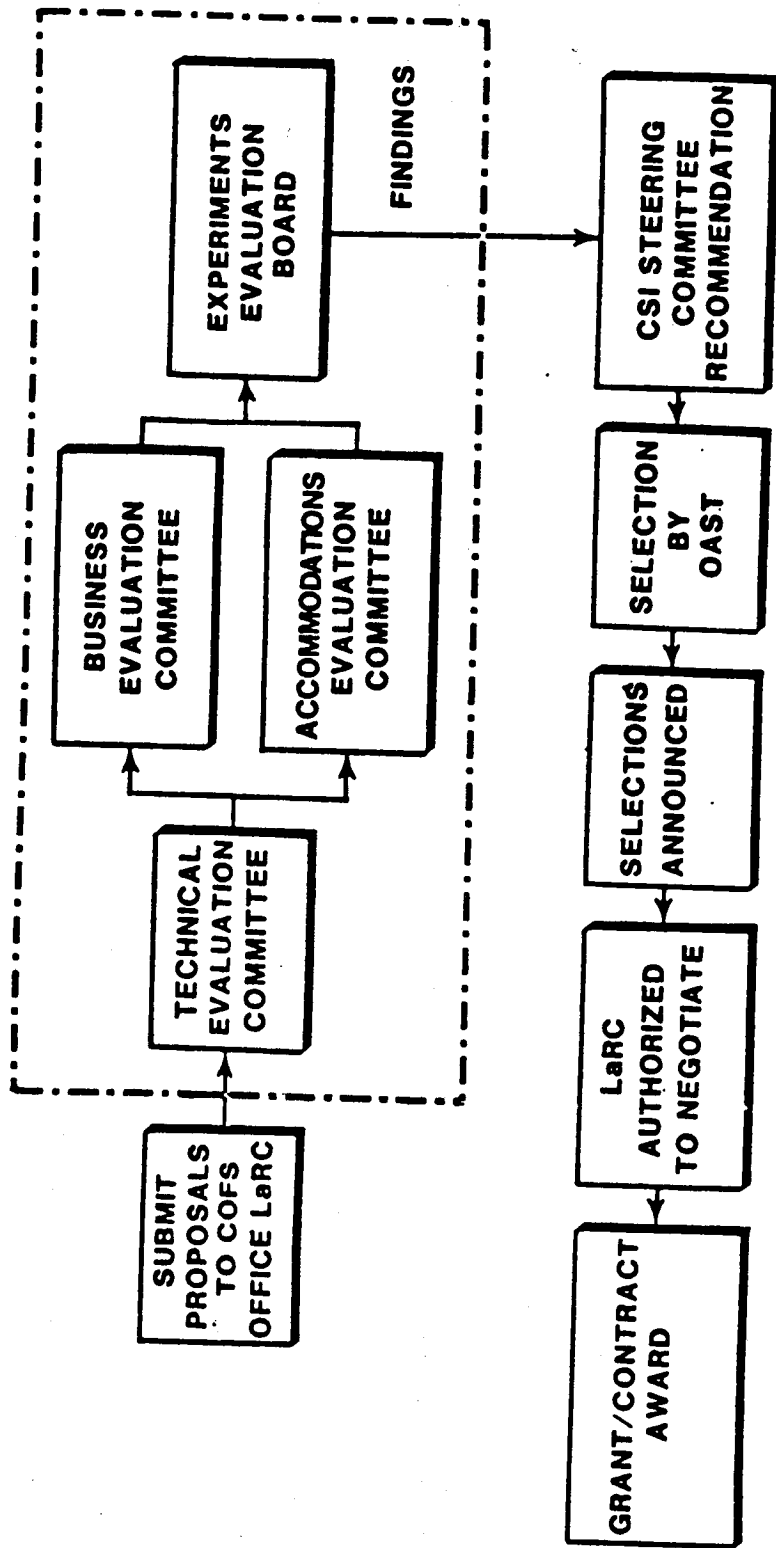
$$p I_\Psi \frac{d^2 u_\Psi}{dt^2} + C I_\Psi \frac{d^3 u_\Psi}{ds^2 dt} - G I_\Psi \frac{d^2 u_\Psi}{ds^2} = \sum_{n=1}^4 g_{\Psi,n} \delta(s-s_n)$$

Beam Elongation

$$p A \frac{d^2 u_z}{dt^2} + C_z A \frac{d^2 u_z}{ds dt} - E A \frac{d^2 u_z}{ds^2} = \sum_{n=1}^4 f_{z,n} \delta(s-s_n)$$

COFS GUEST INVESTIGATOR SELECTION PROCESS

UNIVERSITIES AND INDUSTRY



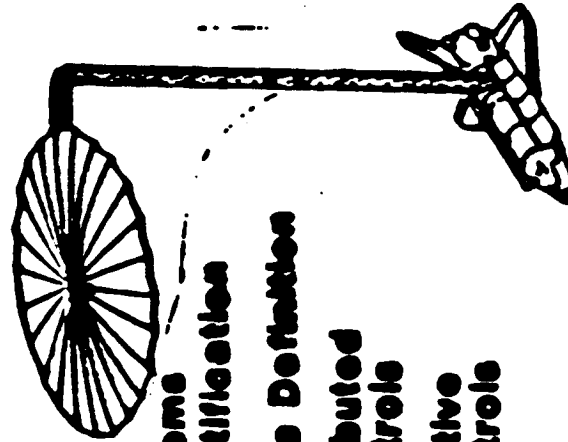
CONTROL OF FLEXIBLE STRUCTURES

COFS I Beam Dynamics & Control

- Systems Identification
- Test Methods
- Distributed Controls

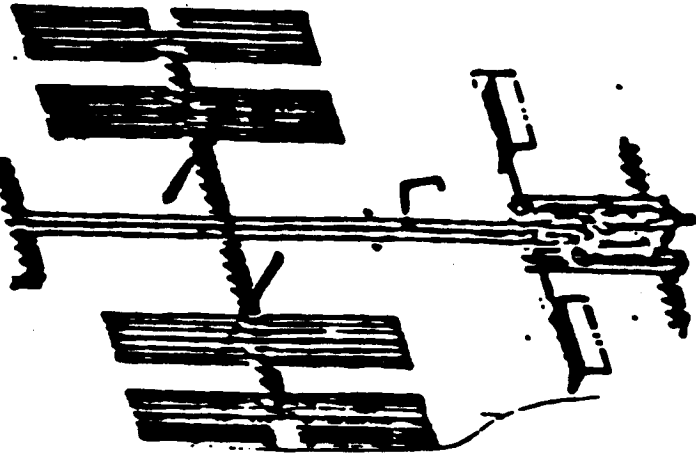


COFS II Three-Dimensional Dynamics & Control



- Systems Identification
- Shape Definitions
- Distributed Controls
- Adaptive Controls

COFS III Multi-Body Dynamics



- Test Methods
- Systems Identification
- Model Sensitivities
- Analysis Validation
- Space Station Supporting Technology

ORIGINAL PAGE IS
OF POOR QUALITY

Issues in Modeling and Controlling the SCOLE Configuration

by

Peter M. Bainum

A.S.S.R. Reddy

Cheick Modibo Diarra

Feiyue Li

Howard University

ISSUES IN MODELING AND CONTROLLING
THE SCOLE CONFIGURATION

by

Peter M. Bainum

A.S.S.R. Reddy

Cheick Modibo Diarra

Feiyue Li

Howard University

Washington, D.C.

3rd Annual SCOLE Workshop

NASA Langley Research Center

Nov. 17, 1986

I. MODELLING OF THE SCOLE CONFIGURATION

- PARAMETRIC STUDY OF THE IN-PLANE SCOLE SYSTEM -
FLOQUET STABILITY ANALYSIS
- THREE DIMENSIONAL FORMULATION OF THE SCOLE SYSTEM DYNAMICS
 - Rotational Equations of Motion
 - Structural Analysis - Boundary Conditions
 - Generic Modal Equations
- WHAT WE CAN LEARN ABOUT THE OPEN LOOP SYSTEM?
 - Consider SCOLE configuration without offset of the mast attachment to the reflector and without flexibility
 - Consider SCOLE configuration without mast flexibility but with offset in the direction of orbit (strawman)
 - Consider SCOLE configuration with offsets in two directions but neglecting mast flexibility
 - Consider general SCOLE system dynamics
- IMPLICATIONS FOR CONTROL STRATEGIES

II. CONTROL ISSUES: ~~WITTAQUSIPIWOO BUNO2 BHT SO SWILLEROM~~

- CONTROL OF LARGE STRUCTURES WITH DELAYED INPUT IN THE CONTINUOUS TIME DOMAIN ~~WITTAQUSIPIWOO BUNO2 BHT SO SWILLEROM~~
- CONTROL WITH DELAYED INPUT IN THE DISCRETE TIME DOMAIN ~~WITTAQUSIPIWOO BUNO2 BHT SO SWILLEROM~~
- CONTROL LAW DESIGN FOR SCOLE USING LQG/LTR TECHNIQUE ~~WITTAQUSIPIWOO BUNO2 BHT SO SWILLEROM~~
- OPTIMAL TORQUE CONTROL FOR SCOLE SLEWING MANEUVERS ~~WITTAQUSIPIWOO BUNO2 BHT SO SWILLEROM~~
 - Kinematical and Dynamical Equations ~~WITTAQUSIPIWOO BUNO2 BHT SO SWILLEROM~~
 - Optimal Control - Two Point Boundary Value Problem ~~WITTAQUSIPIWOO BUNO2 BHT SO SWILLEROM~~
 - to keep the torque constant during the maneuver
 - Estimation of Unknown Boundary Conditions ~~WITTAQUSIPIWOO BUNO2 BHT SO SWILLEROM~~

• Numerical Results ~~WITTAQUSIPIWOO BUNO2 BHT SO SWILLEROM~~

• **Discussion and Further Recommendations**

• ~~WITTAQUSIPIWOO BUNO2 BHT SO SWILLEROM~~

I. MODELLING OF THE SCOLE CONFIGURATION

- ✓
 - PARAMETRIC STUDY OF THE IN-PLANE SCOLE SYSTEM - FLOQUET STABILITY ANALYSIS
 - THREE DIMENSIONAL FORMULATION OF THE SCOLE SYSTEM DYNAMICS
 - Rotational Equations of Motion
 - Structural Analysis - Boundary Conditions
 - Generic Modal Equations
 - WHAT WE CAN LEARN ABOUT THE OPEN LOOP SYSTEM?
 - Consider SCOLE configuration without offset of the mast attachment to the reflector and without flexibility
 - Consider SCOLE configuration without mast flexibility but with offset in the direction of orbit (strawman)
 - Consider SCOLE configuration with offsets in two directions but neglecting mast flexibility
 - Consider general SCOLE system dynamics
 - IMPLICATIONS FOR CONTROL STRATEGIES

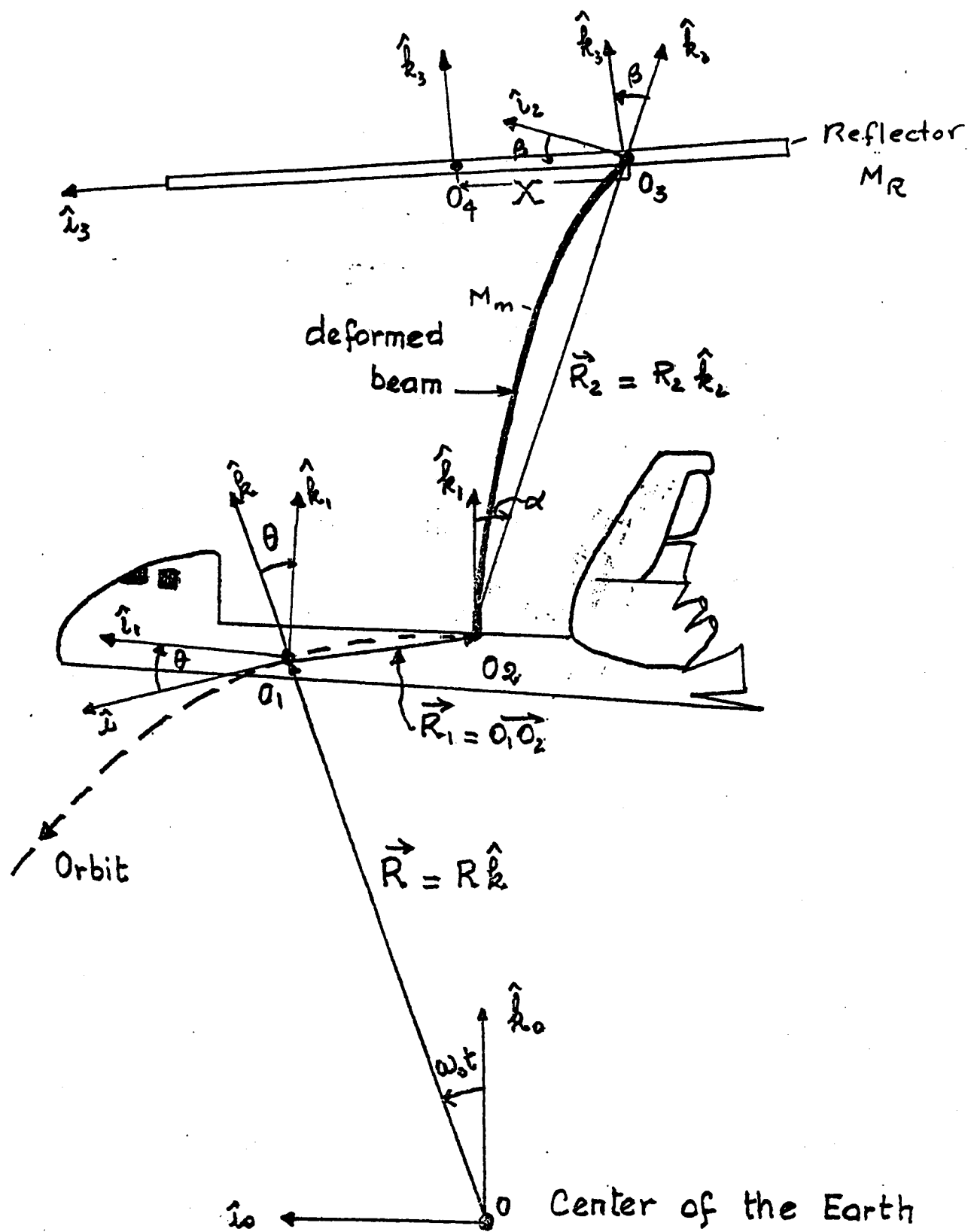


Fig. 2.1. SCOLE System Geometry in the Deformed State (2-D)

Parametric Study of the System

Let us assume that the interface point between the reflector and the mast is at the center of mass of the reflector

$$\rightarrow X = 0 + \lambda = 0 = C_5 = C_6$$

Under this assumption, the equation becomes

$$\begin{aligned} -\theta'' + C_4/c_1 \frac{d}{d\tau} [\theta \cos(\Omega\tau + \phi)] + \Omega^2 C_4/c_1 \cos(\Omega\tau + \phi) \\ = C_4/2c_1 \Omega \sin[\theta(\Omega\tau + \phi)] - \frac{3}{c_1} (I_u - I_{z3}) \theta = 0 \end{aligned} \quad (2.5)$$

which in the absence of gravity gradient, yields the following first integral of the motion:

$$\begin{aligned} -\theta' + C_4/c_1 [\theta \cos(\Omega\tau + \phi) + \Omega C_4/c_1 \sin(\Omega\tau + \phi)] \\ + C_4/4c_1 \cos[\theta(\Omega\tau + \phi)] = K \end{aligned} \quad (2.6)$$

This equation is plotted in the phase plane (θ', θ) for different values of μ and Ω . (Figs. 2.2)

Floquet Analysis

The angular motion about an axis perpendicular to the orbit plane in the absence of gravity gradient is described by:

$$\theta'' = \left[-C_5/c_1 + C_4/c_1 \cos \Omega \tau \right] \theta' - \left[\frac{C_2 \Omega}{c_1} \sin \Omega \tau \right] \theta \quad (2.7)$$

Case 2. No gravity gradient, but offset.

$$p(\tau) = \begin{bmatrix} \frac{c_2}{c_1} \cos \Omega \tau - \frac{c_5}{c_1} & -\frac{c_2}{c_1} \Omega \sin \Omega \tau \\ 1 & 0 \end{bmatrix}$$

$$[\dot{z}(\tau)] = [P(\tau)] [z(\tau)]$$

$$\dot{z}_{11} = P_{11}z_{11} + P_{12}z_{21} \quad (1)$$

$$\dot{z}_{12} = P_{11}z_{12} + P_{12}z_{22} \quad (2)$$

$$\dot{z}_{21} = P_{21}z_{11} + P_{22}z_{21} \quad (3) \text{ which becomes}$$

$$\dot{z}_{21} = z_{11} \text{ since } P_{21} = 1 \text{ and } P_{22} = 0$$

$$\dot{z}_{22} = P_{21}z_{12} + P_{22}z_{22} \quad (4) \text{ which becomes}$$

$$\dot{z}_{22} = z_{12}$$

from (3) $\ddot{z}_{21} = \dot{z}_{11}$, substituted into (1) yields

$$\ddot{z}_{21} = P_{11}\dot{z}_{21} + P_{12}z_{21}$$

similarly from (4) $\ddot{z}_{22} = \dot{z}_{12}$, substituted into (2) yields

$$\ddot{z}_{22} = P_{11}\dot{z}_{22} + P_{12}z_{22}$$

$$\text{since } \frac{c_5}{c_1} = \text{constant} \quad \frac{d}{dt} P_{11} = P_{22}$$

Then

$$\ddot{z}_{21} = P_{11}\dot{z}_{21} + P_{11}z_{21} = \frac{d}{dt} (P_{11}z_{21})$$

$$\text{and} \quad \ddot{z}_{22} = P_{11}\dot{z}_{22} + P_{11}z_{22} = \frac{d}{dt} (P_{11}z_{22})$$

These two last equations are integrated and the following results for z_{21} and z_{22} obtained.

$$\dot{z}_{21} = P_{11}z_{21} + K_1$$

$$\dot{z}_{22} = P_{11}z_{22} + K_2$$

but from (3), $z_{21}(\tau) = z_{11}(\tau)$ and from (4)

$$\dot{z}_{22}(\tau) = z_{12}(\tau)$$

$$\text{Therefore, } \dot{z}_{21}(0) = z_{11}(0) = P_{11}(0)z_{21}(0) + K_1 \rightarrow K_1 = 1$$

$$\text{since } z_{11}(0) = 1 \text{ and } z_{21}(0) = 0$$

$$\begin{aligned}\dot{z}_{22}(0) &= z_{12}(0) = 0 = P_{11}(0)z_{22}(0) + K_2 \\ &\Rightarrow -\frac{c_5}{c_1} + \frac{c_2}{c_1} + K_2 = 0 \text{ or } K_2 = -\frac{c_2}{c_1} + \frac{c_5}{c_1}\end{aligned}$$

The two last equations integrated once, yield

$$\begin{aligned}\dot{z}_{21} &= P_{11}z_{21} + 1 \\ \dot{z}_{22} &= P_{11}z_{22} - \left(\frac{c_2-c_5}{c_1}\right)\end{aligned}$$

ORIGINAL PAGE IS
OF POOR QUALITY

Solution of the first order equations

$$\frac{dz_{22}}{d\tau} - P_{11}z_{22} = -\left(\frac{c_2-c_5}{c_1}\right) \quad (1)$$

The presence of $\frac{dz_{22}}{d\tau}$ and $P_{11}z_{22}$ in the equation suggests a product of the type $\phi(\tau)z_{22}(\tau)$

$$\text{but } \frac{d}{d\tau}(\phi z_{22}) = \frac{d\phi}{d\tau}z_{22} + \phi \frac{d}{d\tau}z_{22} \quad (2)$$

Multiplying (1) by $\phi(\tau)$ yields

$$\phi \frac{dz_{22}}{d\tau} - \phi P_{11}z_{22} = -\phi \left(\frac{c_2-c_5}{c_1}\right)$$

which can become

$$\frac{d}{d\tau}(\phi z_{22}) = -\phi \left(\frac{c_2-c_5}{c_1}\right)$$

if one can find $\phi(\tau)$ (integrating factor) such that

$$\frac{d\phi}{d\tau} = -\phi P_{11}$$

$$\Rightarrow \ln \phi(\tau) = \int -P_{11} d\tau = -\frac{c_2}{c_1 \Omega} \cos \Omega \tau d\tau + \int \frac{c_5}{c_1} d\tau$$

$$\ln \phi(\tau) = -\frac{c_2}{c_1 \Omega} \sin \Omega \tau + \frac{c_5}{c_1} \tau + K$$

$$\text{or } \phi(\tau) = \exp \left[-\frac{c_2}{c_1 \Omega} \sin \Omega \tau \right] \cdot e^{\frac{c_5}{c_1} \tau + K}$$

$$\text{from } \frac{d(z_{22}\phi)}{d\tau} = -\phi \left(\frac{c_2-c_5}{c_1}\right)$$

$$z_{22} = \frac{1}{\phi} \int \phi \left(\frac{c_5-c_2}{c_1}\right) d\tau$$

$$z_{22} = \exp \left[\frac{c_2}{c_1 \Omega} \sin \Omega \tau - \frac{c_5}{c_1} \tau - K \right] \left(\frac{c_5-c_2}{c_1} \right) \int \exp \left[-\frac{c_2}{c_1 \Omega} \sin \Omega \tau + \frac{c_5}{c_1} \tau + K \right] d\tau$$

$$\exp \left[-\frac{c_2}{c_1 \Omega} \sin \Omega \tau \right] \approx 1 - \frac{c_2}{c_1} \tau + \frac{c_2^2}{c_1^2} \tau^2 - \left\{ \left(\frac{c_2}{c_1} \right)^2 - \Omega^2 \frac{c_5}{c_1} \right\} \tau^3/6 + \dots$$

$$\exp \left[\frac{c_5 \tau}{c_1} \right] \approx 1 + \frac{c_5 \tau}{c_1} + \left(\frac{c_5 \tau}{c_1} \right)^2 \cdot \frac{1}{2} + \dots$$

$$\text{Therefore, } \exp \left[-\frac{c_2}{c_1 \Omega} \sin \Omega \tau + \frac{c_5 \tau}{c_1} \right] \approx 1 + \left(\frac{c_5-c_2}{c_1} \right) \tau + \left(\frac{c_5-c_2}{c_1} \right)^2 \tau^2/2 + \dots$$

$$z_{22} = \exp \left[\frac{c_2}{c_1 \Omega} \sin \Omega \tau - \frac{c_5}{c_1} \tau - K \right] \left(\frac{c_5-c_2}{c_1} \right) e^{\frac{c_5 \tau}{c_1}} \left(\tau + \frac{c_5-c_2}{c_1} \tau^2/2 + \left(\frac{c_5-c_2}{c_1} \right)^2 \tau^3/6 + \dots + K \right)$$

$$z_{22}(0) = 1 \Rightarrow \frac{(c_5-c_2)}{c_1} K_1 = 1 \Rightarrow K_1 = \frac{c_1}{c_5-c_2}$$

$$z_{22} = \exp \left[\frac{C_2}{\Omega C_1} \sin \Omega \tau - \frac{C_5}{C_1} \tau \right] \left\{ 1 + \left(\frac{C_5 - C_2}{C_1} \right) \tau + \left(\frac{C_5 - C_2}{C_1} \right)^2 \frac{\tau^2}{2} + \left(\frac{C_5 - C_2}{C_1} \right)^3 \frac{\tau^3}{6} + \dots \right\}$$

$$\text{since } \dot{z}_{22} = z_{12}(\tau) = \exp \left[\frac{C_2}{\Omega C_1} \sin \Omega \tau - \frac{C_5}{C_1} \tau \right] \left\{ \left(\frac{C_5 - C_2}{C_1} \right) + \left(\frac{C_5 - C_2}{C_1} \right)^2 \tau + \dots \right\}$$

$$+ \left(\frac{C_2}{C_1} \cos \Omega \tau - \frac{C_5}{C_1} \right) \exp \left[\frac{C_2}{\Omega C_1} \sin \Omega \tau - \frac{C_5}{C_1} \tau \right] \left\{ 1 + \left(\frac{C_5 - C_2}{C_1} \right) \tau + \left(\frac{C_5 - C_2}{C_1} \right)^2 \frac{\tau^2}{2} + \dots \right\}$$

$$z_{12} = \exp \left[\frac{C_2}{\Omega C_1} \sin \Omega \tau - \frac{C_5}{C_1} \tau \right] \left\{ - \frac{C_2}{C_1} + \frac{C_2}{C_1} \cos \Omega \tau + \left[\left(\frac{C_2 \cos \Omega \tau - C_5}{C_1} \right) \left(\frac{C_5 - C_2}{C_1} \right) \right. \right.$$

$$\left. \left. + \left(\frac{C_5 - C_2}{C_1} \right)^2 \right] \tau + \left[\left(\frac{C_2 \cos \Omega \tau - C_5}{C_1} \right) \left(\frac{C_5 - C_2}{C_1} \right)^2 + \left(\frac{C_5 - C_2}{C_1} \right)^3 \right] \frac{\tau^2}{2} + \dots \right\}$$

$$z_{12}(\tau) = \exp \left[\frac{C_2}{\Omega C_1} \sin \Omega \tau - \frac{C_5}{C_1} \tau \right] \left\{ \frac{C_2}{C_1} (1 + \cos \Omega \tau) + \left(\frac{C_5 - C_2}{C_1} \right) \left(\frac{C_2 \cos \Omega \tau - C_5}{C_1} \right) + \dots \right\}$$

$$z_{12}(\tau) = \exp \left[\frac{C_2}{\Omega C_1} \sin \Omega \tau - \frac{C_5}{C_1} \tau \right] \left[\frac{C_2}{C_1} (\cos \Omega \tau - 1) \right] \left[1 + \frac{C_5 - C_2}{C_1} \tau + \left(\frac{C_5 - C_2}{C_1} \right)^2 \frac{\tau^2}{2} + \dots \right]$$

$$\frac{dz_{21}}{d\tau} = P_{11} z_{21} + 1 \quad \text{where } P_{11} = \frac{C_2}{C_1} \cos \Omega \tau - \frac{C_5}{C_1}$$

$$\text{Integrating factor } \phi : \frac{d\phi}{d\tau} = - \phi' P_{11}$$

$$\rightarrow \phi = \exp \left[- \frac{C_2}{\Omega C_1} \sin \Omega \tau + \frac{C_5}{C_1} \tau + K \right] \quad \text{and}$$

$$z_{21} = \frac{1}{\phi} \int \phi d\tau = \exp \left[\frac{C_2}{\Omega C_1} \sin \Omega \tau - \frac{C_5}{C_1} \tau - K \right] \int \phi d\tau$$

$$\exp \left[- \frac{C_2}{\Omega C_1} \sin \Omega \tau + \frac{C_5}{C_1} \tau \right] \approx 1 + \left(\frac{C_5 - C_2}{C_1} \right) \tau + \left(\frac{C_5 - C_2}{C_1} \right)^2 \frac{\tau^2}{2} + \dots$$

Integrating term by term yields,

$$z_{21} = \exp \left[\frac{C_2}{\Omega C_1} \sin \Omega \tau - \frac{C_5}{C_1} \tau \right] \left[\tau + \left(\frac{C_5 - C_2}{C_1} \right) \frac{\tau^2}{2} + \left(\frac{C_5 - C_2}{C_1} \right)^2 \frac{\tau^3}{6} + \dots + K' \right]$$

$$\text{since } z_{21}(0) = K' = 0 \Rightarrow$$

$$z_{21}(\tau) = \exp \left[\frac{C_2}{\Omega C_1} \sin \Omega \tau - \frac{C_5}{C_1} \tau \right] \left[\tau + \left(\frac{C_5 - C_2}{C_1} \right) \frac{\tau^2}{2} + \left(\frac{C_5 - C_2}{C_1} \right)^2 \frac{\tau^3}{6} + \dots \right]$$

$$z_{21} = z_{11}(\tau) = \exp \left[\frac{C_2}{\Omega C_1} \sin \Omega \tau - \frac{C_5}{C_1} \tau \right] \left\{ 1 + \left(\frac{C_5 - C_2}{C_1} \right) \tau + \left(\frac{C_5 - C_2}{C_1} \right)^2 \frac{\tau^2}{2} + \dots \right\}$$

$$+ \left[\frac{C_2}{C_1} \cos \Omega \tau - \frac{C_5}{C_1} \right] \exp \left[\frac{C_2}{\Omega C_1} \sin \Omega \tau - \frac{C_5}{C_1} \tau \right] \left[\tau + \left(\frac{C_5 - C_2}{C_1} \right) \frac{\tau^2}{2} + \left(\frac{C_5 - C_2}{C_1} \right)^2 \frac{\tau^3}{6} + \dots \right]$$

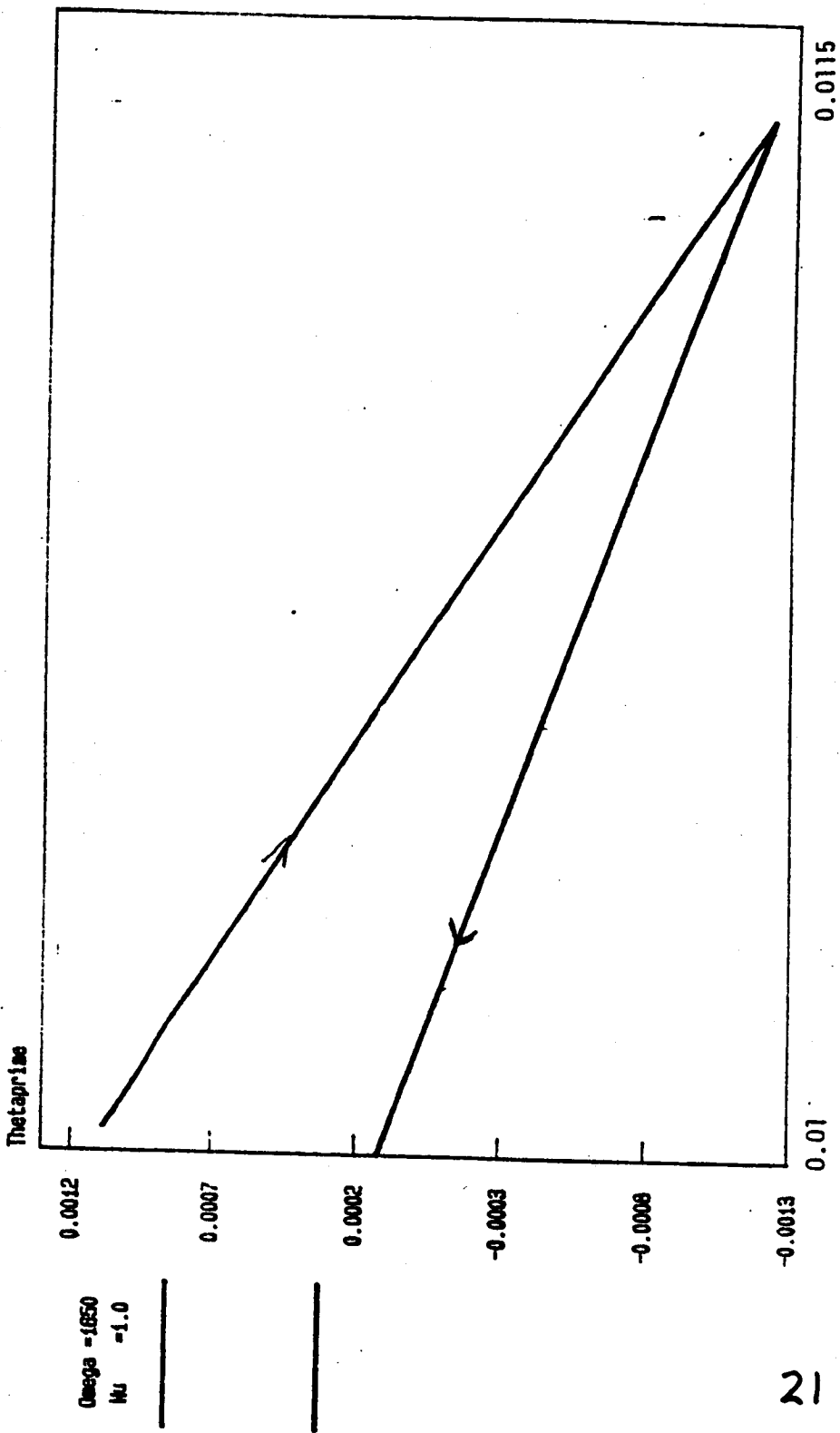
$$z_{11}(\tau) = \exp \left[\frac{C_2}{\Omega C_1} \sin \Omega \tau - \frac{C_5}{C_1} \tau \right] \left[1 + \left(C_5 - C_2 + C_2 \cos \Omega \tau - C_5 \right) \frac{\tau}{C_1} + \dots \right]$$

$$z_{11}(\tau) = \exp \left[\frac{C_2}{\Omega C_1} \sin \Omega \tau - \frac{C_5}{C_1} \tau \right] \left[1 + \frac{C_2}{C_1} (\cos \Omega \tau - 1) \tau + \frac{C_2}{C_1} (C_5 - C_2) (\cos \Omega \tau - 1) \right. \right. \\ \left. \left. + \dots \right] \right]$$

It is seen that $z_{11}(0) = 1$

ORIGINAL PAGE IS
OF POOR QUALITY

PHASE PLANE
Theta_q vs. Theta_{aprime}



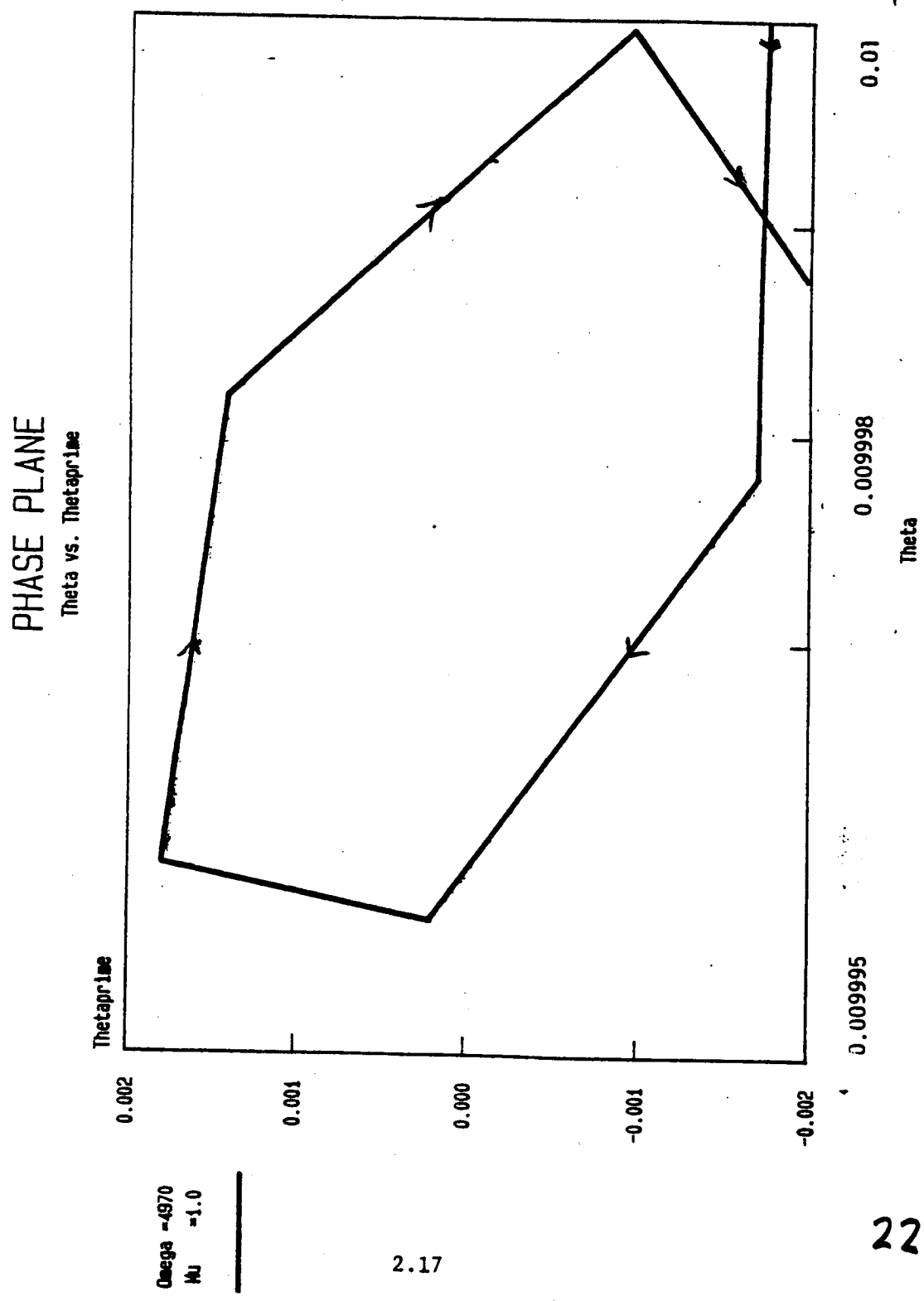


Fig. 2.2b SCOLE System-Phase Plane Trajectories - No Offset, No Gravity Gradient

ORIGINAL PAGE IS
OF POOR QUALITY

$$\Omega = \frac{\omega}{\omega_0}$$

to be multiplied
by 10³

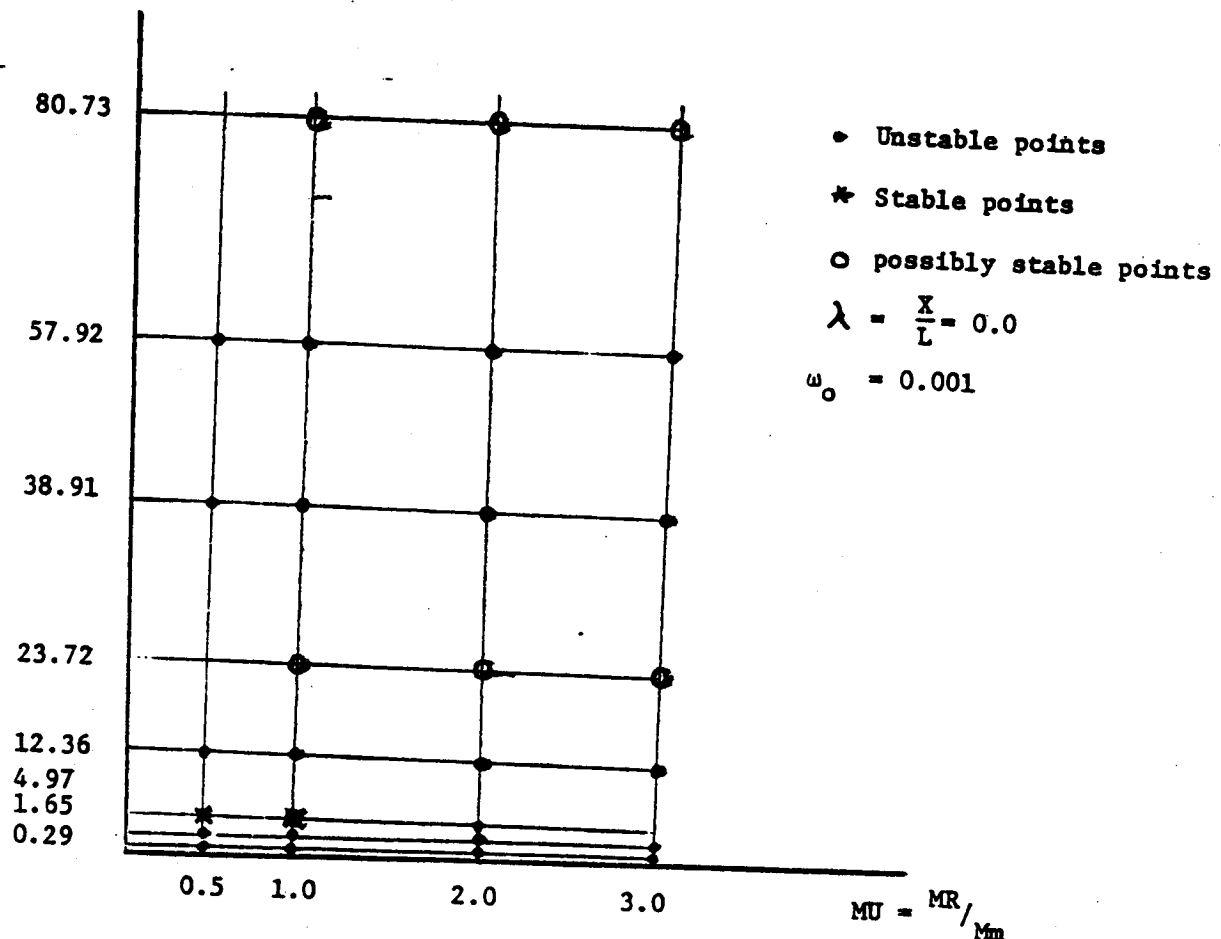


Fig. 2.3 Floquet Stability Diagram - SCOLE Configuration-No Offset
No Gravity Gradient.

$$\Omega = \frac{\omega}{\omega_0}$$

to be multiplied
by 10^3

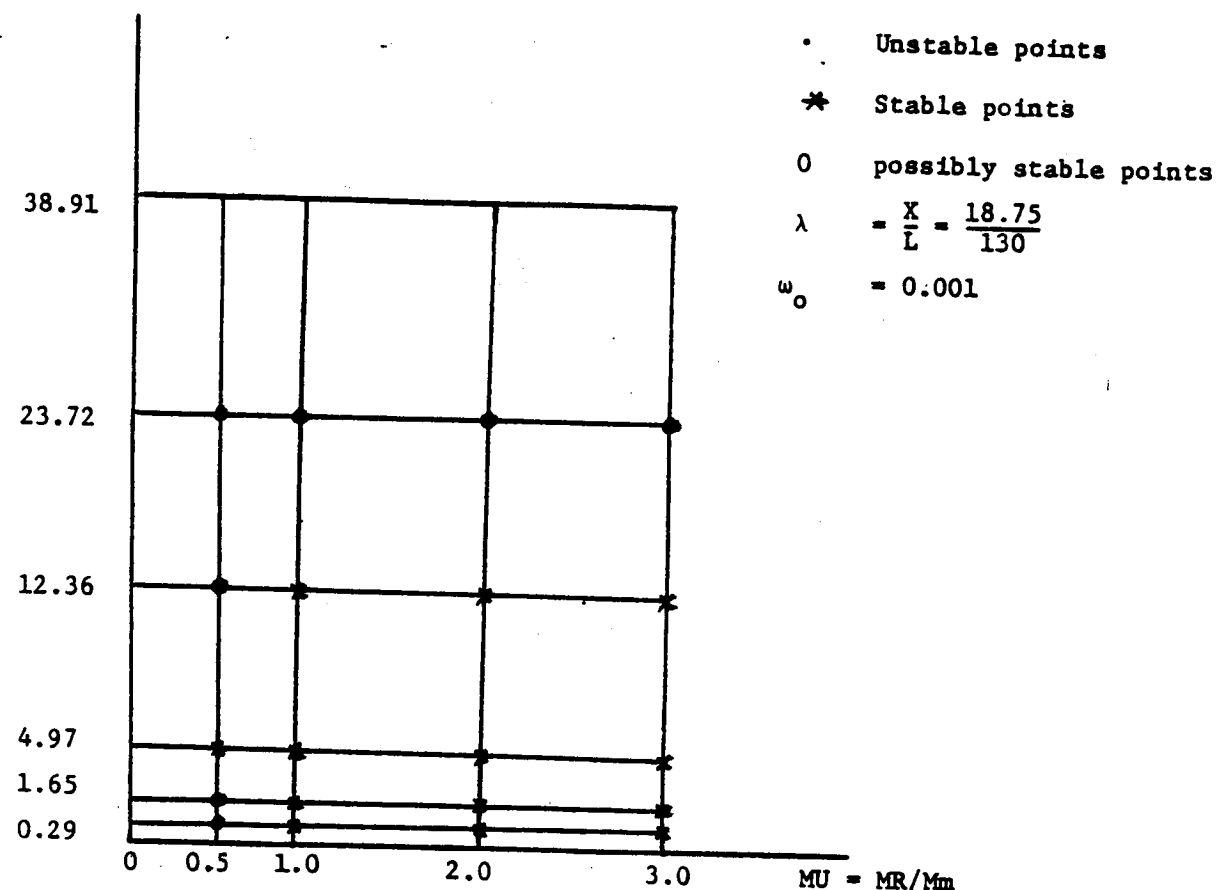


Fig. 2.5 Floquet Stability Diagram - SCOLE Configuration
No Gravity Gradient

$\Omega = \frac{\omega}{\omega_0}$
 to be multiplied
 by 10

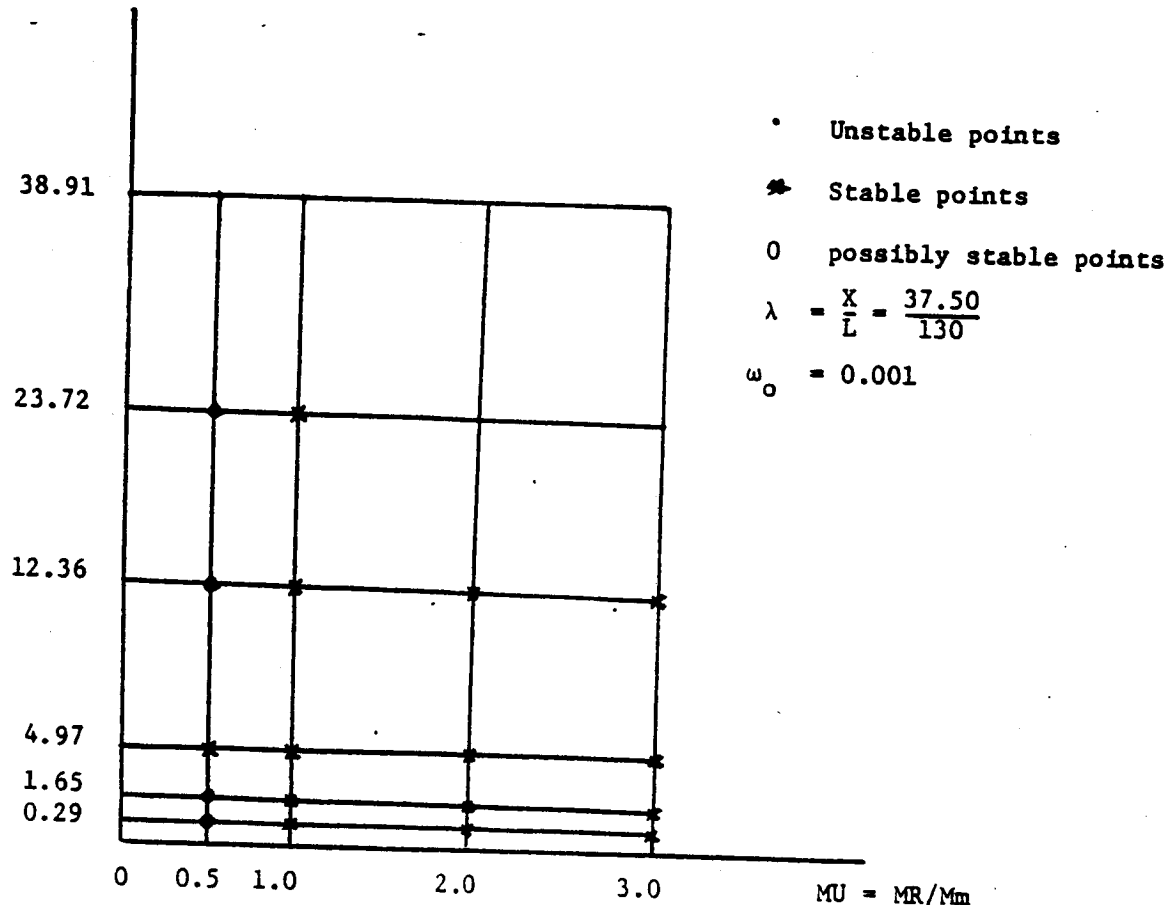


Fig. 2.4 Floquet Stability Diagram - SCOLE Configuration
No Gravity Gradient.

FLOQUET STABILITY ANALYSIS

2D SCOLE OPEN-LOOP SYSTEM

- Offset of the mast attachment point on the reflector results in an increase in the number of stable points for the lower frequencies
- Number of stable points increases for $MR/M_m > 1.0$

I. MODELLING OF THE SCOLE CONFIGURATION

- PARAMETRIC STUDY OF THE IN-PLANE SCOLE SYSTEM -
FLOQUET STABILITY ANALYSIS
- ✓ • THREE DIMENSIONAL FORMULATION OF THE SCOLE SYSTEM DYNAMICS
 - Rotational Equations of Motion
 - Structural Analysis - Boundary Conditions
 - Generic Modal Equations
- WHAT WE CAN LEARN ABOUT THE OPEN LOOP SYSTEM?
 - Consider SCOLE configuration without offset of the mast attachment to the reflector and without flexibility
 - Consider SCOLE configuration without mast flexibility but with offset in the direction of orbit (strawman)
 - Consider SCOLE configuration with offsets in two directions but neglecting mast flexibility
 - Consider general SCOLE system dynamics
- IMPLICATIONS FOR CONTROL STRATEGIES

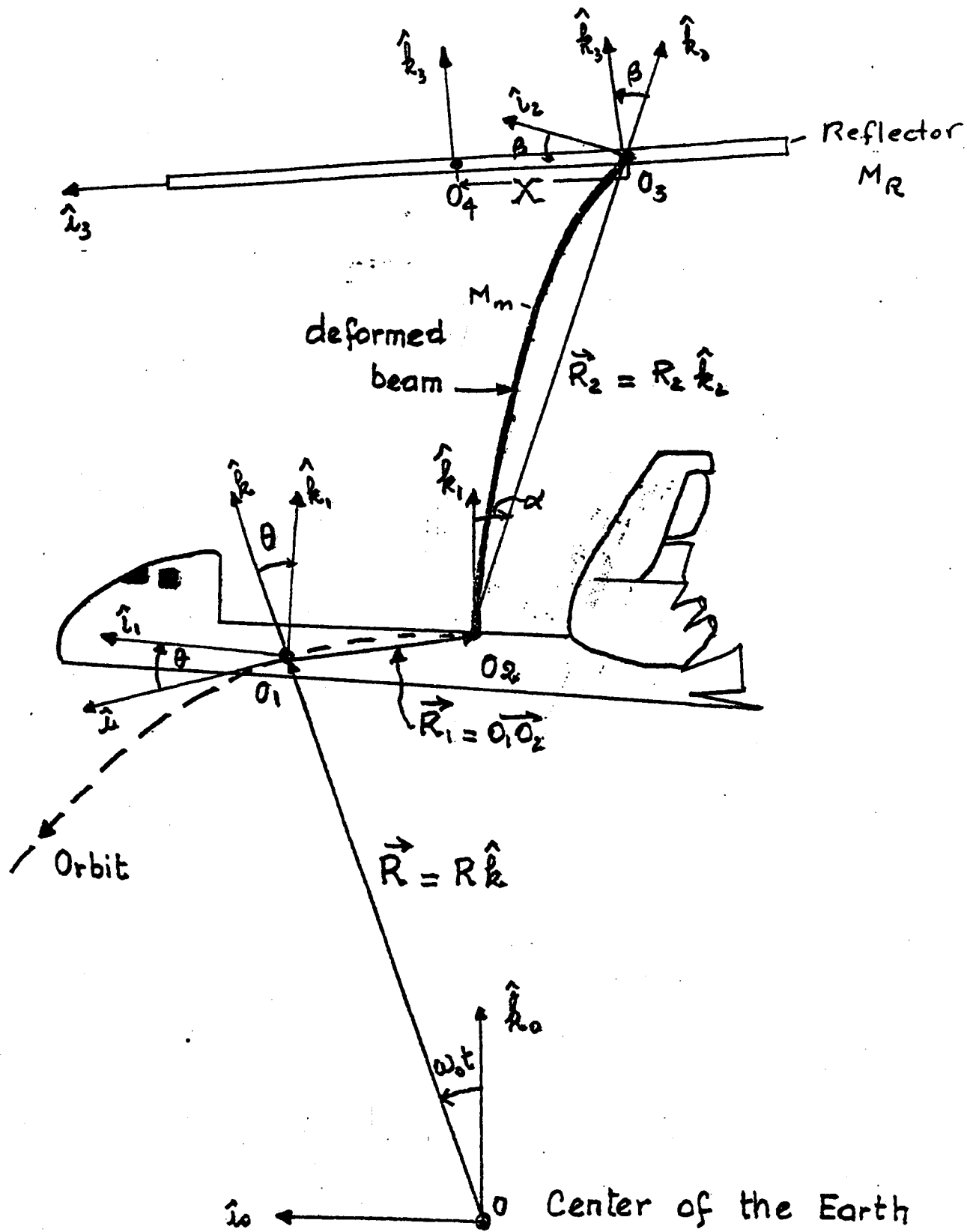


Fig. 2.1. SCOLE System Geometry in the Deformed State (2-D)

A. Angular Momentum of the Shuttle About its Mass Center, G

The angular momentum of the Shuttle, taken as a rigid body in a circular orbit, consists of contributions due to rotation about its center of mass plus the translation along the orbit.

$$\vec{H}_G = \vec{I}_G \vec{\omega}_s / R_o \quad (1.9)$$

where

$$\vec{I}_G = \begin{bmatrix} 905,443 & 0 & 145,393 \\ 0 & 6,784,100 & 0 \\ 145,393 & 0 & 7,086,601 \end{bmatrix} = [I_{ij}]$$

$$\text{in } R(x,y,z) \quad (1.10)$$

$$\vec{\omega}_s / R_o = \omega_x \hat{i} + \omega_y \hat{j} + \omega_z \hat{k} \quad (1.11)$$

B. Angular Momentum of the Beam about G

Consider an element of mass, dm , of the beam located at some point, p , such that $GP = \vec{r}_o + \vec{q} = \vec{r}$

where:

$$(1.12) \quad \vec{r}_o = -zk \text{ is the position vector of } p \text{ in the undeformed state}$$

$$(1.13) \quad \vec{q}(z,t) = u \hat{i} + v \hat{j} \text{ in which, } u \text{ and } v \text{ are the } x \text{ and } y \text{ components of the mode shape vector.}$$

The angular momentum of dm about G , $d \vec{H}_m / G$ is given by:

$$d \vec{H}_m / G = \vec{r} \times \frac{d}{dt} (-Rk + \vec{r}) \Big|_{R_o} dm \quad (1.14)$$

$$d \vec{H}_m / G = (\vec{r} \times \omega_o R \hat{i} + \vec{r} \times \frac{d}{dt} \vec{r} \Big|_{R_o}) dm$$

which is expressed explicitly as:

where $\frac{d\vec{H}_m/G}{dt} = \left\{ (-3\hat{k} + ui + vj) \times \omega_0 R \hat{i} + (-3\hat{k} + ui + vj) \times \frac{d}{dt} (-3\hat{k} + ui + vj) / R_0 \right\} dm$

$$\frac{d\vec{r}}{dt} / R_0 = \frac{d}{dt} (-3\hat{k} + ui + vj) / R_0 = (i - \omega_3 v - 3\omega_y) \hat{i} + (v + \omega_3 u + 3\omega_x) \hat{j} + (\omega_x v - u\omega_y) \hat{k}$$

$$\vec{r} \times \frac{d\vec{r}}{dt} / R_0 = -3(v - \omega_3 v) \hat{j} + 3(v + \omega_3 u) \hat{i} + u(v + \omega_3 u) \hat{k} - u(\omega_x v - u\omega_y) \hat{j} \\ - v(\omega_3 u - \omega_x v) \hat{i} - v(v - \omega_3 v) \hat{k} + 3^2(\omega_3 \hat{j} + \omega_x \hat{i}) + 3(u\omega_x + v\omega_y) \hat{k}$$

After substituting the different terms into equation (1.14), the following expression results:

$$\begin{aligned} \frac{d\vec{H}_m/G}{dt} = & \left\{ [3(v + \omega_3 u) + v(\omega_x v - \omega_y u) + 3^2\omega_x] \hat{i} \right. \\ & + [-3\omega_0 R - 3(v - \omega_3 v) + u(\omega_3 u - \omega_x v) + 3^2\omega_y] \hat{j} \\ & \left. + [-v\omega_0 R + u(v + \omega_3 u) - v(v - \omega_3 v) + 3(u\omega_x + v\omega_y)] \hat{k} \right\} dm \quad (1.15) \end{aligned}$$

Since $u(z, t) = \sum p_x^n(t) s_x^n(z)$ and $v(z, t) = \sum p_y^n(t) s_y^n(z)$,
we consider for one mode in the open-loop situation,

$$\begin{aligned} \dot{u} &= -\omega'_x \sin(\omega'_x t + \alpha) s_x^n(z) \text{ and} \\ \dot{v} &= -\omega'_y \sin(\omega'_y t + \gamma) s_y^n(z) \end{aligned} \quad (1.17)$$

Assuming small elastic displacements such that, $\frac{s_i s_j}{l^2} \ll 1$ and $s_i^2(z)/l^2 \ll 1$, and dividing $\vec{dH_m}/G$ by Ωl^2 , where Ω is an assigned frequency and l a reference length, then,

$$\frac{d\vec{H_m}/G}{\Omega l^2} \approx \frac{1}{\Omega l^2} \int (3\dot{v} + 3\omega_3 u + \omega_3 z^2) \hat{i} + (-3\omega_0 R - 3\dot{u} + \omega_3 z v + z^2 \omega_3) \hat{j} + (-\omega_0 R v + \omega_3 u z + \omega_3 z v) \hat{k} \rho dz \quad (1.18)$$

where ρ is the mass per unit length of the beam. After multiplying both sides of this equation by Ωl^2 , there results:

$$\vec{dH_m}/G = \int (3\dot{v} + 3u\omega_3 + z^2\omega_3) \hat{i} + (-3\omega_0^2 - 3\dot{u} + 3v\omega_3 + z^2\omega_3) \hat{j} + (-vR\omega_0 + 3u\omega_3 + z\omega_3) \hat{k} \rho dz \quad (1.19)$$

The total angular momentum of the mast about G is obtained by integrating (1.19) over the total length of the mast,

$$\vec{H_m}/G = \int_0^l \vec{dH_m}/G \quad (1.20)$$

The ten terms appearing in $\vec{dH_m}/G$ are integrated using integral tables- e.g.

$$\begin{aligned} \int_0^l 3\dot{v} \rho dz &= -g\omega_3' \sin(\omega_3' t + \gamma) \int_0^l 3(A_2 \sin \beta_2 z + B_2 \cos \beta_2 z + C_2 \sinh \beta_2 z \\ &\quad + D_2 \cosh \beta_2 z) dz = \\ &= -g\omega_3' \sin(\omega_3' t + \gamma) \left[A_2 \left(-\frac{\sin \beta_2 l}{\beta_2^2} + \frac{\cosh \beta_2 l}{\beta_2} \right) + B_2 \left(\frac{\sin \beta_2 l}{\beta_2^2} + \frac{\cosh \beta_2 l}{\beta_2^2} - \frac{1}{\beta_2^2} \right) \right. \\ &\quad \left. + C_2 \left(-\frac{\cosh \beta_2 l}{\beta_2^2} + \frac{\sinh \beta_2 l}{\beta_2^2} \right) + D_2 \left(\frac{l \sinh \beta_2 l}{\beta_2} - \frac{\cosh \beta_2 l}{\beta_2^2} + \frac{1}{\beta_2^2} \right) \right] \end{aligned}$$

To simplify the notation, let

f_i(\beta_i) = \left\{ A_i \left(\frac{\ell \cos \beta_i l}{\beta_i} - \frac{\sin \beta_i l}{\beta_i^2} \right) + B_i \left(\frac{\cos \beta_i l}{\beta_i^2} + \frac{\ell \sin \beta_i l}{\beta_i} - \frac{1}{\beta_i^2} \right) \right. \\ \left. + C_i \left(\frac{\sinh \beta_i l}{\beta_i^2} - \frac{\ell \cosh \beta_i l}{\beta_i} \right) + D_i \left(\frac{\ell \sinh \beta_i l}{\beta_i} - \frac{\cosh \beta_i l}{\beta_i^2} + \frac{1}{\beta_i^2} \right) \right\} \quad (1.21)

$$g_i(\beta_i) = A_i \left(\frac{1}{\beta_i} - \frac{\cos \beta_i l}{\beta_i} \right) - B_i \frac{\sin \beta_i l}{\beta_i} - D_i \frac{\sinh \beta_i l}{\beta_i} \\ + C_i \left(\frac{\cosh \beta_i l}{\beta_i} - \frac{1}{\beta_i} \right) \quad (1.22)$$

After substitution of the f_i , g_i and $\frac{M_m}{l}$ for $p_{x,y}$ in the expression of $\vec{H}_{m/G}$, one arrives at:

$$\vec{H}_{m/G} = \frac{M_m}{l} \left\{ \left[\omega_x \cos(\omega_x' t + \alpha) \vec{f}_1 - \omega_y' \sin(\omega_y' t + \gamma) \vec{f}_2 - \omega_x \frac{l^3}{3} \right] \vec{i} \right. \\ + \left[\omega_0 R \frac{l^2}{2} + \omega_x' \sin(\omega_x' t + \alpha) \vec{f}_1 + \omega_y \cos(\omega_y' t + \gamma) \vec{f}_2 - \omega_y \frac{l^3}{3} \right] \vec{j} \\ \left. + \left[\omega_x \cos(\omega_x' t + \alpha) \vec{f}_1 + \omega_y \cos(\omega_y' t + \gamma) \vec{f}_2 + \omega_0 R \cos(\omega_y' t + \gamma) \vec{f}_2 \right] \vec{k} \right\} \quad (1.23)$$

C. Angular Momentum of the Reflector about G.

Since small deflections for the beam are assumed, the reflector can be assumed to be located at a constant distance from G, the Shuttle mass center.

Using the transfer theorem for the angular momentum, (See Appendix IIIA)

$$\vec{H}_{r/G} = \bar{\bar{I}}_{r/o_1} \vec{\omega}_{r/R_o} + M_r \vec{G} \vec{O}_x \frac{d(\vec{O}O_1)}{dt} \quad (1.24)$$

where $\bar{\bar{I}}_{r/o_1}$ and $\vec{\omega}_{r/R_o} = \vec{\omega}_{r/s} + \vec{\omega}_{r/s}$ (1.25) are both expressed in the same coordinate system, $R_2(x_2, y_2, z_2)$, moving with the reflector. In R_2 (principal axes of inertia of the reflector),

$$\bar{\bar{I}}_{r/o_1} = \begin{bmatrix} I_{r_1} & 0 & 0 \\ 0 & I_{r_2} & 0 \\ 0 & 0 & I_{r_3} \end{bmatrix} = \begin{bmatrix} 4,969 & & 0 \\ 0 & 4,969 & 0 \\ 0 & 0 & 9,938 \end{bmatrix} \quad (1.26)$$

$$\vec{\omega}_{r/R_o} = \omega_x \hat{i} + \omega_y \hat{j} + \omega_z \hat{k} + \dot{\psi}_r \hat{i} + \dot{\theta}_r \hat{j} + \dot{\phi}_r \hat{k}_2 \quad (1.27)$$

with $\hat{j}' = \sin \phi_r \hat{i}_2 + \cos \phi_r \hat{j}_2$

therefore,

$$\begin{aligned} \vec{\omega}_{r/R_o} = & (\omega_x + \dot{\psi}_r) \hat{i} + \omega_y \hat{j} + \omega_z \hat{k} + \dot{\theta}_r \sin \phi_r \hat{i}_2 + \dot{\theta}_r \cos \phi_r \hat{j}_2 \\ & + \dot{\phi}_r \hat{k}_2 \end{aligned} \quad (1.28)$$

$$\vec{H}_{r/G} = \omega_1 \vec{I}_r \vec{i}_2 + \omega_2 \vec{I}_{r_2} \vec{j}_2 + \omega_3 \vec{I}_{r_3} \vec{k}_2 + M_r \{ (b\ell + c(r+y)) \vec{i} - (a\ell + c(u+x)) \vec{j} + (b(u+x) - a(v+y)) \vec{k} \} \quad (1.34)$$

Where

$$a = \{ (\omega_0 R + u\ell - \omega_y \ell - \omega_3 v - \omega_3 Y \vec{T}_{11} + X \omega_3 \vec{T}_{21}) + (\omega_1 Y - \omega_2 X) \vec{T}_{31} \}.$$

$$b = \{ \dot{v} - \omega_x \ell + \omega_3 u - \omega_3 Y \vec{T}_{12} + \omega_3 X \vec{T}_{22} + (\omega_1 Y - \omega_2 X) \vec{T}_{32} \}$$

$$c = \{ \omega_x v - \omega_y u - \omega_3 Y \vec{T}_{13} + \omega_3 X \vec{T}_{23} + (\omega_1 Y - \omega_2 X) \vec{T}_{33} \}$$

D. Angular Momentum of the System about G

The angular momentum of the system = the sum of the angular momentum of each component evaluated at the same point

$$\begin{aligned}
 \vec{H}_{\text{System}/G} &= \vec{H}_{S/G} + \vec{H}_{m/G} + \vec{H}_{r/G} \\
 &= (\omega_x I_{11} + \omega_z I_{13}) \hat{i} + (\omega_y I_{22}) \hat{j} + (\omega_x I_{31} + \omega_z I_{33}) \hat{k} \\
 &+ \frac{M_r}{I} \left\{ [\omega_z \cos(\omega_x t + \alpha) \hat{g}_1 - \omega_x' \sin(\omega_x t + \alpha) \hat{g}_2 - \omega_x \frac{I^3}{3}] \hat{i} \right. \\
 &+ \left[\omega_0 R \frac{\ell^2}{2} + \omega_x' \sin(\omega_x t + \alpha) \hat{g}_1 + \omega_z \cos(\omega_x t + \alpha) \hat{g}_2 - \omega_x \frac{I^3}{3} \right] \hat{j} \\
 &+ \left. \left[\omega_x \cos(\omega_x t + \alpha) \hat{g}_1 + \omega_y \cos(\omega_x t + \alpha) \hat{g}_2 - \omega_0 R \cos(\omega_x t + \alpha) \hat{g}_3 \right] \hat{k} \right\} \\
 &+ M_r \left\{ (b\ell + c(v+y)) \hat{i} - (a\ell + c(u+x)) \hat{j} + (b(u+x) - a(v+y)) \hat{k} \right\} \\
 &+ c\omega_1 I_{11} \hat{i}_2 + \omega_2 I_{22} \hat{j}_2 + c\omega_3 I_{33} \hat{k}_2
 \end{aligned} \tag{1.35}$$

In the expression for the total angular momentum, the last term will now be expressed in $R(x, y, z)$ by simply transforming \hat{i}_2 , \hat{j}_2 , and \hat{k}_2 into functions of \hat{i} , \hat{j} , and \hat{k} as follows:

$$\begin{aligned}
 \hat{i}_2 &= \cos \Phi_r \cos \Theta_r \hat{i} + \sin \Phi_r \cos \Theta_r \hat{j} + \sin \Phi_r \sin \Theta_r \hat{k} \\
 \hat{j}_2 &= -\sin \Phi_r \cos \Theta_r \hat{i} + (\cos \Phi_r \cos \Theta_r - \sin \Phi_r \sin \Theta_r \sin \Theta_r) \hat{j} \\
 &\quad + (\sin \Phi_r \sin \Theta_r \cos \Theta_r + \cos \Phi_r \sin \Theta_r) \hat{k} \\
 \hat{k}_2 &= \sin \Theta_r \hat{i} - \cos \Theta_r \sin \Theta_r \hat{j} + \cos \Theta_r \cos \Theta_r \hat{k}
 \end{aligned} \tag{1.36}$$

Rotational Equations of Motion. (Torque Free)

In the linear range,

$$\begin{aligned}
 & \dot{H}_x + \omega_y H_z - \omega_z H_y = 0 \quad (A) \\
 \Rightarrow & \left\{ (\ddot{\psi} - \omega_0 \dot{\phi}) I_{11} + (\ddot{\phi} + \omega_0 \dot{\psi}) I_{13} + \frac{M_r}{\ell} [(\dot{\phi} + \omega_0 \dot{\psi}) \cos(\omega_0 t + \alpha) \dot{q}_1 \right. \\
 & - \omega_x (\dot{\phi} + \omega_0 \dot{\psi}) \sin(\omega_0 t + \alpha) \dot{q}_1 - \omega_y^2 \cos(\omega_0 t + \delta) \dot{q}_2 - (\ddot{\psi} - \omega_0 \dot{\phi}) \dot{q}_3] \\
 & + (\ddot{\psi} - \omega_0 \dot{\phi} + \ddot{\psi}_r - \omega_0 \dot{\phi}_r) \bar{I}_{11} + \omega_0 \dot{\phi}_r \bar{I}_{13} \} + (\omega_0^2 \phi - \omega_0 \dot{\psi}) I_{31} \\
 & + (\omega_0 \dot{\phi} + \omega_0^2 \psi) (I_{22} - I_{33}) \quad) + \frac{M_r}{\ell} [(\omega_0^2 \phi - \omega_0 \dot{\psi}) \cos(\omega_0 t + \alpha) \dot{q}_1 \\
 & + (\omega_0^2 - 2\omega_0 \dot{\theta}) \cos(\omega_0 t + \delta) \dot{q}_2 - (\omega_0 \dot{\theta} - \omega_0^2) R \cos(\omega_0 t + \delta) \dot{q}_2] \\
 & + \omega_0^2 \dot{\psi}_r \bar{I}_{13} - (\dot{\psi}_r \omega_0^2 + \omega_0 \dot{\phi} + \omega_0^2 \psi + \omega_0 \dot{\phi}_r) \bar{I}_{13} + M_r (u + x) / (\theta - \omega_0) \dot{v} \\
 & + \ell (\omega_0^2 \phi - \omega_0 \dot{\psi}) - (\omega_0 \dot{\phi} + \omega_0^2 \psi) u - x (\omega_0^2 \dot{\psi}_r + \omega_0 \dot{\phi}_r + \omega_0^2 \psi + \omega_0 \dot{\phi}) \\
 & + \omega_0^2 \dot{\psi}_r x \} - M_r (v + y) / (\omega_0 \dot{\theta} - \omega_0^2) R + (\theta - \omega_0) \dot{u} + (\omega_0 \dot{\theta} - \omega_0^2) \ell \\
 & + (\omega_0 \dot{\phi} + \omega_0^2 \psi) v + y (\omega_0^2 \dot{\psi}_r + \omega_0 \dot{\phi}_r + \omega_0 \dot{\phi} + \omega_0^2 \psi) - \omega_0^2 \theta_r x \} \\
 & + M_r \ell [\ddot{v} + (\ddot{\psi} - \omega_0 \dot{\phi}) \ell + x (\ddot{\phi} + \omega_0 \dot{\psi} + \ddot{\phi}_r)] + M_r x \omega_0 \dot{v} \\
 & + M_r y [y (\ddot{\psi} + \ddot{\psi}_r - \omega_0 (\dot{\phi} - \dot{\phi}_r)) - x (\ddot{\theta} + \ddot{\theta}_r)] = 0 \quad (1.45)
 \end{aligned}$$

$$\dot{H}_y + \omega_3 H_x - \omega_x H_3 = 0 \quad (8)$$

$$\Leftrightarrow \ddot{\theta} I_{22} + \frac{M_m}{\ell} \left[\omega_x' \cos(\omega_x' t + \alpha) f_1 + (\dot{\phi} + \omega_0 \dot{\psi}) \cos(\omega_y' t + \delta) f_2 \right. \\ - 2\omega_y' (\dot{\phi} + \omega_0 \dot{\psi}) \sin(\omega_y' t + \delta) f_2 - \ddot{\theta} \frac{\ell^3}{3} + \cos(\dot{\psi} - \omega_0 \phi) \cos(\omega_y' t + \delta) (f_2 + g_2 R) \\ + I_{2r} (\ddot{\theta} - \ddot{\theta}_r) - M_r \ell \left[\ddot{u} - \ddot{\theta} \ell - Y (\dot{\phi} + \omega_0 \dot{\psi} + \dot{\phi}_r + \omega_0 \dot{\psi}_r) \right. \\ \left. + \omega_0 \dot{\theta}_r X \right] - 2M_r X \omega_0 \dot{u} - M_r \dot{X} Y (\dot{\psi} - \omega_0 \dot{\phi} + \dot{\psi}_r - \omega_0 \dot{\phi}_r) \\ \left. - M_r X^2 (\ddot{\theta} + \ddot{\theta}_r) - M_r Y (\dot{\psi} - \omega_0 \phi) (\omega_0 R + \omega_0 \ell) \right] = 0 \quad (1.47)$$

$$\dot{H}_3 + \omega_x H_y - \omega_y H_x = 0 \quad (c)$$

$$\Rightarrow \left\{ \begin{aligned} & (\ddot{\psi} - \omega_0 \dot{\phi}) I_{31} + (\ddot{\phi} + \omega_0 \dot{\psi}) I_{33} + \frac{M_m}{\ell} [(\ddot{\psi} - \omega_0 \dot{\phi}) \cos(\omega_x t + \alpha) g_1 \\ & + \omega_z' (\ddot{\psi} - \omega_0 \dot{\phi}) \sin(\omega_x t + \alpha) g_1 + \ddot{\theta} \cos(\omega_y t + \gamma) g_2 - \omega_y' (\ddot{\theta} - \omega_0) \sin(\omega_y t + \gamma) g_2 \\ & + \omega_0 \omega_y' R \sin(\omega_y t + \delta) g_2] + M_r (\mu + X) [\ddot{v} + \ddot{\psi} \ell - \omega_0 \dot{\phi} \ell + \ddot{\phi} u + \dot{\phi} \dot{u} + \omega_0 \dot{\psi} u \\ & + \omega_0 \dot{\psi} \dot{u} + X (\dot{\psi} \omega_0 + \ddot{\phi} + \omega_0 \dot{\psi} + \ddot{\phi}_r - \omega_0 \dot{\psi}_r)] + M_r u [\ddot{v} + (\ddot{\psi} - \omega_0 \dot{\phi}) \ell + (\dot{\phi} + \omega_0 \dot{\psi}) u \\ & + X (\dot{\phi} + \omega_0 \dot{\psi} + \ddot{\phi}_r) - M_r (v + Y) [\ddot{u} - \ddot{\theta} \ell - \dot{\phi} v - \dot{\phi} \dot{v} - \omega_0 \dot{\psi} v - \omega_0 \dot{\psi} \dot{v} \\ & - Y (\dot{\psi} \omega_0 + \ddot{\phi}_r + \omega_0 \dot{\psi} + \ddot{\phi}) + \omega_0 X \dot{\phi}_r] - M_r \dot{v} [\omega_0 R + \dot{u} - (\dot{\phi} - \omega_0) \ell \\ & - (\dot{\phi} + \omega_0 \dot{\psi}) v + \omega_0 \dot{\phi}_r X - Y (\dot{\psi} \omega_0 + \dot{\phi} + \omega_0 \dot{\psi} + \ddot{\phi}_r)] - (\ddot{\psi} - \omega_0 \dot{\phi}) \omega_0 I_{22} \\ & + \frac{M_m}{\ell} (\ddot{\psi} - \omega_0 \dot{\phi}) (\omega_0 R \frac{\ell^2}{2} + \omega_x' \sin(\omega_x t + \alpha) g_1 + \omega_0 \frac{\ell^3}{3}) - \omega_0 (\ddot{\psi} - \omega_0 \dot{\phi}) I_{r2} \\ & - M_r \ell (\ddot{\psi} - \omega_0 \dot{\phi}) (\omega_0 R + \dot{u} + \omega_0 \ell) - M_r (\mu + X)^2 (\ddot{\psi} - \omega_0 \dot{\phi}) + \omega_0 (\ddot{\psi} - \omega_0 \dot{\phi}) \bar{I}_{11} \\ & + \omega_0 (\dot{\phi} + \omega_0 \dot{\psi}) \bar{I}_{13} + \omega_0 \frac{M_m}{\ell} (\dot{\phi} + \omega_0 \dot{\psi}) \cos(\omega_x t + \alpha) g_1 + (\dot{\theta} - \omega_0) \omega_y' \sin(\omega_y t + \gamma) g_2 \\ & - \frac{M_m}{\ell} \ell^2 (\ddot{\psi} - \omega_0 \dot{\phi}) + \omega_0 (\ddot{\psi} - \omega_0 \dot{\phi} + \dot{\psi}_r - \omega_0 \dot{\phi}_r) I_{r1} + \omega_0^2 \ddot{\phi}_r \bar{I}_{1r} \\ & + M_r \omega_0 \int v \ell + (\dot{\psi} + \omega_0 \dot{\phi}) \ell^2 + X \ell (\dot{\psi}_r \omega_0 + \ddot{\phi}_r \\ & + \dot{\phi} + \omega_0 \dot{\psi}) - \omega_0 \dot{\psi}_r X \ell + Y \omega_0 u + Y^2 (\dot{\psi} + \dot{\psi}_r - \omega_0 \dot{\phi} - \omega_0 \dot{\phi}_r) \\ & - X (\dot{\theta} - \omega_0 + \dot{\theta}_r) = 0 \quad (1.49) \end{aligned} \right.$$

2. STRUCTURAL ANALYSIS

A. Governing Differential Equations

The governing partial differential equations for the system (beam) are comprised of two one-plane-bending equations (2.1) and (2.2) and one axial torsion equation, (2.9).

All these equations assume small displacements and slopes, uniform density and distribution of stiffness, and the torsional equation is derived for a circular shaft.

$$\text{for the } x\text{-}z \text{ plane bending: } -\frac{\partial^2(u(z,t))}{\partial t^2} = \frac{\rho A}{EI_x} \frac{\partial^4 u(z,t)}{\partial z^4} \quad (2.1)$$

$$\text{for the } y\text{-}z \text{ plane bending: } -\frac{\partial^2(v(z,t))}{\partial t^2} = \frac{\rho A}{EI_y} \frac{\partial^4 v(z,t)}{\partial z^4} \quad (2.2)$$

where ρ is the density of the beam, A its cross sectional area, and $(EI)_x$, $(EI)_y$ its $(x\text{-}z)$ and $(y\text{-}z)$ plane bending stiffnesses, respectively.

Assuming separation of variables for $u(z,t)$, one may write $u(z,t) = r_x(z)p_x(t)$, and equation (2.1) can then be rewritten as:

$$\ddot{P}_x = -\frac{\rho A}{EI_x} \frac{r_x^{(4)}}{r_x} \quad (2.3)$$

This equation is valid if and only if both sides are equal to a constant: $-\omega_x'^2$

Therefore $\ddot{P}_x + \omega_x'^2 P_x = 0$ (2.4), which integrates into

$P_x(t) = \cos(\omega_x' t + \alpha)$, (2.5); where α is a phase angle.

$$r_x^{(4)} - \omega_x'^2 \frac{\rho A}{EI_x} r_x = 0 \Rightarrow r_x^{(4)} - \beta_x^4 r_x = 0 \quad (2.6)$$

where $\beta_x^4 = \frac{\rho A}{EI_x} \omega_x'^2$

this equation yields.

$$r_x = A_1 \sin \beta_x z + B_1 \cos \beta_x z + C_1 \sinh \beta_x z + D_1 \cosh \beta_x z$$

$$\Rightarrow u(z, t) = \cos(\omega_x' t + \delta) \{ A_1 \sin \beta_x z + B_1 \cos \beta_x z + C_1 \sinh \beta_x z + D_1 \cosh \beta_x z \} \quad (2.7)$$

A similar reasoning enables us to find the solution of equation (2.2) in the following form:

$$v(z, t) = \cos(\omega_y' t + \delta) \{ A_2 \sin \beta_y z + B_2 \cos \beta_y z + C_2 \sinh \beta_y z + D_2 \cosh \beta_y z \} \quad (2.8)$$

Finally the z axis torsional bending is described by:

$$(2.9) \quad \frac{\partial^2 \bar{\Phi}(z, t)}{\partial t^2} = \frac{G}{J} \frac{\partial^2 \bar{\Phi}(z, t)}{\partial z^2} \quad \text{where } G \text{ is}$$

the modulus of rigidity of the beam.

Assuming $\Phi(z, t) = \theta(z) P_z(t)$ and substituting it into equation (2.9) yields:

$$\ddot{\bar{P}}_3 / \bar{P}_3 = - \frac{G}{J} \frac{\bar{\theta}^{(2)}}{\bar{\theta}} = - \omega_3'^2 \quad (2.10)$$

$$\ddot{\bar{P}}_3 / \bar{P}_3 = - \omega_3'^2 \Rightarrow P(t) = \cos(\omega_3' t + \delta) \quad \text{and} \quad (2.11)$$

$$\frac{G}{J} \frac{\bar{\theta}^{(2)}}{\bar{\theta}} = \omega_3'^2 \Rightarrow \bar{\theta}(z) = A_3 \sin \beta_3 z + B_3 \cos \beta_3 z \quad (2.12)$$

Therefore,

$$\bar{\Phi}(z, t) = \cos(\omega_3' t + \delta) \{ A_3 \sin \beta_3 z + B_3 \cos \beta_3 z \} \quad (2.13)$$

B. Boundary Conditions (I-X) and Natural Frequencies of Vibration

The following relationships between shear, moment, and beam displacement are used in the boundary conditions

$$V_x = -\frac{EI}{L^3} u \quad (3)$$

$$V_y = -\frac{EI}{L^3} v \quad (3)$$

$$M_x = -\frac{EI}{L^2} v \quad (2)$$

$$M_y = -\frac{EI}{L^2} u \quad (2) \quad \text{and}$$

$$M_z = \frac{GI_p}{L} - \frac{\partial \phi}{\partial \epsilon}$$

(2.17)

where, V_x = shear force in the x direction

V_y = " " " " y direction

M_x M_y and M_z the moment x , y , and z components, respectively.

I_p is the beam polar moment of inertia. Let M_s be the mass of the Shuttle while M_r is the mass of the reflector. The displacement in the x direction of a point located at $z = 0$ is given by $u(0, t) - \Delta y_o \phi(0, t)$ and that in the y direction by $v(0, t) + \Delta x_o \phi(0, t)$ where Δx_o , Δy_o are the coordinates of the c.m. of the end body (Shuttle).

Now, an attempt will be made to cast the 10 equations describing the boundary conditions into the following matrix form:

$[M] \{A\} = 0$ which has a non-trivial solution only when $\det[M] = 0$.

Since there is no offset at the Shuttle end, $\Delta X_0 = \Delta Y_0 = 0$. Therefore B.C. (I) becomes

$$\frac{EI}{l^3} r_x^{(3)}|_{\varepsilon=0} = + M_s \omega^2 r_x|_{\varepsilon=0}$$

Explicitly

$$(EI/l^3) \beta_1^3 \{-A_1 + C_1\} = M_s \omega^2 \{B_1 + D_1\} \quad (I')$$

B.C. (II) becomes

$$\frac{EI}{l^3} r_y^{(3)}|_{\varepsilon=0} = M_s \omega^2 r_y|_{\varepsilon=0}$$

$$(EI/l^3) \beta_2^3 \{-A_2 + C_2\} = M_s \omega^2 \{B_2 + D_2\} \quad (II')$$

Equation (III')

$$\begin{aligned} & \frac{EI}{l^3} \beta_1^3 \{-A_1 \cos \beta_1 + B_1 \sin \beta_1 + C_1 \cosh \beta_1 + D_1 \sinh \beta_1\} \\ & = -\omega^2 M_r \{-A_1 \sin \beta_1 - B_1 \cos \beta_1 - C_1 \sinh \beta_1 - D_1 \cosh \beta_1 \\ & \quad + \Delta Y_1 A_3 \sin \beta_3 + \Delta Y_1 B_3 \cos \beta_3\} \end{aligned}$$

Equation IV'

$$\begin{aligned} & \frac{EI}{l^3} \beta_2^3 \{ -A_2 \sin \beta_2 + B_2 \sinh \beta_2 + C_2 \cosh \beta_2 + D_2 \sinh \beta_2 \} \\ &= -\omega^2 M_r \{ -A_2 \sin \beta_2 - B_2 \cosh \beta_2 - C_2 \sinh \beta_2 - D_2 \cosh \beta_2 \\ & \quad - \Delta X_1 A_3 \sin \beta_3 - \Delta X_1 B_3 \cosh \beta_3 \} \end{aligned}$$

Equation V'

$$\frac{EI}{l^2} \beta_2^2 \{ -B_2 + D_2 \} = -\omega^2 \left\{ \frac{I_{xys}}{l} \beta_2 (A_2 + C_2) - \frac{I_{xys}}{l} \beta_1 (A_1 + C_1) \right\}$$

Equation VI'

$$\frac{EI}{l^2} \beta_1^2 \{ -B_1 + D_1 \} = -\omega^2 \left\{ \frac{I_{xys}}{l} \beta_1 (A_2 + C_2) + \frac{I_{yys}}{l} \beta_1 (A_1 + C_1) \right\}$$

Equation VII'

$$\begin{aligned} & \frac{EI}{l^2} \beta_2^2 \{ -A_2 \sin \beta_2 - B_2 \cosh \beta_2 + C_2 \sinh \beta_2 + D_2 \cosh \beta_2 \} = \\ & -\omega^2 \left\{ \frac{I_{xys}}{l} \beta_2 (A_2 \cosh \beta_2 - B_2 \sin \beta_2 + C_2 \cosh \beta_2 + D_2 \sinh \beta_2) \right. \\ & \quad \left. - \frac{I_{xys}}{l} \beta_1 (A_1 \cosh \beta_1 - B_1 \sin \beta_1 + C_1 \cosh \beta_1 + D_1 \sinh \beta_1) \right\} \end{aligned}$$

Equation VIII'

$$\begin{aligned} & \frac{EI}{l^2} \beta_1^2 \{ -A_1 \sin \beta_1 - B_1 \cosh \beta_1 + C_1 \sinh \beta_1 + D_1 \cosh \beta_1 \} = \\ & -\omega^2 \left\{ \frac{I_{xys}}{l} \beta_2 (A_2 \cosh \beta_2 - B_2 \sin \beta_2 + C_2 \cosh \beta_2 + D_2 \sinh \beta_2) \right. \\ & \quad \left. - \frac{I_{yys}}{l} \beta_1 (A_1 \cosh \beta_1 - B_1 \sin \beta_1 + C_1 \cosh \beta_1 + D_1 \sinh \beta_1) \right\} \end{aligned}$$

Equation IX

$$\frac{GI_P}{\ell} \beta_3 A_3 = -\omega^2 I_{33s} B_3$$

Equation X

$$\begin{aligned} \frac{GI_P}{\ell} \beta_3 (A_3 \cos \beta_3 - B_3 \sin \beta_3) &= -\omega^2 \left\{ -I_{33r} (A_3 \sin \beta_3 + B_3 \cos \beta_3) \right. \\ &+ M_r (-\Delta X_r [A_2 \sin \beta_2 + B_2 \cos \beta_2 + C_2 \sinh \beta_2 + D \cosh \beta_2]) \\ &+ \Delta Y_r [A_1 \sin \beta_1 + B_1 \cos \beta_1 + C_1 \sinh \beta_1 + D \cosh \beta_1] \left. \right\} \end{aligned}$$

3. GENERIC MODE EQUATIONS

Consider an elemental mass, dm , of the body whose instantaneous position from the center of mass of the Shuttle is r . The equations of motion of dm can be written as

$$\vec{a} dm = L(\vec{q}) + \vec{f}_{dm} + \vec{e}_{dm} \quad (3.1)$$

where \vec{a} is the inertial acceleration of dm ; \vec{f} , the gravitational force per unit mass; \vec{e} , the external force per unit mass; \vec{q} , the elastic displacement of dm ; and L , a linear operator which when applied to the small elastic displacement, \vec{q} , yields the elastic forces acting on dm .

The gravitational force per unit mass \vec{f} , can be expressed as

$$\vec{f} = \vec{f}_0 + \vec{M}r \quad (3.2)$$

where \vec{f}_0 is the gravitational force per unit mass as the center of mass of the body considered and M = matrix operator.

In what follows, the generic mode equations will be derived based on a Newton-Euler formulation. The principal assumptions made in this development are: 1) within each component of the system, the mass and structural properties are uniformly distributed; 2) the material of each component is isotropic; 3) the system is deformed in such a manner that it experiences only small strains (within the linear range); 4) elastic displacements are small as compared with the characteristic linear dimensions of the system; 5) the natural mode shapes of free vibrations of the system are known *à priori*; 6) the system is nominally earth pointing; 7) the system is considered to be closed: no mass transfer across its boundaries.

The vector equation (3.1) can be written in the frame moving with each body as:

$$[\vec{a}_{cm} + \ddot{\vec{r}} + 2\vec{\omega} \times \vec{r} + \dot{\vec{\omega}} \times \vec{r} + \vec{\omega} \times (\vec{\omega} \times \vec{r})] dm = L(\vec{q}) + (\vec{f} + \vec{e}) dm \quad (3.3)$$

Note that $\dot{\vec{r}}$ and $\ddot{\vec{r}}$ are the velocity and acceleration of dm as seen from the body fixed frame. The symbol $\vec{\omega}$ refers to the inertial angular velocity of the body. The instantaneous position vector, \vec{r} , of dm can be written as

$$\vec{r} = \vec{r}_0 + \vec{q} \quad (3.4)$$

where \vec{r}_0 is the position vector of dm with respect to G, center of mass of the Shuttle, in the undeformed state; \vec{q} is the elastic displacement of dm . Hence

$$\dot{\vec{r}} = \dot{\vec{q}} \quad \text{and} \quad \ddot{\vec{r}} = \ddot{\vec{q}} \quad (3.5)$$

For small amplitude elastic displacements, one can write the elastic displacement, \vec{q} , as a superposition of the various modal contributions according to

$$\vec{q} = \sum_{n=1}^{\infty} A_n(t) \vec{\Phi}^{(n)}(\vec{r}_0) \quad (3.6)$$

where $A_n(t) = P^{(n)}(t) (r_x^2 + r_y^2 + \theta^2)^{1/2}$
= modal amplitude

and

$$\vec{\Phi}^{(n)}(\vec{r}_0) = \frac{r_x \hat{i} + r_y \hat{j} + \theta \hat{k}}{\sqrt{r_x^2 + r_y^2 + \theta^2}} \quad (3.7)$$

The mode shape $\vec{\phi}^{(n)}(z)$ is associated with the natural frequency, ω_n , and satisfies the following conditions

$$\int_M \vec{\Phi}^{(m)} \cdot \vec{\Phi}^{(n)} dm = \delta_{mn} M_n \quad (3.8)$$

where M_n is the generalized mass in the n^{th} mode.

$$L(\vec{\Phi}^{(n)}) = -\rho \omega_n^2 \vec{\Phi}^{(n)} \quad (3.9)$$

$$\int_M \vec{\Phi}^{(n)} dm = \vec{0} \quad (3.10)$$

$$\text{and} \quad \int_M \vec{r}_0 \times \vec{\Phi}^{(n)} dm = \vec{0} \quad (3.11)$$

This here assumes that the structural frequencies are much greater than the 1.745 hour/orbit. $\omega_0 = 0.001 \text{ rad/s}$ orbital angular velocity. This enables one to use, with a high degree of accuracy, the mode shape functions corresponding to non-rotating structures. The generic mode equation is obtained by taking the modal components of all internal, external and inertial forces acting on the system, i.e.,

$$\begin{aligned} & \int_M \vec{\Phi}^{(n)} \cdot \left[\vec{a}_{cm} + \ddot{\vec{r}} + 2\vec{\omega} \times \dot{\vec{r}} + \dot{\vec{\omega}} \times \vec{r} + \vec{\omega} \times (\vec{\omega} \times \vec{r}) \right] dm \\ &= \int_M \vec{\Phi}^{(n)} \cdot \left[L(\vec{q})/dm + \vec{f} + \vec{e} \right] dm \end{aligned} \quad (3.12)$$

The various terms appearing in equation (3.12) can now be expanded as follows:

$$\int_M \vec{\Phi}^{(n)} \cdot \vec{a}_{cm} = \vec{a}_{cm} \cdot \int_M \vec{\Phi}^{(n)} dm = \vec{0} \quad (3.13)$$

$$\int_M \vec{\Phi}^{(n)} \cdot \ddot{\vec{r}} dm = \int_M \vec{\Phi}^{(n)} \cdot \ddot{\vec{q}} dm \quad (3.14)$$

$$\int_M \vec{\Phi}^{(n)} \cdot (2\vec{\omega} \times \vec{r}) dm = 2 \int_M \vec{\Phi}^{(n)} \cdot (\vec{\omega} \times \vec{q}) dm \quad (3.15)$$

$$\int_M \vec{\Phi}^{(n)} \cdot (\vec{\omega} \times \vec{r}) dm = \int_M \vec{\Phi}^{(n)} \cdot (\vec{\omega} \times \vec{r}_0) dm + \int_M \vec{\Phi}^{(n)} \cdot (\vec{\omega} \times \vec{q}) dm \quad (3.16)$$

$$\int_M \vec{\Phi}^{(n)} \cdot (\vec{\omega} \times (\vec{\omega} \times \vec{r})) dm = \int_M \vec{\Phi}^{(n)} \cdot \vec{\omega} \times (\vec{\omega} \times \vec{r}_0) dm + \int_M \vec{\Phi}^{(n)} \cdot \vec{\omega} \times (\vec{\omega} \times \vec{q}) dm \quad (3.17)$$

$$\int_M \vec{\Phi}^{(n)} \cdot \frac{L(\vec{q})}{dm} dm = - \omega_n^2 A_n M_n \quad (3.18)$$

$$\begin{aligned} \int_M \vec{\Phi}^{(n)} \cdot \vec{f} dm &= \int_M \vec{\Phi}^{(n)} dm \cdot \vec{f}_0 + \int_M \vec{\Phi}^{(n)} \cdot M \vec{r}_0 dm \\ &+ \int_M \vec{\Phi}^{(n)} \cdot M \vec{q} dm \end{aligned} \quad (3.19)$$

$$\int_M \vec{\Phi}^{(n)} \cdot \vec{e} dm = E_n \quad (3.20)$$

where E_n is the modal contribution of the external forces in the n^{th} mode.

Gravity Gradient Torque, \vec{N} .

Assumed that C_G of entire system coincides with C_G of Shuttle.

($x_G = 0.036 \text{ ft}$; $y_G = -0.063 \text{ ft}$; and $z_G = -0.379 \text{ ft}$)

$$\vec{N} = 3 \omega_0^2 \hat{\alpha}_1 \times \bar{I}_{synt/G} \hat{\alpha}_1$$

$$\bar{I}_{synt/G} = \begin{bmatrix} I_{11} + I_{r1} + M_m b^2/3 & 0 & I_{r3} \\ 0 & I_{22} + I_{r2} + M_m b^2/3 & 0 \\ I_{13} & 0 & I_{33} + I_{r3} \end{bmatrix} =$$

$$\bar{I}_{synt/G} = \begin{bmatrix} I_1 & 0 & I_4 \\ 0 & I_2 & 0 \\ I_4 & 0 & I_3 \end{bmatrix}$$

$$\hat{\alpha}_1 = \sin \theta \cos \phi \hat{i} - (\cos \theta \sin \phi + \sin \theta \cos \phi \cos \psi) \hat{j} + (\sin \theta \cos \phi \sin \psi - \cos \theta \sin \phi) \hat{k}$$

$$\vec{N} = 3 \omega_0^2 \left\{ [\psi (I_3 - I_2)] \hat{i} + [I_4 - \theta (I_1 - I_3)] \hat{j} - I_4 \psi \hat{k} \right\}$$

System with offset.

$$I_{syst/G} = \begin{bmatrix} I_{xx} & -I_{xy} & -I_{xz} \\ -I_{xy} & I_{yy} & -I_{yz} \\ -I_{xz} & -I_{yz} & I_{zz} \end{bmatrix}$$

$$\begin{aligned} \vec{N} = 3\omega_o^2 \left\{ \right. & [I_{yz} + \psi(I_{zz} - I_{yy}) - \theta I_{xy}] \hat{i} \\ & + [I_{xz} - \psi I_{xy} - \theta(I_{xx} - I_{zz})] \hat{j} \\ & \left. + (\theta I_{yz} + \psi I_{xz}) \hat{k} \right\} \end{aligned}$$

I. MODELLING OF THE SCOLE CONFIGURATION

- PARAMETRIC STUDY OF THE IN-PLANE SCOLE SYSTEM - FLOQUET STABILITY ANALYSIS
- THREE DIMENSIONAL FORMULATION OF THE SCOLE SYSTEM DYNAMICS
 - Rotational Equations of Motion
 - Structural Analysis - Boundary Conditions
 - Generic Modal Equations
- ✓ • WHAT WE CAN LEARN ABOUT THE OPEN LOOP SYSTEM?
 - Consider SCOLE configuration without offset of the mast attachment to the reflector and without flexibility
 - Consider SCOLE configuration without mast flexibility but with offset in the direction of orbit (strawman)
 - Consider SCOLE configuration with offsets in two directions but neglecting mast flexibility
 - Consider general SCOLE system dynamics
- IMPLICATIONS FOR CONTROL STRATEGIES

SCOLE (No flexibility, No offset)

$$\begin{aligned}
 & \ddot{\psi} [I_{11} + M_m l^2/3 + M_r l^2 + I_{r1}] + \ddot{\phi} I_{13} - \omega_0 \dot{\phi} [I_{11} - I_{22} + I_{33} \\
 & + I_{r1} - I_{r2} + I_{r3}] + \omega_0^2 \phi I_{31} \\
 & - \omega_0^2 \psi [I_{33} - I_{22} + I_{r3} - I_{r2} + 3(I_3 - I_2) - M_m l^2/3] = 0
 \end{aligned}$$

$$\begin{aligned}
 & \ddot{\psi} I_{31} + \ddot{\phi} (I_{33} + I_{r3}) + \omega_0 \dot{\psi} [I_{11} + I_{33} - I_{22} + I_{r1} + M_m \frac{R\ell}{2} - M_r R\ell \\
 & + I_{r3} - I_{r2}] - \omega_0^2 \phi [I_{11} - I_{22} + I_{r1} - I_{r2} + M_m R\ell/2 - M_r R\ell] \\
 & + \omega_0^2 \psi (I_{13} + 3I_4) = 0
 \end{aligned}$$

$$\ddot{\theta} [I_{22} + I_{r2} + M_r l^2 + M_m l^2/3] + 3\omega_0^2 \theta (I_1 - I_3) - 3\omega_0^2 I_4 = 0$$

The "θ, pitch" equation
decouples from the two others.

and since $I_1 - I_3 < 0$ and $I_{22} + I_{r2} + M_r l^2 - M_m l^2/3 > 0$

⇒ Instability in that d° of freedom.

Furthermore, the last equation is set as:

$$d\ddot{\theta} + e\dot{\theta} + f = 0$$

yields

$$\underline{\theta(t) = A'e^{\sqrt{ed}t} + B'e^{-\sqrt{ed}t} - f/e}$$

The two other equations can be recast in the following state matrix format:

$$\begin{bmatrix} \dot{\phi} \\ \ddot{\phi} \\ \dot{\psi} \\ \ddot{\psi} \end{bmatrix} = \begin{bmatrix} 0 & 1 & 0 & 0 \\ n_3 & -n_4 & -n_1 & -n_2 \\ 0 & 0 & 0 & 1 \\ n_7 & n_8 & n_6 & n_5 \end{bmatrix} \begin{bmatrix} \dot{\phi} \\ \dot{\psi} \\ \dot{\psi} \end{bmatrix}$$

SCOLE (No flexibility but "X" offset)

$$\ddot{\psi} [I_{11} + M_m l_{13}^2 + M_r l^2 + I_{r1}] + \ddot{\phi} (I_{13} + M_r X l) - \omega_o \dot{\phi} [I_{11} - I_{22} \\ + I_{33} + I_{r1} + I_{r3} - I_{rs}] - \omega_o^2 \dot{\phi} (I_{13} + M_r X l) - \omega_o^2 \psi [I_{33} - I_{22} - M_m l_{13}^2 \\ + I_{r3} - I_{r2} - M_r l^2 + 3 (I'_{33} - I'_{yy})] = 0$$

where $I'_{33} = I_{33} + I_{r3} + M_r X^2$ and

$$I'_{yy} = I_{22} + I_{r2} + M_r (X^2 + l^2) + M_m l_{13}^2$$

$$\ddot{\theta} [I_{22} + I_{2r} + M_r (X^2 + l^2) + M_m l_{13}^2] + 3\omega_o^2 \dot{\theta} (I'_{xx} - I'_{33}) - 3\omega_o^2 (I_{13} + M_r X l) \\ = 0$$

where $I'_{xx} = I_{11} + I_{r1} + M_m l_{13}^2 + M_r l^2$

again, the pitch equation decouples from the yaw and roll equations.

Since $I'_{xx} - I'_{33} < 0 \Rightarrow$ Instability in that d^o of freedom.

$$\begin{aligned}
& \ddot{\phi} [I_{33} + I_{r3} + M_r X^2] + \ddot{\psi} [I_{31} + M_r X \ell] + \omega_0^2 \psi [I_{11} - I_{22} \\
& + I_{33} + I_{r1} - I_{r2} + I_{r3} + M_m R \ell_{1/2} - M_r R \ell] - 2\omega_0 \dot{\phi} M_r X \ell \\
& - \omega_0^2 \phi [I_{11} - I_{22} + I_{r1} - I_{r2} - M_r (X^2 + R \ell) + M_m R \ell_{1/2}] \\
& + \omega_0^2 \psi \{ 4(I_{13} + M_r X \ell) \} = 0
\end{aligned}$$

SCOLE with rigid mast and offset

in both the 'X" and 'Y" directions

$$\begin{aligned}
 & \ddot{\psi} [I_{11} + M_m \ell^2/3 + M_r (\ell^2 + Y^2) + I_{r1}] + \ddot{\phi} I_{xz} - \ddot{\theta} M_r X Y \\
 & - \omega_o \dot{\phi} [I_{11} - I_{22} + I_{33} + I_{r1} - I_{r2} + I_{r3}] - \omega_o \dot{\theta} M_r Y (\ell + R) \\
 & - \omega_o^2 \psi [I_{33} - I_{22} + I_{r3} - I_{r2} + M_r (Y^2 - \ell^2) - M_m \ell^2/3 + 3(I_{33} - I_{xx})] \\
 & + \omega_o^2 \phi I_{xz} + 3\omega_o^2 \theta I_{xy} + \omega_o^2 [M_r Y (\ell + R) - 3I_{yz}] = 0
 \end{aligned}$$

$$\begin{aligned}
 & \ddot{\theta} [I_{22} + M_m \ell^2/3 + I_{r2} + M_r (\ell^2 + X^2)] - \ddot{\phi} M_r Y \ell + \ddot{\psi} M_r X Y \\
 & + \omega_o \dot{\phi} M_r X Y + \omega_o^2 \phi M_r Y (\ell + R) + 3\omega_o^2 \psi I_{xy} + 3\omega_o^2 \theta (I_{xx} - I_{zz}) \\
 & - 3\omega_o^2 I_{xz} - \omega_o \dot{\psi} M_m Y R = 0
 \end{aligned}$$

$$\begin{aligned}
 & \ddot{\phi} [I_{33} + I_{r3} + M_r (X^2 + Y^2)] + \ddot{\psi} I_{zx} + \omega_o \dot{\psi} [I_{11} - I_{22} + I_{33} + I_{r1} + M_m R \ell/2 \\
 & - M_r R \ell - I_{r2} + I_{r3}] - \omega_o^2 M_r X Y + \ddot{\theta} M_r Y \ell + M_r X Y \dot{\theta} \omega_o - 3\omega_o^2 \theta I_{yz} \\
 & \omega_o^2 \phi [-M_m R \ell/2 + I_{11} - I_{22} + I_{r1} - I_{r2} + M_r (R \ell - Y^2 + X^2)] + \omega_o^2 \psi (4I_{xz}) = 0
 \end{aligned}$$

IMPLICATIONS FOR LINEAR CONTROL STRATEGIES

After suppression of mast vibrations, linear system eqns. have constant coefficients, control laws can be synthesized based on LQR techniques.

- (A) For the special cases where the in-plane rotational dynamics separate from the out-of-plane dynamics, separate control laws can be generated for pitch and the roll-yaw systems.
- (B) When reflector offset results in coupling between the in-plane and out-of-plane systems, a bias momentum scheme could be considered so that the controllers serve to decouple the system via removal of the relevant coupling terms. Care should be taken so that saturation will not occur.
- (C) Since the vibration frequencies of the mast are much greater than those of the gravity-gradient forced rigid rotational modes, actuators placed at strategic points on the mast could be used for quick removal of the vibrations without inducing substantial disturbances on the rigid modes. Once the mast deformations have been reduced to a specified level, the techniques described in (A) and/or (B) could then be utilized.

II. CONTROL ISSUES:

- ✓ • CONTROL OF LARGE STRUCTURES WITH DELAYED INPUT IN THE CONTINUOUS TIME DOMAIN
- ✓ .. CONTROL WITH DELAYED INPUT IN THE DISCRETE TIME DOMAIN
- ✓ • CONTROL LAW DESIGN FOR SCOLE USING LQG/LTR TECHNIQUE
- OPTIMAL TORQUE CONTROL FOR SCOLE SLEWING MANUEVERS
 - Kinematical and Dynamical Equations
 - Optimal Control - Two Point Boundary Value Problem
 - Estimation of Unknown Boundary Conditions
 - Numerical Results
 - Discussion and Further Recommendations

IV.B STABILITY ANALYSIS OF A SECOND ORDER SYSTEM WITH DELAYED INPUT

The vibration analysis of large space structures is performed using modal analysis and modal coordinates, transforming n coupled second order differential equations or partial differential equations into n decoupled second order differential equations of the form

$$\ddot{x}_i + \omega_i^2 x_i = f_i \quad (1)$$

$i=1, 2, \dots, n$

where x_i = i th modal coordinate

ω_i = i th natural frequency

f_i = influence of the actuators on the i th mode, and the control law of the form

$$f_i = 2\zeta_i \omega_i x_i \quad (2)$$

controls and stabilizes the system (1). The effect of delay in the control force was investigated with numerical simulation for the following numerical example.¹

$$\ddot{x}_i + 6\dot{x}_i(t-h) + 36x_i = 0 \quad (3)$$

It was observed that for delay, $h > 0.15$, instability results.

The analytical verification of the above observation is obtained as follows²:

The roots of the characteristic equation

$$G(s, h) = \sum_{i=0}^n P_i(s) e^{-shi} = 0 \quad (4)$$

can be evaluated from the auxiliary equation

$$\sum_{i=0}^n P_i(s)(1-Ts)^{2i} (1+Ts)^{2n-2i} = 0 \quad (5)$$

where $e^{-j\omega h} = \left[\frac{1-j\omega T}{1+j\omega T} \right]^2$ (6)

Applying the above result to equation (3), the corresponding characteristic equation is given by:

$$G(s, h) = \sum_{i=0}^1 P_i(s) e^{-shi} \quad (7)$$

where $P_0(s) = s^2 + 36$

$$P_1(s) = 6s \quad (8)$$

The auxiliary equation is written as

$$\begin{aligned} T^2 s^4 + (2T + 6T^2) s^3 + (1 + 36T^2 - 12T) s^2 \\ + (72T + 6) s + 36 = 0 \end{aligned} \quad (9)$$

Using the Routh-Hurwitz criterion, Equation (9) has imaginary roots for $T=0.0426$ at $\omega=9.7$. Using relation (6), h can be evaluated as:

$$\omega h = \pi/2 \quad (10)$$

$$\text{or } h = 0.16 \quad (11)$$

It is also brought to our attention³ that the above result can be arrived at without the approximation (6) for a second order system as follows:

The characteristic equation for system (1) with the control law of the form

$$f_i = -2\zeta_i \omega_i x_i(t-h) \quad (12)$$

is written as

$$s^2 + 2\zeta_i \omega_i e^{-hs} s + \omega_i^2 = 0 \quad (13)$$

To evaluate the minimum h for which equation (13) has unstable roots replace s by $j\omega$ as:

$$-\omega^2 + j2\zeta_i \omega_i e^{-j\omega h} \omega + \omega_i^2 = 0 \quad (14)$$

$$\text{Using } e^{-j\omega h} = \cos \omega h - j \sin \omega h, \quad (15)$$

Equation (14) can be written as:

$$(-\omega^2 + 2\zeta_i \omega_i \omega \sin \omega h + \omega_i^2) + j (2\zeta_i \omega_i \cos \omega h) = 0 \quad (16)$$

Thus for equation (16) to be valid

$$\cos wh = 0$$

$$\text{or } wh = \frac{\pi}{2} (2P + 1) \quad (17)$$
$$P = 0, 1, 2, \dots$$

and

$$\omega^2 - 2\zeta_i \omega_i \omega \sin wh - \omega_i^2 = 0 \quad (18)$$

the roots of Equation (18) are

$$\omega = \omega_i \left\{ \zeta_i \sinh \frac{wh}{\omega_i} \pm \sqrt{1 + \zeta_i^2} \right\} \quad (19)$$

Taking the positive ω and substituting into (17)

$$h = \frac{\pi(1+2P)}{2\omega_i \left\{ \zeta_i \sinh \frac{wh}{\omega_i} + \sqrt{1 + \zeta_i^2} \right\}} \quad (20)$$

Thus giving

$$h_{\min} = 0.1618 \quad (21)$$

for the numerical example (3).

Thus the example second order system considered with the natural period of oscillation of 1 second can not tolerate more than 0.16 seconds of delay without becoming unstable. Thus the general problem of delay in control input must be carefully considered in the control system implementation of large space structures.

the beginning. However, the delay in input in the discrete time domain can be relatively easily solved as shown below.¹⁰

The dynamic system described as:

$$x(i+1) = \sum_{j=0}^m A_j x(i-j) + \sum_{j=1}^l B_j u(i-j) \quad (53)$$

can be written as

$$\begin{bmatrix} x(i+1) \\ x(i) \\ x(i-m+1) \\ u(i-1) \\ u(i) \\ u(i-2) \\ \vdots \\ u(i-l+1) \end{bmatrix} = \begin{bmatrix} A_0 & A_1 & \dots & A_m & B_1 & B_2 & \dots & B_l \\ I & 0 & \dots & 0 & 0 & 0 & \dots & 0 \\ 0 & 0 & \dots & I & 0 & 0 & \dots & 0 \\ 0 & 0 & \dots & 0 & 0 & 0 & \dots & 0 \\ 0 & 0 & \dots & 0 & 0 & 0 & \dots & 0 \\ 0 & 0 & & 0 & I & 0 & \dots & 0 \\ 0 & 0 & & 0 & 0 & I & \dots & 0 \\ 0 & 0 & \dots & 0 & 0 & 0 & \dots & 0 \end{bmatrix} \begin{bmatrix} x(i) \\ x(i-1) \\ x(i-m) \\ u(i-1) \\ u(i-2) \\ \vdots \\ u(i-l) \end{bmatrix} + \begin{bmatrix} B_0 \\ 0 \\ 0 \\ I \\ 0 \\ \vdots \\ 0 \end{bmatrix} u(i)$$

ORIGINAL PAGE IS
OF POOR QUALITY

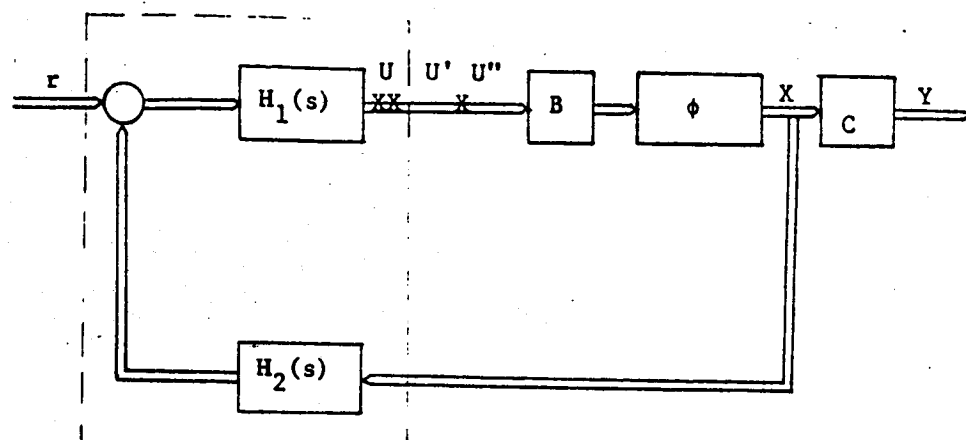
$$z(i+1) \quad \tilde{A} \quad z(i) \quad \tilde{B}$$

(54)

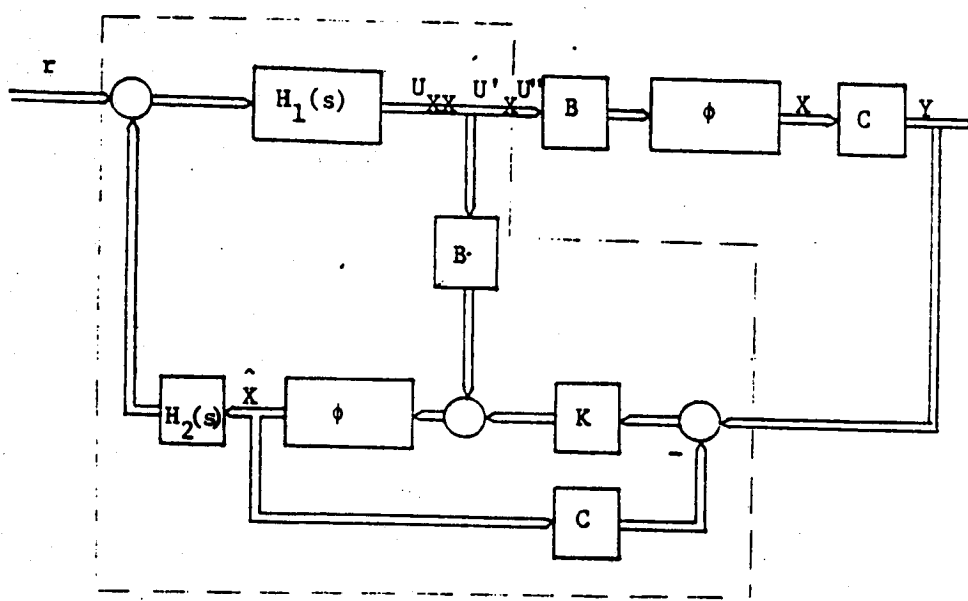
which can be written as:

$$z(i+1) = \tilde{A} z(i) + \tilde{B} u(i) \quad (55)$$

Thus the augmented dynamic system (52) can be solved as a standard control problem. The only disadvantage is the increase in dimensionality of an already large dimensional problem.



a) Full State Feedback



b) Observer Based Implementation

$$\phi = (sI - A)^{-1}$$

IMPORTANT PROPERTIES OF THE TWO TYPES OF IMPLEMENTATIONS:

1. THE CLOSED LOOP TRANSFER FUNCTION MATRICES FROM COMMAND Y TO STATE X ARE IDENTICAL IN BOTH IMPLEMENTATION
2. THE LOOP TRANSFER FUNCTION MATRICES FROM CONTROL SIGNAL U' TO CONTROL SIGNED U (LOOP BROKEN AT XX) ARE IDENTICAL IN BOTH IMPLEMENTATIONS
3. THE LOOP TRANSFER FUNCTION FROM CONTROL SIGNAL U'' TO CONTROL U (LOOPS BROKEN AT POINT X) ARE GENERALLY DIFFERENT. THEY ARE IDENTICAL IF THE OBSERVER DYNAMICS SATISFY:

$$K [I + C (SI - A)]^{-1} = B [C(SI - A)^{-1} B]^{-1} \text{ FOR ALL } S.$$

For Full State Feedback

$$X = \phi B U''$$

For observer Based Implementation

$$\begin{aligned}
 (I + \phi K C) \hat{X} &= \phi B U' + \phi K C \phi B U'' \\
 \hat{X} &= (\phi^{-1} + K C)^{-1} (B U' + K C \phi B U'') \\
 \hat{X} &= (I + \underline{\phi K C})^{-1} \phi (B U' + K C \phi B U'') \\
 &= (I - \phi K (I + C \phi K)^{-1} C) \phi (B U' + K C \phi B U'') \\
 &= \phi [B(C \phi B)^{-1} - K (I + C \phi K)^{-1}] C \phi B U' \\
 &\quad + \phi [K - K (I + C \phi K)^{-1} C \phi K] C \phi B U'' \\
 &= \phi [B(C \phi B)^{-1} - K (I + C \phi K)^{-1}] C \phi B U' \\
 &\quad + \phi [I - (I + C \phi K)^{-1} C \phi K] C \phi B U'' \\
 &= \phi [B(C \phi B)^{-1} - K (I + C \phi K)^{-1}] C \phi B U' \\
 &\quad + \phi [K (I + C \phi K)^{-1}] C \phi B U'' \\
 \end{aligned}$$

use $(I + AB)^{-1} = [I - A(I+BA)^{-1}B]$

An observer Adjustment Procedure:

$$k(q) = \Sigma(q) C^T R^{-1}$$

$$A\Sigma + \Sigma A^T + Q(q) - \Sigma C^T R^{-1} C \Sigma = 0$$

Q and R are treated as design Parameters

[For Kalman Filters, these are noise intensity matrices]

$$Q(q) = Q_0 + q^2 BVB^T$$

$$R = R_0$$

For $q=0$ $K(q)$ is the nominal Kalman gain

For $q \rightarrow \infty$

$$\frac{K R K^T}{q^2} + BVB^T$$

or

$$\frac{K}{q} + B V^{\frac{1}{2}} (R^{\frac{1}{2}})^{-1}$$

II. CONTROL ISSUES:

- CONTROL OF LARGE STRUCTURES WITH DELAYED INPUT IN THE CONTINUOUS TIME DOMAIN
- CONTROL WITH DELAYED INPUT IN THE DISCRETE TIME DOMAIN
- CONTROL LAW DESIGN FOR SCOLE USING LQG/LTR TECHNIQUE
- ✓ • OPTIMAL TORQUE CONTROL FOR SCOLE SLEWING MANUEVERS
 - Kinematical and Dynamical Equations
 - Optimal Control - Two Point Boundary Value Problem
 - Estimation of Unknown Boundary Conditions
 - Numerical Results
 - Discussion and Further Recommendations

N87-17823

Optimal Torque Control for SCOLE Slewing Maneuvers

by

Peter M. Bainum
Feiyue Li
Howard University

OPTIMAL TORQUE CONTROL
FOR SCOLE SLEWING MANUEVERS

P. M. BAINUM AND FEIYUE LI
DEPARTMENT OF MECHANICAL ENGINEERING
HOWARD UNIVERSITY
Washington, D.C. 20059

3rd ANNUAL SCOLE WORKSHOP
NOVEMBER 17, 1986
NASA Langley Research Center
Hampton, Virginia

**Optimal Torque Control
for SCOLE Slewing Maneuvers**

PURPOSE:

**TO SLEW THE SCOLE FROM ONE ATTITUDE TO THE REQUIRED
ATTITUDE, AND MINIMIZE AN INTEGRAL PERFORMANCE INDEX
WHICH INVOLVES THE CONTROL TORQUES.**

CONTENTS:

- 1. KINEMATICAL AND DYNAMICAL EQUATIONS**
- 2. OPTIMAL CONTROL — TWO-POINT BOUNDARY-VALUE PROBLEM
(TPBVP)**
- 3. ESTIMATION OF UNKNOWN BOUNDARY CONDITIONS**
- 4. NUMERICAL RESULTS**
- 5. DISCUSSION AND FURTHER RECOMMENDATIONS**

1. Kinematical and Dynamical Equations

(Rigid SCOLE Configuration)

$$\dot{\mathbf{q}} = (1/2) \tilde{\mathbf{w}} \mathbf{q} \quad (1)$$

$$\mathbf{I} \dot{\mathbf{w}} = -\tilde{\mathbf{w}} \mathbf{I} \mathbf{w} + \mathbf{u} \quad (2)$$

where \mathbf{q} — Euler Parameter Vector $\mathbf{q} = [q_0 \ q_1 \ q_2 \ q_3]^T$

\mathbf{w} — Angular Velocity Vector $\mathbf{w} = [w_1 \ w_2 \ w_3]^T$

\mathbf{u} — Control Torque Vector $\mathbf{u} = [u_1 \ u_2 \ u_3]^T$

$$\tilde{\mathbf{w}} = \begin{bmatrix} 0 & -w_1 & -w_2 & -w_3 \\ w_1 & 0 & w_3 & -w_2 \\ w_2 & -w_3 & 0 & w_1 \\ w_3 & w_1 & -w_2 & 0 \end{bmatrix} \quad \tilde{\mathbf{w}} = \begin{bmatrix} 0 & -w_3 & w_2 \\ w_3 & 0 & -w_1 \\ -w_2 & w_1 & 0 \end{bmatrix}$$

$$\mathbf{I} = \begin{bmatrix} I_{11} & -I_{12} & -I_{13} \\ -I_{12} & I_{22} & -I_{23} \\ -I_{13} & -I_{23} & I_{33} \end{bmatrix}$$

where (Ref.1)

$$I_{11} = 1132533, \quad I_{22} = 7007447, \quad I_{33} = 7113952,$$

$$I_{12} = -7555, \quad I_{13} = 115232, \quad I_{23} = 52293 \quad (\text{slug-ft}^2)$$

or

$$I_{11} = 1535474, \quad I_{22} = 9533821, \quad I_{33} = 9645235,$$

$$I_{12} = -13243, \quad I_{13} = 156193, \quad I_{23} = 73933 \quad (\text{kg-m}^2)$$

Transfer I to a diagonal form by an orthogonal matrix $C^{-1} = C^T$,

$$C = \begin{bmatrix} 3.9993143 & -0.0011151 & 0.0192393 \\ -0.001684 & 0.9273053 & 0.3742533 \\ -0.0132577 & -0.3743042 & 0.9271252 \end{bmatrix}$$

$$C^T I C = \begin{bmatrix} I_1 & & \\ & I_2 & \\ & & I_3 \end{bmatrix} = I_m$$

where subindex, m , represents the principal axes system.

$$I = 1130233, I = 6935292, I = 7137342 \text{ (slug-ft}^2\text{)}$$

From (2), the dynamical equation becomes

$$C^T I C C^T w = -C^T \tilde{w} C C^T I C C^T w + C^T u$$

or

$$I_m \dot{w}_m = -\tilde{w}_m I_m w_m + u_m \quad (3)$$

where

$$u = C u_m, \quad w = C w_m$$

Similarly, we have

$$\dot{q}_m = (1/2) \tilde{w}_m q_m \quad (4)$$

Eq.(3) can be written as

$$\dot{w}_m = -I_m^{-1} \tilde{w}_m I_m w_m + I_m u_m \quad (5)$$

For simplicity, we drop subindex m in the following derivation.

2. Optimal Control Two-Point Boundary-Value Problem (TPBVP)
 Cost Function

$$J = (1/2) \int_{t_0}^{t_f} u^T \dot{u} dt = (1/2) \int_{t_0}^{t_f} u^T u dt$$

The Hamiltonian, H , for the system (4), (5) is

$$H = (1/2) u^T \dot{u} + p^T \dot{q} + r^T \dot{w}$$

By means of Pontryagin's Principle, the necessary conditions for minimizing J , are

$$\dot{p} = - \{ \partial H / \partial q \} \implies \dot{p} = (1/2) \tilde{w} p \quad (6)$$

$$\dot{r} = - \{ \partial H / \partial w \} \implies \dot{r} = [Jw] r + (1/2) [q] p \quad (7)$$

$$\dot{u} = \{ \partial H / \partial u \} \implies u = - \tilde{I}^T r \quad (8)$$

plus (4) and (5), where $p = [p_0 \ p_1 \ p_2 \ p_3]^T$, $r = [r_1 \ r_2 \ r_3]^T$ are the costates corresponding to q and w , respectively.

$$[Jw] = \begin{bmatrix} J & J_2 w_3 & J_3 w_2 \\ J_1 w_3 & J & J_3 w_1 \\ J_1 w_2 & J_2 w_1 & J \end{bmatrix} \quad \begin{array}{l} J = (I_3 - I_2) / I_1 \\ J = (I_1 - I_3) / I_2 \\ J = (I_2 - I_1) / I_3 \end{array}$$

$$[q] = \begin{bmatrix} q_1 & -q_0 & -i_3 & I_2 \\ q_2 & q_3 & -q_0 & I_1 \\ q_3 & -q_2 & I_1 & -q_0 \end{bmatrix}$$

After substitution of u from (8) into (5), we get

$$\dot{w} = - J_{ww} - \tilde{I}^2 r \quad (9)$$

where

$$J_{ww} = [J_1 w_2 w_3 \quad J_2 w_3 w_1 \quad J_3 w_1 w_2]^T$$

Let $z = [q_0 \ q_1 \ q_2 \ q_3 \ \dot{q}_1 \ \dot{q}_2 \ \dot{q}_3 \ \dot{p}_0 \ \dot{p}_1 \ \dot{p}_2 \ \dot{p}_3 \ \dot{r}_1 \ \dot{r}_2 \ \dot{r}_3]^T = [z_1 \ z_2]^T$

$z_1 = [q_0 \ q_1 \ q_2 \ q_3 \ \dot{q}_1 \ \dot{q}_2 \ \dot{q}_3]^T, z_2 = [\dot{p}_0 \ \dot{p}_1 \ \dot{p}_2 \ \dot{p}_3 \ \dot{r}_1 \ \dot{r}_2 \ \dot{r}_3]^T$

Eqs.(4),(5),(7),(9) can be written as

$$\dot{z} = F(z) \quad (1J)$$

The boundary conditions

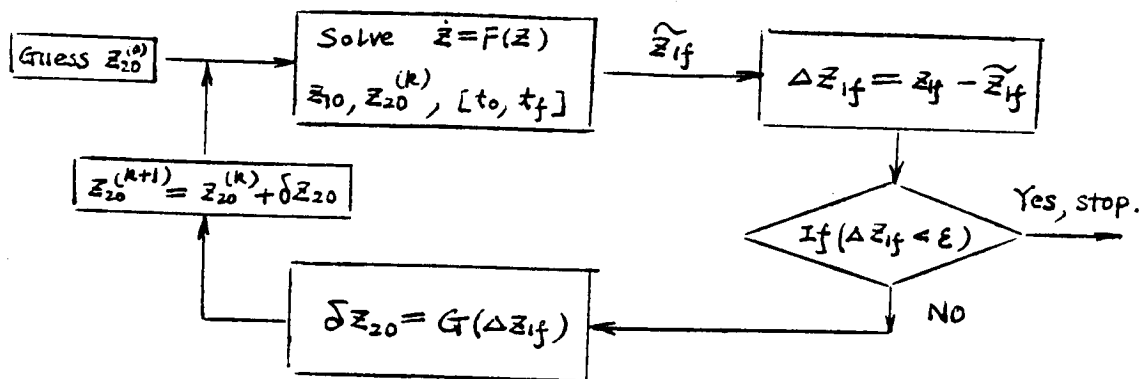
$z_1(t_0), z_1(t_f)$ are known, (11)

$z_2(t_0), z_2(t_f)$ are unknown.

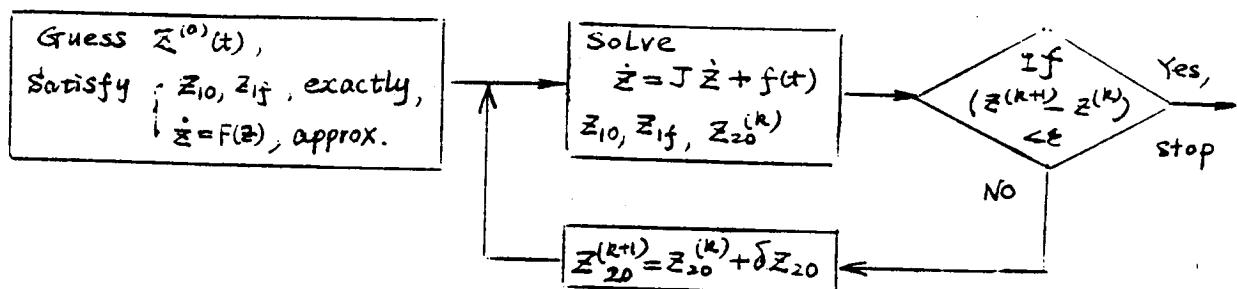
This is the TPBVP. If we find the unknown boundary values, $z_2(t_0)$, then we can integrate (1J) to get r , and from (3) we obtain the control torque vector, u .

Brief Review of Methods

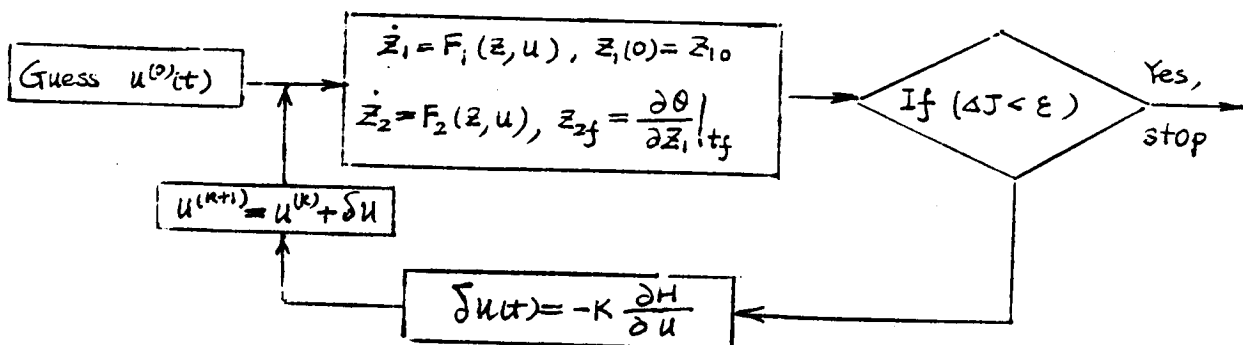
(1) Shooting Methods (Ref. 3)



(2) Quasilinearization Methods (Ref. 3, 4)



(3) Gradient Methods (Ref. 4)



(4) Other Methods (Ref. 2)

$$\text{Minimize } J^2 = \rho^T \rho$$

subject to the terminal constraints $z_1(t_f) = z_{1f}$

3. Estimation of Unknown Boundary Conditions

3.1 Special Case of Slewing Motion

The SCOLE rotates about an arbitrary axis $\vec{\epsilon}$ fixed in both body axes system and inertial space coordinate system, i.e., the Euler rotation. From the physical point of view, the rotation is very simple, its rotation angle is small, and therefore may consumes less energy (torque). In view of our cost function, it is reasonable to think that the optimal slewing is near the Euler rotation. Considering the analytical solution about single principal axis maneuver in Ref.2, we define a rotation angle $\theta(t)$, about an arbitrary axis $\vec{\epsilon}$,

$$\theta(t) = \theta_0 + \dot{\theta}_0 t + (1/2) \ddot{\theta}_0 t^2 + (1/6) \dddot{\theta}_0 t^3 \quad (12)$$

For the given boundary conditions

$$\theta(0) = 0, \quad \dot{\theta}(0) = \dot{\theta}_0, \quad \theta(t_f) = \theta_f, \quad (=2J^\circ), \quad \dot{\theta}(t_f) = \dot{\theta}_f, \quad (13)$$

we have

$$\begin{aligned} \ddot{\theta}_0 &= (6\theta_f/t_f^2) - (4\dot{\theta}_0/t_f) \\ \dddot{\theta}_0 &= -(12\theta_f/t_f^3) + (6\dot{\theta}_0/t_f^2) \end{aligned} \quad (14)$$

After substitution of θ and $\vec{\epsilon}$ into (10), we can get $z_2^{(0)}(0)$, the initial guess of the costates at initial time $t=t_0$.

3.2 Some Properties of the Costates, ρ_i

Since $q^T q = 1$

we have $q^T \rho = \beta^2 = \text{constant}$, but $\beta^2 \neq 1$

β is an unknown which is usually determined by iteration, thus

$[q_f \ w_f]^T \implies 6 \text{ independent conditions}$

$[\rho_i \ r_i]^T \implies 7 \text{ unknowns to be determined}$

Fortunately, for the problem discussed in this paper, we can prove that 1 of the 4 unknowns ρ_i can be arbitrarily selected.

4. Numerical Results

Without loss of generality, we choose

$$\mathbf{q} = [1 \ 0 \ 3 \ 3]^T, \ \mathbf{q} = [q_{0f} \ q_{1f} \ q_{2f} \ q_{3f}]^T$$

so

$$\theta_f = 2 \arccos(q_{0f}), \ \epsilon_j = q_{jf} \operatorname{sign}(q_{0f}) / \sqrt{1 - q_{0f}^2}, \ j=1,2,3$$

or

$$q_{0f} = \cos(\theta_f/2), \ q_{jf} = \epsilon_j \sin(\theta_f/2), \ j=1,2,3$$

where θ_f, ϵ_j , can be chosen according to the practical problem.

For example, $\epsilon_{M_1} = 3.87463125, \ \epsilon_{M_2} = 3.159326134, \ \epsilon_{M_3} = 3.454357417$

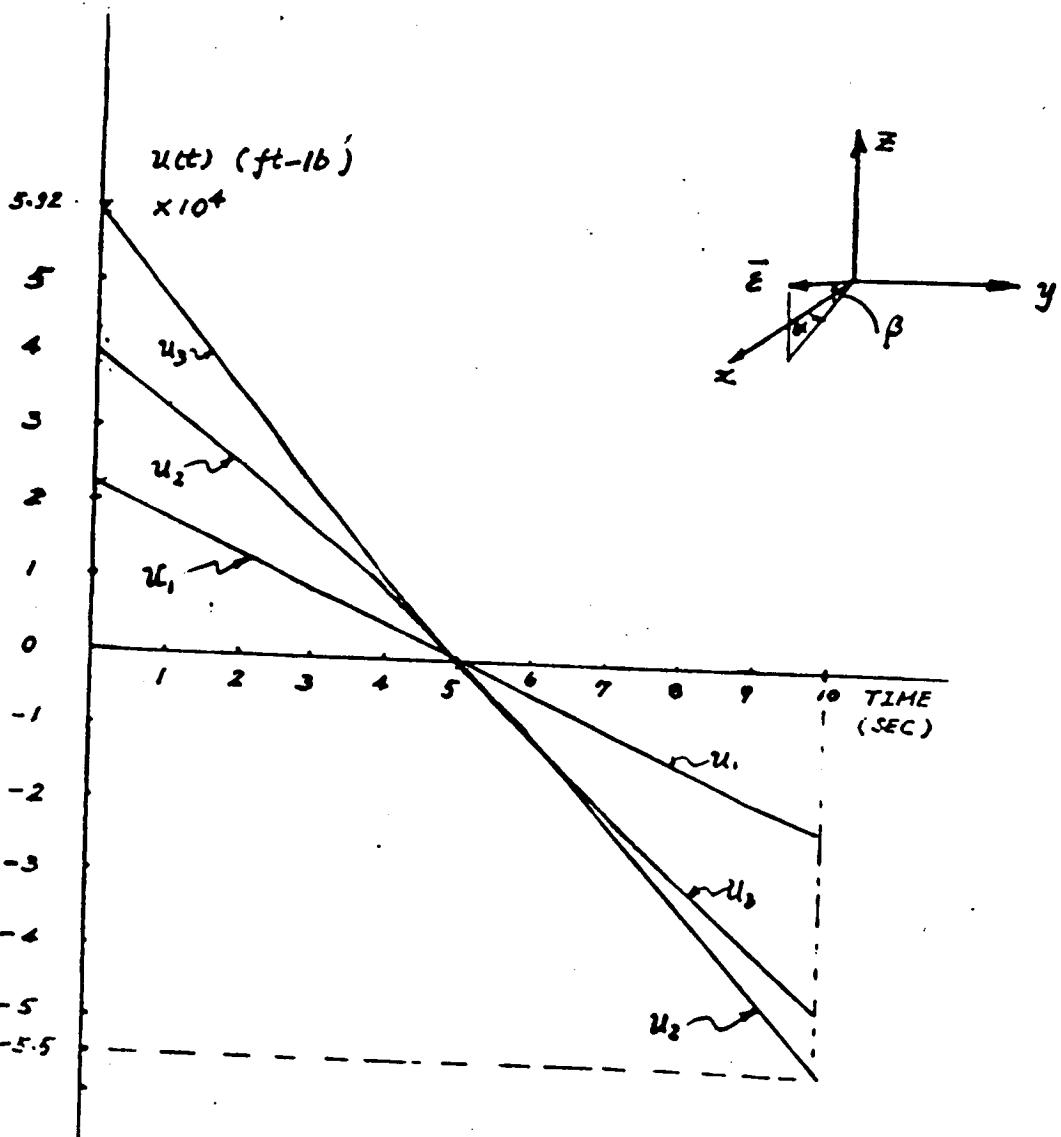


Fig. 2. CONTROL TORQUE

Table I Slewing Data and Boundary Values

$I_1 = 1133283 \quad I_2 = 5035292 \quad I_3 = 7137342 \quad (\text{slug-ft}^2)$			
States			
	Initial	Final	
q_0	1		0.93483775
q_1	3		0.15187820
q_2	3		0.32935137
q_3	3		0.07893337
w_1	3		3
w_2	3		3
w_3	3		3
Costates ($p_0 = 0$) $\times 10^{12}$			
No. of Iter.	p_1	p_2	p_3
0	-0.009360927	-0.069113961	-0.193909345
1	-0.009526333	-0.039331742	-0.201133079
2	-0.009632339	-0.039403392	-0.201193294
3	-0.009602836	-0.039403936	-0.201193267
4	-0.009632806	-0.039408936	-0.201193267
r_1 r_2 r_3			
0	-0.023402267	-0.172734931	-0.484773363
1	-0.023757945	-0.105295499	-0.501347327
2	-0.023705126	-0.105472413	-0.501933771
3	-0.023705305	-0.105472654	-0.501933773
4	-0.023705305	-0.105472654	-0.501933773

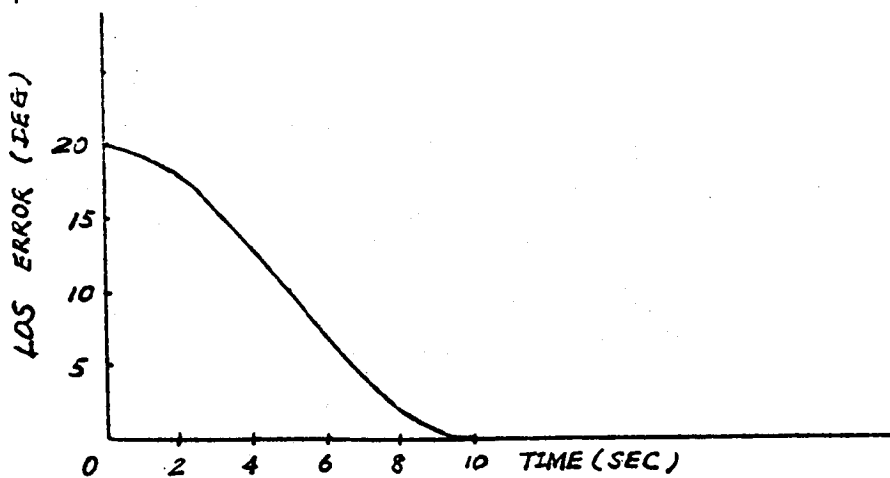


FIG. 1. LINE-OF-SIGHT ERROR

5. Discussion and Further Recommendations

(1) Consider the Distribution of ω on the Shuttle and the Reflector.

(2) Time-Optimal Slewing, (Rigid Configuration),
Cost Function

$$J = \int_{t_0}^{t_f} dt$$

Solve the TP3VP by Shooting Methods

(3) Include the Flexibility in the Problems.

$$z = [q_0 \ q_1 \ q_2 \ q_3 \ \omega_1 \ \omega_2 \ \omega_3 \ \alpha_1 \ \alpha_2 \ \dots \ \alpha_n \ \beta_0 \ \beta_1 \ \beta_2 \ \dots]^T$$

[1 x 14 + 2n]

n = No. of flexible appendage nodes included

ORIGINAL PAGE IS
OF POOR QUALITY

REFERENCES

- [1] Taylor,L.N. and Balakrishnan,A.V., "A Mathematical Problem and a Spacecraft Control Laboratory Experiment(SCOLE) Used to Evaluate Control Laws for Flexible Spacecraft...NAS/IEEE Design Challenge," Jan., 1984.
- [2] Junkins,J.L., and Turner,J.D. "Optimal Continuous Torque Attitude Maneuvers", J. Guidance and Control, Vol.3, No.3, May-June,1983, pp210-217.
- [3] Knowles,G. "An Introduction to Applied Optimal Control", Academic Press, New York, 1981.
- [4] Andrew P. Sage and Chelsea C. White,III "Optimum System Control", 2nd ed., Prentice-Hall,Inc. Englewood Cliffs. New Jersey 07632, 1977.

N87-17824

Mathematical Modeling of SCOLE Configuration with Line-of-Sight Error as the Output

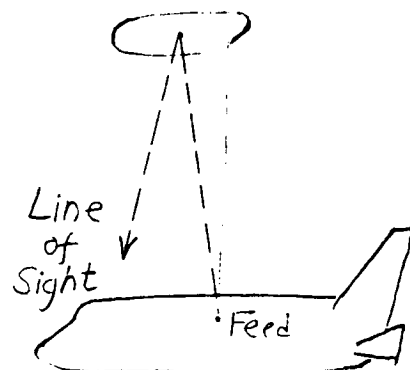
by

**S. M. Joshi
NASA Langley
Research Center**

PRECEDING PAGE BLANK NOT FILMED

Mathematical Modeling of the SCOLE Configuration with Line-of Sight Error as the output

S. M. Joshi



I-SCOLE Linear Model

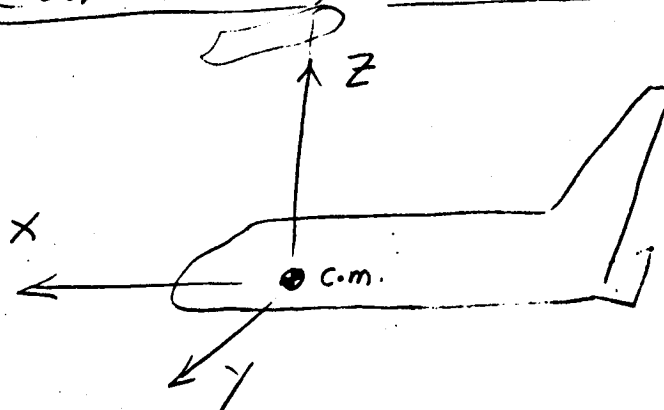
3 - Rigid-body modes + 10 Flex. modes
(order = 26)

5 inputs $[M_x, M_y, M_z, F_x, F_y]$
Moments applied /
at shuttle
Forces
Applied at
reflector

3 output $y = \Delta L.O.S.$

(3-dim. error in Line-of-sight vector)

Coordinate System: D. Roberts



Units : FPS System

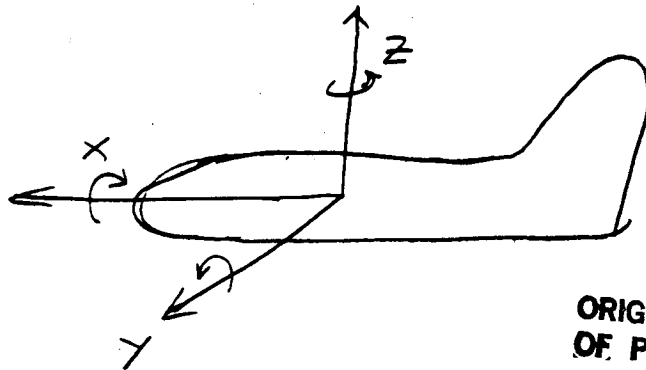
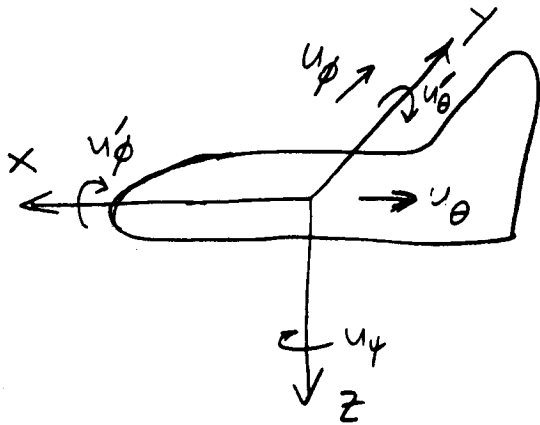
Expression for linearized LOS error

If everything is in Robertson's coordinate system, the linearized LOS error is:

$$\Delta_{\text{LOS}} = \begin{bmatrix} -L\theta_3 + r_y\psi_3 + u_\theta(L) - u_\theta(0) + r_y u_\psi(L) - 2Lu_\theta'(L) \\ L\phi_3 + r_x\psi_3 + u_\phi(L) - u_\phi(0) + r_x u_\psi(L) - 2Lu_\phi'(L) \\ -r_x\theta_3 - r_y\phi_3 - r_x u_\theta(L) + r_y u_\phi(L) \end{bmatrix}$$

(Where ϕ_3, θ_3, ψ_3 are the rigid-body angles about x, y, z axes).

u_θ, u_ϕ are elastic deflections, $u'_\theta, u'_\phi, u'_\psi$ are elastic angular deflections



ORIGINAL PAGE IS
OF POOR QUALITY

Taylor's coordinate system

Robertson's system



X-defl. $-u_\theta$

Y-defl. u_ϕ

Angular defl. (about X) u'_ϕ

Angular defl. (about Y) u'_θ

Angular defl. (about Z) u'_4

Coordinates of refl. c.m. rel. to shuttle

$(r_x, r_y, -L)$

$$r_x = 18.75 \\ r_y = -32.5, L = 130.$$

X-defl. u_θ

Y-defl. u_ϕ

Angular defl. (about X-axis) $-u'_\phi$

Angular defl. (about Y-axis) u'_θ

Angular defl. (about Z-axis) u'_4

86

S. M. Jashi
Nov. '86

LOAD MAP - CONTROL

CYB 224000 CM STORAGE USED

CYBER LOADER 1.5-552 86/11/04 16:00:24

69 TABLE NOTES

A (26 x 26)

The diagram illustrates a rigid-body system with 12 degrees of freedom (DOFs). The system is divided into three main parts: a base, a middle section, and a top section. The base is labeled with q_1, q_2, q_3, q_4 . The middle section is labeled with q_5, q_6, q_7, q_8 . The top section is labeled with $q_9, q_{10}, q_{11}, q_{12}$. The base is further divided into two parts: 'rigid-body' (labeled q_1, q_2, q_3) and 'parts' (labeled q_4). The middle section is divided into two parts: 'rigid-body' (labeled q_5, q_6, q_7) and 'parts' (labeled q_8). The top section is divided into two parts: 'rigid-body' (labeled q_9, q_{10}, q_{11}) and 'parts' (labeled q_{12}). The 'rigid-body' parts are grouped together, and the 'parts' are grouped together, with a bracket indicating they are part of the same rigid-body system.

11

ORIGINAL PAGE IS
OF POOR QUALITY

Cont.

$A_{26 \times 26}$ (Contd. from
previous page)

0.0000000000000000

Row 16

-4-

88

B (26x5)

$$\begin{bmatrix} 0. & 0. & 0. & 0. & 0. \\ 0. & 0. & 0. & 0. & 0. \\ 0. & 0. & 0. & 0. & 0. \\ 0. & 0. & 0. & 0. & 0. \\ 0. & 0. & 0. & 0. & 0. \end{bmatrix}$$

$$\begin{bmatrix} 0.08486E-06 & -10610E-08 & 14337E-07 & -59958E-08 & -11476E-03 \\ -10610E-08 & 0.14272E-06 & -10662E-06 & 0.10586E-05 & 0.11794E-05 \\ 0.14337E-07 & -10662E-06 & 0.14681E-06 & -0.46726E-05 & 0.77638E-06 \\ 0. & 0. & 0. & 0. & 0. \\ -1.46847E-03 & -0.67762E-03 & 0.48084E-04 & 0.19876E+01 & -0.62670E-01 \\ 0. & 0. & 0. & 0. & 0. \\ 0.51993E-02 & -4.5857E-04 & -0.26144E-04 & 0.14599E+00 & 0.20166E+01 \\ 0. & 0. & 0. & 0. & 0. \\ -0.32276E-03 & -0.73059E-04 & -0.30638E-04 & 0.10032E+01 & -0.56127E+00 \\ 0. & 0. & 0. & 0. & 0. \\ 0.71189E-03 & -0.54433E-04 & 0.35905E-07 & 0.27669E+00 & 0.48924E+00 \\ 0. & 0. & 0. & 0. & 0. \\ -0.18690E-03 & -0.43101E-04 & 0.21200E-06 & -0.91695E-01 & 0.51600E-01 \\ 0. & 0. & 0. & 0. & 0. \\ 0.12068E-03 & -0.93335E-05 & 0.24059E-09 & -0.15570E+00 & -0.26696E+00 \\ 0. & 0. & 0. & 0. & 0. \\ -0.62175E-04 & -0.14263E-04 & 0.14394E-06 & -0.37195E+00 & 0.21355E+00 \\ 0. & 0. & 0. & 0. & 0. \\ 0.65351E-04 & -0.35004E-05 & -0.33458E-10 & 0.10385E+00 & 0.17688E+00 \\ 0. & 0. & 0. & 0. & 0. \\ -0.25440E-04 & -0.58553E-05 & -0.19444E-07 & 0.31226E+00 & -0.16050E+00 \\ 0. & 0. & 0. & 0. & 0. \\ 0.23310E-04 & -0.17993E-05 & 0.56658E-11 & -0.76610E-01 & -0.13216E+00 \end{bmatrix}$$

-5-

$$U = \begin{bmatrix} M_x \\ M_y \\ M_z \\ F_x \\ F_y \end{bmatrix}_{5 \times 1}$$

ORIGINAL PAGE IS
OF POOR QUALITY

$$C (3 \times 26) \quad y = [A \cdot 0.5]_{3 \times 1}$$

$$\begin{bmatrix} 0. & -0.13000E+03 & -0.22200E+02 & 0. \\ -0.40647E+00 & 0.57773E+00 & 0.13941E+01 & 0. \\ 0.36432E-01 & 0.421907E+00 & -0.26795E-01 & 0. \\ 0.13000E+03 & 0.48750E+02 & 0. & 0. \\ -0.25707E+00 & -0.68594E+00 & 0.79447E+00 & 0. \\ 0.28930E-01 & 0.11102E+00 & 0.11240E-01 & 0. \\ 0.32200E+02 & -0.10750E+02 & 0.19527E+00 & 0. \\ -0.65548E-01 & 0.75790E-01 & 0.29226E-01 & 0. \\ -0.37941E-02 & 0. & 0.19829E-02 & 0. \end{bmatrix}$$

$$\begin{bmatrix} 0. & 0. & 0. & 0. \\ -0.154352E+00 & 0. & -0.88903E-01 & 0. \\ 0. & -0.26795E-01 & 0. & -0.55986E+00 & 0. \\ 0. & 0. & -0.93453E-02 & 0. & 0.86560E+00 & 0. \\ 0. & 0. & 0.10136E+00 & 0. & -0.30609E+00 & 0. \\ 0. & 0. & 0.11240E-01 & 0. & -0.38918E-01 & 0. \\ 0. & 0. & 0.19527E+00 & 0. & 0.76339E-01 & 0. \\ 0. & 0. & 0.29226E-01 & 0. & -0.78259E-01 & 0. \end{bmatrix}$$

II- SCOLE - Flexible linear model

(10 Flex. modes only)

8 Inputs } as described
14 Outputs }

Coordinate system: D. Robertson's

FPS Units

Note: For control of LOS using Δ LOS measurements, the previous model which includes rigid + 10 flex modes should be adequate. The following model is provided for those wishing to use additional inputs or outputs. This can be accomplished by selecting appropriate elements of "B" and "C" matrices. Note that the following model contains only flex. modes since its purpose is to supplement the previous (rigid + elastic) model.

S. John
5/12/85
Orientation (Dec '84)

ScalE-Flexible model (no model)

(The state, input, output variables are defined in the *stroke_wfs presentation* (Dec '84))

NO. 06 MODELS. 10M. 20M. 0 1. 14
A MATRIX

NO. OF NODES = 10N = 20 N = 0 L = 14
 A MATRIX (2x7x2x7)

$$X = \begin{bmatrix} q_1 & q_2 & q_3 & q_4 & q_5 & q_6 & q_7 \\ q_8 & q_9 & q_{10} & q_{11} & q_{12} & q_{13} & q_{14} \end{bmatrix}$$

N87-17825

Slew Maneuver Dynamics of the Spacecraft Control Laboratory Experiment

by

**Y. P. Kakad
Univ. of No. Carolina
at Charlotte**

SLEW MANEUVER DYNAMICS OF THE
SPACECRAFT CONTROL LABORATORY EXPERIMENT (SCOLE)

Y. P. KAKAD

DEPT. OF ELECTRICAL ENGINEERING
UNIVERSITY OF NORTH CAROLINA AT CHARLOTTE
CHARLOTTE, N.C. 28223

$$C = \begin{bmatrix} \cos\theta_2 \cos\theta_3 & -\cos\theta_2 \sin\theta_3 & \sin\theta_2 \\ (\sin\theta_1 \sin\theta_2 \cos\theta_3 & (-\sin\theta_1 \sin\theta_2 \sin\theta_3 & -\sin\theta_1 \cos\theta_2 \\ + \sin\theta_1 \cos\theta_2) & + \cos\theta_1 \cos\theta_2) & \\ (-\cos\theta_1 \sin\theta_2 \cos\theta_3 & (\cos\theta_1 \sin\theta_2 \sin\theta_3 & \cos\theta_1 \cos\theta_2 \\ + \sin\theta_3 \sin\theta_1) & + \cos\theta_3 \sin\theta_1) \end{bmatrix} \quad (1)$$

where if $\vec{i}, \vec{j}, \vec{k}$ represent the dextral set of orthogonal unit vectors fixed in the body-fixed frame, then θ_1 is the rotation of \vec{i} , θ_2 is the rotation of \vec{j} and θ_3 is the rotation of \vec{k} .

The angular velocity of the orbiter can be transformed from the inertial frame to the body-fixed frame for the body-three angles as

$$\underline{\omega} = M^T \underline{\dot{\theta}} \quad (2)$$

The total kinetic energy expression of the system can be given as [4]

$$T = T_0 + T_1 + T_2 \quad (3)$$

where T_0 is the kinetic energy of the shuttle and is given as

$$T_0 = 1/2 m_1 \underline{\underline{V}}^T \underline{\underline{V}} + 1/2 \underline{\underline{\omega}}^T \underline{\underline{I}}_1 \underline{\underline{\omega}} \quad (4)$$

The kinetic energy of the flexible beam is T_1 and it

$$\begin{aligned}
 T_1 = & \frac{1}{2} m V_0^T V_0 + \frac{1}{2} \underline{\omega}^T \underline{J} \underline{\omega} - m V_0^T \underline{\underline{C}} \underline{\omega} + \frac{1}{2} \frac{\dot{d}^T}{-} \frac{\dot{d}}{dm} dm \\
 & + V_0^T \int \dot{d} dm + \underline{\omega}^T \int \dot{\underline{a}} dm + \frac{1}{2} \begin{bmatrix} \dot{u}_x & \dot{u}_y & \dot{u}_\psi \end{bmatrix} dI \\
 & \begin{bmatrix} \dot{u}_x \\ \dot{u}_y \\ \dot{u}_\psi \end{bmatrix} \quad (5)
 \end{aligned}$$

$$T_1 = 1/2 \underline{m} \underline{V}_0^T \underline{V} + 1/2 \underline{\omega}^T \underline{J} \underline{\omega} - \underline{m} \underline{V}_0^T \underline{\tilde{C}} \underline{\omega} + \underline{m} \sum_{i=1}^n \dot{q}_i^2 + \underline{V}_0^T \underline{\dot{\alpha}} \\ + \underline{\omega}^T \underline{\beta} + 1/4 \rho \left[\sum_{i=1}^n p_{5i} \dot{q}_i^2 + \sum_{i=1}^n p_{6i} \dot{q}_i^2 \right] \quad (6)$$

where

$$u_x = \sum_{i=1}^n \phi_{xi}(s) q_i(t) \\ u_y = \sum_{i=1}^n \phi_{yi}(s) q_i(t) \\ u_\psi = \sum_{i=1}^n \phi_{\psi i}(s) q_i(t) \quad (7)$$

and

$$p_{1i} = \int_0^L \phi_{xi}(s) ds \\ p_{2i} = \int_0^L \phi_{yi}(s) ds \\ p_{3i} = \int_0^L s \phi_{xi}(s) ds \\ p_{4i} = \int_0^L s \phi_{yi}(s) ds \\ p_{5i} = \int_0^L (s \phi_{xi}')^2 ds \\ p_{6i} = \int_0^L (s \phi_{yi}')^2 ds \quad (8)$$

and

$$\dot{\underline{\alpha}}(t) = \begin{bmatrix} n \\ i=1 p_{1i} \dot{q}_i \\ n \\ i=1 p_{2i} \dot{q}_i \\ 0 \end{bmatrix} \quad (9)$$

$$\dot{\underline{\beta}}(t) = \begin{bmatrix} n \\ i=1 p_{4i} \dot{q}_i \\ n \\ i=1 p_{3i} \dot{q}_i \\ 0 \end{bmatrix} \quad (10)$$

The kinetic energy T_2 , of the tip mass (the reflector) is

$$\begin{aligned} T_2 = & 1/2 m_2 \underline{v}_0^T \underline{v}_0 - m_2 \underline{v}_0^T \tilde{\underline{a}}(L) \underline{\omega} + m_2 \underline{v}_0^T \dot{\underline{d}}(L) \\ & - 1/2 m_2 \underline{\omega}^T \tilde{\underline{a}}(L) \tilde{\underline{a}}(L) \underline{\omega} + m_2 \underline{\omega}^T \tilde{\underline{a}}(L) \dot{\underline{d}}(L) \\ & + 1/2 m_2 \dot{\underline{d}}^T(L) \dot{\underline{d}}(L) + 1/2 \underline{\Omega}^T I_2 \underline{\Omega} \end{aligned} \quad (11)$$

where

$$\underline{\Omega} = \underline{\omega} + \begin{bmatrix} \dot{u}_x'(L) \\ \dot{u}_y'(L) \\ \dot{u}_\psi(L) \end{bmatrix} \quad (12)$$

$$\begin{aligned}
 T = & \frac{1}{2} m_2 \underline{V}_0^T \underline{V}_0 - m_2 \underline{V}_0^T \tilde{\underline{a}}(L) \underline{\omega} + m_2 \underline{V}_0^T \dot{\underline{d}}(L) \\
 & - \frac{1}{2} m_2 \underline{\omega}^T \tilde{\underline{a}}(L) \tilde{\underline{a}}(L) \underline{\omega} + m_2 \underline{\omega}^T \tilde{\underline{a}}(L) \dot{\underline{d}}(L) \\
 & + \frac{1}{2} m_2 \left[\sum_{i=1}^n \sum_{j=1}^n \phi_{x_i}(L) \phi_{x_j}(L) \dot{q}_i \dot{q}_j + \sum_{i=1}^n \sum_{j=1}^n \phi_{y_i}(L) \phi_{y_j}(L) \dot{q}_i \dot{q}_j \right] \\
 & + \frac{1}{2} \dot{\underline{P}}^T \underline{I}_2 \dot{\underline{P}} + \frac{1}{2} \underline{\omega}^T \underline{I}_2 \underline{\omega}
 \end{aligned} \tag{13}$$

where

$$\dot{\underline{P}} = \left[\sum_{i=1}^n \dot{\phi}_{x_i}(L) \dot{q}_i(t) \quad \sum_{i=1}^n \dot{\phi}_{y_i}(L) \dot{q}_i(t) \quad \sum_{i=1}^n \dot{\phi}_{\psi_i}(L) \dot{q}_i(t) \right] \tag{14}$$

Substituting \underline{V}_0 , \underline{V}_1 and \underline{V}_2 from the foregoing equations into equation (3), the total kinetic energy expression can be written as

$$\begin{aligned}
 T = & \frac{1}{2} m_0 \underline{V}^T \underline{V} + \underline{\omega}^T \underline{H} \underline{V} + \frac{1}{2} \underline{\omega}^T \underline{I}_0 \underline{\omega} + \underline{V}^T \underline{A}_1 \dot{\underline{q}} \\
 & + \underline{\omega}^T \underline{A}_2 \dot{\underline{q}} + \frac{1}{2} \dot{\underline{q}}^T \underline{A}_3 \dot{\underline{q}}
 \end{aligned} \tag{15}$$

where

$$m_0 = m_1 + \rho L + m_2 \quad (16)$$

$$H = (\rho L + m_0) \tilde{r} + m_2 \tilde{a}(L) + \rho L \tilde{c} \quad (17)$$

$$I_0 = I_1 + J + I_2 \quad (18)$$

and also

$$A_1 \dot{\underline{q}} = \dot{\underline{a}} + m_2 \dot{\underline{d}}(L) \quad (19)$$

$$A_2 \dot{\underline{q}} = \tilde{r} \dot{\underline{a}} + \dot{\underline{b}} + m_2 \tilde{r} \dot{\underline{d}}(L) + m_2 \tilde{a}(L) \dot{\underline{d}}(L) \quad (20)$$

$$A_3 = \begin{bmatrix} & & 0 \\ & & \\ \rho L + m_2 + p_{5i} + p_{6i} & & \\ & & \\ & 0 & \end{bmatrix} + \phi^T(L) I_2 \phi(L) \quad (21)$$

The matrix $\phi^T(L)$ is given as

$$\phi^T(L) = \begin{bmatrix} \phi_{1x}'(L) & 0 & 0 \\ 0 & \phi_{1y}'(L) & 0 \\ 0 & 0 & \phi_{1\psi}'(L) \\ \dots & \dots & \dots \\ \dots & \dots & \dots \\ \phi_{ix}'(L) & 0 & 0 \\ 0 & \phi_{iy}'(L) & 0 \\ 0 & 0 & \phi_{i\psi}'(L) \end{bmatrix} \quad (22)$$

$$\underline{m}_0 \dot{\underline{v}} - \underline{H} \dot{\underline{\omega}} + \underline{A}_1 \ddot{\underline{q}} = \underline{N}_1 + \underline{F}(t) \quad (26)$$

where the nonlinear term N_1 is given as

$$\begin{aligned} \underline{N}_1 &= -\underline{C}^T \dot{\underline{C}} (\underline{m}_0 \dot{\underline{v}} - \underline{H} \dot{\underline{\omega}} + \underline{A}_1 \dot{\underline{q}}) \\ &= \dot{\underline{\omega}} (\underline{m}_0 \dot{\underline{v}} - \underline{H} \dot{\underline{\omega}} + \underline{A}_1 \dot{\underline{q}}) \end{aligned} \quad (27)$$

Similarly, using equation (2) and the chain rule in the Lagrange's equations, the rotational equations are obtained as

$$\dot{\underline{H}} \dot{\underline{V}} + I_0 \dot{\underline{\omega}} + \underline{A}_2 \ddot{\underline{q}} = \underline{G}(t) + \underline{N}_2 \quad (28)$$

where $G(t)$ is the net moment about the mass center of the orbiter and is given as

$$\underline{G} = \underline{G}_0 + (\underline{r} + \underline{a}) \times \underline{F}_2 \quad (29)$$

and the nonlinear term N_2 is given in terms of transformations M and C , and $\underline{\omega}$, \underline{v} and $\underline{\theta}$. The vibration equations of the beam can be obtained by again using Lagrange's equations and the potential energy function

$$U = 1/2 \underline{q}^T K \underline{q} \quad (30)$$

where the stiffness matrix K is given as

$$K = \begin{bmatrix} 4 \\ \frac{EI(\beta^2)}{L^3} \end{bmatrix} \quad (31)$$

The vibration equations are

$$\underline{A}_1^T \dot{\underline{V}} + \underline{A}_2^T \dot{\underline{\omega}} + \underline{A}_3 \ddot{\underline{q}} = -K \underline{q} \quad (32)$$

$$I_0 \dot{\underline{\omega}} + A_2 \ddot{\underline{q}} = \underline{G}(t) + \underline{N}_2(\underline{\omega}) \quad (33)$$

$$A_2^T \dot{\underline{\omega}} + A_3 \ddot{\underline{q}} = -K\underline{q} \quad (34)$$

Equation (33) can be rewritten as

$$\dot{\underline{\omega}} = I_0^{-1} [\underline{G} + \underline{N}_2(\underline{\omega}) - A_2 \ddot{\underline{q}}] \quad (35)$$

The first three Euler parameters are defined as

$$\underline{\varepsilon} \triangleq \begin{bmatrix} \varepsilon_1 \\ \varepsilon_2 \\ \varepsilon_3 \end{bmatrix} = \underline{\lambda} \sin \psi/2 \quad (36)$$

$$\varepsilon_4 \triangleq \cos \psi/2 \quad (37)$$

$$\frac{d\underline{\varepsilon}}{dt} \triangleq 1/2 (\varepsilon_4 \dot{\underline{\omega}} + \underline{\varepsilon} \times \underline{\omega}) \quad (38)$$

$$\frac{d\varepsilon_4}{dt} = -1/2 \underline{\omega} \cdot \underline{\varepsilon} \quad (39)$$

$$\dot{\underline{\omega}} = 2 (\varepsilon_4 \frac{d\underline{\varepsilon}}{dt} - \dot{\varepsilon}_4 \underline{\varepsilon} - \underline{\varepsilon} \times \frac{d\underline{\varepsilon}}{dt}) \quad (40)$$

$$\dot{\underline{\varepsilon}} = \frac{d\underline{\varepsilon}}{dt} = \underline{h} (\underline{\varepsilon}, \underline{\omega}) \quad (41)$$

ONE PAGE IS
OF POOR QUALITY

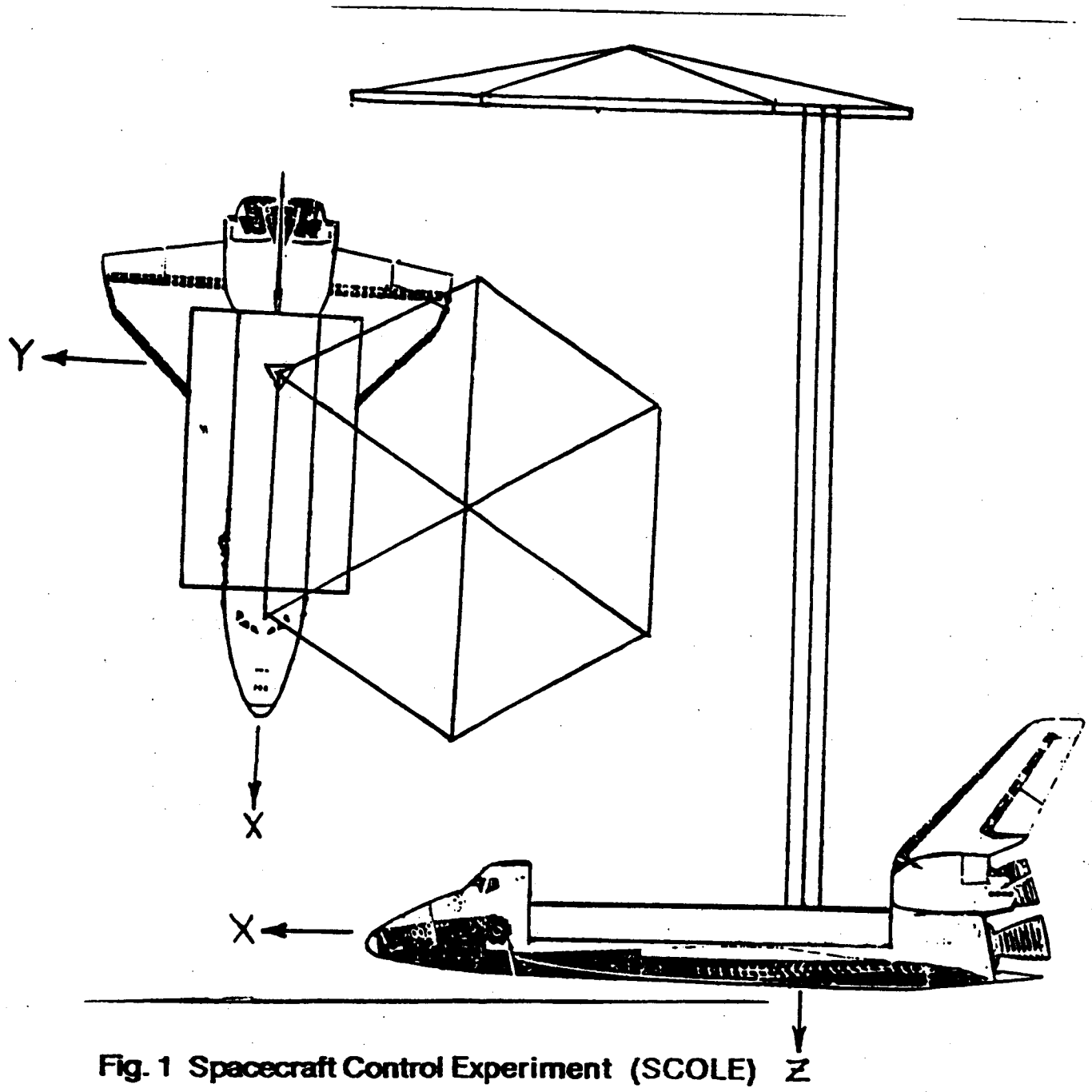
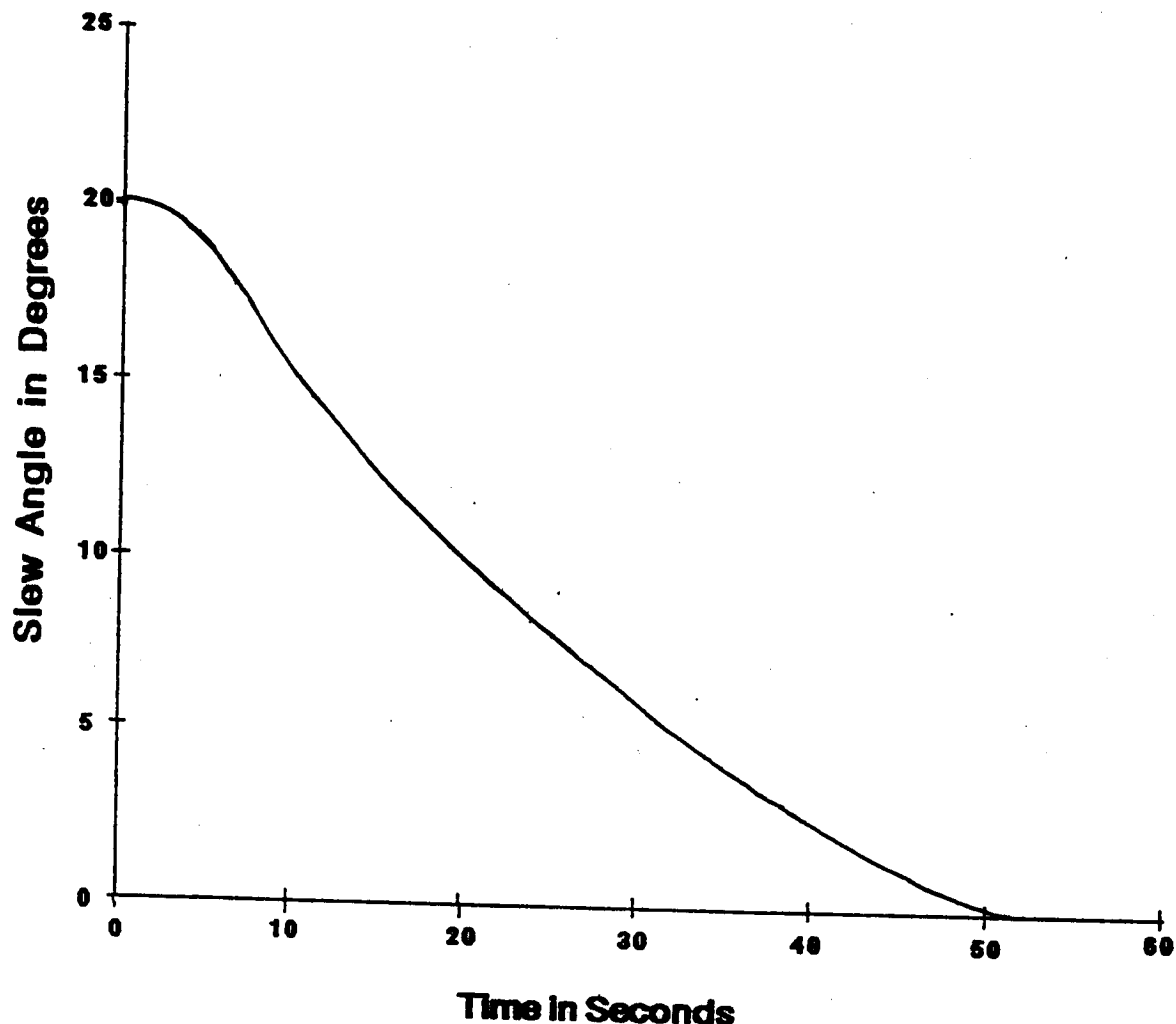
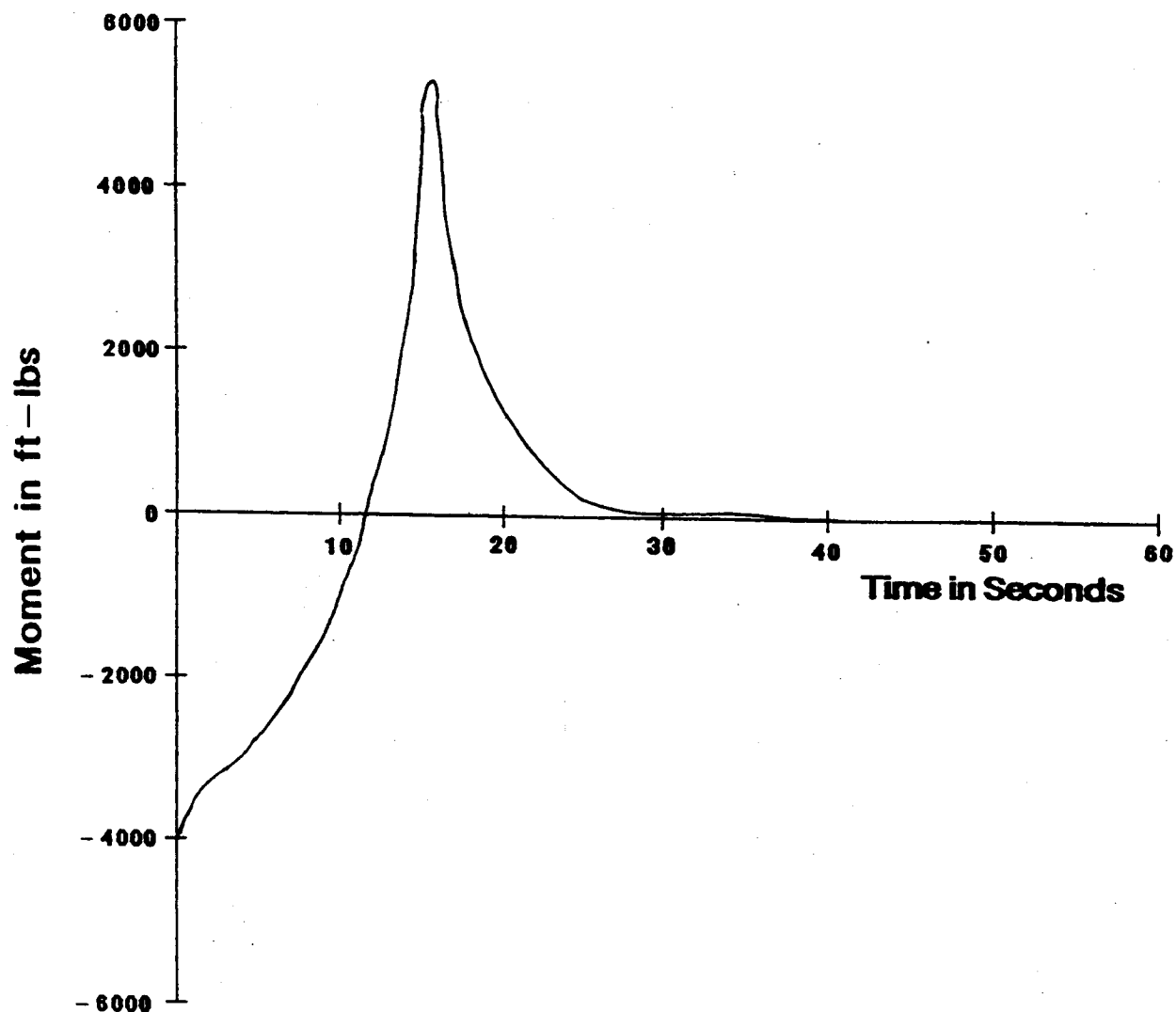


Fig. 1 Spacecraft Control Experiment (SCOPE) 2



**Fig. 6 Slew Angle vs. Time
(Axis of Rotation)**
 $3i + j + 5k$



**Fig. 7 Moment Component G_1 vs. Time
(Axis of Rotation)**

$$3i + j + 5k$$

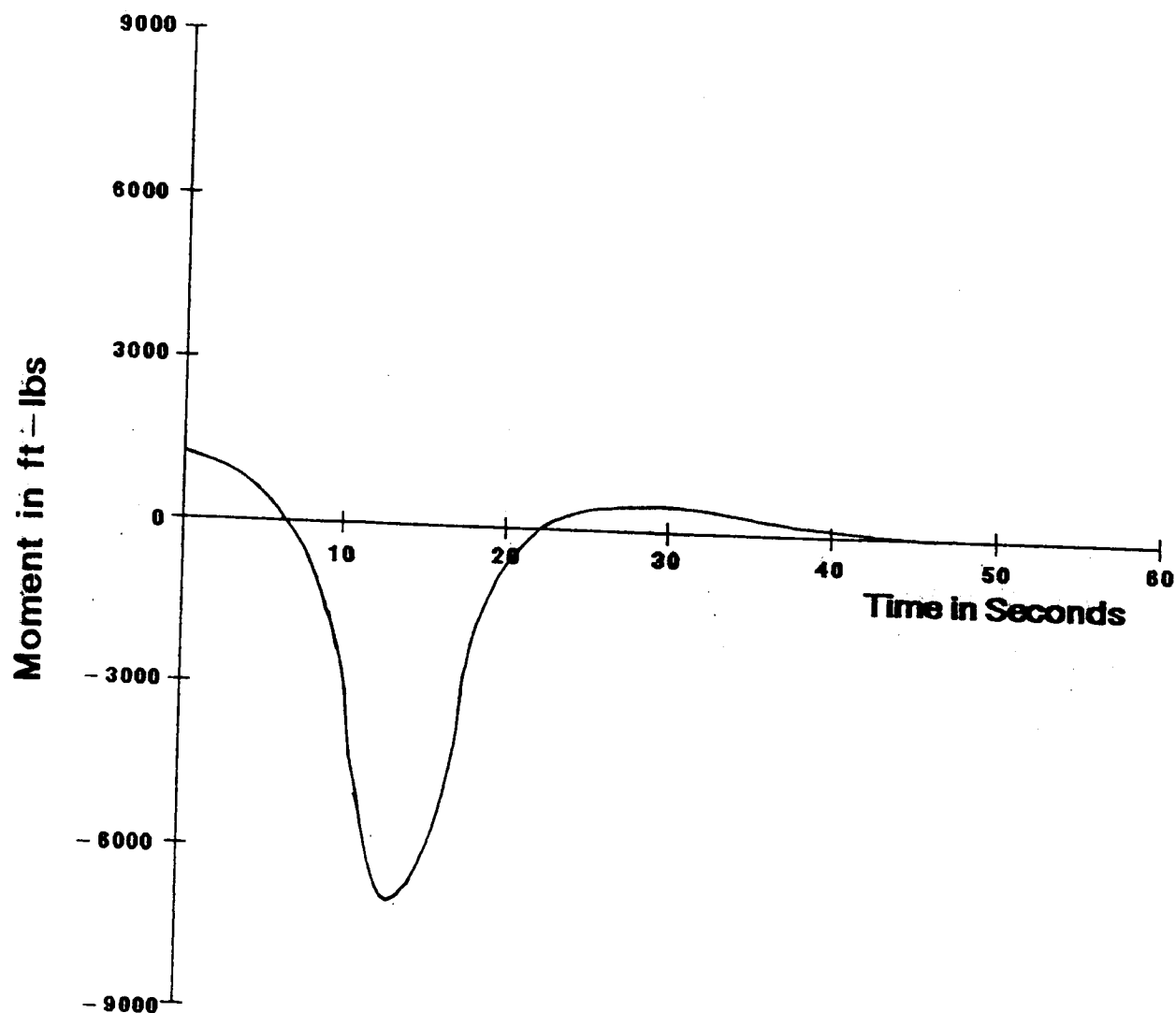


**Fig. 8 Moment Component G_2 vs. Time
(Axis of Rotation)**

$3i + j + 5k$

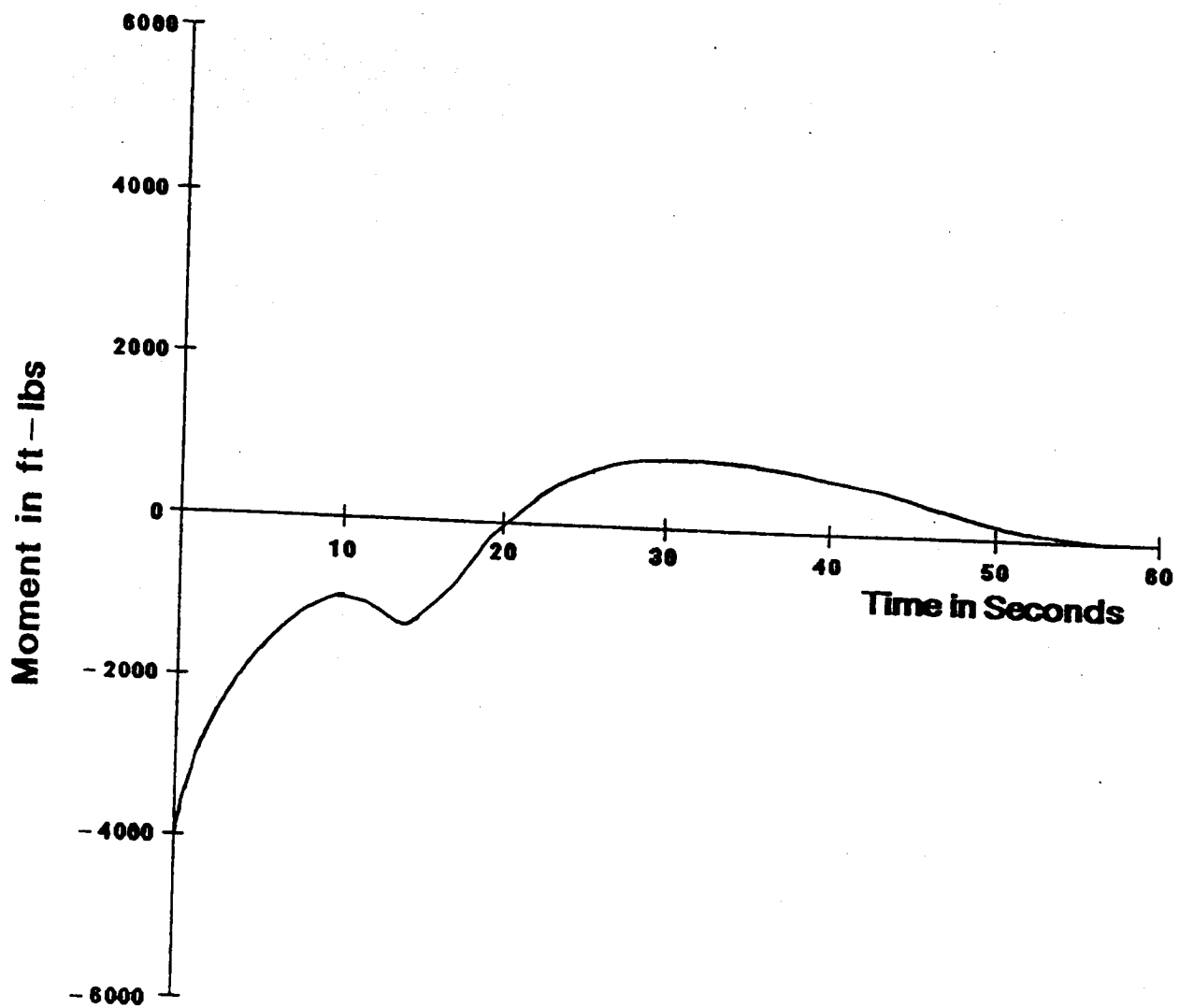


**Fig. 9 Moment Component G_3 vs. Time
(Axis of Rotation)**

$$3i + j + 5k$$

108

Modeling and Identification of SCOLE

by

L. Meirovitch

M. A. Norris

**Virginia Polytechnic
Institute and State Univ**

RECORDED PAGE 42346 NOT FILMED

THIRD ANNUAL SCOLE WORKSHOP

MODELING AND IDENTIFICATION OF SCOLE

L. Meirovitch and M. A. Norris

Department of Engineering Science and Mechanics
Virginia Polytechnic Institute and State University

Blacksburg, VA 24061

6

VECTOR DIFFERENTIAL EQUATION FOR DISTRIBUTED STRUCTURES

$$\mathcal{L} \underline{u}(P, t) + M \ddot{\underline{u}}(P, t) = \underline{f}(P, t), \quad P \in D$$

Boundary conditions: $B_i \underline{u}(P, t) = 0, \quad i = 1, 2, \dots, p, \quad P \in S$

$\underline{u}(P, t)$ = displacement vector at point P in the domain D

\mathcal{L} = stiffness operator matrix with entries of maximum order $2p$

M = mass density matrix

$\underline{f}(P, t)$ = control force density vector

B_i = boundary differential operator matrices with entries of maximum order $2p-1$

||

DISCRETIZATION (IN SPACE) OF THE DISTRIBUTED STRUCTURE

Shuttle and reflector are assumed to be rigid.

Cable is discretized by the Rayleigh-Ritz method (resulting in a small number of degrees of freedom):

$$u_x(z, t) = \sum_{r=1}^n \phi_{xr}(t) a_{xr}(t), \quad u_y(z, t) = \sum_{r=1}^n \phi_{yr}(t) a_{yr}(t), \quad 0 < z < L_1$$

u_x, u_y = displacements in the x and y direction, respectively.

ϕ_{xr}, ϕ_{yr} = admissible functions

a_{xr}, a_{yr} = generalized coordinates

L_1 = length of cable

DISCRETIZATION (IN SPACE) OF THE DISTRIBUTED STRUCTURE (CONT'D)

Because the identification and control problems are based on actual displacements of various points, the mast is discretized by the finite element method:

$$\underline{u}(z, t) = \begin{bmatrix} u_x(z, t) \\ u_y(z, t) \\ \theta_z(z, t) \end{bmatrix} = L(z) \underline{w}_j(t), \quad (j-1)h < z < jh$$

u_x, u_y = bending displacements

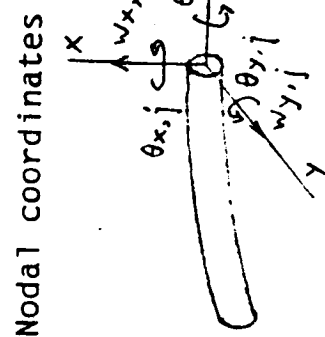
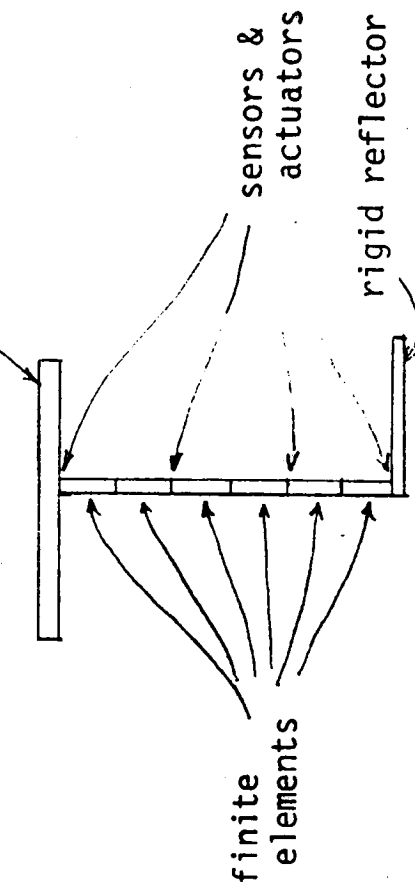
θ_z = torsional displacement

$L(z)$ = matrix of interpolation functions

$\underline{w}_j(t)$ = vector of nodal coordinates = vector of actual displacements at nodal points

DISCRETIZATION (IN SPACE) OF THE DISTRIBUTED STRUCTURE (CONT'D)

Finite element model rigid shuttle



Element nodal vector

$$\underline{w}_j(t) = [w_{x,j-1} \ \theta_{x,j-1} \ w_{y,j-1} \ \theta_{y,j-1} \ w_{z,j-1} \ \theta_{z,j-1} \ w_{x,j} \ \theta_{x,j} \ w_{y,j} \ \theta_{y,j} \ w_{z,j} \ \theta_{z,j}]^T$$

(2)

DISCRETIZATION (IN SPACE) OF THE DISTRIBUTED STRUCTURE (CONT'D)

The cable is represented by four degrees of freedom.

The shuttle has three rotational degrees of freedom.

The mast is divided into six finite elements, each requiring five degrees of freedom. Hence the model has 37 degrees of freedom.

The discretized system equations of motion: $\ddot{M}\underline{q}(t) + \ddot{K}\underline{q}(t) = \ddot{F}(t)$

$\underline{q}(t)$ = generalized displacement vector

M, K = mass, stiffness matrices

$\ddot{F}(t)$ = control vector

$$\underline{q}(t) = [a_{x1} \ a_{y1} \ a_{x2} \ a_{y2} \ \theta_{x0} \ \theta_{y0} \ \theta_{z0} \ \theta_{x1} \ \theta_{y1} \ \theta_{z1} \ \dots \ \theta_{x6} \ \theta_{y6} \ \theta_{z6}]^T$$

PARAMETER IDENTIFICATION

Assume that the shuttle is fixed and identify the mast parameter. Use a perturbation technique in conjunction with frequency response.

$$\text{Harmonic excitation: } \underline{F}(t) = \underline{F}^e e^{i\omega t}, \quad e = 1, 2, \dots, m$$

$$\text{Frequency response: } [\underline{K} - (\omega^e)^2 M] \underline{q}^e = \underline{F}^e$$

$$\text{Perturbation technique: } M = M_0 + \Delta M, \quad K = K_0 + \Delta K \rightarrow \underline{p} = \underline{p}_0 + \Delta \underline{p}$$
$$\underline{p} = [m_1 \ m_2 \ \dots \ m_6 \ EI_{x1} \ EI_{y1} \ GJ_{z1} \ \dots \ EI_{x6} \ EI_{y6} \ GJ_{z6}]^T = \text{actual parameter vector}$$

\underline{p}_0 = postulated parameter vector

$\Delta \underline{p}$ = parameter perturbation vector

Actual, or perturbed, frequency response:

$$[\underline{K}_0 + \Delta K - (\omega^e)^2 (M_0 + \Delta M)] (\underline{q}_0^e + \Delta \underline{q}^e) = \underline{F}^e, \quad e = 1, 2, \dots, m$$

PARAMETER IDENTIFICATION (CONT'D)

$$\left. \begin{array}{l} q_0^e = \text{response amplitude computed on the basis of} \\ \text{postulated model} \\ q_{\tilde{z}}^e = \text{actual response amplitude} \end{array} \right\} q_{\tilde{z}}^e = q_0^e + \Delta q^e$$

$$\text{Parameter perturbations: } \Delta M = \sum_{\xi=1}^6 \frac{\partial M}{\partial p_{\xi}} \Delta p_{\xi}, \quad \Delta K = \sum_{\xi=7}^{24} \frac{\partial K}{\partial p_{\xi}} \Delta p_{\xi}$$

$$\left. \begin{array}{l} 1 - (\omega^e)^2 \frac{\partial M}{\partial p_{\xi}} \Delta p_{\xi}, \quad \xi = 1, 2, \dots, 6 \\ B_{\xi}^e = \left\{ \begin{array}{l} \frac{\partial K}{\partial p_{\xi}} \Delta p_{\xi}, \quad \xi = 7, 8, \dots, 24 \end{array} \right. \end{array} \right\}$$

$$\text{Identification algorithm: } B^e \Delta p_{\tilde{z}} = C_{\tilde{z}}^e, \quad C_{\tilde{z}}^e = [K_0 - (\omega^e)^2 M_0] \Delta q^e, \quad e = 1, 2, \dots, m$$

$$B = [B^e], \quad C_{\tilde{z}} = [C_{\tilde{z}}^e] \rightarrow B \Delta p_{\tilde{z}} = C_{\tilde{z}} + \Delta p = (B^T B^{-1}) B^T C_{\tilde{z}}$$

PARAMETER IDENTIFICATION (CONT'D)

If the measured output is not the whole state, use Kalman filter to estimate the state. First estimation is based on the postulated model:

$$\dot{\underline{x}}(t) = A\underline{x}(t) + B[\underline{F}(t) + \underline{v}(t)]$$

$$\underline{x}(t) = [\underline{q}^T(t) \quad \dot{\underline{q}}^T(t)]^T, \quad A = \begin{bmatrix} 0 & 1 \\ -M_0^{-1}K_0 & 0 \end{bmatrix}, \quad B = \begin{bmatrix} 0 \\ M_0^{-1} \end{bmatrix}$$

$\underline{v}(t)$ = excitation (actuator) noise vector

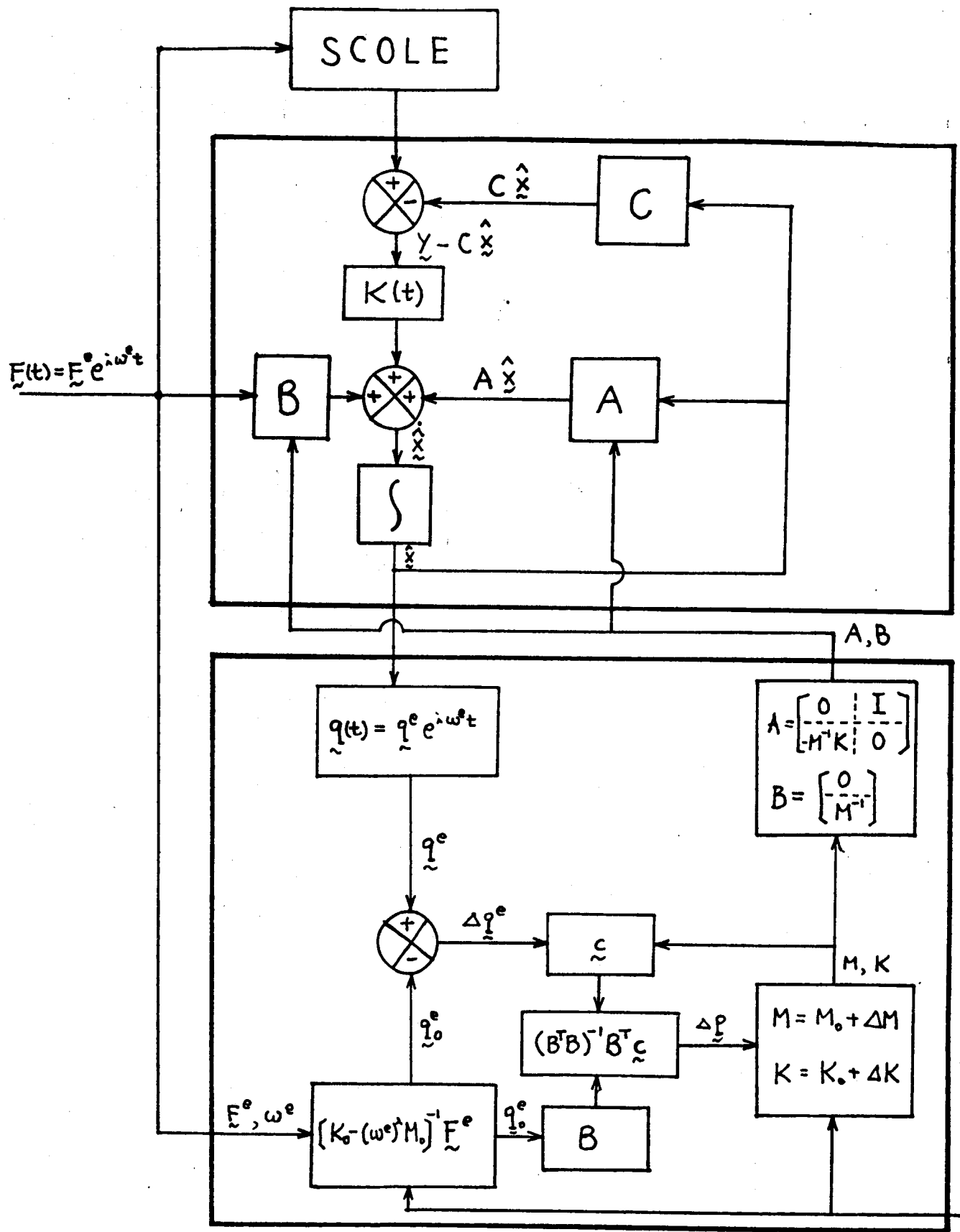
Kalman filter: $\dot{\hat{\underline{x}}}(t) = A\hat{\underline{x}}(t) + B\underline{F}(t) + K(t)[\underline{y}(t) - \hat{C}\hat{\underline{x}}(t)]$

$$\underline{y}(t) = C\underline{x}(t) + \underline{w}(t) = \text{output vector}$$

$$\underline{w}(t) = \text{measurement (sensor) noise vector}$$

The finite-element based identification routine and the Kalman filter work together in a closed-loop fashion.

Identification process is carried out iteratively: identified model becomes postulated model for the new iteration cycle.



120

On Incorporating Damping and Gravity Effects in Models...

by

Larry Taylor
NASA Langley
Research Center

and

Terry Leary
Eric Stewart
Geo. Washington U.

PRECEDING PAGE BLANK NOT FILMED

**On Incorporating Damping and Gravity Effects in Models of
Structural Dynamics of the SCOLE Configuration**

by

Lawrence W. Taylor, Jr

Terry Leary

Eric Stewart

Presented at
The 3rd Annual SCOLE* Workshop
NASA Langley Research Center
Hampton, Virginia
November 17, 1986

*Spacecraft Control Laboratory Experiment(SCOLE)

On Incorporating Damping and Gravity Effects in Models of Structural Dynamics of the SCOLE Configuration

ABSTRACT

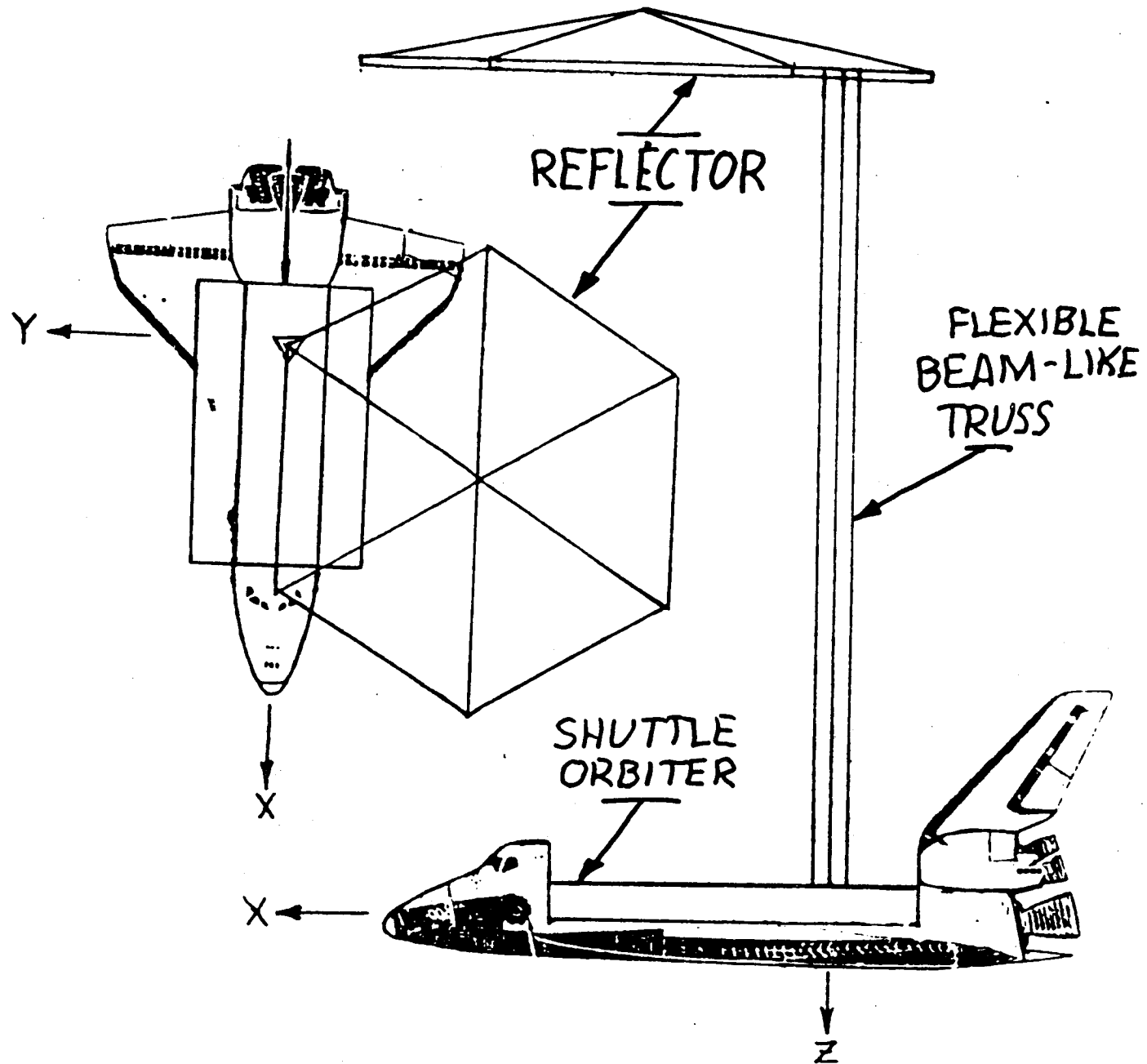
The damping for structural dynamics models of flexible spacecraft is usually ignored and then added after modal frequencies and mode shapes are calculated. It is common practice to assume the same damping ratio for all modes, although it is known that damping due to bending and that due to torsion are different. Mass effects on damping are sometimes ignored.

It is the purpose of this paper to examine two ways of including damping in the modeling process from its onset. First, the partial derivative equations of motion are analyzed for a pinned-pinned beam with damping. The end conditions are altered to handle bodies with mass and inertia for the SCOLE configuration. Second, a massless beam approximation is used for the modes with low frequencies, and a clamped-clamped system is used to approximate the modes for arbitrarily high frequency. The model is then modified to include gravity effects and is compared with experimental results.

OUTLINE

- Introductory Remarks
- SCOLE Configuration
- Partial Differential Equations
- Pinned-Pinned System with Damping
- Free-Free System with End Bodies & Damping
- Massless Beam Approximation
- Gravity Effects
- Comparison of Model Frequencies
- Concluding Remarks

CONFIGURATION



Equations of Motion

Shuttle (and Reflector) Body

$$\dot{\bar{w}}_1 = -\bar{I}_1^{-1} (\bar{w}_1 I_1 w_1 - M_1 - M_{1, \text{Beam}})$$

$$\dot{v}_1 = (F_1 + F_{1, \text{Beam}}) / m_1$$

$$\dot{T}_1^T = -\bar{w}_1 T_1^T$$

Roll (and Pitch) Beam Bending

$$p A_\phi \frac{d^2 u_\phi}{dt^2} - C I_\phi \frac{d^3 u_\phi}{ds^2 dt} + E I_\phi \frac{d^4 u_\phi}{ds^4} = \sum_{n=1}^4 [f_{\phi,n} \delta(s-s_n) + g_{\phi,n} \frac{d\delta}{ds}(s-s_n)]$$

Yaw Beam Torsion

$$p I_\Psi \frac{d^2 u_\Psi}{dt^2} + C I_\Psi \frac{d^3 u_\Psi}{ds^2 dt} - G I_\Psi \frac{d^2 u_\Psi}{ds^2} = \sum_{n=1}^4 g_{\Psi,n} \delta(s-s_n)$$

Beam Elongation

$$p A \frac{d^2 u_z}{dt^2} + C_z A \frac{d^2 u_z}{ds dt} - E A \frac{d^2 u_z}{ds^2} = \sum_{n=1}^4 f_{z,n} \delta(s-s_n)$$

Damping Considerations

- The Classical Damping, $\frac{du^5}{ds^4 dt}$ Yields Excessive Excessive Damping at Higher Mode Numbers
- The Term, $\frac{du^3}{ds^2 dt}$ is Consistent with experimental Data.
- The Practice of Post-Analysis Addition of Damping Ignores Effects of Mass, Stress Type.
- Damping Must be Included from the Start.

Distributed Parameter Model of SCOLE with "Proportional Damping"

- Start with Pinned-Pinned Beam with Damping
- Add Bodies with Inertia at Ends
- Model Acceleration of Frame as Inertial Loading
- Extend in Three Dimensions to
SCOLE Configuration.
- Yields Infinite-Order, Modal, State Equations.

Distributed Parameter System

$$\frac{d}{dt} \begin{bmatrix} \mathbf{q} \\ \dot{\mathbf{q}} \end{bmatrix} = \begin{bmatrix} 0 & I \\ A_{21}^* & A_{22}^* \end{bmatrix} \begin{bmatrix} \mathbf{q} \\ \dot{\mathbf{q}} \end{bmatrix} + \begin{bmatrix} 0 \\ B_2 \end{bmatrix} \begin{bmatrix} M_1 \\ M_4 \\ F_1 \\ F_4 \end{bmatrix}$$

$$A_{21}^* = \{B_M \begin{bmatrix} I_1 & 0 \\ 0 & I_4 \end{bmatrix} R\}^{-1} [A + B \begin{bmatrix} -pA & 0 \\ \frac{pA}{L} & \frac{pA}{L} \end{bmatrix} Q]$$

$$A_{22}^* = \{B_M \begin{bmatrix} I_1 & 0 \\ 0 & I_4 \end{bmatrix} R\}^{-1}$$

$$B_{22}^* = \{B_M \begin{bmatrix} I_1 & 0 \\ 0 & I_4 \end{bmatrix} R\}^{-1} [-B_M B_W \begin{bmatrix} -pA & 0 \\ \frac{pA}{L} & \frac{pA}{L} \end{bmatrix} + B_A]$$

$$A = \begin{bmatrix} 0 & 1 \\ -\omega_1 - 2\delta\omega_1 & \\ & 0 & 1 \\ & -\omega_2 - 2\delta\omega_2 & \\ & & 0 & 1 \\ & & -\omega_3 - 2\delta\omega_3 & \\ & & & \ddots \\ & & & \ddots \end{bmatrix}$$

$$B_M = \begin{bmatrix} 0 & 0 \\ \frac{2\pi^2}{\rho AL^3} & -\frac{2\pi^2}{\rho AL^3} \\ 0 & 0 \\ \frac{8\pi^2}{\rho AL^3} & \frac{8\pi^2}{\rho AL^3} \\ 0 & 0 \\ \frac{18\pi^2}{\rho AL^3} & -\frac{18\pi^2}{\rho AL^3} \\ \vdots & \vdots \end{bmatrix} \quad B_W = \begin{bmatrix} 0 & 0 \\ -\frac{8}{\rho AL} & -\frac{4}{\rho A} \\ 0 & 0 \\ 0 & \frac{4}{\rho A} \\ 0 & 0 \\ -\frac{8}{\rho AL} & -\frac{4}{\rho A} \\ \vdots & \vdots \end{bmatrix}$$

$$R = \begin{bmatrix} 0 & 1 & 0 & 1 & 0 & 1 & 0 & 1 & 0 & 1 & \dots \\ 0 & -1 & 0 & 1 & 0 & -1 & 0 & 1 & 0 & -1 & 0 & \dots \end{bmatrix}$$

$$B_A = \left[\begin{array}{c|c} -B_M & B_W \begin{bmatrix} \frac{\rho A}{m_1} & 0 \\ \frac{\rho A}{Lm_1} & \frac{\rho A}{Lm_4} \end{bmatrix} \end{array} \right]$$

$$Q = \begin{bmatrix} 0 & 0 \\ -\frac{EI\pi^2}{L^2} & \frac{EI\pi^2}{L^2} \\ 0 & 0 \\ -\frac{4EI\pi^2}{L^2} & -\frac{4EI\pi^2}{L^2} \\ 0 & 0 \\ \vdots & \vdots \end{bmatrix}$$

Massless Beam Model

- **Exact Static Deflection**
- **Approximates Low-Frequency Modes**
- **Nonlinear Kinematics**
- **Linearized State Space, Modal Model**
- **Classical Damping(Working Proportional)**
- **Extended to n-Body Network**

Gravity Effects

- Assume Cubic Deflection of Beam
- Express Potential Energy due to the Raising of End Body
- Relate to Stiffness Matrices of the Massless Beam Model
- Incorporate Gravity Effects in the Stiffness Matrices
- Gravity Effects Larger than Structural Stiffness

Equations of Motion

$$\dot{\mathbf{x}} = \mathbf{Ax} + \mathbf{Bu}$$

$$\mathbf{A} = \begin{bmatrix} 0 & a_{12} & 0 & a_{14} & 0 & a_{16} & 0 & a_{18} \\ 1 & 0 & 0 & 0 & 0 & 0 & 0 & 0 \\ 0 & a_{32} & 0 & a_{34} & 0 & a_{36} & 0 & a_{38} \\ 0 & 0 & 1 & 0 & 0 & 0 & 0 & 0 \\ 0 & a_{52} & 0 & a_{54} & 0 & a_{56} & 0 & a_{58} \\ 0 & 0 & 0 & 0 & 1 & 0 & 0 & 0 \\ 0 & a_{72} & 0 & a_{74} & 0 & a_{76} & 0 & a_{78} \\ 0 & 0 & 0 & 0 & 0 & 0 & 1 & 0 \end{bmatrix}$$

$$B = \begin{bmatrix} b_{11} & b_{12} & b_{13} & b_{14} \\ 0 & 0 & 0 & 0 \\ b_{31} & b_{32} & b_{33} & b_{34} \\ 0 & 0 & 0 & 0 \\ b_{51} & b_{52} & b_{53} & b_{54} \\ 0 & 0 & 0 & 0 \\ b_{71} & b_{72} & b_{73} & b_{74} \\ 0 & 0 & 0 & 0 \end{bmatrix}$$

$$x = \begin{bmatrix} w_1 \\ E_1 \\ V_1 \\ R_1 \\ w_4 \\ E_4 \\ V_4 \\ R_4 \end{bmatrix} \quad u = \begin{bmatrix} F_1 \\ \Pi_1 \\ F_4 \\ \Pi_4 \end{bmatrix}$$

$$a_{12} = I_1^{-1} [-M_U \tilde{r}_1 + M_{\angle} + \tilde{r}_1 F_{\angle} - \tilde{r}_1 F_U \tilde{r}_1] = -a_{16}$$

$$a_{14} = I_1^{-1} [M_U + \tilde{r}_1 F_U] = -a_{18}$$

$$a_{32} = \frac{1}{m_1} [-F_U \tilde{r}_1 + F_{\angle}] = -a_{36}$$

$$a_{34} = \frac{1}{m_1} [F_U] = -a_{38}$$

$$a_{52} = I_4^{-1} [-M_U \tilde{r}_4 + M_{\angle} + \tilde{r}_4 F_{\angle} - \tilde{r}_4 F_U \tilde{r}_4] = -a_{56}$$

$$a_{54} = I_4^{-1} [M_U + \tilde{r}_4 F_U] = -a_{58}$$

$$a_{72} = \frac{1}{m_4} [-F_U \tilde{r}_4 + F_{\angle}] = -a_{76}$$

$$a_{74} = \frac{1}{m_4} [F_U] = -a_{78}$$

I - Moment of Inertia

m - Mass

r - Coordinates of attach point

\tilde{r} - Cross product operator, $r \times$

$M_U, M_{\angle}, F_U, F_{\angle}$ - Stiffness Matrices

1 - Denotes the Shuttle body

4 - Denotes the reflector body

u, \angle - Beam deflection and slope

Stiffness Matrices

$$\partial \mathbf{r}^B = \mathbf{U}^B \mathbf{M}^B \quad \partial \mathbf{u}^B$$

$$\left[\begin{array}{ccc} -\frac{12EI}{L^3} - \frac{86W}{5L} * \left[\mathbf{U}^B \mathbf{M}^B \right] & 0 & 0 \\ 0 & -\frac{12EI}{L^3} - \frac{6W}{5L} * \left[\mathbf{U}^B \mathbf{M}^B \right] & 0 \\ 0 & 0 & -\frac{EA}{L} \end{array} \right] = \mathbf{P}^B$$

$$\left[\begin{array}{ccc} 0 & 0 & -\frac{6EI}{L^2} * \left[\mathbf{U}^B \mathbf{M}^B \right] \\ 0 & 0 & -\frac{6EI}{L^2} * \left[\mathbf{U}^B \mathbf{M}^B \right] \\ 0 & 0 & -\frac{EA}{L} \end{array} \right] = \mathbf{Q}^B$$

$$\left[\begin{array}{ccc} \frac{6EI}{L^2} & 0 & 0 \\ 0 & \frac{6EI}{L^2} & 0 \\ 0 & 0 & 0 \end{array} \right] = \mathbf{K}^B$$

ORIGINAL PAGE IS
OF POOR QUALITY

subject to joint
displacements of support point

* Gravity Effect
- Sagging of object due to weight of object

in rotates the left elector body
about deflection and slope

136

Stiffness Matrices

$$M_U = \begin{bmatrix} -\frac{4EI}{L} - \frac{2WL^*}{15} & 0 & 0 \\ 0 & -\frac{4EI}{L} - \frac{2WL^*}{15} & 0 \\ 0 & 0 & -\frac{GJ}{L} \end{bmatrix}$$

$$M_U = \begin{bmatrix} 0 & \frac{6EI}{L^2} + \frac{W^*}{10} & 0 \\ \frac{6EI}{L^2} + \frac{W^*}{10} & 0 & 0 \\ 0 & 0 & 0 \end{bmatrix}$$

* Gravity Effect

PROGRAM TWO800
REAL 11,14,11IN,14IN,M1,M4,MU,MANG,L,MASS1,MASS4
DIMENSION 11(13),11IN(13),14(13),14IN(13),R(588),RAT1(7),
*RAT1T(13),RAT4(7),RAT4T(13),FU(13),FANG(13),MU(13),MANB(13),
*DUM(588),DUN(588),ERREAL(30),EIMAG(30),EVEC(588),DUO(588)
C..... DEFINE INERTIA MATRICES.....
CALL SET(11,24,24)
CALL SET(11,3,3)
11(5)=995443.
11(7)=-145393.
11(9)=6789100.
11(11)=-145393.
11(13)=7886601.
CALL SPIT(11,3H 11)
CALL MAKE(DUM,11)
CALL INUR(11,11IN)
CALL MAKE(11,DUM)
CALL SET(14,3,3)
14(5)=4969.
14(9)=4969.
14(13)=9938.
CALL SPIT(14,3H 14)
CALL MAKE(DUM,14)
CALL INUR(14,14IN)
CALL MAKE(14,DUM)
C..... DEFINE ATTACH POINT VECTOR, MATRIX.
CALL SET(RAT1,3,1)
CALL TILDA(RAT1,RAT1T)
CALL SET(RAT4,3,1)
RAT4(5)=-18.75
RAT4(6)=32.5
CALL TILDA(RAT4,RAT4T)
MASS4=12.42
C..... ADD HALF OF BEAM MASS TO REFLECTOR BODY...
AD=MASS4/(MASS4+12.42*.5)
CALL ADD(AD,RAT4T,-1.,RAT4T,DUM)
CALL SPIT(DUM,4H DUM)
CALL MULT(DUM,DUM,DUN)
CALL SPIT(DUM,4H DUN)
CALL ADD(1.,14,-12.42,DUN,14)
AD=.5*12.42/(12.42+.5*12.42)
CALL ADD(AD,RAT4T,-1.,RAT4T,DUM)
CALL MULT(DUM,DUM,DUN)
CALL ADD(1.,14,-6.21,DUN,14)
CALL SPIT(14,5H 14NU)
CALL INUR(14,14IN)
MASS1=6366.46+.09556*130./2.
MASS4=MASS4+.09556*130/2.
C..... BEAM SECTION CHARACTERISTICS.....
EI=400000000.
GJ=400000000.
EA=100000000.
L=130.
C..... SET UP FORCE/DEFLECTION MATRIX.....
CALL SET(FU,3,3)
FU(5)=-12.*EI/(L*L*L)
FU(9)=-12.*EI/(L*L*L)
FU(13)=-EA/L
C..... SET UP FORCE/SLOPE ANGLE MATRIX.....
CALL SET(FANG,3,3)
FANG(6)=6.*EI/(L*L)
FANG(8)=FANG(6)
C..... SET UP MOMENT/DEFLECTION MATRIX.....
CALL MAKE(MU,FANG)

C.....SET UP MOMENT/SLOPE ANGLE MATRIX.....

```
CALL SET(MANG,3,3)
MANG(5)=-4.*EI/L
MANG(9)=-4.*EI/L
MANG(13)=-GJ/L
CALL SPIT(FU,3H FU)
CALL SPIT(FANG,5H FANG)
CALL SPIT(MU,3H MU)
CALL SPIT(MANG,3H MANG)
```

C.....CALCULATE ELEMENTS IN "A" MATRIX.....

```
CALL MULT(RAT1T,FU,DUM)
CALL MULT(DUM,RAT1T,DUM)
CALL MULT(RAT1T,FANG,DUM)
CALL ADD(1.,DUM,-1.,DUM,DUM)
CALL ADD(1.,MANG,1.,DUM,DUM)
CALL MULT(MU,RAT1T,DUM)
CALL ADD(-1.,DUM,1.,DUM,DUM)
CALL MULT(11IN,DUM,DUM)
CALL INSERT(1,4,DUM,A)
CALL ADD(-1.,DUM,0.,DUM,DUM)
CALL INSERT(1,16,DUM,A)
CALL MULT(RAT1T,FU,DUM)
CALL ADD(1.,MU,1.,DUM,DUM)
CALL MULT(11IN,DUM,DUM)
CALL INSERT(1,18,DUM,A)
CALL ADD(-1.,DUM,0.,DUM,DUM)
CALL INSERT(1,22,DUM,A)
CALL IDENT(DUM,3)
CALL INSERT(4,1,DUM,A)
CALL INSERT(10,7,DUM,A)
CALL INSERT(16,13,DUM,A)
CALL INSERT(22,19,DUM,A)
CALL MULT(FU,RAT1T,DUM)
CALL ADD(-1.,DUM,1.,FANG,DUM)
AD=1./MASS1
CALL ADD(AD,DUM,0.,DUM,DUM)
CALL INSERT(7,4,DUM,A)
CALL ADD(-1.,DUM,0.,DUM,DUM)
CALL INSERT(7,16,DUM,A)
CALL ADD(AD,FU,0.,FU,DUM)
CALL INSERT(7,10,DUM,A)
CALL ADD(-1.,DUM,0.,DUM,DUM)
CALL INSERT(7,22,DUM,A)
```

C.....A52.....

```
CALL MULT(RAT4T,FU,DUM)
CALL MULT(DUM,RAT4T,DUM)
CALL MULT(RAT4T,FANG,DUM)
CALL ADD(1.,DUM,-1.,DUM,DUM)
CALL ADD(1.,DUM,1.,MANG,DUM)
CALL MULT(MU,RAT4T,DUM)
CALL ADD(-1.,DUM,1.,DUM,DUM)
CALL MULT(14IN,DUM,DUM)
CALL INSERT(13,16,DUM,A)
CALL ADD(-1.,DUM,0.,DUM,DUM)
CALL INSERT(13,4,DUM,A)
CALL MULT(RAT4T,FU,DUM)
CALL ADD(1.,DUM,1.,MU,DUM)
CALL MULT(14IN,DUM,DUM)
CALL INSERT(13,22,DUM,A)
CALL ADD(-1.,DUM,0.,DUM,DUM)
CALL INSERT(13,10,DUM,A)
CALL MULT(FU,RAT4T,DUM)
CALL ADD(-1.,DUM,1.,FANG,DUM)
AD=1./MASS4
CALL ADD(AD,DUM,0.,DUM,DUM)
CALL INSERT(19,16,DUM,A)
```

ORIGINAL PAGE IS
OF POOR QUALITY

```
CALL ADD(-1.,DUM,0.,DUM,DUM)
CALL INSERT(19,4,DUM,A)
CALL ADD(AD,FU,0.,FU,DUM)
CALL INSERT(19,22,DUM,A)
CALL ADD(-1.,DUM,0.,DUM,DUM)
CALL INSERT(19,18,DUM,A)
C.....CALCULATE EIGEN VALUES, MODE SHAPES.....
CALL EIGEN(A,EREA1,E1MAG,EVEC,IERR)
CALL SPIT(EREA1,SH REAL)
CALL SPIT(E1MAG,SH IMAG)
123 FORMAT(110,E15.6)
C.....PRINT NON-ZERO ELEMENTS OF "A" MATRIX.....
DO 10 I=4,580
IF(R(I)**2- .0000000001>11,11,12
12 PRINT 123,I,R(I)
11 CONTINUE
10 CONTINUE
END
—E01/TOP—
??
```

ORIGINAL PAGE IS
OF POOR QUALITY

	1	2	3
11	.9054E+06	.0000E+00	.1454E+06
2	.0000E+00	.6789E+07	.0000E+00
3	-.1454E+06	.0000E+00	.7087E+07
	4341883E+28		
14	1	2	3
1	.4969E+04	.0000E+00	.0000E+00
2	.0000E+00	.4969E+04	.0000E+00
3	.0000E+00	.0000E+00	.9038E+04
	2453788E+12		
DUM	1	2	3
1	.0000E+00	.0000E+00	-.1083E+02
2	.0000E+00	.0000E+00	-.6250E+01
3	.1083E+02	.6250E+01	.0000E+00
DUN	1	2	3
1	-.1174E+03	-.6771E+02	.0000E+00
2	-.6771E+02	-.3905E+02	.0000E+00
3	.0000E+00	.0000E+00	-.1564E+03
14NU	1	2	3
1	.9342E+04	.2523E+04	.0000E+00
2	.2523E+04	.6424E+04	.0000E+00
3	.0000E+00	.0000E+00	.1577E+05
	8458959E+12		
FU	1	2	3
1	-.2185E+03	.0000E+00	.0000E+00
2	.0000E+00	.2185E+03	.0000E+00
3	.0000E+00	.0000E+00	-.7692E+06
FANG	1	2	3
1	.0000E+00	.1420E+05	.0000E+00
2	.1420E+05	.0000E+00	.0000E+00
3	.0000E+00	.0000E+00	.0000E+00
MU	1	2	3
1	.0000E+00	.1420E+05	.0000E+00
2	.1420E+05	.0000E+00	.0000E+00
3	.0000E+00	.0000E+00	.0000E+00
MANG	1	2	3
1	-.1231E+07	.0000E+00	.0000E+00
2	.0000E+00	-.1231E+07	.0000E+00
3	.0000E+00	.0000E+00	-.3077E+06
PEARL	1		
1	-.1344E-04		
2	-.9690E-06		
3	-.2861E-08		
4	-.6211E-14		
5	.6211E-14		
6	.2861E-08		
7	.9690E-06		
8	.1344E-04		
9	.0000E+00		
10	.0000E+00		
11	.0000E+00		
12	.0000E+00		
13	.0000E+00		
14	.0000E+00		
15	.0000E+00		
16	.0000E+00		
17	.0000E+00		
18	.0000E+00		
19	.0000E+00		
20	.0000E+00		
21	.0000E+00		
22	.0000E+00		

23 .0000E+00
24 .0000E+00
1MAG 1
1 .0000E+00
2 .0000E+00
3 .0000E+00
4 .0000E+00
5 .0000E+00
6 .0000E+00
7 .0000E+00
8 .0000E+00
9 .8682E-09
10 -.8682E-09
11 .1398E-05
12 -.1398E-05
13 .1621E+01
14 -.1621E+01
15 .2328E+01
16 -.2328E+01
17 .5821E+01
18 -.5821E+01
19 .1124E+02
20 -.1124E+02
21 .1617E+02
22 -.1617E+02
23 .3764E+03
24 -.3764E+03
8 -.136379E+01
10 -.699510E-02
15 .157361E-01
20 .136379E+01
22 .699510E-02
27 -.157361E-01
33 -.181286E+00
38 .289176E-02
45 .181286E+00
50 -.289176E-02
56 -.279884E-01
58 -.435624E-01
63 .322851E-03
68 .279884E-01
70 .435624E-01
75 -.322851E-03
77 .100000E+01
102 .100000E+01
127 .100000E+01
158 -.342839E-01
178 .342839E-01
183 -.342839E-01
195 .342839E-01
208 -.120708E+03
220 .120708E+03
227 .100000E+01
252 .100000E+01
277 .100000E+01
296 .753974E+05
297 .433556E+05
298 .101820E+02
302 .667765E+00
303 -.170050E+01
304 .231538E+04
306 -.753974E+05
309 -.433556E+05
310 -.101820E+02
314 -.667765E+00
315 .170050E+01

ORIGINAL PAGE IS
OF POOR QUALITY

316 - .231538E+04
320 .433556E+05
321 .252605E+05
322 .578424E+02
326 - .247271E+01
327 .667765E+00
328 .133588E+04
332 - .433556E+05
333 - .252605E+05
334 - .678424E+02
338 .247271E+01
339 - .667765E+00
348 - .133588E+04
344 .168886E+02
345 .292737E+02
346 .390243E+02
358 - .450364E+00
351 - .259825E+00
356 - .168886E+02
357 - .292737E+02
358 - .390243E+02
362 .450364E+00
363 .259825E+00
377 .100000E+01
402 .100000E+01
427 .100000E+01
441 - .762218E+03
442 - .381109E+03
446 .117264E+02
453 .762218E+03
454 .381109E+03
458 - .117264E+02
464 - .762218E+03
466 - .219870E+03
471 .117264E+02
476 .762218E+03
478 .219870E+03
483 - .117264E+02
488 .134182E+07
489 .774127E+06
496 .412868E+05
500 - .134182E+07
501 - .774127E+06
508 - .412868E+05
527 .100000E+01
552 .100000E+01
577 .100000E+01

ORIGINAL PAGE IS
OF POOR QUALITY

REVERT NORMAL END.

Static Deflection

<u>Number of Modes</u>	<u>Error in Deflection</u>
1	39%
2	24
3	17
4	13
5	11
6	9
7	8
8	7
9	6
:	:
67	1

Comparison of Modal Frequencies

Mode	P.D.E.	Finite El.	Lumped Mass *Clamped
1	.278	.276	.258
2	.314	.301	.370
3	.812	.810	.926
4	1.18	1.18	1.79
5	2.05	2.05	2.57
6	4.76	4.77	4.28*
7	5.51	5.52	4.28*
8	12.3	12.4	11.89*

SCOLE Experiment Modal Characteristics



Large
Amplitude

Small
Amplitude

Imaginary
Part, $j\omega$

30

20

10

0

5th Mode

□□□

4th Mode

3rd Mode

◇◇◇

2nd Mode

△△△

1st Mode

Proportional Damping
(Constant Damping Ratio)

-.03

-.02

-.01

Real Part, σ

Concluding Remarks

- An Infinite-Order State Space Model was Developed which Incorporates "Proportional" Damping.
- A Lumped Mass Model of SCOLE was Developed which Includes Gravity Effects and Classical Damping. Extended to n-Body Modeling.
- Modal Frequencies are Compared for the SCOLE using Different Methods.
- Items Remain to be Addressed Before SCOLE Modeling is Complete.

REFERENCES

1. Taylor, Lawrence W., Jr. and A. V. Balakrishnan (1983). A Mathematical Problem and a Spacecraft Control Laboratory Experiment (SCOLE) Used to Evaluate Control Laws for Flexible Spacecraft.....NASA/IEEE Design Challenge. Fourth VPI&SU/AIAA Symposium on Dynamics and Control of Large Structures. Blacksburg, Virginia. Also presented at the First Annual SCOLE Workshop. December, 1984. NASA Langley Research Center. Hampton, Virginia.
2. Robertson, Daniel K. (1985). Three-Dimensional Vibration Analysis of a Uniform Beam with Offset Inertial Masses at the Ends. NASA Technical Memorandum 86393
3. Poelaert, D. (1983). DISTEL, A Distributed Element Program for Dynamic Modelling and Response Analysis of Flexible Structures. Fourth VPI&SU/AIAA Symposium on Dynamics and Control of Large Structures, Blacksburg, Virginia.
4. Joshi, Suresh M. (1983). A Modal Model for SCOLE Structural Dynamics. First Annual SCOLE Workshop. NASA Langley Research Center, Hampton, Virginia.
5. Balakrishnan, A. V. (1986). Functional Analysis of the SCOLE Problem. To be published.
6. Bishop, R. E. D. and D. C. Johnson (1960). The Mechanics of Vibration. Cambridge University Press. Cambridge
7. Naidu, D. S. and A. K. Rao (1985). Singular Perturbation Analysis of Discrete Control Systems. Lecture Notes in Mathematics. Springer-Verlag Berlin
8. Taylor, Lawrence W., Jr., William T. Suit and Marna H. Mayo (1984) A Program to Form a Multidisciplinary Data Base and Analysis for Dynamic Systems. AIAA Flight Mechanics Conference, Seattle, Washington. August 20-23, 1984.

N87-17828

Finite Element Model of SCOLE Laboratory Configuration

by

**Beth Lee
Jeffrey P. Williams
Dean Sparks
NASA Langley
Research Center**

REPORT - 1978

**FINITE ELEMENT MODEL OF SCOLE
LABORATORY CONFIGURATION**

Beth Lee

Jeffrey P. Williams

Dean Sparks, Jr.

NASA Langley Research Center

Mail Stop 161

Hampton, VA 23665

(804)-865-4591

MODEL DESCRIPTION

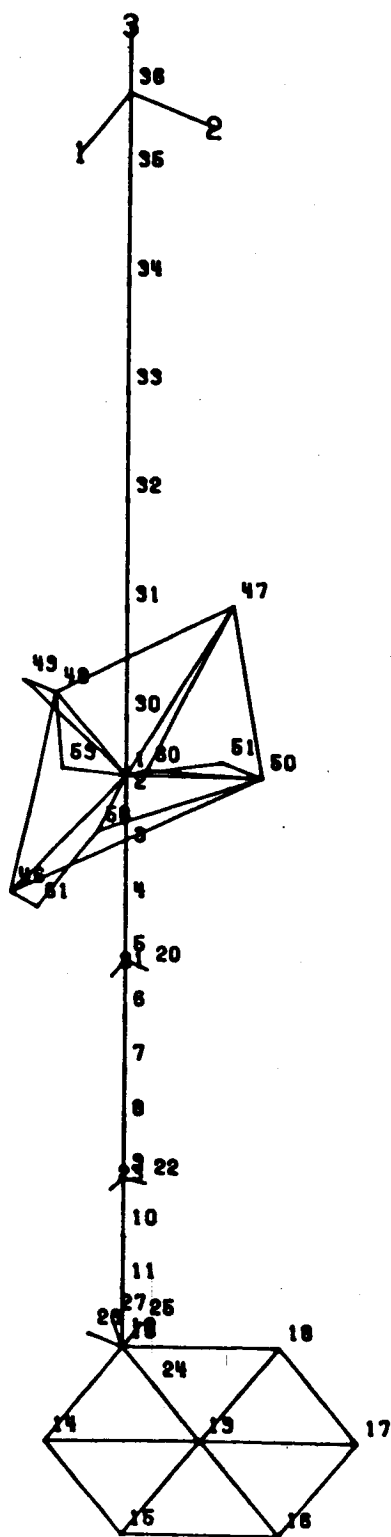
DEFINE ELEMENT PROPERTIES :

- MATERIAL CONSTANTS
MODULUS OF ELASTICITY,
POISSON'S RATIO,
DENSITY
- MAST, REFLECTOR, RIGID LINKS AS BEAM ELEMENTS
- CABLE AS BAR ELEMENT (AXIAL STIFFNESS ONLY)
- SHUTTLE AS VERY STIFF BEAM (ASSUME RIGID)

JOINT LOCATIONS AND CONNECTIONS :

- 44 JOINTS TOTAL, 7 FOR CABLE, 12 FOR MAST, 6 FOR REFLECTOR AND REST FOR RIGID MASSES

JOINT LOCATIONS



SCOLE

152

0 3
SCALE

MODEL DESCRIPTION (Continued)

TWO BOUNDARY CONDITIONS MODELLED:

**CASE 1—SUSPENDED (6 DOF FOR ALL JOINTS
EXCEPT TOP OF CABLE)**

**CASE 2— CANTILEVERED CABLE, SHUTTLE
PLATFORM FIXED IN ALL DOF**

INCLUDE RIGID MASSES AND CONNECTIONS :

- ACTUATORS
- SENSORS
- SHUTTLE PLATFORM AND COMPONENTS

CALCULATIONS :

- STIFFNESS AND MASS MATRICES
- INITIAL STRESSES (DUE TO GRAVITY
LOADING)
- STATIC DISPLACEMENTS AND REACTIONS
- EIGEN SOLUTIONS — FREQUENCIES AND
MODE SHAPES

FREQUENCY DATA FOR CANTILEVERED CASE (FIG 1,2)

MODE	FREQ (HZ)		DELTA-%	EAL/LAB RATIO
	EAL	LAB		
1	0.443	0.44	0.7	1.01
2	0.447	0.44	1.6	1.02
3	1.504	1.54	2.3	0.98
4	2.913	3.00	3.0	0.97
5	4.345	4.36	0.3	0.99
6	6.821	3.08	121.5	2.21

FREQUENCY DATA FOR SUSPENDED CASE (FIG 3,4)

MODE	FREQ (HZ)		DELTA-%	EAL/LAB RATIO
	EAL	LAB		
6	0.566	0.55	2.9	1.03
7	0.638	0.65	1.8	0.98
8	1.514	1.62	6.5	0.93
9	2.940	3.10	5.0	0.95

RATIO OF SUSPENDED TO CANTILEVERED FREQUENCIES (FIG 5,6)

MODE*	EAL	LAB
1	1.28	1.25
2	1.43	1.48
3	1.01	1.05
4	1.01	1.03

* NOTE: SUSPENDED MODES 6-9 CORRESPOND TO CANTILEVERED MODES 1-4

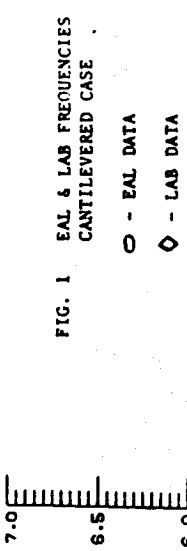


FIG. 2 RATIO OF EAL TO LAB FREQUENCIES
CANTILEVERED CASE

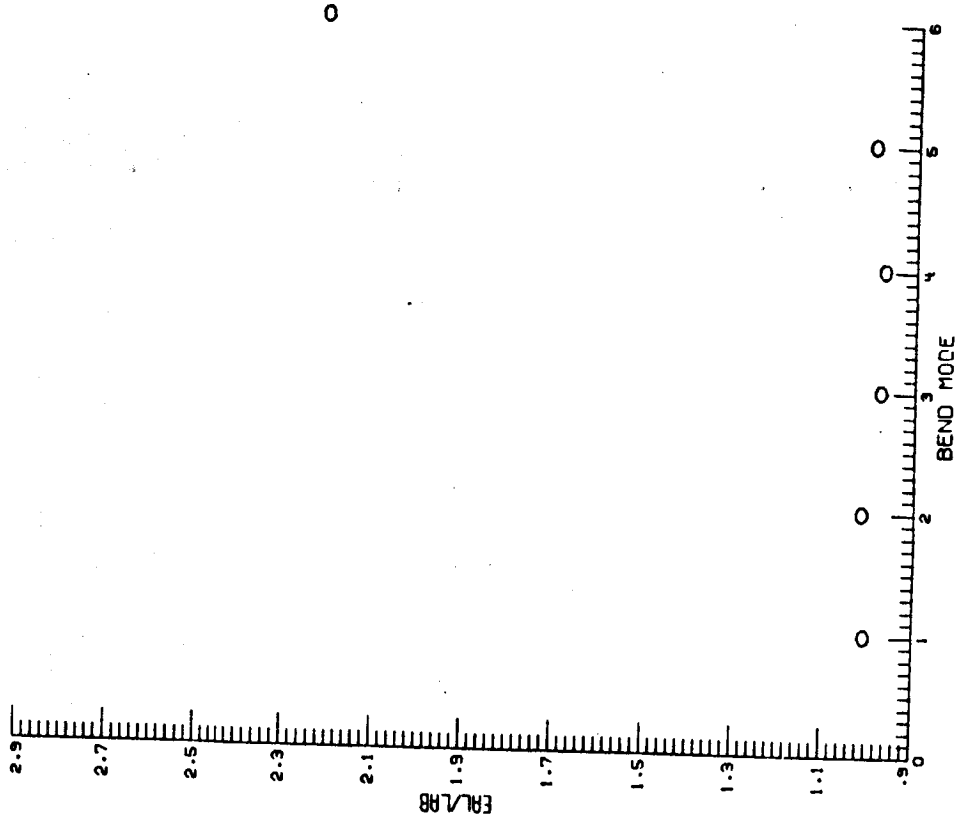


FIG. 3 EAL & LAB FREQUENCIES
SUSPENDED CASE

○ - EAL DATA
◊ - LAB DATA

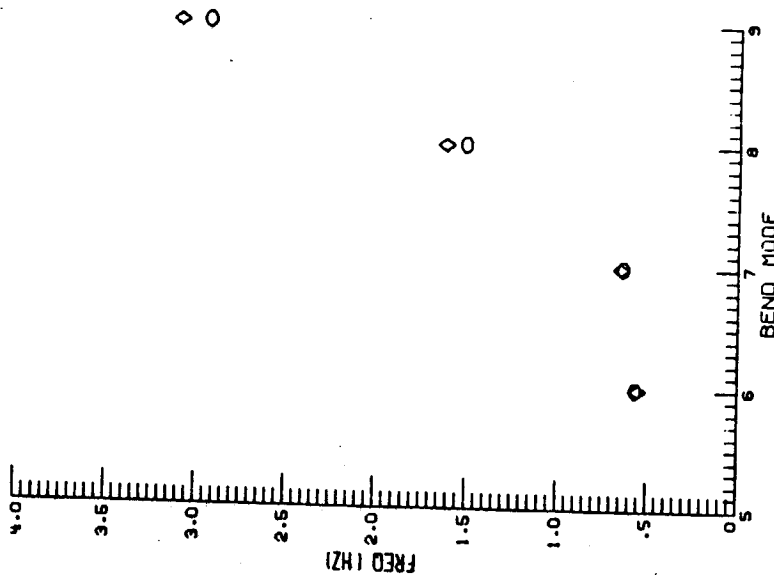
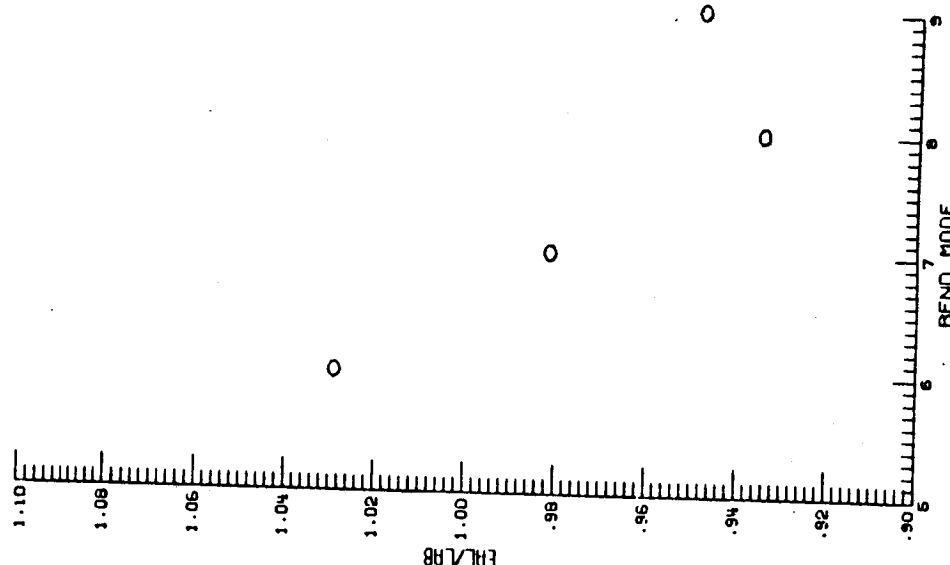


FIG. 4 RATIO OF EAL TO LAB FREQUENCIES
SUSPENDED CASE

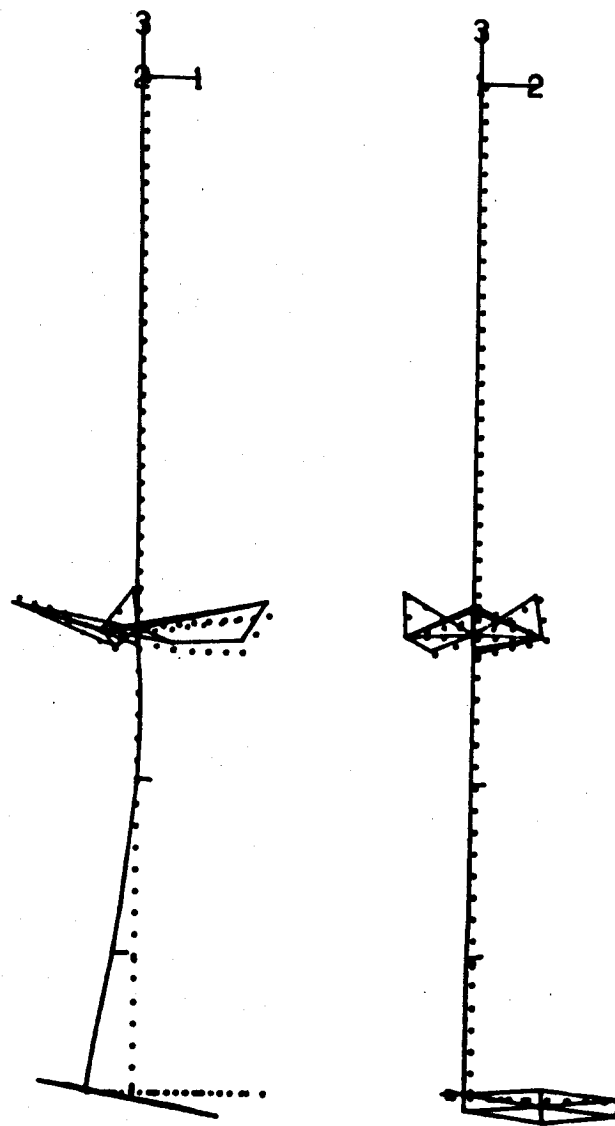
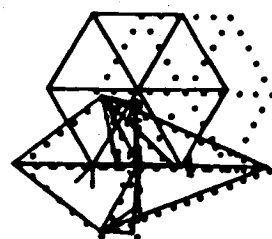


EAL PLOT 1st PITCH
SUSPENDED CASE

MODE. FREQ (HZ)

• 5657 X10 + 0 0

ID= 1 / 1 / 6



157

SCOPE VIBRATIONAL MODE SHAPE 6

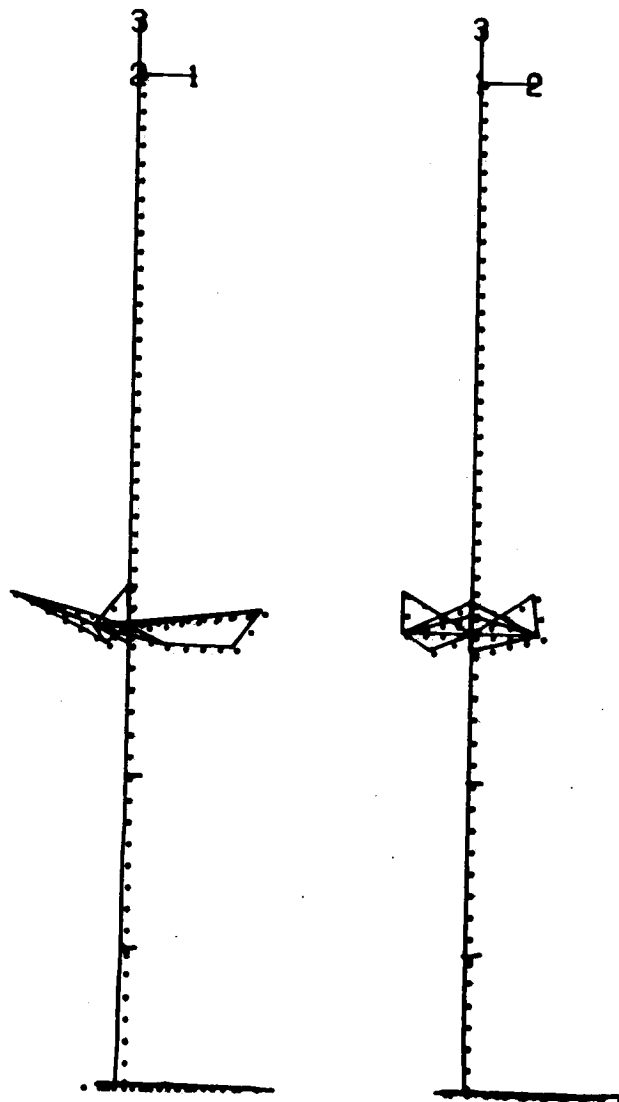
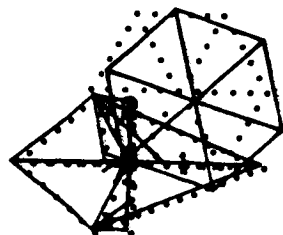
0
SCALE

EAL PLOT 1st TORSIONAL
SUSPENDED CASE

MODE. FREQ (HZ)

1513 X10 + 0 1

ID= 1 / 1 / 8



SCOPE VIBRATIONAL MODE SHAPE 8

158

0
SCAL F

FIG. 5 RATIO OF LAB FREQUENCIES
SUSPENDED/CANTILEVERED

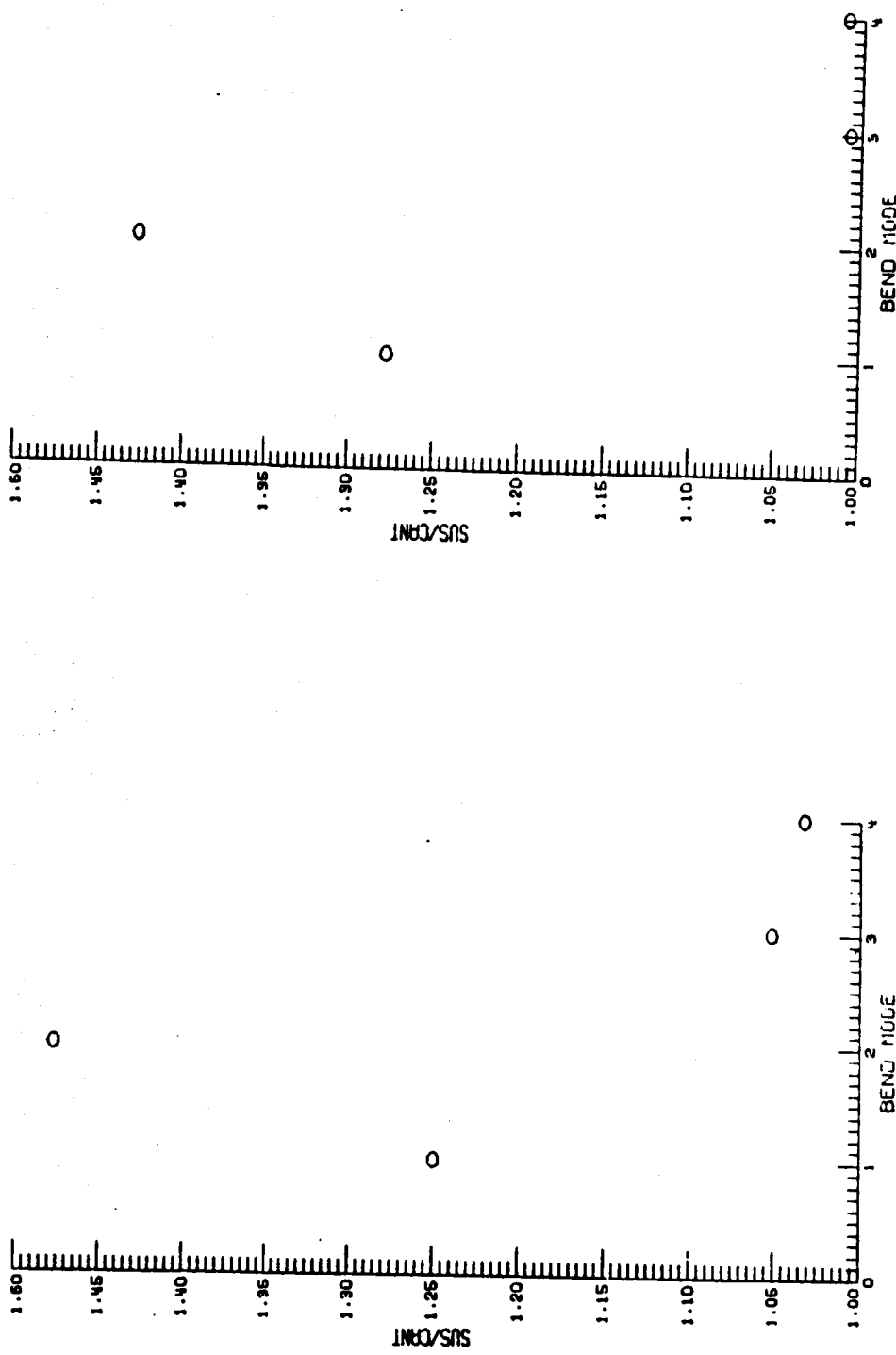


FIG. 6 RATIO OF EAL FREQUENCIES
SUSPENDED/CANTILEVERED

COMMENTS

- EAL, LAB DATA IN GOOD AGREEMENT
- HIGHER MODES TEND TO HAVE SLIGHTLY LARGER DIFFERENCES BETWEEN EAL & LAB RESULTS
- FOR HIGHER MODES, FREQUENCIES OF THE SUSPENDED AND CANTILEVERED CASES ARE SIMILAR; THE MODE SHAPES ARE ALSO CLOSE

CONCLUSIONS

- EAL, LAB FREQUENCY DATA MATCH WELL**
- NEED TO GET MORE ACCURATE MEASUREMENTS FROM LAB, AND WITH MORE MODES FOR BETTER COMPARISON COMPUTER MODEL & LAB**
- FOR HIGHER MODES, THE CANTILEVERED CONDITION MAY BE SUBSTITUTED FOR THE SUSPENDED, THUS REDUCING THE NUMBER OF NODES AND DOF'S IN COMPUTATION**

Model Reference Control of Distributed Parameter Systems: Application to the SCOLE Problem

by

H. Kaufman

D. Minnick

M. Balas

A. Musalem

**Rensselaer Polytechnic
Institute**

PRECEDING PAGE BLANK NOT FILMED

MODEL REFERENCE CONTROL
OF DISTRIBUTED PARAMETER SYSTEMS
WITH APPLICATION TO THE SCOLE PROBLEM

BY

H. KAUFMAN

D. MINNICK

M. BALAS

A. MUSALEM

ELECTRICAL, COMPUTER AND SYSTEMS ENGINEERING DEPARTMENT

RENSSELAER POLYTECHNIC INSTITUTE
TROY, NEW YORK 12180-3590

OUTLINE

- INTRODUCTION
- MODEL REFERENCE CONTROL OF LUMPED LINEAR SYSTEMS
 - THEORY
 - SCOPE APPLICATION
- MODEL REFERENCE CONTROL OF DPS
 - THEORY
 - SCOPE APPLICATION
- CONCLUSIONS AND RECOMMENDATIONS

INTRODUCTION

SCOLE MODELS

LUMPED: 16th ORDER WITH 5 FLEXIBLE AND 3 RIGID BODY MODES

DISTRIBUTED: 3 PARTIAL DIFFERENTIAL EQUATIONS FOR ROLL,
PITCH, YAW BEAM BENDING

LUMPED MODEL

$$\dot{x} = Ax + Bu$$

$$y = Cx$$

$$x^T = (\underline{u}_1^T, \dots, \underline{u}_8^T, \underline{\phi}_{RB}^T, \underline{\theta}_{RB}^T, \underline{\psi}_{RB}^T)$$

$$y_F^T = (\underline{\phi}_s^T, \underline{\theta}_s^T, \underline{\psi}_s^T, \underline{\phi}_r^T, \underline{\theta}_r^T, \underline{\psi}_r^T, \zeta_x, \zeta_y)$$

$$y^T = y_F^T + (\underline{\phi}_{RB}^T, \underline{\theta}_{RB}^T, \underline{\psi}_{RB}^T, \underline{\phi}_{RB}^T, \underline{\theta}_{RB}^T, \underline{\psi}_{RB}^T, 0, 0)$$

$$\underline{u}^T = (\underline{I}_s, \underline{f}_r, \underline{I}_r)$$

OBJECTIVE: IF $\phi_{RB}(0) = 20^\circ$

$\phi_{RB} \rightarrow 0$ IN ABOUT 10 SEC.

$|T| \leq 10,000$

$|f| \leq 800$

DISTRIBUTED MODEL

ROLL BEAM BENDING:

$$PA \frac{\partial^2 u_\phi}{\partial t^2} + 2\zeta_\phi \sqrt{PA} EI_\phi \frac{\partial^3 u_\phi}{\partial s^2 \partial t} + EI_\phi \frac{\partial^4 u_\phi}{\partial s^4} = \sum_{n=1}^4 [f_{\phi,n} \delta(s-s_n) + g_{\phi,n} \frac{\partial \delta}{\partial s}(s-s_n)]$$

PITCH BEAM BENDING:

$$PA \frac{\partial^2 u_\theta}{\partial t^2} + 2\zeta_\theta \sqrt{PA} EI_\theta \frac{\partial^3 u_\theta}{\partial s^2 \partial t} + EI_\theta \frac{\partial^4 u_\theta}{\partial s^4} = \sum_{n=1}^4 [f_{\theta,n} \delta(s-s_n) + g_{\theta,n} \frac{\partial \delta}{\partial s}(s-s_n)]$$

YAW BEAM TORSION:

$$PI_\psi \frac{\partial^2 u_\psi}{\partial t^2} + 2\zeta_\psi I_\psi \sqrt{GP} \frac{\partial^3 u_\psi}{\partial s^2 \partial t} + GI_\psi \frac{\partial^4 u_\psi}{\partial s^4} = \sum_{n=1}^4 [g_{\psi,n} \frac{\partial \delta}{\partial s}(s-s_n)]$$

MODEL REFERENCE CONTROL OF LUMPED LINEAR SYSTEMS

THEORY

$$\left. \begin{array}{l} \dot{x}_p = A_p x_p + B_p u_p \\ y_p = C_p x_p \end{array} \right\} \text{PROCESS}$$

$$\left. \begin{array}{l} \dot{x}_m = A_m x_m + B_m u_m \\ y_m = C_m x_m \end{array} \right\} \text{REFERENCE MODEL}$$

DESIRE

$$y_p \rightarrow y_m$$

DEFINE IDEAL STATE AND CONTROL

$$\dot{x}_p^* = A_p x_p^* + B_p u_p^*$$

$$y_p^* = C_p x_p^*$$

$$\text{WHERE } y_p^* = C_m x_m = y_m$$

WILL FORCE $x_p \rightarrow x_p^*$

$$\Rightarrow y_p \rightarrow y_p^* = y_m$$

ASSUME

$$x_p^* = s_{11} x_M + s_{12} u_M$$

$$u_p^* = s_{21} x_M + s_{22} u_M$$

THEN

$$s_{11} A_M - A_p s_{11} = B_p s_{21}$$

$$s_{11} B_M - A_p s_{12} = B_p s_{22}$$

$$C_p s_{11} = C_M$$

$$C_p s_{12} = 0$$

APPLY

$$u_p = u_p^* + K(y_m - y_p)$$

THEN

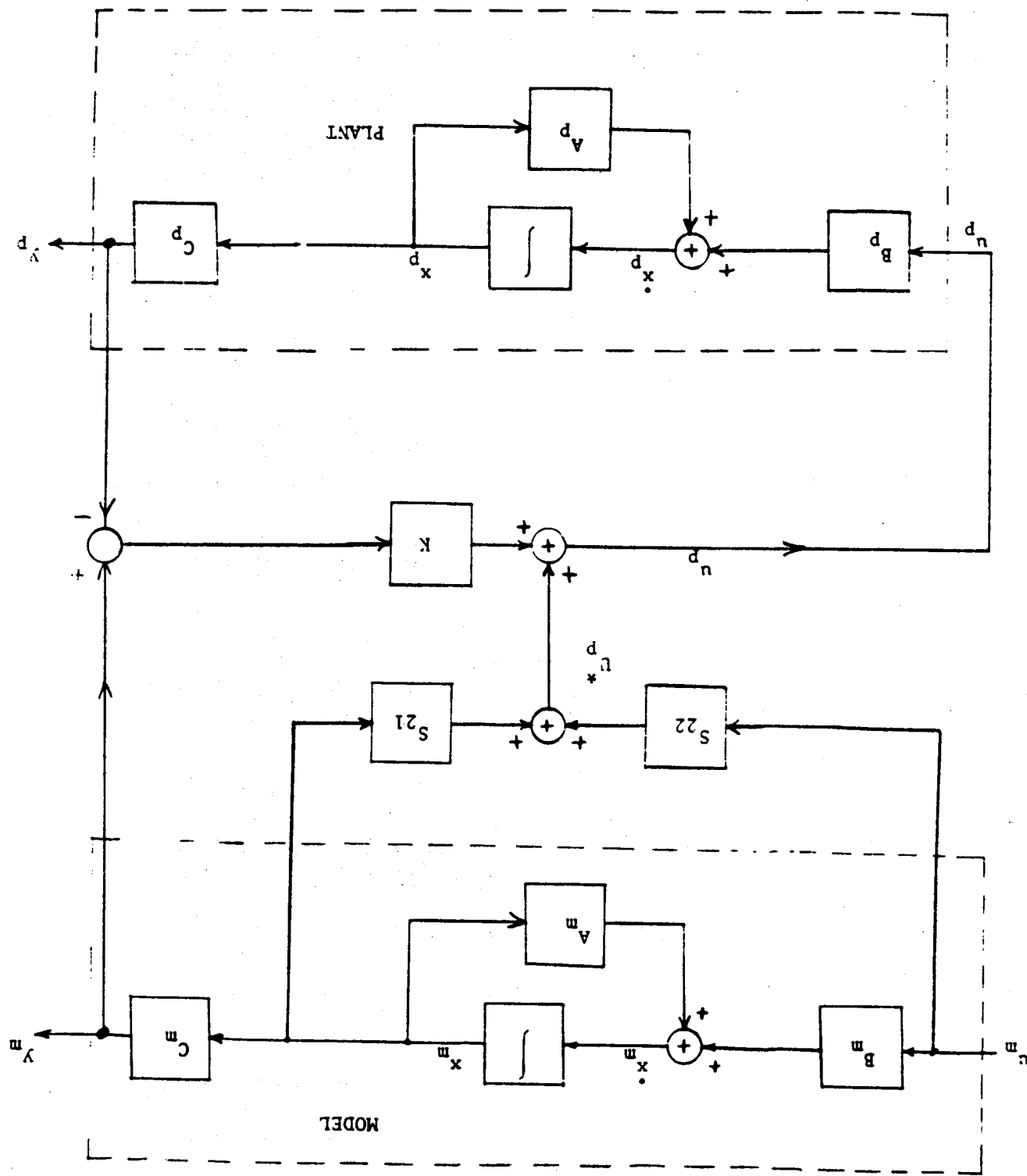
$$\dot{e} = (A_p - B_p K C_p)e$$

WHERE

$$e = x_p^* - x_p$$

∴ CHOOSE K TO STABILIZE $(A_p - B_p K C_p)$

Figure 1: System block diagram.



SPECIAL CASE (PMF)

$$x_p \rightarrow x_m$$

$$\text{OR } C_p = C_m = 1$$

$$u_p = S_{21} x_m + S_{22} u_m + K(x_m - x_p)$$

$$B_p S_{21} = A_m - A_p$$

$$B_m = B_p S_{22}$$

$$(A_p - B_p K) \text{ STABLE}$$

SCOPE APPLICATION OF LUMPED MODEL FOLLOWING

OBSERVATIONS

- EIGHT CONTROLS
- EIGHT OUTPUT MODES TO BE CONTROLLED

PROCEDURES

- PMF
 $x_p \rightarrow x_m$
- OUTPUT FOLLOWING
 $y_p \rightarrow y_m$

SPECIAL CASES: 8 outputs

CASE I: Consider only positions:

$$Y_P^T = \left[\theta_S + \theta_{RB}, \theta_S + \theta_{RB}, \psi_S + \psi_{RB}, \xi_X, \xi_Y, \theta_r + \theta_{RB}, \theta_r + \theta_{RB}, \psi_r + \psi_{RB} \right]^T$$

CASE II: Position and LOS Vectors

$$Y_P^T = \left[\theta_S + \theta_{RB}, \theta_S + \theta_{RB}, \psi_S + \psi_{RB}, \xi_X, \xi_Y, E_1, E_2, E_3 \right]^T$$

E_1, E_2, E_3 - LOS VECTOR COMPONENTS

Note: $R_{LOS} = (R_{LOS})_{NOM} + \Delta$, where $\Delta = \begin{bmatrix} E_1 \\ E_2 \\ E_3 \end{bmatrix}$

$$E_1 = -130 \theta_{RB} - 32.2 \psi_{RB} + \xi_X - 32.2 \psi_r - 260 \theta_r$$

$$E_2 = 130 \theta_{RB} + 18.75 \psi_{RB} + \xi_Y + 18.75 \psi_r - 260 \theta_r$$

$$E_3 = -18.75 \theta_{RB} + 32.2 \psi_{RB} - 18.75 \theta_r - 32.2 \theta_r$$

INITIAL CONDITIONS

Two sets of I.C.'s for each case

CASE I (a):

Choose θ_{RBi} , θ_{RBF} , θ_{RBi} , θ_{RBF} so that $\epsilon_{LOS}(0) = 20^\circ$, $\epsilon_{LOS}(t_f) = 0^\circ$

$$\Rightarrow \theta_{RBi} = 0.1063 \text{ rad} ; \theta_{RBF} = -0.245 \text{ rad}$$

$$\theta_{RBi} = -0.1115 \text{ rad} ; \theta_{RBF} = -0.1115$$

$$t_f = 10 \text{ sec.}$$

$$\Rightarrow Y_0^T = [0.0163 , -0.1115 , 0 , 0 , 0 , 0.1063 , -0.1115 , 0] \text{ T}$$

STATE I.C.'S:

$$Y_p(0) = C_p X_p(0) \text{ ---- Solve for } X_p(0)$$

Model I.C.'S

$$Y_p \rightarrow Y_m , Y_p(0) = Y_m(0)$$

$$\Rightarrow X_{m1}^T = [0.1063 , -0.1115 , 0 , 0] \text{ T}$$

COMMAND

$$H(i, \alpha) = 1.0 , T \rightarrow 0. i = 1, 2, \dots, 8$$

I.C.'s (cont.)

CASE I (b):

$$\theta_{RB} = 0.34 \text{ rad} = 20^\circ$$

$$\psi_{RB} = \theta_{RB} = 0.0$$

$$\Rightarrow y_p^T(0) = [0.34, 0, 0, 0, 0, 0.34, 0, 0]^T$$

Model:

$$x_m^T = [0.34, 0, 0, 0]^T$$

COMMAND:

$$U_{m_i}(0) = 0.0, T \geq 0, i = 1, \dots, 8$$

I. C."s (cont.)

CASE II (a): Same objective as in CASE I (a)

$$Y_P^T(0) = [0.1063, -0.1115, 0, 0, 14.49, 13.82, 5.51]^T$$

$$X_M^T(0) = [0.1063, -0.1115, 0, 0, 1]$$

$$\Rightarrow Y_M(0) = Y_P(0)$$

$$U_{m_i} = 1.0, i \geq 0, i = 1, \dots, 8$$

CASE II (b): Same objective as in CASE I (b)

$$Y_P^T(0) = [0.34, 0, 0, 0, 44.2, 10.948]^T$$

$$X_M^T = [0.34, 0, 0, 0, 1]^T$$

MODEL

In both cases: 4 states

$$\dot{X}_M = A_M X_M + B_M U_M$$

$$A_M = \text{DIAG } [A_1 \ A_2 \ A_3 \ A_4] = [-.15, -0.10, -0.10, -0.10]^T$$

$$Y_M^T = [Y_{M1} \ Y_{M2} \ \dots \ Y_{M8}]^T$$

CASE I (a, b):

$$C_M = \begin{bmatrix} 1 & 0 & 0 & 0 \\ 0 & 1 & 0 & 0 \\ 0 & 0 & 1 & 0 \\ 0 & 0 & 0 & 1 \end{bmatrix}$$

CASE II (a, b):

$$C_M = \begin{bmatrix} 1 & 0 & 0 & 0 \\ 0 & 1 & 0 & 0 \\ 0 & 0 & 1 & 0 \\ 0 & 0 & 0 & 1 \end{bmatrix}$$

Matrix BM:

Cases I (a), II (a):

$$B_M = \begin{bmatrix} -3.67 \times 10^{-2} & 0 & 0 & 0 & 0 & 0 \\ 0 & -1.115 \times 10^{-2} & 0 & 0 & 0 & 0 \\ 0 & 0 & 0 & 0 & 0 & 0 \\ 0 & 0 & 0 & 0 & 0 & 0 \\ 0 & 0 & 0 & 0 & 0 & 0 \end{bmatrix}$$

Cases II (b), II (b):

$$B_M = \{0\}$$

SYSTEM I.C.'S: RESULTS

CASE I (a):

$$y_p^T(0) = y_m^T(0) = [0.1063 \ -0.1115, 0, 0, 0, 0.1063, -0.1115, 0]^T$$

$$x_p^T(0) = [0, 0, 0, 0, 0, 0, 0, 0, 0.1063, 0, -0.1115, 0, 0, 0]^T$$

$$x_p^{*T}(0) = [0, -0, 0, 0, 0, 0, 0, 0, 0.1063, -0.05269, -0.1115, 0, 0, 0]^T$$

CASE I (b):

$$y_p^T(0) = y_m^T(0) = [0.34, 0, 0, 0, 0.34, 0, 0]^T$$

$$x_p^T(0) = [0, 0, 0, 0, 0, 0, 0, 0, 0.34, 0, 0, 0, 0, 0]^T$$

$$x_p^{*T}(0) = [0, 0, 0, 0, 0, 0, 0, 0, 0.34, -0.051, 0, 0, 0, 0]^T$$

CASE II (a):

$$Y^T(o) Y^T_M(o) = [0.1063, -0.1115, 0, 0, 0, 14.49, 13.82, 5.51]^T$$

$$x_1^T(0) = [0.118, 0, -0.0186, 0, -0.1087, 0, -0.0042, 0, -0.022, 0, 0.1063, 0; -0.1115, 0, 0]^T$$

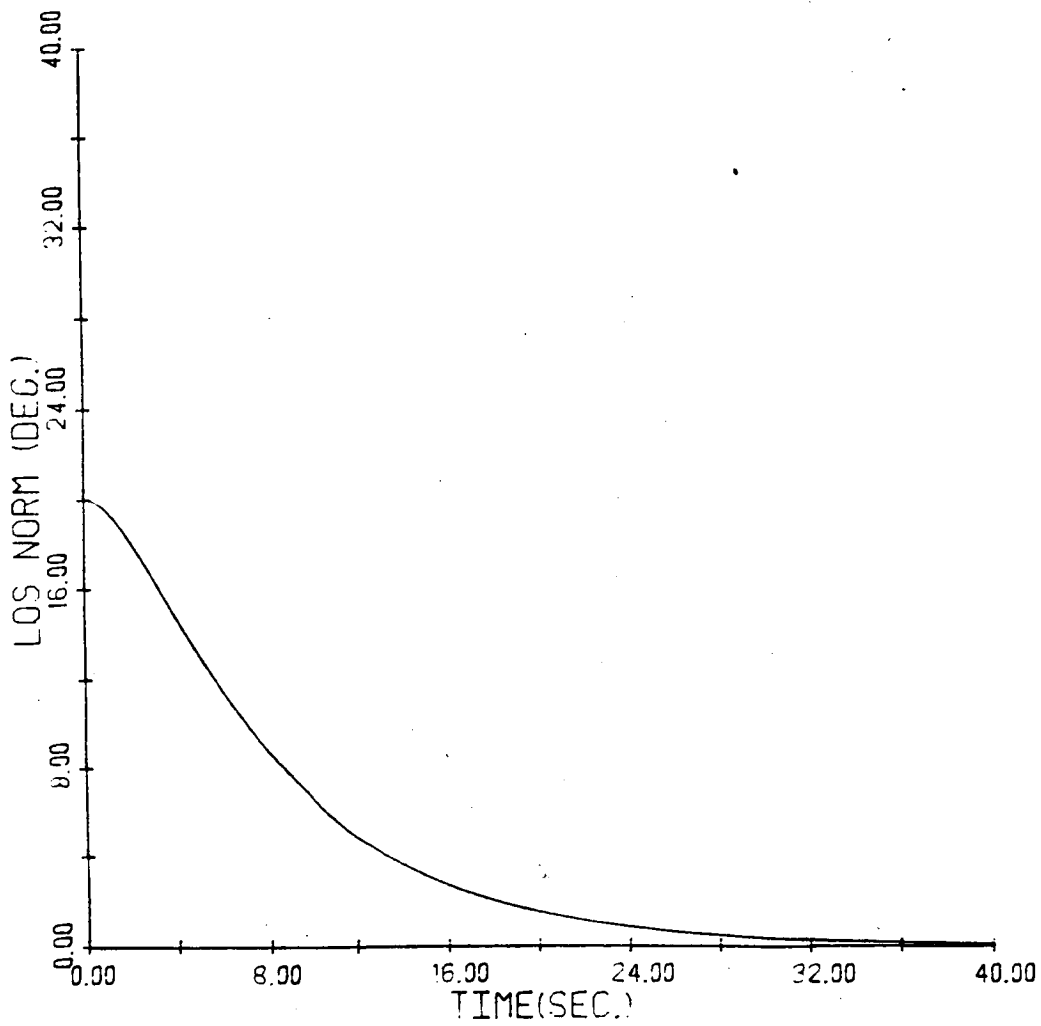
CASE II (b):

$$Y_P^T(0) = Y_M^T(0) = [0.34, 0, 0, 0, 0, 0, 0, 0, 0, 0, 0, 0]^T$$

$$x_p^* (0) = [0, 0, 0, 0, 0, 0, 0, 0, 0, 0, 0, 0, 0, 0]^T$$

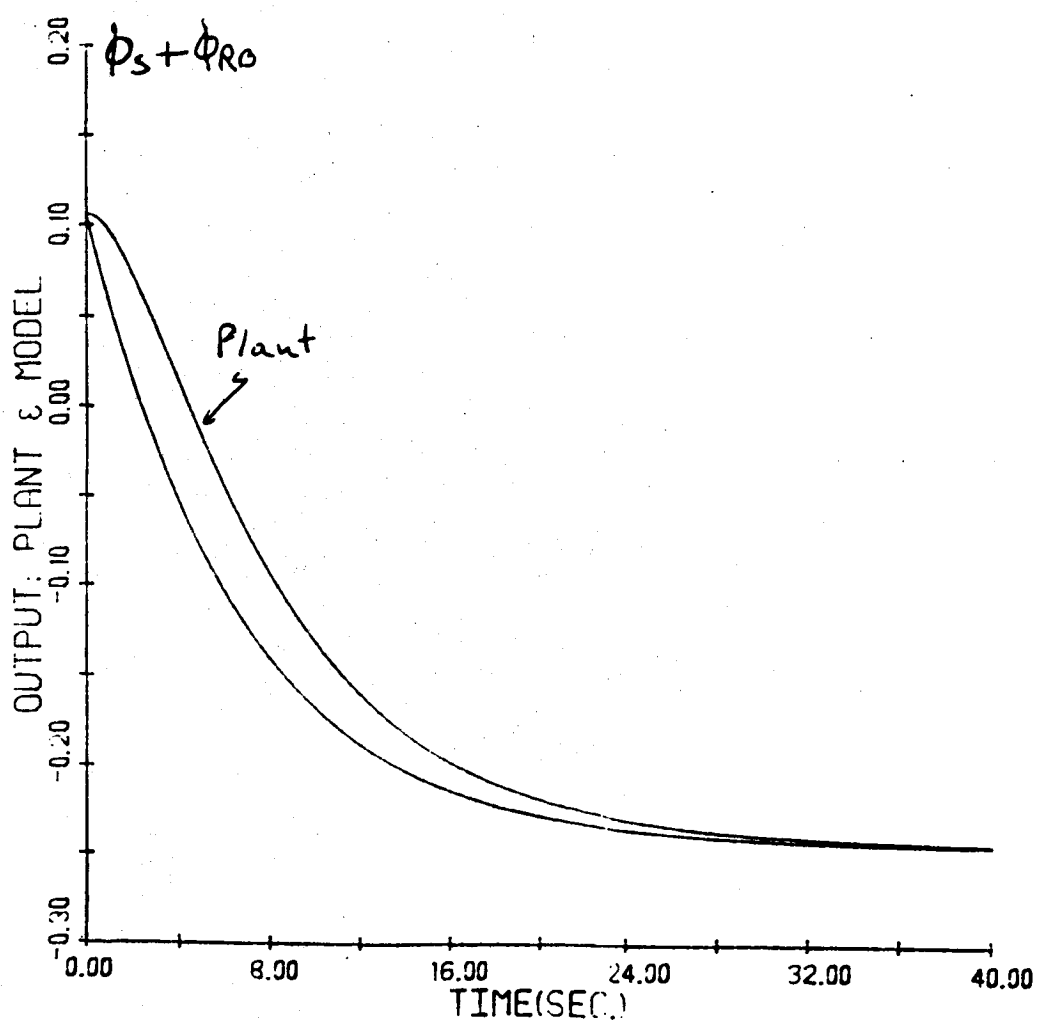
LOS ERROR : CASE II(a)

$$\epsilon_{\text{LOS}} = \sin^{-1} \left[\frac{\|\mathbf{B}_r \times \mathbf{T}_i \bar{\mathbf{R}}_{\text{LOS}}\|}{\|\bar{\mathbf{R}}_{\text{LOS}}\|} \right]$$

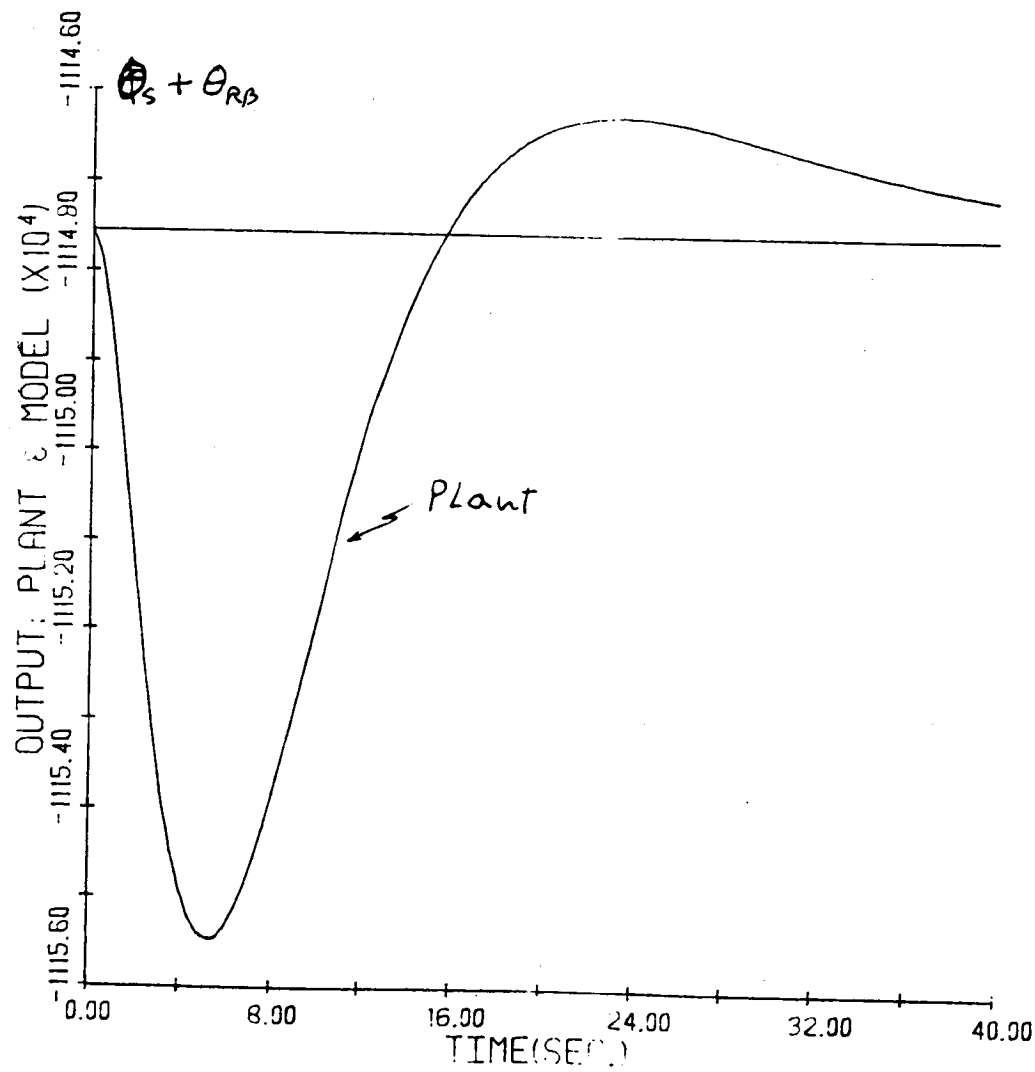


OUTPUT : PLANT and Model

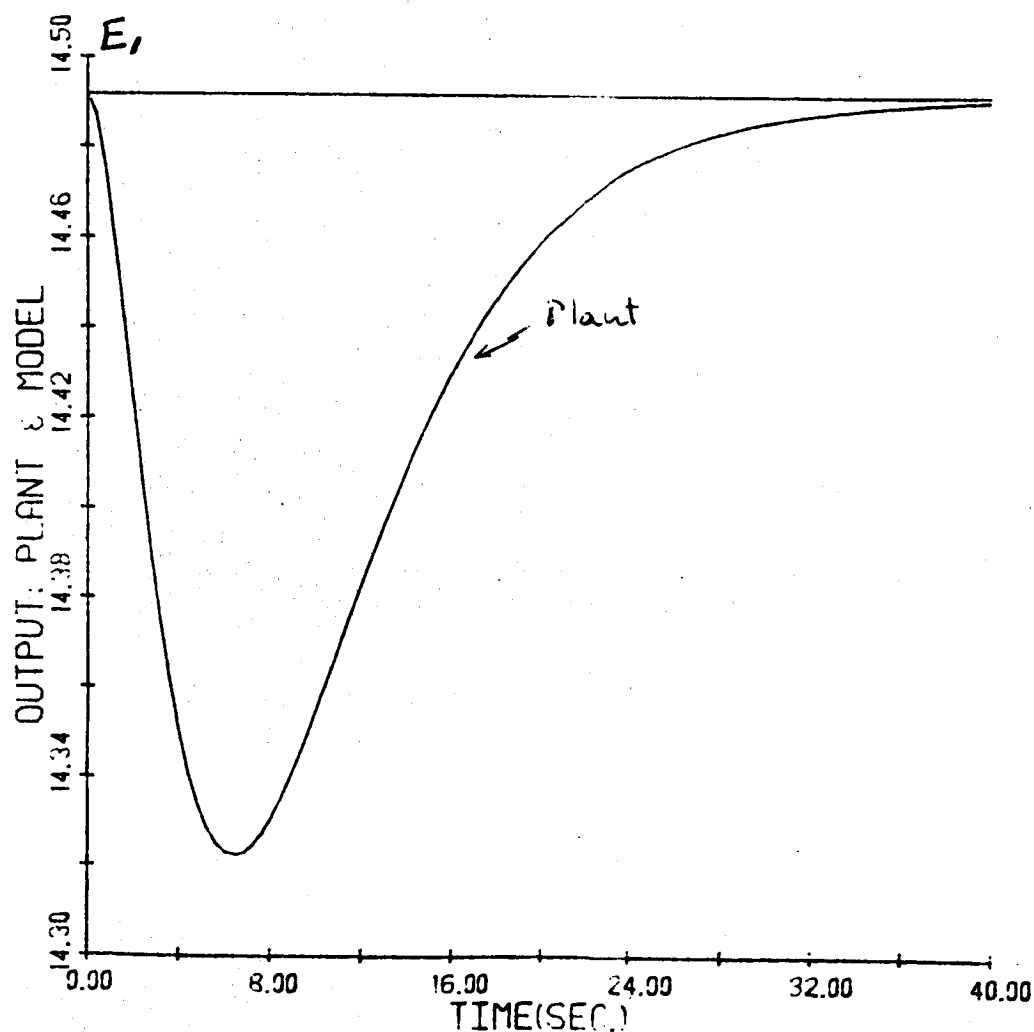
Case II (a)



OUTPUT: PLANT and Model
Case II (a)



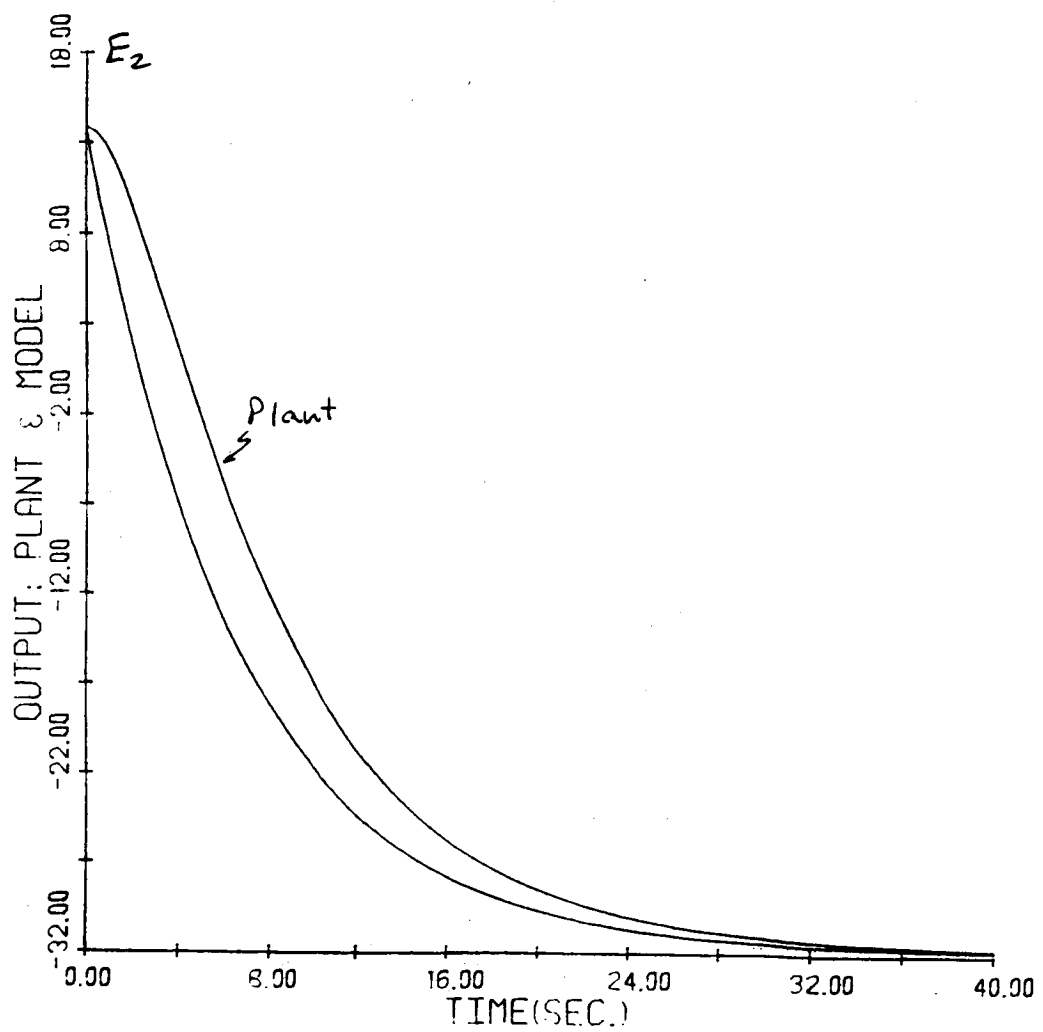
OUTPUT: PLANT and Model
CASE II(a): 1st Component of LOS



C-3

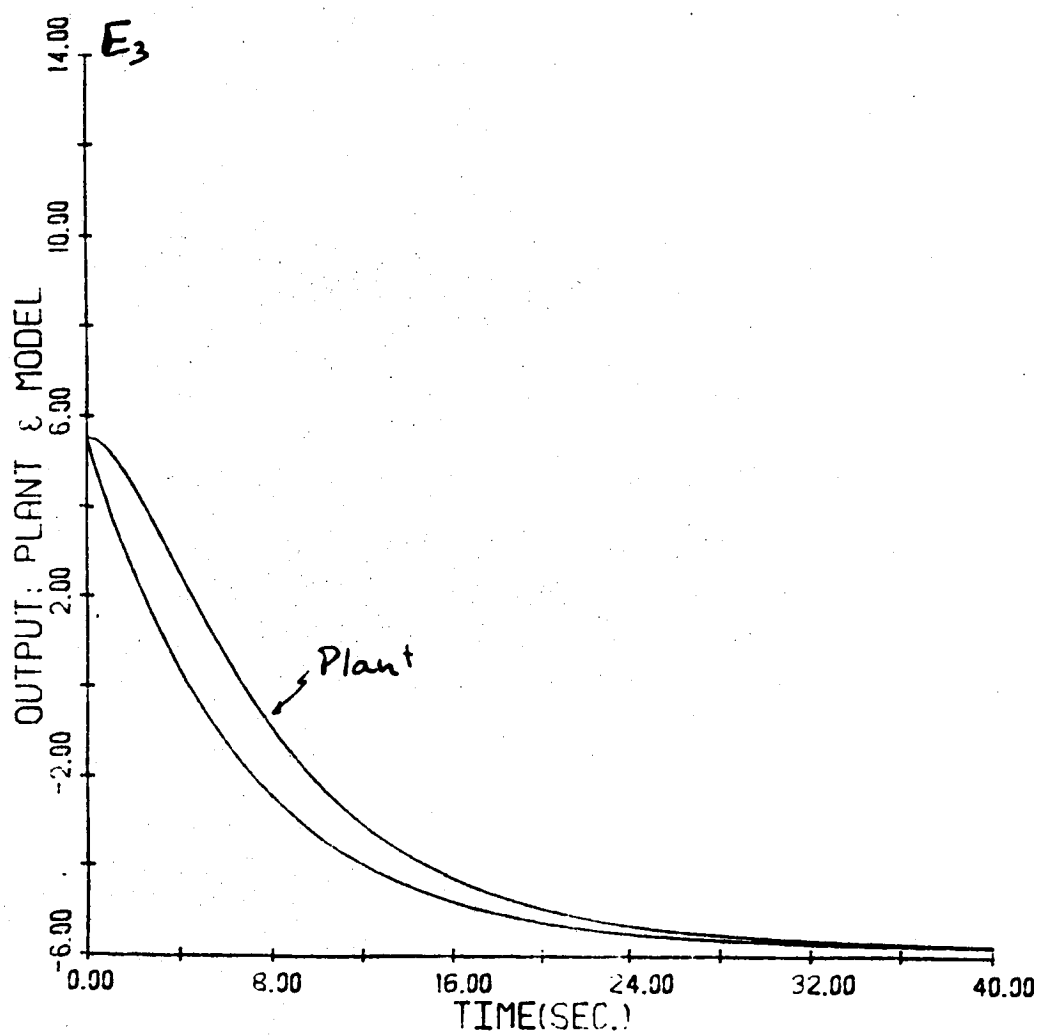
187

OUTPUT : PLANT and Model
CASE II(a) : 2nd Component of LOS

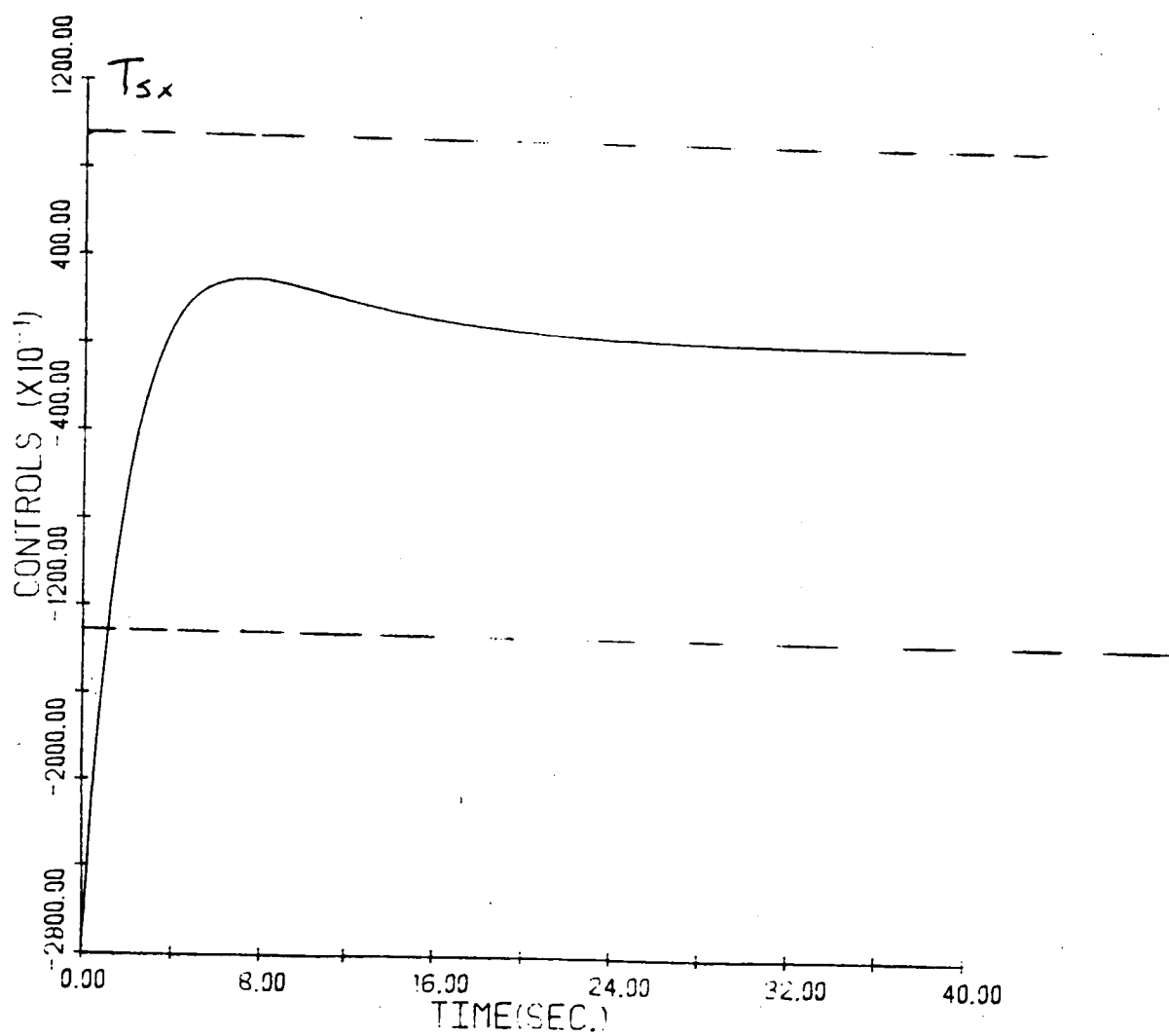


OUTPUT : PLANT and Model

CASE II(a) : 3rd Component of LOS

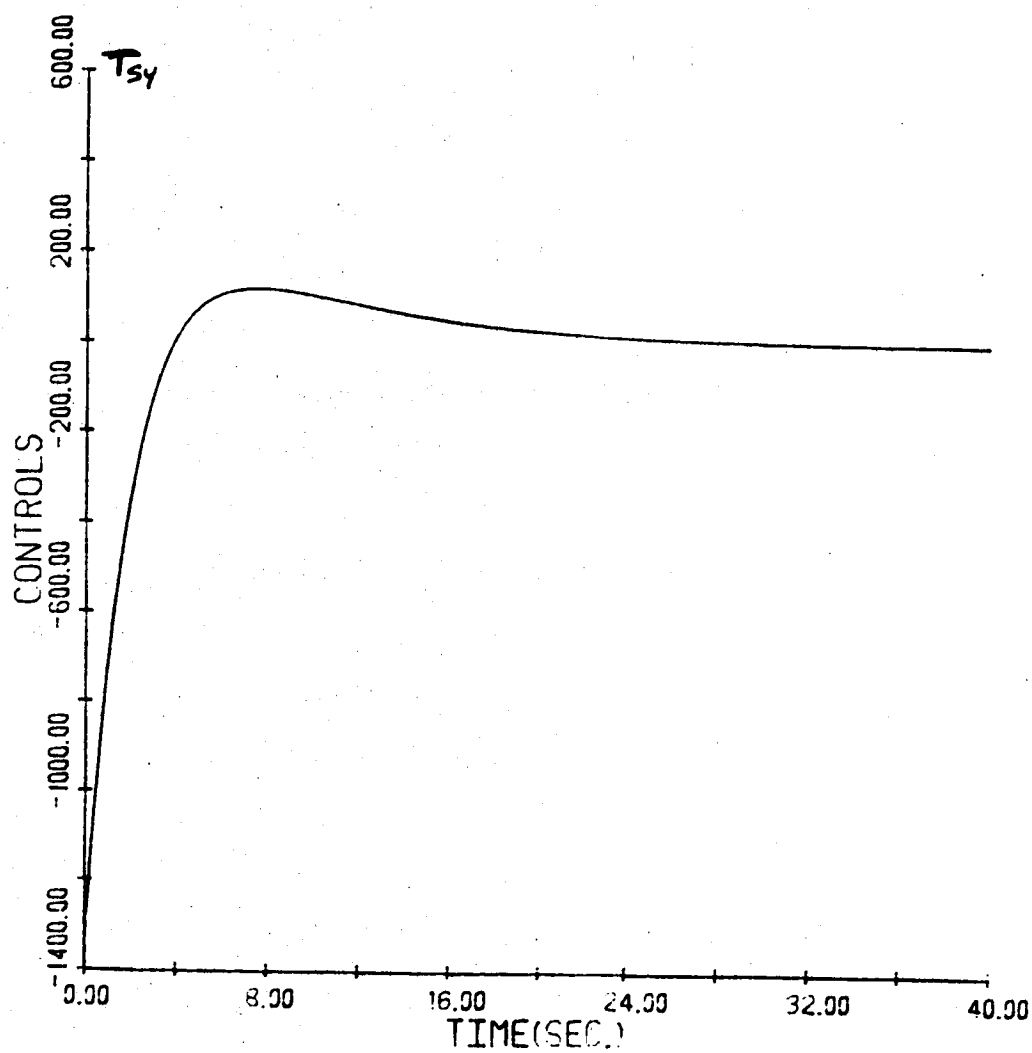


CONTROL : CASA II(a)

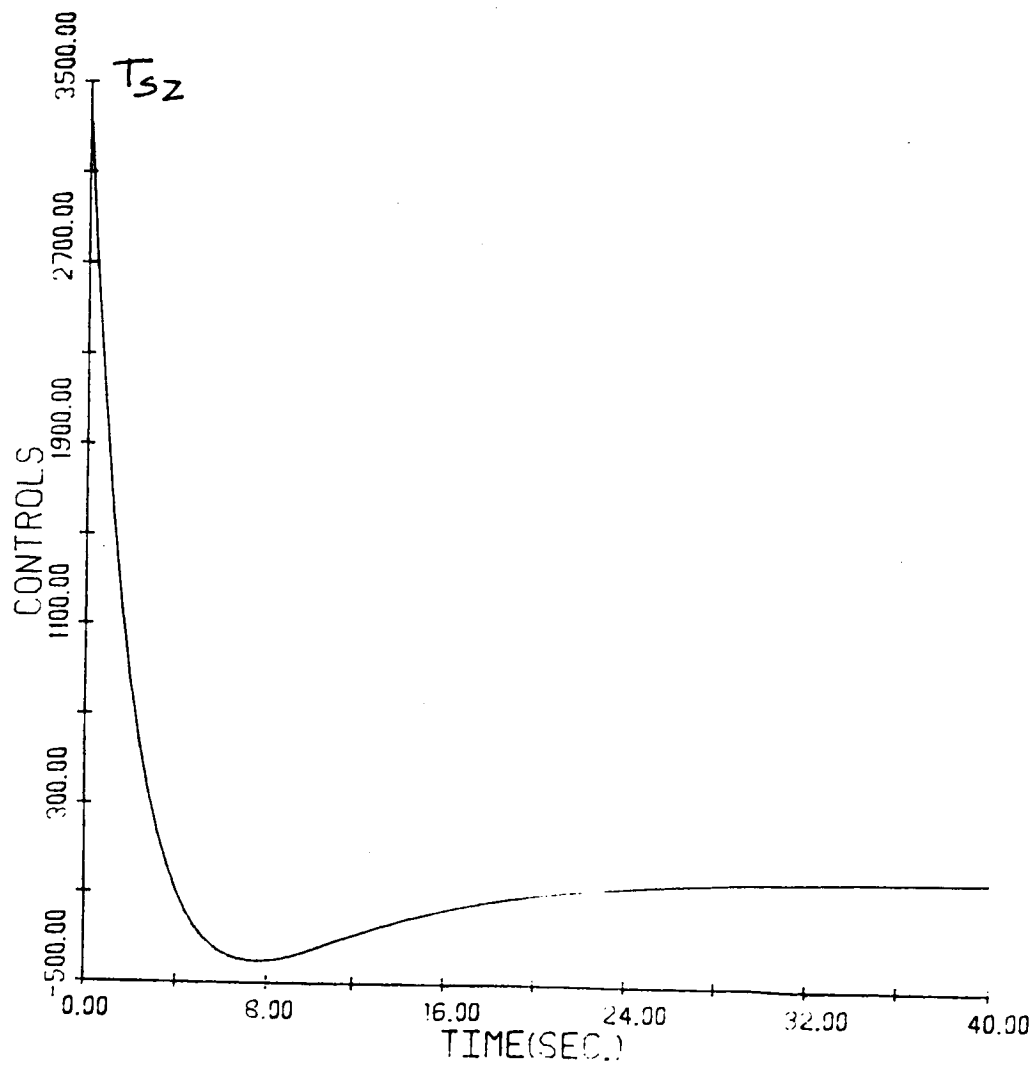


190

CONTROL : CONTROL : CASE II(a)



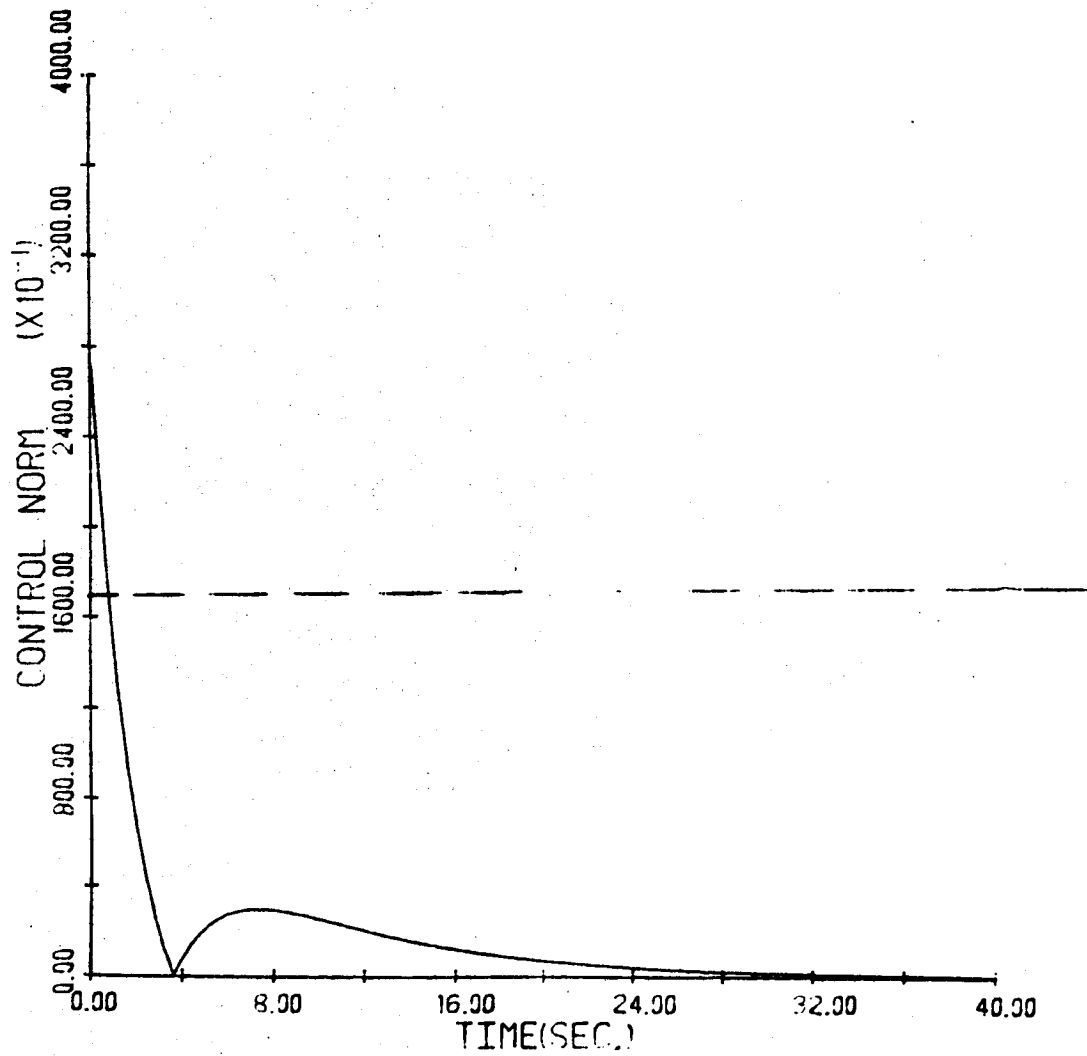
CONTROL: CASE II (a)



192

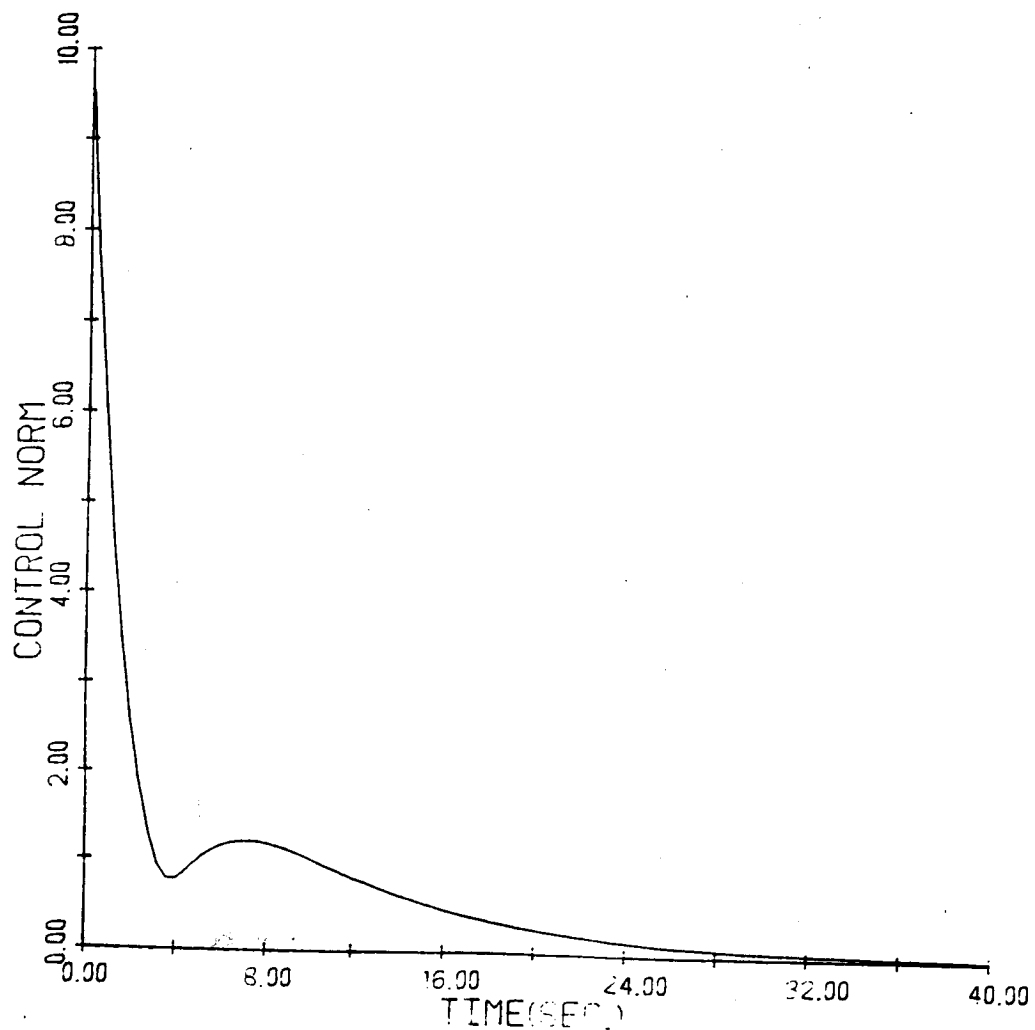
NORM OF MOMENTS AT SHUTTLE : CASE II(a)

$$= (T_{Sx}^2 + T_{Sy}^2 + T_{Sz}^2)^{1/2}$$



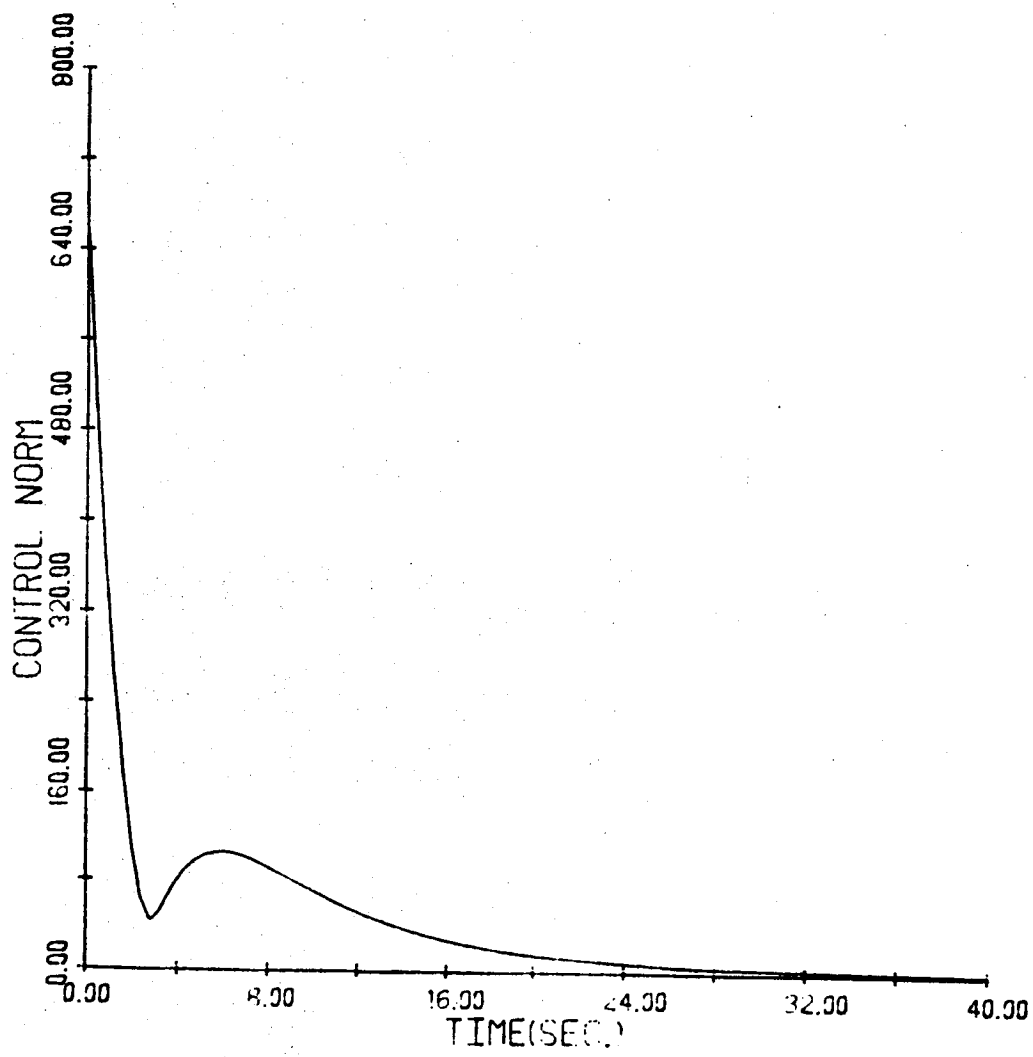
NORM of FORCES AT REFLECTOR : CASE II(2)

$$= (f_{nx}^2 + f_{ny}^2)^{1/2}$$

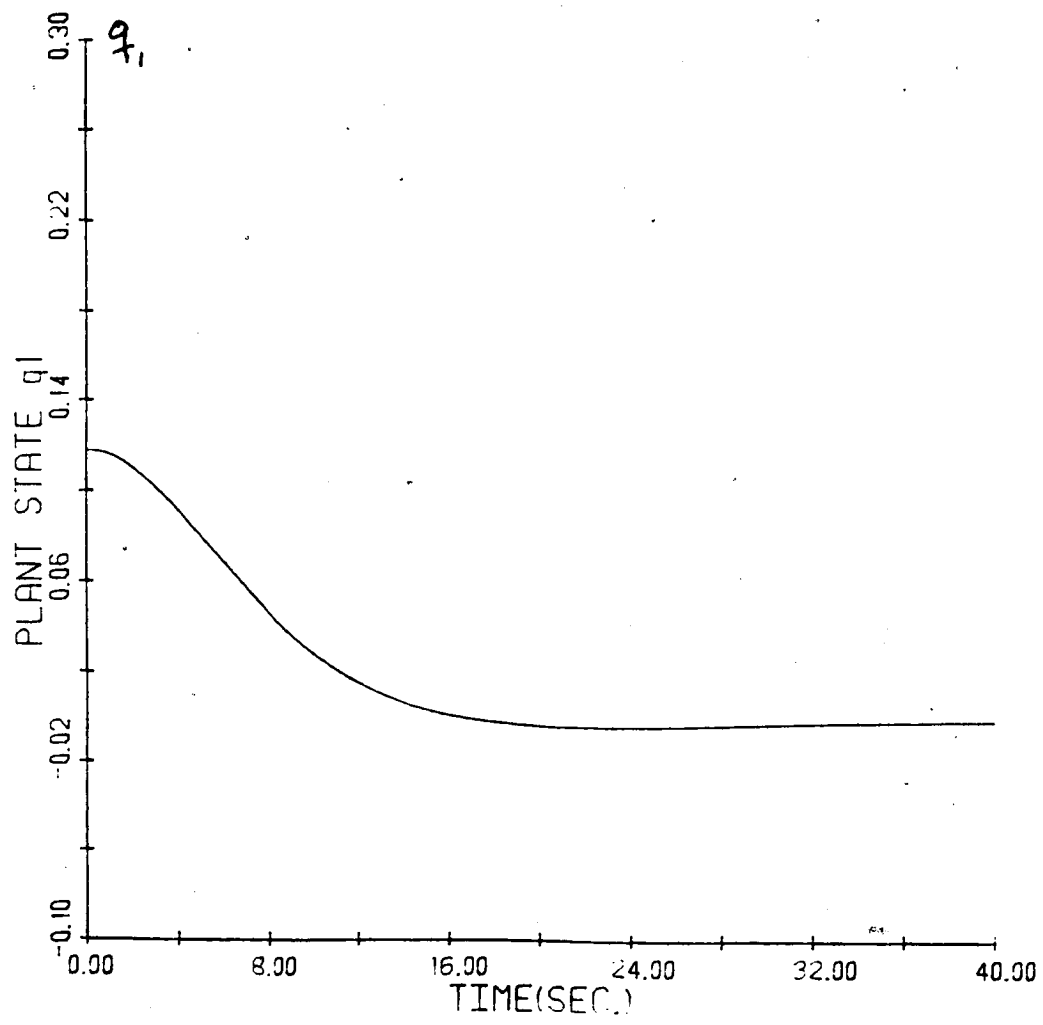


NORM OF MOMENTS AT REFLECTOR: CASE II(a)

$$= (T_{rx}^2 + T_{ry}^2 + T_{rz}^2)^{1/2}$$



PLANT STATE : CASE II(a)



196

MODEL REFERENCE CONTROL OF DISTRIBUTED SYSTEMS

$$m(x)u_{tt}(x,t) + D_0u_t(x,t) + A_0u(x,t) = f(x,t)$$

$$v_1 = u(x,t)$$

$$\text{BC} \quad v_1'''(0) = v_1'''(L) = 0$$

$$v_2 = \frac{\partial}{\partial t} u(x,t)$$

$$\text{and } v_2'''(0) = v_2'''(L) = 0$$

$$\dot{\underline{y}} = \underline{Ay} + \underline{B}f(x,t)$$

$$A = \begin{bmatrix} 0 & 1 \\ -A_0 & -D_0 \\ \hline \overline{m(x)} & \overline{m(x)} \end{bmatrix}$$

$$B = \begin{bmatrix} 0 \\ \hline \frac{1}{\overline{m(x)}} \end{bmatrix}$$

$$y = Cv$$

CONTROL PROBLEM FORMULATION

GIVEN THE DPS, IT IS DESIRED TO FIND A FINITE DIMENSIONAL CONTROLLER

SO THAT THE OUTPUT $y(t)$ "FOLLOWS" A DESIRABLE OUTPUT TRAJECTORY $y_m(t)$.

$$\dot{q} = A_m q + B_m u_m$$

$$y_m = C_m q$$

SOLUTION TO DPS MRC PROBLEM

DEFINE IDEAL STATE AND CONTROL v^* , f^*

$$\frac{\partial v^*(t)}{\partial t} = A v^*(t) + B f^*(t)$$

$$y^*(t) = C v^*(t)$$

$$y^*(t) = y_m(t) = C_m q(t)$$

$$v^*(t) = S_{11}(x) q(t) + S_{12}(x) u_m(t)$$

$$f^*(t) = S_{21} q(t) + S_{22} u_m(t)$$

$$y^*(t) = C S_{11} q + C S_{12} u_m = y_m = C_m q$$

$$S_{11}(x) A_m = A S_{11}(x) + B S_{21}$$

$$S_{11} B_m = A S_{12}(x) + B S_{22}$$

$$C S_{11} = C_m$$

$$C S_{12} = 0$$

$$\dot{e} = \dot{v}^* - \dot{v} =$$

$$Av^* + Bf^* - Av - Bf =$$

$$Ae + B(f^* - f)$$

THIS EQUATION SUGGESTS THAT THE ACTUAL MODEL FOLLOWING

CONTROL (f) BE DEFINED AS:

$$\begin{aligned}f &= f^* + G(y_m - y) \\&= f^* + G(C q_m - Cv) \\&= f^* + G C (v^* - v) \\&= f^* + G C e\end{aligned}$$

SUBSTITUTION OF (3.14) INTO (3.13) GIVES:

$$\dot{e} = (A - B G C)e$$

FOR ILLUSTRATIVE PURPOSES WE WILL CONTROL

$$\omega_4 = \dot{v}'(t, 1.) = y_1$$

$$\omega_1 = \dot{v}'(t, 0) = y_2$$

AND

$$y_3 = v(t, s_o) + \alpha \dot{v}(t, s_o)$$

WHERE

$$0 < s_o < L$$

THUS

$$C = \begin{bmatrix} 0 & \frac{\partial}{\partial s} [\delta(s-L)] \\ 0 & \frac{\partial}{\partial s} \delta(s) \\ \delta(s-s_o) & \alpha \delta(s-s_o) \end{bmatrix}$$

REFERENCE MODEL

$$\dot{q} = a_m q + b_m u_m$$

$$y_{m1} = c_1 q$$

$$y_{m2} = c_2 q$$

$$y_{m3} = c_3 q$$

UNDER THE ASSUMPTION THAT $u_m = 0$,

$$v_1^* = S_{11}^1(s) q(t)$$

$$v_2^* = S_{11}^2(s) q(t)$$

$$f_1^* = S_{21}^1 q$$

$$f_2^* = S_{21}^2 q$$

$$f_3^* = S_{21}^3 q$$

ILLUSTRATIVE APPLICATION TO SCOLE
ROLL BEAM BENDING EQUATION

ASSUMPTIONS: PROOF MASSES AND DAMPING NEGIGIBLE, REFLECTION MASS NEGIGIBLE

$$PA \ddot{v}(t,s) + EI v''''(t,s) = f_1 \delta(s-1) + f_2 \delta'(s) + f_3 \delta'(s-L)$$

$$f_1 = F_y$$

$$f_2 = M_i$$

$$f_3 M_y$$

CASE 1: (ignore shuttle mass)

$$v''(t,0) = v''(t,L) = 0$$

$$v''''(t,0) = v''''(t,L) = 0$$

CASE 2: Simple-free (shuttle mass \rightarrow infinity)

$$v(t,0) = 0 \quad v'(0,t) = 0$$

$$v''(t,L) = 0 \quad v''''(t,L) = 0$$

CASE 1 Free-Free

$$S_{11}^{-1}(s) =$$

$$\begin{aligned}
 & + S_{21} \frac{1}{K} \sum \frac{x_K(L)}{(PA a_m^2 + EI K^4)} x_K^2(L) x_K(s) \\
 & + S_{21} \frac{2}{K} \sum \frac{-x_K(0)}{(PA a_m^2 + EI K^4)} x_K^2(L) x_K(s) \\
 & + S_{21} \frac{3}{K} \sum \frac{-x_K(L)}{(PA a_m^2 + EI K^4)} x_K^2(L) x_K(s)
 \end{aligned}$$

WHERE $x_K(s) = \left[\begin{array}{l} \left(\frac{\sinh(KL) - \sin(KL)}{\cos(KL) - \cosh(KL)} (\cosh ks + \cos ks) \right) \\ + \sinh(ks) + \sin(ks) \end{array} \right]$

SOLVING THE EQUATIONS OF MOTION

$$v(t, s) = \sum_{n=1}^{\infty} Q_n(s) y_n(t)$$

$$EI \frac{d^4 Q_n(s)}{ds^4} - w_n^2 P A Q_n(s) = 0 \quad n = 1, 2, \dots, \infty$$

$$\begin{aligned} Q_n(s) &= A \sin k_n s + B \cos k_n s + C \sinh k_n s \\ &+ D \cosh k_n s \end{aligned}$$

CASE 1

$$Q_n(s) = \begin{bmatrix} \sinh k_n L & -\sin k_n L \\ \cos k_n L & -\cosh k_n L \end{bmatrix} (\cosh k_n s + \cos k_n s) \\ + \sin k_n s + \sinh k_n s$$

CASE

$$Q_n(s) = \frac{1}{N_n} \begin{bmatrix} \sin k_n L & +\sinh k_n L \\ \cos k_n L & +\cosh k_n L \end{bmatrix} (\cos k_n s - \cosh k_n s) \\ + \sin k_n s \quad \sinh k_n s$$

CGT GAIN SOLUTION

Output matrix values

$$\text{Note: } S_{11}(0) = \frac{c_1}{A_m}$$

$$S_{11}(L) = \frac{c_2}{A_m}$$

$$S_{11}(s) = \frac{c_3}{1 + \alpha A_m}$$

Want $S_{11}(s)$ to be ideal initial beam shape

Case 1

$$c_1 = 0.00251$$

$$c_2 = -0.00251$$

$$c_3 = 0.09596$$

Case 2

$$c_1 = 0.002$$

$$c_2 = -0.001456$$

$$c_3 = 0.092$$

REFERENCE MODEL SELECTION

PURPOSE: TO DAMP OUT THE STRUCTURAL VIBRATIONS WITHIN TEN
SECONDS WITHOUT VIOLATING THE CONTROL MAGNITUDE
CONSTRAINTS.

$$\dot{q}(t) = \emptyset \cdot 4q(t)$$

$$y_{m1}(t) = c_{m1}q(t)$$

$$y_{m2}(t) = c_{m2}q(t)$$

$$y_{m3}(t) = c_{m3}q(t)$$

$$q(\emptyset) = 1$$

RESULTS

- o FEEDBACK GAINS
- o FEEDFORWARD GAINS
- o SIMULATIONS

PARAMETER	VALUE
L = Beam Length	130.0 ft
α = weighting factor	0.25
s = additional beam sensor location	65.0 ft
EI	4.0×10^7 lb-ft ²
PA	0.09556 slugs/ft

TABLE 5.1 : SCOLE BEAM PARAMETERS

MODE # n	k_n	ω_n (rad/sec)	f_n (HZ)
1	4.73	27.085	4.311
2	7.853	74.658	11.882
3	10.996	146.378	23.297
4	14.173	243.181	38.703
5	17.274	361.236	57.492

TABLE 5.2 : NATURAL FREQUENCIES FOR CASE I

MODE # n	k_n	ω_n (rad/sec)	f_n (Hz)
1	3.927	18.669	2.971
2	7.069	60.495	9.628
3	10.210	126.199	20.085
4	13.352	215.823	34.349
5	16.493	329.310	52.411

TABLE 5.3 : NATURAL FREQUENCIES FOR CASE II

RECALL THAT FOR TRUE STABILITY WE NEED

$$\underline{f} = f^* + G(y_m - y) = f^* + GC(v^* - v)$$

THIS SYSTEM WILL BE STABLE FOR

$$G = \begin{bmatrix} G_{11} & 0 & 0 \\ 0 & G_{22} & 0 \\ 0 & 0 & G_{33} \end{bmatrix}$$

$$G_{11} > 0$$

FEEDBACK GAINS (NO SENSOR AT s_0)

CASE I

SET A : $g_{11} = 1210.0$ $g_{22} = 1730.0$ $g_{33} = 0.0$

SET B : $g_{11} = 600.0$ $g_{22} = 850.0$ $g_{33} = 0.0$

SET C : $g_{11} = 60.0$ $g_{22} = 85.0$ $g_{33} = 0.0$

CASE II

SET A : $g_{11} = 950.0$ $g_{22} = 300.0$ $g_{33} = 0.0$

SET B : $g_{11} = 475.0$ $g_{22} = 150.0$ $g_{33} = 0.0$

SET C : $g_{11} = 95.0$ $g_{22} = 30.0$ $g_{33} = 0.0$

# modes in series	s_{21}^1	s_{21}^2	s_{21}^3
3	-690.946	-1641.531	-9785.292
4	-690.954	-1044.241	-9188.201
5	-669.460	-1236.139	-8678.003
6	-669.401	-949.532	-8391.477
7	-641.403	-1145.781	-7803.666
8	-641.402	-982.676	-7640.603
9	-631.98	-1066.760	-7320.688
10	-631.916	-959.505	-8279.688
AVERAGE	-658.000	-1127.700	-8279.000

CGT Gains for Case 1

# modes in series	s_{21}^1	s_{21}^2	s_{21}^3
3	-355.878	-1141.894	-6309.016
4	-332.129	-805.507	-5354.048
5	-318.384	-1007.015	-4986.424
6	-316.305	-791.389	-4776.447
7	-303.601	-953.259	-4463.880
8	-300.262	-856.221	-4300.704
9	-295.713	-924.748	-4184.084
10	-294.991	-937.512	-4166.822
AVERAGE	-314.235	-926.750	-4817.250

Staurois

Case I : Free-Free

$$\begin{array}{llll} G_{11} = 1210 & G_{22} = 1731 & G_{33} = 0 \\ S_{\text{eff}} = -669.0 & S_{\text{eff}} = -949.5 & S_{\text{eff}} = -8391.5 \end{array}$$

Case II : Simple-Free

$$\begin{array}{llll} G_{11} = 950 & G_{22} = 300 & G_{33} = 0 \\ S_{\text{eff}} = -316.3 & S_{\text{eff}} = -791.4 & S_{\text{eff}} = -4776.4 \end{array}$$

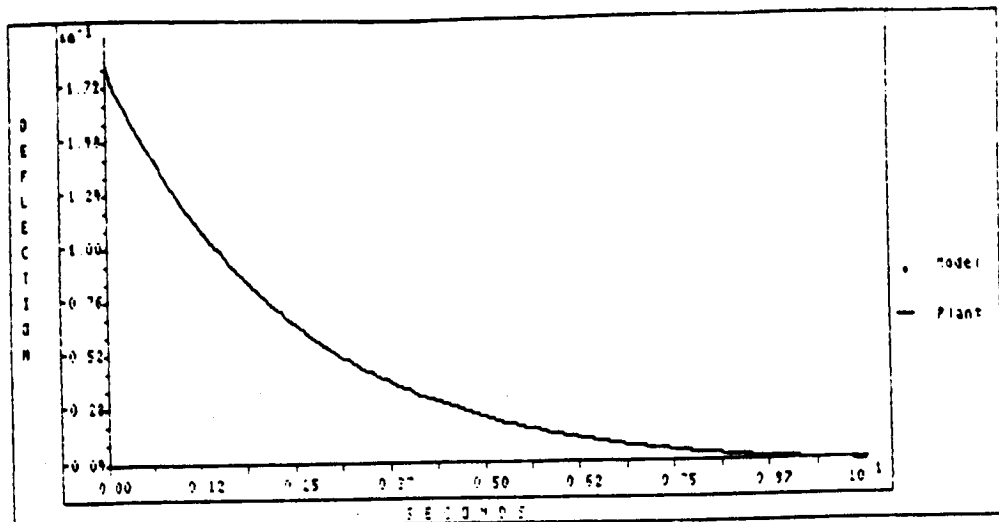


Figure 5.11 Case I : Perfect Model Following-
CGT Gains for 6 Modes

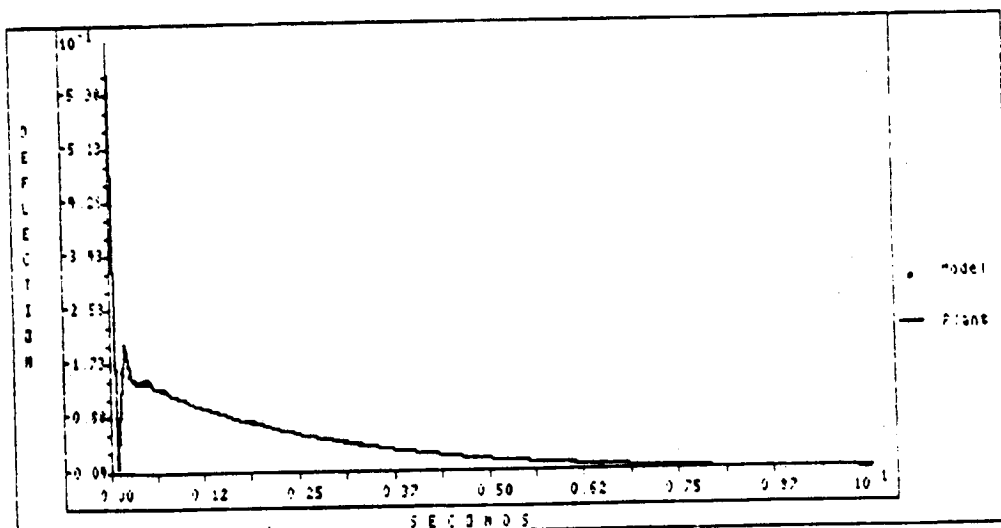


Figure 5.12 Case I : Tracking -
CGT Gains for 4 Modes

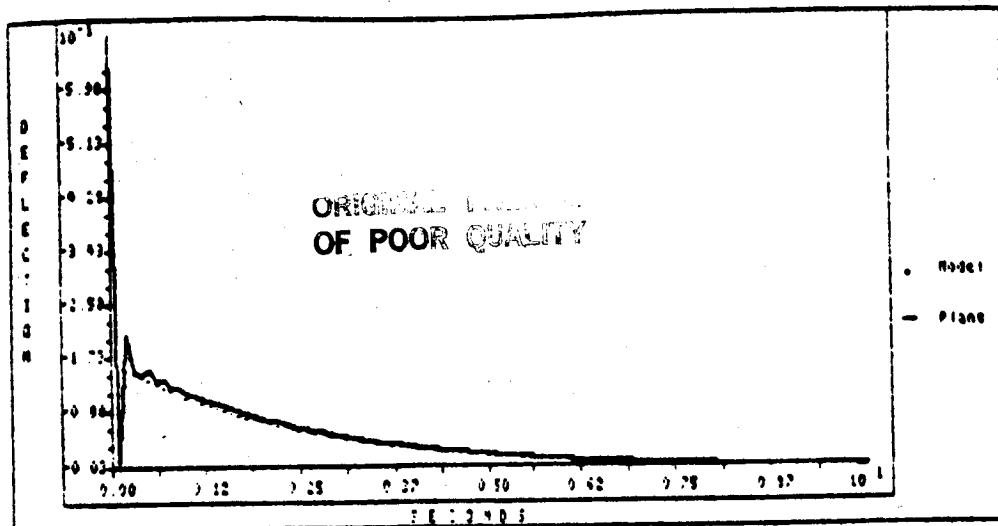


Figure 5.13 Case I : Tracking -
CGT Gains for 6 Modes

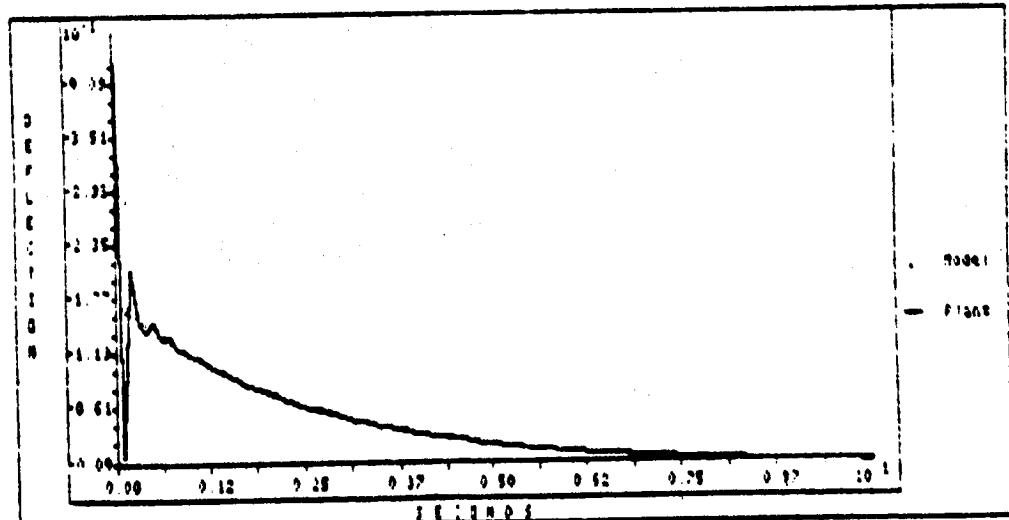


Figure 5.14 Case I : Tracking -
CGT Gains for Ave Modes

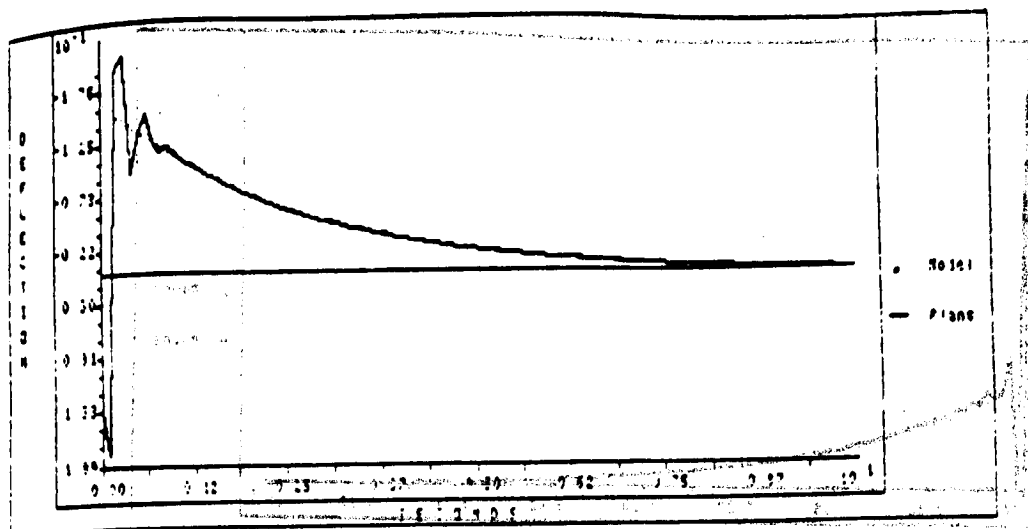


Figure 5.15 Case II : Tracking -
CGT Gains for 4 Modes

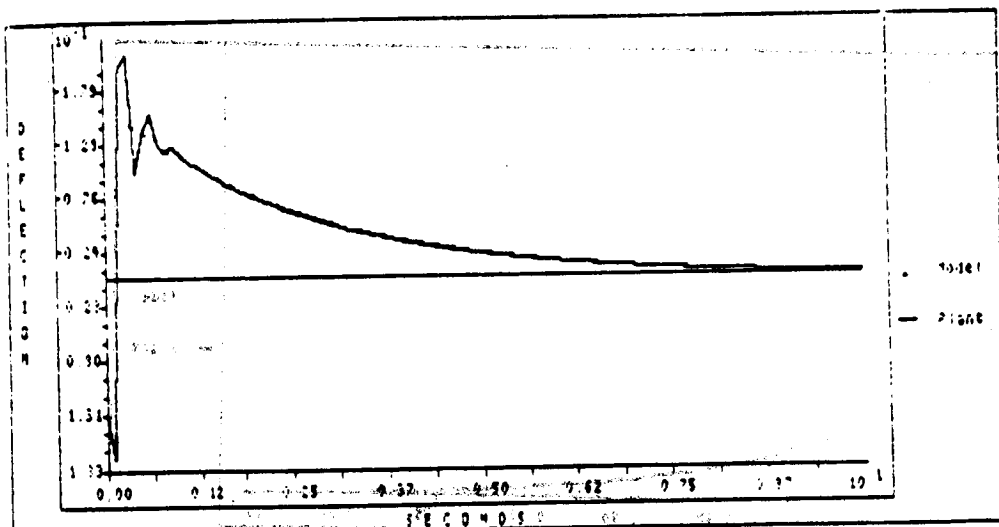


Figure 5.16 Case II : Tracking -
CGT Gains for 6 Modes

ORIGINAL PAGE IS
OF POOR QUALITY

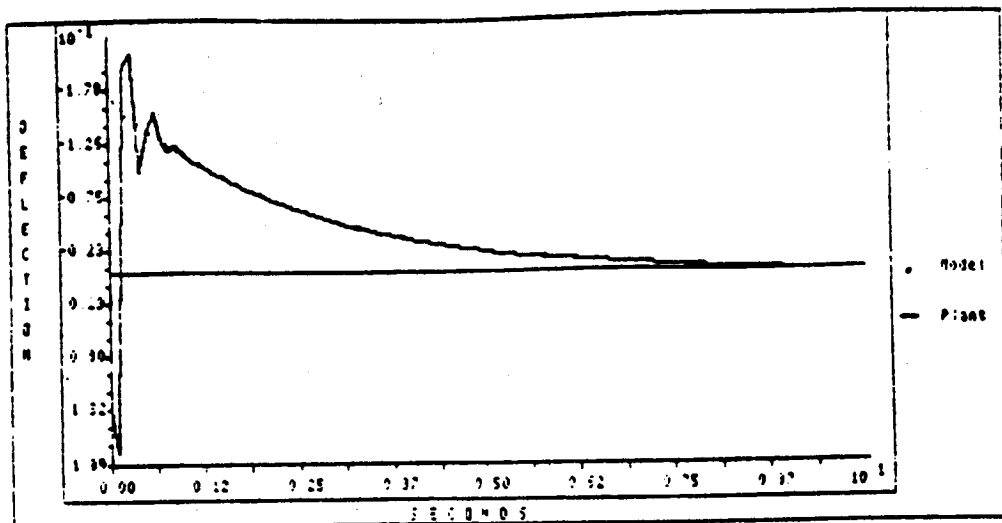


Figure 5.17 Case II : Tracking -
CGT Gains for Ave Modes

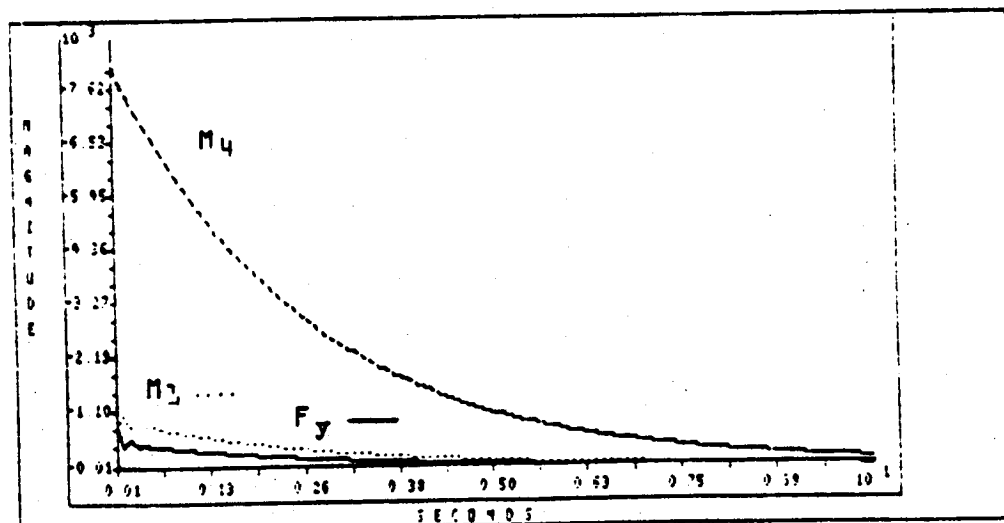


Figure 5.18 Case I : Controls -
CGT Gains for 6 Modes

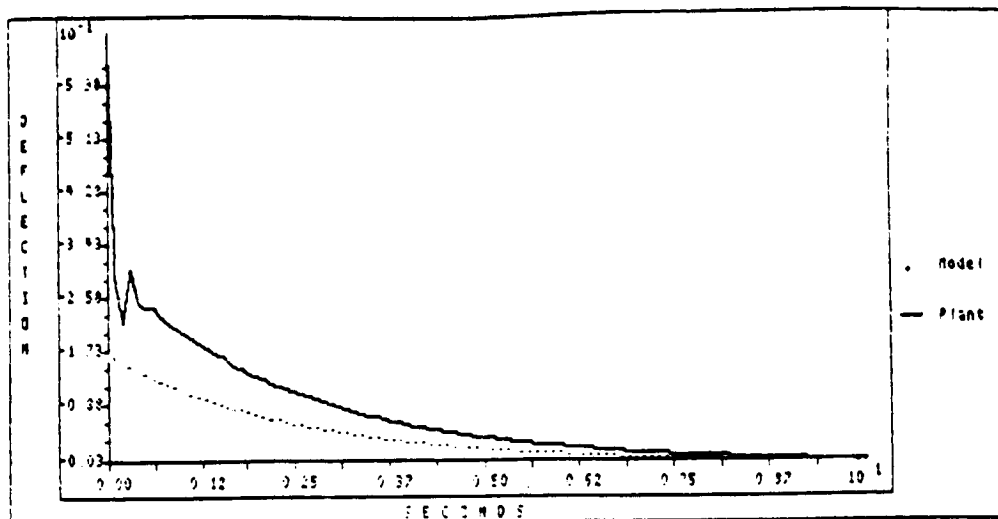


Figure 5.19 Case I : Parameter Variation -
CGT Gains for 6 Modes

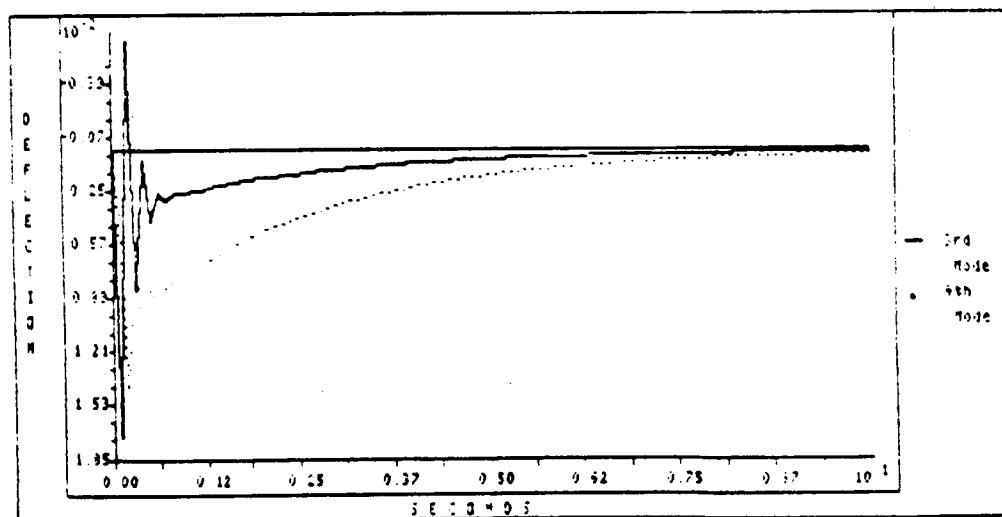


Figure 5.20 Case I : Control Spillover -
Beam Deflection for 3rd and 4th Modes,
CGT Gains for 6 Modes

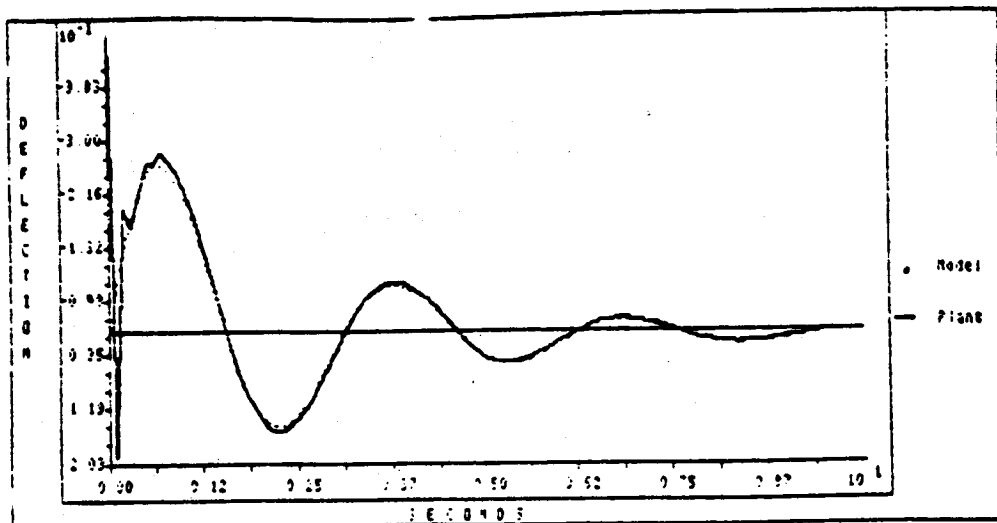


Figure 5.21 Case I : Tracking -
Reference Model $2.04 e^{-4t} \sin (2.04t)$,
CGT Gains for 6 Modes

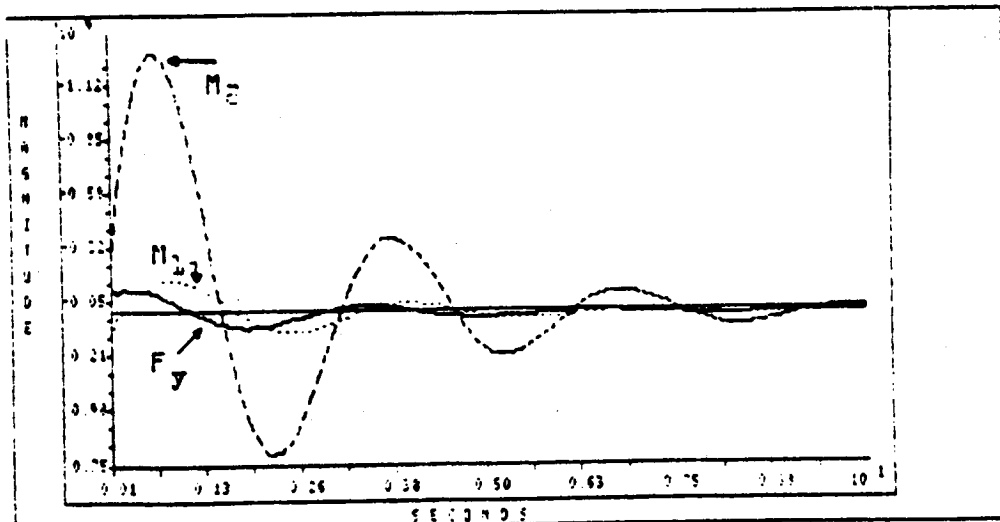


Figure 5.22 Case I : Controls -
Reference Model $2.04 e^{-4t} \sin (2.04t)$,
CGT Gains for 6 Modes

CONCLUSIONS

1. A MODEL FOLLOWING PROCEDURE USING CGT THEORY WAS DEVELOPED FOR APPLICATION TO DPS SYSTEMS.
2. THE DESIGN PROCEDURE RESULTS IN A FINITE-DIMENSIONAL CONTROLLER THAT GIVES OUTPUT FOLLOWING AND FULL STATE STABILITY.
3. THE MODEL FOLLOWING CONTROLLER'S APPLICATION TO A MODELS OF THE SCOLE WAS SHOWN.
4. THROUGH SIMULATIONS, IT WAS DEMONSTRATED THAT SATISFACTORY TRACKING OF A DESIRED TRAJECTORY CAN BE ACHIEVED.
5. EXCITATION OF HIGHER ORDER MODES BY THE CONTROLLER AND PARAMETER VARIATIONS DO NOT ADVERSELY AFFECT THE SYSTEM PERFORMANCE.

PLANNED ACTIVITIES

- o DEVELOPMENT OF OUTPUT FEEDBACK FOR LUMPED MODEL CONTROLLER
- o DEVELOPMENT OF CONTROLS FOR THE PITCH AND YAW TORSION EQUATION
- o TESTING OF THE CONTROLLERS, IN THE PRESENCE OF NOISY SENSORS.
- o ADAPTIVE CONTROL

**Proof-Mass Actuator
Placement Strategies
for Regulation of Flexure
During the SCOLE Slew**

by

**Shalom (Mike) Fisher
Naval Research Lab**

PRECEDING PAGE BLANK NOT FILMED

**PROOF-MASS ACTUATOR
PLACEMENT STRATEGIES FOR
REGULATION OF FLEXURE DURING
THE SCOLE SLEW MANEUVER**

Shalom ("Mike") Fisher
Naval Research Laboratory

November 17, 1986

STATEMENT OF THE REGULATOR PROBLEM

**HOW DO DIFFERENT ACTUATOR PLACEMENT
STRATEGIES AFFECT BEAM FLEXURE DURING
LOS SLEW MANEUVER AND SETTLING**

OBJECTIVES OF THIS ANALYSIS

- *Immediate*

1. To find the best placement for the actuators.
2. To determine the importance of placement, i.e., what is the sensitivity of beam flexure to actuator placement.

- *Ultimate*

1. To "close the loop" and apply regulation to the experimental test model of SCOLE.
2. To achieve the design challenge goal of .02 degrees LOS pointing error.

PROCEDURES OF THIS ANALYSIS

- NASTRAN finite element model for flexible beam with 21 grid points on beam Reflector and shuttle body assumed to be rigid
- Nonlinear DISCOS simulation of 20 degree slew
- Closed-loop linear quadratic regulator (LQR)
- Regulator uses:
 1. Proof mass actuators on boom
Maximum force is 10 lbs.
Maximum stroke is 1 foot.
 2. Thruster moments on shuttle body
Thruster forces on reflector

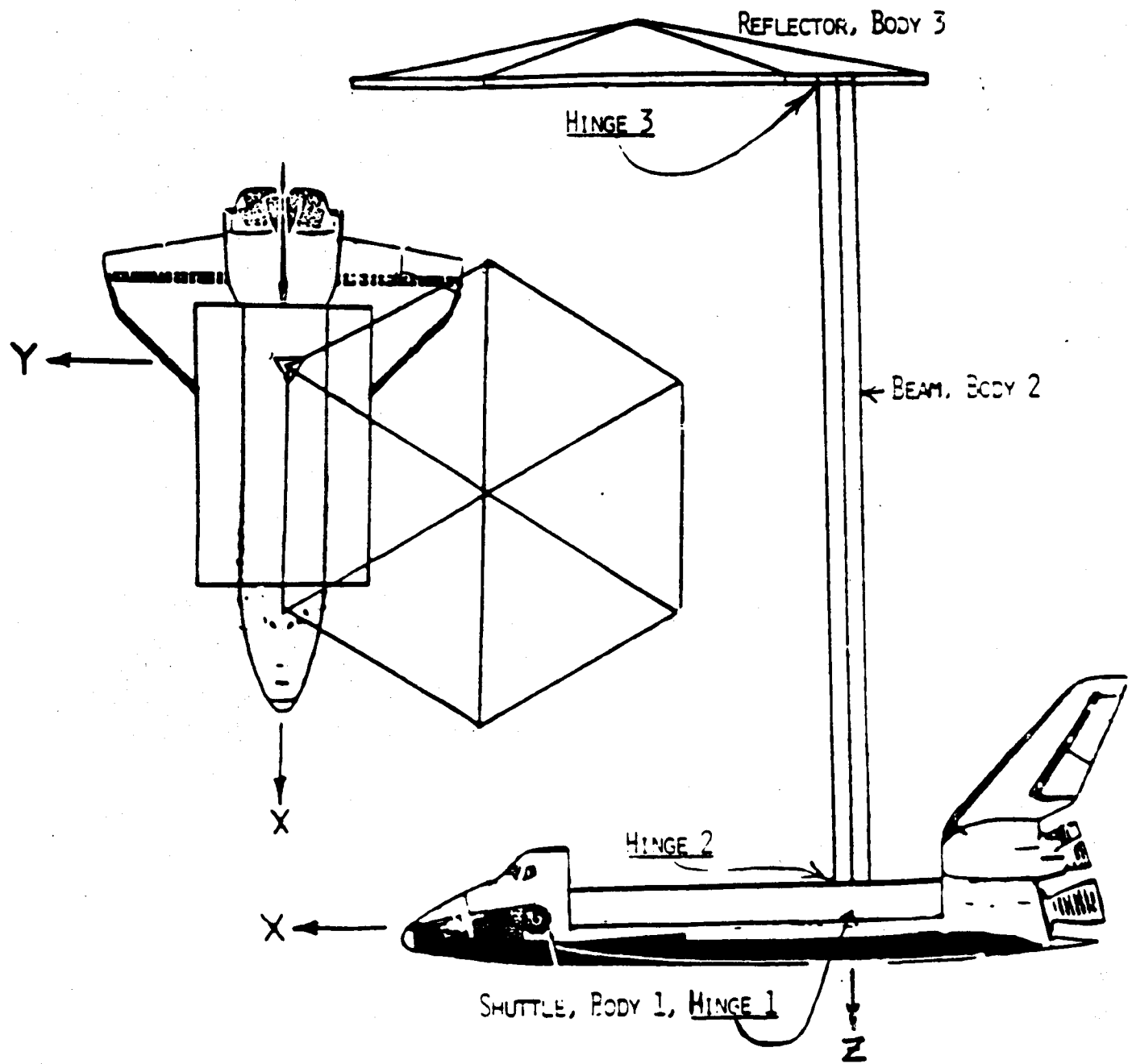
BRIEF CONCLUSIONS FROM SIMULATION

1. Maximum relative orientation of reflector to shuttle, due to flexure during the simulation, is reduced by a factor of four by the proof-mass actuators.
2. Maximum flexure amplitude is insensitive to changes in actuator locations.
3. Damping of the flexure oscillations is sensitive to changes in actuator placement.
4. Good actuator placements can generate an overdamping in the flexure oscillations.

DISCOOS SIMULATION: RIGID BODIES CONNECTED BY HINGES

MASS AND MOMENT OF INERTIA PROVIDED BY USER FOR EACH BODY

LOCATION OF HINGES AND SENSORS



COMPONENTS OF THE ANALYSIS

1. Nastran finite element model of beam, 40 nodes or grid points
21 on beam itself, including end points.
12 lowest modes retained for simulation.
2. DISCOS nonlinear simulation
open loop commanded slew about minimum principal axis
10,000 ft-lbs torque on shuttle, 22 lbs force on reflector
Bang-bang control law, slewing time = 11.3 secs.
3. LQ regulator, using ORACLS
control algebraic Riccati equation (CARE)
No noise or time delay in sensors or actuators

LQ REGULATOR FOR FLEXIBLE BEAM

- Purpose: To maintain the flexible beam in a nominally unbent position during the large angle slew
- Method: Linear quadratic regulator (LQR) matrices computed offline via ORACLS.
- Linearized system equation: $\dot{x}(t) = Ax(t) + Bu(t)$
 - $x(t)$: components are modal amplitudes and rates
 - A : system matrix (from DISCOS)
 - B : input matrix, determined by actuator placements
 - $u(t)$: input forces, commanded by regulator control
- Cost functional to be minimized:

$$J = \int_0^\infty [x^T(s)Qx(s) + u^T(s)Ru(s)]ds$$

LQ REGULATOR (CONTINUED)

- Objectives in minimizing cost functional:
 1. Maximize regulator performance
 2. 10lb limitation on actuator force

- Solve control algebraic Riccati equation :

$$0 = Q + A^T P + P A - P B R^{-1} B^T P$$

set $Q = I$ and $R = rI$, with $r = 10^{-5}$ or 10^{-6}

- Input force vector $u(t)$ is given by:

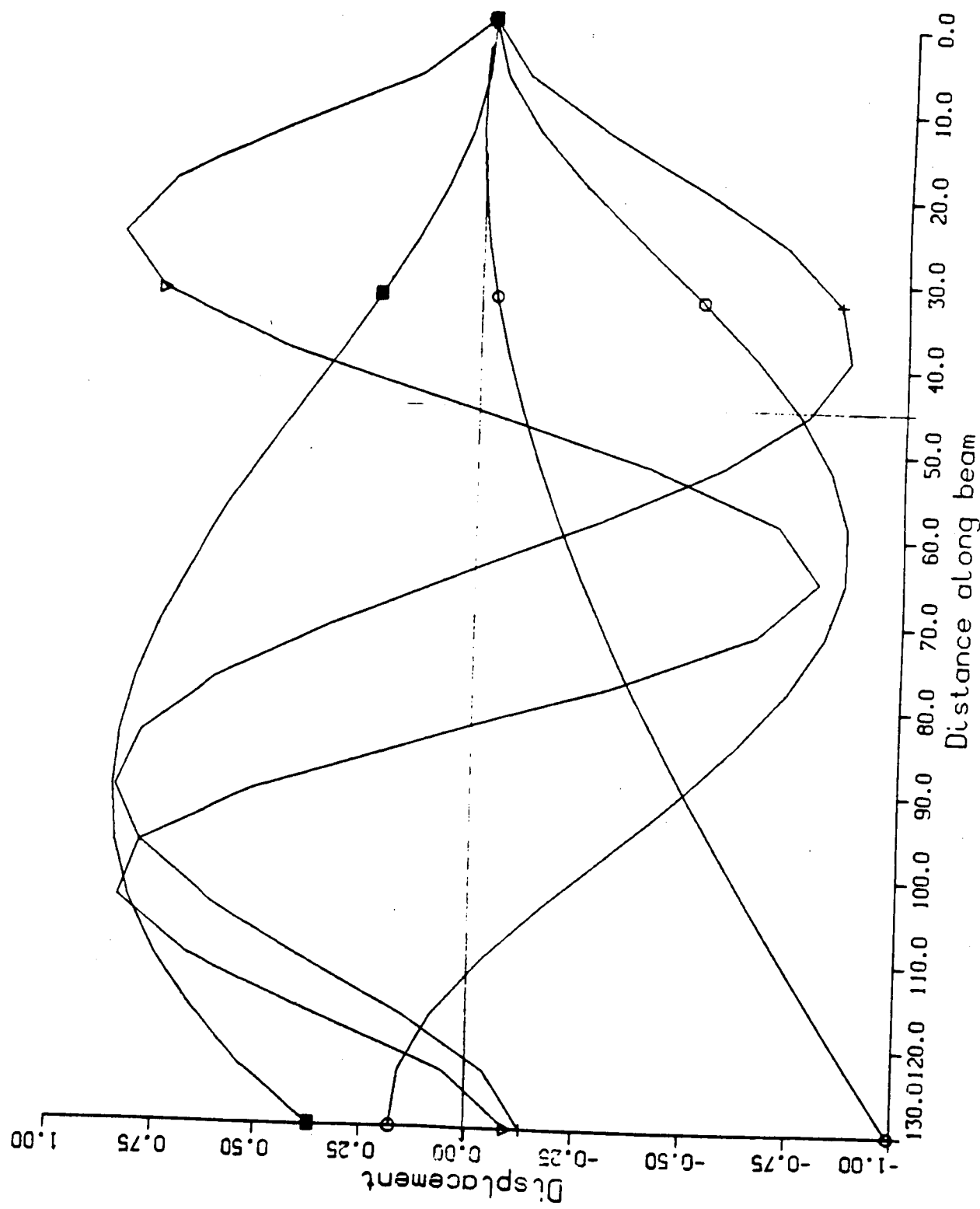
$$u(t) = -R^{-1}B^T P x(t)$$

$u(t)$ is recalculated each time step in DISCOS
from current value of $x(t)$ and offline,
predetermined values of R , B , and P .

TABLE I: MODES OF THE SYSTEM AS COMPUTED BY NASTRAN

MODE NUMBER	MODE TYPE	ANGULAR FREQ.	FREQ. IN HZ
1	PITCH	1.746	0.278
2	ROLL	1.969	0.313
3	YAW	5.105	0.182
4	ROLL	7.410	1.179
5	PITCH	12.848	2.045
6	ROLL	29.459	4.689
7	PITCH	34.263	5.453
8	ROLL	74.670	11.884
9	PITCH	78.883	12.555
10	COMPRESSION	106.281	16.915
11	ROLL	142.467	22.674
12	PITCH	145.618	23.176

Modal displacement in Y of roll modes



- INPUT MATRIX B

B is of the form : $[B]_{i,k} = \phi_{i,k}$

where $\phi_{i,k}$ is input influence coefficient on i^{th} mode from actuator at location k (21 grid points on beam)

6 degrees of freedom, 3 translational, 3 rotational,

$$\phi_{i,k} = (\phi_x \ \phi_y \ \phi_z \ \phi_\theta \ \phi_\phi \ \phi_\psi)_{i,k}$$

ϕ_x is x displacement of i^{th} mode at location k

- Degree of controllability, ρ , with 2 actuators at l and n

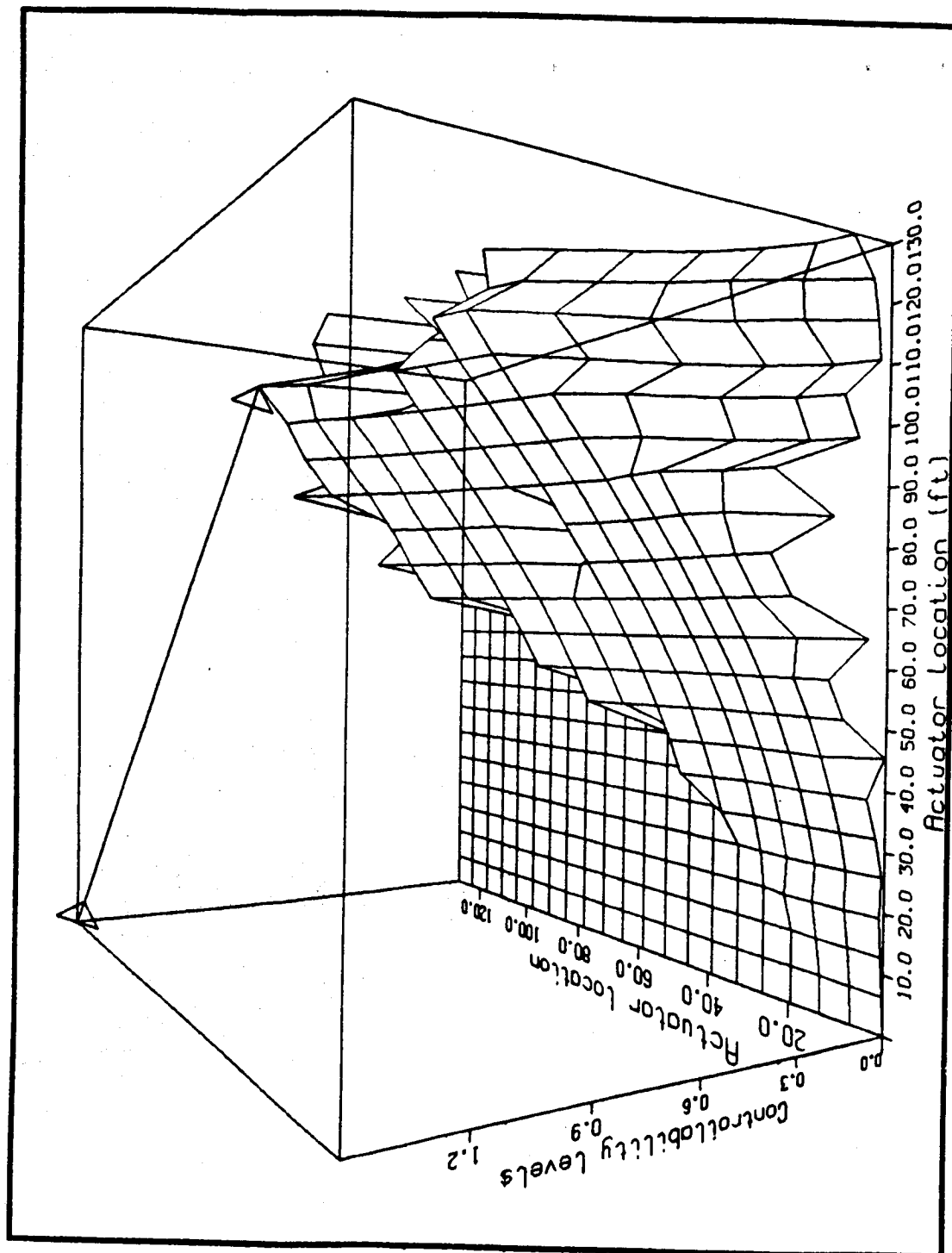
$$\rho = \min_i [\varepsilon \cdot (|\phi_{i,l}| + |\phi_{i,n}|) + |\phi_{i,1}| + |\phi_{i,21}|]$$

ε = ratio of actuator influence to thruster influence

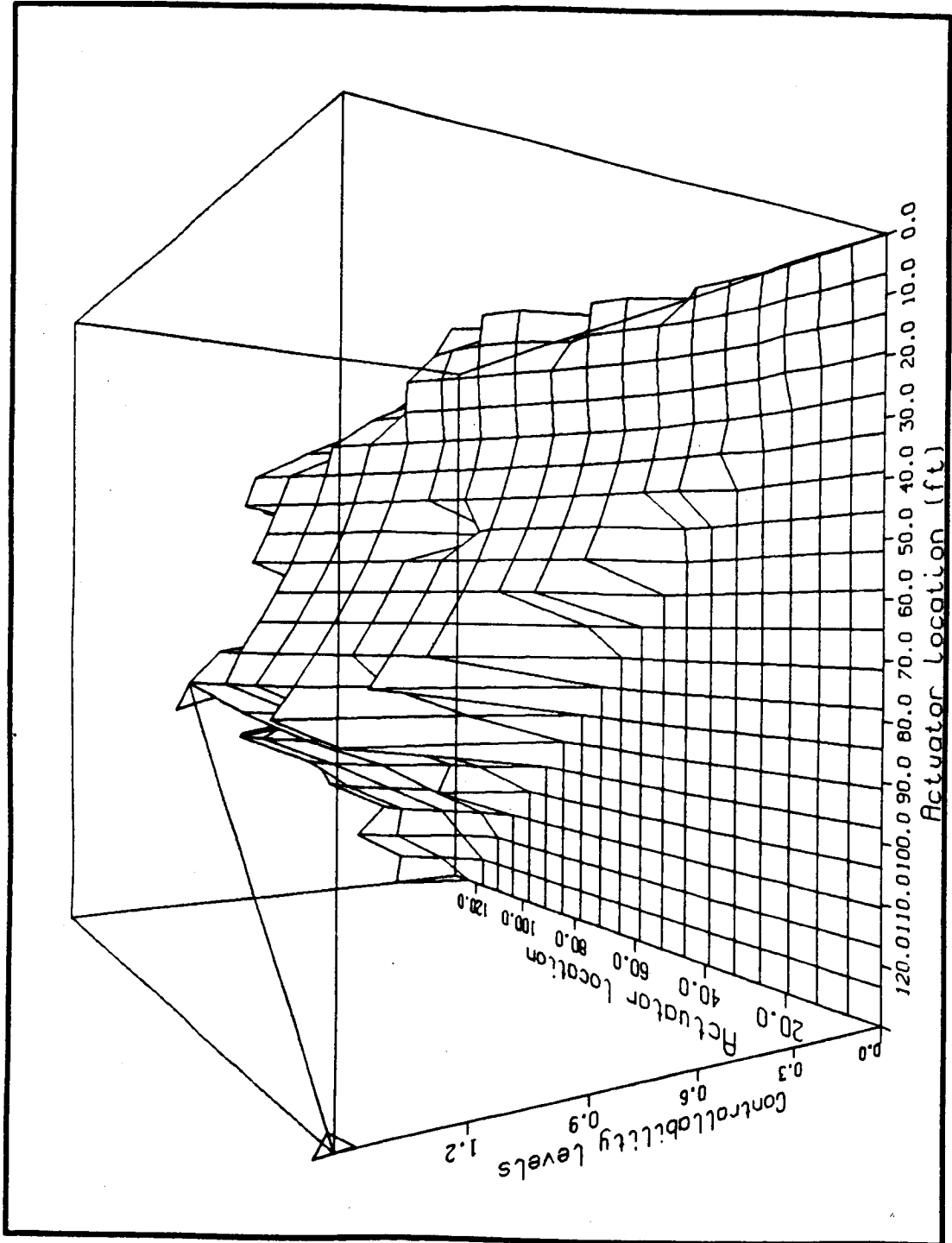
TABLE 2: ACTUATOR LOCATIONS FOR MAXIMUM CONTROLLABILITY

CASE	Joint #	ACTUATOR 1		Joint #	ACTUATOR 2	
		Location	Location		Location	Location
No Thrusters						
Actuators/Thrusters = 10	12	104	ft	17	16	71.5
Actuators/Thrusters = 1	11	110.5			17	78
Actuators/Thrusters = 0.1	14	91			17	71.5
Actuators/Thrusters = 0.01	13	97.5			17	71.5
	16	78			16	78

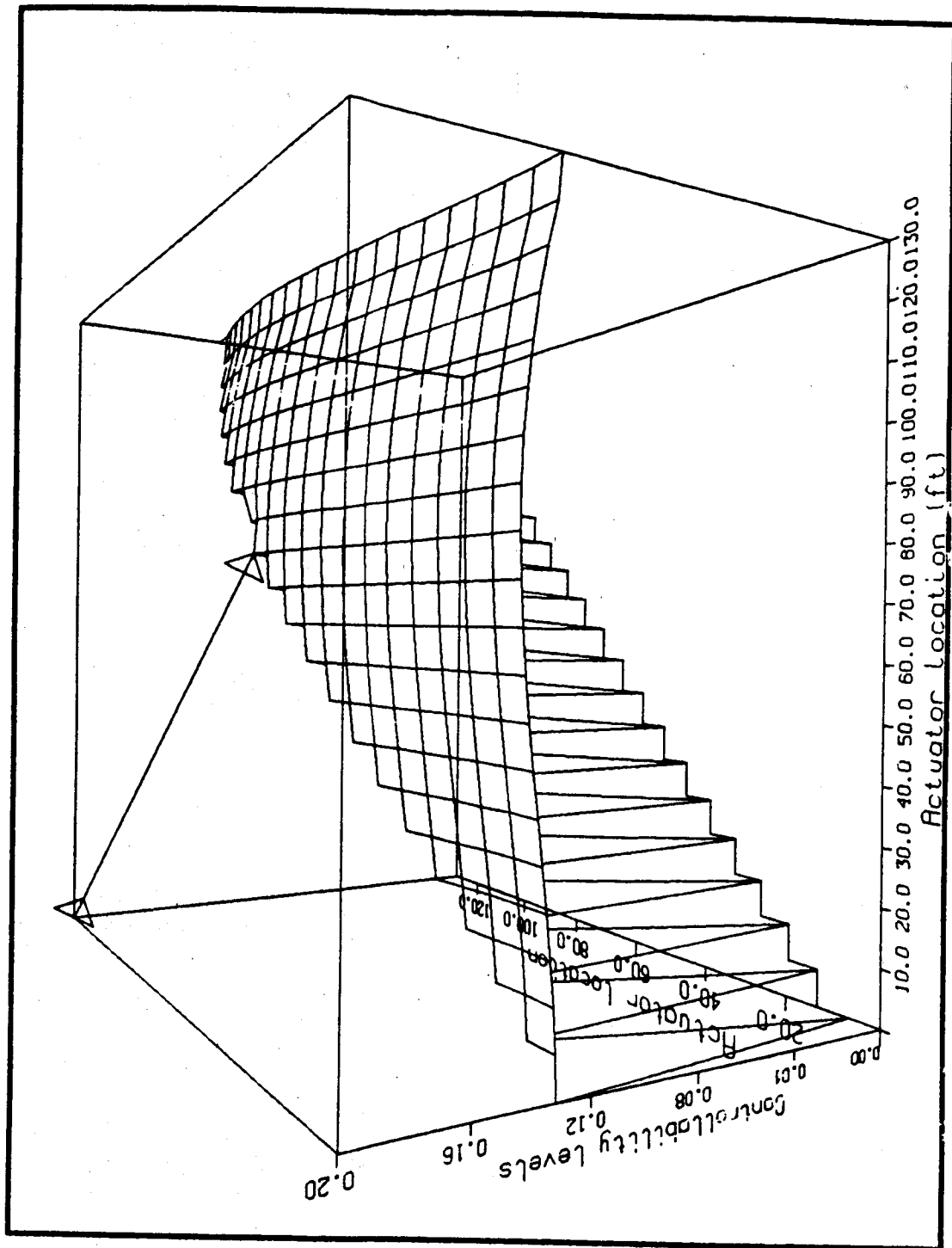
Controllability surface, X view



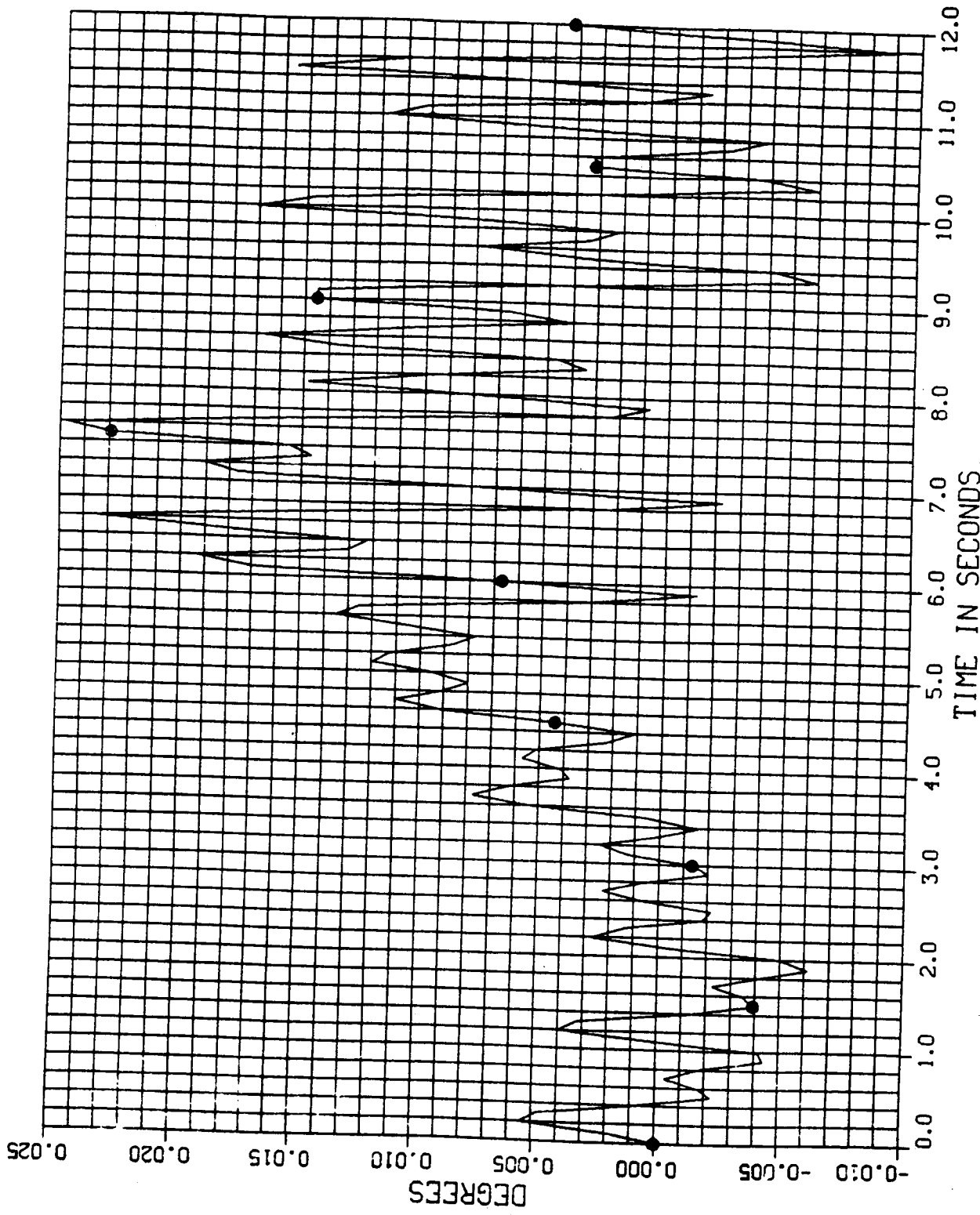
Controllability surface, Y view



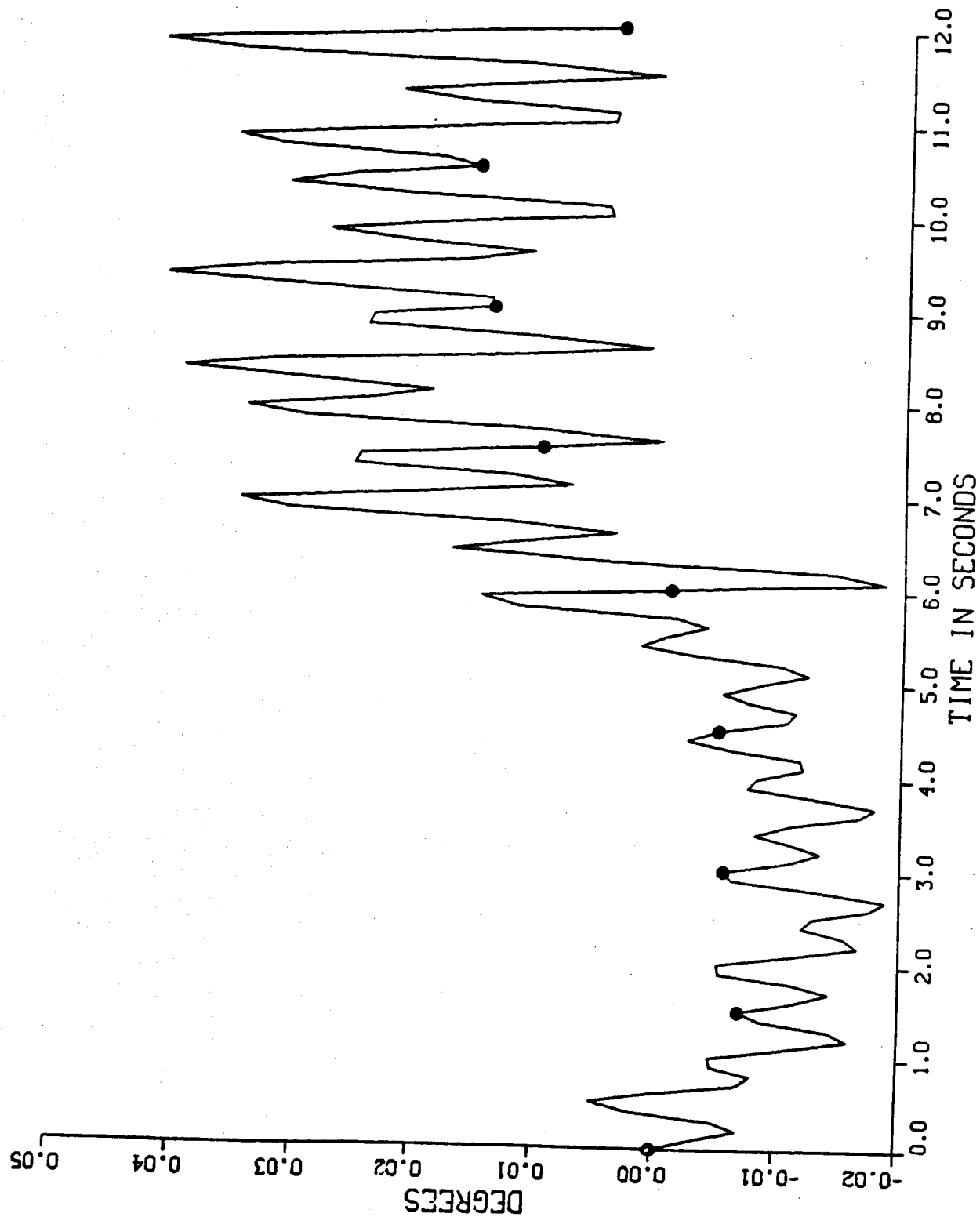
Controllability surface, X view



ROLL OF ANTENNA RELATIVE TO SHUTTLE VERSUS TIME



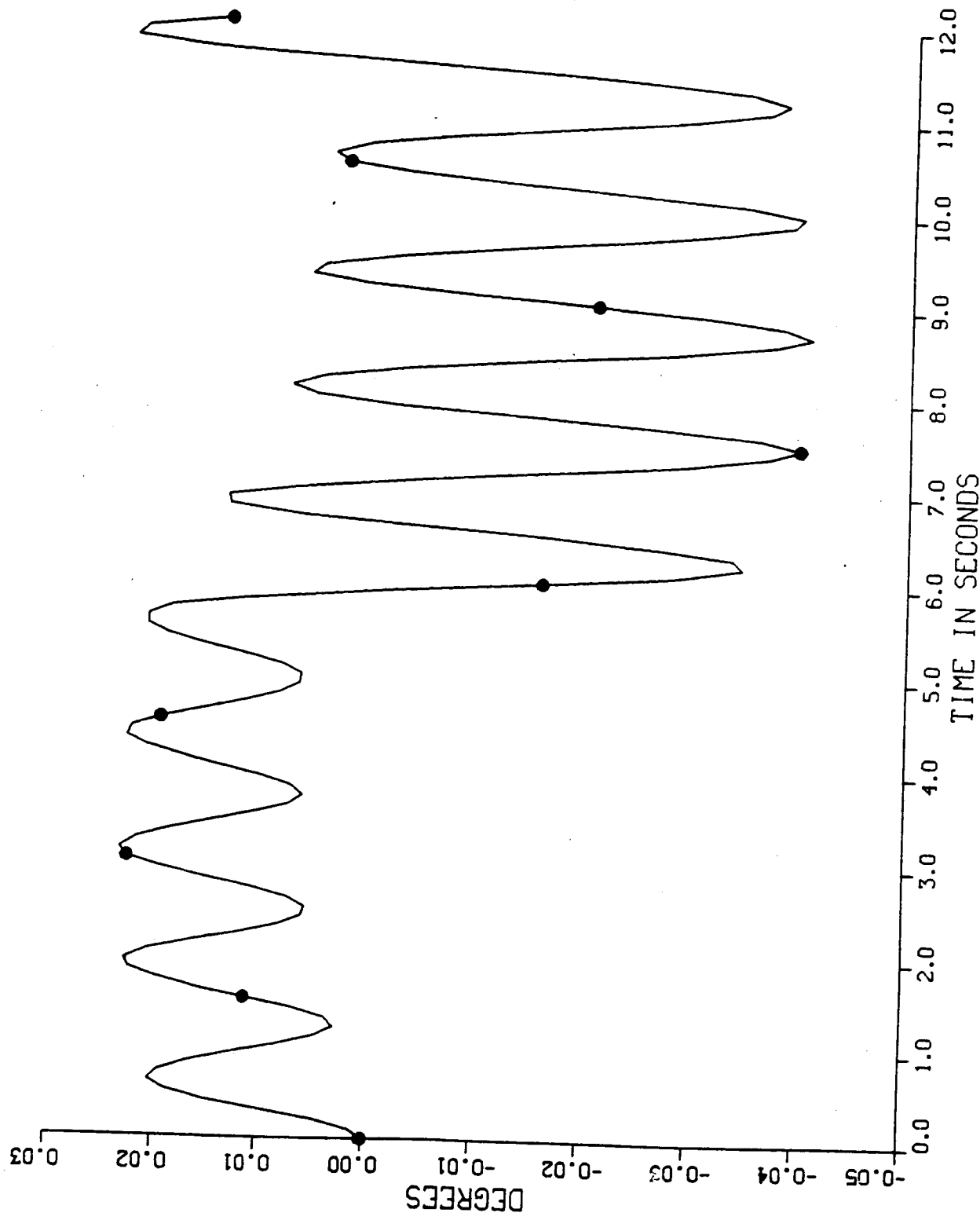
246



ORIGINAL PAGE IS
OF POOR QUALITY

247

LINE OF MINIMUM RELATIVE INERTIA VERSUS TIME

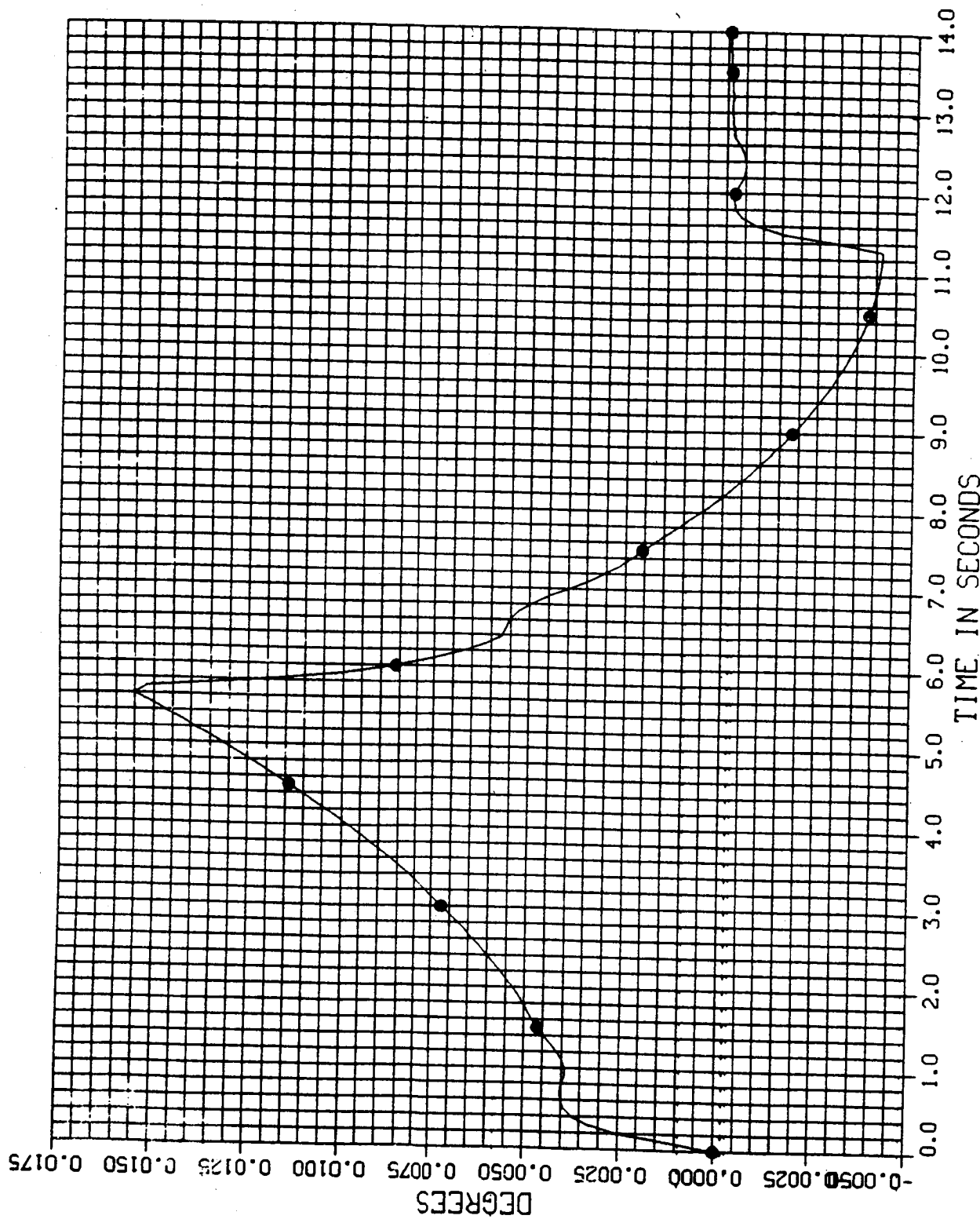


248

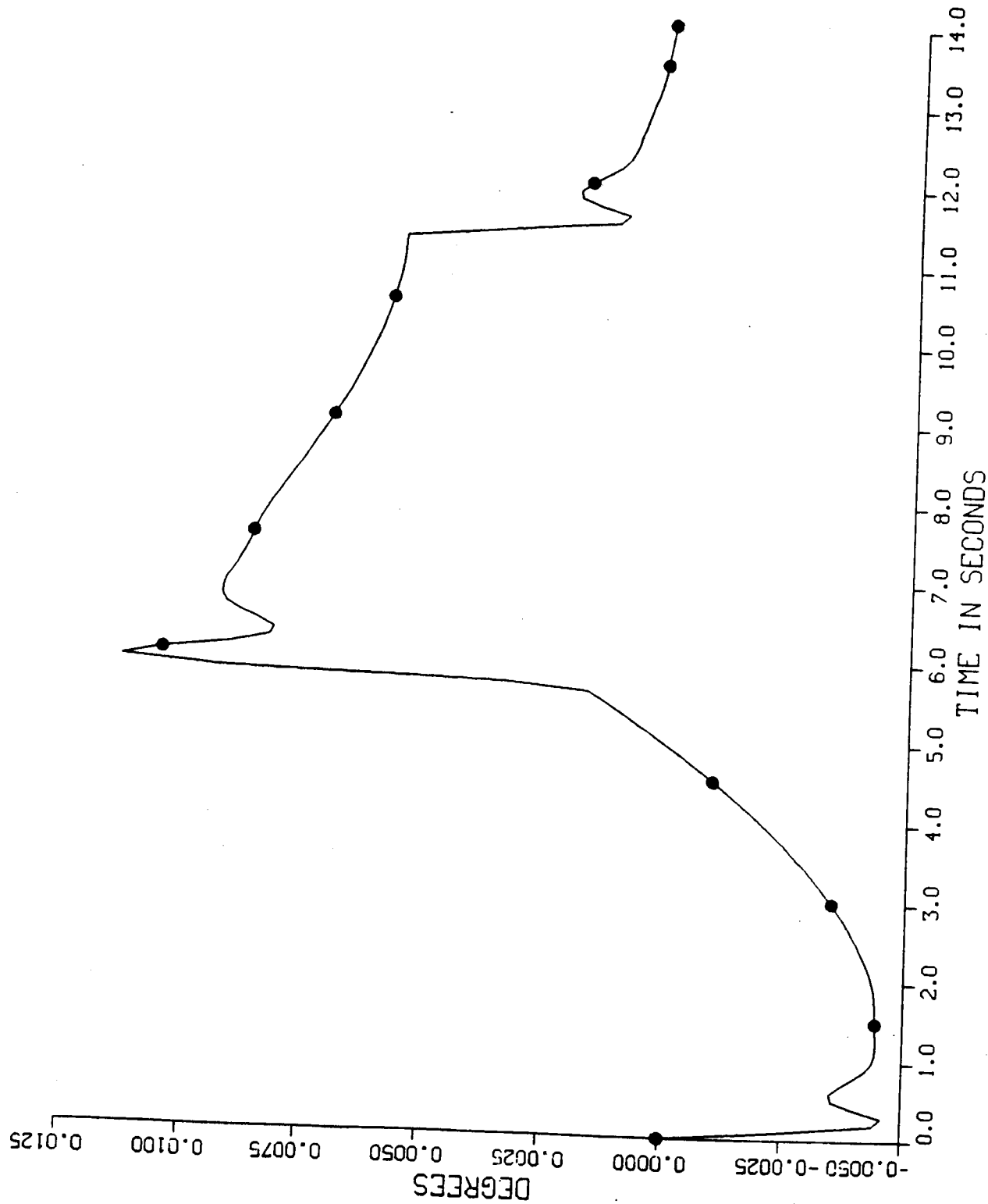
ORIGINAL PAGE IS
OF POOR QUALITY

ROLL OF ANILINH KELHIVE IN SHUTTLE VERSUS TIME

ORIGINAL PAGE IS
OF POOR QUALITY

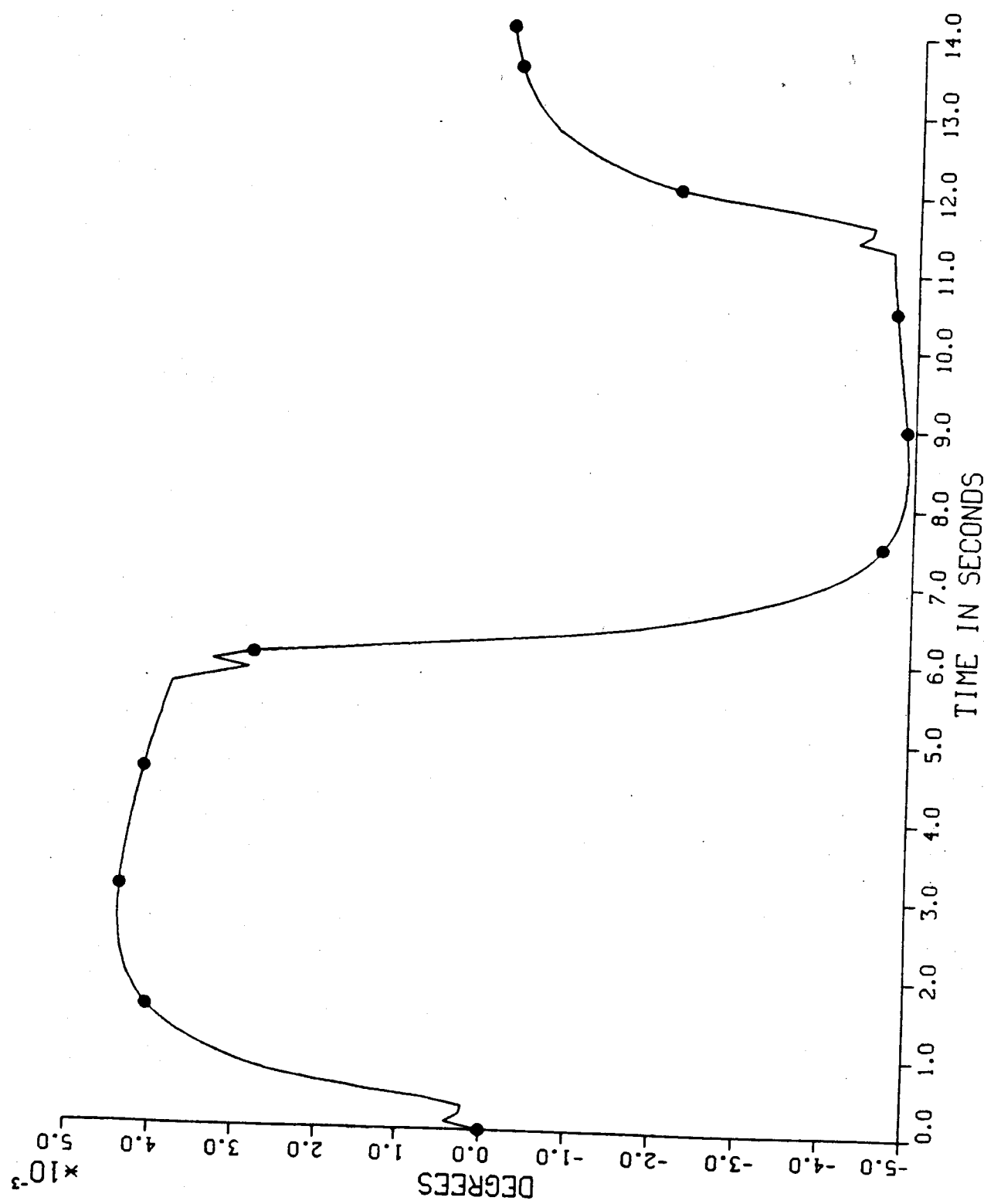


RIGHT CUSCULUS TITIUS IN HABITUS

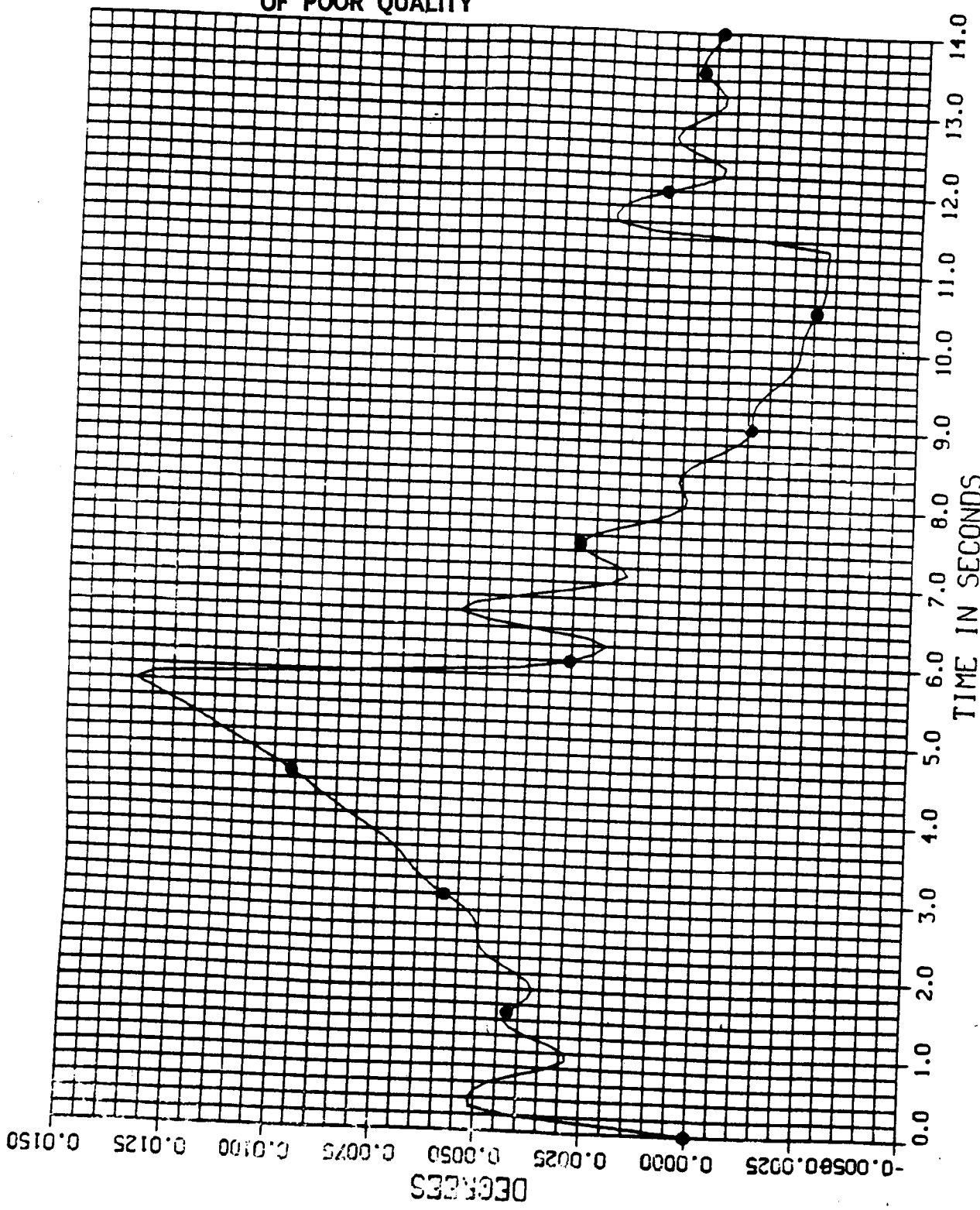


250

YAW OF ANTENNA RELATIVE TO SHUTTLE VERSUS TIME

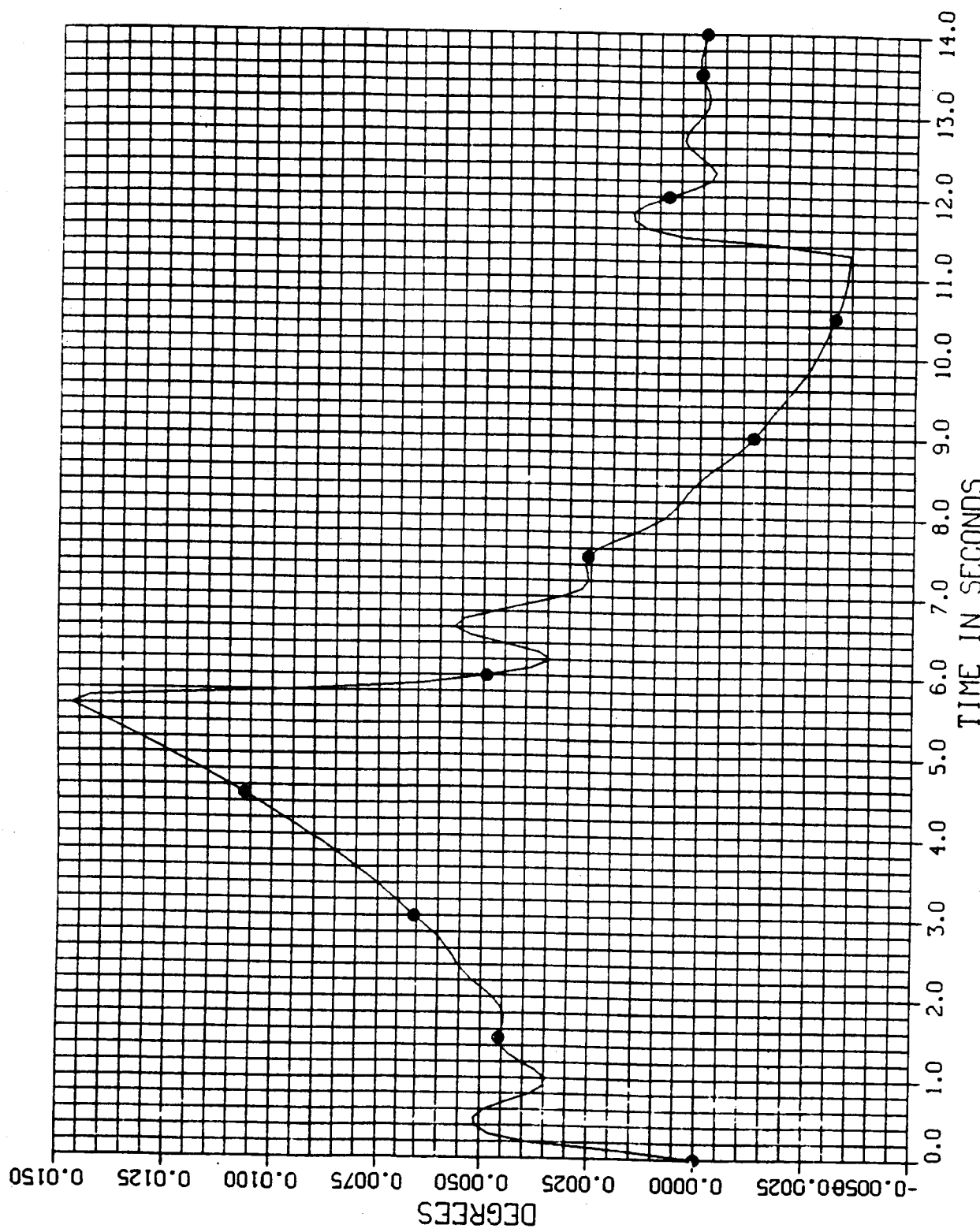


ORIGINAL PAGE IS
OF POOR QUALITY

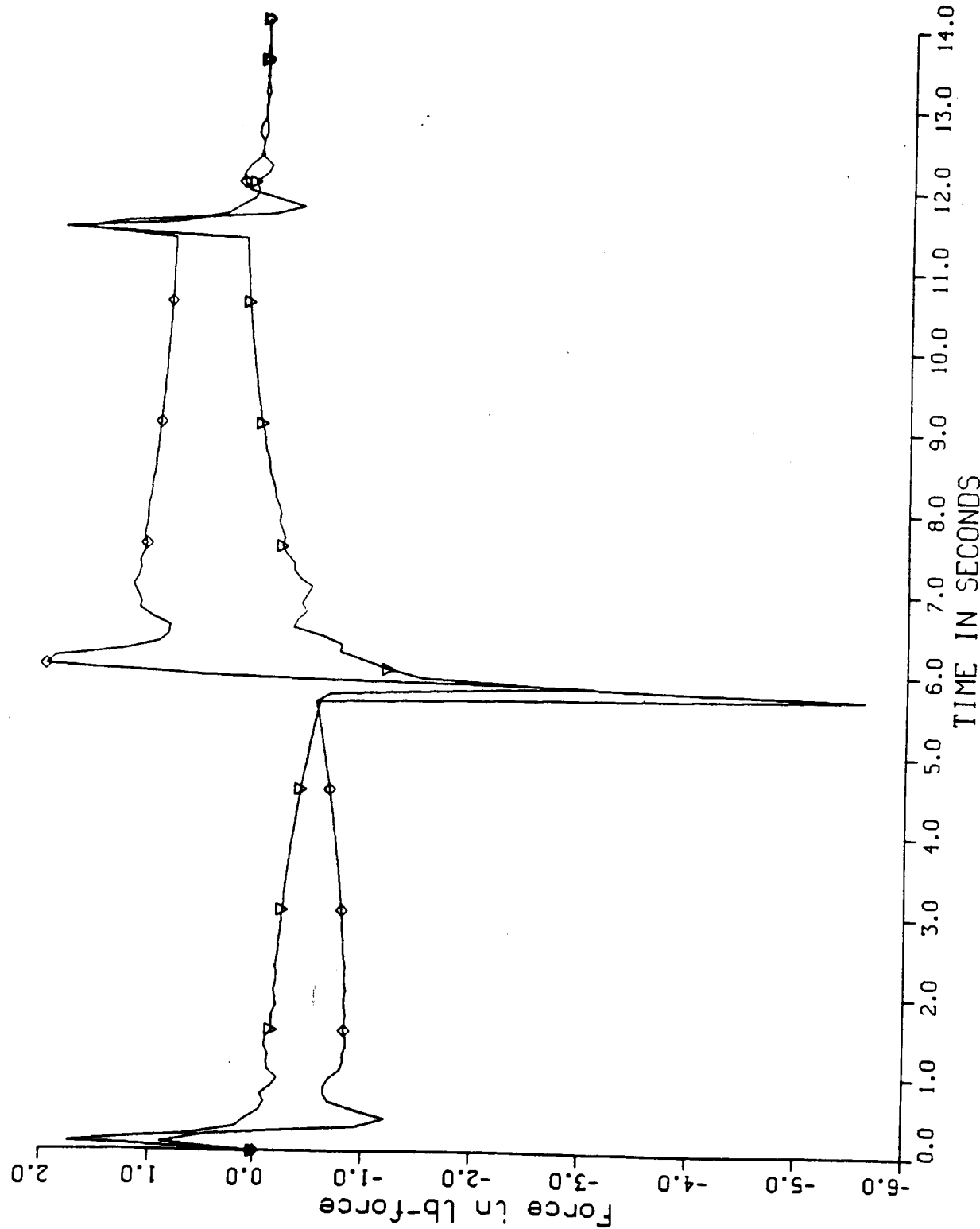


ROLL OF ANTENNA RELATIVE TO SHUTTLE VERSUS TIME 4 Oct 2001 452138.5

ORIGINAL PAGE IS
OF POOR QUALITY

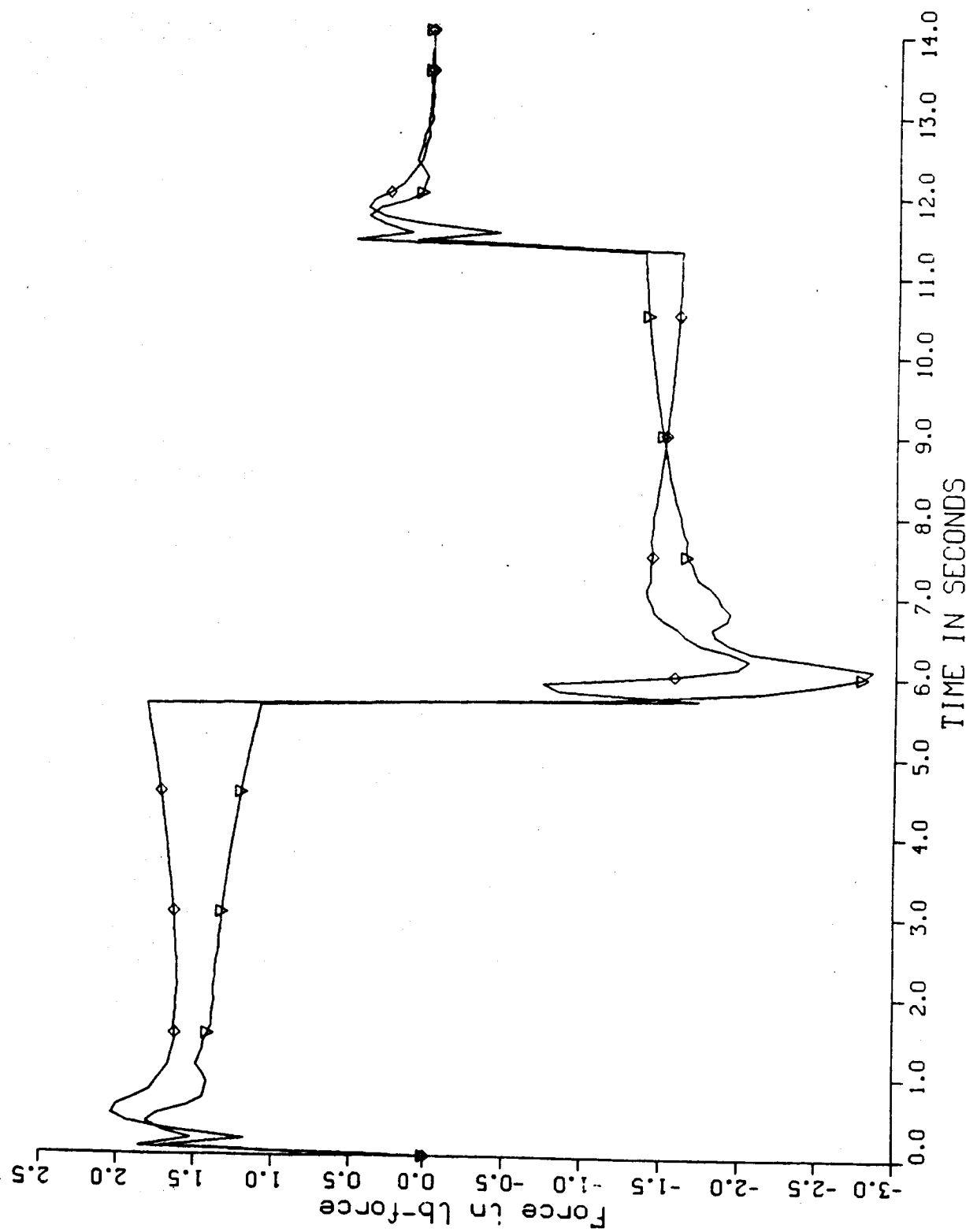


Proof mass forces near base of beam
Structures at 1/24 + 16444

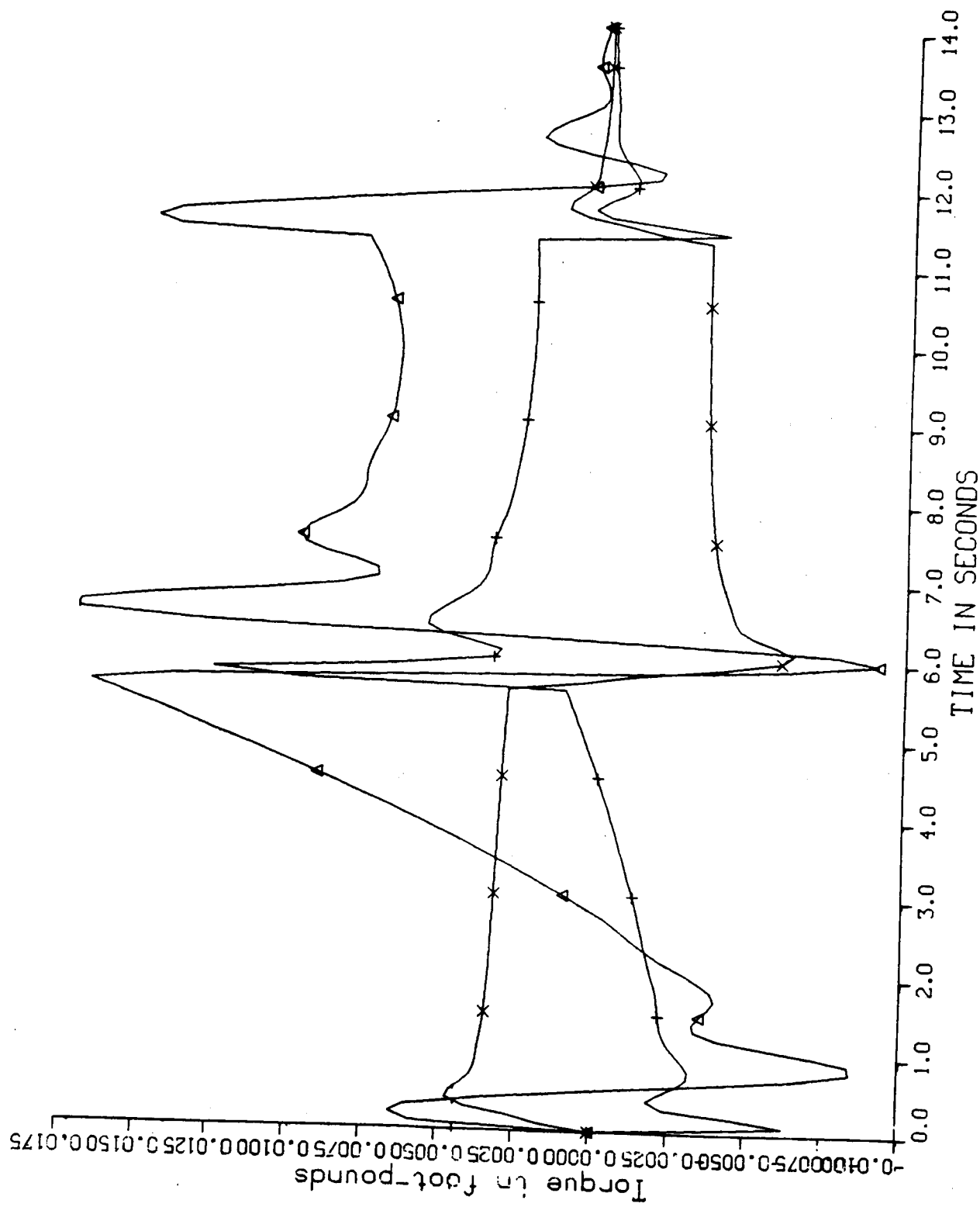


Proof mass forces applied near top of beam At-tors at $7\frac{1}{2}$ ft + 104 ft.

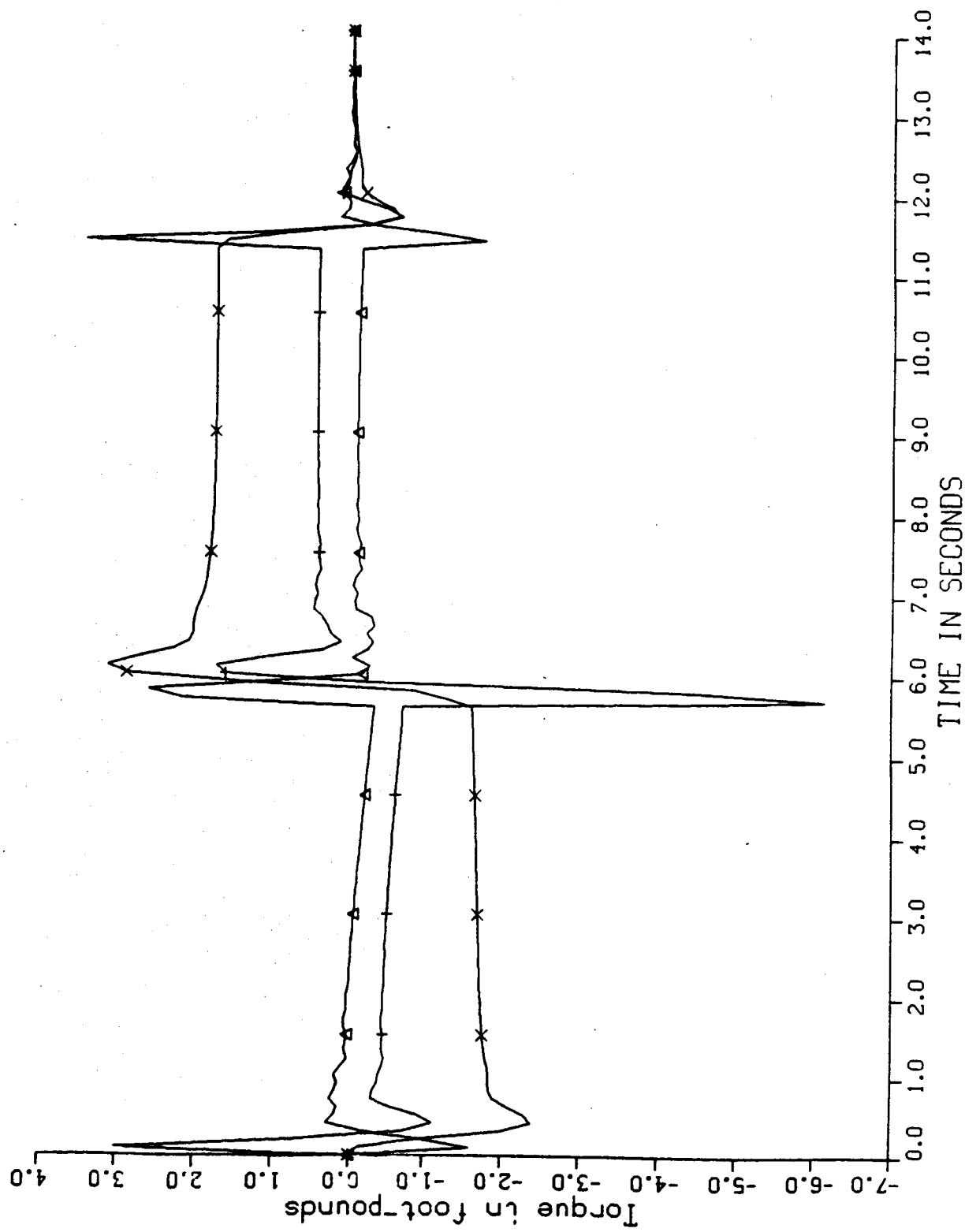
ORIGINAL PAGE IS
OF POOR QUALITY



Torques applied at base of beam

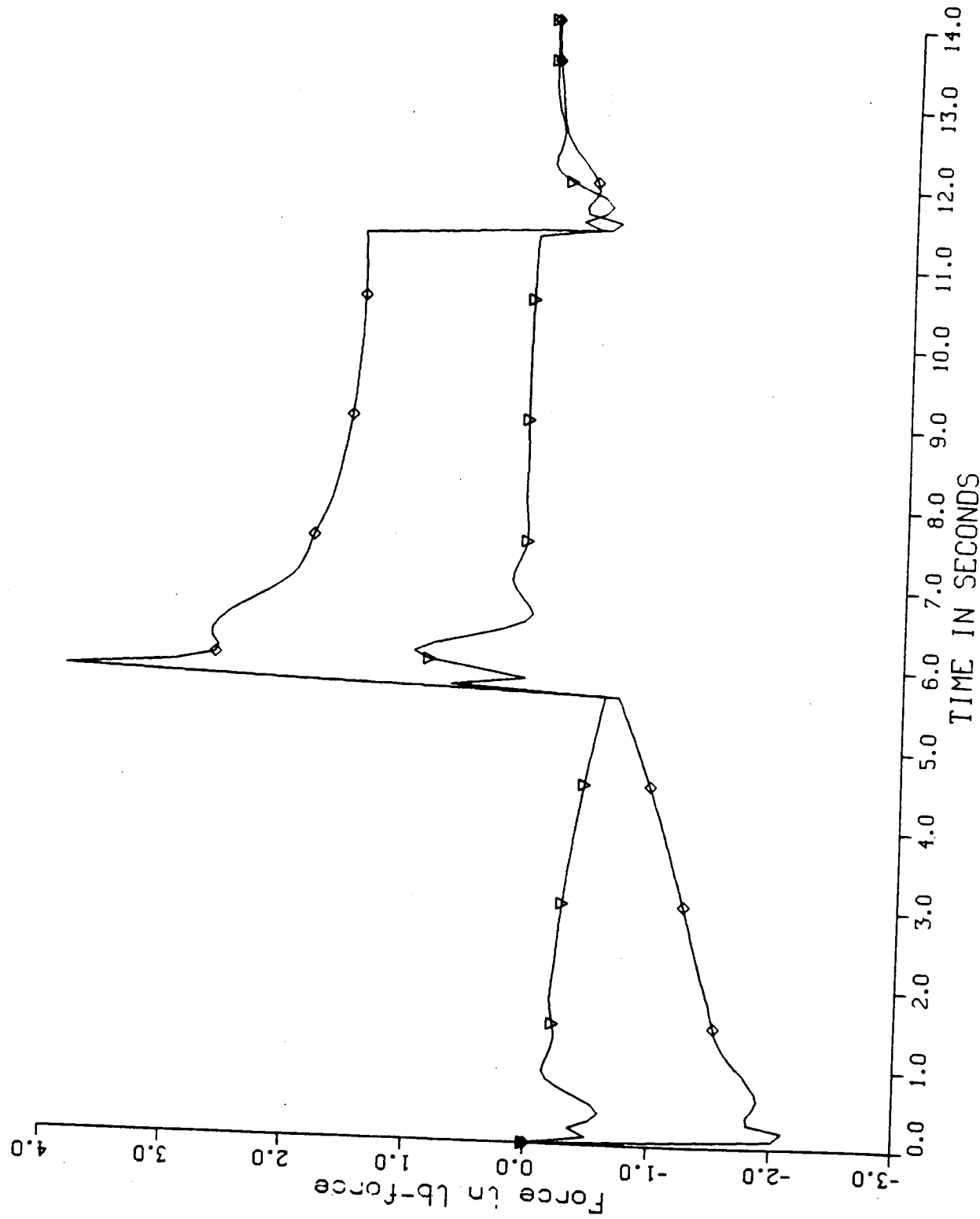


Control torques applied at reflector



Forces applied at reflector

— 1 —



CONCLUSIONS

1. PROOF-MASS ACTUATORS CAN REDUCE FLEXURE AMPLITUDE AND DAMP OSCILLATIONS
2. AMPLITUDE OF DEFORMATIONS DURING SLEW IS RELATIVELY INSENSITIVE TO PLACEMENT OF ACTUATORS
3. DAMPING FACTOR OF OSCILLATIONS IS SENSITIVE TO PLACEMENT OF ACTUATORS
4. DEGREE OF CONTROLLABILITY METHOD INDICATES MOST EFFECTIVE PLACEMENT FOR ACTUATORS

FUTURE DIRECTIONS

1. INCLUDE NOISE AND TIME DELAYS
IN SENSORS AND ACTUATORS
KALMAN FILTER.
2. "CLOSE THE LOOP" BY SIMULATING THE
EXPERIMENTAL TEST MODEL OF SCOLE.

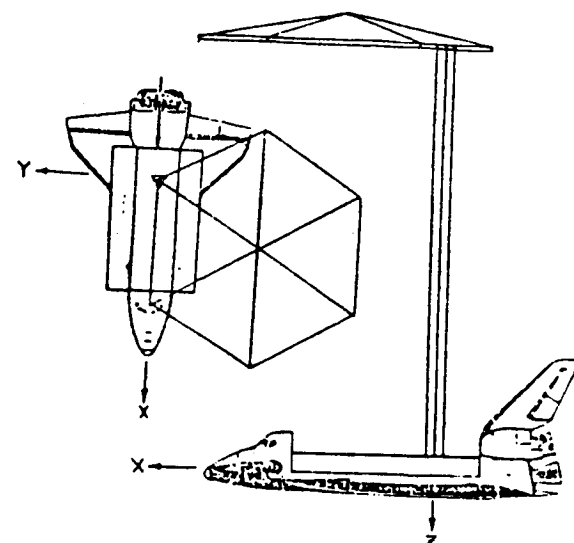
N87-17831

Active Damping of Vibrations in SCOLE Excited by Slewing

by

**Jiguang Gene Lin
Control Research Corp.**

ACTIVE DAMPING OF VIBRATIONS IN SCOPE
EXCITED BY MINIMUM-TIME RAPID SLEWING



JIGUAN GENE LIN
CONTROL RESEARCH CORPORATION
LEXINGTON, MA 02173

INTRODUCTION

HIGHLIGHTS OF NUMERICAL RESULTS

MINIMUM-TIME RAPID LOS POINTING SLEW FOR SCOLE

ADAPTATION OF LOS ERROR EXPRESSION

CONCEPT OF "MODAL DASHPOTS"

MODAL-DASHPOT VIBRATION CONTROLLERS
-- DESIGN AND SIMULATION RESULTS

CONCEPT OF "MODAL SPRINGS"

MODAL-SPRING VIBRATION CONTROLLERS
-- DESIGN AND SIMULATION RESULTS

COMBINED USE OF MODAL DASHPIOTS AND SPRINGS
-- MORE DESIGN AND SIMULATION RESULTS

CONCLUSIONS

HIGHLIGHTS OF NUMERICAL SIMULATION RESULTS

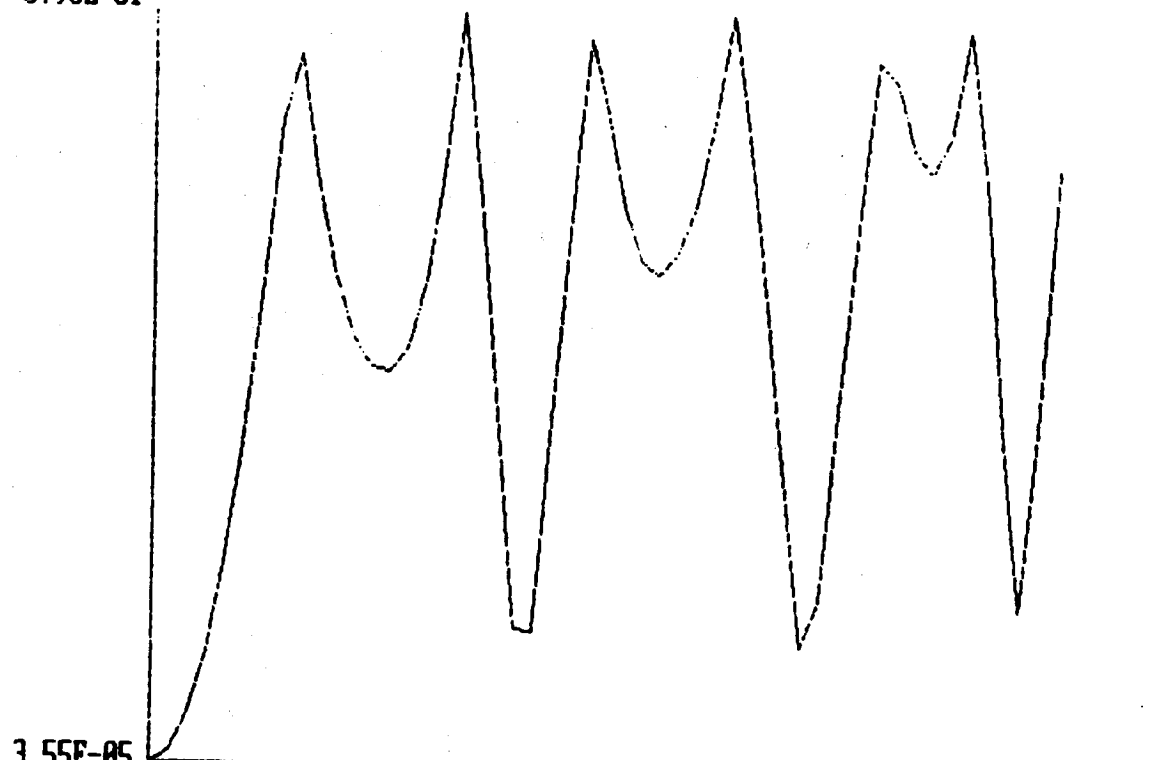
F0000: BPB SLEW EXCITATION 10,000 lb-ft on Shuttle, 800 lb on Refl.
F0010: ACTIVE DAMPING AFTER EXCITATION 5 deg/sec rate lim

F0100: ACTIVE STIFFENING DURING EXCITATION
F2100: ACTIVE DAMPING & STIFFENING
DURING EXCITATION
F3100: SAME

F0110: ACTIVE DAMPING & STIFFENING
DURING AND AFTER EXCITATION
F2110: SAME
F3110: SAME

F125: BB SLEW EXCITATION; 10,000 lb-ft on Shuttle
25 lb on Reflector

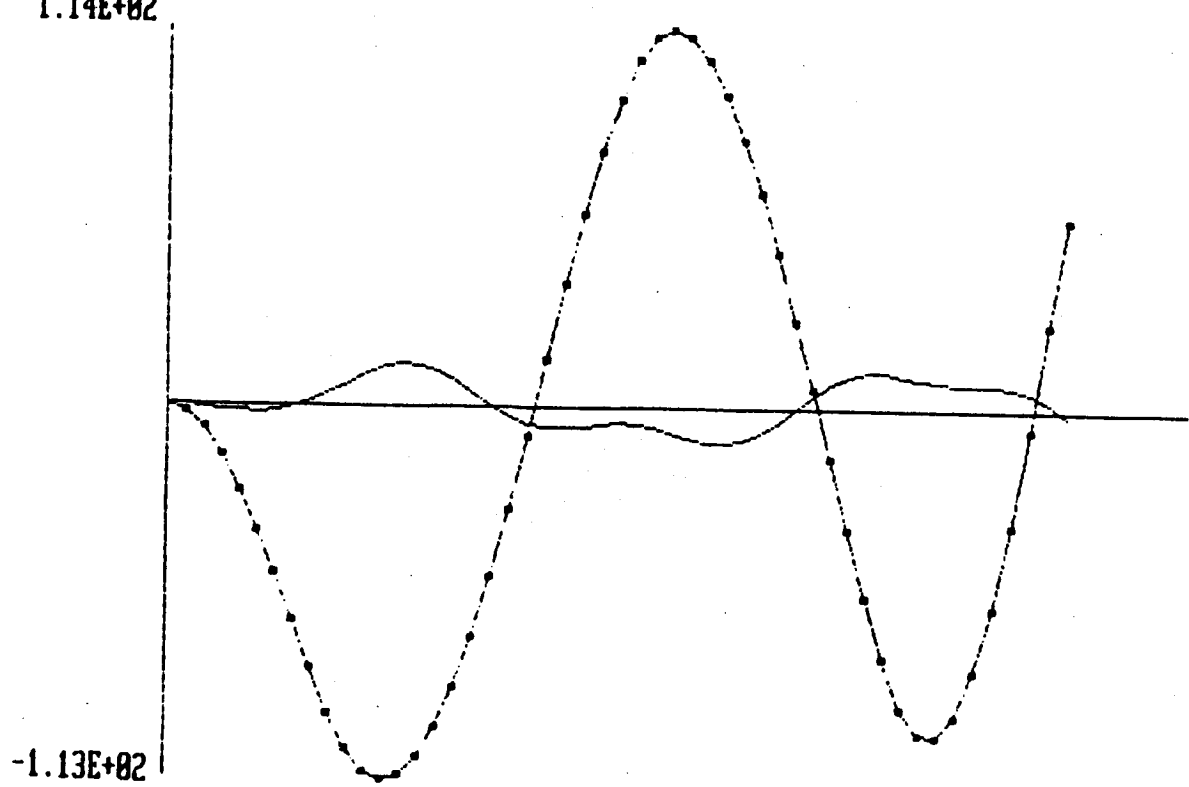
8.98E+01



LOS ERROR (DEG) RUN TIME= 4.892 pf0000.6na

LCOPY

1.14E+02

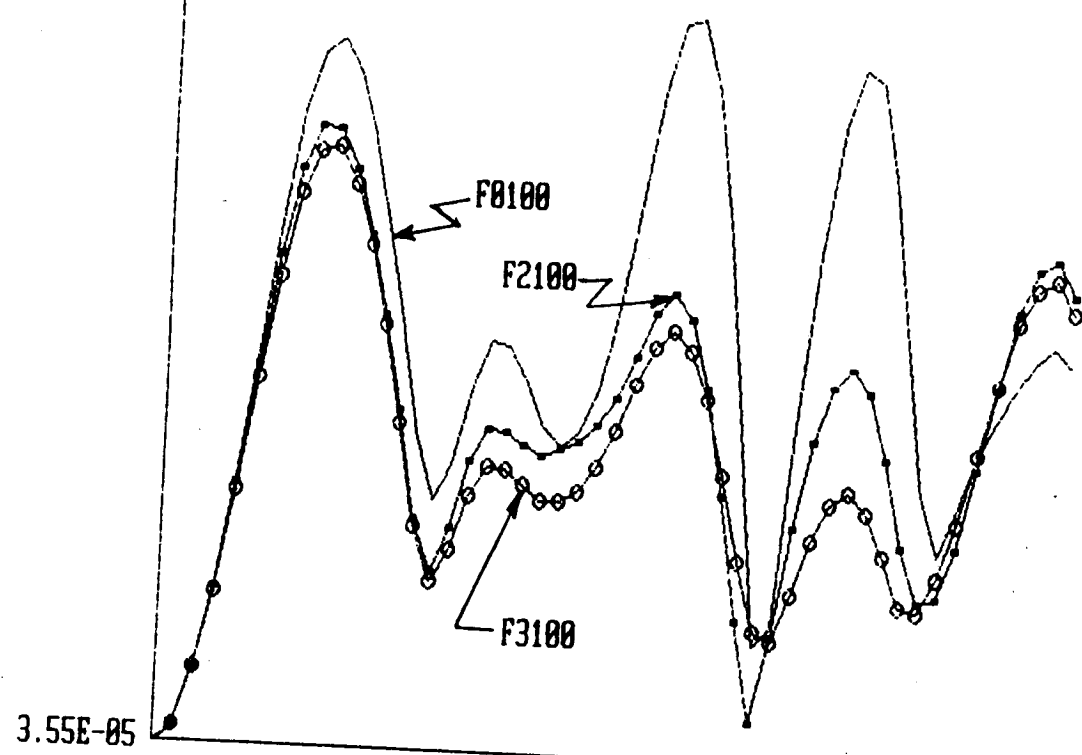


Y14 RUN TIME = 4.892 pf0000.6na

1 runov

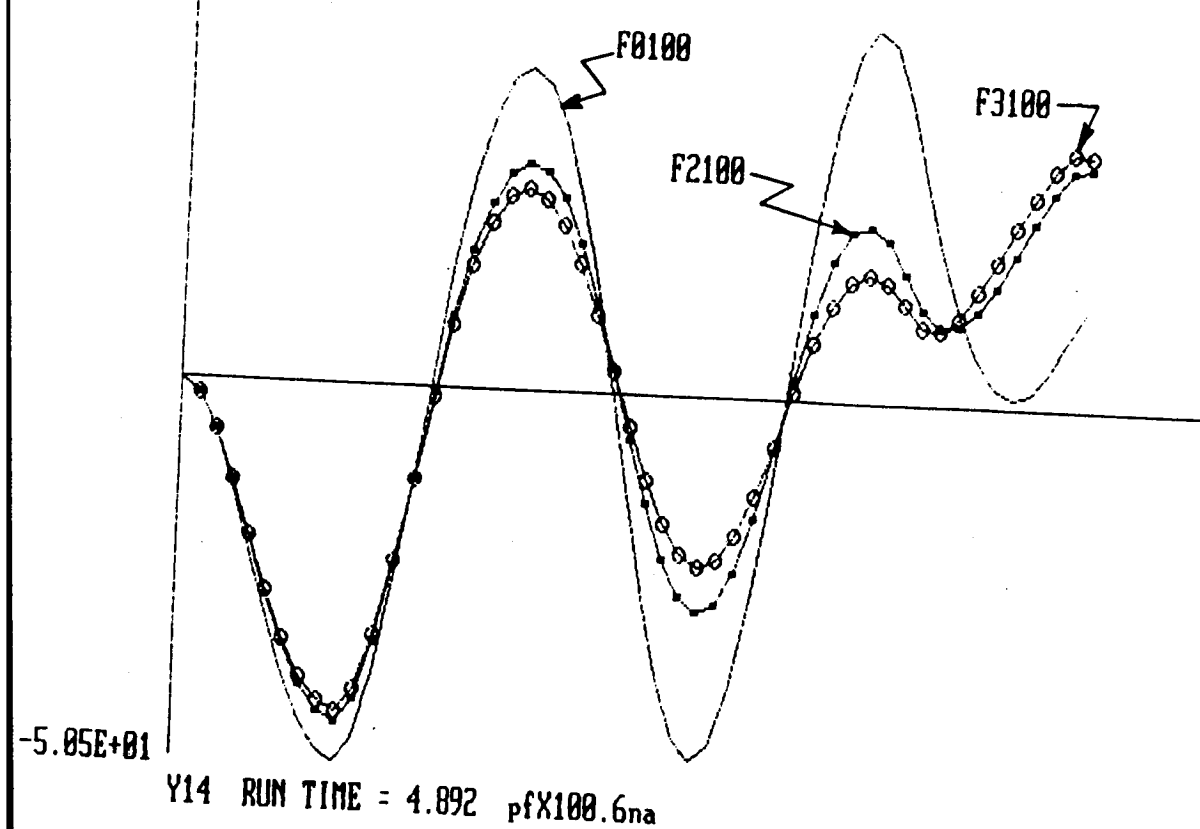
265

5.95E+01

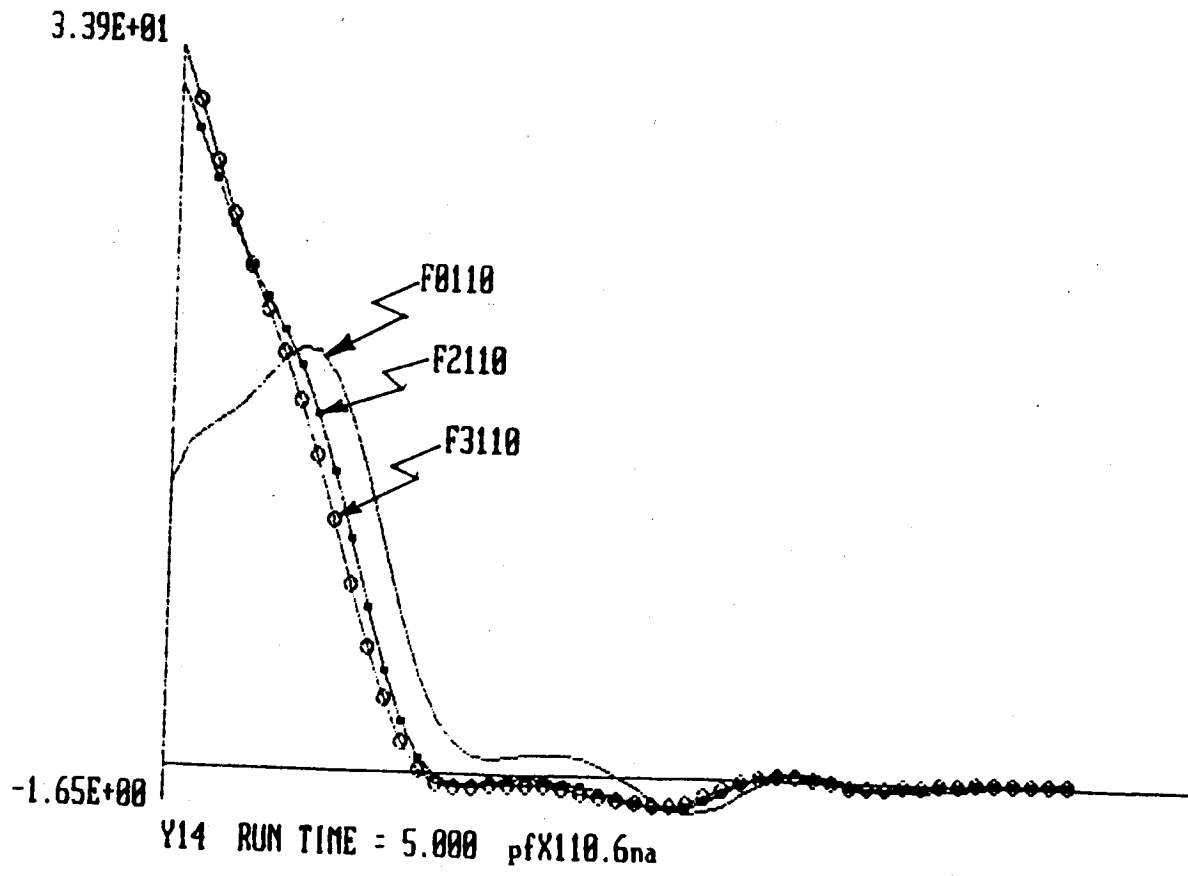
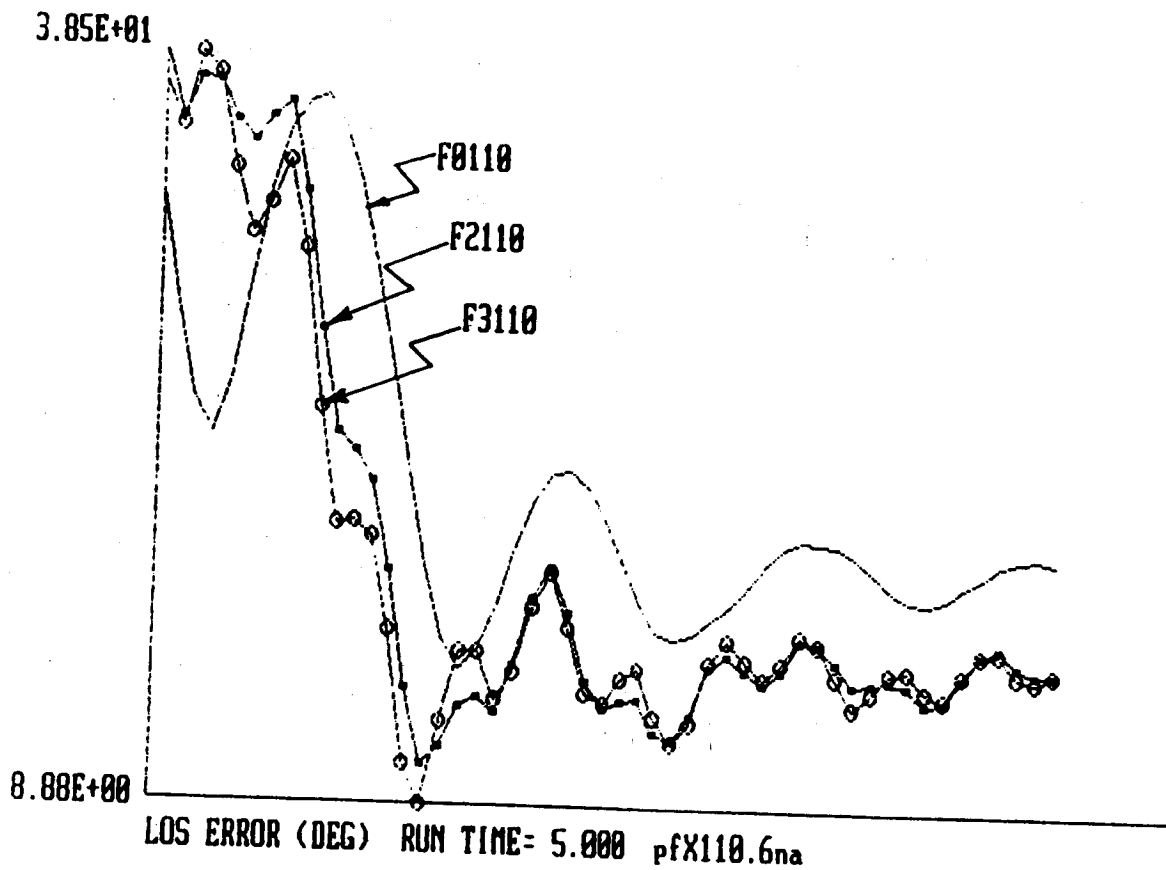


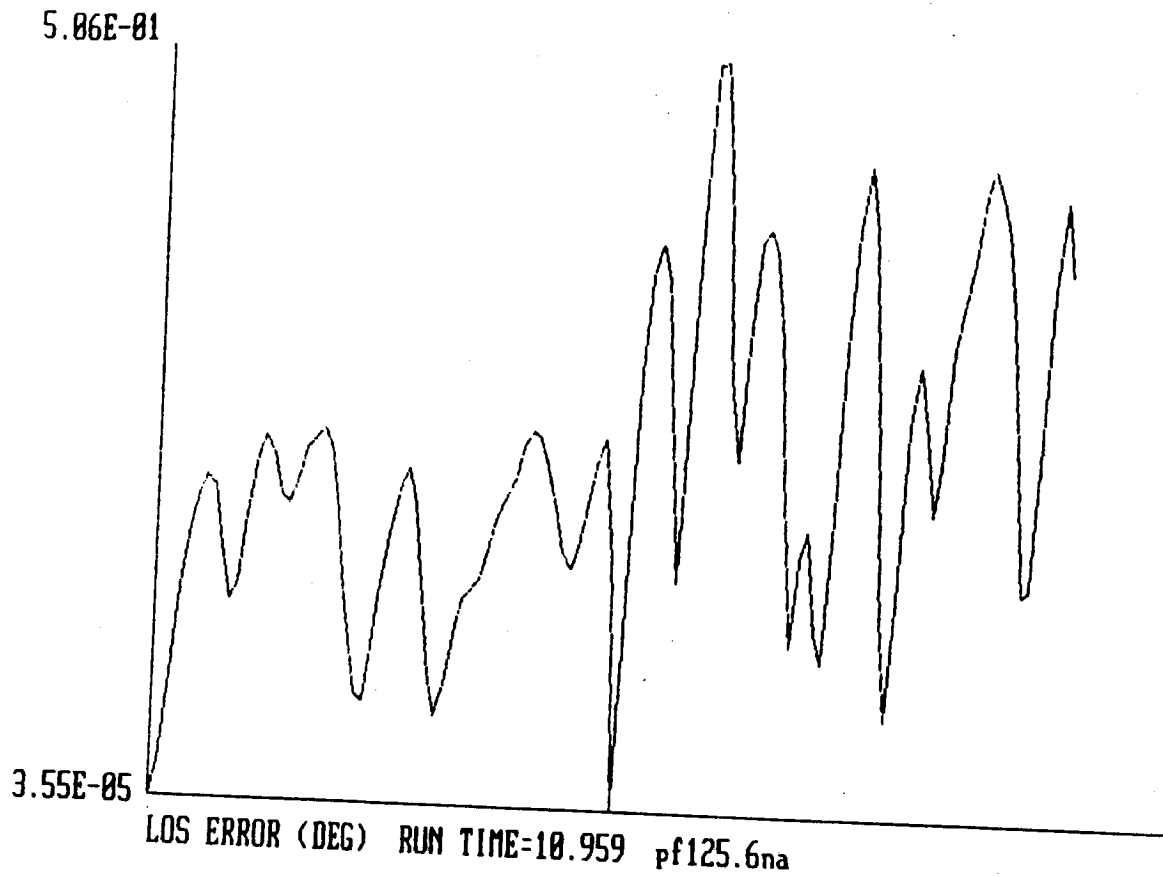
LOS ERROR (DEG) RUN TIME= 4.892 pfX100.6na

5.01E+01



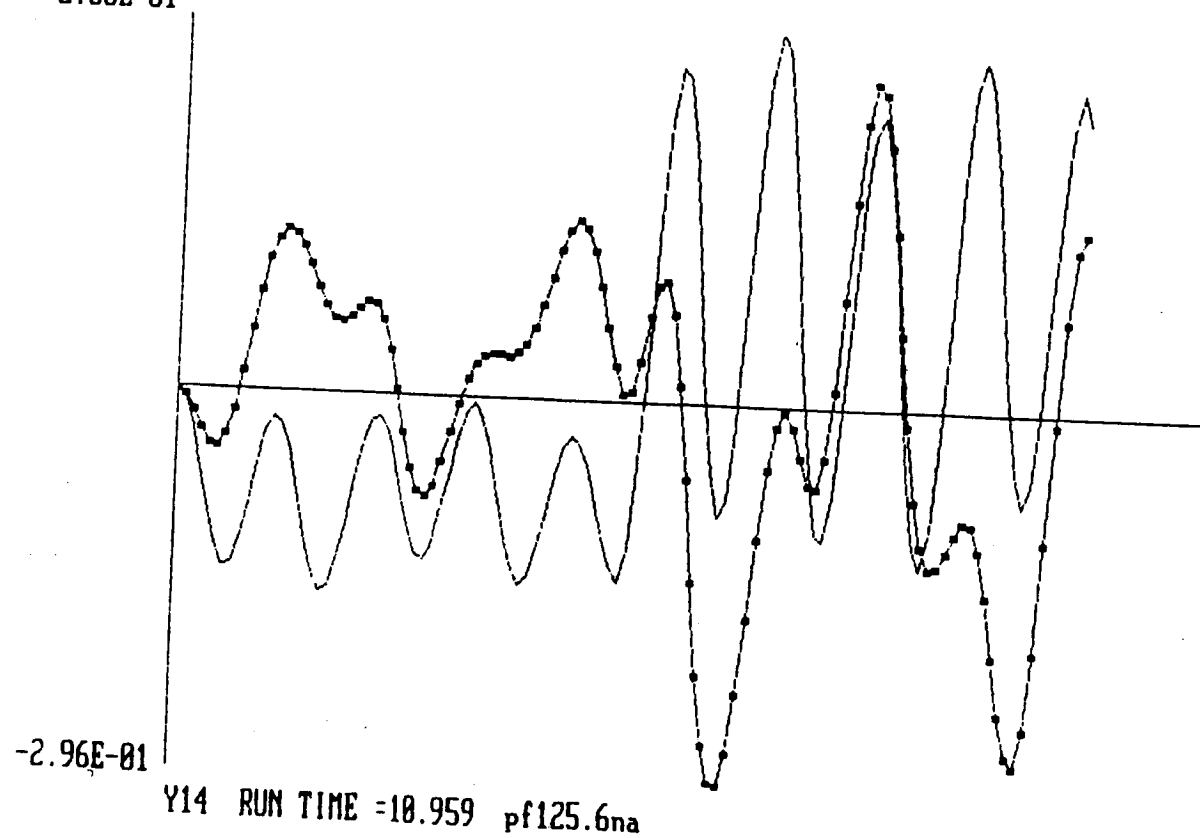
Y14 RUN TIME = 4.892 pfX100.6na





LCOPY

2.88E-01



LCOPY

268

LINE-OF-SIGHT ERROR--GENERAL VECTOR EXPRESSION

o $\underline{F_R} = \text{RAY OF EMISSION} = \underline{R_R} - \underline{R_F}$

$\underline{F' R} = \text{REFLECTED RAY} = \text{LOS VECTOR} = \underline{R_{LOS}}$

o $\underline{RF'} = \underline{F_R} + 2\underline{RR'}$ SINCE

$$\underline{F_R} + \underline{RF'} = \underline{FF'} ; \quad \underline{F_R} + \underline{RR'} = \underline{FR'} ; \quad \underline{FF'} = 2\underline{FR'}$$

o $\underline{RR'} = (\underline{RF} \cdot \underline{R_A})\underline{R_A} = -(\underline{F_R} \cdot \underline{R_A})\underline{R_A}$

o IN UN-NORMALIZED FORM:

$$\underline{R_{LOS}} = \underline{RF'} = \underline{R_R} - \underline{R_F} - 2[(\underline{R_R} - \underline{R_F}) \cdot \underline{R_A}]\underline{R_A}$$

o TRANSFORMING TO INERTIAL FRAME,
FORMING CROSS-PRODUCT WITH TARGET DIRECTION,

$$\begin{aligned} ||\underline{D_T} \times \underline{T_1 R_{LOS}}|| &= ||\underline{D_T}|| \cdot ||\underline{T_1 R_{LOS}}|| \cdot |\sin \epsilon_{LOS}| \\ &= ||\underline{R_{LOS}}|| \cdot |\sin \epsilon_{LOS}| \end{aligned}$$

o TAKING PRINCIPAL VALUE

$$\epsilon_{LOS} = \pm \sin^{-1} [||\underline{D_T} \times \underline{T_1 R_{LOS}}|| \cdot ||\underline{R_{LOS}}||]$$

LINE-OF-SIGHT ERROR -- GENERAL MATRIX EXPRESSION

O $\mathbf{R}_A = \begin{bmatrix} R_{Ax} \\ R_{Ay} \\ R_{Az} \end{bmatrix}$ IN REFLECTOR'S BODY AXES

O $\mathbf{R}_R - \mathbf{R}_F = \begin{bmatrix} 18.75 \\ -32.5 \\ -130 \end{bmatrix} - \begin{bmatrix} 3.75 \\ 0 \\ 0 \end{bmatrix} = \begin{bmatrix} 15 \\ -32.5 \\ -130 \end{bmatrix}$

O $(\mathbf{R}_R - \mathbf{R}_F)^T \mathbf{R}_A = [15 \ -32.5 \ -130] \begin{bmatrix} R_{Ax} \\ R_{Ay} \\ R_{Az} \end{bmatrix}$
 $= 15R_{Ax} - 32.5R_{Ay} - 130R_{Az}$

$$\boxed{\mathbf{R}_{LOS} = \begin{bmatrix} 15 \\ -32.5 \\ -130 \end{bmatrix} - 2(15R_{Ax} - 32.5R_{Ay} - 130R_{Az}) \begin{bmatrix} R_{Ax} \\ R_{Ay} \\ R_{Az} \end{bmatrix}$$

$$= \begin{bmatrix} -2(15R_{Ax} - 32.5R_{Ay} - 130R_{Az})R_{Ax} + 15 \\ -2(15R_{Ax} - 32.5R_{Ay} - 130R_{Az})R_{Ay} - 32.5 \\ -2(15R_{Ax} - 32.5R_{Ay} - 130R_{Az})R_{Az} - 130 \end{bmatrix}}$$

O $\mathbf{D}_T = \begin{bmatrix} 0 \\ 0 \\ 1 \end{bmatrix} \quad [\mathbf{D}_T \mathbf{x}] = \begin{bmatrix} 0 & -1 & 0 \\ 1 & 0 & 0 \\ 0 & 0 & 0 \end{bmatrix}$

$$[\mathbf{T}_1 \mathbf{R}_{LOS}] = \begin{bmatrix} (\mathbf{T}_1 \mathbf{R}_{LOS})_x \\ (\mathbf{T}_1 \mathbf{R}_{LOS})_y \\ (\mathbf{T}_1 \mathbf{R}_{LOS})_z \end{bmatrix} \quad [\mathbf{D}_T \mathbf{x} \ \mathbf{T}_1 \mathbf{R}_{LOS}] = \begin{bmatrix} -(\mathbf{T}_1 \mathbf{R}_{LOS})_y \\ (\mathbf{T}_1 \mathbf{R}_{LOS})_x \\ 0 \end{bmatrix}$$

$$||\mathbf{D}_T \mathbf{x} \ \mathbf{T}_1 \mathbf{R}_{LOS}|| = \sqrt{[(\mathbf{T}_1 \mathbf{R}_{LOS})_x]^2 + [(\mathbf{T}_1 \mathbf{R}_{LOS})_y]^2}$$

MORE ON LOS ERROR EXPRESSION --

INCLUSION OF MAST BENDING AND TORSION

$$R_R - R_F = R_T - T_1^T T_4 R_B - R_F$$

WHERE

$$R_T = \begin{bmatrix} \text{BEND}_x \\ \text{BEND}_y \\ -\sqrt{130^2 - \text{BEND}_x^2 - \text{BEND}_y^2} \end{bmatrix}$$

$$R_B = \begin{bmatrix} 18.75 \\ -32.5 \\ 0 \end{bmatrix} \quad R_F = \begin{bmatrix} 3.75 \\ 0 \\ 0 \end{bmatrix}$$

$$\text{BEND}_x = u_x(4) - u_x(1)$$

$$\text{BEND}_y = u_y(4) - u_y(1)$$

⋮
⋮
⋮
⋮

$$LOS_x = -(T_1 R_{LOS})_y = -T_{1ry} R_{LOS}$$

$$= \left[2T_{4yz} T_{4xz}, -1 + 2T_{4yz}^2, -2T_{4yz} T_{4zz} \right] T_1 \left[R_T - R_F \right] \\ + T_{4ry} R_B$$

$$LOS_y = (T_1 R_{LOS})_x = T_{1rx} R_{LOS}$$

$$= \left[1 - 2T_{4xz}^2, -2T_{4xz} T_{4yz}, -2T_{4xz} T_{4zz} \right] T_1 \left[R_T - R_F \right] \\ + T_{4rx} T_B$$

DYNAMICS:

$$M \frac{d^2 x}{dt^2} + D \frac{dx}{dt} + K x = f$$

FORCE (TORQUE) ACTUATORS AND VELOCITY SENSORS:

$$f = B_F u$$

$$y = C_V \frac{dx}{dt}$$

NORMAL MODAL REPRESENTATION $x = \Phi \eta$:

$$\frac{d^2 \eta}{dt^2} + \Delta \frac{d\eta}{dt} + \Omega^2 \eta = \Phi^T B_F u$$

$$y = C_V \Phi \frac{d\eta}{dt}$$

WHERE

$$\Omega^2 = \text{DIAG}[\omega_i^2] = \Phi^T K \Phi$$

$$\Delta = \Phi^T D \Phi$$

CONTROL LAW FOR CONSTANT-GAIN
VELOCITY-OUTPUT FEEDBACK:

$$u = -G y$$

FULL-ORDER CLOSED-LOOP SYSTEM EQUATION:

$$\frac{d^2 \eta}{dt^2} + \underbrace{(\Delta + \Phi^T B_F G C_V \Phi)}_{\Delta^*} \frac{d\eta}{dt} + \Omega^2 \eta = 0$$

MODAL-DASHPOT APPROACH

DESIGN TO ACHIEVE INDEPENDENT
DAMPING AUGMENTATION FOR EACH MODE IN A
REDUCED-ORDER MODEL

LET ξ_i BE DAMPING RATIO DESIRED OF MODELED MODE i

SET $\underbrace{\Omega_M^T B_F G C_v \Omega_M}_{\Delta_M^*} = \text{DIAG}[\underbrace{2\xi_i \omega_i}_{\delta_i^*}]$

THEN SOLVE FOR FEEDBACK GAIN MATRIX G ,

$$G = (\Omega_M^T B_F)^T \text{DIAG}[\underbrace{2\xi_i \omega_i}_{\delta_i^*}] (C_v \Omega_M)^T$$

USING THE PSEUDO-INVERSES $(\cdot)^T$ DEFINED AS FOLLOWS

$$(\Omega_M^T B_F)^T = (\Omega_M^T B_F)^T [(\Omega_M^T B_F) (\Omega_M^T B_F)^T]^{-1}$$

$$(C_v \Omega_M)^T = [(\Omega_M^T B_F)^T (C_v \Omega_M)]^{-1} (\Omega_M^T B_F)^T$$

- NEVER DESTABILIZE LARGE FLEXIBLE SPACE STRUCTURES WHEN THE ACTUATORS ARE CO-LOCATED WITH THE SENSORS
- WITHIN THE REDUCED-ORDER DESIGN MODEL, ANY AMOUNT OF DAMPING DESIRED CAN BE ADDED TO ANY MODE EXACTLY

NUMERICAL ANALYSIS OF VIBRATION MODES

1. LOS ERROR DUE TO UNIT INITIAL MODAL DISPLACEMENT

MODE	1	2	3	4	5	6	7	8	9	10
PEAK	.37	.53	.54	.93	1.3	.14	.51	.002	.18	.03
	====>	5,	4,	3,	2,	7,	1,	9,	6,	10,

2. MODAL DISPLACEMENT DUE TO RAPID POINTING SLEW

MODE	1	2	3	4	5
PEAK	21.6	603	41.2	13.7	0.49
	====>	2,	3,	1,	4,

WHICH MODES REALLY REQUIRE ACTIVE CONTROL?

NEED AN ALTERNATIVE AND MORE INDICATIVE MEASURE !!!

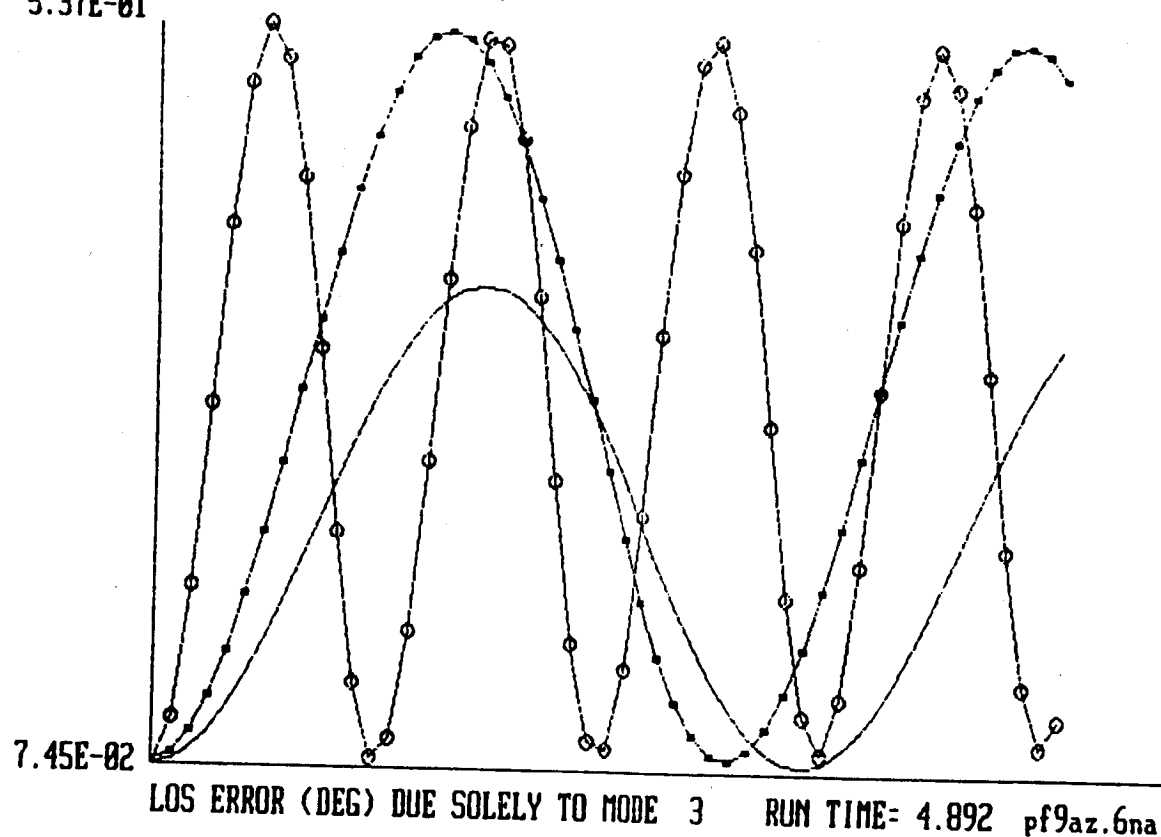
3. LOS ERROR SOLELY DUE TO EACH MODE EXCITED BY THE SLEW

MODE	1	2	3	4	5
PEAK	3.26	88.6(?)	9.57	6.53	0.33
	====>	2,	3,	1,	4 (OR 4, 1), 5, 7, 6, ...

A SOUND MEASURE OF THE SIGNIFICANCE OF EACH MODE:

INPUT (SLEW EXCITATION) AND OUTPUT (LOS ERROR)
DULY COMBINED

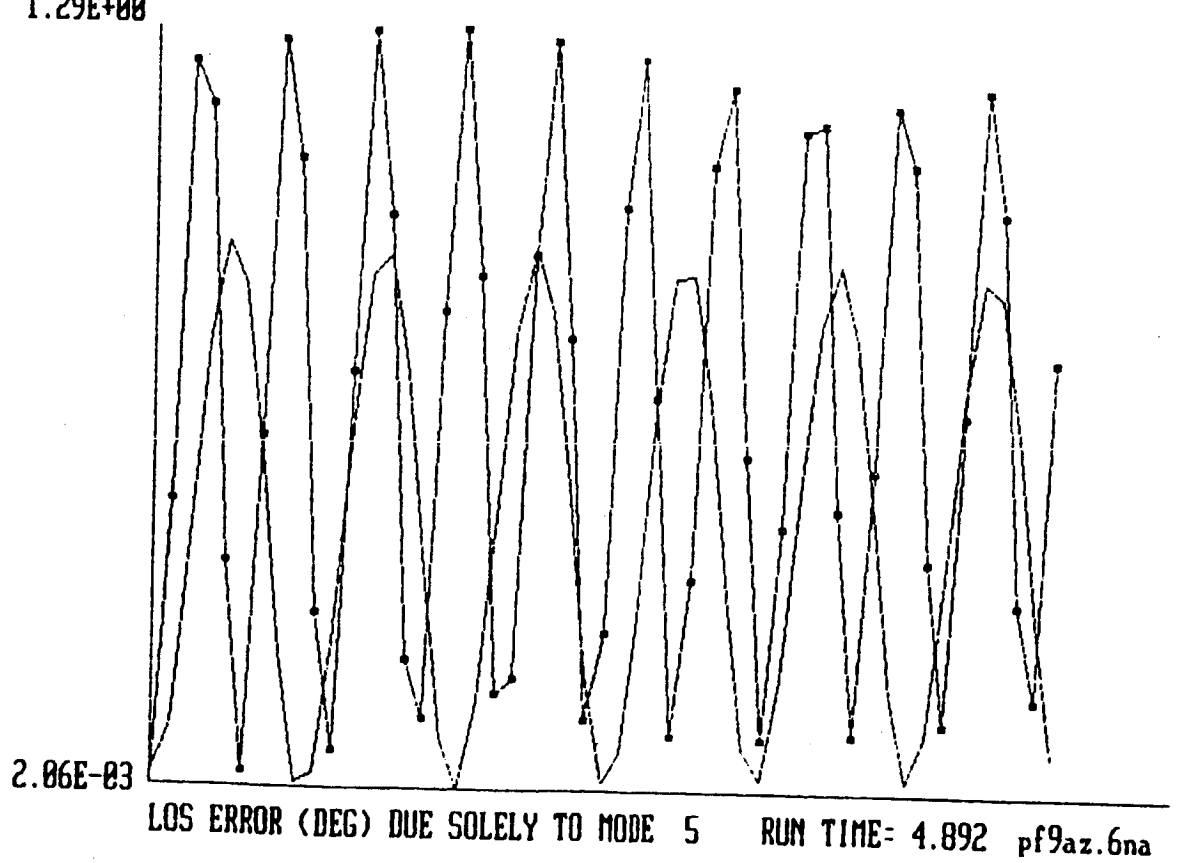
5.37E-01



LOS ERROR (DEG) DUE SOLELY TO MODE 3 RUN TIME = 4.892 pf9az.6na

LCOPY

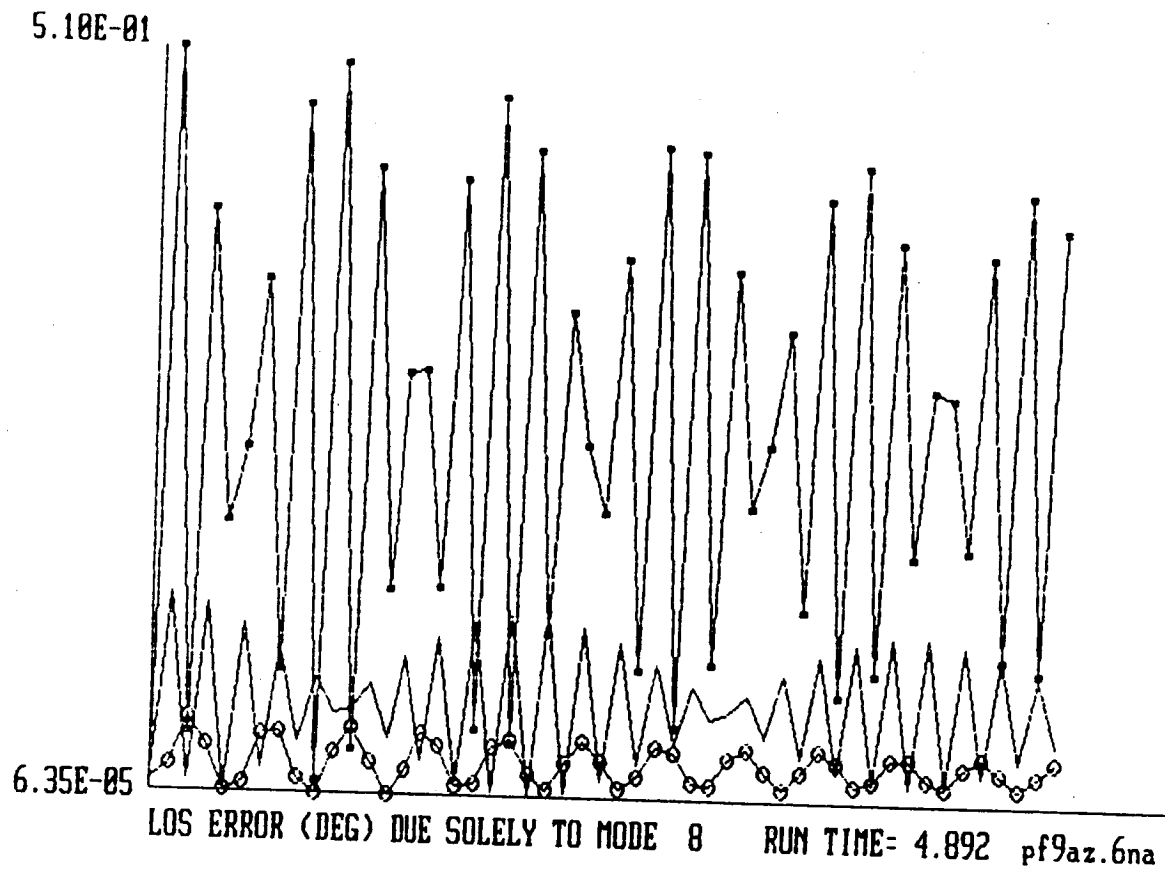
1.29E+00



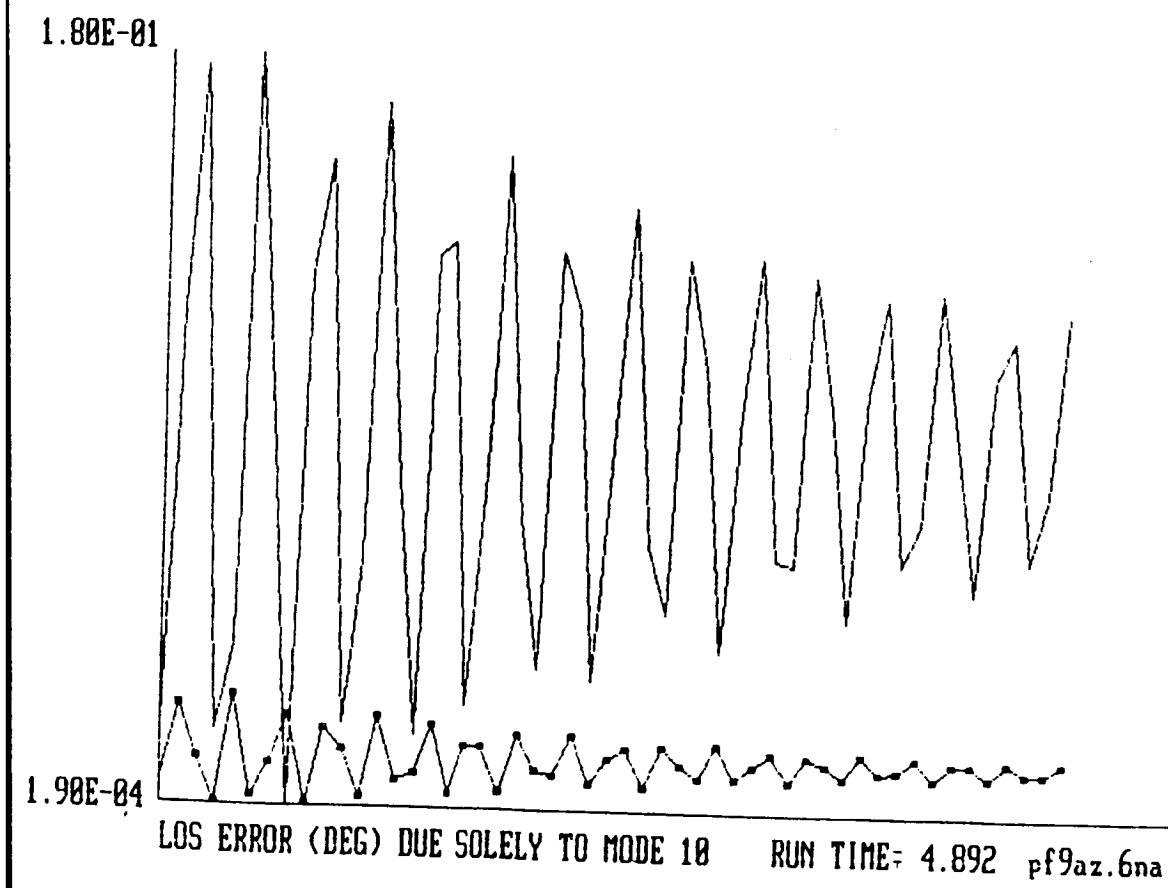
LOS ERROR (DEG) DUE SOLELY TO MODE 5 RUN TIME = 4.892 pf9az.6na

LCOPY

275

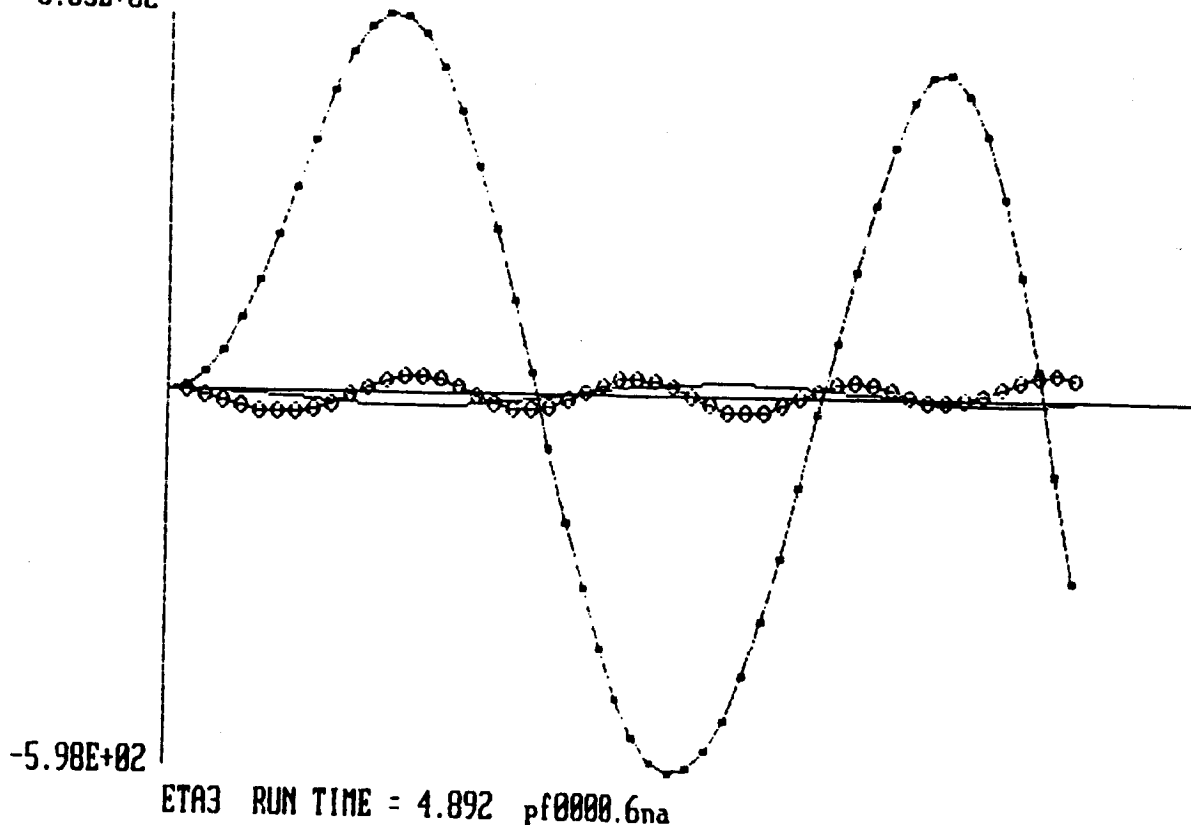


LCOPY



LCOPY

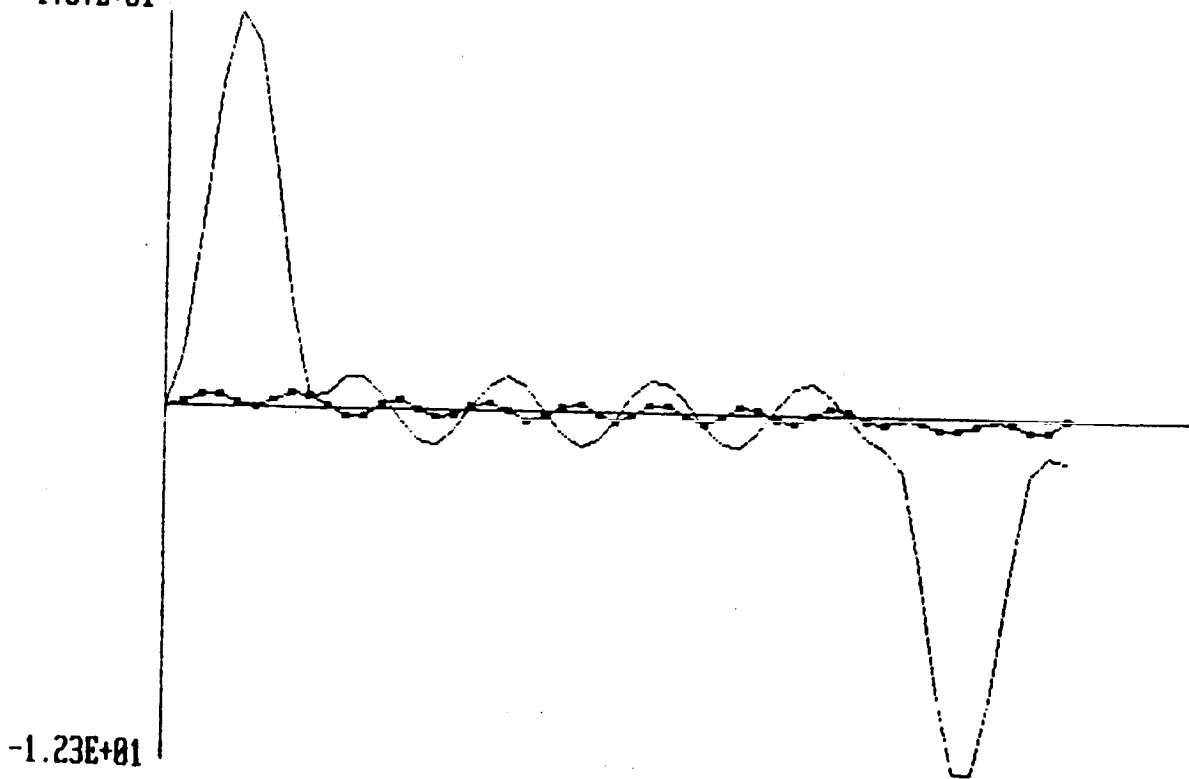
6.03E+02



ETA3 RUN TIME = 4.892 pf0000.6na

LCOPY

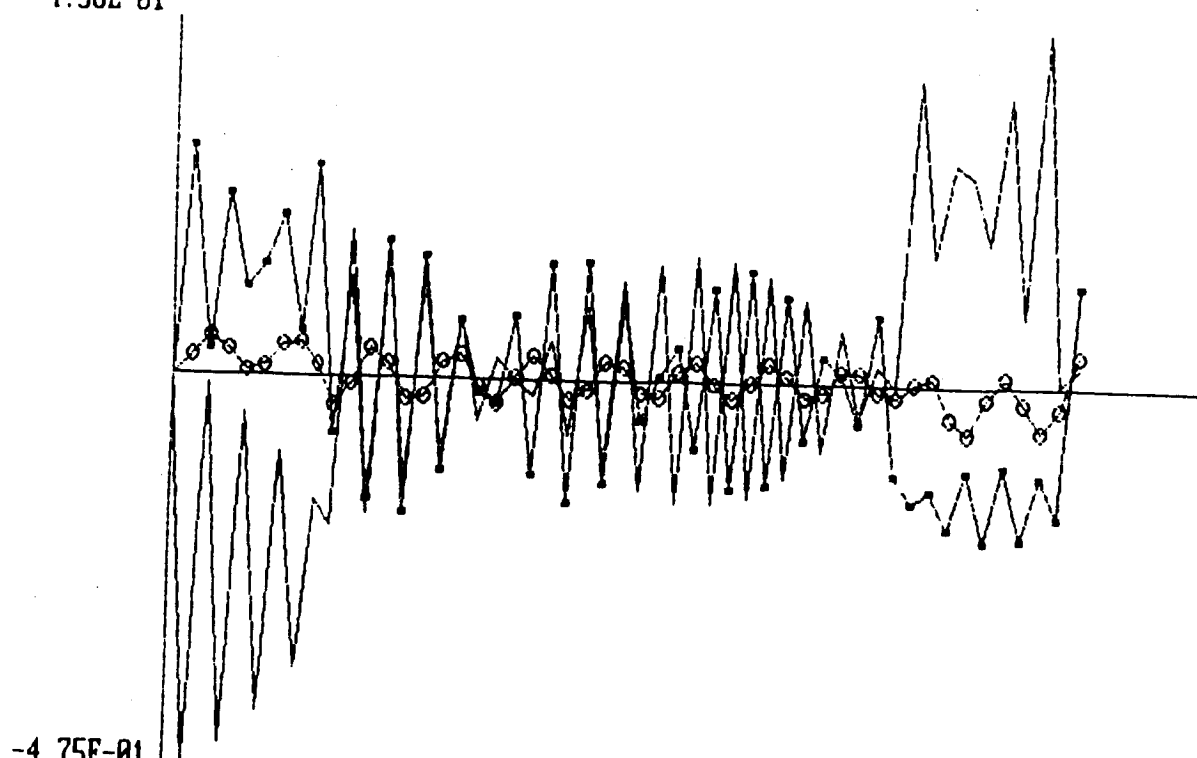
1.37E+01



ETA5 RUN TIME = 4.892 pf0000.6na

LCOPY

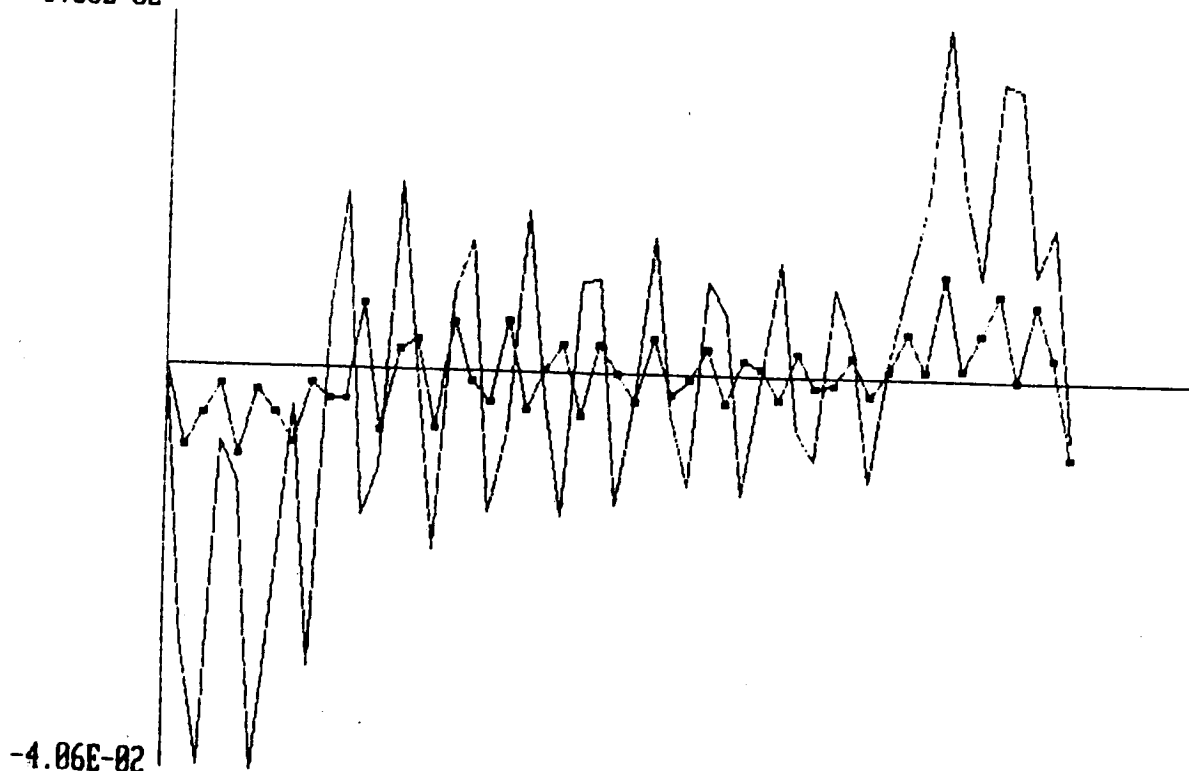
277



ETA8 RUN TIME = 4.892 pf0000.6na

LCOPY

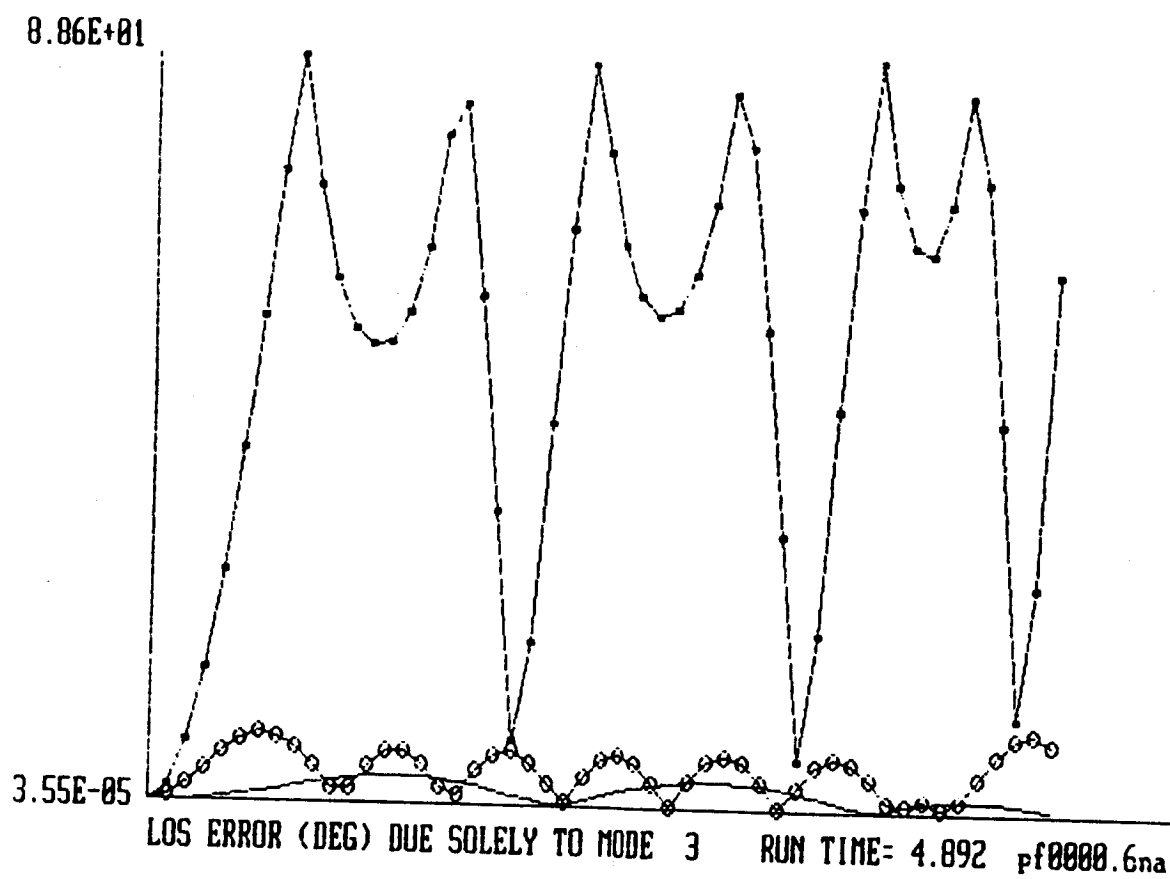
3.56E-02



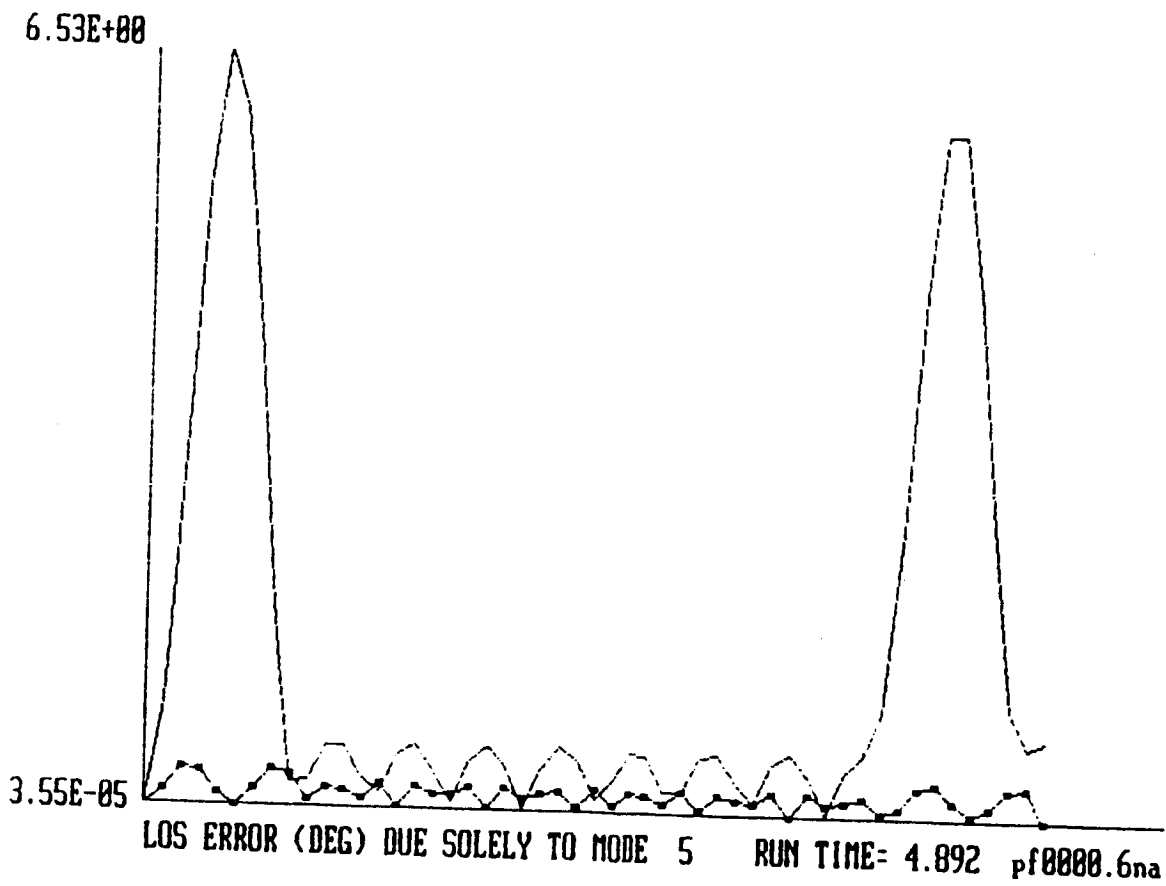
ETA10 RUN TIME = 4.892 pf0000.6na

LCOPY

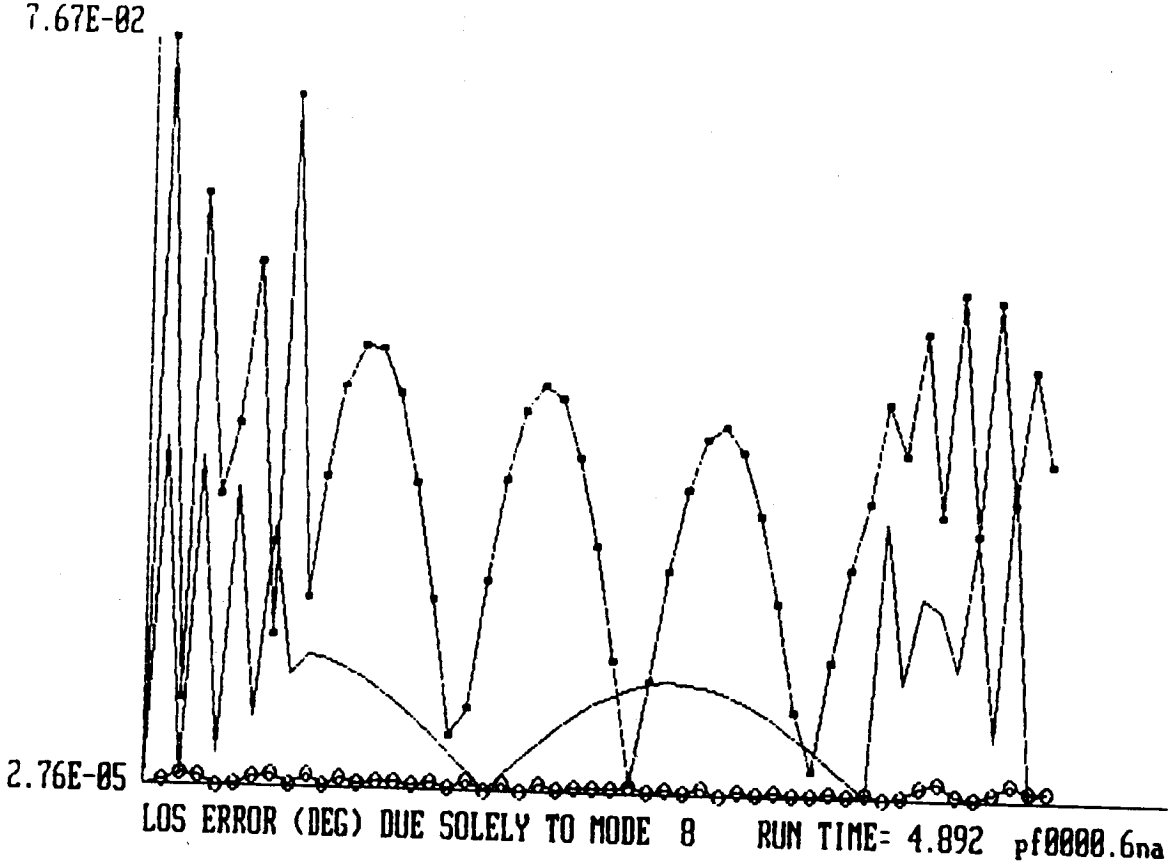
278



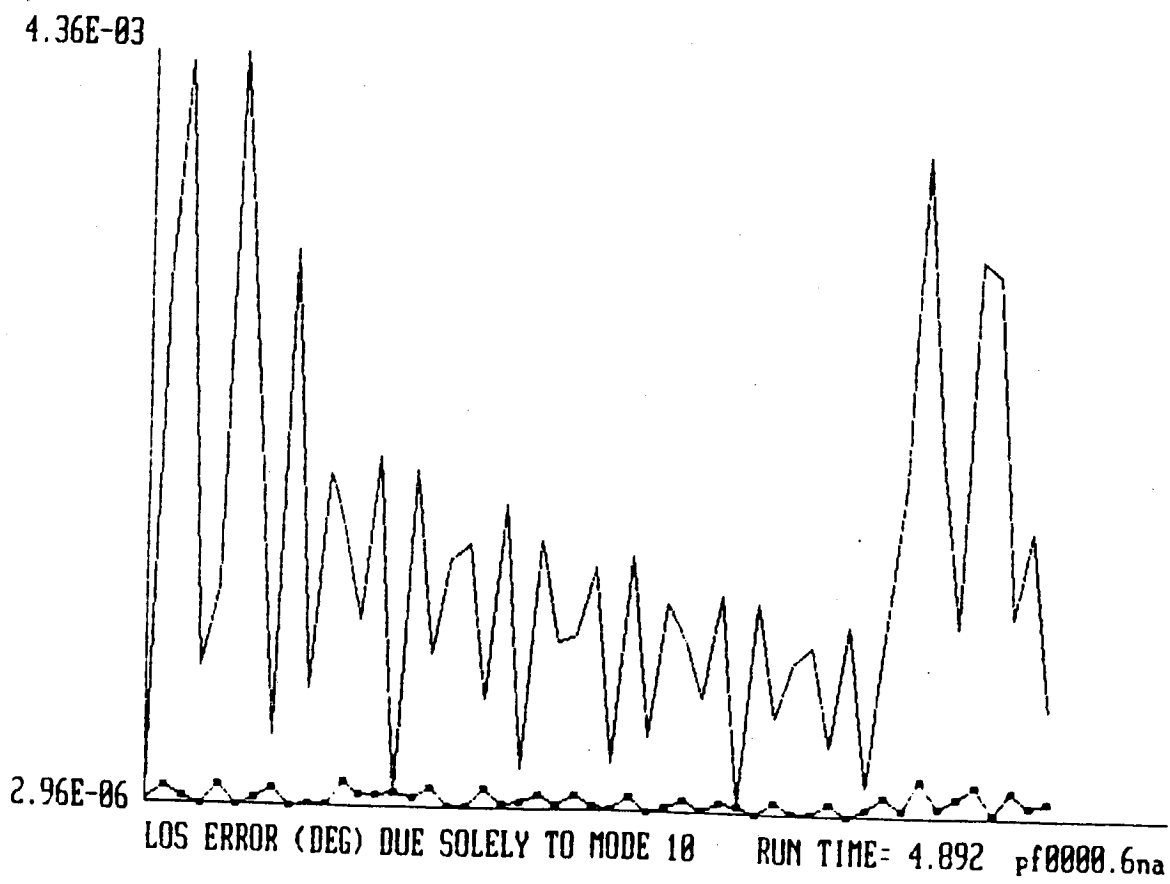
LCOPY



LCOPY



LCOPY



LCOPY

280

ACTUATOR/SENSOR INFLUENCE ON FIRST 10 MODES

MODE ACT. 1 - 3 MODE ACT. 4 - 6 MODE ACT. 7 - 8 MODE ACT. 9 - 12

2	0.30019961E-02	5	0.36487188E-01	2	0.14311218E+01	2	0.10711402E+00
4	0.41220308E-03	4	0.25172627E-01	1	0.14061384E+01	1	0.10338868E+00
1	0.40146321E-03	3	0.15999462E-01	3	0.81986851E+00	3	0.10171293E+00
3	0.19184369E-03	2	0.15595800E-01	4	0.39743480E+00	4	0.69439910E-01
5	0.11186474E-03	7	0.14711439E-01	7	0.30395976E+00	9	0.68373762E-01
6	0.69881789E-04	1	0.13037169E-01	9	0.25503686E+00	8	0.67025743E-01
7	0.36829457E-04	9	0.57048416E-02	6	0.21852742E+00	5	0.63191518E-01
8	0.26261532E-04	6	0.34139471E-02	8	0.14623879E+00	10	0.46103600E-01
9	0.15072107E-04	8	0.12352261E-02	10	0.10801539E+00	6	0.39935779E-01
10	0.13497747E-04	10	0.63637015E-03	5	0.74399590E-01	7	0.32263912E-01

MODE SEN. 1 - 3 MODE SEN. 4 - 6 MODE SEN. 7 - 8 MODE SEN. 9 - 12

2	0.28690067E-03	5	0.34890966E-02	2	0.13466856E+00	2	0.10711402E+00
4	0.39390128E-04	3	0.32387748E-02	1	0.12736945E+00	1	0.10338868E+00
1	0.39113598E-04	4	0.24055073E-02	3	0.12407852E+00	3	0.10171293E+00
3	0.18940789E-04	2	0.15346858E-02	4	0.38158901E-01	4	0.69439910E-01
5	0.10689848E-04	7	0.14879148E-02	7	0.36793593E-01	9	0.68373762E-01
6	0.66779044E-05	1	0.13531352E-02	9	0.30879460E-01	8	0.67025743E-01
7	0.35194691E-05	9	0.67911280E-03	6	0.20832075E-01	5	0.63191518E-01
8	0.25095521E-05	6	0.32624099E-03	8	0.14005536E-01	10	0.46103600E-01
9	0.14402938E-05	8	0.11804001E-03	10	0.10299906E-01	6	0.39935779E-01
10	0.12898448E-05	10	0.60812166E-04	5	0.90737212E-02	7	0.32263912E-01

MODAL-DASHPOT MD. 1

PART 1: LINEAR VELOCITY FEEDBACK GAIN GLUR

2 FORCE ACTUATOR ON REFLECTORS

--> U₇ (X AXIS); U₈ (Y AXIS)

2 LINEAR VELOCITY SENSORS AT REFLECTOR END

--> Y₁₅ (X AXIS); Y₁₆ (Y AXIS)

2 "MODELED MODES" FOR DAMPING AUGMENTATION

MODE 1: $\delta_1^* = 2 \times 60 \times \omega_1 = 2.0964$

--> TIME CONSTANT= 0.95 SEC

MODE 2: $\delta_2^* = 2 \times 67 \times \omega_2 = 2.6389$

--> TIME CONSTANT= 0.76 SEC

PART 2: ANGULAR VELOCITY FEEDBACK GAIN GAUR

3 TORQUE ACTUATORS ON REFLECTOR

--> U₄ (X AXIS); U₅ (Y AXIS); U₆ (Z AXIS)

3 ANGULAR VELOCITY SENSORS AT REFLECTOR END

--> Y₁₀ (X AXIS); Y₁₁ (Y AXIS); Y₁₂ (Z AXIS)

3 "MODELED MODES" FOR DAMPING AUGMENTATION

MODE 3: $\delta_3^* = 2 \times 3 \times \omega_3 = 0.3065$

--> TIME CONSTANT= 6.53 SEC

MODE 4: $\delta_4^* = 2 \times 3 \times \omega_4 = 0.4470$

--> TIME CONSTANT= 4.47 SEC

MODE 5: $\delta_5^* = 2 \times 3 \times \omega_5 = 0.7742$

--> TIME CONSTANT= 2.58 SEC

DYNAMICS: $M \frac{d^2 x}{dt^2} + D \frac{dx}{dt} + K x = f$

FORCE (TORQUE) ACTUATORS AND DISPLACEMENT SENSORS:

$$f = B_F u \quad y = C_D \frac{dx}{dt}$$

CONTROL LAW FOR DISPLACEMENT-OUTPUT FEEDBACK:

$$u = -G_D y$$

FULL-ORDER CLOSED-LOOP SYSTEM EQUATION:

$$\frac{d^2 \eta}{dt^2} + \Delta \frac{d\eta}{dt} + (\Omega^2 + \Phi^T B_F G C_D \Phi) \eta = 0$$

MODAL-SPRING APPROACH

DESIGN TO AUGMENT STIFFNESS TO EACH MODE
OF A REDUCED-ORDER MODEL

LET $\omega_{i\text{NEW}}$ BE DESIRED FREQUENCY FOR MODELED MODE i

SET $\Phi_M^T B_F G C_D \Phi_M = \text{DIAG}[\omega_{i\text{NEW}}^2 - \omega_i^2]$

$$= \text{DIAG}[\sigma_i]$$

THEN SOLVE FOR FEEDBACK GAIN MATRIX G ,

$$G = (\Phi_M^T B_F)^T \text{DIAG}[\sigma_i] (C_D \Phi_M)^T$$

USING THE PSEUDO-INVERSES $(\cdot)^T$ DEFINED AS FOLLOWS

$$(\Phi_M^T B_F)^T = (\Phi_M^T B_F)^T \left[(\Phi_M^T B_F) (\Phi_M^T B_F)^T \right]^{-1}$$

$$(C_D \Phi_M)^T = \left[(C_D \Phi_M)^T (C_D \Phi_M) \right]^{-1} (C_D \Phi_M)^T$$

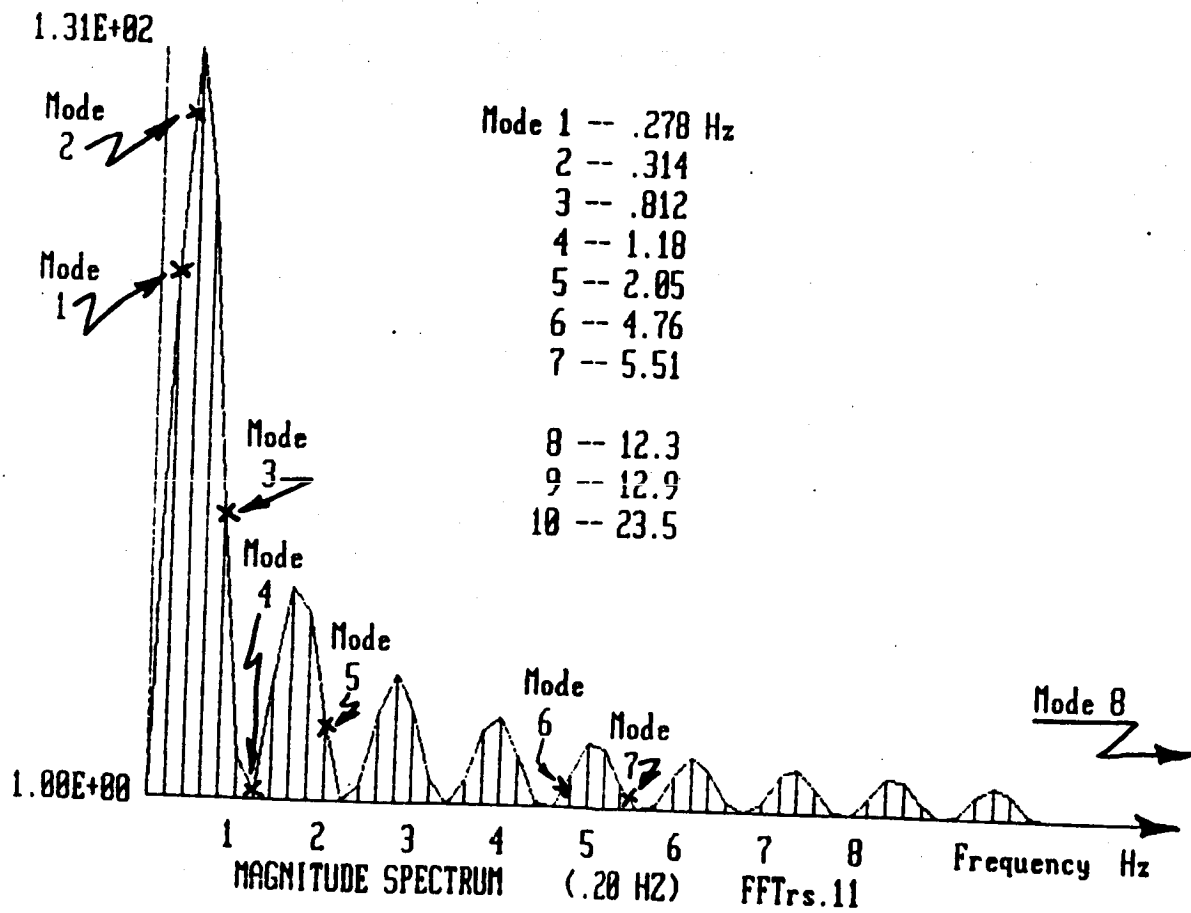
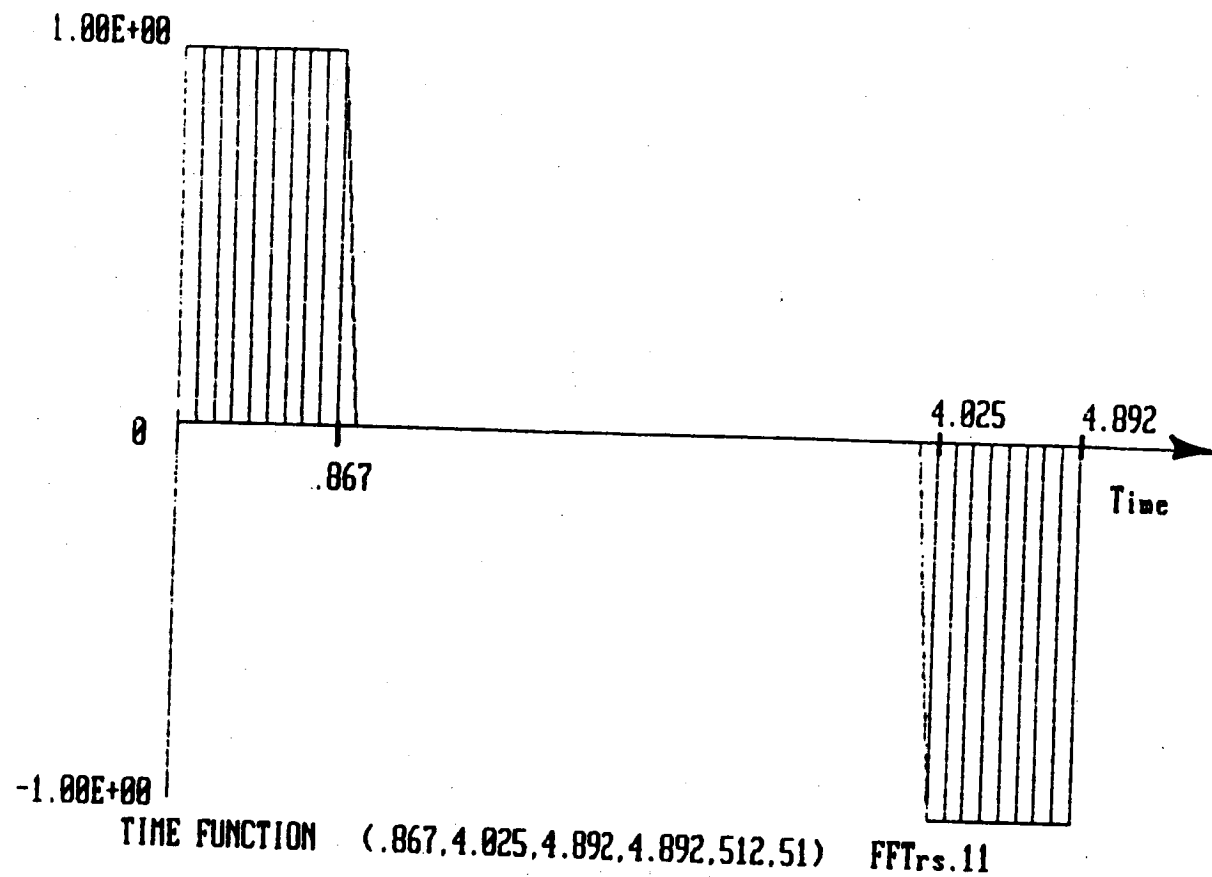
PRE-DESIGN ANALYSES -- MODAL SPRINGS

PLACEMENT OF Z-AXIS PROOF-MASS ACTUATORS

- 1 AT REFLECTOR END
-- PEAK OF MODES 1, 2, 3
- 1 AT 92FT FROM SHUTTLE (70.77% LENGTH)
-- PEAK OF MODE 4

FFT ANALYSIS OF BPB SLEW DISTURBANCE

=> SHIFT MODES 2 & 3 UP AND AWAY !!!
AVOID CONTROL SPILLOVER TO MODE 1 !
IGNORE MODE 4



MODAL-SPRING MS.1

LINEAR DISPLACEMENT FEEDBACK GAIN GLDM

2 2-AXIS PROOF-MASS ACTUATORS ON MAST:

1 AT REFLECTOR END

--> U_9 (X AXIS); U_{10} (Y AXIS)

1 AT 92 FT FROM SHUTTLE (70.77% LENGTH)

--> U_{11} (X AXIS); U_{12} (Y AXIS)

4 LINEAR DISPLACEMENT SENSORS ON MAST:

CO-LOCATED WITH PROOF-MASS ACTUATORS

--> Y_{13} , Y_{17} (X AXIS);

Y_{14} , Y_{18} (Y AXIS)

3 "MODELED MODES" FOR STIFFNESS AUGMENTATION

MODE 1: $\sigma_1^* = 0$

MODE 2: $\sigma_2^* = (2\pi \times 0.7)^2 - (2\pi \times 0.3136)^2$
= 15.4627

MODE 3: $\delta_3^* = (2\pi \times 0.85)^2 - (2\pi \times 0.812)^2$
= 2.4290

MODAL-DASHPOT MD.2

LINEAR VELOCITY FEEDBACK GAIN GLUM

2 2-AXIS PROOF-MASS ACTUATORS ON MAST:

1 AT REFLECTOR END

--> U_9 (X AXIS); U_{10} (Y AXIS)

1 AT 92 FT FROM SHUTTLE (70.77% LENGTH)

--> U_{11} (X AXIS); U_{12} (Y AXIS)

4 LINEAR VELOCITY SENSORS ON MAST:

CO-LOCATED WITH PROOF-MASS ACTUATORS

--> Y_{15} , Y_{19} (X AXIS);

Y_{16} , Y_{20} (Y AXIS)

3 "MODELED MODES" FOR DAMPING AUGMENTATION

MODE 1: $\delta_1^* = 2 \times 2.7 \times \omega_1 = 0.0943$

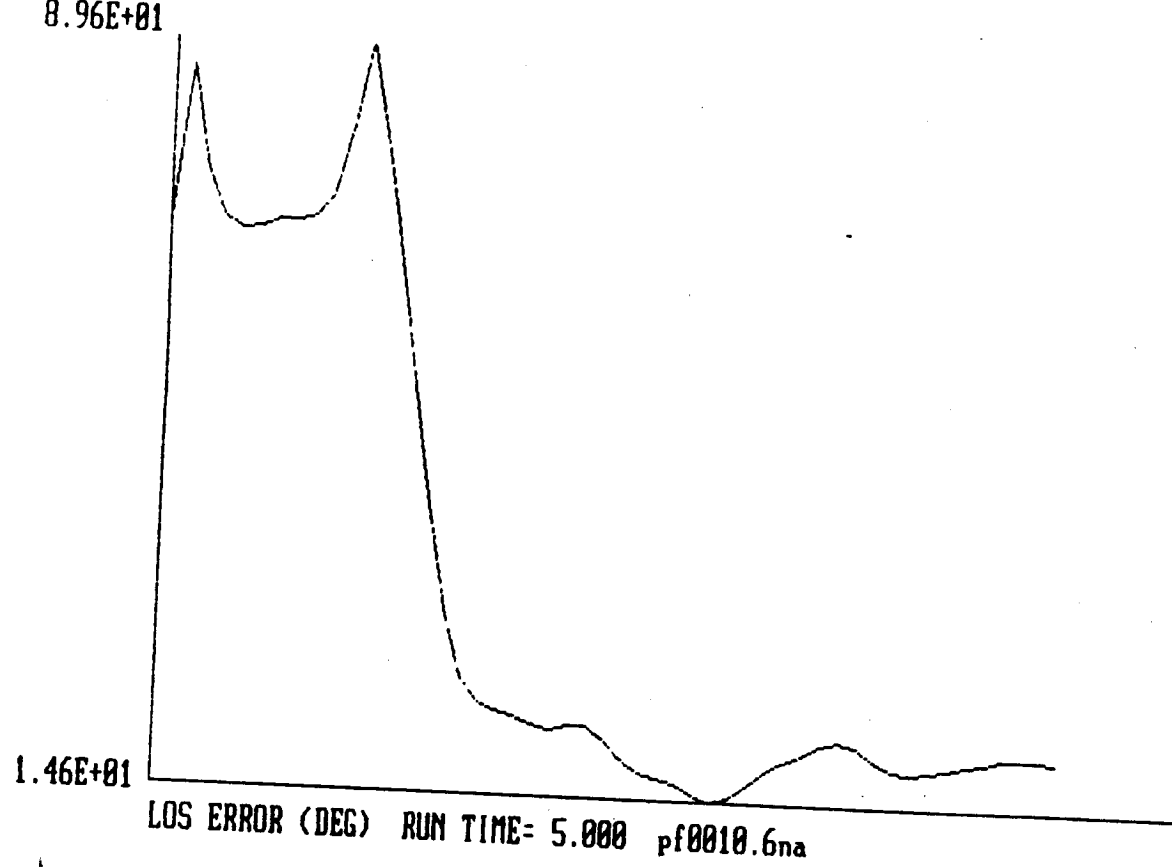
MODE 2: $\delta_2^* = 2 \times 2.7 \times \omega_2(\text{NEW}) = 0.2375$

MODE 3: $\delta_3^* = 2 \times 2.7 \times \omega_3 = 0.2758$

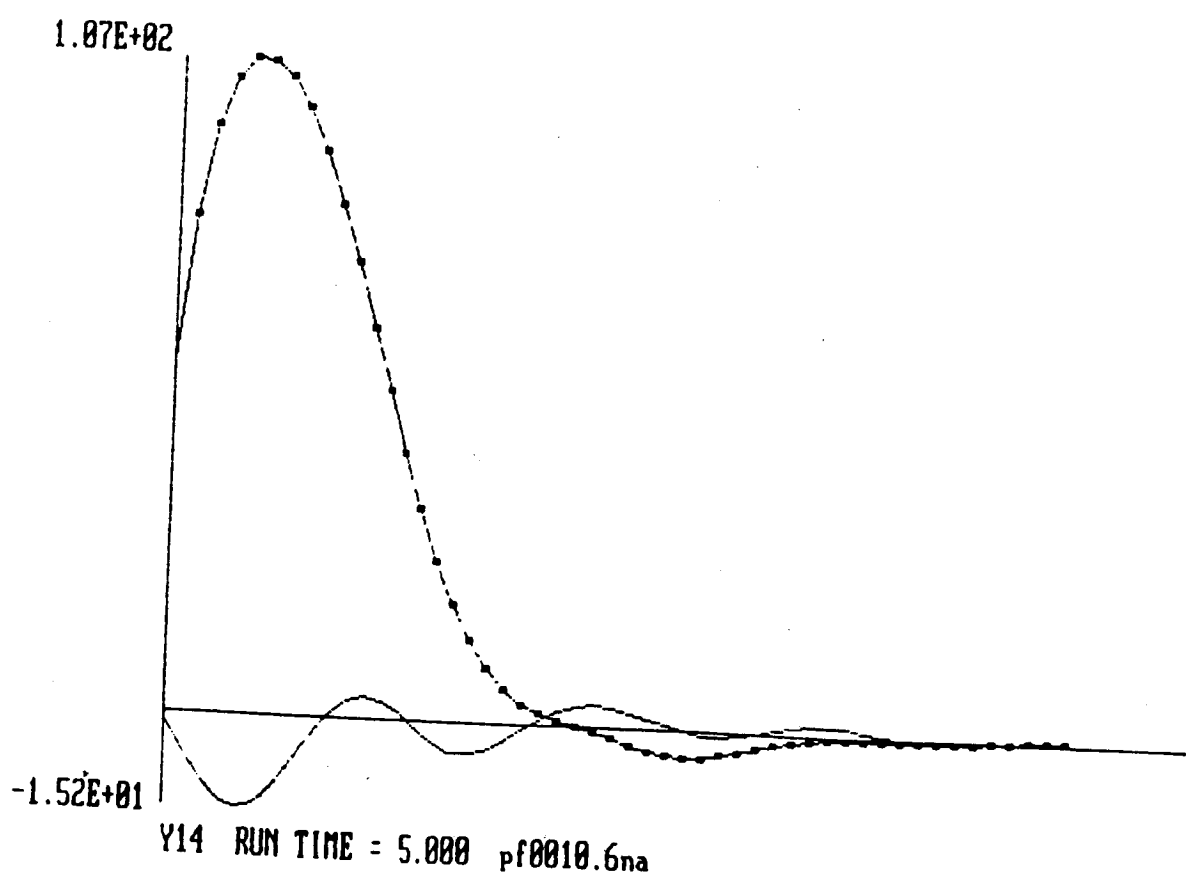
MODAL-DASHPOT MD.3

PART 1: LINEAR VELOCITY FEEDBACK GAIN GLUM

PART 2: ANGULAR VELOCITY FEEDBACK GAIN GAUR

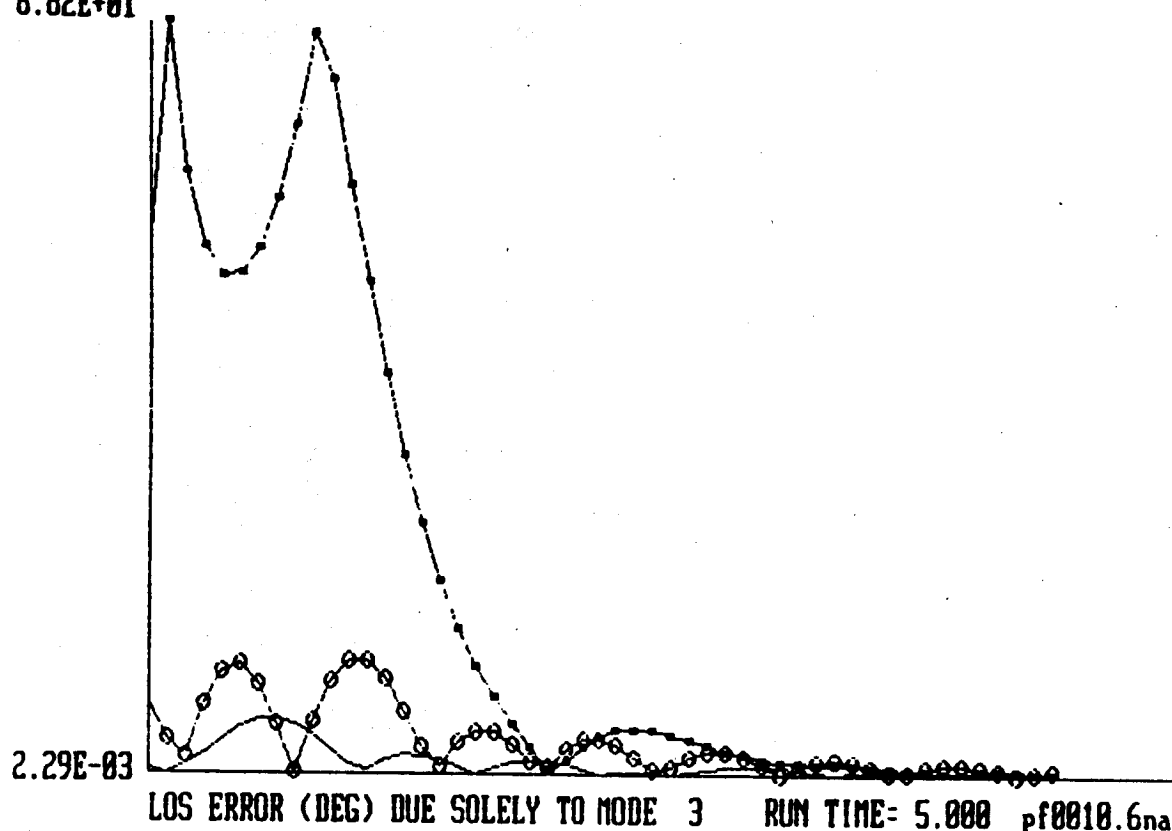


LCOPY



LCOPY

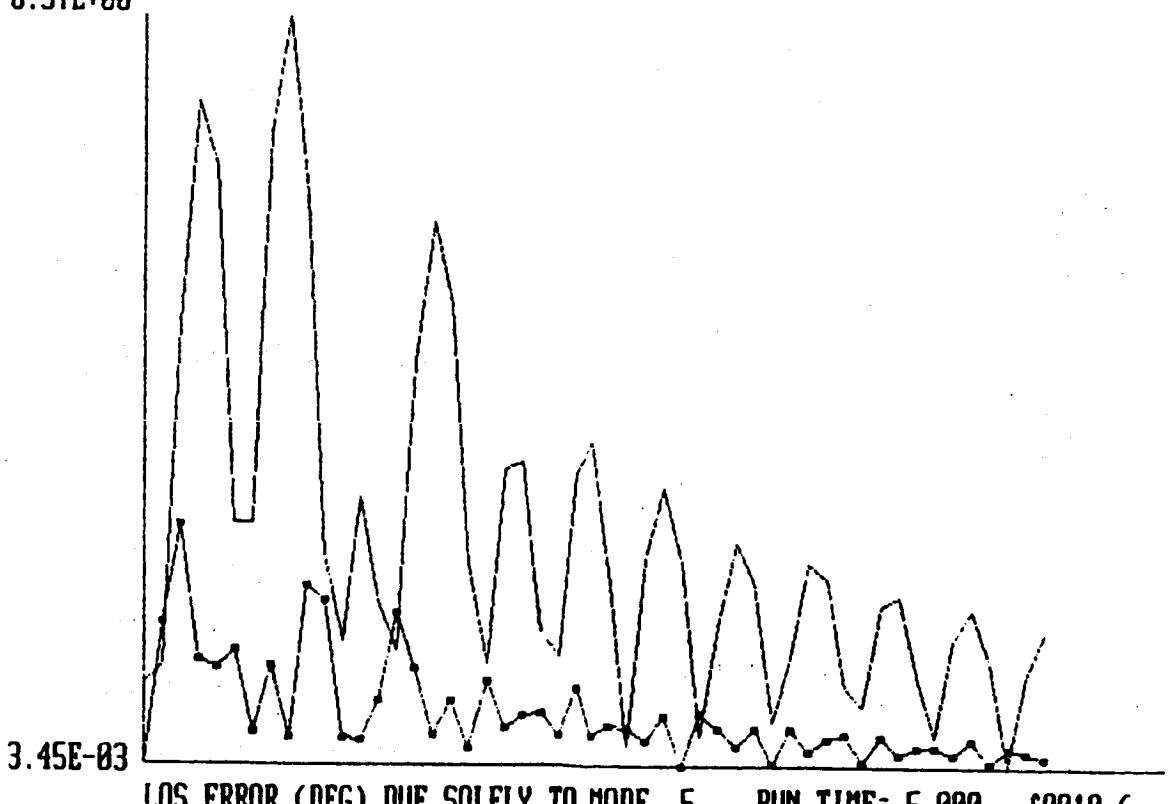
8.82E+01



LOS ERROR (DEG) DUE SOLELY TO MODE 3 RUN TIME= 5.000 pf0010.6na

LCOPY

6.37E+00

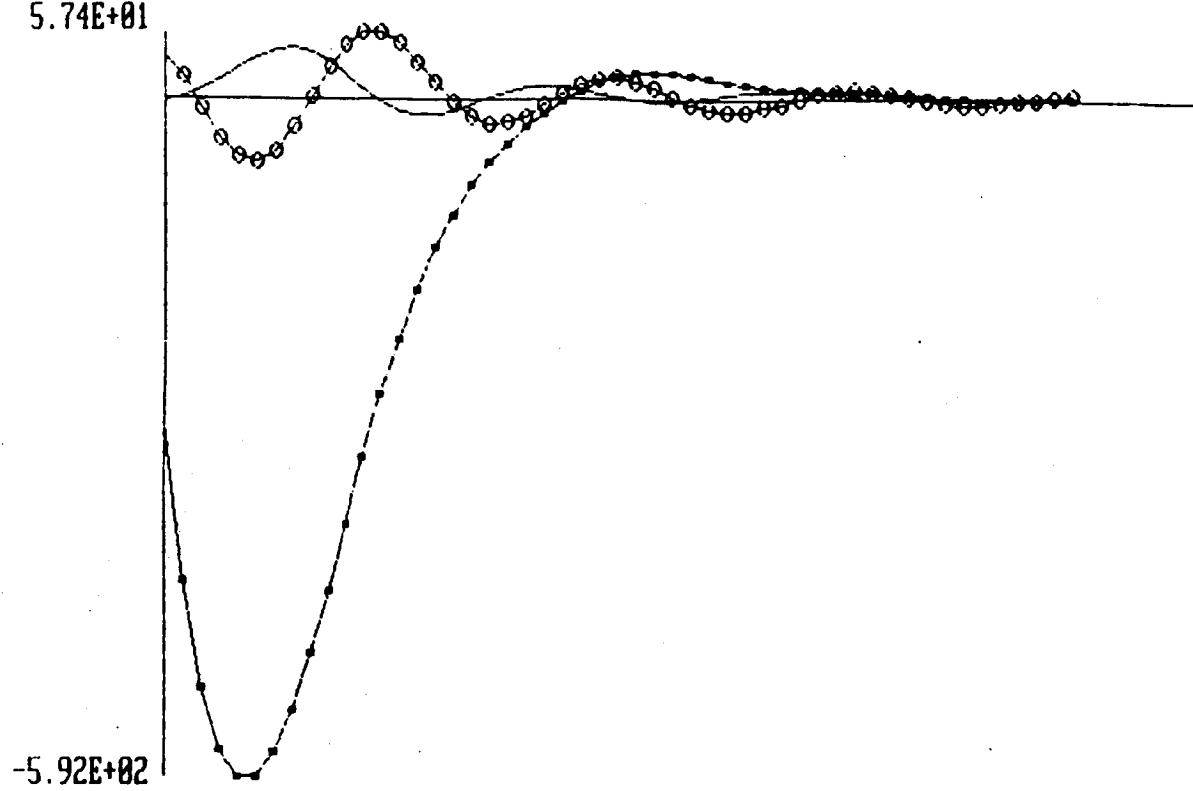


LOS ERROR (DEG) DUE SOLELY TO MODE 5 RUN TIME= 5.000 pf0010.6na

LCOPY

289

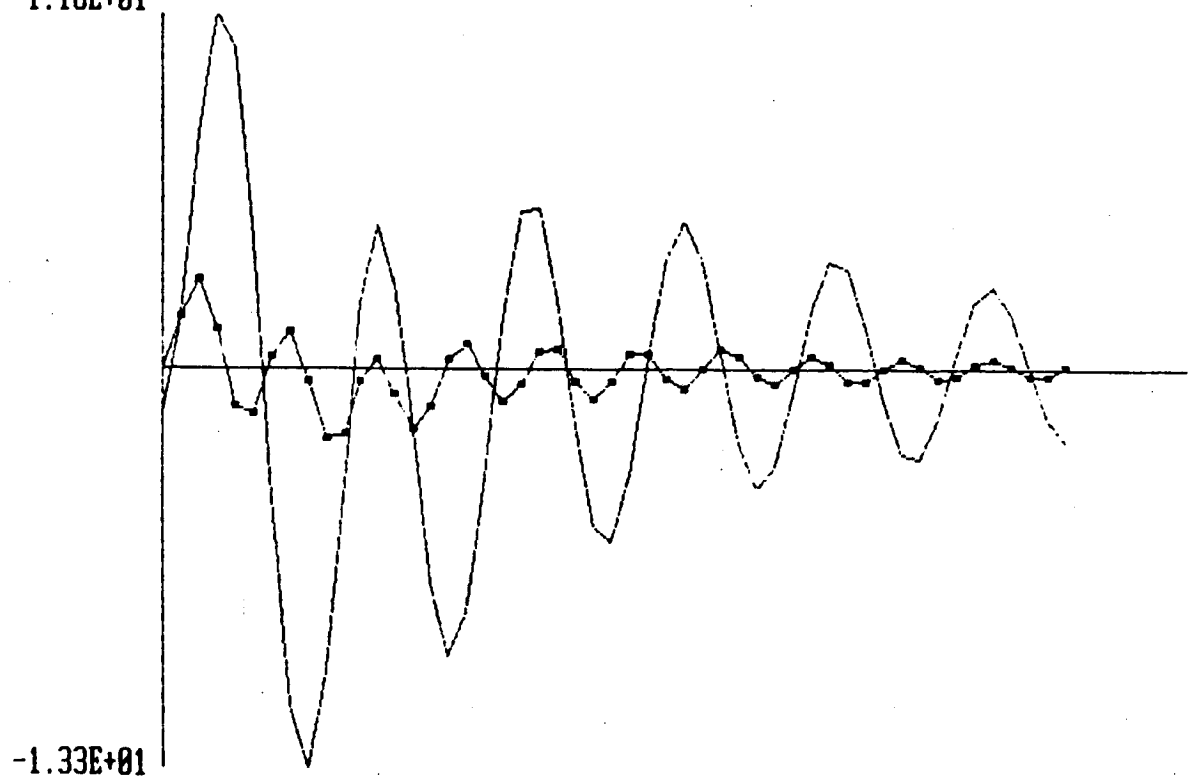
5.74E+01



ETA3 RUN TIME = 5.000 pf0010.6na

LCOPY

1.18E+01



ETA5 RUN TIME = 5.000 pf0010.6na

LCOPY

290

5.95E+01

3.55E-05

LOS ERROR (DEG) RUN TIME= 4.892 pf0100.6na

LCOPY

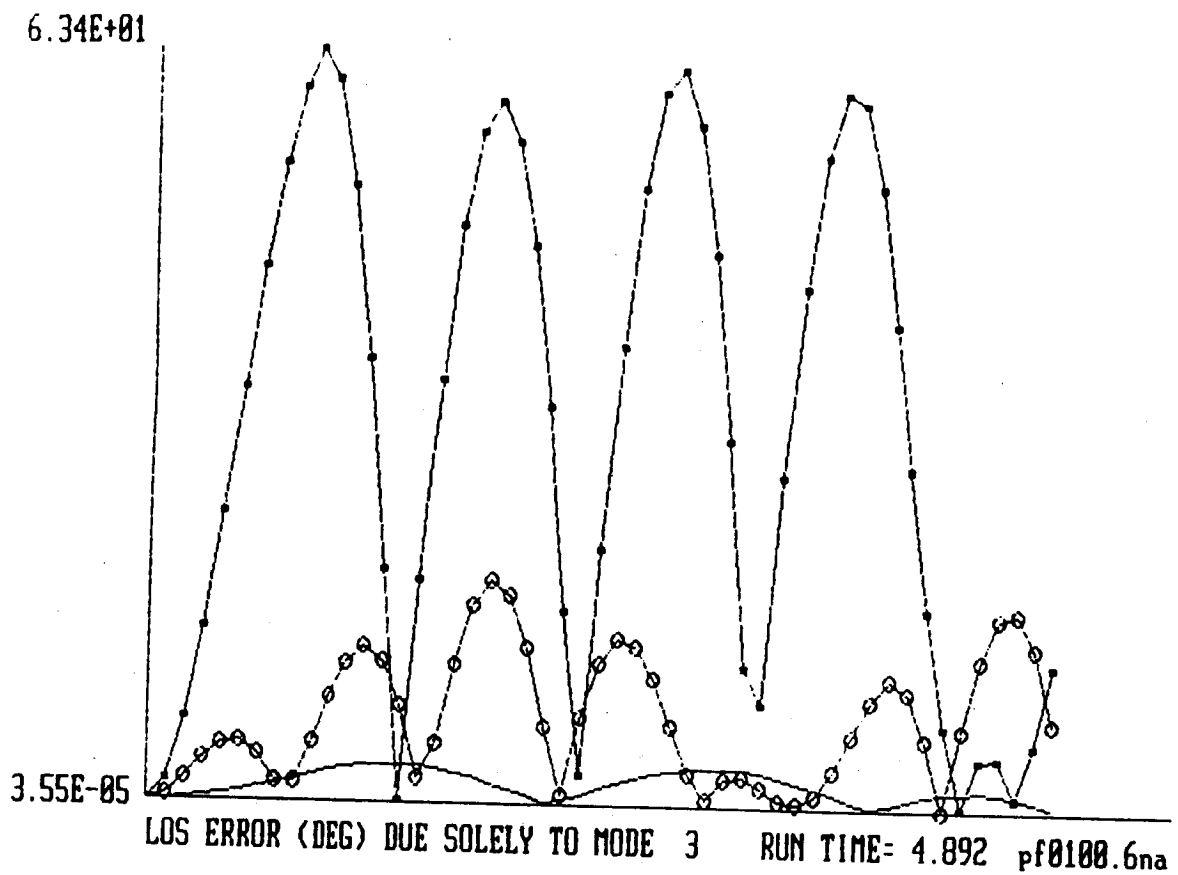
5.01E+01

-5.05E+01

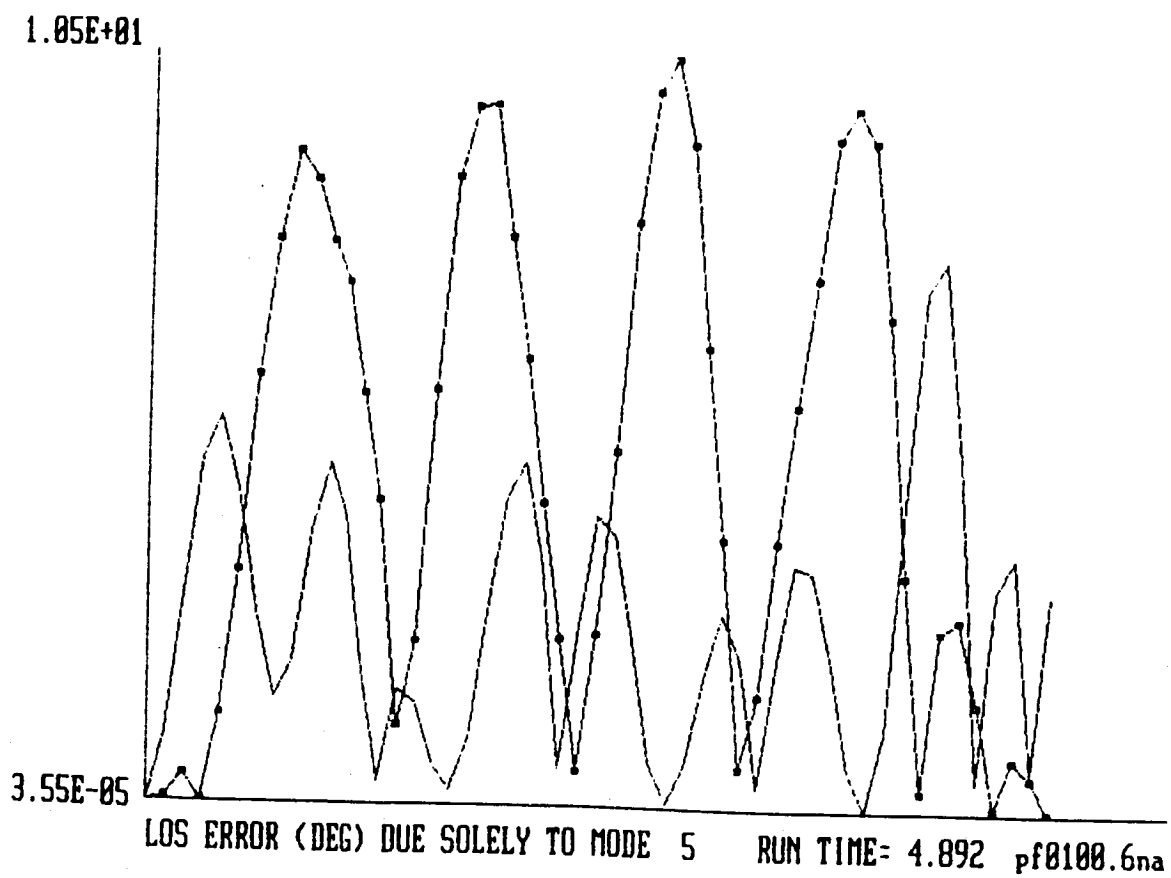
Y14 RUN TIME = 4.892 pf0100.6na

LCOPY

291



LCOPY



LCOPY

292

2.76E+02

-2.78E+02

ETA3 RUN TIME = 4.892 pf0100.6na

LCOPY

1.48E+01

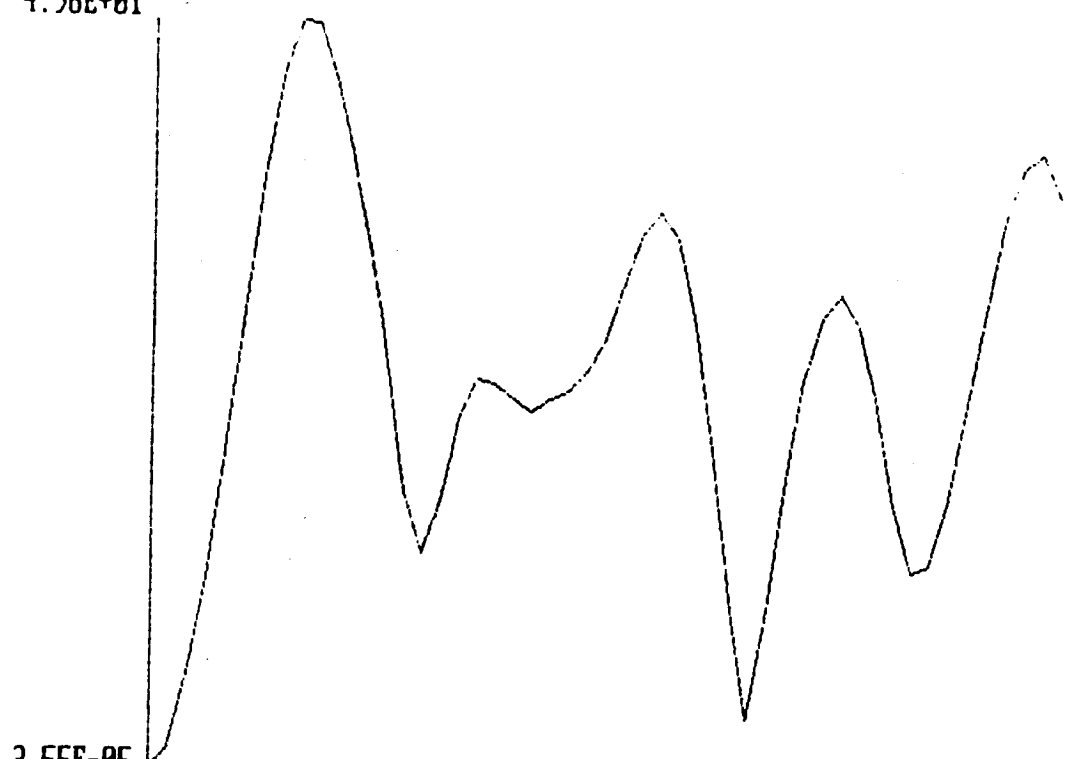
-1.61E+01

ETA5 RUN TIME = 4.892 pf0100.6na

LCOPY

293

4.98E+01

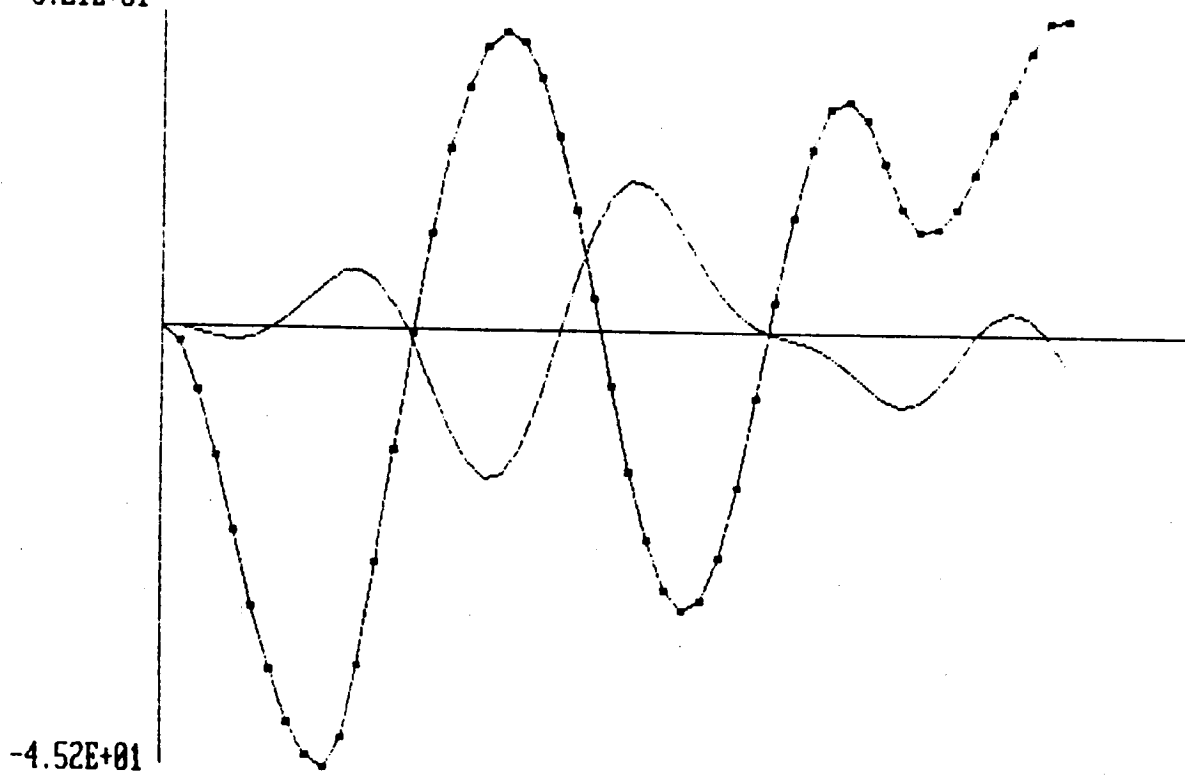


3.55E-05

LOS ERROR (DEG) RUN TIME= 4.892 pf2100.6na

LCOPY

3.21E+01



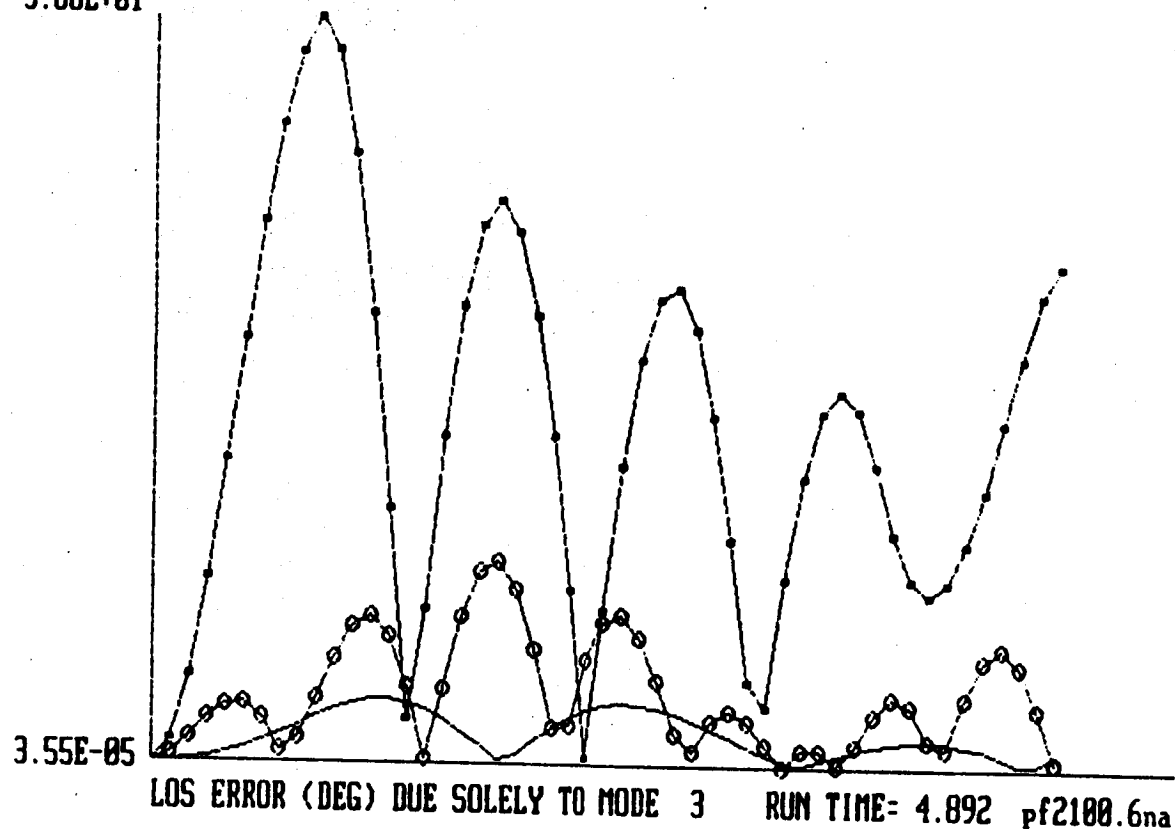
-4.52E+01

Y14 RUN TIME = 4.892 pf2100.6na

LCOPY

294

5.68E+01

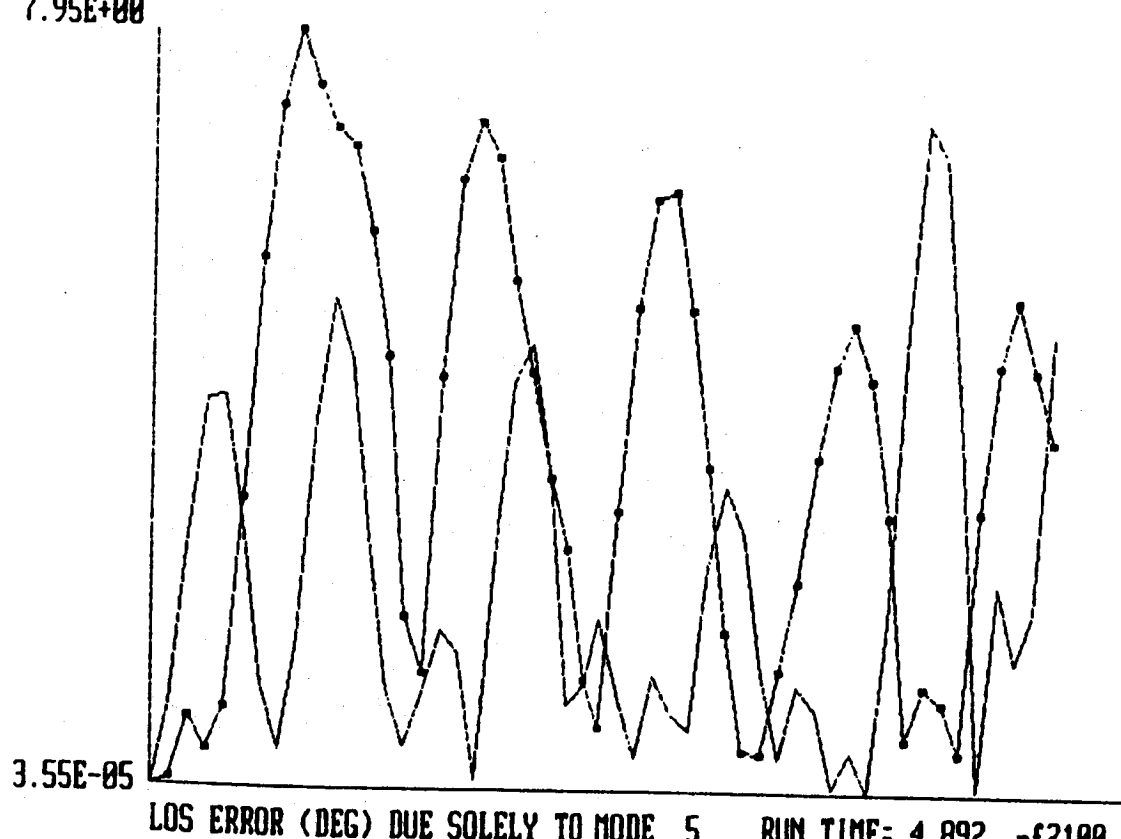


LOS ERROR (DEG) DUE SOLELY TO MODE 3

RUN TIME= 4.892 pf2100.6na

LCOPY

7.95E+00

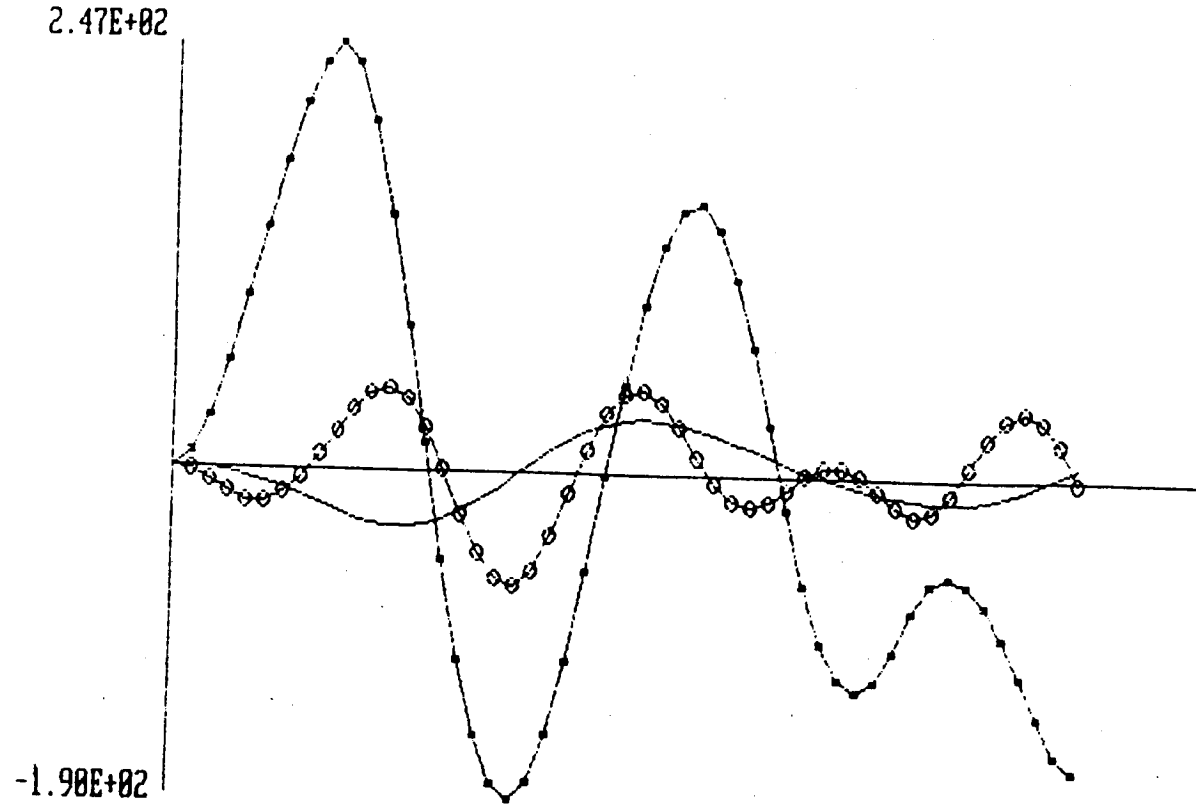


LOS ERROR (DEG) DUE SOLELY TO MODE 5

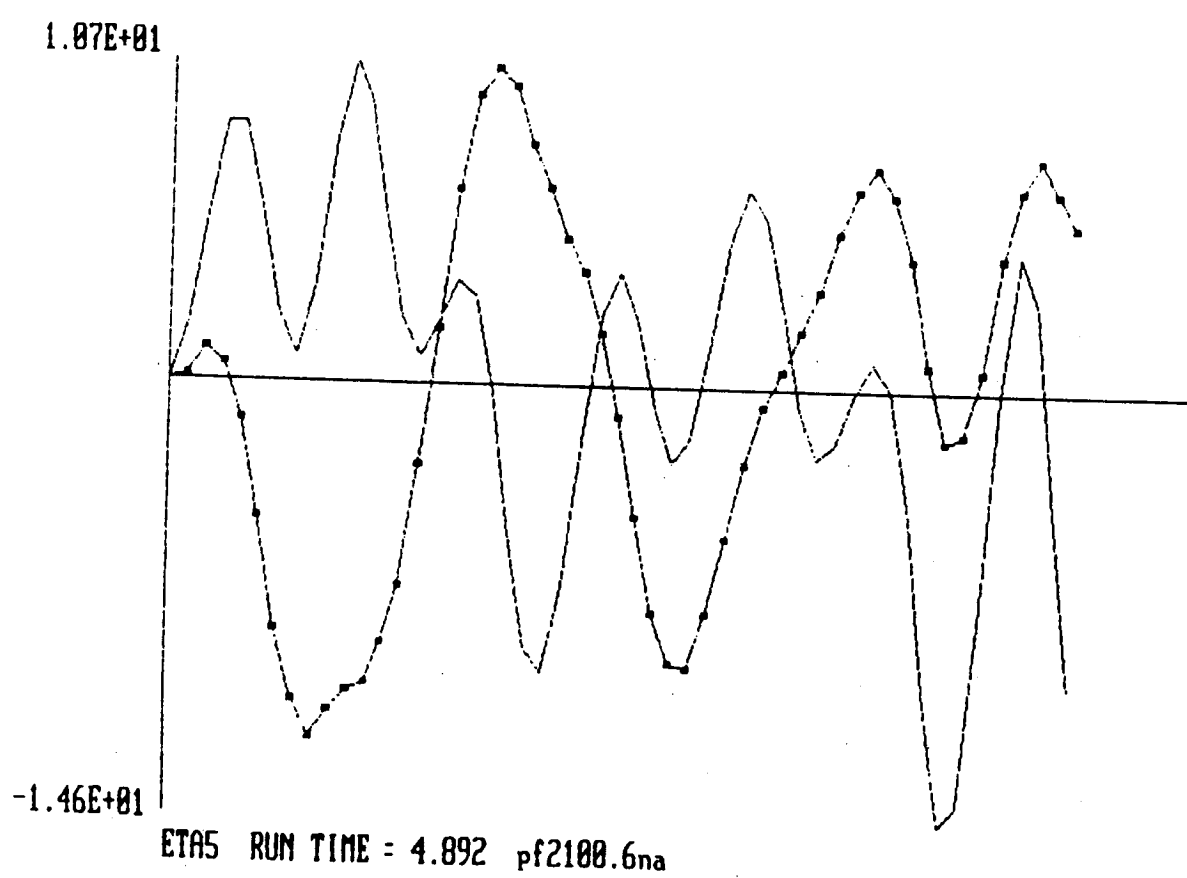
RUN TIME= 4.892 pf2100.6na

1 runn

295

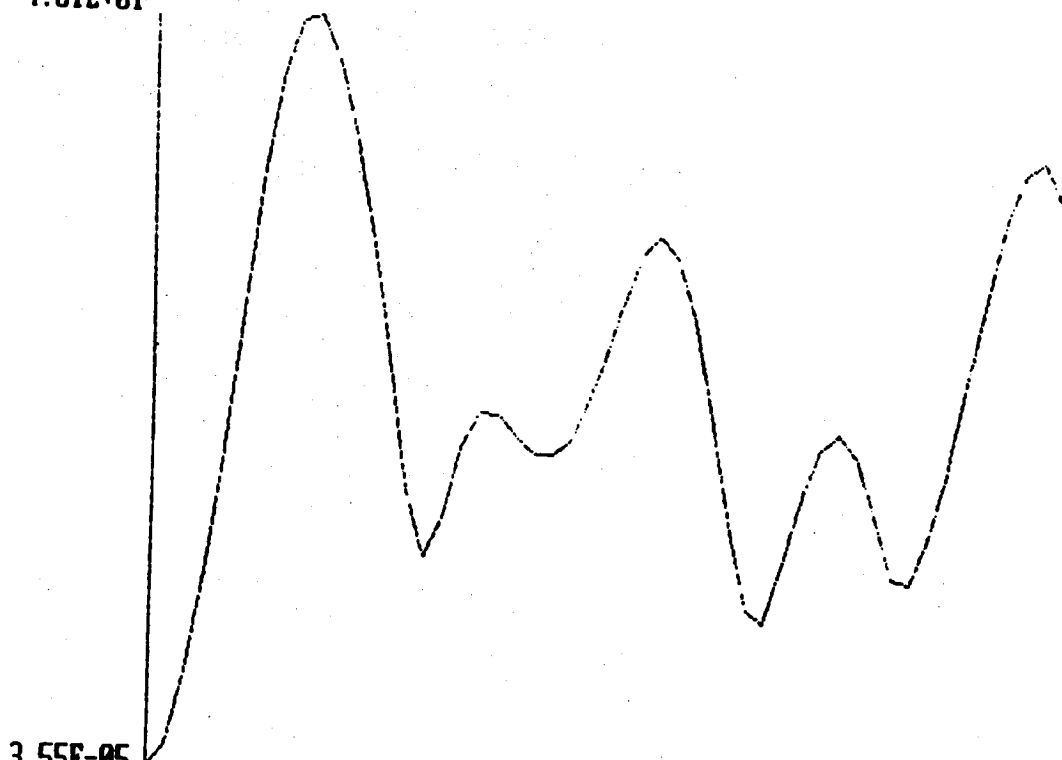


LCOPY



ICOPY

4.81E+01

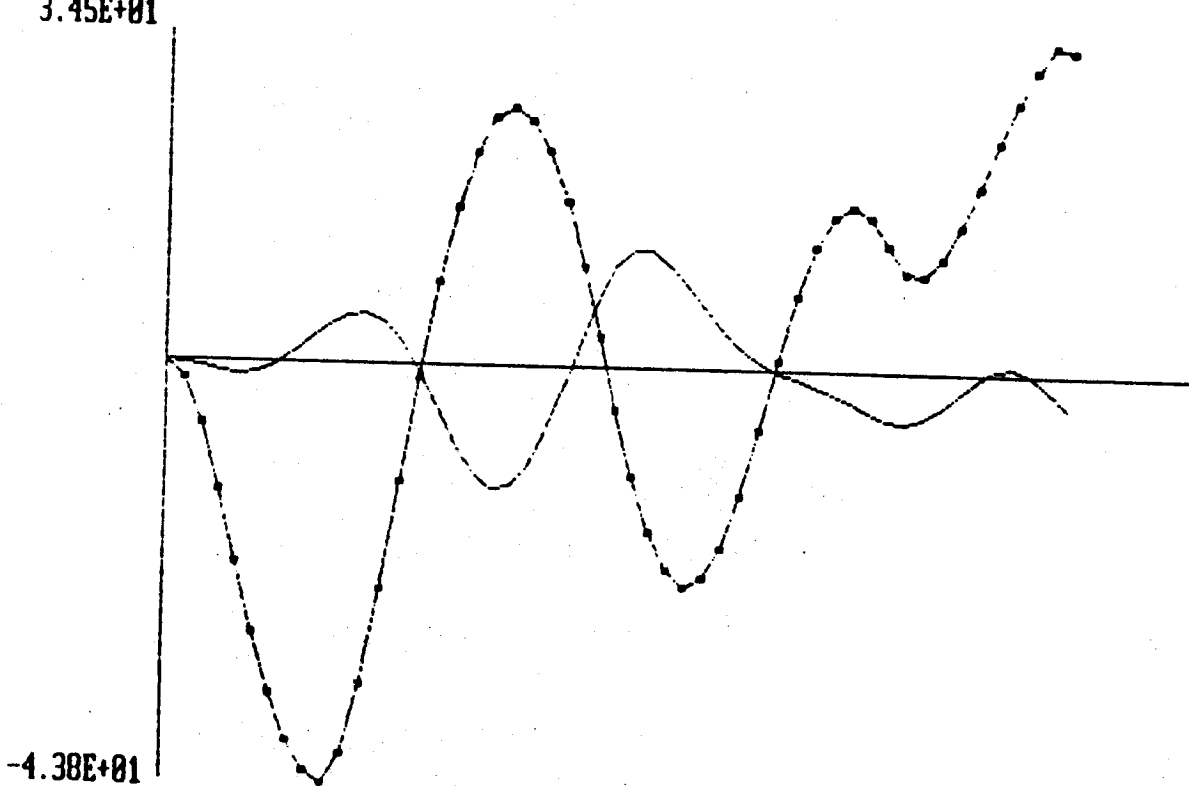


3.55E-05

LOS ERROR (DEG) RUN TIME= 4.892 pf3100.6na

LCOPY

3.45E+01

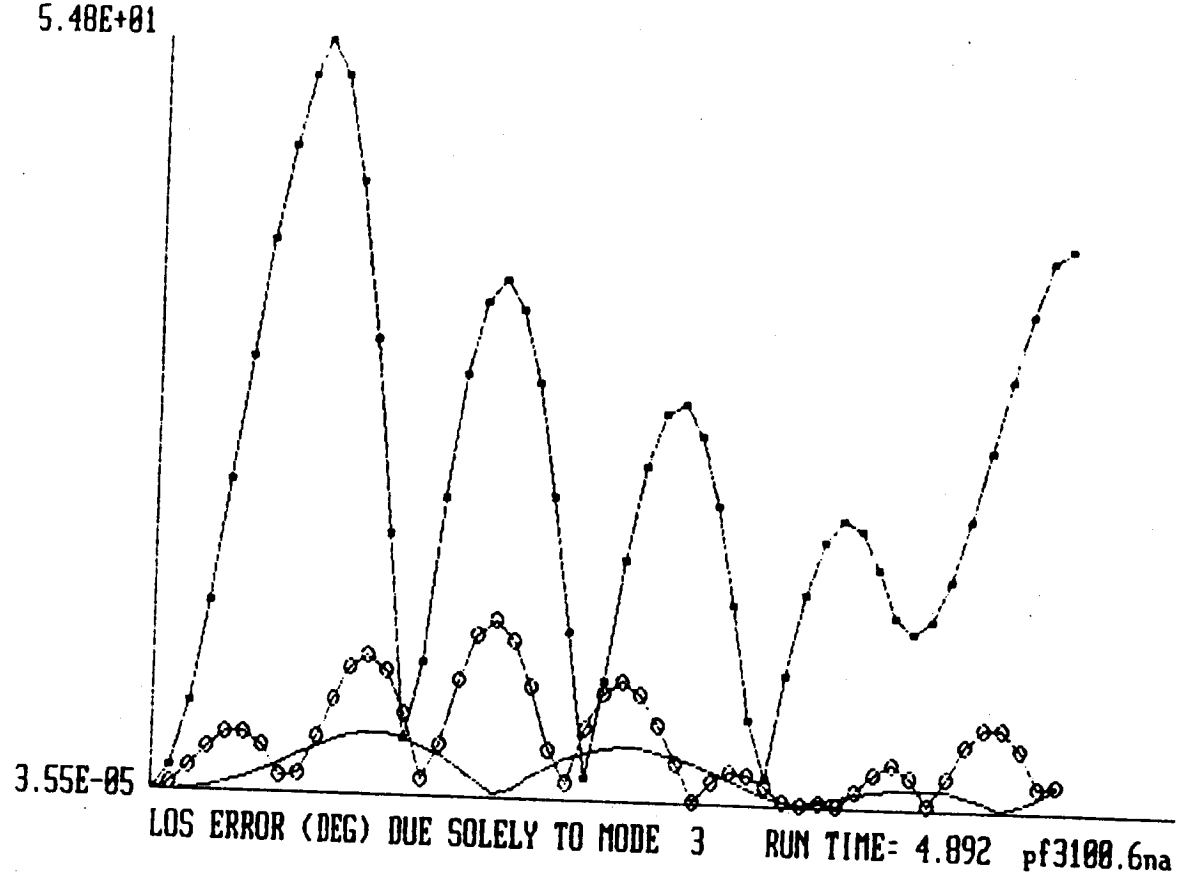


-4.38E+01

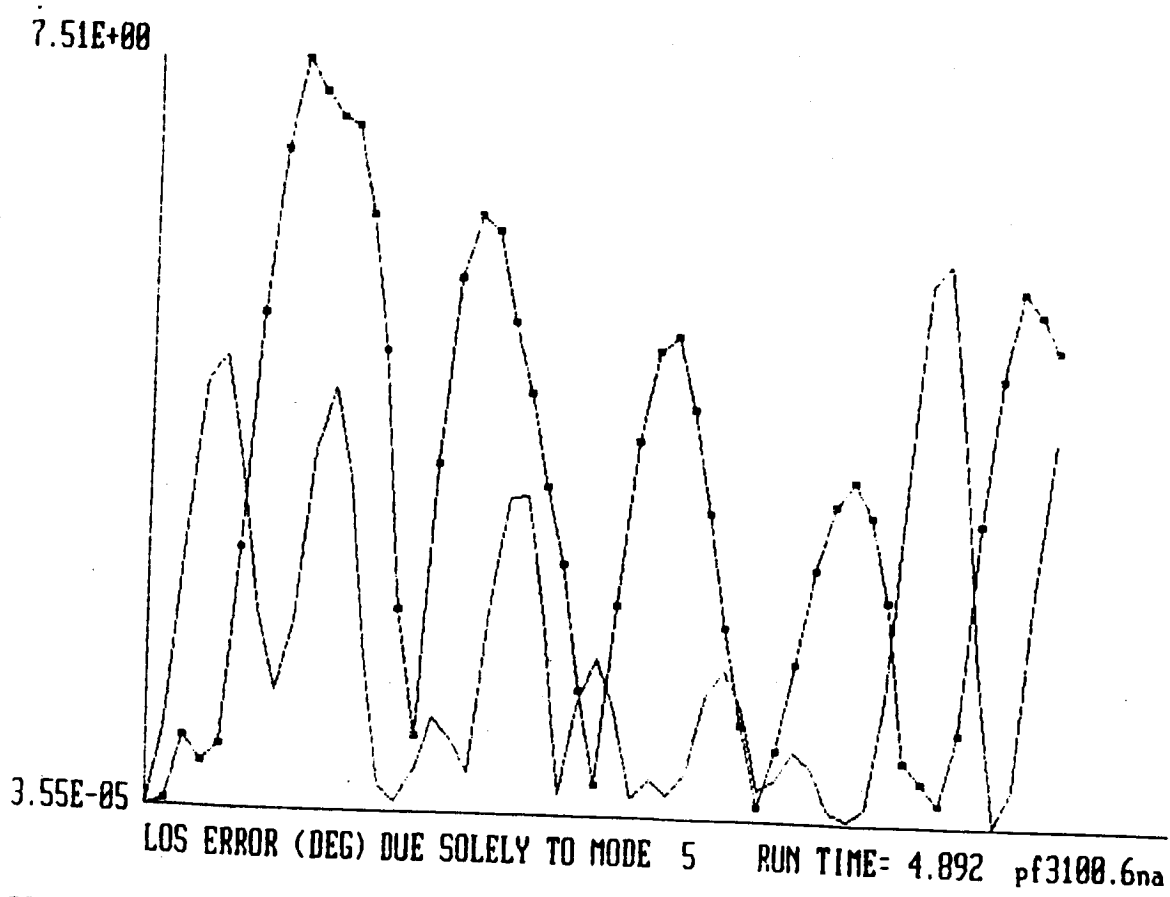
Y14 RUN TIME = 4.892 pf3100.6na

1 FNPV

297

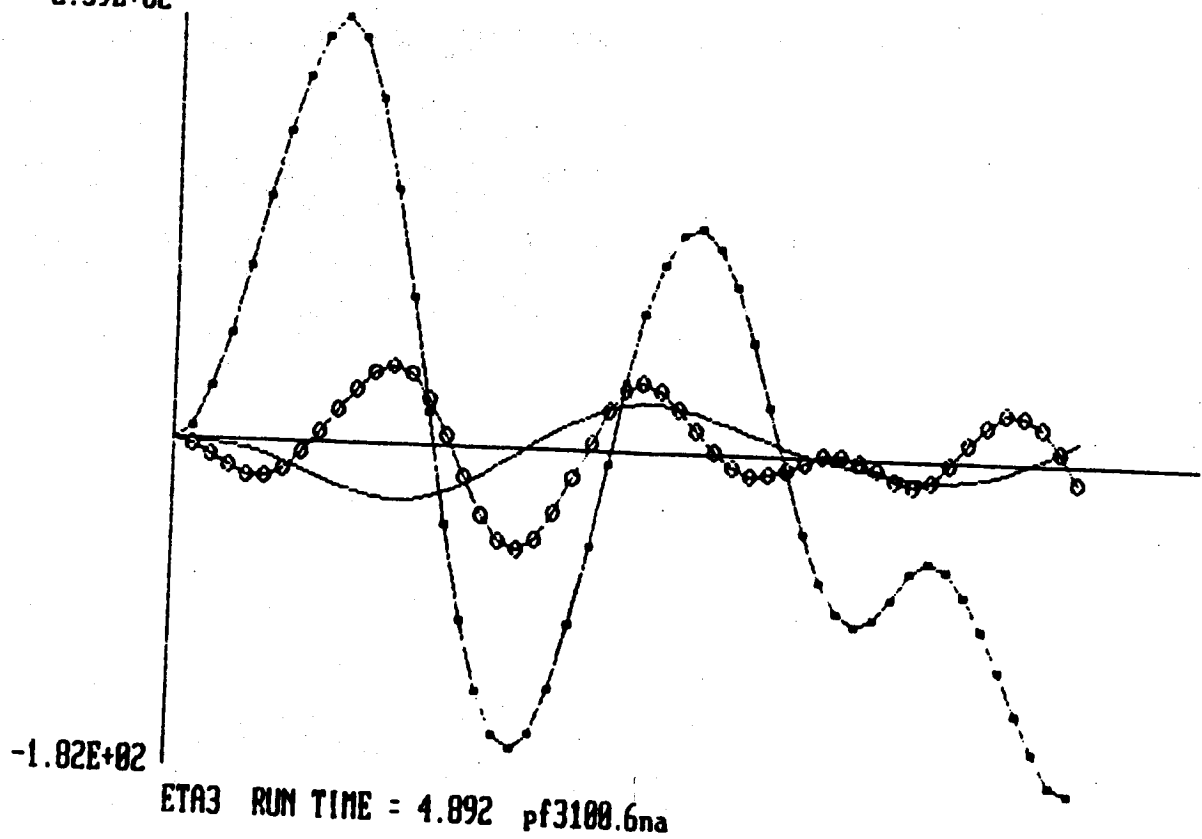


LCOPY



LCOPY

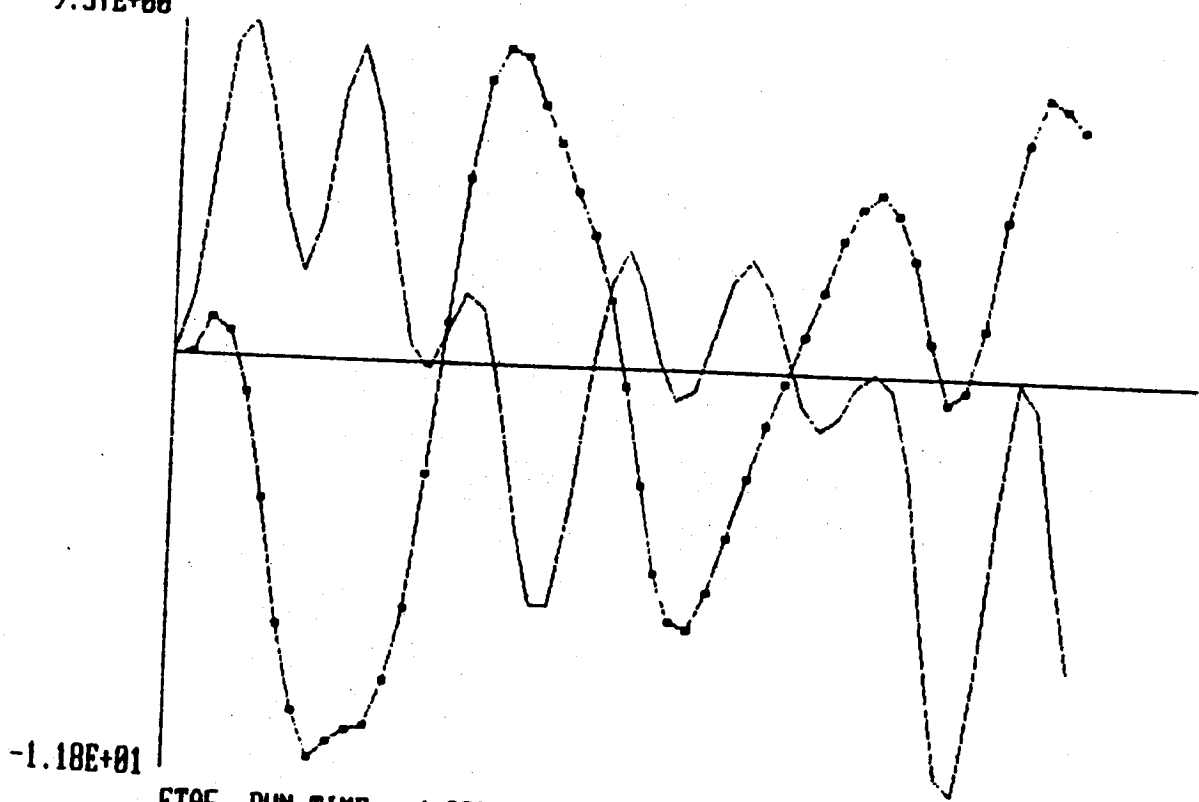
2.39E+02



ETA3 RUN TIME = 4.892 pf3100.6na

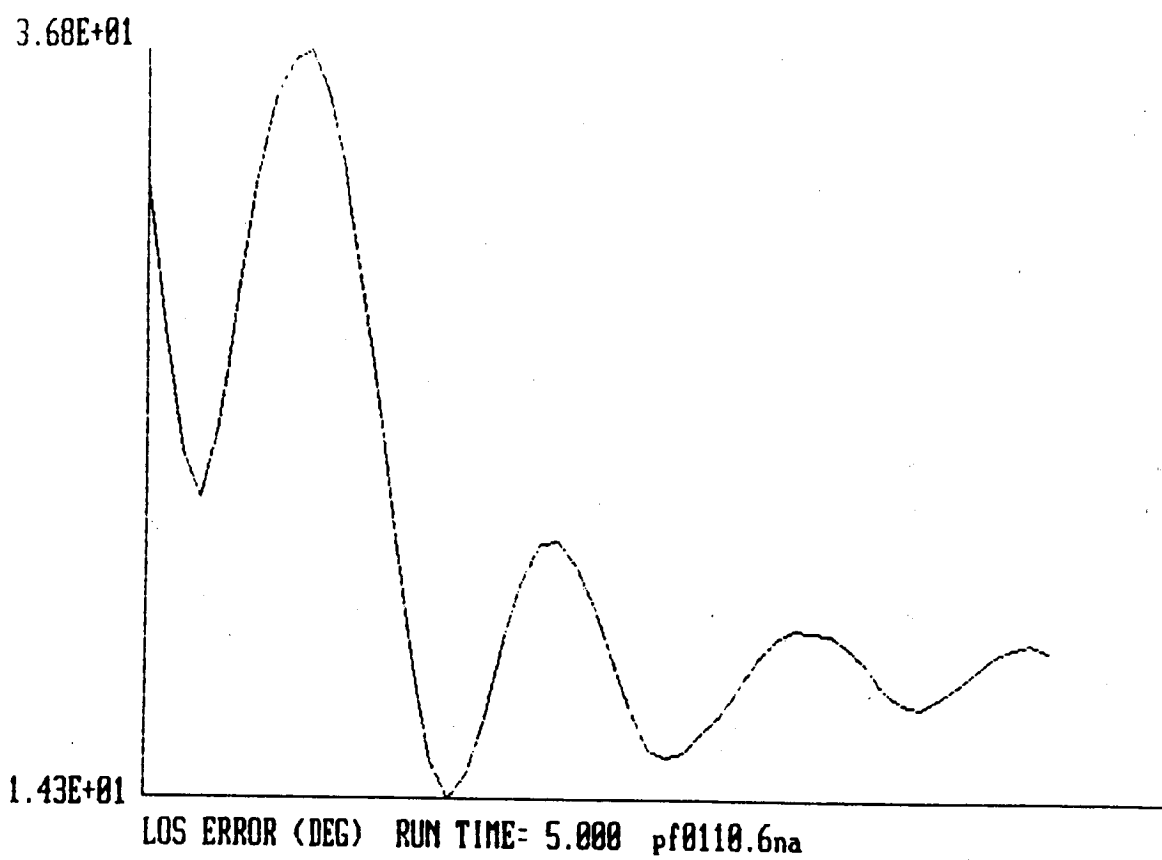
LCOPY

9.57E+00

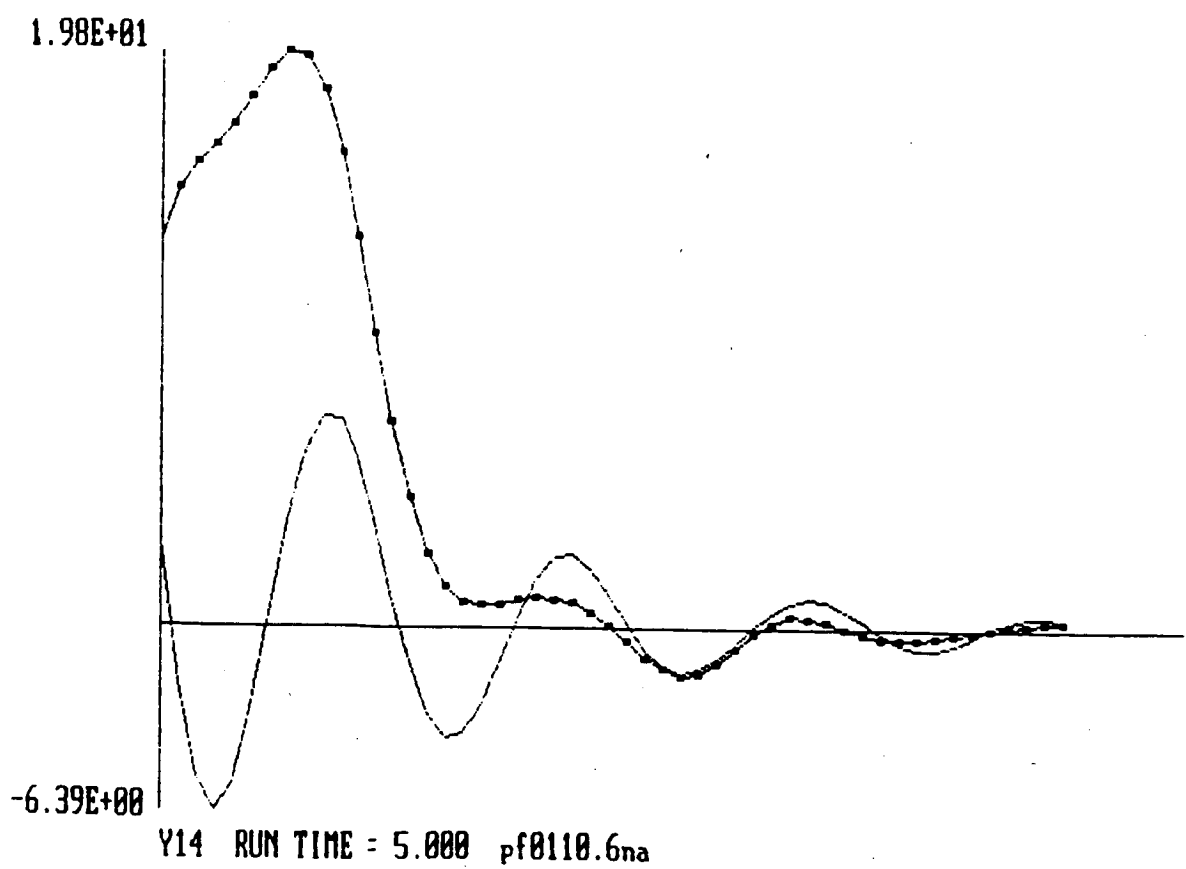


ETAS5 RUN TIME = 4.892 pf3100.6na

LCOPY



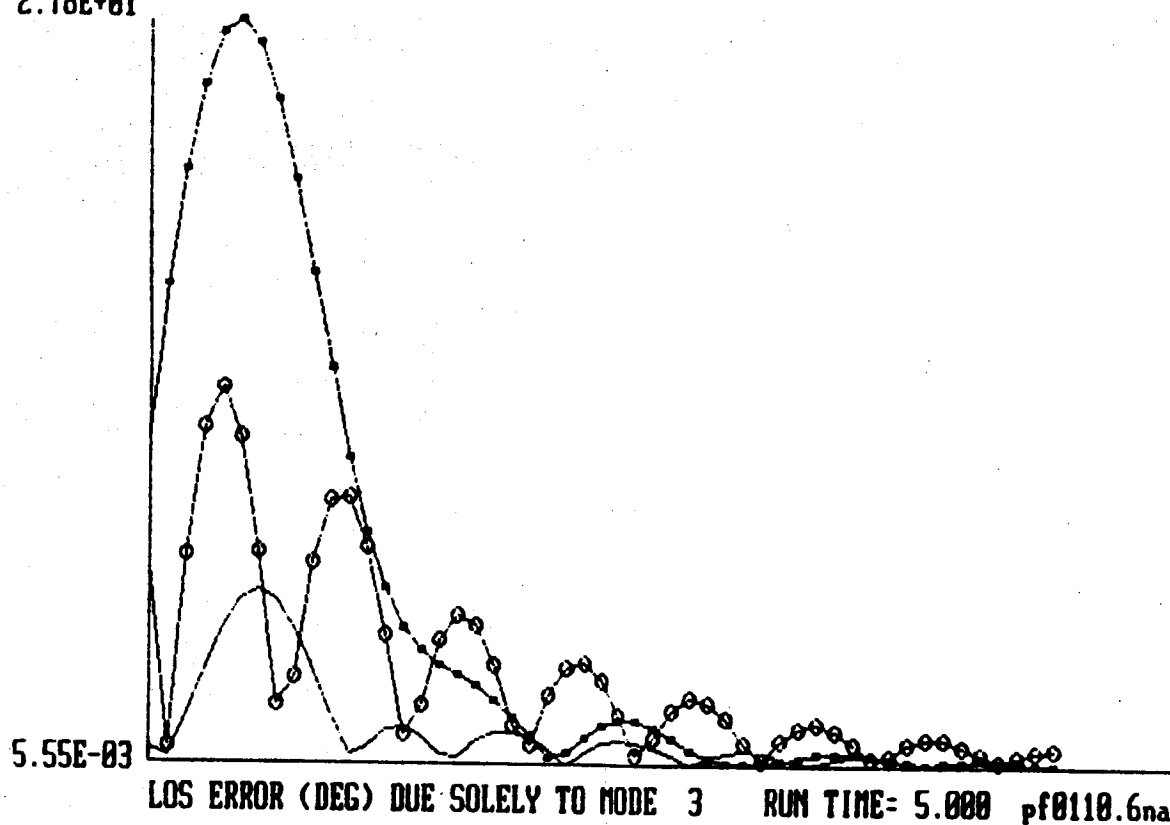
LCOPY



ICOPY

300

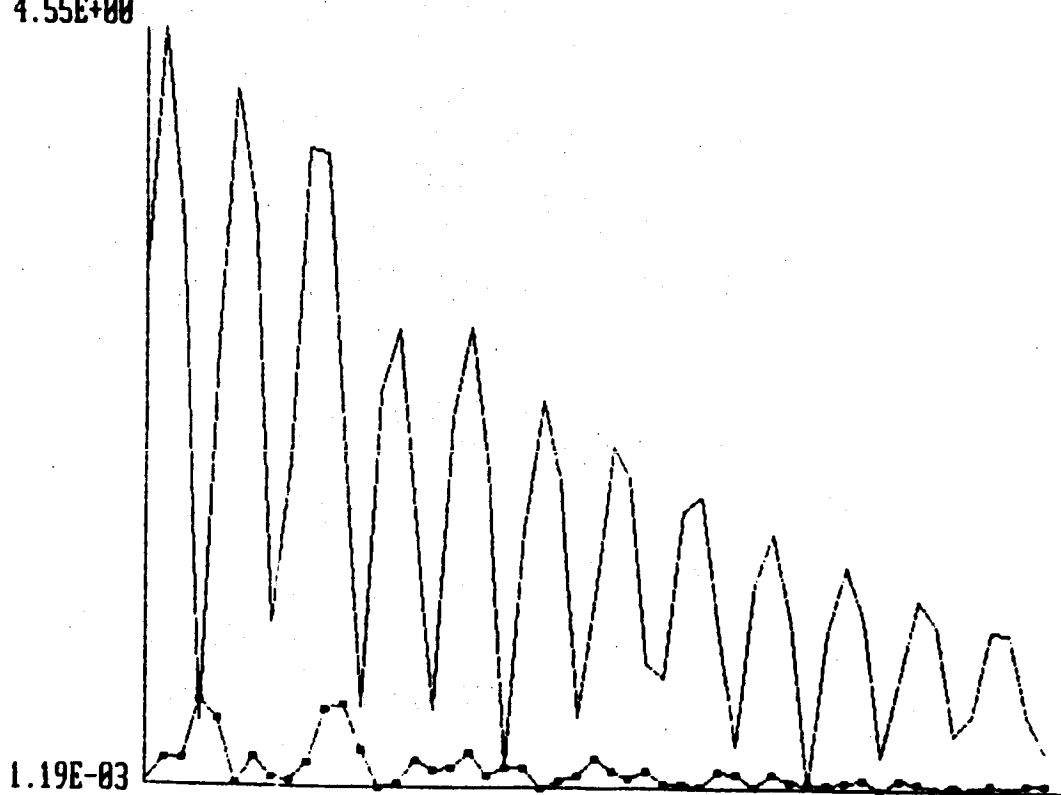
2.78E+01



LOS ERROR (DEG) DUE SOLELY TO MODE 3 RUN TIME= 5.000 pf0110.6na

LCOPY

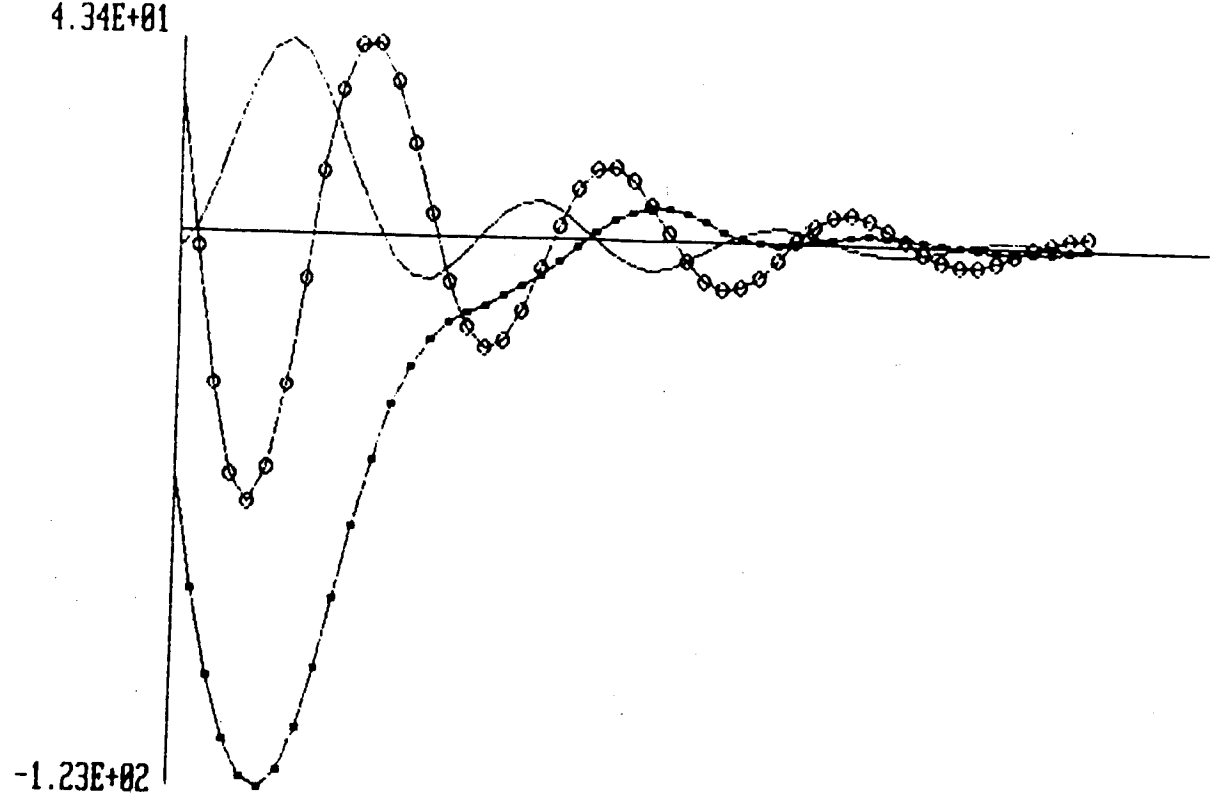
4.55E+00



LOS ERROR (DEG) DUE SOLELY TO MODE 5 RUN TIME= 5.000 pf0110.6na

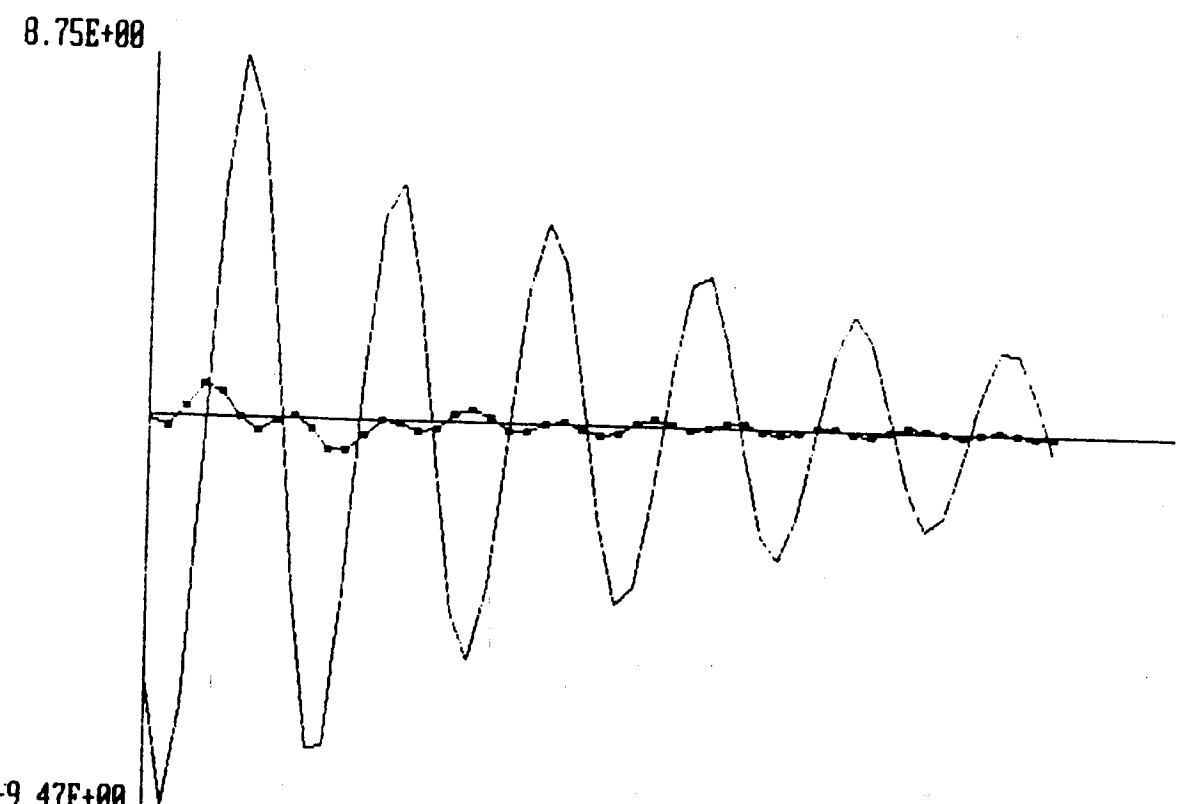
LCOPY

301



ETA3 RUN TIME = 5.000 pf0110.6na

LCOPY

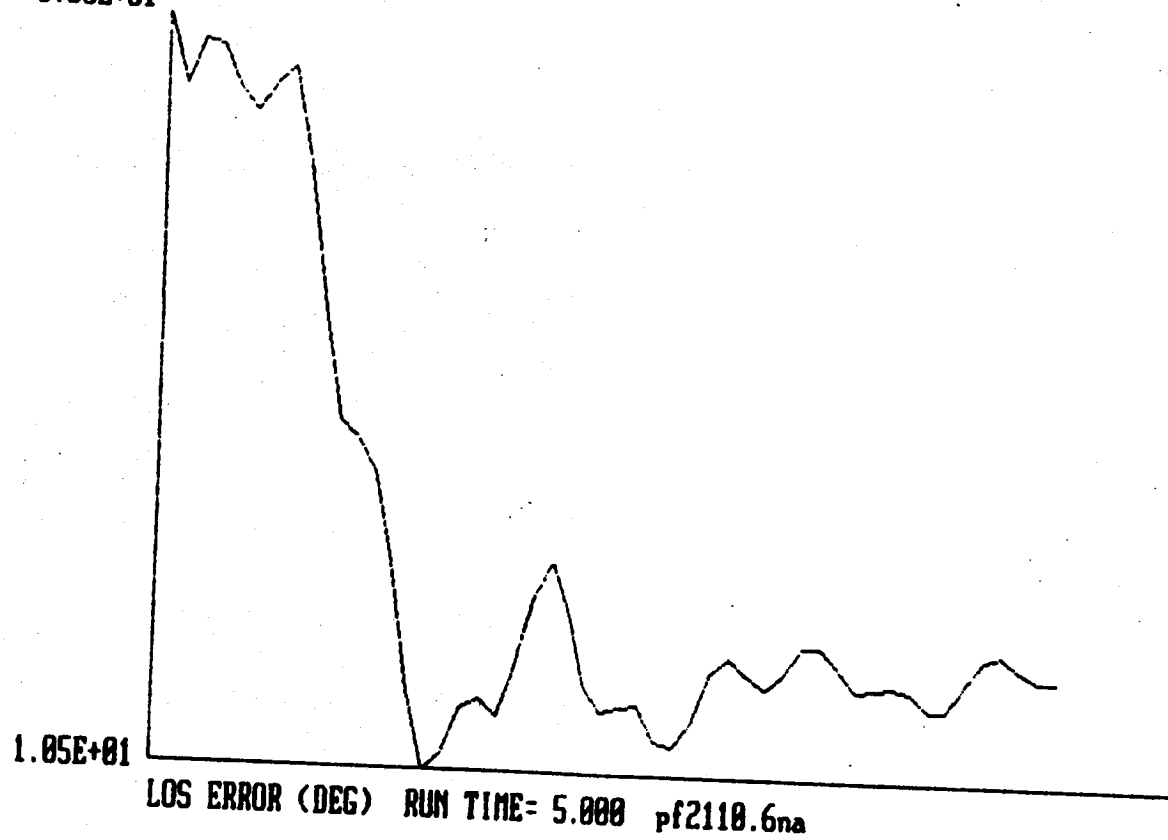


ETAS RUN TIME = 5.000 pf0110.6na

LCOPY

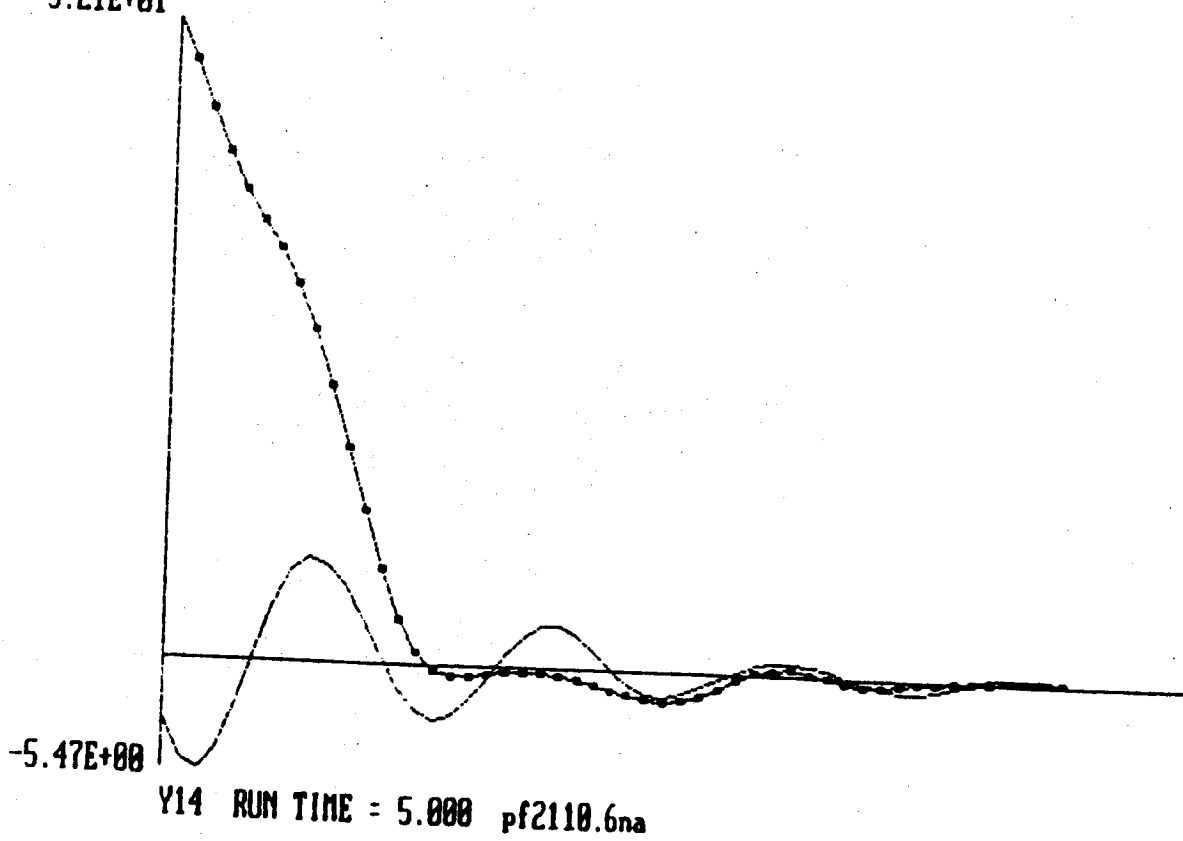
302

3.85E+01



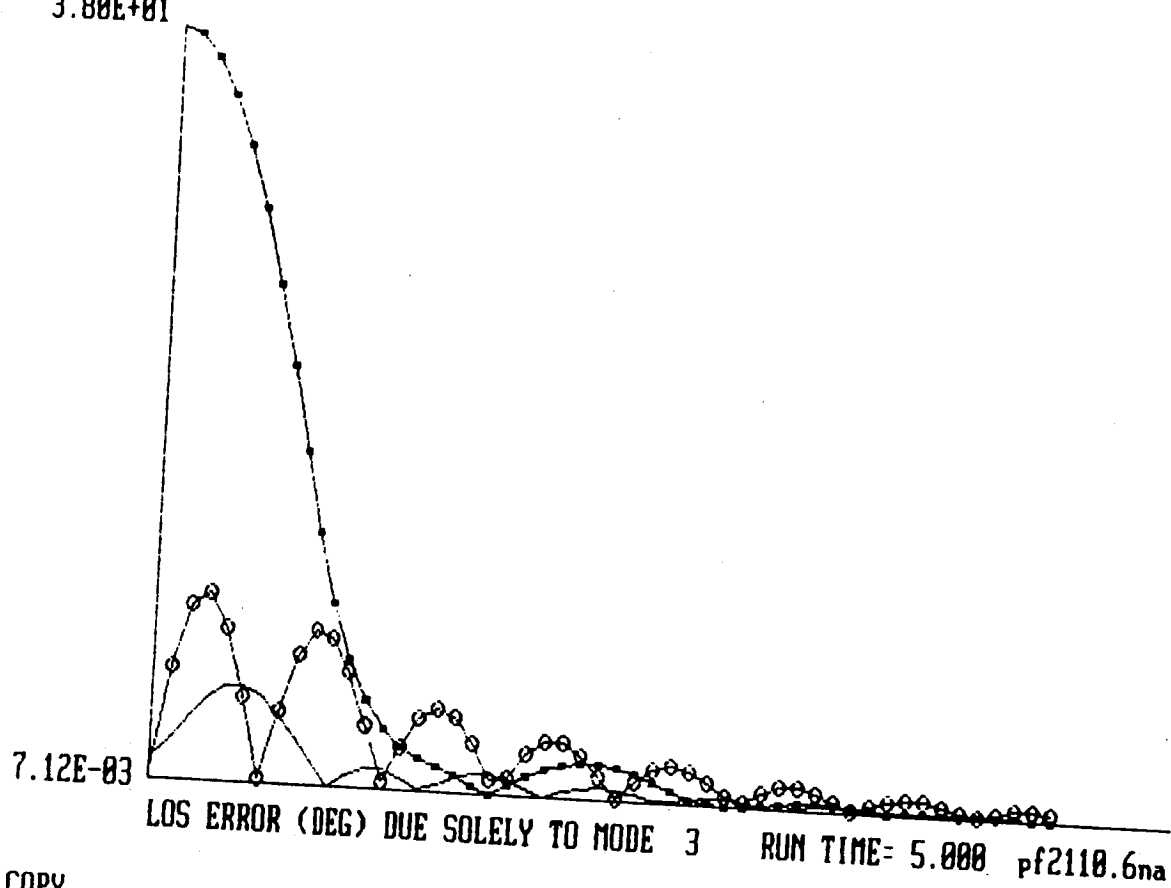
LCOPY

3.21E+01

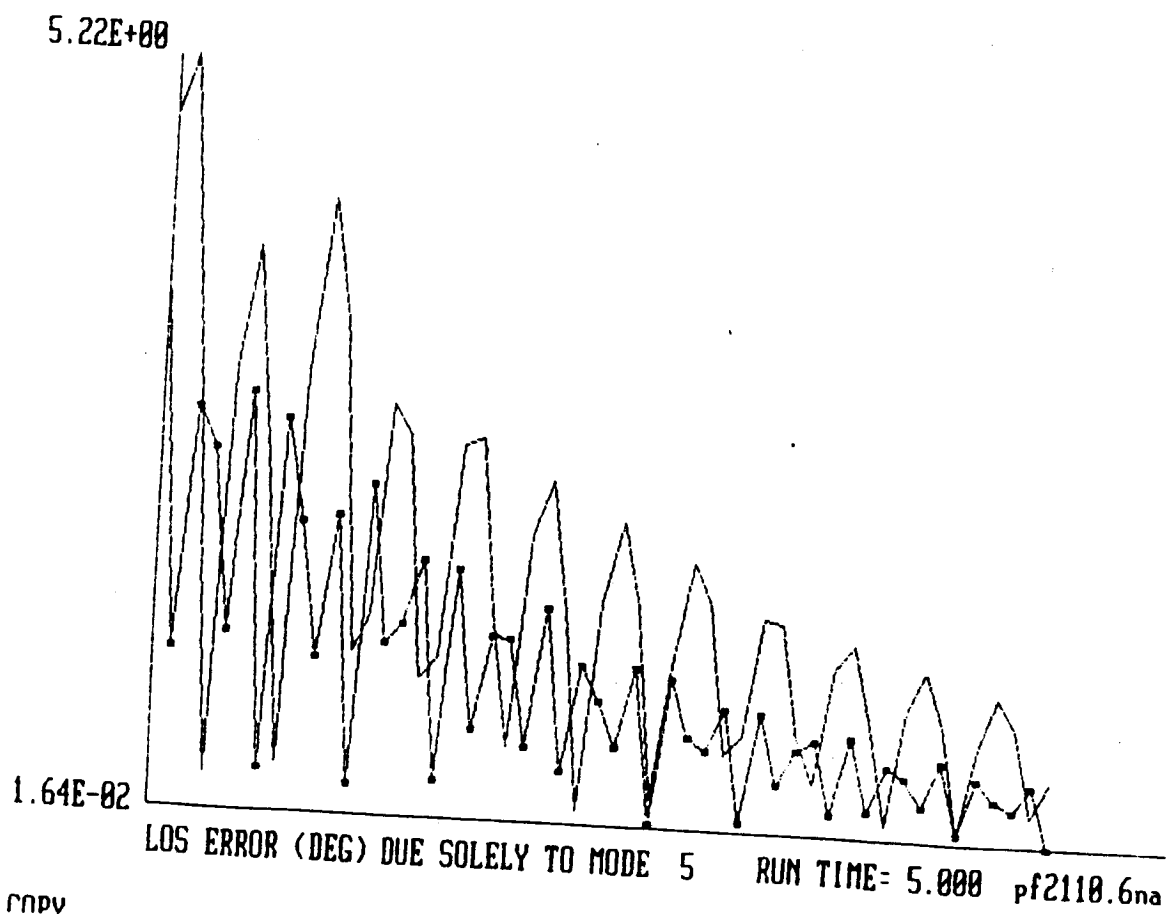


LCOPY

303



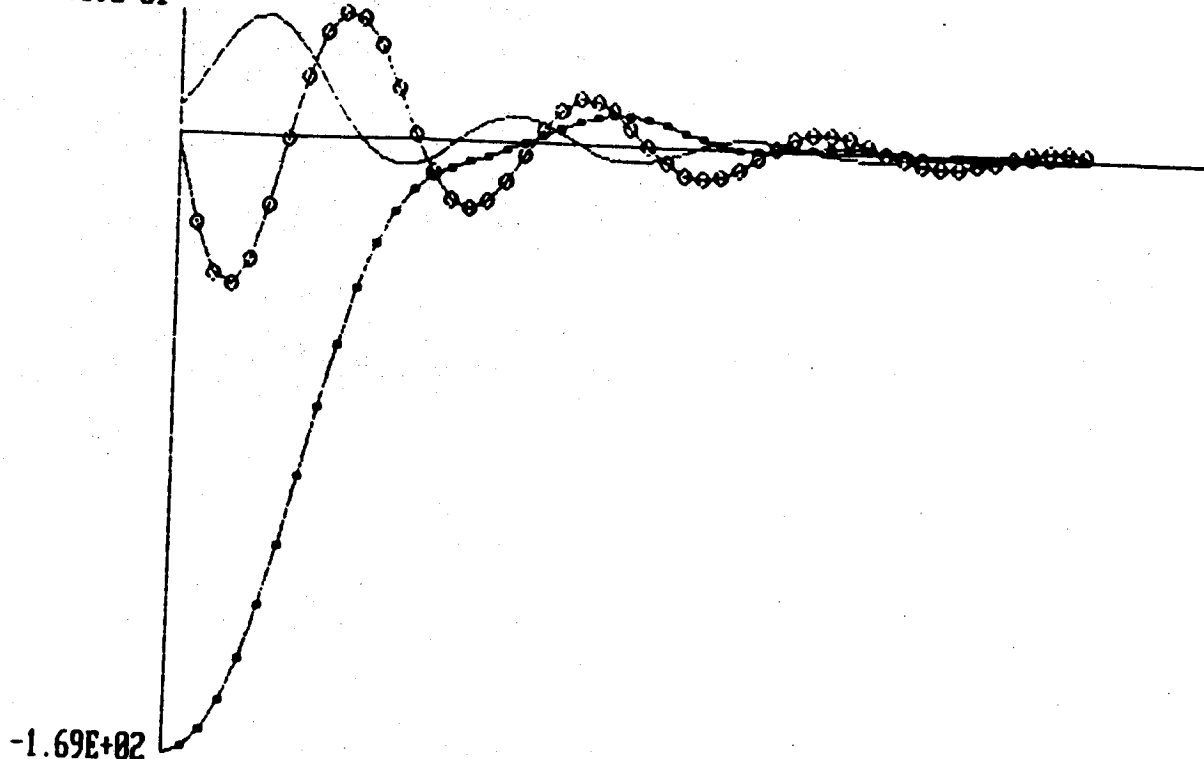
LCOPY



LCOPY

304

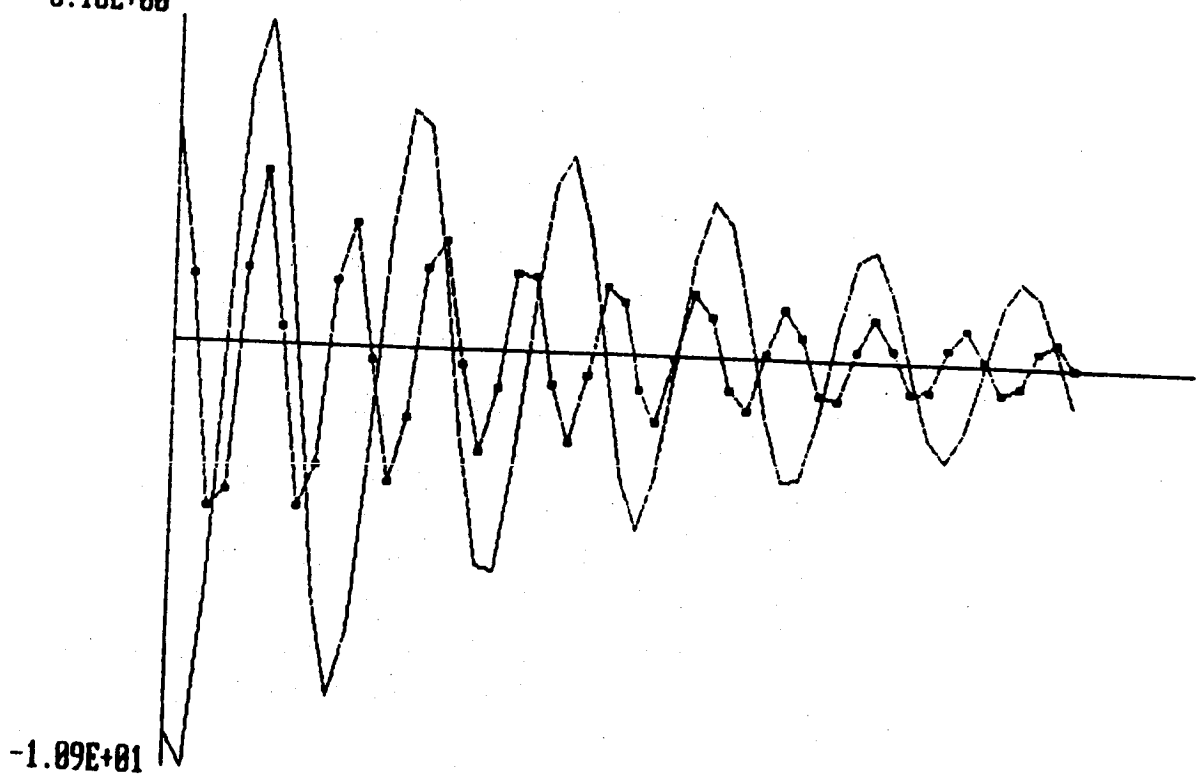
3.39E+01



ETA3 RUN TIME = 5.000 pf2110.6na

LCOPY

8.18E+00

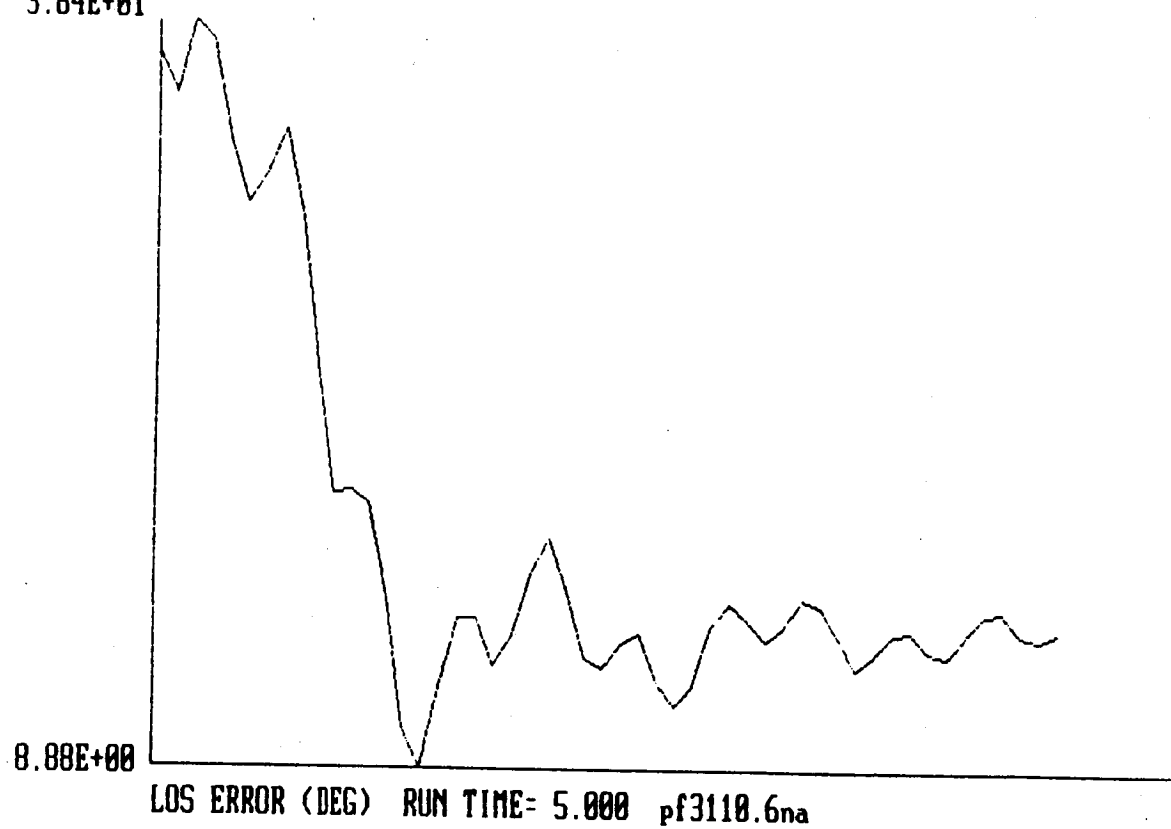


ETA5 RUN TIME = 5.000 pf2110.6na

LCOPY

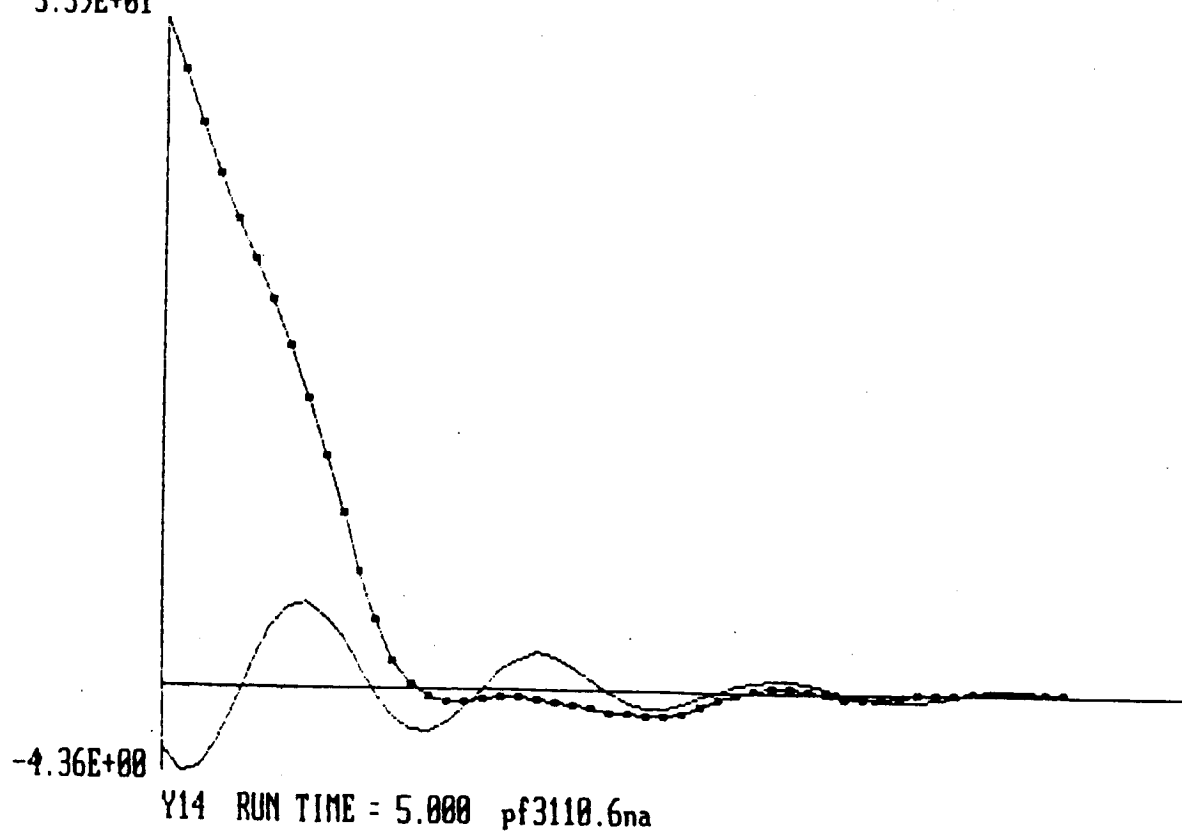
305

3.84E+01



LCOPY

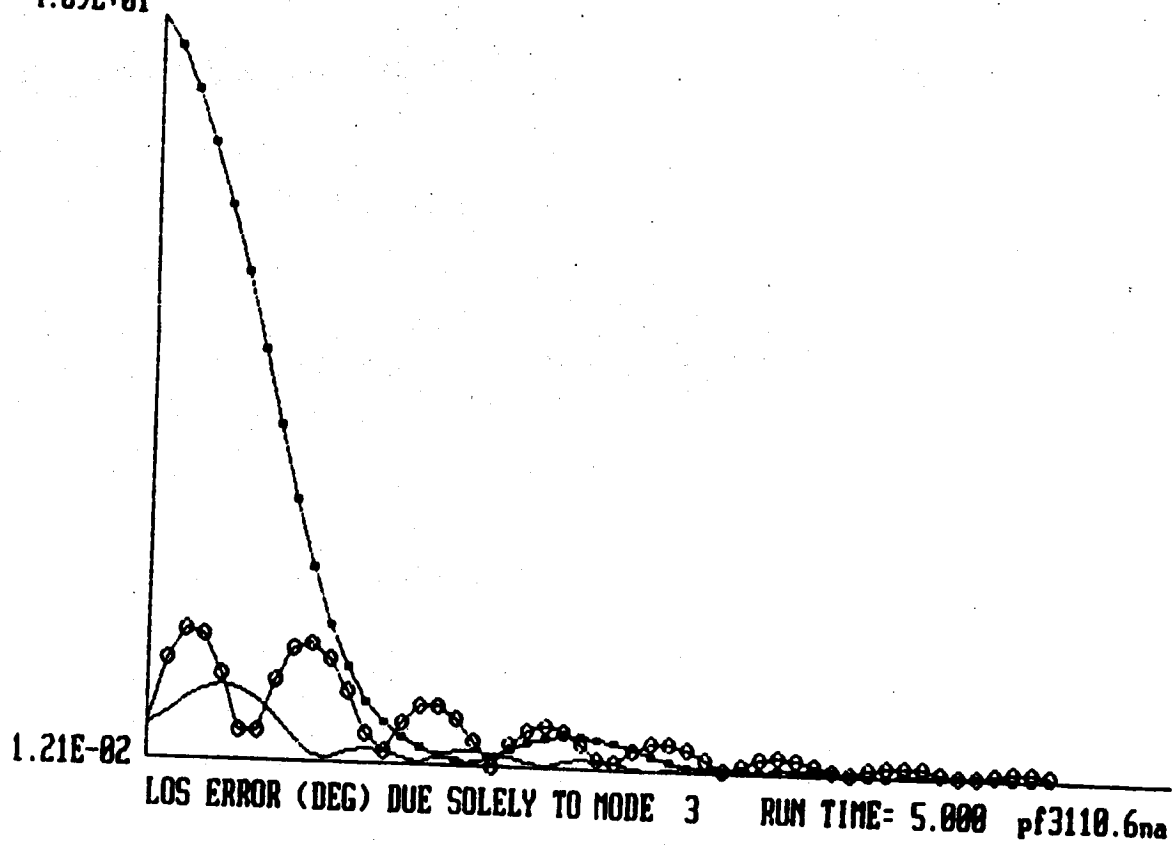
3.39E+01



LCOPY

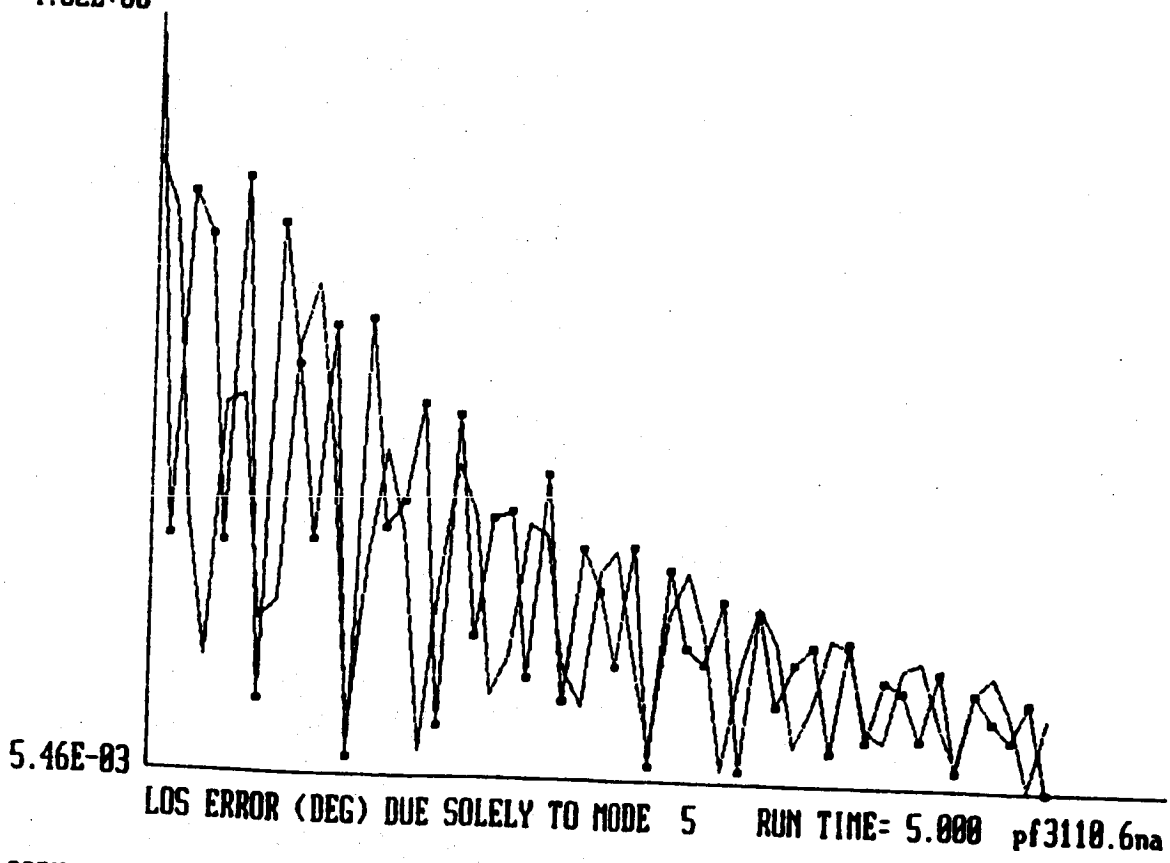
306

4.89E+01



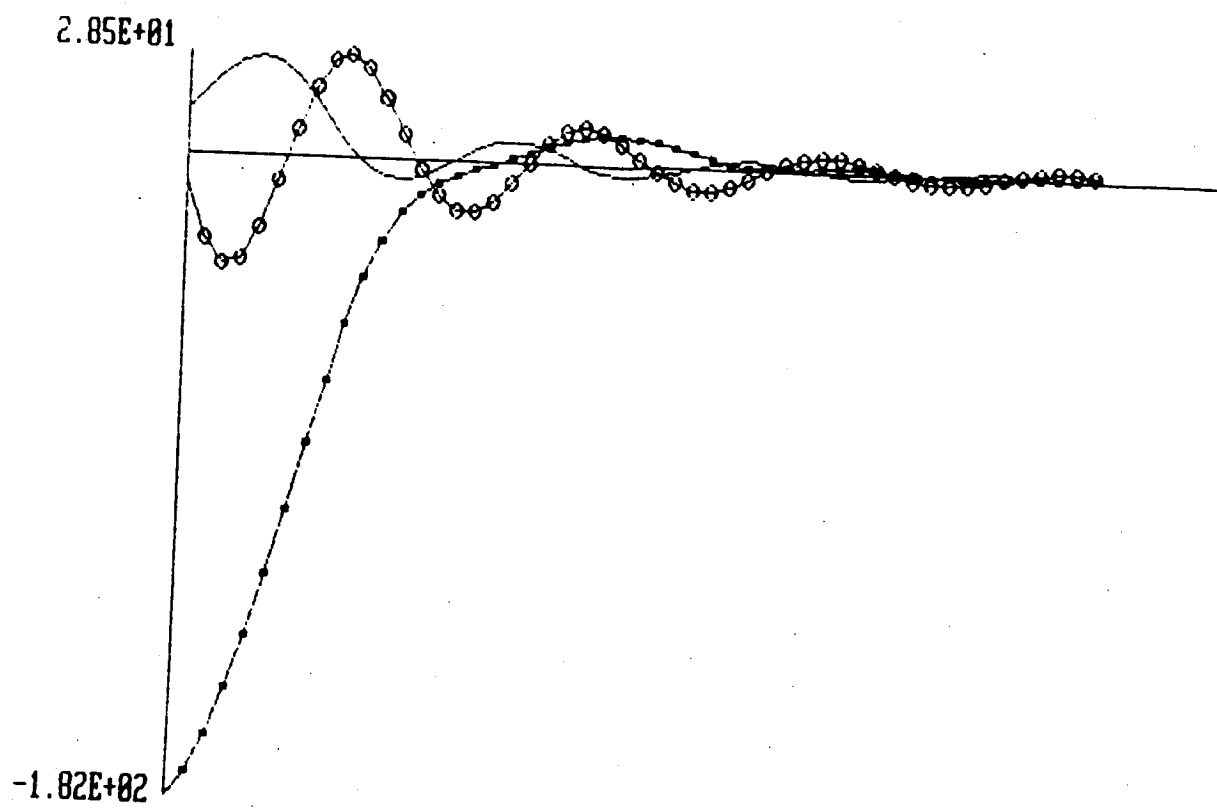
LCOPY

4.82E+00

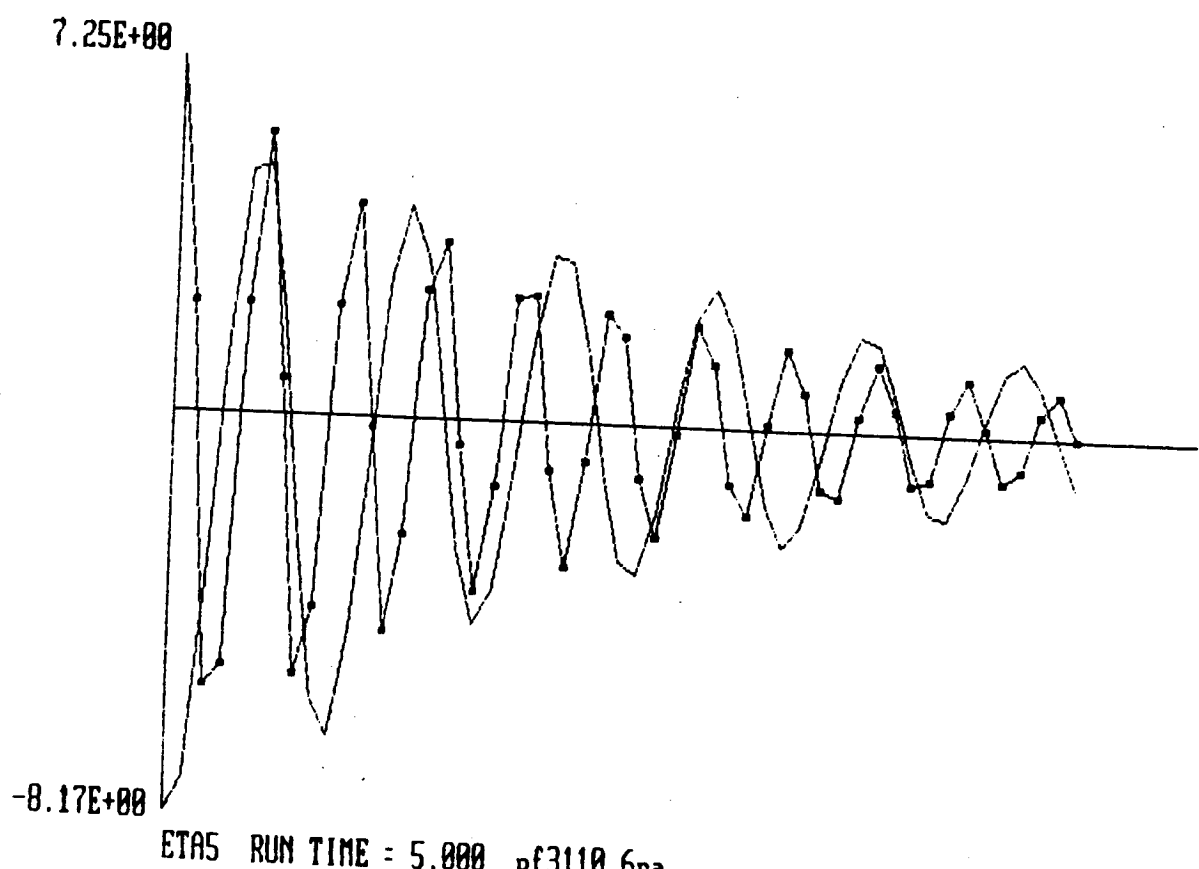


LCOPY

307



LCOPY



LCOPY

308

CONCLUSIONS

GENERAL:

- MODAL-DASHPOT AND MODAL-SPRING CONTROLLERS PROVIDE QUICK AND EFFECTIVE VIBRATION CONTROL-- EVEN EXCITED BY MOST VIOLENT, BANG-BANG TYPE
- HIGH-GAIN PROBLEMS CAN BE AVOIDED BY PROPER SELECTION OF "MODELED MODES" AND PROPER LEVEL OF AUGMENTATION
- MODAL DASHPOTS AND MODAL SPRINGS MOST EFFECTIVE DURING THE INITIAL PERIOD OF LARGE VIBRATIONS-- NEED LQG/LTR HIGH-PERFORMANCE CONTROLLERS FOR PRECISION POINTING/STABILIZATION LATER
- LOS ERROR DUE SOLELY TO EACH MODE EXCITED BY THE DISTURBANCE PROVIDES A SOUND MEASURE OF IMPORTANCE OF INDIVIDUAL MODES-- CORRECT SELECTION OF MODES TO CONTROL

SPECIFIC ON THE NUMERICAL SIMULATIONS:

- USING MODAL DASHPOTS AFTER EXCITATION GREATLY REDUCED EXCESSIVE LOS JITTER AND MAST BENDING (F0010 VS F0000)
 - MAY REQUIRE LARGE CONTROL FORCES AND MOMENTS
 - NOT BE VERY PRECISE
 - BUT ARE FAST AND EFFECTIVE
- USING MODAL SPRINGS DURING EXCITATION PREVENTED EXCESSIVE LOS JITTER AND MAST BENDING (F0100 VS F0000)
- USING MODAL DASHPOTS WITH MODAL SPRINGS DURING EXCITATION FURTHER REDUCED JITTER AND BENDING (F2100 & F3100 VS F0100)
- APPROPRIATE USE OF MODAL DASHPOTS AND SPRINGS BOTH DURING AND AFTER EXCITATION SUPPRESSED LOS JITTER AND MAST BENDING EFFECTIVELY AND QUICKLY (F0110, F2110 & F3110 VS F0000)
- MORE ACTIVE DAMPING DURING EXCITATION MAY NOT BE BETTER, HOWEVER (F3110 VS F2110)
 - MAY REQUIRE MORE CONTROL FORCES AND MOMENTS, SUPPRESS LESS LOS JITTER, LESS MAST BENDING

ISSUES NEEDED TO BE ADDRESSED:

- COUPLING OF RIGID-BODY DYNAMICS**
- INTEGRATED DESIGN WITH LQG/LTR FOR HIGH PRECISION**
 - MODAL DASHPOTS AND SPRINGS AS INNER LOOP
 - TO ENHANCE STABILITY AND ROBUSTNESS
 - LQG/LTR AS OUTER LOOP TO ENHANCE PRECISION
- TOTAL TIME FOR THE REQUIRED ACCURACY
IN LOS POINTING AND STABILIZATION**
- EVALUATION ON THE LABORATORY APPARATUS**

312

N87-17832

Control of SCOLE

by

L. Meirovitch

M. A. Norris

**Virginia Polytechnic
Institute & S. U.**

PRECEDING PAGE BLANK NOT FILMED

313

THIRD ANNUAL SCOLE WORKSHOP

CONTROL OF SCOLE

L. Meirovitch and M. A. Norris

Department of Engineering Science and Mechanics
Virginia Polytechnic Institute and State University
Blacksburg, VA 24061

MODAL CONTROL

The object is to control the SCOLE using a relatively low order model.

$$\text{Discretized model: } \underline{M}\dot{\underline{q}}(t) + \underline{K}\underline{q}(t) = \underline{F}(t) + \underline{v}(t)$$

$\underline{q}(t)$ = relatively high-dimensional configuration vector

$\underline{v}(t)$ = actuator noise vector

Drastic truncation of the model is proposed by means of a modal expansion.

$$\text{Open-loop eigenvalue problem: } \underline{K}\underline{u}_i = \omega_i^2 \underline{M}\underline{u}_i, \quad i = 1, 2, \dots, n$$

$$\text{Eigenvalue orthonormality: } \underline{u}_j^T \underline{M} \underline{u}_i = \delta_{ij}, \quad \underline{u}_j^T \underline{K} \underline{u}_i = \omega_i^2 \delta_{ij}$$

$$\text{Modal truncation: } \underline{q}(t) = \sum_{i=1}^C \underline{u}_i \underline{\eta}_i(t) = \underline{U}_C \underline{\eta}(t)$$

$\underline{U}_C = [\underline{u}_1 \ \underline{u}_2 \ \dots \ \underline{u}_C]$ = truncated modal matrix

$\underline{\eta}(t)$ = C -dimensional modal vector

MODAL CONTROL (CONT'D)

Truncated modal equations: $\ddot{\eta}_i(t) + \omega_i^2 \eta_i(t) = f_i(t) + v_i(t), \quad i = 1, 2, \dots, c$

$$f_i(t) = \underline{u}_i^T \underline{F}(t) = \text{modal control}$$

$$v_i(t) = \underline{u}_i^T \underline{v}(t) = \text{modal actuator noise}$$

Modal state equations: $\dot{\underline{x}}_i(t) = A_i \underline{x}(t) + B_i [f_i(t) + v_i(t)], \quad i = 1, 2, \dots, c$

$$A_i = \begin{bmatrix} 0 & 1 \\ -\omega_i^2 & 0 \end{bmatrix}, \quad B_i = \begin{bmatrix} 0 \\ 1 \end{bmatrix}$$

Actual output vector: $\underline{y}(t) = C \underline{x}(t) + \underline{w}(t)$

$C = s \times 2c$ matrix with c elements of a given row obtained from U_C
and the balance equal to zero

$\underline{x}(t)$ = overall modal state

$\underline{w}(t)$ = measurement (sensor) noise vector

(3)

MODAL CONTROL (CONT'D)

Modal Kalman filter: $\dot{\hat{x}}(t) = \hat{A}\hat{x}(t) + Bf(t) + K(t)[y(t) - \hat{c}\hat{x}(t)]$

A = block-diag A_i , B = block-diag B_i

K = estimator gain matrix

To determine the matrix K , it is necessary to solve first a $2C \times 2C$ matrix Riccati equation for given actuator and sensor noise intensities.

INDEPENDENT MODAL-SPACE CONTROL (IMSC)

Linear (proportional and rate feedback) control:

$$f_i = -h_i \dot{\eta}_i - g_i \ddot{\eta}_i$$

h_i, g_i = modal gains

Nonlinear control (on-off):

$$f_i = -k_i \dot{\eta}_i \geq d_i; \quad 0, \quad |\dot{\eta}_i| < d_i; \quad k_i, \dot{\eta}_i \leq d_i$$

$2d_i$ = width of the deadband region

k_i = magnitude of the modal control force

INDEPENDENT MODAL-SPACE CONTROL (IMSC) (CONT'D)

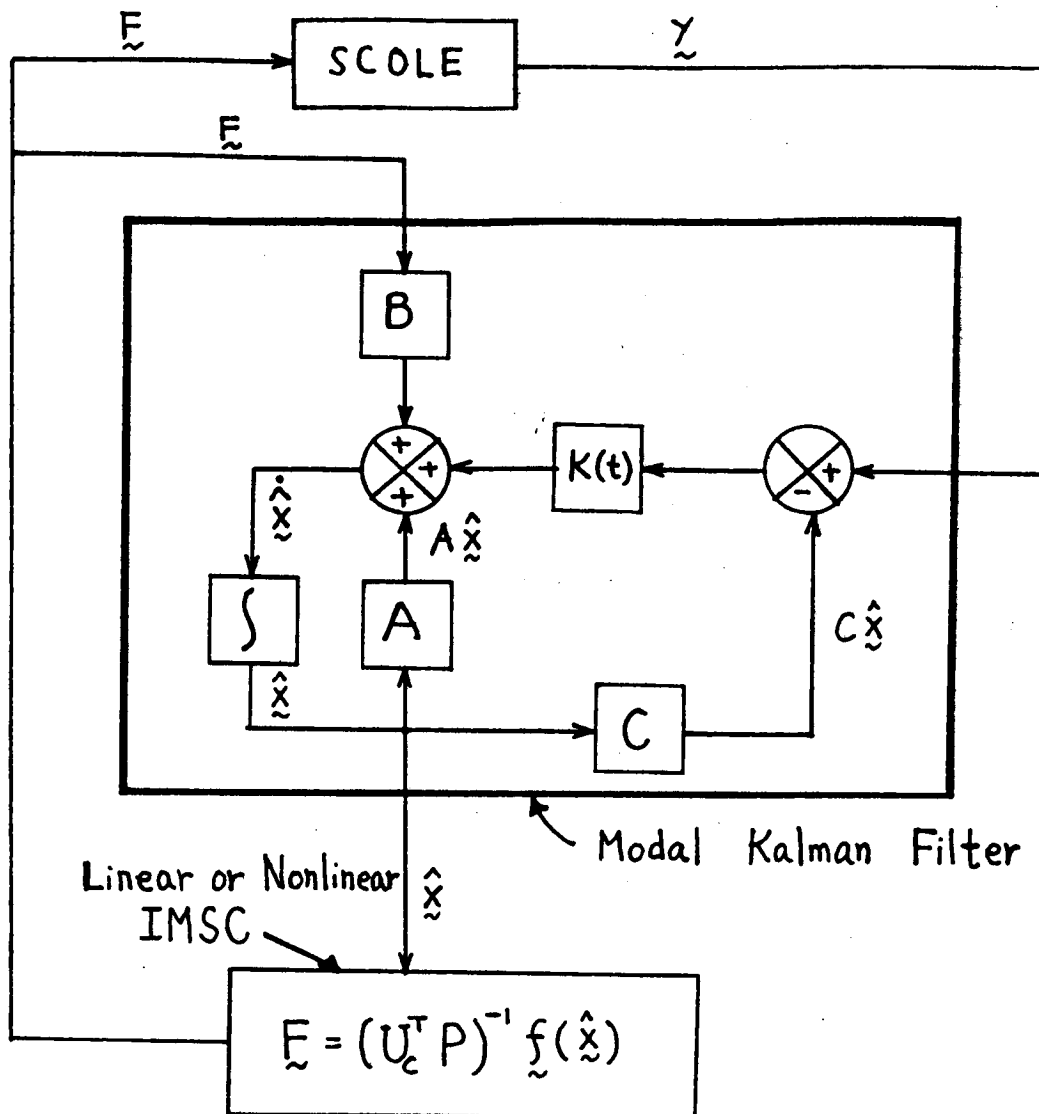
Synthesis of actual controls: let the number of controlled modes coincide with the number of actuators.

Because $\underline{F}(t)$ is of smaller dimension than $\underline{q}(t)$, let

$$M\underline{q}(t) + K\underline{q}(t) = P[\underline{F}(t) + \underline{y}(t)], \quad P = n \times c$$

$$\underline{f}(t) = U_C^T P \underline{F}(t) + \underline{F}(t) = (U_C^T P)^{-1} \underline{f}(t)$$

∴ The components of $\underline{F}(t)$ are linear combinations of the components of $\underline{f}(t)$. When the modal control is nonlinear, the components of $\underline{F}(t)$ are quantized and have the appearance of staircase functions



N87-17833 4

Regulation of the SCOLE Configuration

by

**Gregory A. Norris
Emmanuel G. Collins
Robert E. Skelton
Purdue University**

REGULATION OF

THE SCOLE CONFIGURATION

INVESTIGATORS

Gregory A. Norris

Emmanuel G. Collins

Robert E. Skelton

PERFORMANCE REQUIREMENTS

- (I) MAINTAIN RMS OF THE STEADY STATE LINE-OF-SIGHT (LOS) ERROR WITHIN A SPECIFIED BOUND.
- (II) MAINTAIN STEADY STATE ACTUATOR VARIANCES AS CLOSE AS POSSIBLE TO SPECIFIED BOUNDS.

ORIGINAL SCOPE CONFIGURATION

- LOCATION OF 2 PROOF MASS ACTUATORS NOT SPECIFIED.
- 42 SENSORS PROVIDED.

OBJECTIVES

- (I) DETERMINE LOCATIONS FOR PROOF MASS ACTUATORS.
- (II) DETERMINE A REDUCED SET OF SENSORS.
- (III) DESIGN A CONTROL LAW TO MEET PERFORMANCE REQUIREMENTS FOR LOS ERROR AND ACTUATORS.

- SOLUTIONS TO THE 3 PROBLEMS ARE INTERDEPENDENT.
- CHOICE OF ACTUATORS AND SENSORS INFLUENCES CONTROL LAW.
- CHOICE OF CONTROL LAW INFLUENCES SENSOR AND ACTUATOR SELECTION.

LINEARIZED DYNAMICAL MODEL

VECTOR SECOND ORDER MODAL FORM

$$\ddot{\eta} + D\dot{\eta} + \Omega^2 \eta = \bar{B}(u+w)$$

output vector y

$$y_1 = LOS_x, \quad y_2 = LOS_y, \quad y_3 = LOS_z$$

$$E(\text{LOS error})^2 = (Ey_1^2 + Ey_2^2 + Ey_3^2)^{1/2}$$

$$y = C_p \eta$$

measurement vector z

$z_{p,r} = \text{position \& rate measurement vector}$

$$= P_p \dot{\eta} + P_v \dot{\eta} + v_{p,r}$$

$z_a = \text{acceleration measurement vector}$

$$= Q\eta + v_a$$

$$= Q(-\Omega^2 \eta - D\eta + \bar{B}u + \bar{B}w) + v_a$$

$$z = \begin{bmatrix} z_{p,r} \\ z_a - Q\bar{B}u \end{bmatrix} = M_p \dot{\eta} + M_v \dot{\eta} + v$$

where

$$M_p = \begin{bmatrix} P_p & 0 \\ 0 & -Q\Omega^2 \end{bmatrix}$$

$$M_v = \begin{bmatrix} P_v & 0 \\ 0 & -QD \end{bmatrix}$$

$$v = \begin{bmatrix} v_{p,r} \\ v_a + Q\bar{B}w \end{bmatrix}$$

=> ASSOCIATED SENSOR NOISE (v) & ACTUATOR NOISE (w) ARE CORRELATED

- MODEL OBTAINED USING CUBIC BEAM ELEMENT SHAPE FUNCTIONS FOR BEAM BENDING AND LINEAR SHAPE FUNCTION FOR BEAM TWIST.
- 32 MODES IN ORIGINAL MODEL.
- MODAL COST ANALYSIS USED TO REDUCE TO 23 MODE DESIGN AND EVALUATION MODEL.

MODAL COST ANALYSIS

modal cost	rank	mode no.	modal cost	freq. (hz)	mode type
1	1	1	infinite	0	Rigid body
2	2	2	infinite	0	Rigid body
3	3	3	infinite	0	Rigid body
4	5	5	.911e+07	.299e+00	Bending (roll)
5	7	7	.363e+07	.118e+01	Bending
6	4	4	.336e+07	.276e+00	Bending (pitch)
7	6	6	.138e+07	.811e+00	Bending
8	8	8	.955e+06	.205e+01	Bending
9	10	10	.673e+04	.551e+01	Bending
10	9	9	.556e+04	.478e+01	Bending
11	11	11	.246e+02	.123e+02	Bending
12	14	14	.365e+01	.243e+02	Bending
13	17	17	.245e+01	.395e+02	Twist
14	12	12	.305e+00	.129e+02	Bending
15	16	16	.116e+00	.390e+02	Bending
16	15	15	.349e-01	.256e+02	Bending
17	26	26	.995e-02	.109e+03	Bending
18	25	25	.377e-02	.103e+03	Bending
19	13	13	.376e-02	.237e+02	Bending
20	29	29	.174e-02	.140e+03	Bending
21	35	35	.836e-03	.215e+03	Bending
22	20	20	.597e-03	.586e+02	Bending
23	28	28	.370e-03	.139e+03	Bending
24	23	23	.125e-03	.617e+02	Bending
25	19	19	.310e-04	.561e+02	Bending
26	34	34	.275e-04	.215e+03	Bending
27	32	32	.617e-05	.175e+03	Bending
28	31	31	.294e-05	.175e+03	Bending
29	27	27	.131e-05	.135e+03	Twist
30	24	24	.140e-07	.106e+03	Twist
31	30	30	.134e-07	.167e+03	Twist
32	33	33	.413e-08	.200e+03	Twist
33	22	22	.298e-10	.811e+02	Bending
34	18	18	.340e-11	.515e+02	Twist
35	21	21	.226e-13	.702e+02	Twist

• FIRST 5 FLEXIBLE MODES DOMINATE MODAL COST

• BEAM BENDING DOMINATES MODAL COST

CONTROL LAW DESIGN VIA
THE OUTPUT VARIANCE ASSIGNMENT ALGORITHM

- ITERATIVE ALGORITHM DEVELOPED BY SKELTON AND DELORENZO
- OBJECTIVE IS TO CHOOSE DIAGONAL Q AND R IN THE LQG COST FUNCTIONAL

$$v = E_{\infty} (y^T Q y + u^T R u)$$

S.T. THE LQG CONTROL LAW SATISFIES

$$E_{\infty} y_i^2 = \sigma_i^2 \quad (\text{or } < \sigma_i^2) \quad \forall i = 1 \dots n_y$$

WHILE MINIMIZING

$$\sum_{i=1}^{n_u} \frac{E_{\infty} u_i^2}{\mu_i^2}.$$

bounds on input variances

SENSOR AND ACTUATOR SELECTION
VIA INPUT/OUTPUT COST ANALYSIS

- SUBOPTIMAL APPROACH.
- BASED ON DECOMPOSING COST FUNCTION

$$v = E_{\infty}(y^T Q y + u^T R u)$$

as

$$v = \sum_{i=1}^{n_y} v_i^y + \sum_{i=1}^{n_u} v_i^u$$
$$v = \sum_{i=1}^{n_u} v_i^w + \sum_{i=1}^{n_z} v_i^v$$

- DEFINES ACTUATOR EFFECTIVENESS,

$$v_i^{\text{act}} = v_i^u - v_i^w$$

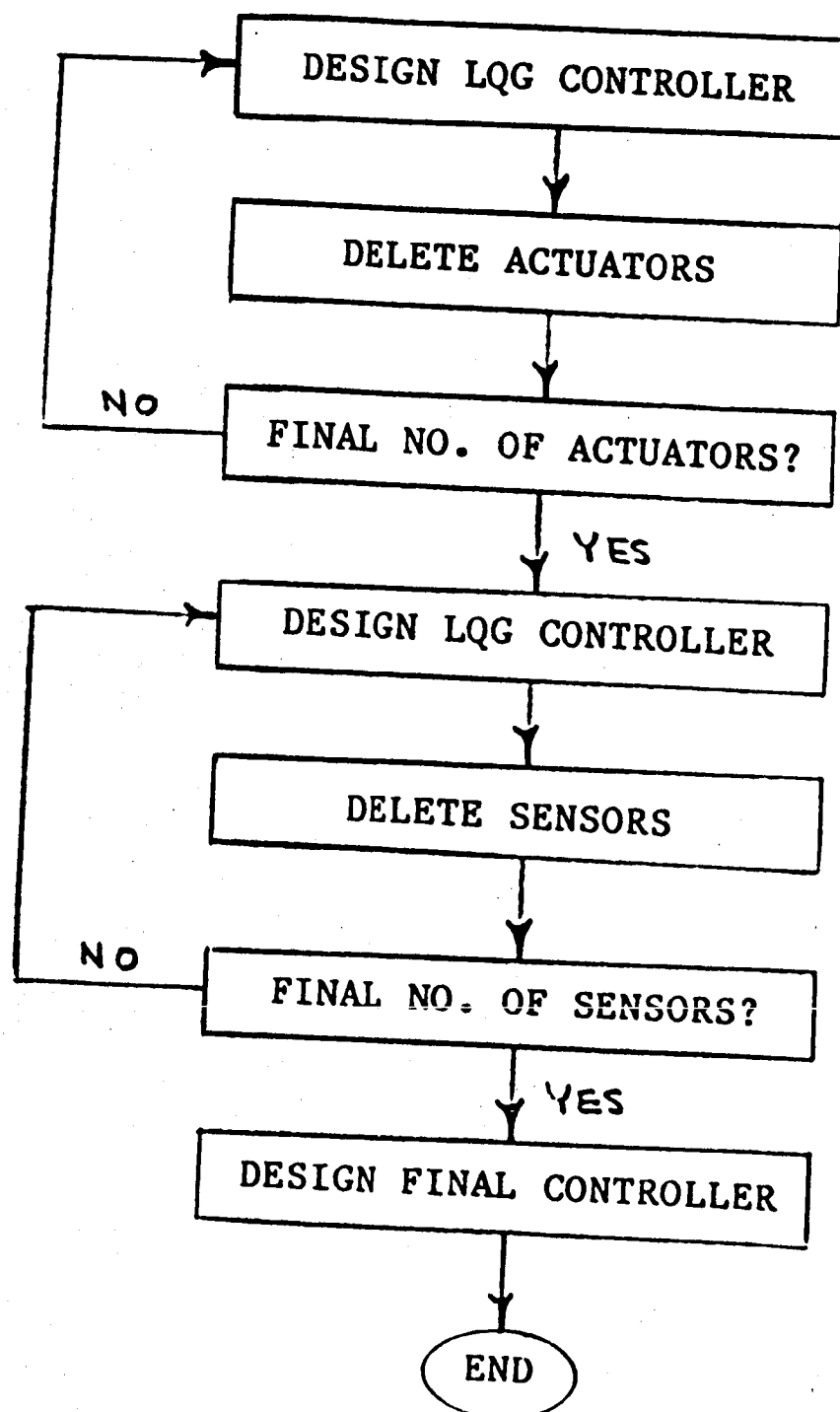
AND SENSOR EFFECTIVENESS

$$v_i^{\text{sen}} = v_i^v$$

- DELETES ACTUATOR(S) OR SENSOR(S) WITH LOWEST EFFECTIVENESS VALUES.

SOLUTION PROCEDURE

- BEGIN WITH LARGE SET OF PROOF MASS ACTUATORS AT FIXED LOCATIONS



SOME RESULTS

ORIGINAL SCOPE PROPOSAL

$\text{rms(los error)} < .02 \text{ deg}$

OUR FINDINGS

if noise through shuttle cmgs only:

$\text{rms(los error)} > .045 \text{ deg}$

if equivalent noise through all actuators:

$\text{rms(los error)} > .075 \text{ deg}$

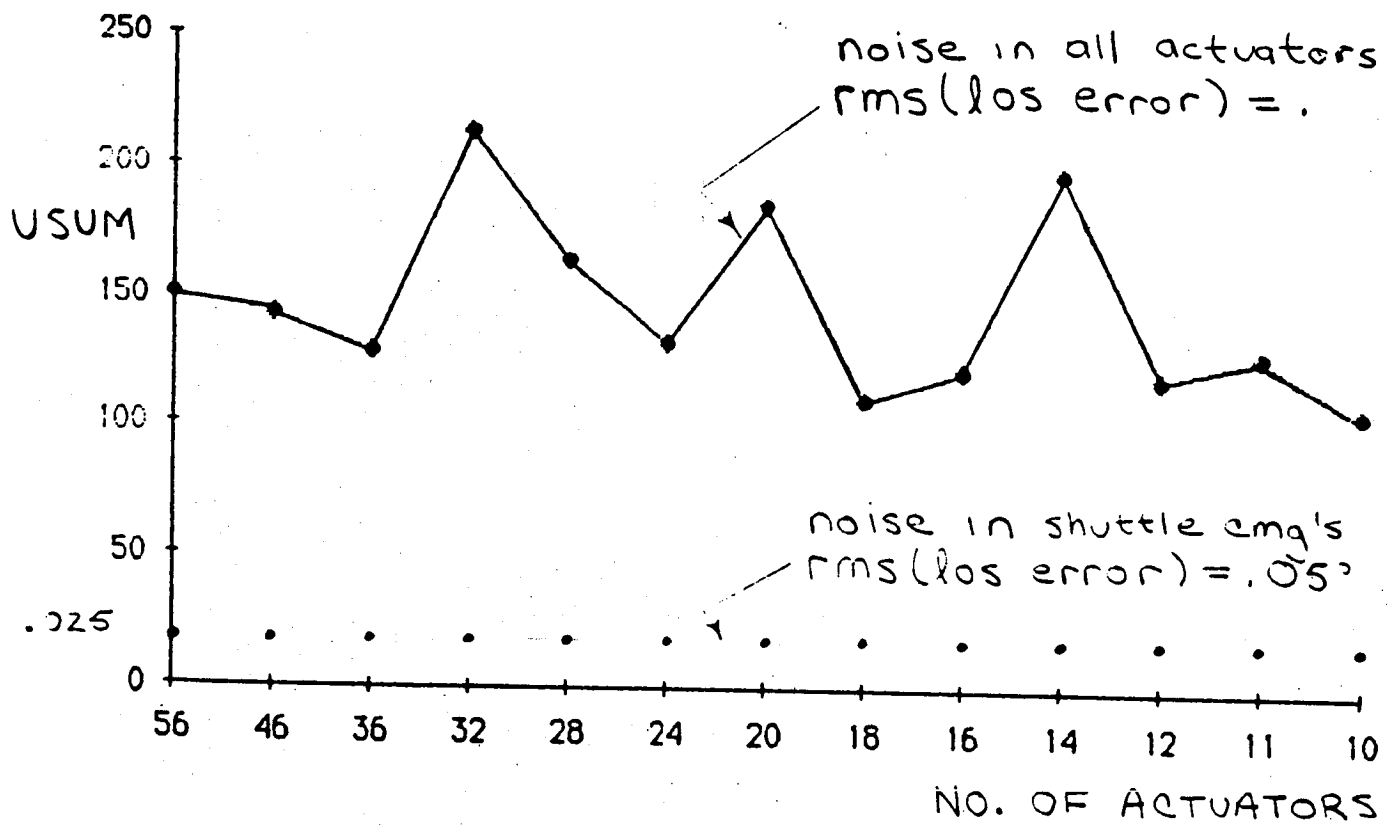
CONCLUSIONS

- ORIGINAL SPECS ON LOS ERROR ARE NOT ACHIEVABLE.
- MUST MODIFY LOS SPECS.

ACTUATOR SELECTION

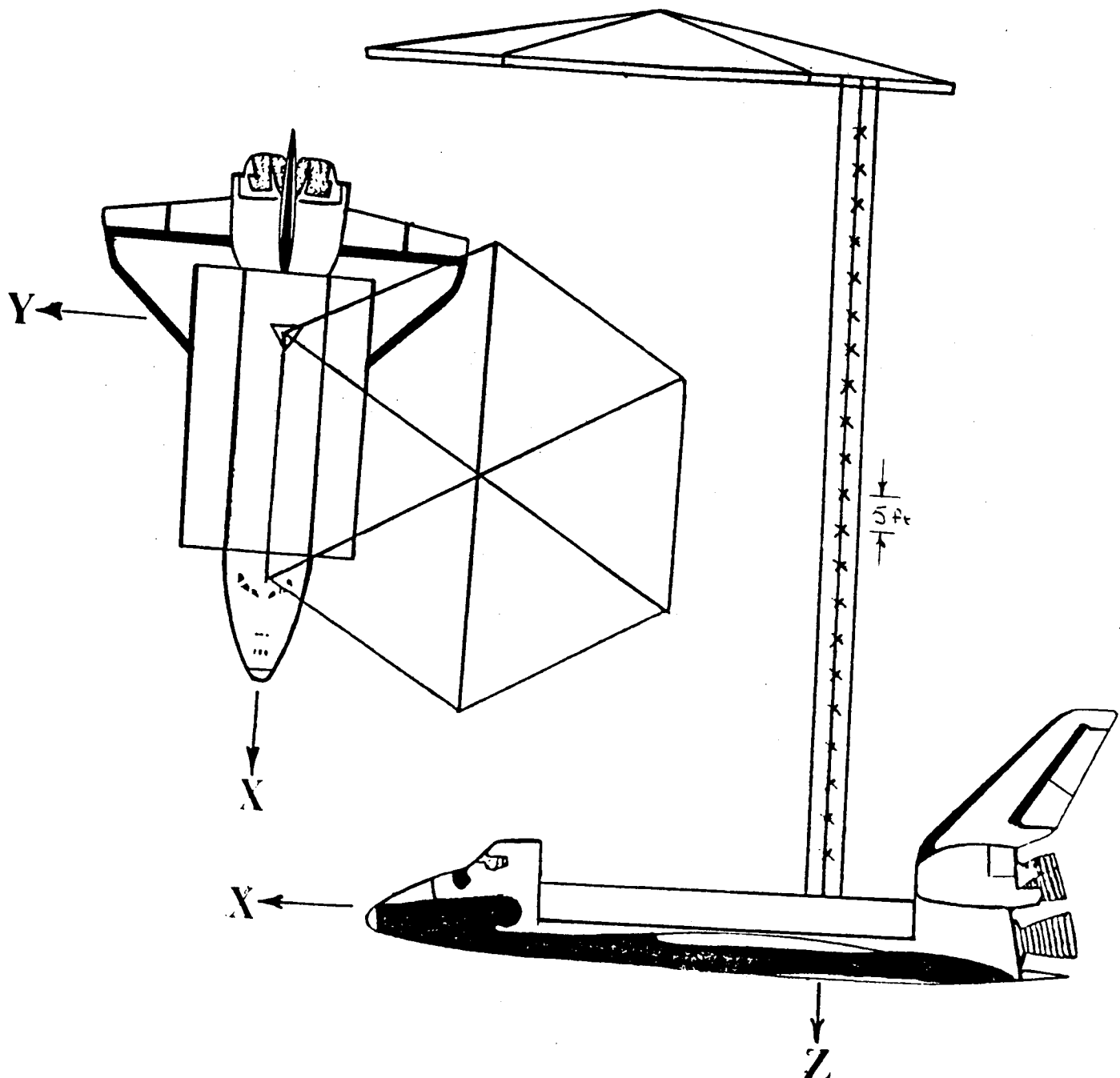
DEFINE

$$USUM = \sum_{i=1}^n \frac{E_{ui}^2}{\mu_i^2} = \text{dimensionless measure of total control effort}$$



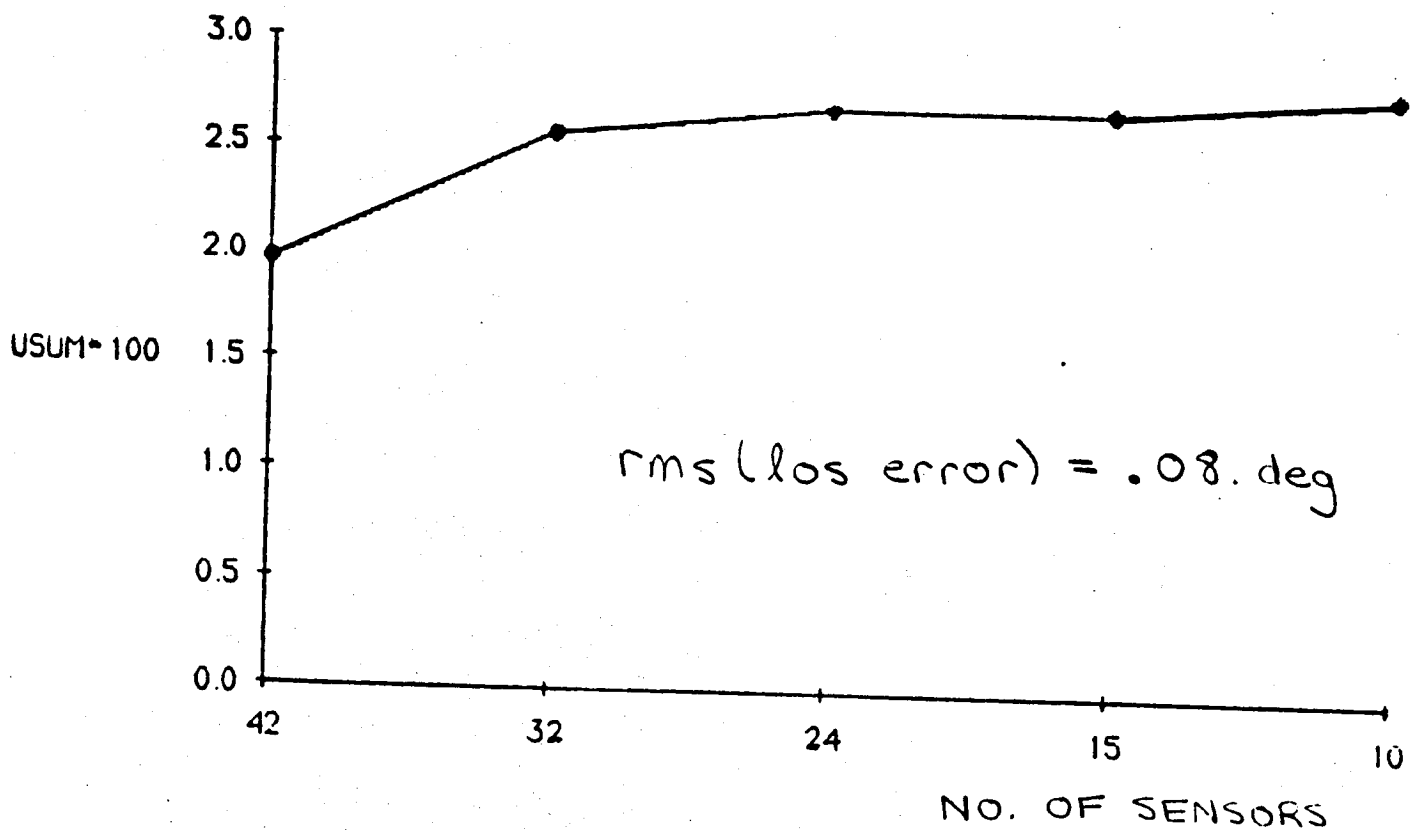
FINDINGS

- BY USING REDUCED SET OF ACTUATORS THERE IS A 50% SAVINGS IN CONTROL EFFORT (AS MEASURED BY USUM).



- PROOF MASS ACTUATORS NEAR TOP OF THE BEAM ARE MORE EFFECTIVE

SENSOR SELECTION



- GOOD PERFORMANCE MAY BE ACHIEVED WITH A MUCH SMALLER SET OF SENSORS.

CONCLUSIONS

(I) RMS(LOS ERROR) \leq .02 DEG IS NOT ACHIEVABLE.

RMS(LOS ERROR) \leq .05 DEG IS ACHIEVABLE IF NOISE IS ONLY THROUGH SHUTTLE CMG'S.

RMS(LOS ERROR) \leq .08 DEG IS ACHIEVABLE IF (EQUIVALENT) NOISE IS THROUGH ALL ACTUATORS.

(II) PROOF MASS ACTUATORS SHOULD BE PLACED NEAR TOP OF MAST.

(III) GOOD PERFORMANCE MAY BE ACHIEVED WITH A (SIGNIFICANTLY) REDUCED SET OF SENSORS.

Evaluation of On-Line Pulse Control for Vibration Suppression in Flexible Spacecraft

by

G. A. Bekey

S. F. Masri

R. K. Miller

Univ. of So. California



EVALUATION OF ON-LINE PULSE CONTROL FOR VIBRATION SUPPRESSION IN FLEXIBLE SPACECRAFT

G.A. Bekey, S.F. Masri, R.K. Miller

University of Southern California
Los Angeles, CA

OUTLINE

I. Objective

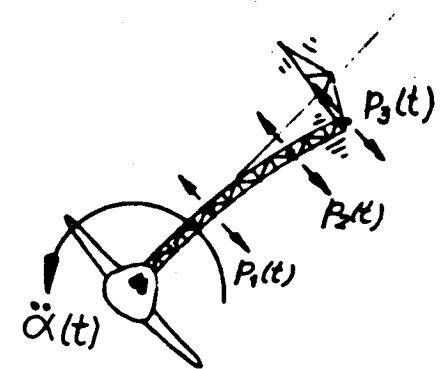
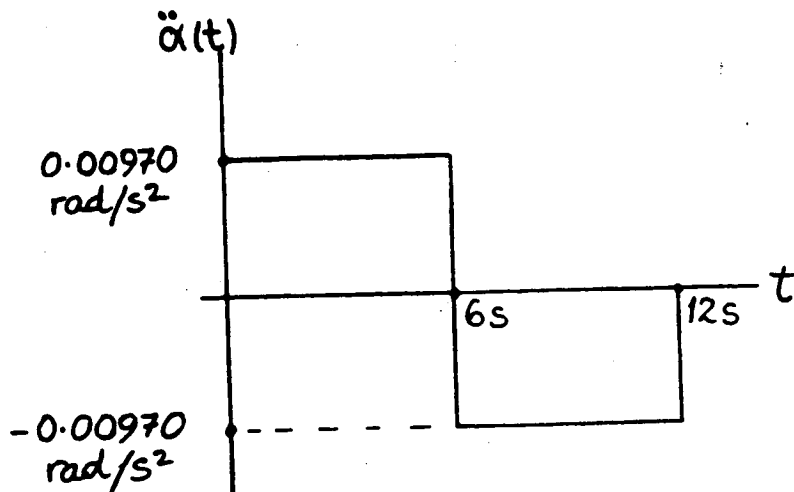
II. Modeling Issues

- Beam vs. Truss
- NL-FEM, numerical problems

III. Control Issues

- ED Pulse Actuator Development
- Pseudo Pulse Algorithm Dev.
- Large NL Simulation Problems

OVERALL OBJECTIVE



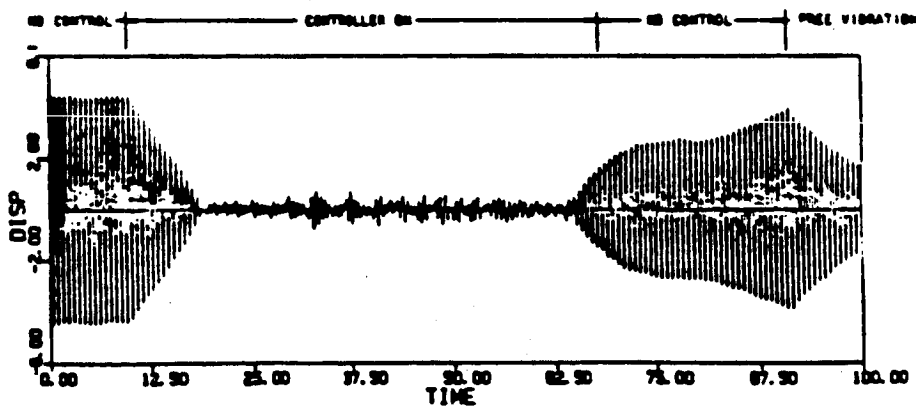
(Gene Lin, 1984 SCOLE Mtg.)

Minimum Time 20°
Slew Maneuver

Mass-Ejection Pulse Control Strategy:

$$P_i(t) = \begin{cases} -c_i \operatorname{sgn}(v_i) |v_i|^{n_i} & t_{0_i} < t < (t_{0_i} + T_{d_i}) \\ 0 & (t_{0_i} + T_{d_i}) < t < t_{0_{i+1}} \end{cases}$$

Typical Experimental Results:

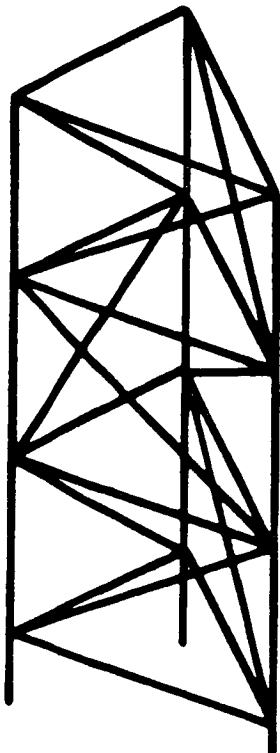


MODELLING ISSUES

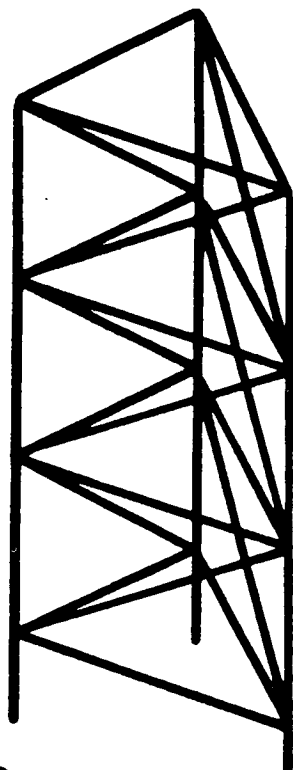


1. Continuous Beam vs. Truss

- Axial / Torsional Coupling
- Local Member Participation in Modes
- Parametric Resonance Problems



Alternating Bay
Diagonals



Mast Flight Beam

Identical Bay
Diagonals

LINEAR TRUSS RESULTS

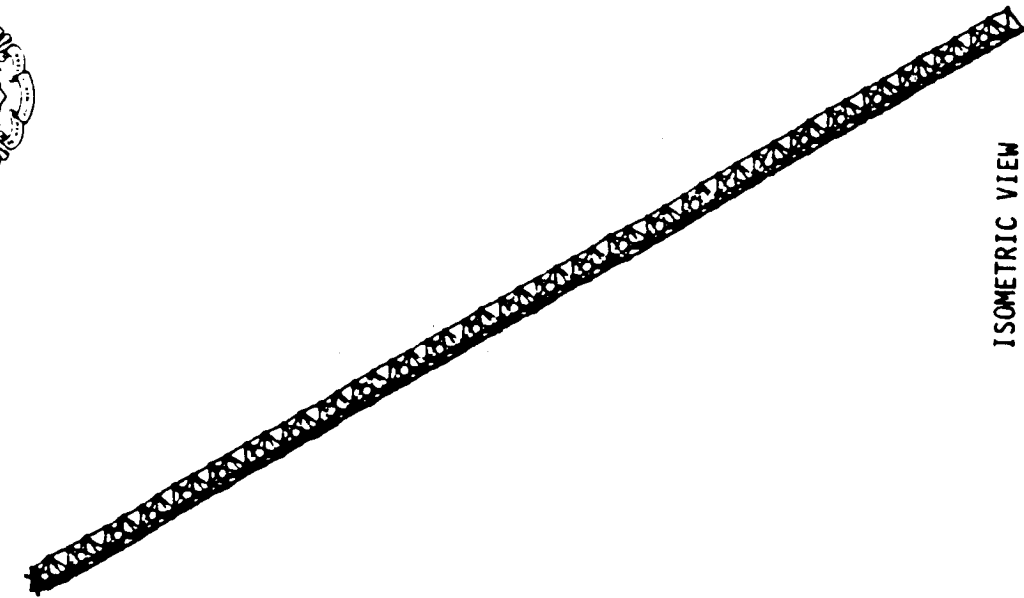


2. Linear Finite Element Model Characteristics

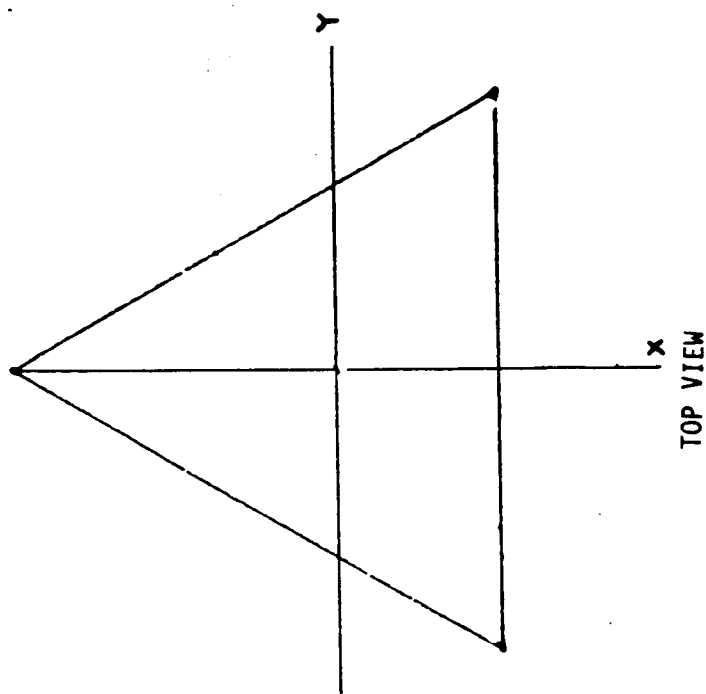
- COFS-I Hardware Configuration
- 54 Bays, 60m
- 171 nodes, 486 elements, 522 D. of F.
- July 1986 data for member characteristics from Astro Aerospace Corp. / Harris Corp.
- Match modal results with Astro/Harris
- Transient Response Simulations:
 - Rayleigh damping: $\zeta_1 = 1\%$, $\zeta_{12} = 10\%$
 - Sine-sweep, tip excitation
 - Nonstationary Random, tip excitation
 - Harmonic, base excitation



NUMBER OF NODES = 171
NUMBER OF TRUSS ELEMENTS = 486
NUMBER OF BEAM ELEMENTS (WITH END RELEASE) = 18
NUMBER OF DEGREES OF FREEDOM = 522



ISOMETRIC VIEW



FRONT VIEW

FIG. 1. NONLINEAR THREE-DIMENSIONAL FINITE ELEMENT MODEL OF COFS I MAST



NASA RESULTS
MAST ON RIGID BASE

USC RESULTS
MAST ON RIGID BASE

MODE	FREQUENCY (HZ)	TYPE	FREQUENCY (HZ)	TYPE
1	0.18	1st Bending in Y	0.18	1st Bending in Y
2	0.20	1st Bending in X	0.20	1st Bending in X
3	1.77	2nd Bending in Y	1.60	2nd Bending in Y
4	1.97	2nd Bending in X	1.72	2nd Bending in X
5	2.18	1st Torsion	2.37	1st Torsion
6	5.47	3rd Bending in Y	4.72	3rd Bending in Y
7	6.07	3rd Bending in X	5.07	3rd Bending in X
8	8.12	2nd Torsion	7.70	2nd Torsion
9	11.23	4th Bending in Y	9.29	4th Bending in Y
10	12.44	4th Bending in X	9.93	4th Bending in X
11	12.62	1st Compression	12.49	1st Compression
12	13.51	3rd Torsion	12.82	3rd Torsion

FIG. 3. FIRST 12 NATURAL FREQUENCIES AND MODE SHAPES OBTAINED BY DETERMINING THE EIGEN VALUES AND EIGENVECTORS CORRESPONDING TO THE LINEARIZED VERSION OF THE FINITE ELEMENT MODEL SHOWN IN FIG. 1.



NOTE: TORSIONAL MODE PLOTS APPEAR DISTORTED DUE TO PLOTTING ALGORITHM. ACTUAL MODE SHAPES INCLUDE NEGLIGIBLE BATTEN DEFORMATIONS.

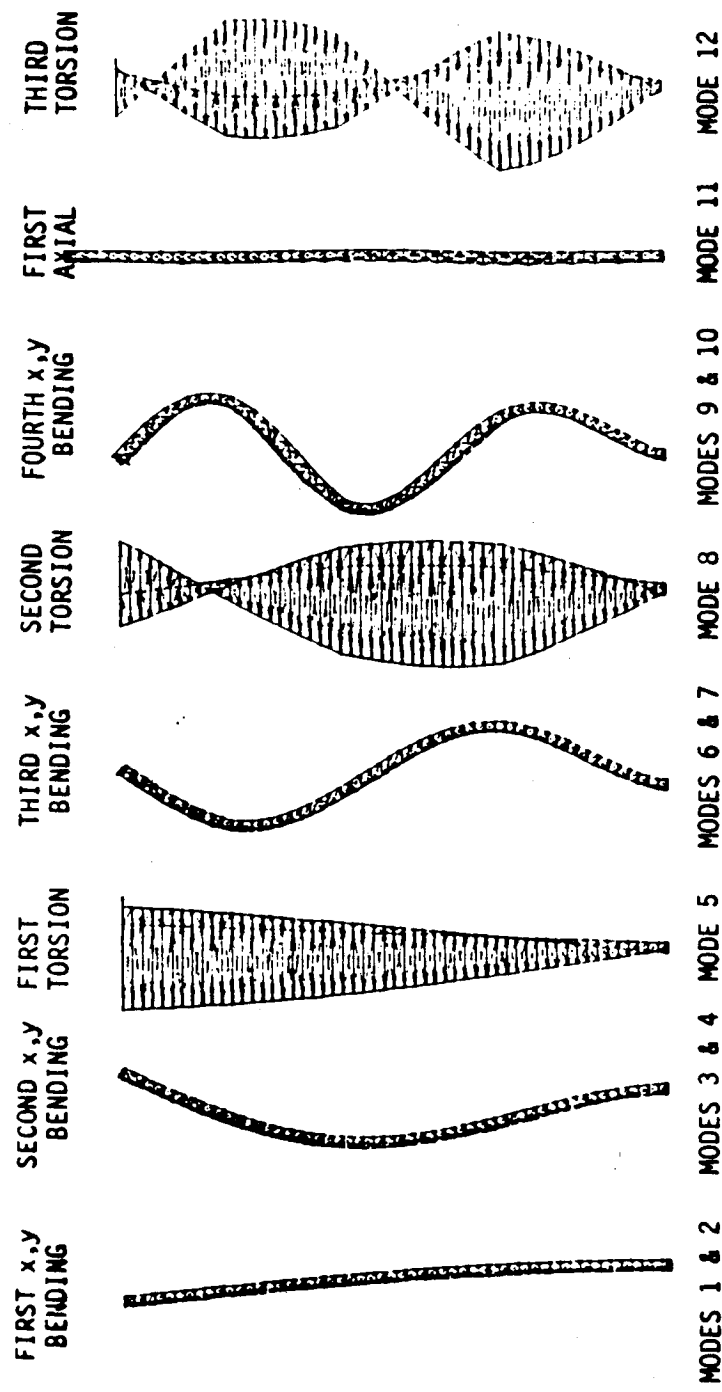
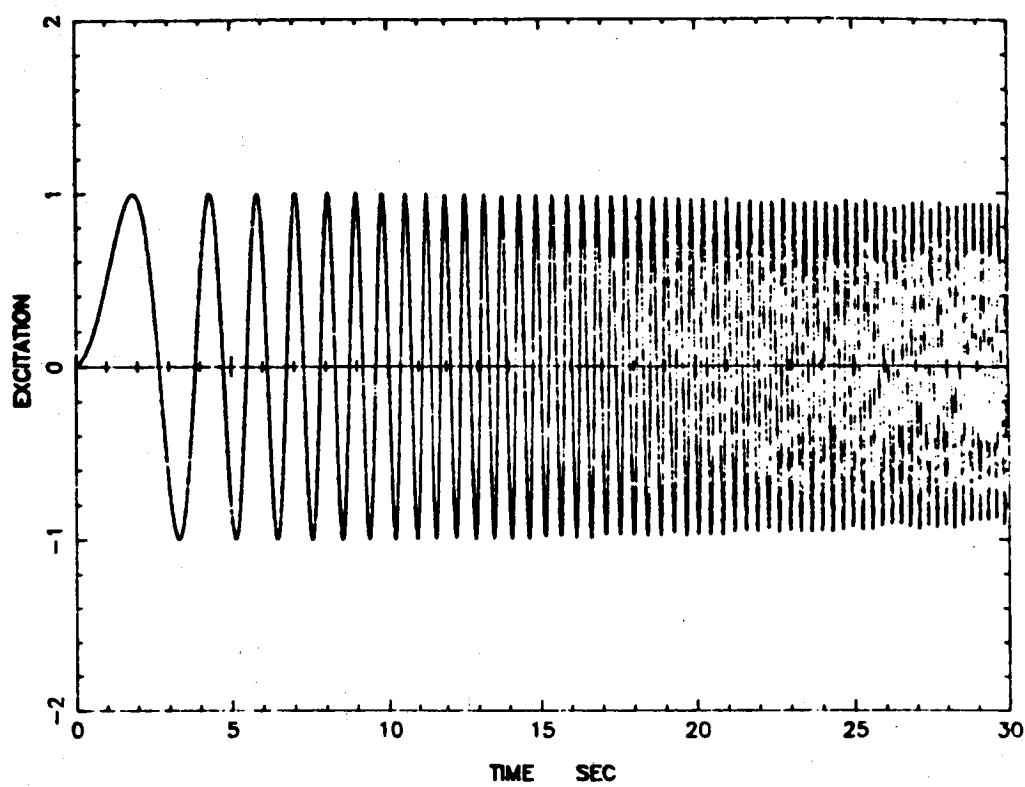
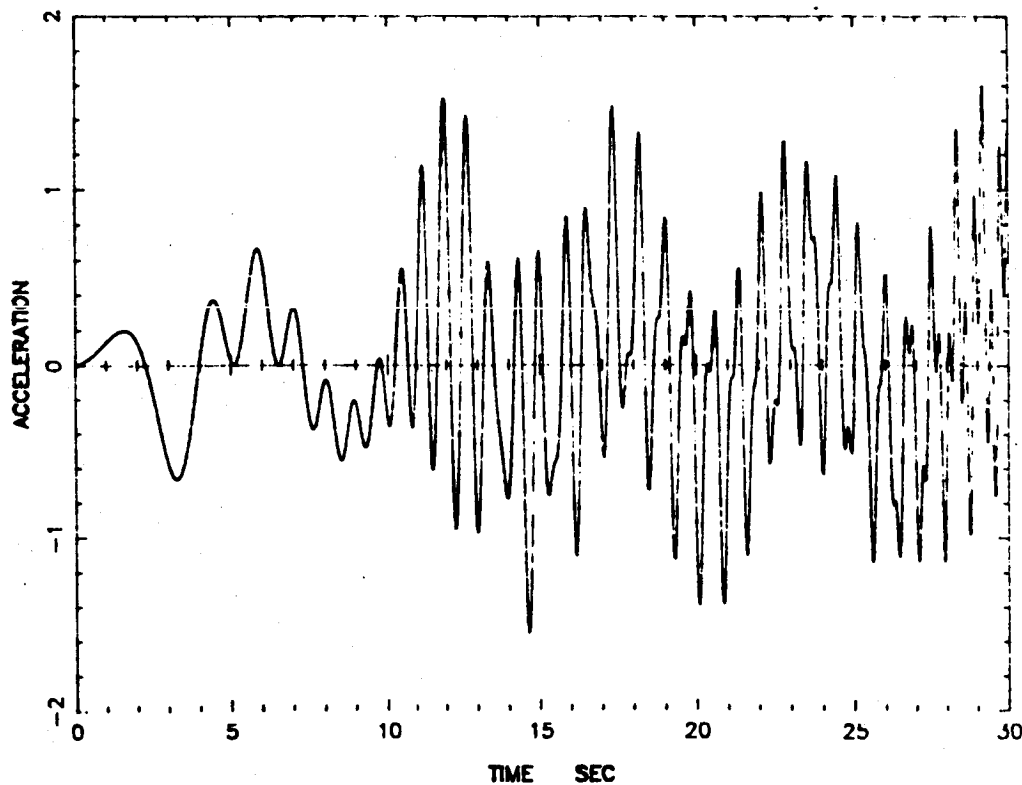


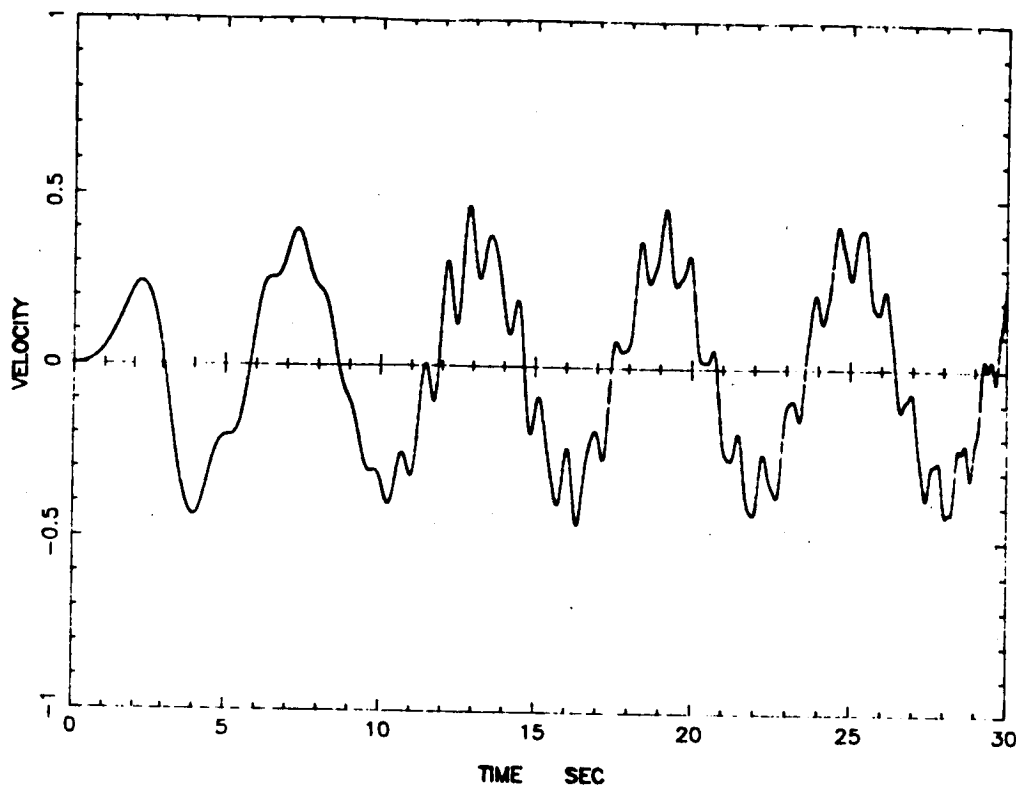
FIG. 4. REPRESENTATIVE MODE SHAPES CORRESPONDING TO THE LINEARIZED VERSION OF THE USC NONLINEAR COFS I MAST FINITE ELEMENT MODEL.



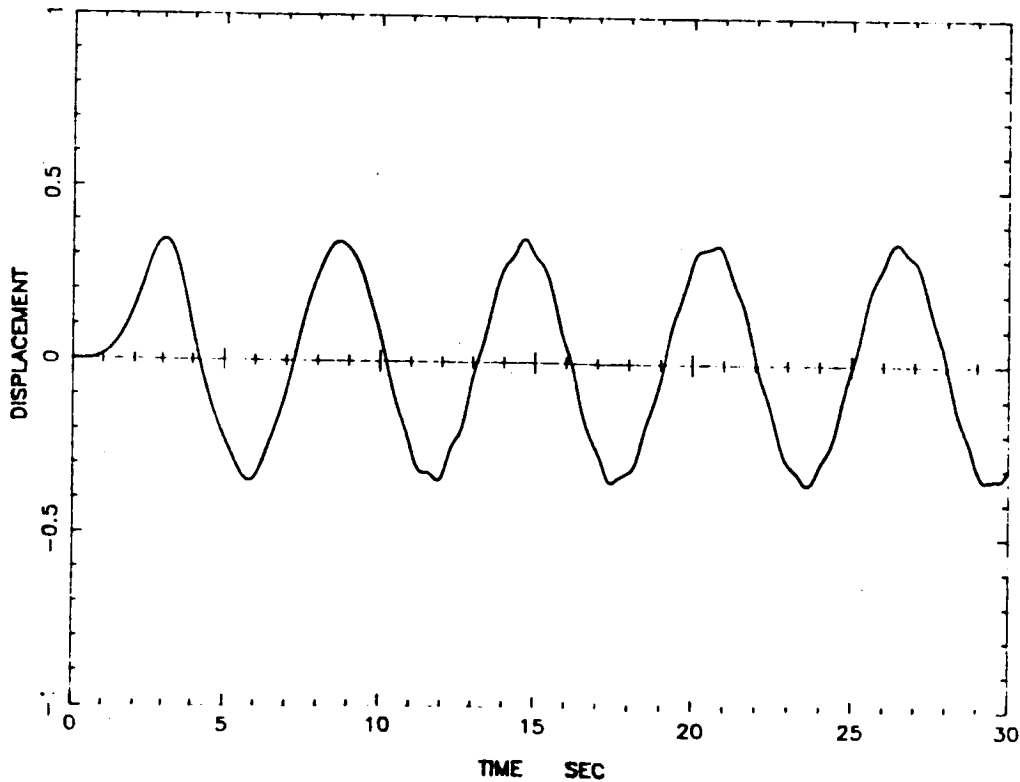
Swept Sine Response - Tip Excit.



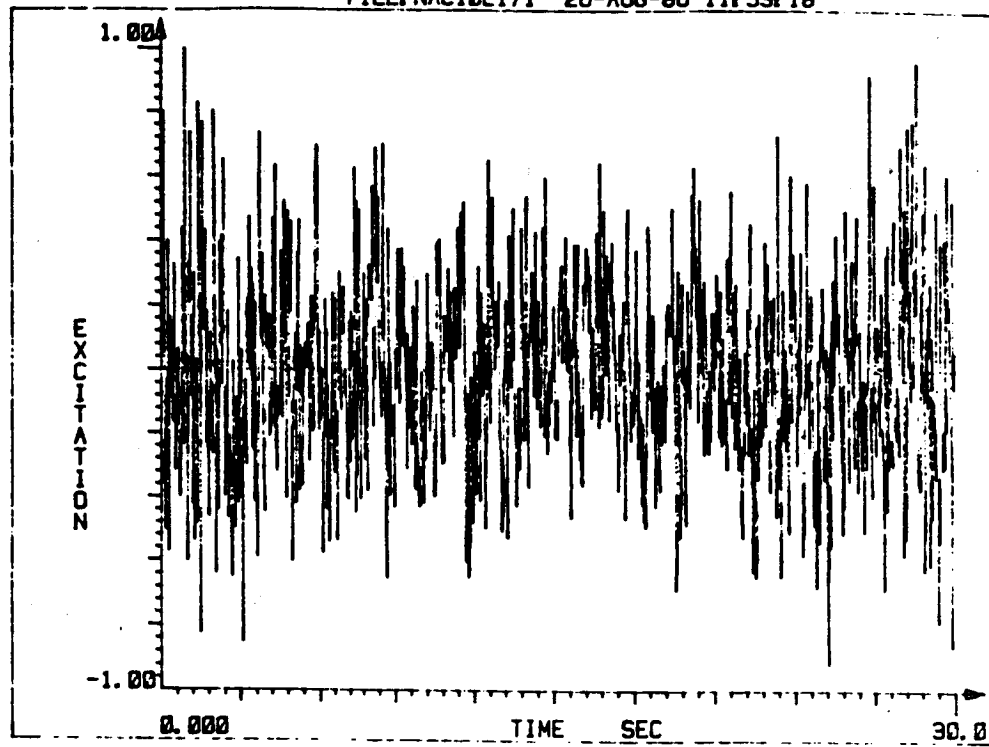
345



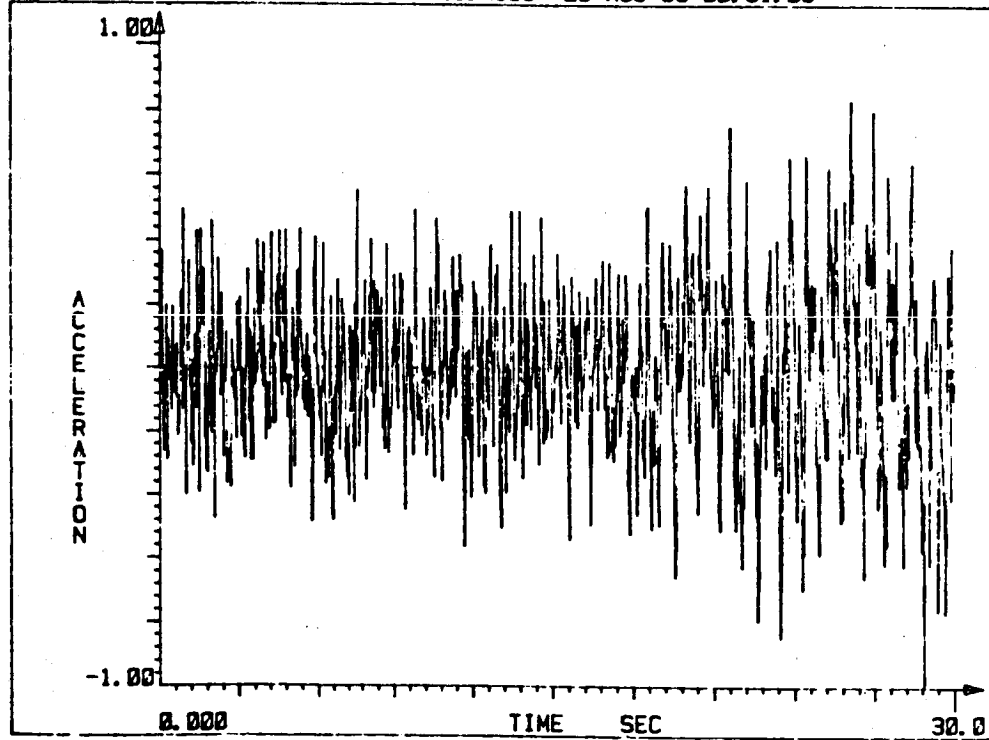
Swept Sine Response - Tip Excit.

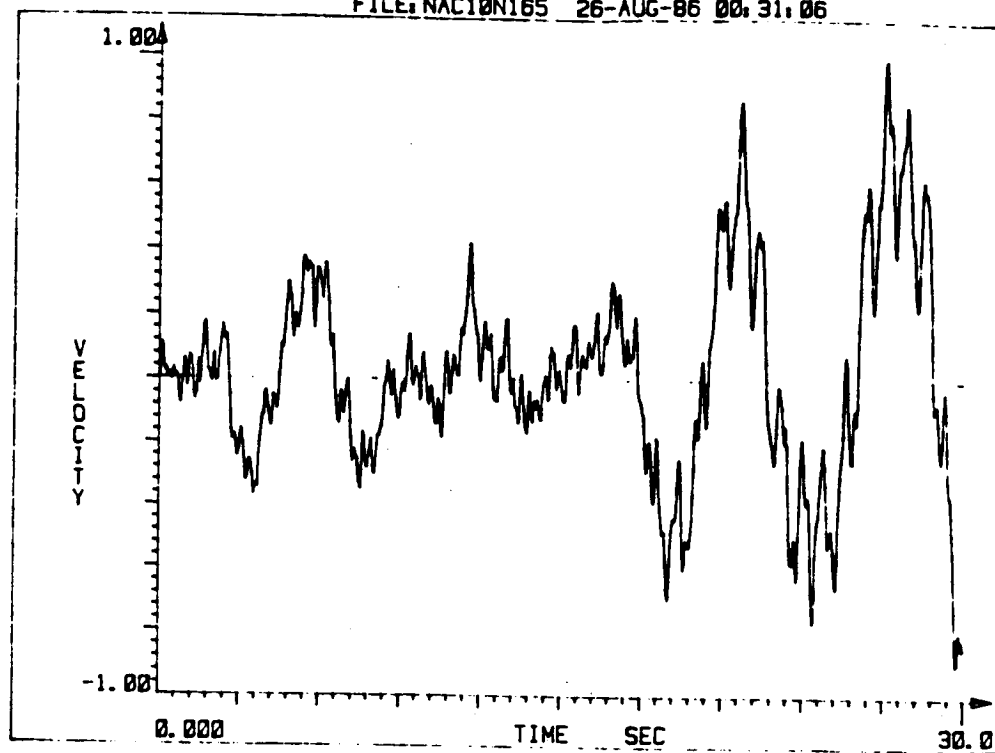


346

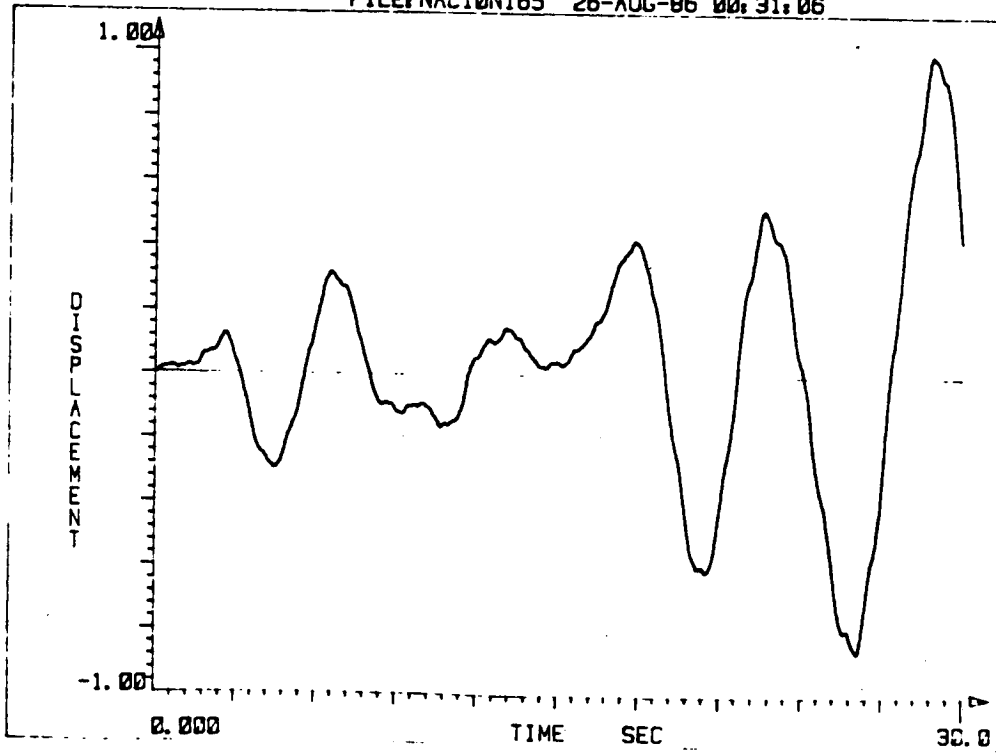


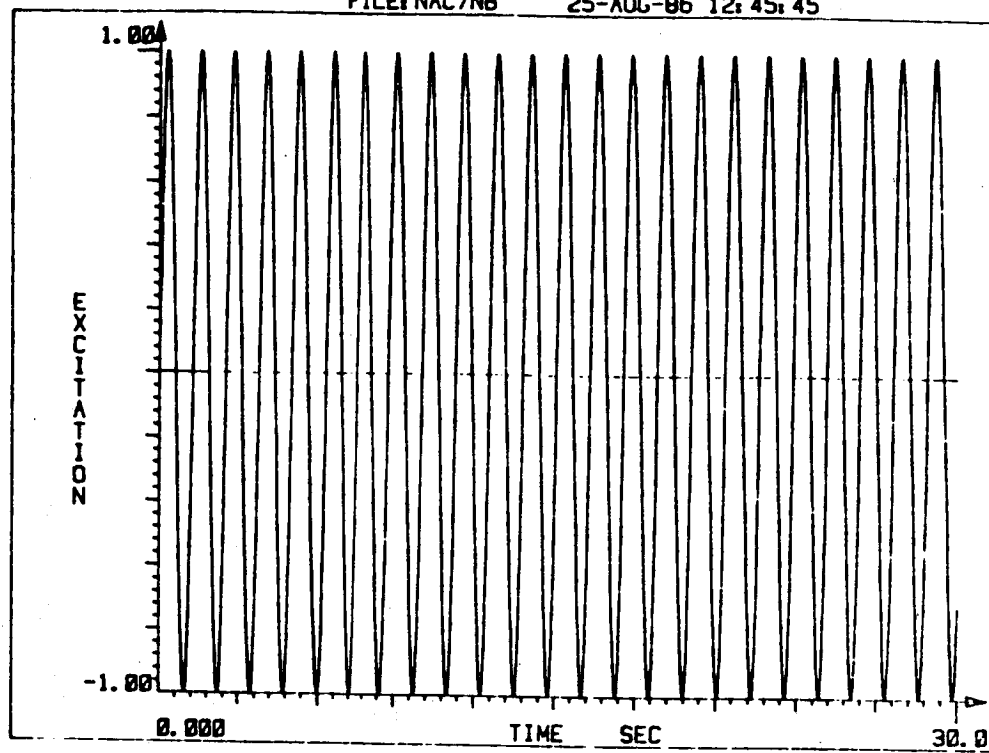
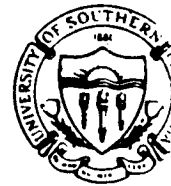
Nonstationary Random Response - Tip Excit



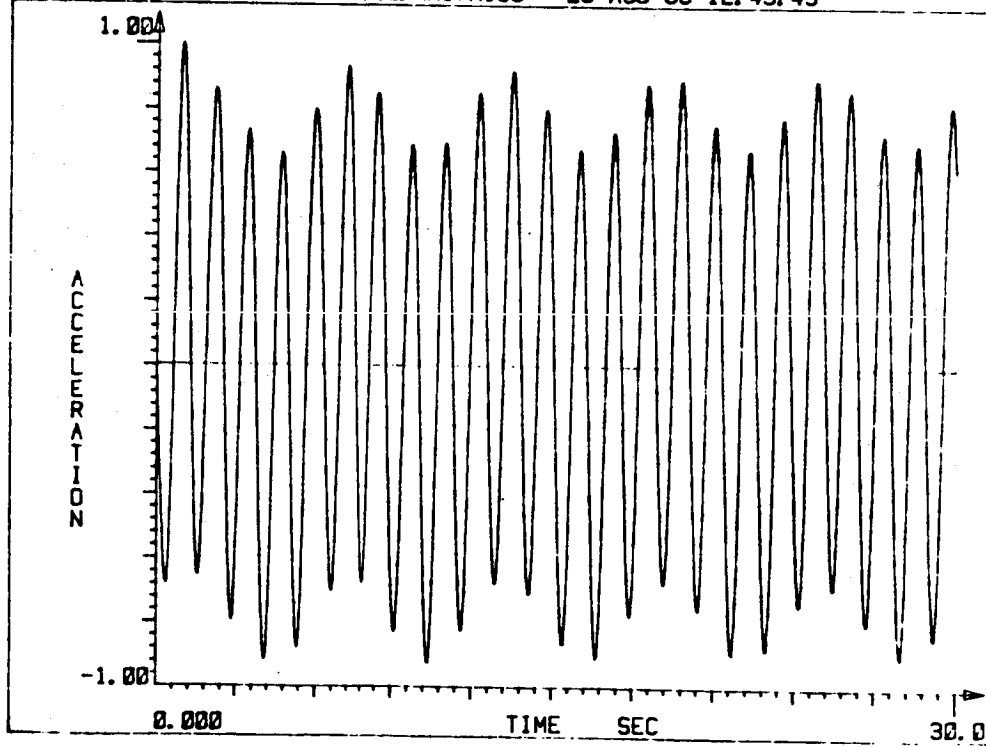


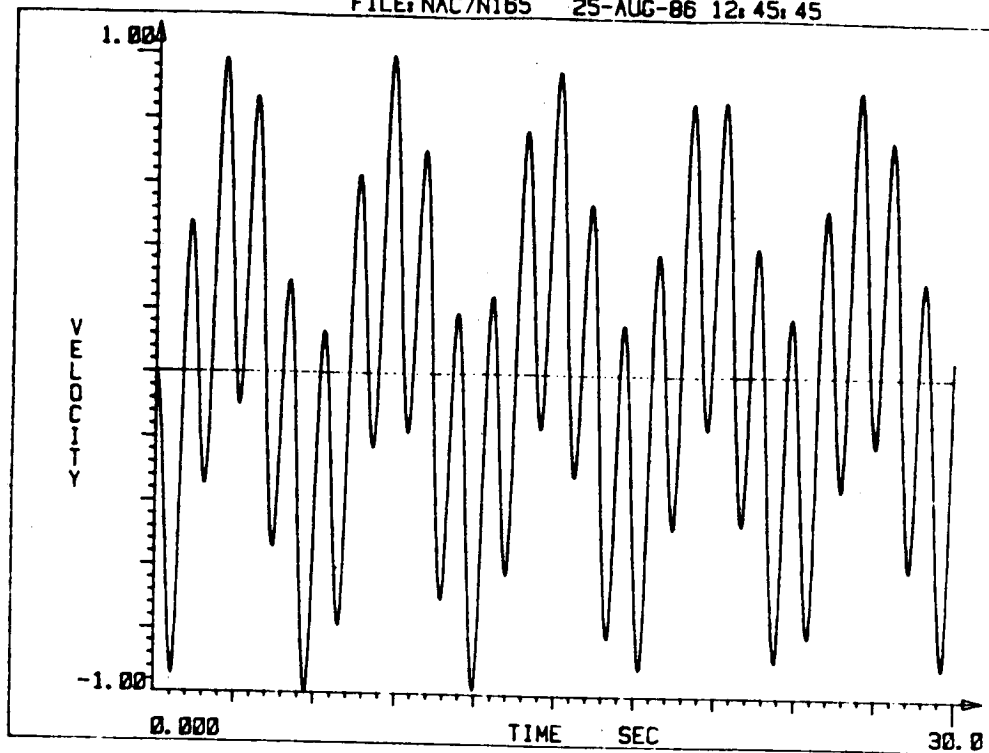
Nonstationary Random Response-Tip Excit.



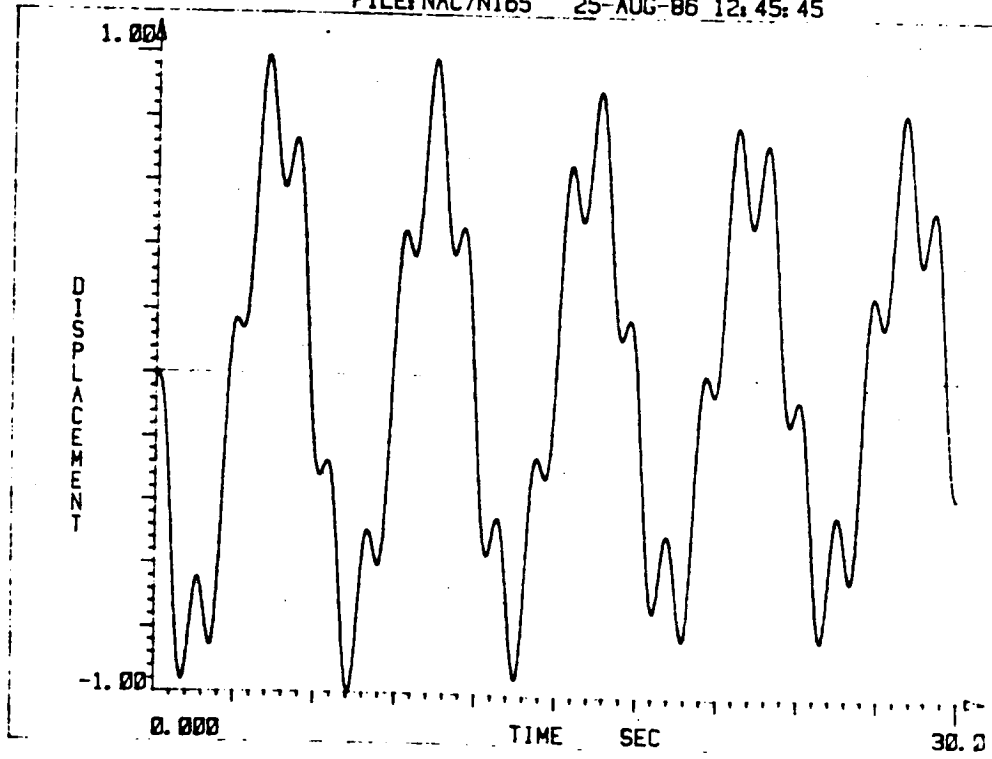


Harmonic Response - Base Excit.





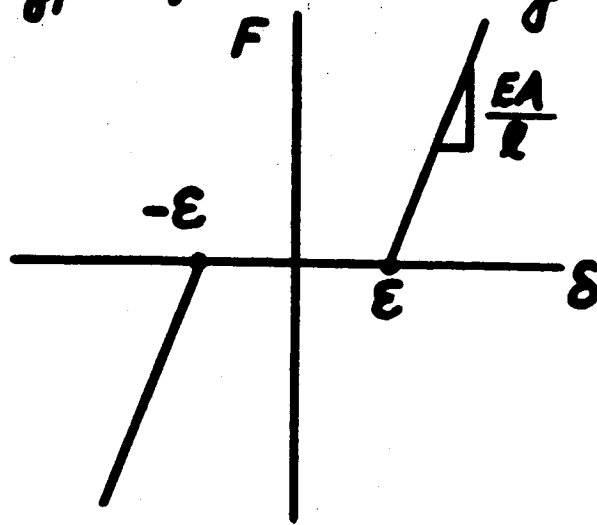
Harmonic Response - Base Excit.



NONLINEAR FINITE ELEMENT MODEL



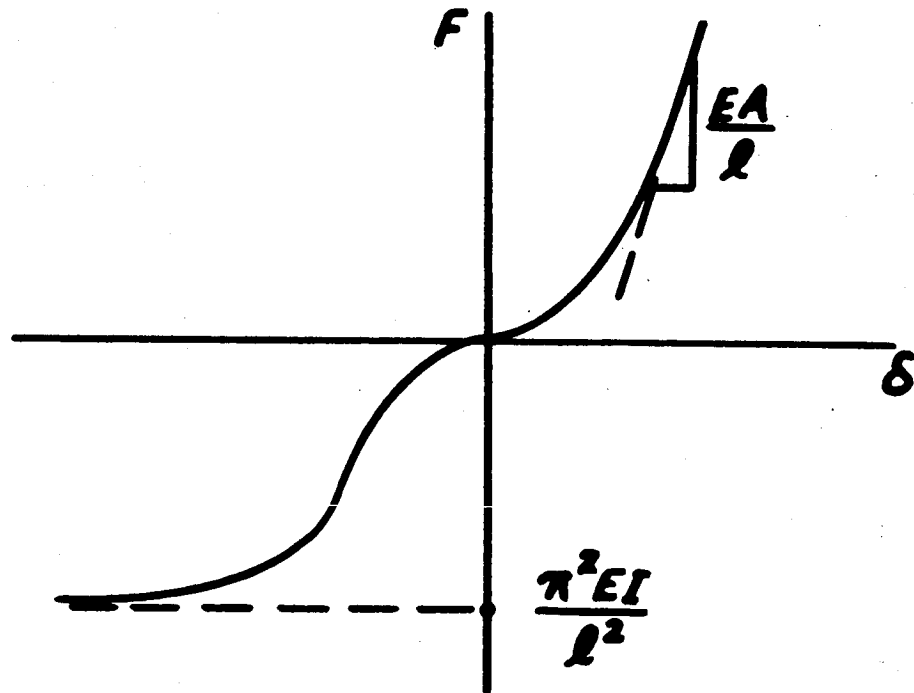
3. Type of Nonlinearity



$$\begin{aligned}
 \left(\frac{\delta}{\epsilon}\right) &= \frac{1}{2} + \\
 0.57|f| & \left[\frac{2}{3} - \ln(1.14f) \right]; \\
 0 \leq |f| & \leq 0.63 \\
 &= 0.86; \quad |f| > 0.63 \\
 \left(f \leq \frac{F}{E\ell\epsilon}\right) &
 \end{aligned}$$

Crude Joint Clearance

Hertzian Joint Contact



Joint Contact + Strut Buckling

NONLINEAR SIMULATION PROBLEMS



1. Excessive CPU Time

- 92+ Hours for $T=3$ Fundamental Periods on VAX 11/750
- Small Δt ($\approx \tau_{12}/1000$) required for numerical stability

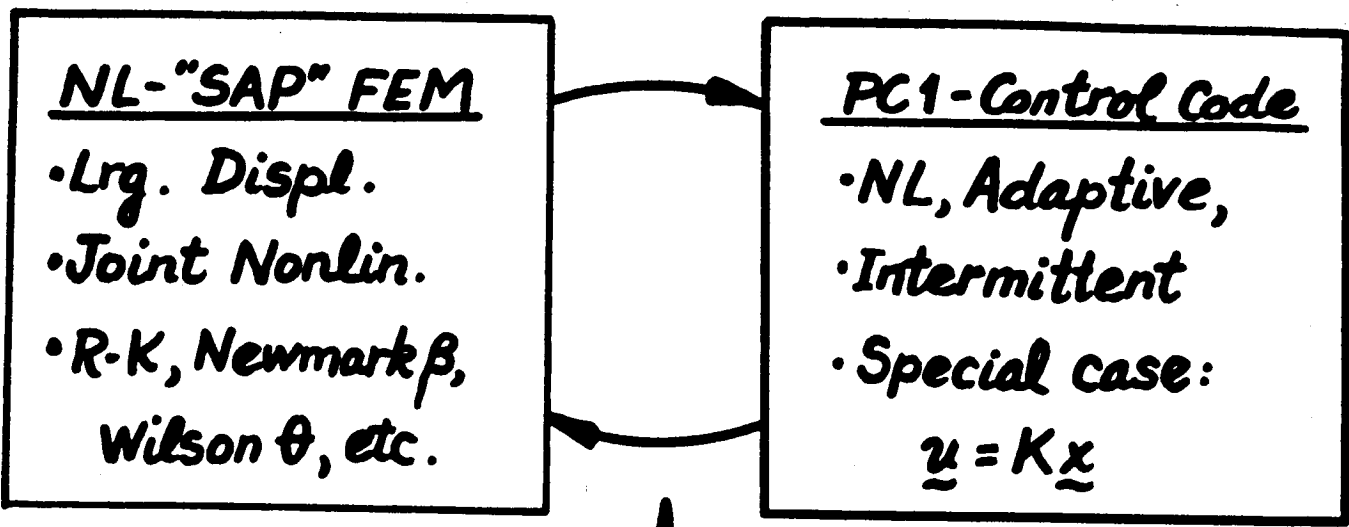
2. Model Order Reduction Necessary

- Nonparametric "RONN" Model - in process
- Parametric/Superelement Model - in process
- Validity ???

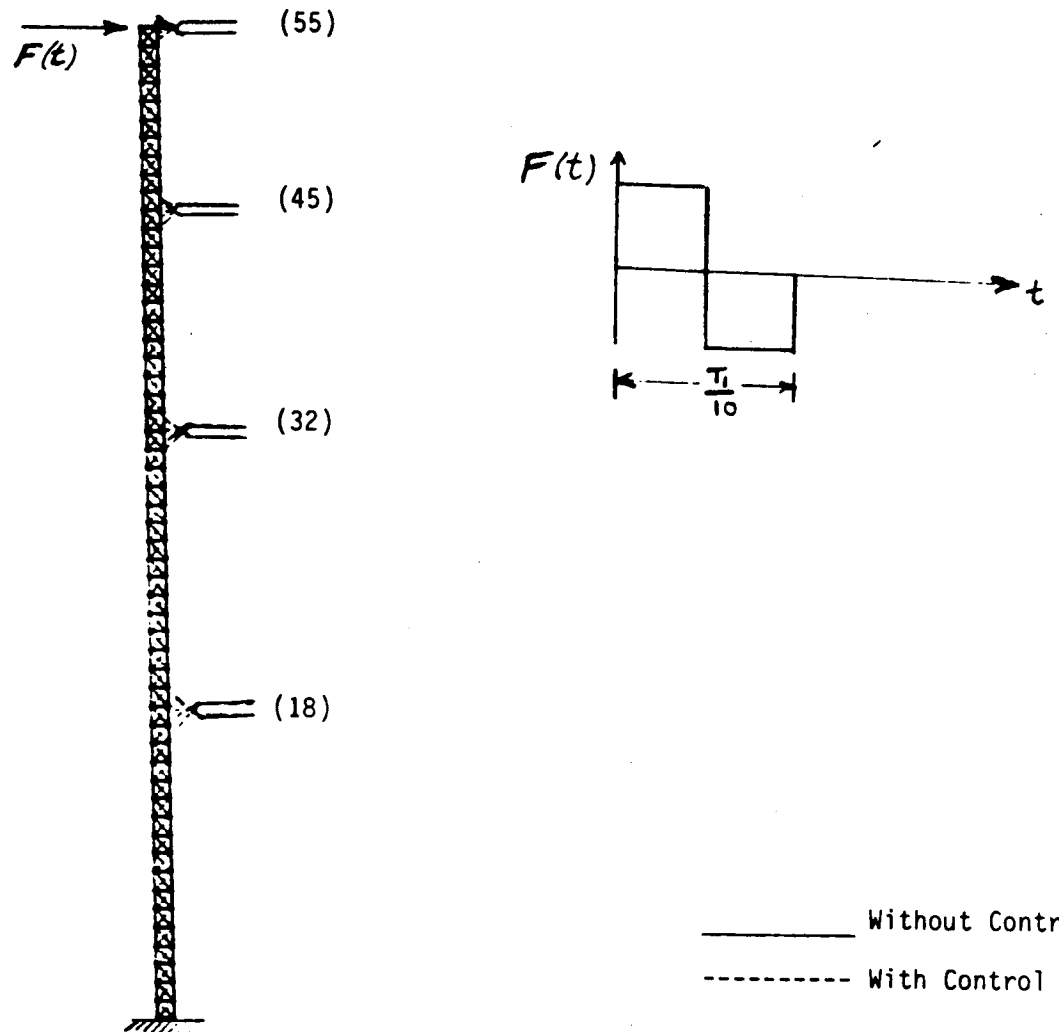


CONTROL ISSUES

1. Simulation Progress

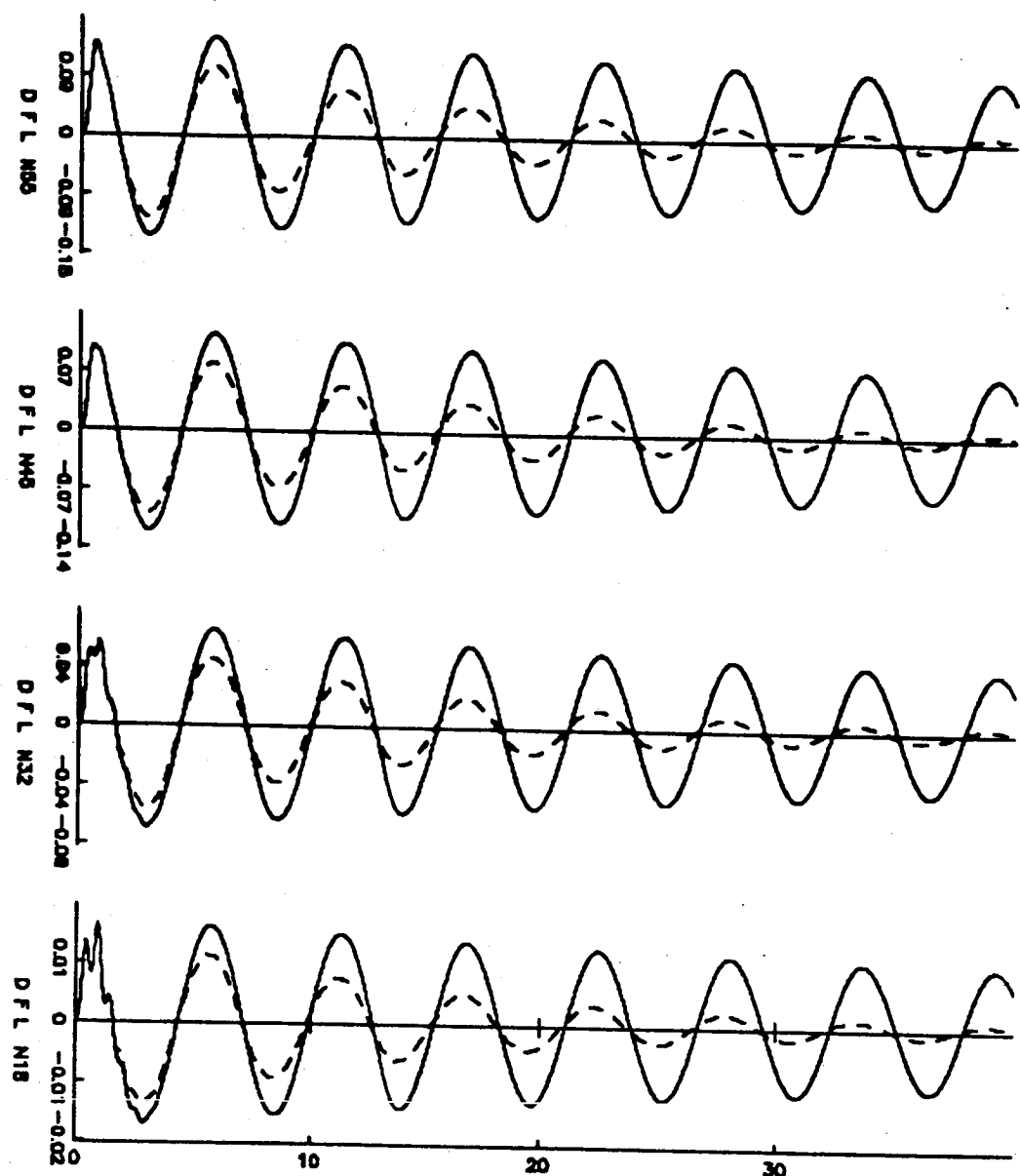


1. Time step interrupt req'd.
2. Excess storage for state variables
3. Stability and restart capability for time-stepping algorithms



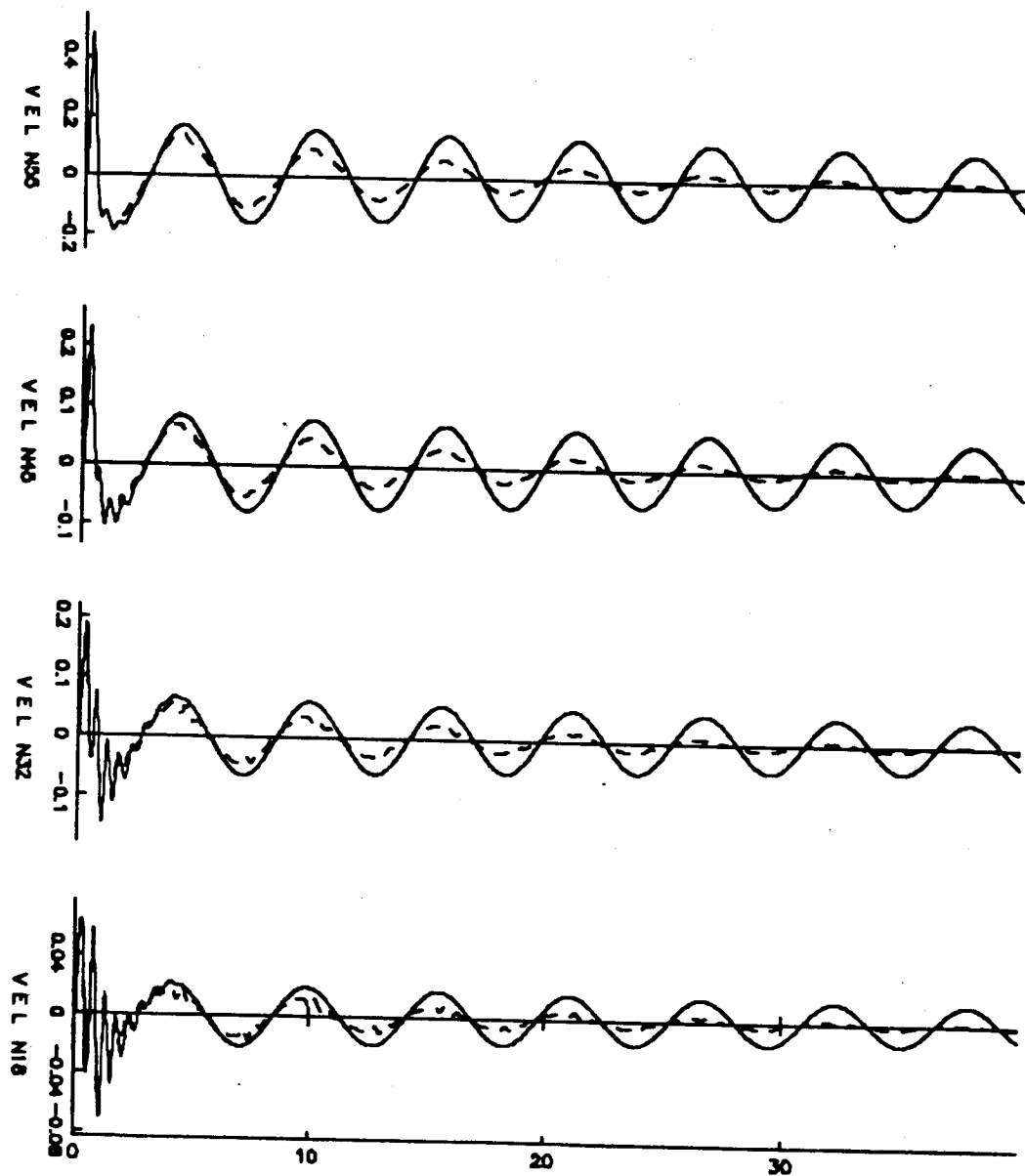
THREE-DIMENSIONAL FINITE ELEMENT MODEL OF COFS I MAST

$C=100$ $n=1$ $T_d=0.2$



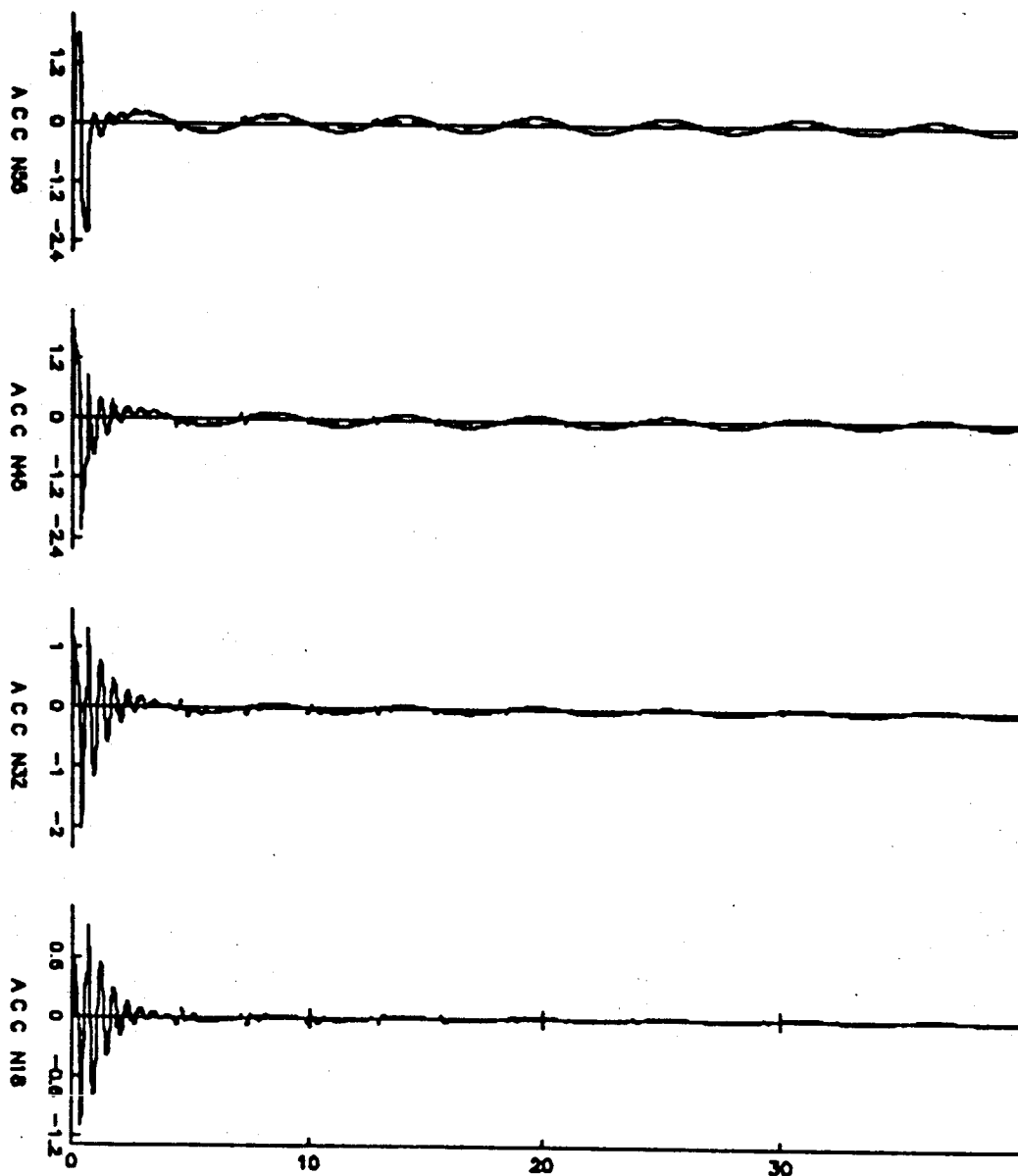
Displacement Response with and without Control

$C=100$ $n=1$ $T_d=0.2$



Velocity Response with and without Control

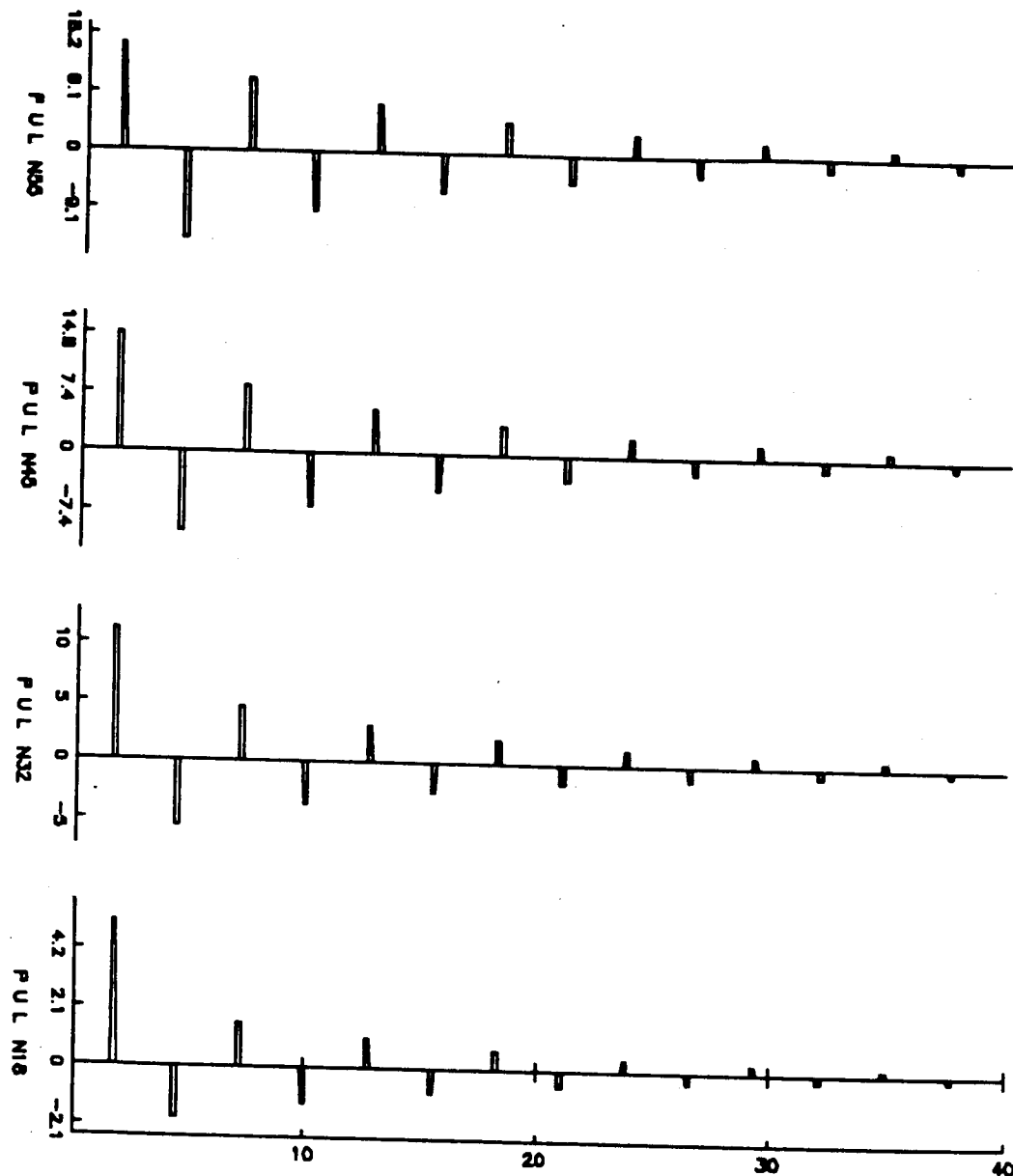
$C=100$ $n=1$ $T_d=0.2$



Acceleration Response with and without Control



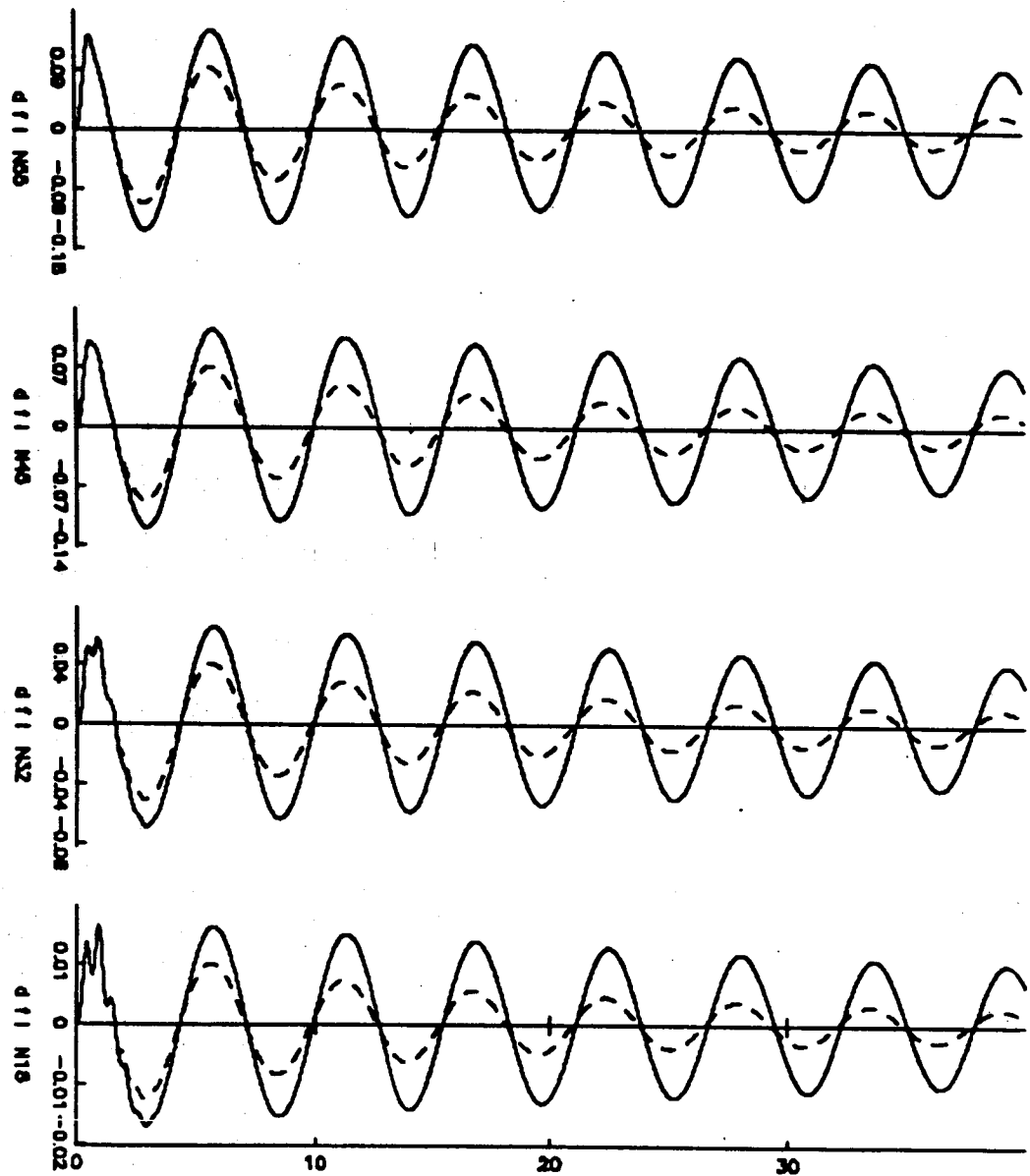
$C=100$ $n=1$ $T_d=0.2$



Pulse Control Forces



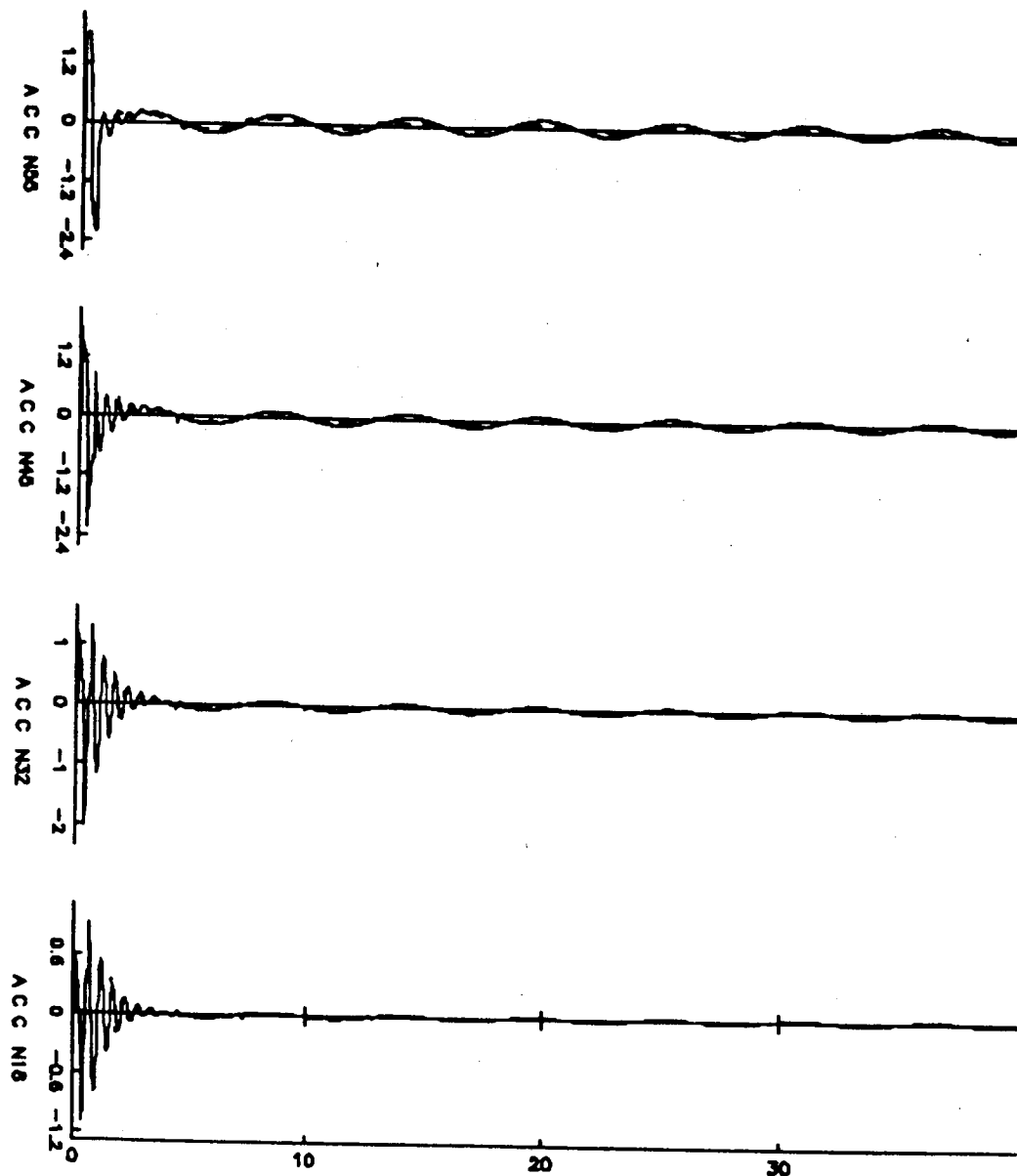
$C=100$ $n=2$ $T_d=0.2$



Displacement Response with and without Control



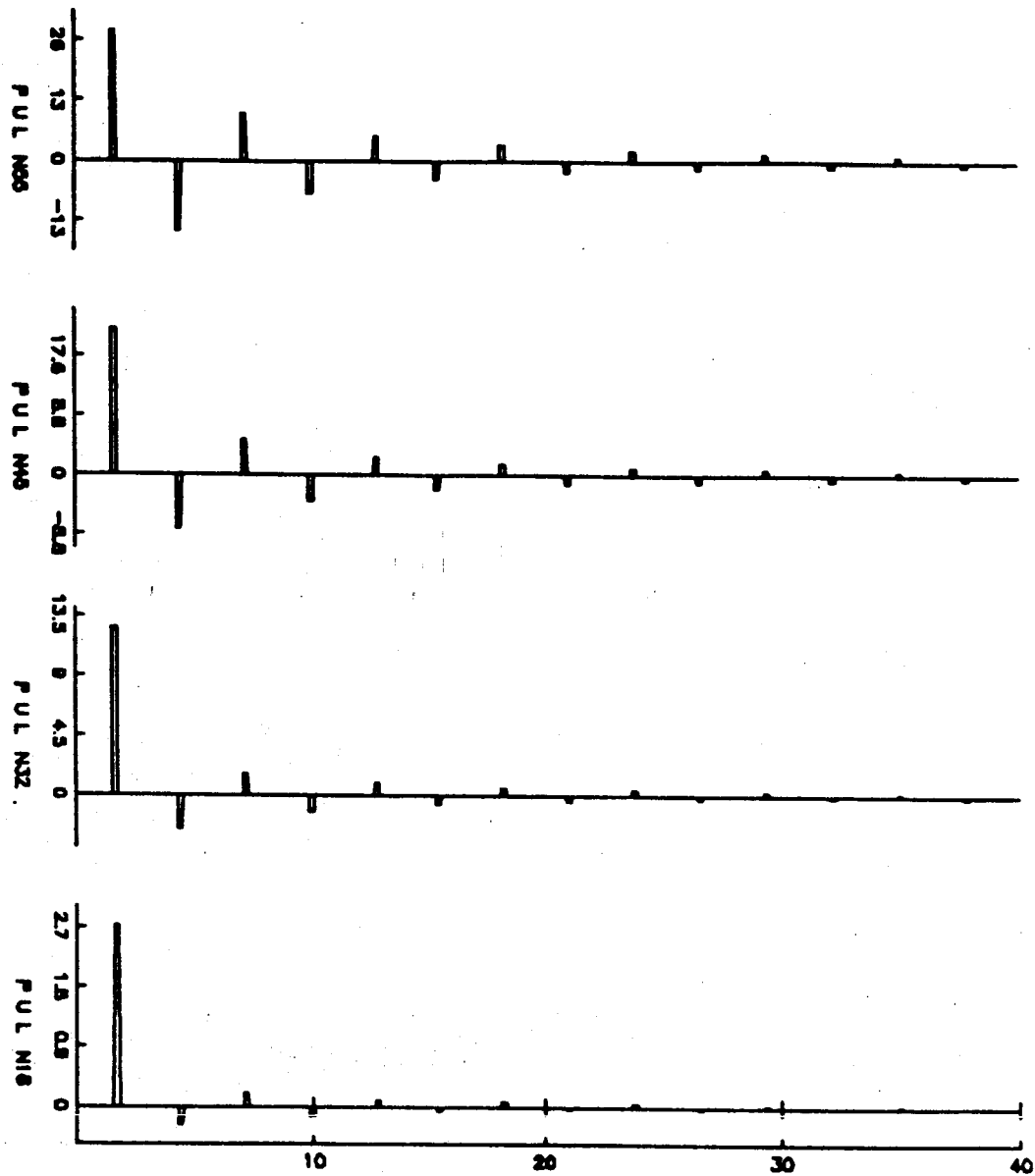
$C=100$ $n=2$ $T_d=0.2$



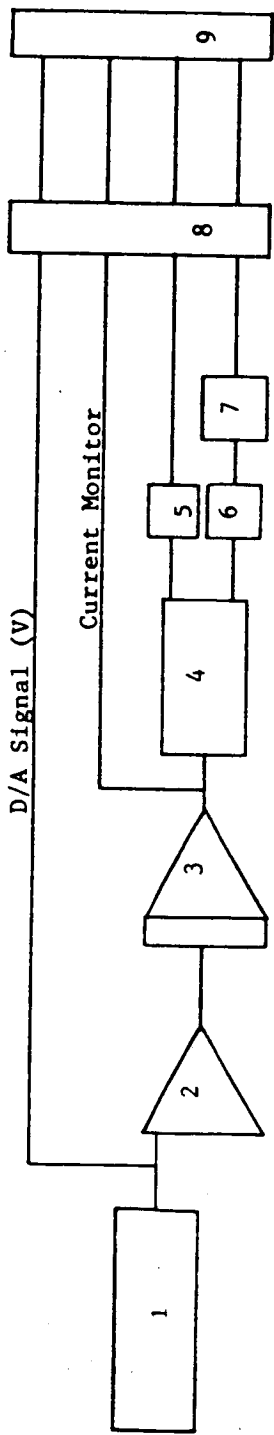
Acceleration Response with and without Control



$C=100$ $n=2$ $T_d=0.2$



Pulse Control Forces



1. PC - XT
2. Operational Amplifier (X2)
3. Power Amplifier
4. Shaker
5. XCDR1 (LVDT)
6. XCDR2 (Piezoresistive accelerometer)
7. Signal Conditioning
8. Digital Filter
9. A/D Converter

TIME HISTORY OF INPUT SIGNAL & RESPONSE



acceleration

input signal

1.00

-1.00

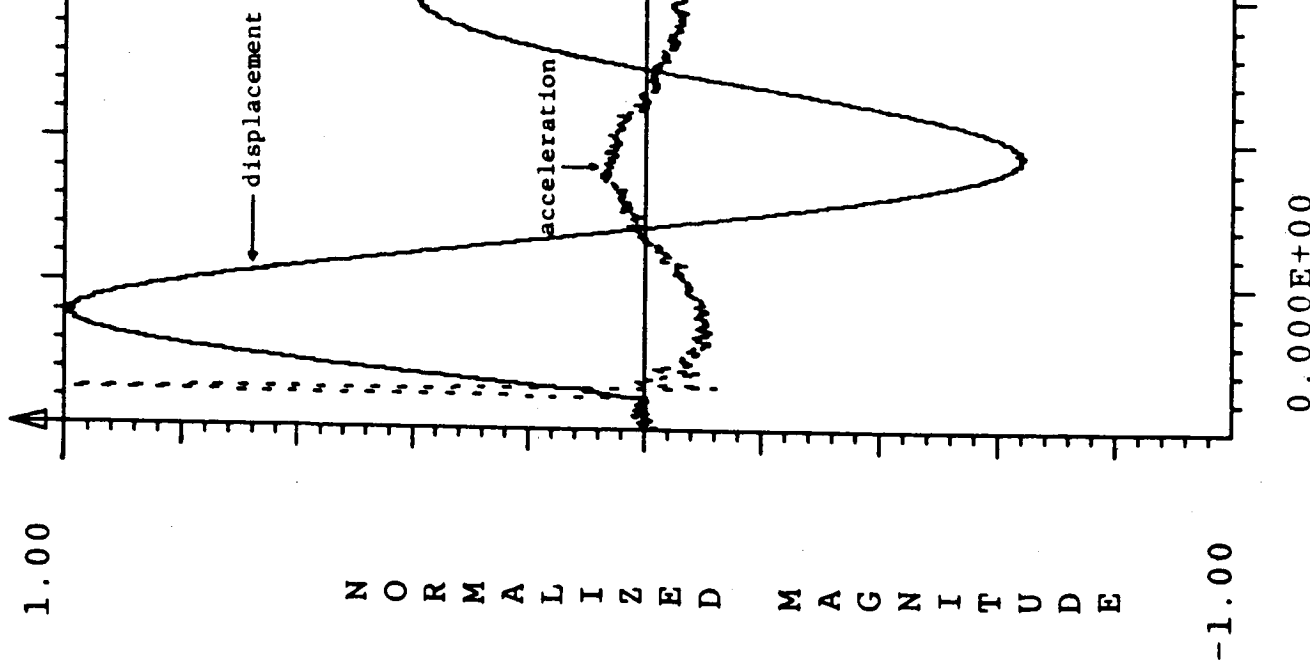
N O R M A L I Z E D M A G N I T U D E

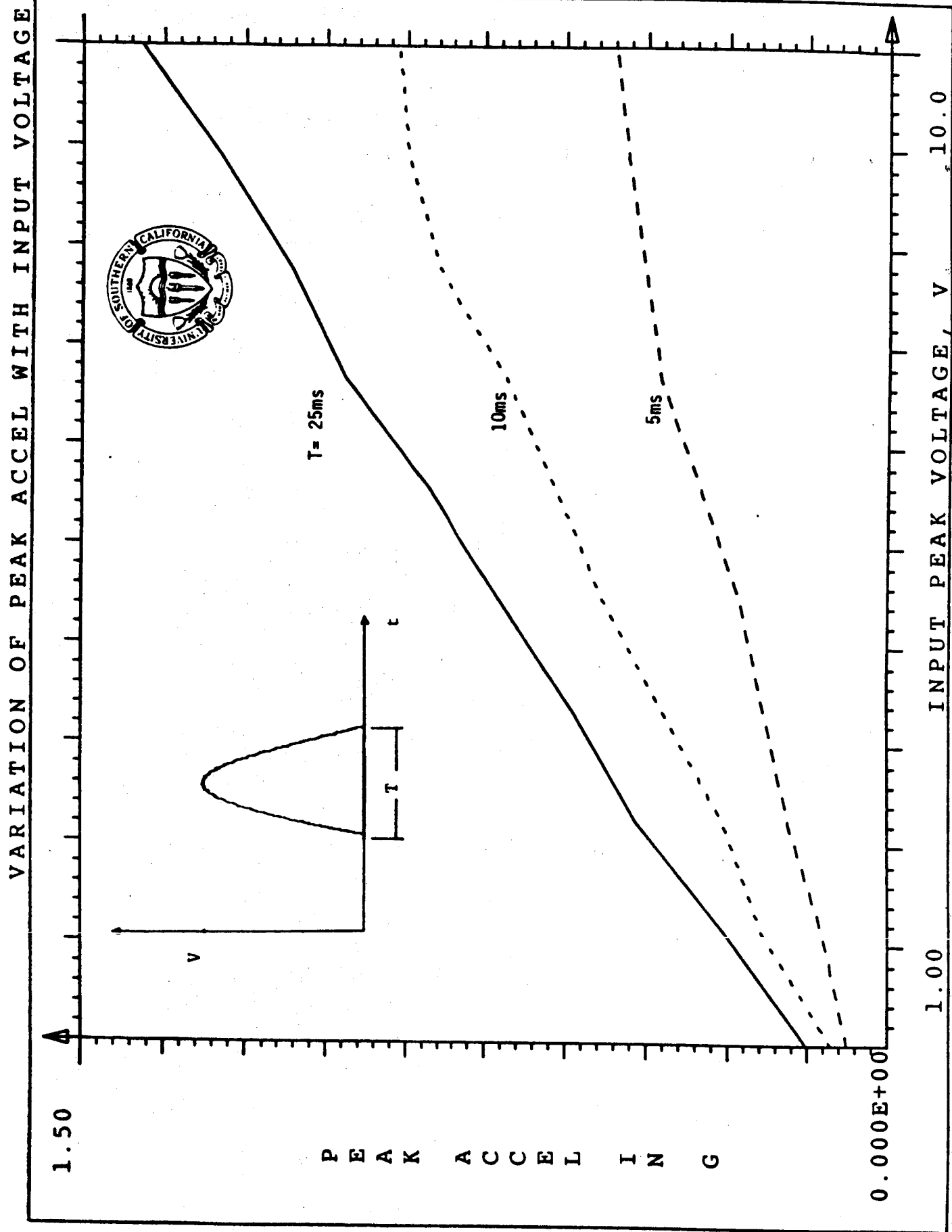
0.000E+00

TIME

0.500

TIME HISTORY OF RESPONSE





N87-17835

ACTIVE STABILITY AUGMENTATION OF LARGE SPACE STRUCTURES:
A STOCHASTIC CONTROL PROBLEM

A.V. Balakrishnan
Department of Electrical Engineering
UCLA

Paper to be presented at the IFAC Conference on Stochastic Control,
Vilnius, May 1986.

Research supported in part under NASA grant no. NAG 1-464.

PRECEDING PAGE BLANK NOT FILMED

28833-678

368

1. Introduction

In the 1987-1990 period NASA has planned several ground and flight experiments with the eventual objective of deploying large flexible structures in space. A currently active precursor is the SCOLE experiment [1]. Here the problem is that of slewing an offset antenna on a long (130 ft.) flexible beam-like truss attached to the space shuttle, with rather stringent pointing accuracy requirements ($\pm .02$ degrees). This paper examines the relevant methodology aspects in robust feedback-control design for stability augmentation of the beam using on-board sensors. We frame it as a stochastic control problem - boundary control of a distributed parameter system described by partial differential equations. While the framework is mathematical, the emphasis is still on an engineering solution.

The fact that the deployment is in space makes model uncertainty the major consideration in control design. Particularly serious in this regard is for instance the modelling of inherent damping in the system long known to be difficult [2], and a still unresolved problem even in theory. Hence robustness becomes a must feature, even at the expense of optimality. Another aspect is the complexity of computation, making any simulation study a costly undertaking.

The overall model involving both slewing and beam stabilization is still not well understood. Hence the two problems -- of slewing and stabilization -- are best studied, at least in initial efforts such as reported here, separately. We attempt stabilization at the termination of the slewing so that in particular the system is essentially linear except for a small nonlinear term contributed by the kinematic nonlinearity. It should be noted that at present

PRECEDING PAGE BLANK NOT FILMED

we do not have a stochastic time-optimal control theory adequate for optimal slewing based on sensor data.

An abstract mathematical formulation is developed in Section 2 as a nonlinear wave equation in a Hilbert space. We show that the system is controllable and develop a feedback control law that is robust in the sense that it does not require quantitative knowledge of system parameters. The stochastic control problem that arises in instrumenting this law using appropriate sensors is treated in Section 3. Using an Engineering first approximation which is valid for "small" damping, formulas for optimal choice of the control gain are developed.

2. Abstract Formulation

We are concerned with the mast stabilization problem only and the model we use assumes that the angular velocity of the shuttle-antenna system is small enough to be neglected. We model the mast as a thin prismatic beam. There is then the question of whether a finite-element model or a continuum (involving partial differential equations) model should be used. Here we deal only with the latter, the basic governing equations being beam bending and torsion equations with controls at the boundaries.

With reference to Figure 1, the beam of length L is along the Z axis, z being zero at the shuttle end. $u_\phi(\cdot)$, $u_\theta(\cdot)$ will denote the displacements along the $Y-Z$, $X-Z$ planes and $u_\psi(\cdot)$ the angular deflection about the Z axis. In addition proof-mass controllers are provided at points s_1 and s_2 , on the beam, the locations to be chosen optimally. Control moments are applied at both ends as well as control forces at the reflector center. The various moments of inertia and masses are specified in [1], [2].

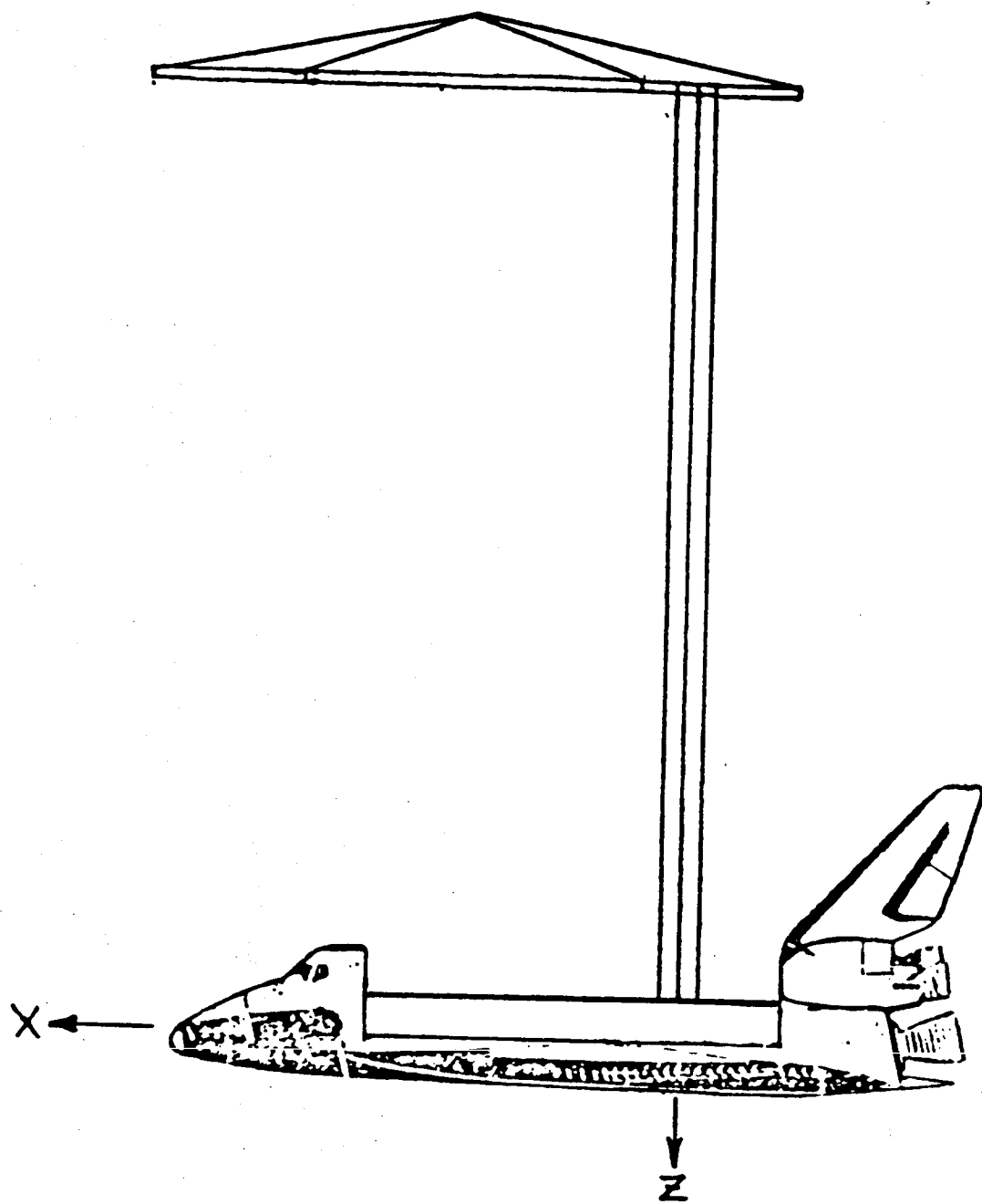


FIGURE 1
SHUTTLE/ANTENNA CONFIGURATION

We first develop an abstract mathematical model. We define

$$H = L_2[0, L]^3 \times \mathbb{R}^{14} \quad 0 < L < \infty$$

with the usual inner-product thereon denoted $[,]$. We fix the points $0 < s_2 < s_3 < L$ and define a linear operator A into H with domain D in H defined as follows. We use $u_\phi(\cdot)$, $u_\theta(\cdot)$, $u_\psi(\cdot)$ to denote the functions in $L_2[0, L]^3$. Thus an element x in H is denoted

$$\begin{aligned} & u_\phi(\cdot) \\ & u_\theta(\cdot) \\ & u_\psi(\cdot) \\ & x_4 \\ & \vdots \\ & x_{17} \end{aligned}$$

The domain D consists of elements x such that $u_\phi', u_\theta', u_\psi' \in L_2[0, L]$ and $u_\phi''(\cdot)$ has L_2 -derivatives in $[0, s_2]$, $[s_2, s_3]$ and $[s_3, L]$; similarly for $u_\theta(\cdot)$; $u_\psi(\cdot)$ such that $u_\psi'(\cdot)$ and $u_\psi''(\cdot) \in L_2[0, L]$; the remaining components of x are specified as

$$\begin{aligned} x_4 &= u_\phi(0+) & x_{11} &= u_\phi'(L-) \\ x_5 &= u_\theta(0+) & x_{12} &= u_\theta'(L-) \\ x_6 &= u_\phi(L-) & x_{13} &= u_\psi(L-) \\ x_7 &= u_\theta(L-) & x_{14} &= u_\phi(s_2) \\ x_8 &= u_\phi'(0+) & x_{15} &= u_\theta(s_2) \\ x_9 &= u_\theta'(0+) & x_{16} &= u_\phi(s_3) \\ x_{10} &= u_\psi(0+) & x_{17} &= u_\theta(s_3) \end{aligned}$$

Thus at least for x in D , we may identify the finite-dimensional part as the "boundary." The operator A is then defined by

$$y = Ax$$

where the functional part (in $L_2[0, L]^3$) is given by

$$EI_{\phi} u_{\phi}'''(\cdot)$$

$$EI_{\theta} u_{\theta}'''(\cdot)$$

$$-GI_{\psi} u_{\psi}''(\cdot)$$

and the boundary part by:

$$y_4 = EI_{\phi} u_{\phi}'''(0+)$$

$$y_{11} = EI_{\phi} u_{\phi}''(L-)$$

$$y_5 = EI_{\theta} u_{\theta}'''(0+)$$

$$y_{12} = EI_{\theta} u_{\theta}''(L-)$$

$$y_6 = -EI_{\phi} u_{\phi}'''(L-)$$

$$y_{13} = GI_{\psi} u_{\psi}'(L-)$$

$$y_7 = -EI_{\theta} u_{\theta}'''(L-)$$

$$y_{14} = EI_{\phi} (u_{\phi}'''(s_2+) - u_{\phi}'''(s_2-))$$

$$y_8 = -EI_{\phi} u_{\phi}''(0+)$$

$$y_{15} = EI_{\theta} (u_{\theta}'''(s_2+) - u_{\theta}'''(s_2-))$$

$$y_9 = -EI_{\theta} u_{\theta}''(0+)$$

$$y_{16} = EI_{\phi} (u_{\phi}'''(s_3+) - u_{\phi}'''(s_3-))$$

$$y_{10} = -GI_{\psi} u_{\psi}'(0+)$$

$$y_{17} = EI_{\theta} (u_{\theta}'''(s_3+) - u_{\theta}'''(s_3-))$$

It may then be verified that D is dense and A is self-adjoint and nonnegative definite. Moreover A has a compact resolvent with a complete orthonormal set of eigenfunctions (modes). Zero is an eigenvalue.

The control system dynamics can then be characterized as a nonlinear wave-equation:

$$M\ddot{x}(t) + Ax(t) + K(\dot{x}(t)) + Bu(t) = 0 \quad (2.1)$$

where M is a 17×17 nonsingular nonnegative definite matrix, and defines self-adjoint positive definite linear operator H onto H . The control $u(\cdot)$ is in R^{12} , and

$$Bu = x$$

$$x = \text{col. } [0, 0, 0, 0, 0, u_1, u_2, u_3, u_4, u_5, u_6, u_7, u_8, u_9, u_{10}, u_{11}, u_{12}]$$

We have thus only "boundary" control. The nonlinearity is kinematic:

$$K(x) = \begin{vmatrix} 0 \\ 0 \\ 0 \\ 0 \\ 0 \\ 0 \\ \Omega_1 \bullet I_1 \Omega_1 \\ \Omega_4 \bullet I_4 \Omega_4 \\ 0 \\ 0 \\ 0 \\ 0 \end{vmatrix}$$

where

$$\Omega_1 = \text{col } (x_8, x_9, x_{10})$$

$$\Omega_4 = \text{col } (x_{11}, x_{12}, x_{13})$$

I_1, I_4 are symmetric positive definite (moment) matrices and

\bullet denotes vector cross-product.

Two relevant properties of the function $K(\cdot)$ are:

$$(i) [K(x), x] = 0$$

$$(ii) \|K(x)\| \leq \text{const. } \|x\|^2$$

We do allow for "state noise" and let

$$N(t) = \begin{vmatrix} N_1(t) \\ N_2(t) \\ N_3(t) \end{vmatrix}$$

$$FN(t) = x(t)$$

where $N(t)$ is white Gaussian with spectral density matrix Λ , and the components of $x(t)$ are defined by

$$\begin{aligned} x_i(t) &= 0 & i = 1, \dots, 7 \\ x_8(t) &= N_1(t) \\ x_9(t) &= N_2(t) \\ x_{10}(t) &= N_3(t) \\ x_i(t) &= 0 & i > 10. \end{aligned}$$

Note that the "boundary" values are part of the state.

State-space Form

With

$$Y(t) = \begin{vmatrix} x(t) \\ \dot{x}(t) \end{vmatrix}$$

we go over to the state-space form:

$$\dot{Y}(t) = AY(t) + K(Y(t)) + Bu(t) + F(N(t)) \quad (2.2)$$

where

$$A = \begin{bmatrix} 0 & I \\ -M^{-1}A & 0 \end{bmatrix}$$

$$Bu(t) = \begin{vmatrix} 0 \\ -M^{-1}Bu(t) \end{vmatrix}$$

and in the notation

$$Y = \begin{vmatrix} y_1 \\ y_2 \end{vmatrix}, \quad Y \in H \times H$$

we have

$$K(Y) = \begin{vmatrix} 0 \\ -M^{-1}K(y_2) \end{vmatrix}$$

$$F_N(t) = \begin{vmatrix} 0 \\ -M^{-1}F_N(t) \end{vmatrix}$$

As is well known, we can introduce a new inner product, the "energy" inner product

$$[Y, Z]_E = [\sqrt{A} y_1, \sqrt{A} z_1] + [My_2, z_2]$$

on $R(A) \times H$. $R(A)$ is the orthogonal complement of the null space of A .

We denote the completed space by H_E . We shall from now on consider only H_E . We have:

$$A + A^* = 0$$

and of course A has a compact resolvent and we have an orthogonal decomposition of H_E given by

$$Y = \sum_1^{\infty} p_k Y \quad (2.3)$$

where p_k is a two-dimensional projection for each k , $p_k H_E$ spanned by

$$\phi_j^+ = \begin{vmatrix} \phi_k \\ i\omega_k \phi_k \end{vmatrix}$$

$$\phi_k^- = \begin{vmatrix} \phi_k \\ -i\omega_k \phi_k \end{vmatrix}$$

where

$$A\phi_k = \omega_k^2 M\phi_k, \quad \omega_k^2 > 0, \quad \omega_k^2 \rightarrow \infty; \quad (2.4)$$

$$[M\phi_k, \phi_j] = \delta_j^k.$$

Let $S(t)$ denote the semigroup generated by A . Then we have the representation:

$$S(t)y = \sum_1^{\infty} S(t) p_k y$$

$$p_k S(t) p_k = S(t) p_k.$$

More explicitly, if

$$S(t)y = \begin{vmatrix} y_1(t) \\ y_2(t) \end{vmatrix}.$$

Then

$$y_2(t) = \dot{y}_1(t)$$

and

$$y_1(t) = \sum_1^{\infty} [y_1, M\phi_k] \phi_k \cos \omega_k t + \sum_1^{\infty} [y_2, M\phi_k] \phi_k \frac{\sin \omega_k t}{\omega_k} \quad (2.5)$$

Note that it is required that y_1 satisfy:

$$\sum_1^{\infty} [y_1, M\phi_k]^2 \omega_k^2 < \infty.$$

It is easy to establish existence and uniqueness of solution for the integral version of (2.2):

$$\begin{aligned} Y(t) &= S(t)Y(0) + \int_0^t S(t-\sigma) B u(\sigma) d\sigma + \int_0^t S(t-\sigma) F N(\sigma) d\sigma \\ &\quad + \int_0^t S(t-\sigma) K(Y(\sigma)) d\sigma, \end{aligned} \quad (2.6)$$

without invoking any nonlinear semigroup theory, by just Picard iteration. See [3].

We can now state the basic result that yields a robust feedback-control law for the deterministic system (seeing $F = 0$).

Theorem 2.1.

Let P be any 12×12 symmetric nonnegative definite nonsingular matrix. Then the feedback control

$$u(t) = -P B^* Y(t) \quad (2.7)$$

is such that the "closed-loop" system

$$\dot{Y}(t) = AY(t) - B_P B^* Y(t) + K(Y(t)) \quad (2.8)$$

is globally asymptotically stable. That is to say

$$\|Y(t)\|_E \rightarrow 0 \quad \text{as } t \rightarrow \infty$$

Proof. We refer to [4] for a proof. The proof exploits the fact that (A, B) is controllable in an essential way. In particular the semigroup $S_B(t)$ generated by $(A - B_P B^*)$ is strongly stable: that is to say:

$$\|S_B(t)Y\|_E \rightarrow 0 \quad \text{as } t \rightarrow \infty.$$

We also obtain that

$$\int_0^{\infty} (P B^* S_B(t) Y, B^* S_B(t) Y) dt = \frac{1}{2} \|Y\|_E^2. \quad (2.9)$$

The control law is also optimal for the quadratic cost functional:

$$\int_0^{\infty} \|\sqrt{P} B^* Y(t)\|^2 dt + \int_0^{\infty} \|u(t)\|^2 dt$$

for the linear system

$$\dot{Y}(t) = AY(t) + B\sqrt{P} u(t)$$

3. Stochastic Control

To instrument the control law

$$\begin{aligned} u(t) &= PB^* \dot{x}(t) \\ &= P \dot{b}(t) \end{aligned} \quad (3.1)$$

We need to assume co-located (rate) sensors. The sensor output $v(t)$ would then be:

$$v(t) = \dot{b}(t) + N_0(t) \quad (3.2)$$

where $N_0(t)$ represents the sensor noise, modelled as white Gaussian with (12×12) spectral density matrix D . In terms of the state-space representation (2.2), we can rewrite (3.2) as

$$v(t) = CY(t) + N_0(t) \quad (3.2)$$

where

$$C = B^*$$

and C is of course finite-dimensional. If we assume that the separation principle applies, a reasonable choice of control law would be

$$u(t) = \hat{P} \dot{b}(t) \quad (3.3)$$

where, E denoting conditional expectation:

$$\hat{b}(t) = E[\dot{b}(t) \mid v(s), s \leq t]$$

and of course

$$\hat{b}(t) = C \hat{Y}(t)$$

where $\hat{Y}(t)$ is the Kalman state estimate:

$$\hat{Y}(t) = E[Y(t) \mid v(s), s \leq t].$$

Even if we were to neglect the nonlinear term $K(\cdot)$, this would require an infinite-dimensional Kalman filter, which even if we could instrument it, would depend on quantitative knowledge of the system parameters. Hence this filter would need to be simplified in considerable measure, in favor of robustness.

The simplest version would be one that did not distort $\dot{b}(t)$ and thus would lead to the control law:

$$u(t) = Pv(t) . \quad (3.4)$$

We are thus introducing a noise input into the system which may excite higher-order modes. Let us therefore study the system response which is now given by the stochastic equation:

$$\dot{Y}(t) = (A - B_P B^*) Y(t) - B_P N_0(t) + K(Y(t)) + F_N(t) \quad (3.5)$$

This can be expressed as an integral equation:

$$Y(t) = Y_0(t) + \int_0^t S_B(t-\sigma) K(Y(\sigma)) d\sigma \quad (3.6)$$

where

$$Y_0(t) = S_B(t)Y(0) - \int_0^t S_B(t-\sigma) B_P N_0(\sigma) d\sigma + \int_0^t S_B(t-\sigma) F_N(\sigma) d\sigma \quad (3.7)$$

We note that because $K(\cdot)$ is locally Lipschitzian, we may solve (3.6) by Picard iteration:

$$Y_{n+1} = Y_0(t) + \int_0^t S_B(t-\sigma) K(Y_n(\sigma)) d\sigma . \quad (3.8)$$

We omit the details; see [3]. More important to us is actually (3.7).

We want to show that the process $Y_0(\cdot)$ is asymptotically stationary and

evaluate its covariance function. Following [5], since $S_B(\cdot)$ is strongly stable, it is only necessary to show that for Y in H_E :

$$\int_0^\infty [S_B(\sigma)BPD\bar{P}^*S_B(\sigma)^*Y, Y]_E d\sigma < \infty \quad (3.9)$$

and also that

$$\int_0^\infty [S_B(\sigma)F\Lambda F^*S_B(\sigma)^*Y, Y]_E d\sigma < \infty. \quad (3.10)$$

For this purpose we note that $S_B(t)^*$ is strongly stable with generator

$$A^* - B\bar{P}B^*$$

and analogous to (2.9) we have that

$$\int_0^\infty \|\sqrt{P}B^*S_B(t)^*Y\|^2 dt = \frac{1}{2} \|Y\|_E^2.$$

Hence

$$\int_0^\infty \|\sqrt{D}P\bar{B}^*S_B(t)^*Y\|^2 dt \leq \frac{\|D\|}{2} \|P\| \|Y\|_E^2 < \infty.$$

Since

$$\|F^*S_B(t)^*Y\| \leq \|B^*S_B(t)^*Y\|$$

we also obtain (3.10). For Y, Z in H_E let

$$[R(t,s)Y, Z] = E([Y_0(t), Y][Y_0(s), Z]).$$

Then we have that

$$R(t,s) = S_B(t-s) R(s,s), \quad t \geq s$$

and hence it follows that

$$\lim_{L \rightarrow \infty} R(t+L, s+L) = S_B(t-s) R_\infty, \quad t \geq s \quad (3.11)$$

where

$$[R_\infty Y, Y] = \int_0^\infty \|\sqrt{D}P\bar{B}^*S_B(t)^*Y\|^2 dt + \int_0^\infty \|\sqrt{A}F^*S_B(t)^*Y\|^2 dt. \quad (3.12)$$

The process $Y_0(\cdot)$ is thus asymptotically stationary with covariance operator

$$S_B(t-s)R_\infty \quad t \geq s$$

We note that R_∞ is not necessarily nuclear, even though $R(t,t)$ will be if $R(0,0)$ is. Indeed taking

$$D = dI; \quad P = I$$

we obtain that

$$\int_0^\infty \|\sqrt{D}PB^*S_B(t)*Y\|^2 dt = \frac{d}{2} \|Y\|_E^2.$$

From (3.8) we can show that the process $Y(t)$ is asymptotically stationary, since $Y_n(\cdot)$ will have this property for each n . Since it would appear that the nonlinearity is small, we shall now concentrate our attention on the linear approximation $Y_0(\cdot)$.

The eigenfunctions of $(A - BPB^*)$ are approximately the same as that of A and the eigenvalues are

$$\sigma_k \pm i\omega_k; \quad \frac{\sigma_k}{\omega_k} \ll 1.$$

where

$$2\sigma_k = [Pb_k, b_k]. \quad (3.13)$$

Hence

$$[R_\infty \phi_k^+, \phi_k^+]_E = \omega_k^2 \frac{([DPb_k, Pb_k] + [F^*\phi_k, F^*\phi_k])}{[Pb_k, b_k]} \quad (3.14)$$

which is thus the noise energy in the k th mode. We see that increasing P increases the damping but also increases the noise excitation. In practice one would want a compromise between increasing damping at selected low order modes but keeping the noise excitation at higher order modes within bound. Clearly further work is needed before any attempt at control design.

We may also mention one point of purely theoretical interest. To characterize the distributions of the noise response of a nonlinear system described by ordinary differential equations one uses the Fokker-Planck-Kolmogorov equations which are partial differential equations. In (3.5) we have a nonlinear partial differential equation; it would be of interest to develop a corresponding tool to study the distributions.

REFERENCES

- [1] SCOLE Workshop Proceedings, 1984. Compiled by L.W. Taylor. NASA Langley FRC, Hampton, Virginia, 23665.
- [2] S. Timoshenko, D.H. Young and W. Weaver, Jr.: Vibration Problems in Engineering, 4th edition. New York: John Wiley, 1974.
- [3] A.V. Balakrishnan: A Mathematical Formulation of the SCOLE Control Problem, Part 1. NASA CR-172581.
- [4] A.V. Balakrishnan: On a Large Space Structure Control Problem, Proceedings of the IFIP Working Conference on Control of Systems Governed by Partial Differential Equations, Gainesville, Florida, 1986. (To be published.)
- [5] A.V. Balakrishnan: Applied Functional Analysis, 2nd edition. Springer-Verlag, 1981.

384

The SCOLE Design Challenge

by

**Larry Taylor
NASA Langley
Research Center
and
A. V. Balakrishnan
U. C. L. A.**

SCOLE - SCD

JUNE 1984

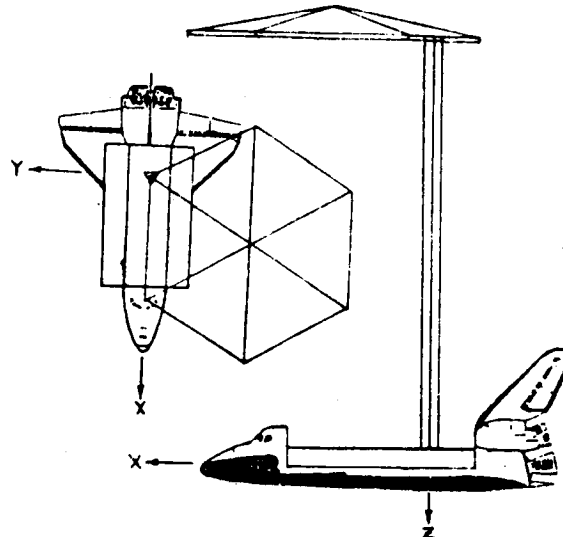
A MATHEMATICAL PROBLEM AND A SPACECRAFT CONTROL LABORATORY
EXPERIMENT (SCOLE) USED TO EVALUATE CONTROL LAWS FOR
FLEXIBLE SPACECRAFT... NASA/IEEE DESIGN CHALLENGE

by

Lawrence W. Taylor, Jr.
Spacecraft Control Branch
NASA Langley Research Center
Hampton, VA 23665

and

A. V. Balakrishnan
Chairman, IEEE Subcommittee on Large Space Structures, COLSS
System Sciences Department
University of California at Los Angeles
Los Angeles, CA



NASA

IEEE

A MATHEMATICAL PROBLEM AND A SPACECRAFT CONTROL LABORATORY
EXPERIMENT (SCOPE) USED TO EVALUATE CONTROL LAWS FOR
FLEXIBLE SPACECRAFT... NASA/IEEE DESIGN CHALLENGE

by

Lawrence W. Taylor, Jr.
Spacecraft Control Branch
NASA Langley Research Center
Hampton, VA 23665

and

A. V. Balakrishnan
Chairman, IEEE Subcommittee on Large Space Structures, COLSS
System Sciences Department
University of California at Los Angeles
Los Angeles, CA

SUMMARY

The problem of controlling large, flexible space systems has been the subject of considerable research. Many approaches to control system synthesis have been evaluated using computer simulation. In several cases, ground experiments have also been used to validate system performance under more realistic conditions. There remains a need, however, to test additional control laws for flexible spacecraft and to directly compare competing design techniques. In this paper an NASA program is discussed which has been initiated to make direct comparisons of control laws for, first, a mathematical problem, then an experimental test article is being assembled under the cognizance of the Spacecraft Control Branch at the NASA Langley Research Center with the advice and counsel of the IEEE Subcommittee on Large Space Structures. The physical apparatus will consist of a softly supported dynamic model of an antenna attached to the Shuttle by a flexible beam. The control objective will include the task of directing the line-of-sight of the Shuttle/antenna configuration toward a fixed

target, under conditions of noisy data, limited control authority and random disturbances. The open competition started in the early part of 1984. Interested researchers are provided information intended to facilitate the analysis and control synthesis tasks. A workshop is planned for early December at the NASA Langley Research Center to discuss and compare results.

INTRODUCTION

Many future spacecraft will be large and consequently quite flexible. As the size of antennae is increased, the frequencies of the first flexible modes will decrease and overlap the pointing system bandwidth. It will no longer be possible to use low gain systems with simple notch filters to provide the required control performance. Multiple sensors and actuators, and sophisticated control laws will be necessary to ensure stability, reliability and the pointing accuracy required for large, flexible spacecraft.

Control of such spacecraft has been studied with regard given to modeling, order reduction, fault management, stability and dynamic system performance. Numerous example applications have been used to demonstrate specific approaches to pertinent control problems. Both computer simulations and laboratory experiment results have been offered as evidence of the validity of the approaches to control large, flexible spacecraft. Concerns remain, however, because of the chronic difficulties in controlling these lightly damped large-scale systems. Because of these concerns and because of the desire to offer a means of comparing technical approaches directly, an NASA/IEEE Design Challenge is being offered. An

experimental test article is being assembled under the cognizance of the Spacecraft Control Branch at the NASA Langley Research Center with the advice and counsel of the IEEE (COLSS) Subcommittee on Large Space Structures. This Spacecraft Control Laboratory Experiment (SCOLE) will serve as the focus of a design challenge for the purpose of comparing directly different approaches to control synthesis, modeling, order reduction, state estimation and system identification.

The configuration of the SCOLE will represent a large antenna attached to the Space Shuttle orbiter by a flexible beam. This configuration was chosen because of its similarity to proposed space flight experiments and proposed space-based antenna systems. This paper will discuss the "Design Challenge" in terms of both a mathematical problem and a physical experimental apparatus. The SCOLE program is not part of any flight program.

SYMBOLS

a	acceleration vector ft/sec ²
A	beam cross section area
c	observation matrix
d	noise contaminating direction cosine matrix measurements
e	line-of-sight error
E	modulus of elasticity
f	concentrated force expressions
F ₄	force vector
g	concentrated moment expressions
GI	torsional rigidity
I	moment of inertia matrix for entire Shuttle/antenna configuration

I_1	moment of inertia matrix, Shuttle body
I_4	moment of inertia matrix, reflector body
I_ϕ	beam cross section moment of inertia, roll bending
I_θ	beam cross section moment of inertia, pitch bending
I_ψ	beam polar moment of inertia, yaw torsion
L	length of the reflector mast, beam
M_1	control moment applied to the Shuttle body
M_4	control moment applied to the reflector body
M_D	disturbance moment applied to the Shuttle body
m	mass of entire Shuttle/antenna configuration
m_1	mass of Shuttle body
m_4	mass of reflector body
ρ	mass density of beam
s	beam position variable
T_1	direction cosine matrix, Shuttle body () _{earth} = $T_1()$ _{Shuttle body}
T_4	direction cosine matrix, reflector body () _{earth} = $T_4()$ _{reflector body}
v_1	inertial velocity, Shuttle body
v_4	inertial velocity, reflector body
u_ϕ	lateral deflection of beam bending in y-z plane
u_θ	lateral deflection of beam bending in x-z plane
u_ψ	angular deflection of beam twisting about z axis
X, Y, Z	position variables
Δ	displacement of proof-mass actuator
δ	line-of-sight pointing requirement
ϵ	noise contaminating angular velocity measurements

θ, ϕ, ψ pitch, roll, heading
 ζ damping ratio
 τ noise contaminating acceleration measurements
 ω_1 angular velocity of Shuttle body
 ω_4 angular velocity of reflector body

DISCUSSION

The objective of the NASA-IEEE Design Challenge concerning the control of flexible spacecraft is to promote direct comparison of different approaches to control, state estimation and systems identification. The design challenge has principal parts, the first using a mathematical model, and the second using laboratory experimental apparatus. The specific parts of the Spacecraft Control Laboratory Experiment (SCOLE) program will be discussed in detail.

Control Objectives

The primary control task is to rapidly slew or change the line-of-sight of an antenna attached to the space Shuttle orbiter, and to settle or damp the structural vibrations to the degree required for precise pointing of the antenna. The objective will be to minimize the time required to slew and settle, until the antenna line-of-sight remains within the angle δ . A secondary control task is to change direction during the "on-target" phase to prepare for the next slew maneuver. The objective is to change attitude and stabilize as quickly as possible, while keeping the line-of-sight error less than δ .

Math Model Dynamics

The initial phase of the design challenge will use a mathematical model of the Shuttle orbiter/antenna configuration. It is necessary to obtain a balance, of course, between complex formulations which might be more accurate and simplified formulations which ease the burden of analysis.

The dynamics are described by a distributed parameter beam equation with rigid bodies, each having mass and inertia at either end. One body represents Space Shuttle orbiter; the other body is the antenna reflector. The equations for the structural dynamics and Shuttle motion are formed by adding to the rigid-body equations of motion, beam-bending and torsion equations. The boundary conditions at the ends of the beam contain the forces and moments of the rigid Shuttle and reflector bodies. The nonlinear kinematics couples the otherwise uncoupled beam equations. Additional terms represent the action of two, 2-axis proof-mass actuators at locations on the beam chosen by the designer.

The rigid-body equations of motion for the Shuttle body are given by:

$$\dot{\omega}_1 = - I_1^{-1} (\tilde{\omega}_1 I_1 \omega_1 + M_1 + M_D + M_{B,1})$$

$$\dot{v} = \frac{F_{B,1}}{m_1}$$

Similarly, for the reflector body,

$$\dot{\omega}_4 = - I_4^{-1} (\tilde{\omega}_4 I_4 \omega_4 + M_4 + M_{B,4})$$

$$\dot{v}_4 = \frac{F_4 + F_{B,4}}{m_4}$$

The direction cosine matrices defining the attitudes of the Shuttle and reflector bodies are given by:

$$\dot{T}_1^T = - \tilde{\omega}_1 T_1^T$$

$$\dot{T}_4^T = - \tilde{\omega}_4 T_4^T$$

The direction cosine matrices defining the attitudes of the Shuttle and the reflector bodies are related to the beam end conditions.

$$T_4 = \begin{bmatrix} 1 & 0 & 0 \\ 0 & \cos\Delta\phi & -\sin\Delta\phi \\ 0 & \sin\Delta\phi & \cos\Delta\phi \end{bmatrix} \begin{bmatrix} \cos\Delta\theta & 0 & \sin\Delta\theta \\ 0 & 1 & 0 \\ -\sin\Delta\theta & 0 & \cos\Delta\theta \end{bmatrix} \begin{bmatrix} \cos\Delta\Psi & -\sin\Delta\Psi & 0 \\ \sin\Delta\Psi & \cos\Delta\Psi & 0 \\ 0 & 0 & 1 \end{bmatrix} T_1$$

where:

$$\Delta\Psi = u_\Psi \Big|_{s=L} - u_\Psi \Big|_{s=0}$$

$$\Delta\theta = \frac{\partial u_\theta}{\partial s} \Big|_{s=L} - \frac{\partial u_\theta}{\partial s} \Big|_{s=0}$$

$$\Delta\phi = \frac{\partial u_\phi}{\partial s} \Big|_{s=L} - \frac{\partial u_\phi}{\partial s} \Big|_{s=0}$$

The equations of motion for the flexible beam-like truss connecting the reflector and Shuttle bodies consist of standard beam bending and torsion partial differential equations with energy dissipative terms which enable damped modes with constant characteristics for fixed, though dynamic, end conditions. The system of equations can be viewed as driven by changing end conditions and forces applied at the locations of the proof-mass actuators.

ROLL BEAM BENDING:

$$PA \frac{\partial^2 u_\phi}{\partial t^2} - 2\zeta_\phi \sqrt{PA EI_\phi} \frac{\partial^3 u_\phi}{\partial s^2 \partial t} + EI_\phi \frac{\partial^4 u_\phi}{\partial s^4} = \sum_{n=1}^4 [f_{\phi,n} \delta(s-s_n) + g_{\phi,n} \frac{\partial \delta}{\partial s} (s-s_n)]$$

PITCH BEAM BENDING:

$$PA \frac{\partial^2 u_\theta}{\partial t^2} - 2\zeta_\theta \sqrt{PA EI_\theta} \frac{\partial^3 u_\theta}{\partial s^2 \partial t} + EI_\theta \frac{\partial^4 u_\theta}{\partial s^4} = \sum_{n=1}^4 [f_{\theta,n} \delta(s-s_n) + g_{\theta,n} \frac{\partial \delta}{\partial s} (s-s_n)]$$

YAW BEAM TORSION:

$$PI_\psi \frac{\partial^2 u_\psi}{\partial t^2} + 2\zeta_\psi I_\psi \sqrt{GP} \frac{\partial^3 u_\psi}{\partial s^2 \partial t} + GI_\psi \frac{\partial^2 u_\psi}{\partial s^2} = \sum_{n=1}^4 g_{\psi,n} \delta(s - s_n)$$

where:

$$f_{\phi,1} = m_1 \frac{\partial^2 u_\phi}{\partial t^2} \Big|_{s=0} \quad \{ \text{SHUTTLE BODY FORCE} \}$$

$$f_{\phi,2} = m_2 \frac{\partial^2 u_\phi}{\partial t^2} \Big|_{s=s_2} + m_2 \frac{\partial^2 \Delta_\phi,2}{\partial t^2} \quad \{ \text{PROOF-MASS ACTUATOR FORCE} \}$$

$$f_{\phi,3} = m_3 \frac{\partial^2 u_\phi}{\partial t^2} \Big|_{s=s_3} + m_3 \frac{\partial^2 \Delta_{\phi,2}}{\partial t^2}$$

{PROOF-MASS ACTUATOR}

$$f_{\phi,4} = m_4 \frac{\partial^2 u_\phi}{\partial t^2} \Big|_{s=130} - I_{zz,4} \frac{\partial^2 u_\psi}{\partial t^2} / 32.5 + F_y$$

{REFLECTOR BODY FORCE}

$$f_{\theta,1} = m_1 \frac{\partial^2 u_\theta}{\partial t^2} \Big|_{s=s_1}$$

{SHUTTLE BODY FORCE}

$$f_{\theta,2} = m_2 \frac{\partial^2 u_\theta}{\partial t^2} \Big|_{s=s_2} + m_2 \frac{\partial^2 \Delta_{\theta,2}}{\partial t^2}$$

{PROOF-MASS ACTUATOR FORCE}

$$f_{\theta,3} = m_3 \frac{\partial^2 u_\theta}{\partial t^2} \Big|_{s=s_3} + m_3 \frac{\partial^2 \Delta_{\theta,2}}{\partial t^2}$$

{PROOF-MASS ACTUATOR FORCE}

$$f_{\theta,4} = m_4 \frac{\partial^2 u_\theta}{\partial t^2} \Big|_{s=130} - I_{zz,4} \frac{\partial^2 u_\psi}{\partial t^2} / 18.75 - F_x$$

{REFLECTOR BODY FORCE}

$$\begin{pmatrix} g_{\phi,1} \\ g_{\theta,1} \\ g_{\psi,1} \end{pmatrix} = I_1 \dot{\omega}_1 + \omega_1 I_1 \omega_1 + M_1 + M_D \quad \{ \text{SHUTTLE BODY, MOMENTS} \}$$

$$\begin{pmatrix} g_{\phi,2} \\ g_{\theta,2} \\ g_{\psi,2} \end{pmatrix} = 0 \quad \{ \text{PROOF-MASS ACTUATOR, MOMENT} \}$$

$$\begin{pmatrix} g_{\phi,3} \\ g_{\theta,3} \\ g_{\psi,3} \end{pmatrix} = 0 \quad \{ \text{PROOF-MASS ACTUATOR, MOMENT} \}$$

$$\begin{pmatrix} g_{\phi,4} \\ g_{\theta,4} \\ g_{\psi,4} \end{pmatrix} = I_4 \dot{\omega}_4 + \omega_4 I_4 \omega_4 + M_4 + \tilde{R}_B F_{B,4} \quad \{ \text{REFLECTOR BODY, MOMENT} \}$$

The angular velocity of the reflector body is related to the Shuttle body by:

$$\omega_4 = \left[\begin{array}{c} \frac{\partial^2 u_\phi}{\partial s \partial t} \\ \hline s=L \end{array} \right] - \left[\begin{array}{c} \frac{\partial^2 u_\phi}{\partial s \partial t} \\ \hline s=0 \end{array} \right] + \omega_1 \quad \tilde{R}_B = \begin{pmatrix} 0 & 130 & 0 \\ -130 & 0 & 0 \\ 0 & 0 & 0 \end{pmatrix}$$

The line-of-sight error described in figure 2 is affected by both the pointing error of the Shuttle body and the misalignment of the reflector due to the deflection of the beam supporting the reflector. The line-of-sight is defined by a ray from the feed which is reflected at the center of the reflector. Its direction in the Shuttle body coordinates is given by:

$$R_{LOS} = \frac{-R_R + R_F + 2 \left[R_A^T (R_R - R_F) \cdot R_A \right]}{\left\| R_R - R_F - 2 \left[R_A^T R_R - R_F \right] \cdot R_A \right\|}$$

where:

R_F is the feed location (3.75, 0, 0)

R_R is the location of the center of the reflector (18.75, -32.5, -130) *in an undeflected state*.

R_A is a unit vector in the direction of the reflector axis in Shuttle body coordinates

The vector R_A can be related to the direction cosine attitude matrices for the Shuttle body, T_1 , and the reflector body, T_4 , by

$$R_A = \begin{bmatrix} T_1^T \\ T_4^T \end{bmatrix} \begin{pmatrix} 0 \\ 0 \\ 1 \end{pmatrix}$$

The relative alignment of the reflector to the Shuttle body is given by $T_1^T T_4$ which is a function of the structural deformations of the beam.

The line-of-sight error, e , is the angular difference between the target direction, given by the unit vector, D_T , and the line-of-sight direction in Earth axes, $T_1 R_{LOS}$.

$$e = \text{ARCSIN } |D_T \times T_1 R_{LOS}| \quad \text{or} \quad \text{ARCSIN } |\tilde{D}_T T_1 R_{LOS}|$$

Computer programs are available which generate time histories of the rigid body and the mode shapes and frequencies for the body-beam-body configuration for "pitch" bending, "roll" bending and "yaw" twisting. Since the modes are based on solving explicitly the distributed parameter equations (without damping and without kinematic coupling) there is no limit to the number of modal characteristic sets that can be generated by the program. It will be the analyst's decision as to how many modes need to be considered.

Laboratory Experiment Description

The second part of the design challenge is to validate in the laboratory, the system performance of the more promising control system designs of the first part. The experimental apparatus will consist of a dynamic model of the Space Shuttle orbiter with a large antenna reflector attached by means of a flexible beam. The dynamic model will be extensively instrumented and will have attached force and moment generating devices for control and for disturbance generation. A single, flexible tether will be used to suspend the dynamic model, allowing complete angular freedom in yaw, and limited freedom in pitch and roll. An inverted position will be used to let the reflector mast to hang so that gravity effects on mast bending will be minimized. The dynamics of the laboratory model will of necessity be different from the mathematical model discussed earlier.

Design Challenge, Part One

For part one of the design challenge, the following mathematical problem is addressed. Given the dynamic equations of the Shuttle/antenna configuration, what control policy minimizes the time to slew to a target and to stabilize so that the line-of-sight (LOS) error is held, for a time, within a specified amount, δ . During the time that the LOS error is within δ , the attitude must change 90° to prepare for the next slew maneuver. This was previously referred to as the sescondary control task. The maximum moment and force generating capability will be limited. Advantage may be taken of selecting the most suitable initial alignment of the Shuttle/antenna about its assigned initial RF axis, line-of-sight. Random, broad band-pass disturbances will be applied to the configuration. Two proof-mass, force actuators may be positioned anywhere along the beam. The design guidelines are summarized below:

1. The initial line-of-sight error is 20 degrees.

$$e(0) = 20 \text{ degrees}$$

2. The initial target direction is straight down.

$$D_T = \begin{pmatrix} 0 \\ 0 \\ 1 \end{pmatrix}$$

3. The initial alignment about the line-of-sight is free to be chosen by the designer. Advantage may be taken of the low value of moment of inertia in roll. The Shuttle/antenna is at rest initially.
4. The objective is to point the line-of-sight of the antenna and stabilize to within 0.02 degree of the target as quickly as possible.

$$\delta = 0.02 \text{ degree}$$

5. Control moments can be applied at 100 Hz sampling rate to both the Shuttle and reflector bodies of 10,000 ft-lb for each axis. The commanded moment for each axis is limited to 10,000 ft-lb. The actual control moment's response to the commanded value is first-order with a time constant of 0.1 second.

For the rolling moment applied to the Shuttle body:

$$-10^4 \leq M_{X,1,command} \leq 10^4$$

$$M_{X,1}(n+1) = e^{-0.1} M_{X,1}(n) + (1 - e^{-0.1}) M_{X,1,command}(n)$$

Equations for other axes and for the reflector body are similar.

6. Control forces can be applied at the center of the reflector in the X and Y directions only. The commanded force in a particular direction is limited to 800 lbs. The actual control force's response to the commanded value is first-order with a response time of 0.1 second.

For the side force applied to the reflector body:

$$-800 \leq F_{Y,command} \leq 800$$

$$F_Y(n+1) = e^{-0.1} F_Y(n) + (1 - e^{-0.1}) F_{Y,command}(n)$$

Equations for X-axis are similar.

7. Control forces using two proof-mass actuators (each having both X and Y axes) can be applied at two points on the beam. The strokes are limited to ± 1 ft, and the masses weight 10 lbs each. The actual stroke follows a first-order response to limited commanded values.

For the X-axis of the proof-mass actuator at s_2 :

$$-1 \leq \Delta_{X,2,\text{command}} \leq 1$$

$$\Delta_{X,2}(n+1) = e^{-0.1} \Delta_{X,2}(n) + (1 - e^{-0.1}) \Delta_{X,2,\text{command}}(n)$$

Equations for other axes and locations are similar.

8. The inertial attitude direction cosine matrix for the Shuttle body lags in time the actual values by 0.01 second and are made at a rate of 100 samples per second. Each element of the direction cosine measurement matrix is contaminated by additive, uncorrelated Gaussian noise having an rms value of 0.001. The noise has zero mean.

$$T_{s,\text{measured}}(n+1) = T_{s,\text{true}}(n) + \begin{bmatrix} d_{11}(n) & d_{12}(n) & d_{13}(n) \\ d_{21}(n) & d_{22}(n) & d_{23}(n) \\ d_{31}(n) & d_{32}(n) & d_{33}(n) \end{bmatrix}$$

where:

$$E\{d_{ij}(n)\} = 0$$

$$E\{d_{ij}(n)d_{kL}(n)\} = 0 \quad \text{for } i \neq k \text{ or } j \neq L$$

$$E\{d_{ij}(n)d_{ij}(n+k)\} = 0 \quad \text{for } k \neq 0$$

$$= [0.001]^2 \quad \text{for } k = 0$$

9. The angular velocity measurements for both the Shuttle and reflector bodies pass through a first-order filter with 0.05 sec time constant and lag in time the actual values by 0.01 second and are made at a rate of 100 samples per second. Each rate measurement is contaminated by additive, Gaussian, uncorrelated noise having an rms value of 0.02 degree per second. The noise has zero mean.

For example:

$$\omega_{1,X,\text{measured}}^{(n+1)} = \omega_{1,X,\text{filtered}}^{(n)} + \varepsilon_{1,X}^{(n)}$$

$$E\{\varepsilon_{1,X}^{(n)} \varepsilon_{1,X}^{(n+k)}\} = 0 \quad \text{for } k \neq 0$$

$$= (.02)^2 \quad \text{for } k = 0$$

where

$$\dot{\omega}_{1,X,\text{filtered}} = -20 \omega_{1,X,\text{filtered}} + 20 \omega_{1,X,\text{true}}$$

10. Three-axis accelerometers are located on the Shuttle body at the base of the mast and on the reflector body at its center. Two-axes (X and Y) accelerometers are located at intervals of 10 feet along the mast. The acceleration measurements pass through a first-order filter with a 0.05 second time constant and lag in time the actual values by 0.01 second, and are made at a rate of 100 samples per second. Each measurement is contaminated by Gaussian additive, uncorrelated noise having an rms value of 0.05 ft/sec².

For example:

$$a_{1,X,\text{measured}}^{(n+1)} = a_{1,X,\text{filtered}}^{(n)} + \tau_{1,X}^{(n)}$$

$$E\{\tau_{1,X}^{(n)} \tau_{1,X}^{(n+k)}\} = 0 \quad \text{for } k \neq 0$$

$$= (0.05)^2 \quad \text{for } k = 0$$

where:

$$\dot{a}_{1,X,\text{filtered}} = -20 a_{1,X,\text{filtered}} + 20 \omega_{1,X,\text{true}}$$

11. Gaussian, uncorrelated step-like disturbances are applied 100 times per second to the Shuttle body in the form of 3-axes moments, having rms values of 100 ft-lbs. These disturbances have zero mean.

For example:

$$E\{M_{D,X}^{(n)} M_{D,X}^{(n+k)}\} = 0 \quad \text{for } k \neq 0$$

$$= (100)^2 \quad \text{for } k = 0$$

In summary, the designer's task for part one is to: (1) derive a control law for slewing and stabilization, coded in FORTRAN; (2) select an initial attitude in preparation for slewing 20 degrees; and (3) select two positions for the 2-axes proof-mass actuators. An official system performance assessment computer program will be used to establish the time required to slew and stabilize the Shuttle/antenna configuration.

Design Challenge, Part Two

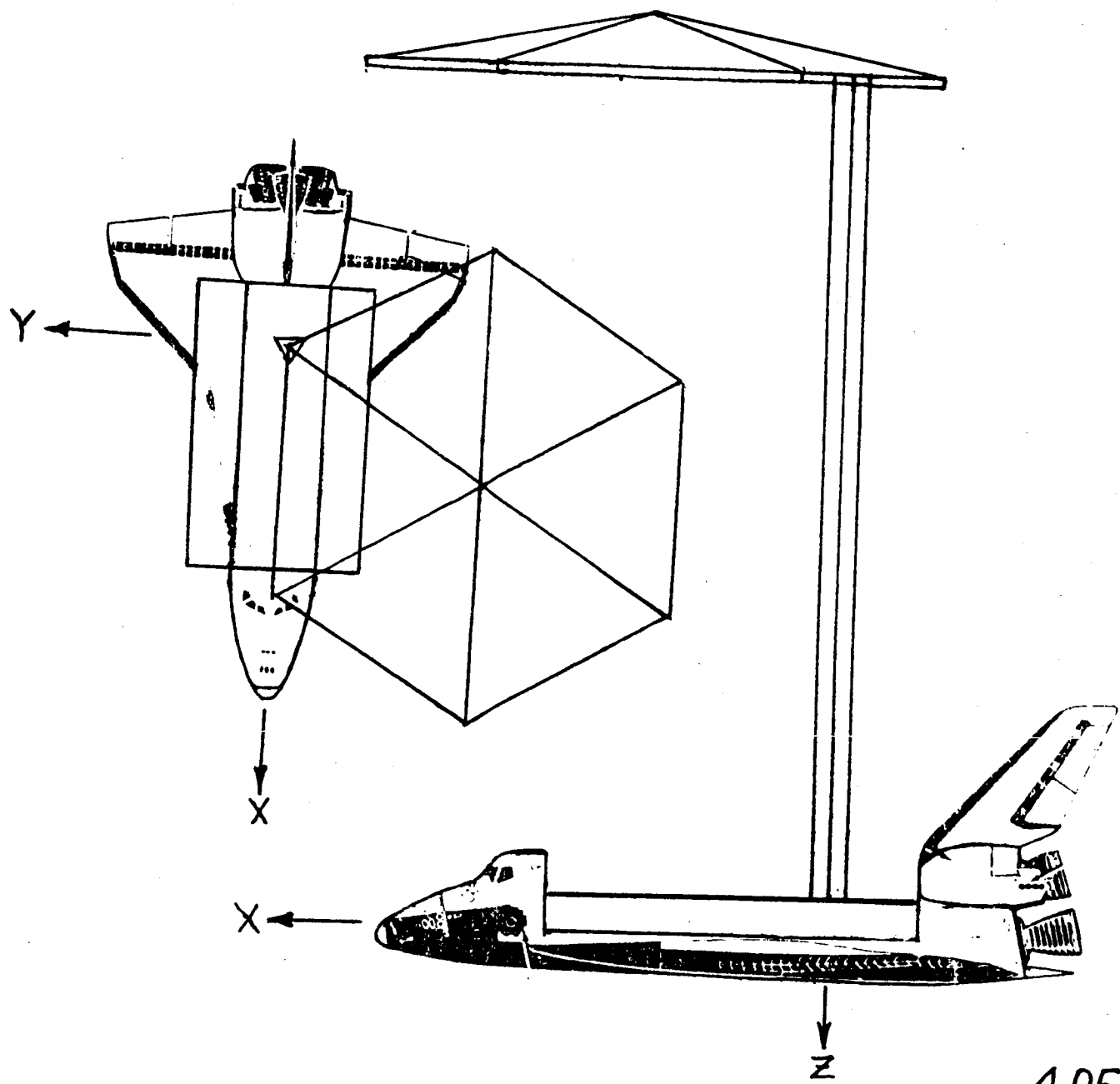
As in part one, the task is to minimize the time to slew and stabilize a Shuttle/antenna configuration. The difference is that in part two of the design challenge, a physical laboratory model will be used instead of the dynamic equations of part one. The constraints on total moment and force generation capability will apply to part two, as for part one. Again, the analyst may select the initial alignment about the assigned initial RF line-of-sight. Disturbances will be injected into the Shuttle/antenna model. The designer's task will be similar to that for part one.

CONCLUDING REMARKS

A Design Challenge, in two parts, has been offered for the purpose of comparing directly different approach to controlling a flexible Shuttle/antenna configuration. The first part of the design challenge uses only mathematical equations of the vehicle dynamics; the second part uses a physical laboratory model of the same configuration. The Spacecraft Control Laboratory Experiment (SCOLE) program is being conducted under the cognizance of the Spacecraft Control Branch at the NASA Langley Research Center. The NASA/IEEE Design Challenge has the advice and counsel of the IEEE-COLSS Subcommittee on Large Space Structures. Workshops will be held to enable investigators to compare results of their research.

Figure 1. Drawing of the Shuttle/Antenna Configuration.

SPACECRAFT CONTROL LAB EXPERIMENT (SCOLE)



The moment of inertia becomes:

$$I = \begin{bmatrix} I_{xx} & -I_{xy} & -I_{xz} \\ -I_{xy} & I_{yy} & -I_{yz} \\ -I_{xz} & -I_{yz} & I_{zz} \end{bmatrix} = \begin{bmatrix} 1,132,508 & 7,555 & -115,202 \\ 7,555 & 7,007,447 & -52,293 \\ -115,202 & -52,293 & 7,113,962 \end{bmatrix}$$

$$I_1 = \begin{bmatrix} 905,443 & 0 & -145,393 \\ 0 & 6,789,100 & 0 \\ -145,393 & 0 & 7,086,601 \end{bmatrix}$$

$$I_4 = \begin{bmatrix} 4,969 & 0 & 0 \\ 0 & 4,969 & 0 \\ 0 & 0 & 9,938 \end{bmatrix}$$

$$m = 6391.30 \text{ slugs}$$

$$m_1 = 6366.46 \text{ slugs}$$

$$m_2 = 0.3108 \text{ slugs}$$

$$m_3 = 0.3108 \text{ slugs}$$

$$m_4 = 12.42 \text{ slugs}$$

$$\begin{aligned} PA &= 0.09556 \text{ slugs/ft} \\ I_\phi &= 4.0 \times 10^7 \text{ lb-ft}^2 \\ &= .003 \\ &= 0.9089 \text{ slug-ft} \\ &= 4.0 \times 10^7 \text{ lb-ft}^2 \\ &= .003 \end{aligned}$$

$$\begin{aligned} PA &= 0.09556 \text{ slugs/ft} \\ EI_\theta &= 4.0 \times 10^7 \text{ lb-ft}^2 \\ \zeta_\theta &= .003 \end{aligned}$$

MASS CHARACTERISTICS

CG LOCATION, FT X Y Z	WEIGHT, LB	I_{XX} $SLG-FT^2$	I_{YY} $SLG-FT^2$	I_{ZZ} $SLG-FT^2$	I_{XY} $SLG-FT^2$	I_{XZ} $SLG-FT^2$	I_{YZ} $SLG-FT^2$
SHUTTLE 0 0 0	205,000	905,443	6,789,100	7,086,601	0	145,393	0
MAST, CG 0 0 -65.	400	17,495	17,495	0	0	0	0
REFLECTOR, CG 18.75 -32.5 -130.	400	4,969	4,969	9,938	0	0	0
REFLECTOR, ATTACHMENT POINT		18,000	9,336	27,407	-7,570	0	0
TOTAL .036 -.063 -.379	205,800	1,132,508	7,007,447	7,113,962	-7,555	115,202	52,293

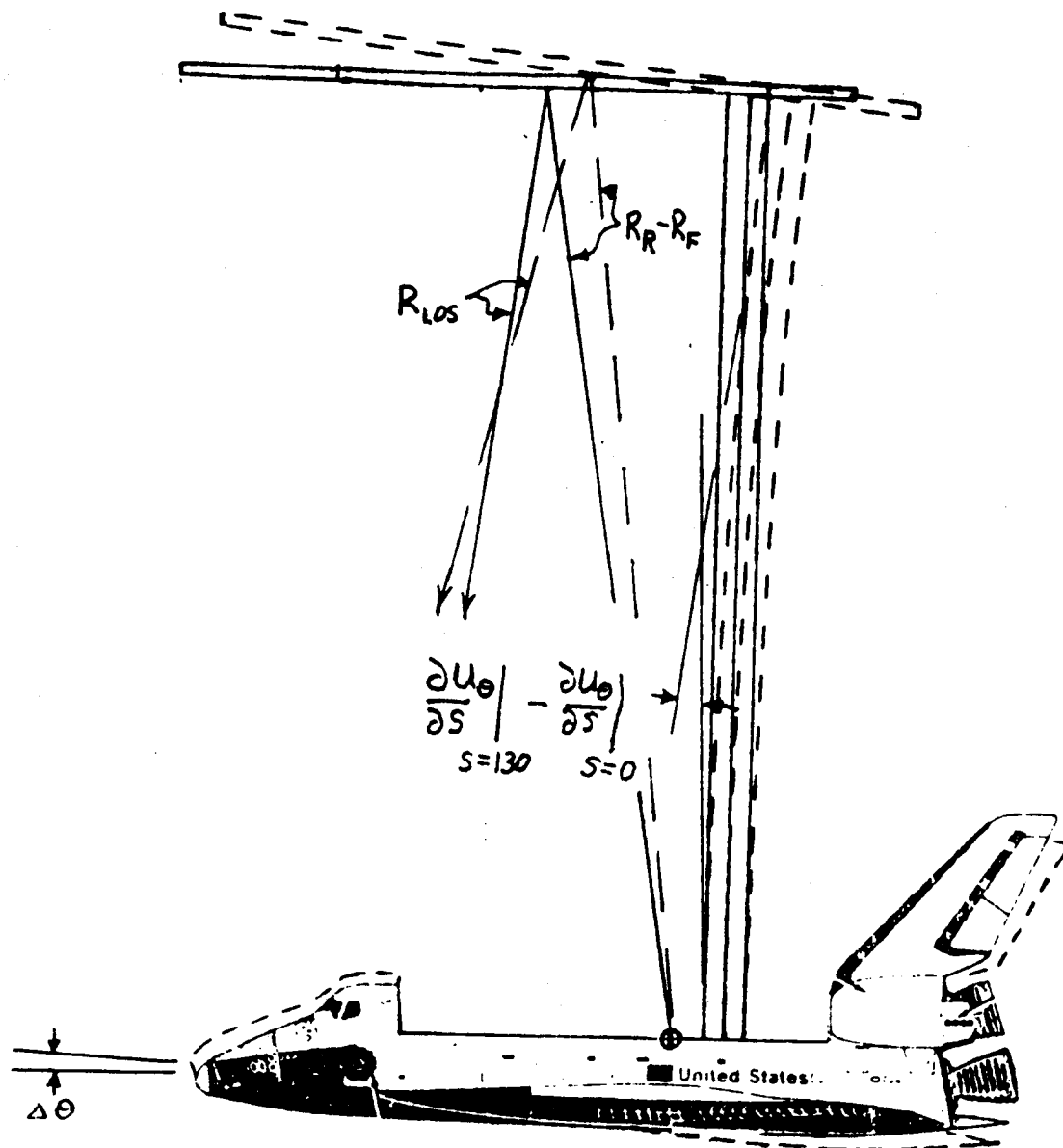
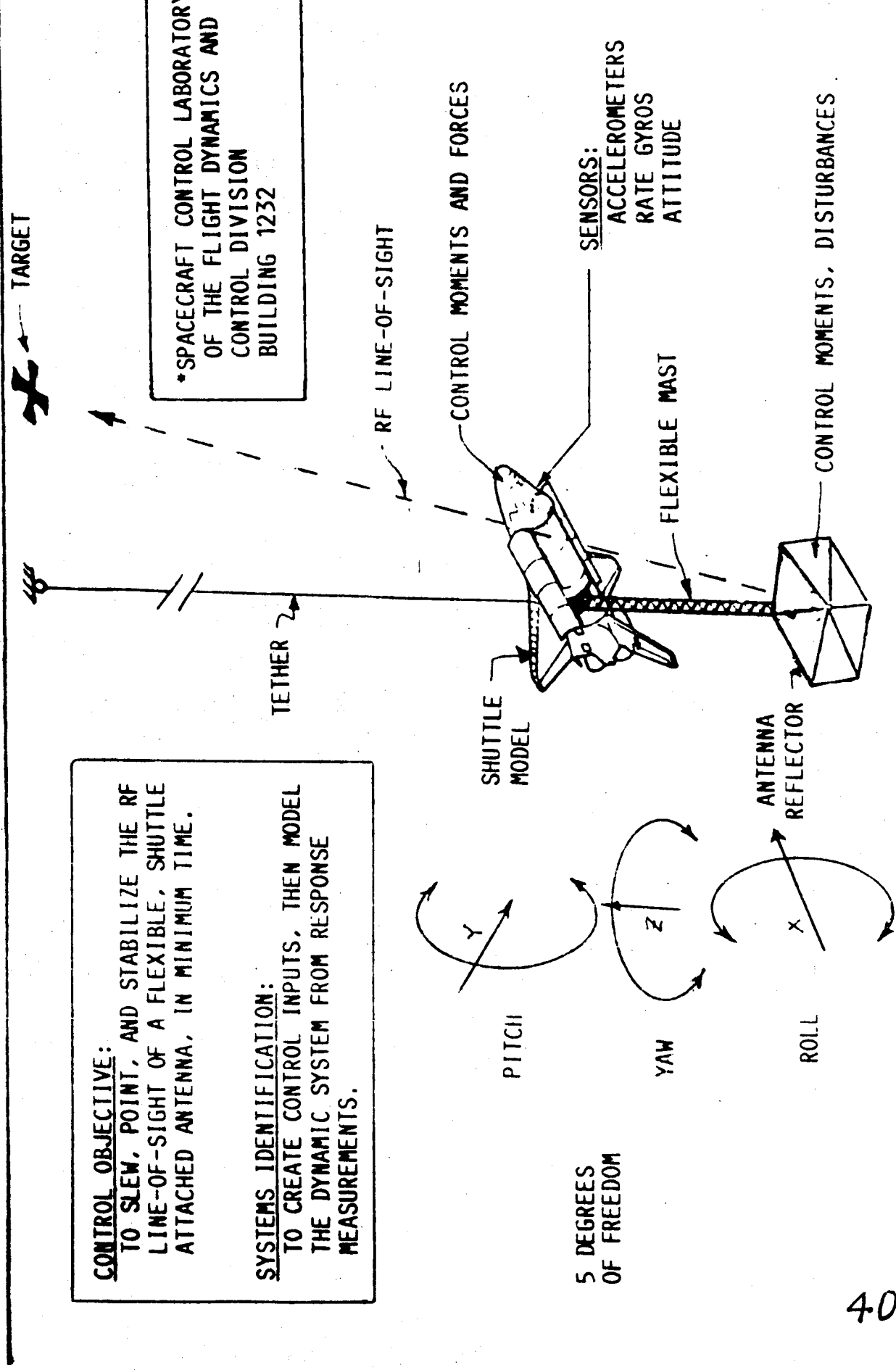


Figure 2.- Schematic of the effect of bending on the line-of-sight pointing error.

Figure 3. SPACECRAFT CONTROL LABORATORY EXPERIMENT (SCOLE)



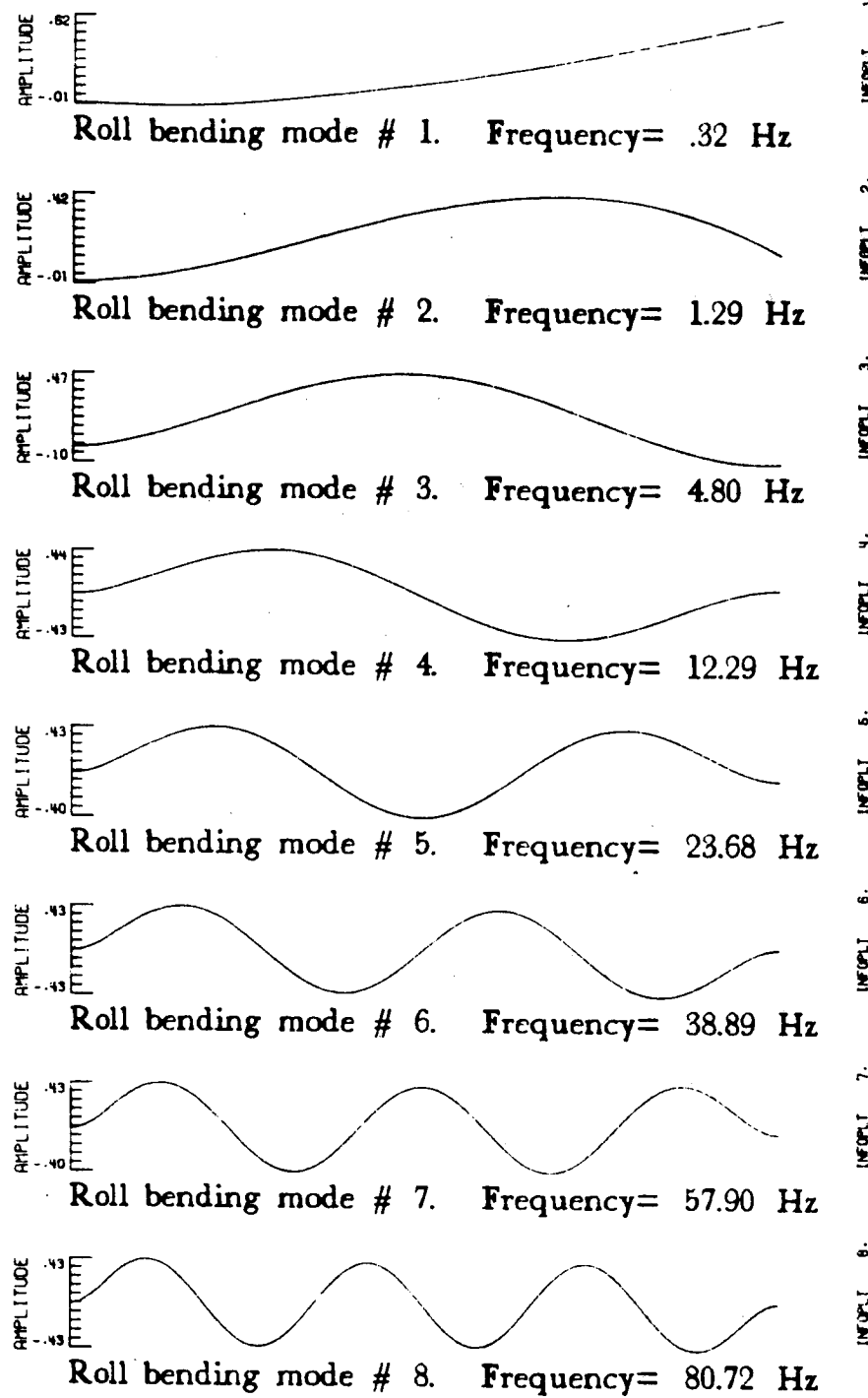


Figure 4a.- Plots of normalized roll bending mode shapes for SCOLE configuration.

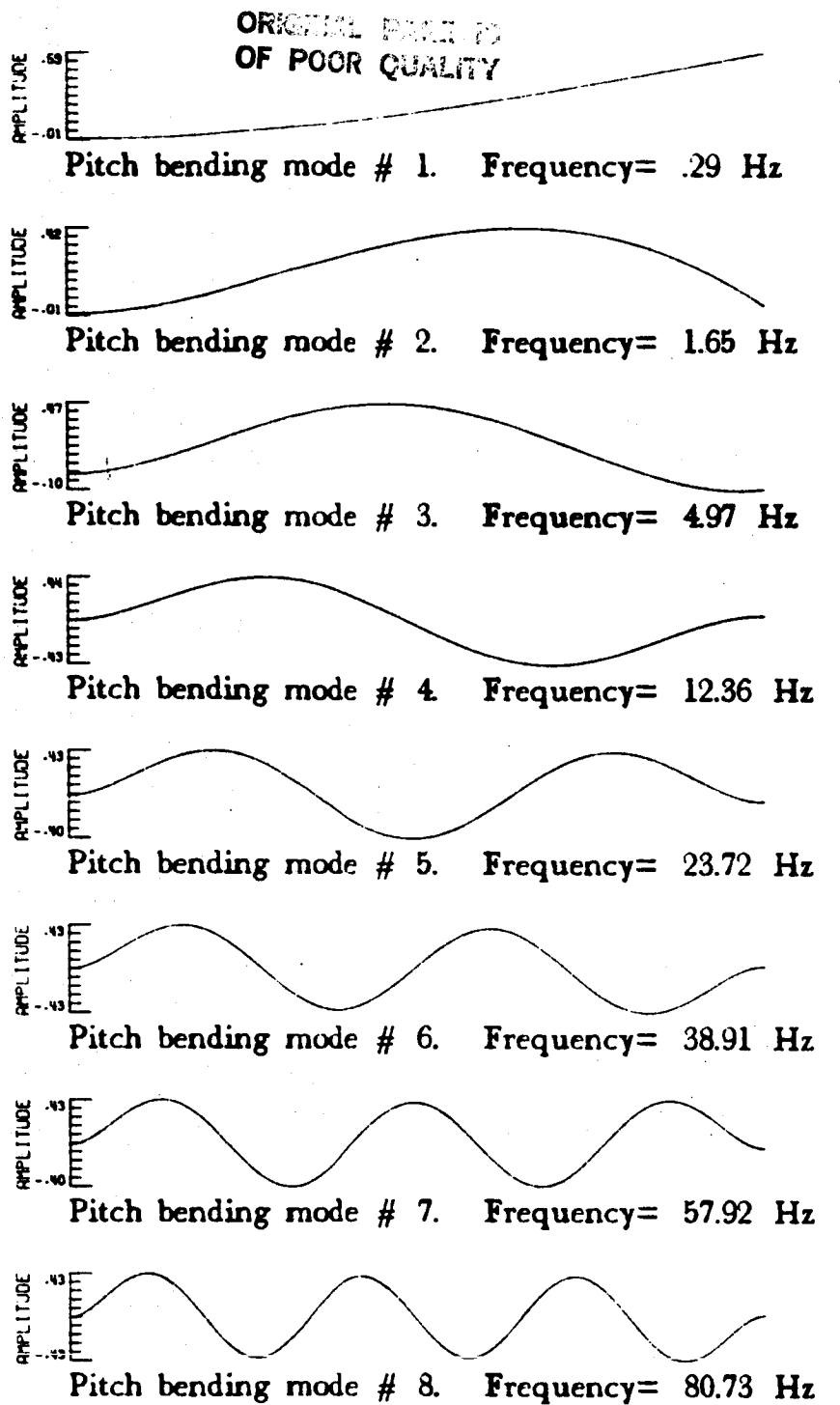


Figure 4b.- Plots of normalized pitch bending mode shapes for SCOLE configuration.

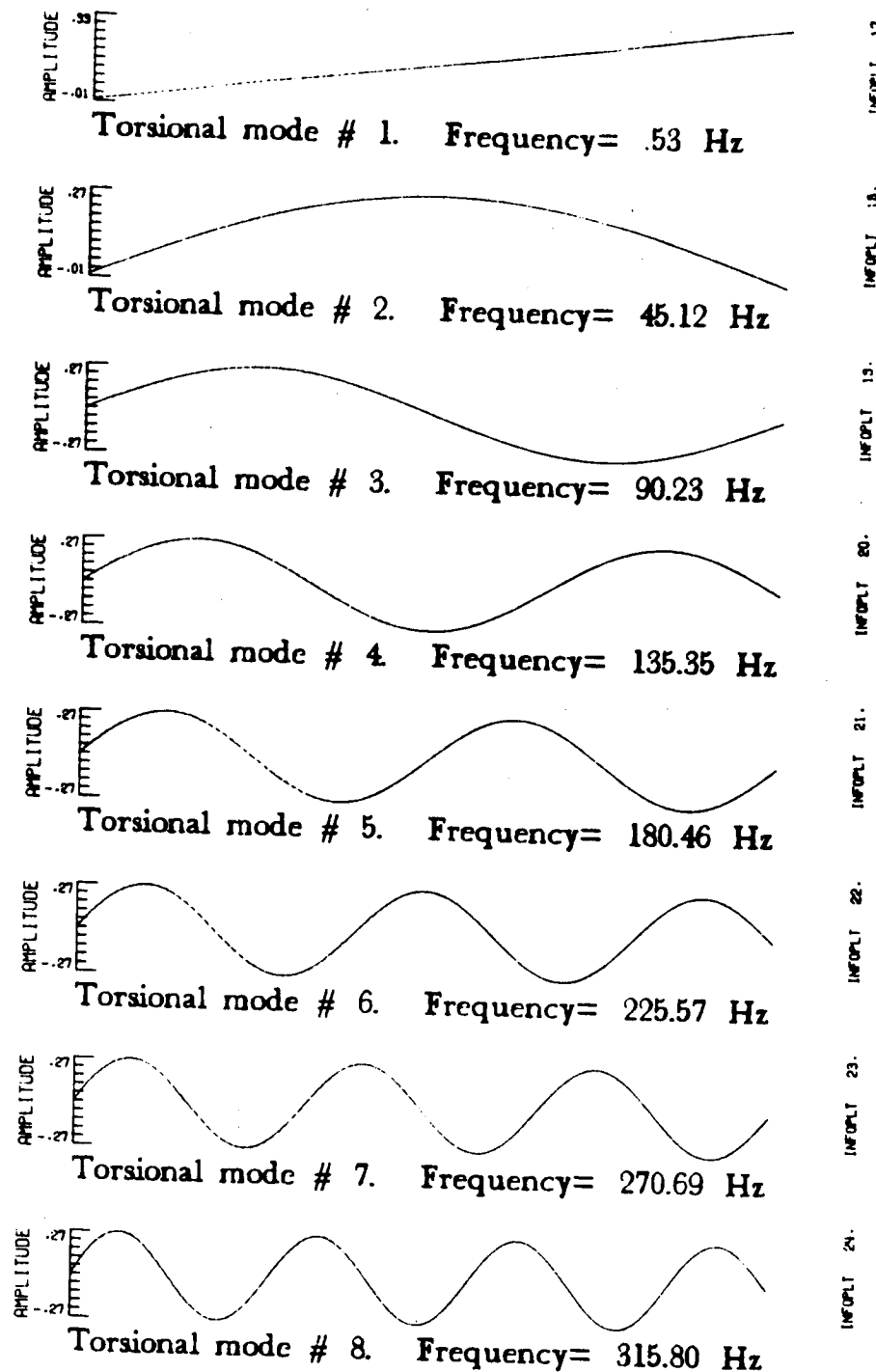


Figure 4c.- Plots of normalized torsional mode shapes for SCOLE configuration.

Description of the Spacecraft Control Laboratory Experiment (SCOLE) Facility

by

**Jeffrey P. Williams
Rosemary A. Rallo
NASA Langley
Research Center**

SCOLE - 1

SUMMARY

The Spacecraft Control Laboratory Experiment is a facility for the investigation of control techniques for large flexible spacecraft. The control problems to be studied are slewing maneuvers and pointing operations. The facility implements the salient characteristics of a flexible satellite with distributed sensors and actuators.

The flexible satellite is represented by a continuous structure consisting of a large mass and inertia connected to a small mass and inertia by a slender, flexible beam. The structure is suspended by a single cable mounted to a universal joint at the system C. G. The sensors for the experiment consist of aircraft quality rate sensors and servo-accelerometers. The shuttle attitude will be determined through a combination of inertial measurements and optical sensing techniques. Actuators for the experiment consist of Control Moment Gyros, reaction wheels, and cold gas thrusters. Computational facilities consist of micro-computer-based central processing units with appropriate analog interfaces for implementation of the primary control system, the attitude estimation algorithm and the CMG steering law. Details of the experimental apparatus and the system software are presented in this paper.

ABSTRACT

A laboratory facility for the study of control laws for large flexible spacecraft is described in the following paper. The facility fulfills the requirements of the Spacecraft Control Laboratory Experiment (SCOLE) design challenge for a laboratory experiment, which will allow slew maneuvers and pointing operations. The structural apparatus is described in detail sufficient for modelling purposes. The sensor and actuator types and characteristics are described so that identification and control algorithms may be designed. The control implementation computer and real-time subroutines are also described.

INTRODUCTION

A modelling and control design challenge for flexible space structures has been presented to the technical community by the NASA and IEEE (ref. 1). The Spacecraft Control Laboratory Experiment (SCOLE) was constructed to provide a physical test bed for the investigation and validation techniques developed in response to the design challenge. The control problems to be studied are slewing maneuvers and pointing operations. The slew is defined as minimum time maneuver to bring the antenna line-of-sight (LOS) pointing to within an error limit of the pointing target. The second control objective is to rotate about the line of sight and stabilize about the new attitude while keeping the LOS error within the bound δ . The SCOLE problem is defined as two design challenges. The first challenge is to design control laws, using a given set of sensors and actuators, for a mathematical model of a large antenna attached to the space shuttle by a long flexible mast. The second challenge is to design and implement the control laws on a structural model of the system in a laboratory environment. This report gives preliminary specifications of the laboratory apparatus so that interested investigators may begin design and simulation for the laboratory experiment.

The laboratory experiment shown in figure 1 attempts to implement the definition of the modelling and control design challenge within reasonable limits of the 1-g atmospheric environment. The experimental facility exhibits the essential SCOLE characteristics of a large mass/inertia (space shuttle model) connected to a

small mass/inertia (antennae reflector) by a flexible beam. Control sensors and actuators are typical of those which the control designer would have to deal with on an actual spacecraft. Some trades are made in terms of structure, sensors, actuators, and computational capability in order to develop the experiment in a timely and cost-effective manner. To this end, the basic structure is made of homogeneous, continuous elements. It is suspended from a steel cable with the positive z-axis of the shuttle pointing up, thus minimizing the static bending of the antenna mast. The suspension point is a two-degree-of-freedom gimbal for pitch and roll with yaw freedom supplied by the suspension cable. The sensors are aircraft quality rate sensors and servo-accelerometers. The shuttle attitude will be determined through a combination of inertial measurements and optical sensing techniques.

The shuttle control moments are provided by a pair of two-axis control moment gyros (CMG's). Mast-mounted control torques can be applied by a pair of two-axis reaction wheels. The reflector-based forces are provided by solenoid-actuated cold-air thrusters. Reflector mounted torque devices are a trio of high-authority reaction wheels. Computational facilities consist of micro-computer-based central processing units with appropriate analog interfaces for implementation of the primary control system, the attitude estimation algorithm, and the CMG steering law. All of the elements which make up the SCOLE experiment are described in detail in the following text.

The description of the apparatus covers five major groups: The basic structural elements are described and pertinent dimensions and structural properties are provided. The sensor locations and their dynamic properties are presented. The actuator locations and estimated dynamic properties are also given. The mass properties of the combined structure, sensor and actuator system are given. Finally, the computing system and analog interfaces are described.

The contents of this report are considered accurate at the time of publication. All of the planned SCOLE components are implemented and are available to the user at a raw signal level. However, due to continued refinement of some of the components, specific details of the system may change over the life-time of the experimental apparatus.

STRUCTURES

The SCOLE is comprised of three basic structures, the shuttle, the mast, and the reflector panel. The assembly of these individual components and the global reference frame are shown in figure 2.

The shuttle planform is made from a 13/16-inch steel plate and has overall dimensions of 83.8 by 54.0 inches. Its total weight is 501.7 pounds. The shuttle's center-of-mass is located 3.4 inches below the experiment's point of suspension, and 26.8 inches forward of the tail edge (fig. 3).

The mast is 120 inches long. It is made from stainless steel tubing and weighs 4.48 pounds. One-inch thick manifolds are mounted to the mast at each end. The assembly of these parts and their dimensions are shown in figure 4.

The reflector panel is hexagonal in shape, made from welded aluminum tubing, and weighs 4.76 pounds (fig. 5). It is located 126.6 inches below the SCOLE's point of suspension. The center of the reflector is located at 12.0 inches in the x direction and 20.8 inches in the y direction from the end of the mast.

The complete system is suspended from an 11-foot cable attached at the system center-of-gravity via a universal joint. Roll and pitch rotational freedom is provided by pillow-block ball bearings which have an estimated break-out torque of 0.1 ft-lb. The universal joint is shown in figure 6. It is fixed to the shuttle plate, and the system center-of-gravity is made to coincide with the center-of-rotation by means of an adjustable counter balance system.

SENSORS

The sensors for the experiment consists of nine servo-accelerometers and two, 3-axis rotational rate sensing units. An optical sensor will provide yaw attitude of the shuttle. The power supplies for these sensors are mounted on the shuttle plate to minimize the number of large gauge wires which must cross the universal joint suspension point. Only a single 115 VAC cable and 33 signal wires cross the universal joint. The wires for the sensors are routed on the shuttle and along the mast.

Accelerometers

All nine accelerometers have a frequency response which is nearly flat up to 350 Hz. Linearity is within 0.17 percent of the full-scale output. A typical calibration is presented in figure 7. Individual calibrations are available on request.

The shuttle-mounted accelerometers shown in figure 8a sense the x, y, and z accelerations. These sensors are distributed away from the suspension point to aid inertial attitude estimation. The locations and sensitive axis are shown in figure 8b.

The mast-mounted accelerometers shown in figure 9a sense x and y acceleration at locations about one-third of the mast length from each end. The positions and sensing axis of the devices are shown in figure 9b.

The reflector-mounted accelerometers are shown in figure 10a. They are positioned in the center of the reflector below the thrusters and sense the x and y accelerations. The coordinates and sensing axis of the devices are shown in figure 10b.

Rate Sensors

The rotational rate sensors are three-axis, aircraft-quality instruments. The frequency response is approximately flat to 1 Hz and -6 db at 10 Hz. Linearity is about 0.6 percent full scale. A typical calibration is shown in figure 11. The range is 60 deg/sec for the yaw and pitch axis and 360 deg/sec. for roll. The threshold is 0.01 deg/sec.

The shuttle-mounted rate sensor package, shown in figure 12a, senses three-axis, rigid body angular rates of the shuttle plate. Its coordinates and sensing axis are presented in figure 12b.

The mast-mounted rate sensor package, shown in figure 13a, senses three-axis angular rates at the reflector end of the mast. Its coordinates and sensing axis are presented in figure 13b.

The sensor information required for control system design is summarized in Table I. The sensor type is listed in column 2, and its sensed variable is listed in column 3. The analog interface channel is listed next. The coordinates of the parts with respect to the universal joint are listed in the next three columns. The sensitivities in terms of analog-to-digital converter units are listed next. The error list shows the RMS deviation of the rate sensors or the percentage of full-scale linearity error for the accelerometers. The linear range of the instruments is listed in the next-to-last column.

OPTICAL SENSOR

An optical sensor will be provided to determine yaw attitude of the shuttle. The optical sensor is a planar photo-diode with appropriate optics mounted on the ground. The outputs of the sensor are proportional to the position of an infrared light source on the shuttle. The sensor data is processed by a dedicated microcontroller and then sent to the main CPU over a serial data link for transformation to attitude angles. No photographs or calibration data are available for this device.

ACTUATORS

The actuators consist of both proportional and on-off controllers. Shuttle attitude control is provided by a pair of two-axis control moment gyros (CMG's). Mast vibration suppression can be achieved with a pair of orthogonally mounted reaction wheel actuators positioned at two stations on the mast. Reflector forces are provided by four cold gas jets. Reflector torques are provided by three orthogonally mounted reaction wheels at the end of the mast. As with the sensors, all devices are inertial, and the power supplies and amplifiers are mounted on the shuttle. Fifteen command signal wires cross the universal joint. All actuators were manufactured in house.

Control Moment Gyros

The CMG's each have two gimbals which are equipped with individual direct drive DC torque motors. The momentum wheel is mounted in the inner gimbal and driven by two permanent magnet DC motors. The nominal operational momentum is about 2.5 ft-lb-sec. The gimbal torque motors are driven by current amplifiers so the output torque will be proportional to the command voltage sent to the amplifier. The gimbal torquers will produce ± 1.5 ft-lbs at frequencies up to 1kHz. The gimbals are instrumented with tachometers and sine-cosine potentiometers to facilitate decoupled control of the shuttle attitude angles. A dedicated computer will be used to control the CMG gimbals. Routines will be provided so that users may command decoupled shuttle torques or gimbal torque commands.

The sensitivity calibration curve of a typical gimbal motor is shown in figure 14. No other calibration data are available for the CMG's.

The forward CMG is shown in figure 15a. Note that the outer gimbal is fixed and parallel to the pitch axis of the shuttle. The inner gimbal is nominally oriented so that the spin axis of the momentum wheel is parallel to the shuttle z-axis. The second CMG is mounted at the rear of the shuttle so that the outer gimbal is

parallel to the z-axis. The inner gimbal is nominally oriented so that the rotor spin axis is parallel to the shuttle x-axis. The coordinates and nominal axis of actuation of the CMG's are shown in figure 15b.

Reaction Wheels

The mast-mounted reaction wheels consist of aluminum disks with inertia of about $0.00027 \text{ lb-ft-sec}^2$ mounted directly on the drive shaft of a 20 oz-in permanent magnet DC motor. The motors are powered by high bandwidth current amplifiers. A torque sensitivity plot is presented in figure 16. No other calibration data are available. A typical reaction wheel assembly is shown in figure 17a. The two actuator locations and their axis of actuation are shown in figure 17b.

The mast end mounted reaction wheels consist of DC permanent magnet pancake motors which are mounted with the armature fixed to the structure. The stator and case of the motor are allowed to rotate via a slip ring assembly, thus providing high inertia mass to fixed mass efficiency.

The motors are powered by high bandwidth current amplifiers. The torque capability of these devices is estimated to be about 50 oz-in. No sensitivity plot or other calibration data is presently available. The three-axis reaction wheel assembly is shown in figure 18a. The actuator locations and their axis of actuation are shown in figure 18a.

Thrusters

The control forces on the reflector are provided by solenoid actuated cold gas jets. The thrusters are mounted in the center of the reflector and act in the x-y plane. The jets are supplied by a compressed air tank mounted on the shuttle. The pressurized air travels through the mast to the solenoid manifold, which gates the air flow between the regulated supply tank and the thrusters as shown in figure 19. Thrust is initiated by opening the solenoid with a discrete command. The rise time and transient oscillation of thrust is shown in figure 20. The magnitude and duration of the thrust before the air supply is depleted at 60-psi nozzle pressure is shown in figure 21. The pertinent data from figures 20 and 21 are tabulated in Table II.

The thrusters are shown in figure 22a. Their location and axis of actuation are shown in figure 22b.

The actuator information required for control system design is summarized in Table III. The actuator type and direction of action are listed in Column 2. The analog interface channels are listed in Column 3. The coordinates of the devices are listed in the next three columns. The sensitivities of the actuators in terms of digital-to-analog converter units are shown in Column 7. An estimate of the thruster RMS deviations exhibited in figure 19 is presented as error data. No other error data are available. The maximum range of the system actuators is shown in the next-to-last column.

MASS PROPERTIES

The position and weight of the various pieces of equipment, which collectively form the SCOLE apparatus, are cataloged in Table IV. Distances are measured from the point of suspension to the approximate center-of-mass of each component. Each major component is listed in the second column of the table. The x, y, z coordinates are listed next. The weight of each component is listed in Column 6. The remaining columns are the mass moments and moments of inertia. The totals for the complete system are presented on the bottom row.

COMPUTER SYSTEM

The main computer for control law implementation will be a micro-computer based on the Motorola M68000 microprocessor. The computer has 2.0 M-byte of random access memory and a 40 M-byte hard disk. The operating system is based on UNIX with C, Fortran and Pascal compilers available for applications programming. The computer has 12 serial ports and 1 parallel port. Terminals are connected on four of the ports and an answer-only modem is attached to another. One port is used for an originate-only modem. A line printer is attached to another port. The optical sensor is connected to a serial port. The IBM PC, which is used to drive the CMG's, is also connected to a serial port.

Analog interfaces consist of a four-bit, output-only discrete channel: an 8 bit discrete output port, an 8-bit discrete input port, 8 digital-to-analog converters, and 64 analog-to-digital converters. All converters are 12-bit devices with a range of +/-10v. These interfaces are shown schematically in figure 23. The CMG control software required for the PC should be relatively transparent to the controls designer who will be operating on the CRDS computer.

Subroutines for accessing the analog interfaces and setting the digital sampling interval are described in Appendix A. The most commonly used routines are listed below.

For accessing the analog devices:

getadc - read the analog-to-digital converters
setdac - set the digital-to-analog converters
thrust - set the cold-gas thrusters.

To control the sampling interval:

rtime - sets the sample period marks the beginning
of a real-time loop.

A time-line of the synchronization of the sample interval using the routine rtime and the analog interface routine usage is shown in figure 24. The basic operation is as follows:

The user first calls rtime with flag=.true., and a valid sample interval. After setting the timer period, the routine starts the user's real-time routine and the interval clock. The user routine will use some or all of the subroutine calls shown. When the user computations and actuator commands are complete, the routine must return to the top of the real-time loop and once again call rtime. If this occurs before the end of the sample interval, the time-out condition will be inhibited and rtime will wait for the next rising edge of the sample interval clock and then return

to the calling program. If the user computations take longer than the sample interval, a time-out condition will be signaled to the operator when `rtime` is called. The user may choose to ignore the condition and continue or may take specific steps to alleviate the condition.

The procedure for logging on to the computer is as follows:

Set communication parameters to 1200 baud, 7 bit, even parity.
Dial in to the Langley data communication switching system at 804-865-4037. When connected, type a carriage return.
To the system prompt "ENTER RESOURCE CODE" type "acrl."
Wait until "GO" and the "name:" prompt appear on the screen.
Type in your log-in information. All investigators will be given a three-letter log-in name (usually the university affiliation).

Some useful system commands are listed below:

To transfer a file to the experiment computer from a smart terminal, type `cat > filename <cr>` and then enable the upload function of the local terminal. When the upload is complete, type `<ctrl>d`.
To transfer a file from the experiment computer to a smart terminal, type `cat filename` then enable the download function of the local terminal and type a `<cr>`.

To list the contents of a directory, type `l <cr>`.

To look at a file, type `p filename`.

To compile a FORTRAN program and link with real-time system commands and TCS graphics, type `frt filename`.

Note: `filename` must have the extension `.for`. The executable code will be under `filename` without the `.for` extension. To run, simply type `filename` without any extension.

To list the system commands, type `l /bin`. To get a description of any command, type `describe command`.

System user guides will be available upon request from the Spacecraft Control Branch, M/S 161, NASA Langley Research Center, Hampton, VA, 23665-5225. Other details for operating in a real-time mode will be provided at the time of implementation.

CONCLUDING REMARKS

The SCOLE laboratory facility is an experimental apparatus which permits ground-based investigation of identification and control algorithms for large space structures. The facility exhibits structural dynamics similar to those expected on the large satellites. The sensors and actuators are typical of those, which may be used on an operational satellite. The computational system is reasonably sized with current technology processors and permits ready access to the facility for interested investigators.

The description of the structural assembly, the sensor and actuator configuration, and software provided in this paper should be sufficient for SCOLE investigators to begin designing identification and control algorithms for the SCOLE facility.

APPENDIX

REAL-TIME SYSTEM SUBROUTINES

Analog I/O system command.

NAME:

getadc Samples the analog-to-digital converters.

COMMAND:

getadc [-s]

DESCRIPTION:

This command is used to sample the analog-to-digital converters and display selected channels at the terminal. The +/- 10.0 volt input range is scaled to +/- 1.0 units so a single bit is worth .00049 units. The channels to be displayed are selected with the **-s** option. This option displays a menu which allows the user to set the print flags for the individual ADC channels. Specific choices are:

- 1) turn on all print flags,
- 2) turn off all print flags,
- 3) turn on a range of print flags,
- 4) turn off a range of print flags,
- 5) display current print flags,
- 6) save current print flags.

If the command is executed without the **-s** option, the last set of print flags is used to selectively display the ADC channels.

USES:

getadc.flags

DIRECTORY:

/bin

SOURCE:

/usr/csc/ele/getadc.c

422

Analog I/O system command.

NAME:

getadc Samples the analog-to-digital converters.

COMMAND:

getadc [-s]

DESCRIPTION:

This command is used to sample the analog-to-digital converters and display selected channels at the terminal. The +/- 10.0 volt input range is scaled to +/- 1.0 units so a single bit is worth .00049 units. The channels to be displayed are selected with the **-s** option. This option displays a menu which allows the user to set the print flags for the individual ADC channels. Specific choices are:

- 1) turn on all print flags,
- 2) turn off all print flags,
- 3) turn on a range of print flags,
- 4) turn off a range of print flags,
- 5) display current print flags,
- 6) save current print flags.

If the command is executed without the **-s** option, the last set of print flags is used to selectively display the ADC channels.

USES:

getadc.flags

DIRECTORY:

/bin

SOURCE:

/usr/csc/ele/getadc.c

Analog I/O system command.

NAME:

setdac Sets the digital-to-analog converters.

COMMAND:

setdac [-s] [-0]

DESCRIPTION:

This command is used to set the voltage on a range of digital-to-analog output channels. The +/- 1.0 unit output range is scaled to +/- 10.0 volts so a single unit is worth .0049 volts. The channels to be set are selected by executing the command with the **-s** option. This option displays a request for the range of channels to be set, and then queries for individual channel values in terms of units. All DAC channels may be set to zero by executing the command with the **"-0"** option.

USES:

Nothing.

DIRECTORY:

/bin

SOURCE:

/usr/csc/ele/setdac.c

UNOS system command.

NAME:

lterm Terminal emulator.

COMMAND:

term [-s] [-S]

DESCRIPTION:

This command connects the user terminal to the Langley central data communication switch at 1200 baud. This is a dumb terminal emulator which provides rudimentary file transfer capabilities. No attempt is made to emulate control codes of any particular terminal for editing purposes.

The emulator commands are as follow:

- @ Return to UNOS (operating system.)
- ! To download a file.
- ^ To upload a file.
- To execute a system command.
- ? For help.

The options are:

-s 300 baud
-S 900 baud

Upload means to transfer a file from the Charles River computer to the remote computer. The remote computer must have some mechanism for receiving the text.

Download means to transfer a file from the remote computer to the Charles River computer. No attempt is made to check for existence of the receiving file name before saving the downloaded file.

USES:

/doc/cmds/lterm.help

DIRECTORY:

/bin

SOURCE:

/jpw/lterm.c

Analog I/O system command.

NAME:

8751_test Test the serial communication link to the 8751 boards.

COMMAND:

8751_test

DESCRIPTION:

This command facilitates verification and calibration of the 8751 micro-controller interface over the RS-232 serial ports. The command queries for voltages to be output by the digital-to-analog converters on the 8751 boards. The data input is in terms of units with 2047 equal to 9.9951 volts and -2048 equal to -10.0000 volts. If the input line contains only one value, all active boards are sent that value. Otherwise, individual values are sent.

USES:

motint()
motsub()

DIRECTORY:

/bin

SOURCE:

/usr/rdb/8751_test.for

426

Analog I/O system subroutine.

NAME:

getadc() (C callable) Sample a range of analog-to-digital converters.

CALL:

```
int error, first_adc, last_adc;  
float adc_data_pointer;  
int getadc( first_adc, last_adc, &adc_data_pointer)  
error = getadc(first_adc, last_adc, &adc_data_pointer)
```

DESCRIPTION:

This subroutine samples a range of analog-to-digital converters. The +/- 10.0 volt input range is scaled to +/- 1.0 units so a single bit is worth .00049 units. The arguments are:

first_adc (int) First converter to be sampled (numbering starts from zero.)

last_adc (int) Last converter to be sampled (maximum is 63.)

&adc_data_pointer (*) Starting location for storing sample data. Data are floating point values with a range of +/- 1.0.

RETURNS:

error = 0 indicates valid transfer.

error = indicates bad range.

USES:

Nothing

LIBRARY: None

SOURCE:

/usr/csc/ele/getadc_c.c

427

Analog I/O system subroutine.

NAME:

setdac() (C callable) Set a range of digital-to-analog converters.

CALL:

```
int error, first dac, last dac;  
float dac data pointer;  
int setdac( first dac, last dac, & dac data pointer )
```

DESCRIPTION:

This subroutine sets a range of digital-to-analog converters. The +/- 1.0 unit output range is scaled to +/- 10.0 volts so a single unit is worth .0049 volts. The arguments are:

```
first dac      (int)      First converter to be set (numbering starts from  
                           zero.)  
last_dac      (int)      Last converter to be set (maximum is 7.)  
&dac_data_pointer (*) Starting location DAC data. Data are floating point  
                           values with a range of +/- 1.0.
```

RETURNS:

```
error = 0  Indicates valid transfer.  
error =-1  Indicates bad range.  
error > 0  Indicates "error" number of data words out of range.
```

USES:

Nothing.

LIBRARY:

None.

SOURCE:

/usr/csc/ele/setdac_c.c

Analog I/O system subroutine.

NAME:

`getadc()` (Fortran callable) Sample a range of analog-to-digital converters.

CALL:

```
integer error, getadc
error = getadc(first_adc, last_adc, adc_data_array)
```

DESCRIPTION:

This subroutine samples a range of analog-to-digital converters. The +/- 10.0 volt input range is scaled to +/- 1.0 units so a single bit is worth .00049 units. The arguments are:

`first_adc` (integer) First converter to be sampled (numbering starts from zero.)

`last_adc` (integer) Last converter to be sampled (maximum is 63.)

`adc_data_array` (real) Starting location for storing sample data. Data are floating point values with a range of +/- 1.0.

RETURNS:

`error = 0` indicates valid transfer.
`error ==-1` indicates bad range.

USES:

`getadc_w.j.`

LIBRARY:

`/lib/acrl_rt_lib_f.j`

SOURCE:

`/usr/csc/ele/getadc_f.c`

Analog I/O system subroutine.

setdac() (Fortran callable) Set a range of digital-to-analog converters.

CALL:

```
integer error, setdac
error = setdac( first_dac, last_dac, dac_data_array )
```

DESCRIPTION:

This subroutine sets a range of digital-to-analog converters. The +/- 1.0 unit output range is scaled to +/- 10.0 volts so a single unit is worth .0049 volts. The arguments are:

```
first_dac (integer) First converter to be set (numbering starts
from zero.)
last_dac (integer) Last converter to be set (maximum is 7.)
dac_data_array (real) Starting location DAC data. Data are floating point
values with a range of +/- 1.0.
```

RETURNS:

```
error = 0 Indicates valid transfer.
error == -1 Indicates bad range.
error > 0 Indicates "error" number of data words out of range.
```

USES:

setdac_w.j

LIBRARY:

/lib/acrl_rt_lib_f.j

SOURCE:

/usr/csc/ele/setdac_f.c

Analog I/O system subroutine.

NAME:

motsub() (Fortran callable) Send scaled voltages to the 8751 micro-controllers which in turn set individual DACs.

CALL:

```
integer torque
call motsub ( torque )
```

DESCRIPTION:

This subroutine sends the motor torque command data to the 8751 micro-controller boards which in turn load the data into the digital-to-analog converters.

torque(6) (integer) Array of dimension 6 which contains the scaled data to be output on the 8751 DAC's. The range of the data is +2047 for +9.9951 volt output to -2048 for -10.0000 volt output.

REQUIRES:

Call to motint.

RETURNS:

Nothing.

USES:

motsub_w.j

LIBRARY:

/lib/acrl_rt_lib_f.j

SOURCE:

/jpw/8751COM/torsub.c

Analog I/O system subroutine.

NAME:

finish() (Fortran callable) Close serial ports to 8751s.

CALL:

finish()

DESCRIPTION:

This subroutine closes the serial communication lines to the 8751s. There are no arguments.

RETURNS:

Nothing.

USES:

finish_w.j.

LIBRARY:

/lib/acrl_rt_lib_f.j

SOURCE:

/jpw/8751COM/torsub.c

432

Analog I/O system subroutines.

NAME:

thrust (Fortran callable) Set the discrete ports to activate the thrusters.

CALL:

```
integer*2 thrust = thrust ( x,y )
```

DESCRIPTION:

This subroutine sets the states of the four discrete outputs on the Parallel Interface/Timer. It was designed for the thrusters on the SCOLE facility. The arguments can have one of three values: 1, 0, or -1 corresponding to positive, none, and negative thrust respectively.

The arguments are:

x (integer) State of x thruster.

y (integer) State of y thruster.

REQUIRES:

Nothing.

RETURNS:

Nothing.

USES:

thrust_w.j

LIBRARY:

/lib/acrl_rt_lib_f.

SOURCE:

/jpw/TIMER/pitdsc.j

Analog I/O system subroutine.

NAME:

rtime() (fortran callable) Mark the start of the real-time loop and change the sample time interval if required.

CALL:

```
call rtime(tau,flag,k)
```

DESCRIPTION:

An internal memory mapped timer is used to control the timing of real-time operations in the Charles River Computer. The programmable clock is required to generate a start pulse and a stop pulse for each sampling interval of the control process. The maximum interval is eighty-five seconds and the minimum interval is 5 micro-seconds. The timer is a Motorola M68230 Parallel Interface Timer (PI/T) which provides versatile double buffered parallel interfaces and 24-bit programmable timer for M68000 systems.

Note: The call to rtime() should be made just inside the real time loop. The arguments are:

tau (real) is the sample period,
flag (logical) is the indicator to either maintain the same value of tau or pass in a new value,
k (integer) is the timeout parameter. If k is returned from rtime containing a 1, this indicates a normal return. If k is returned a 0, a timeout has occurred, and appropriate action should be taken. The user must supply his/her own timeout procedure.

REQUIRES:

Nothing.

RETURNS:

k

LIBRARY:

/lib/acrl_rt_lib_f.j
Add "/jpw/rtime.obj" to FORTRAN compile command.

USES:

tmset()
init()
rtwate()
cktim()
pint_w.j

SOURCE:

/jpw/TIMER/pint.c
/jpw/TIMER/pint_w.m
/jpw/rtime.for

434

REFERENCES

1. Taylor, L. W., Jr., and Balakrishnan, A. V.: A Laboratory Experiment Used To Evaluate Control Laws for Flexible Spacecraft...NASA/IEEE Design Challenge, June 1983, pp.1-2.

ORIGIN OF POOR QUALITY

TABLE I. SENSOR PARAMETERS FOR CONTROL SYSTEM DESIGN

Component No.	Type	Sensed Variable	Signal Source	X Coord. (Inches)	Y Coord. (Inches)	Z Coord. (Inches)	Sensitivity	Error	Range	Bias
1	Rate Gyro	1 s roll s pitch s yaw	ADC 0 ADC 1 ADC 2	27.8	0.0	-5.3	0.0393 units/s ⁻¹ 0.2351 units/s ⁻¹ 0.2354 units/s ⁻¹	.58 deg/n rms 0.55 deg/n rms 0.53 deg/s rms	+/-360 (deg/s)	2.458 v
2	Rate Gyro	2 r roll r pitch r yaw	ADC 3 ADC 4 ADC 5	0.0	0.0	-129.3	0.0395 units/s ⁻¹ 0.2300 units/s ⁻¹ 0.2300 units/s ⁻¹	0.43 deg/n rms 0.10 deg/n rms 0.12 deg/n rms	+/-360 (deg/s) +/-60 (deg/s) +/-60 (deg/s)	2.361 v 2.564 v
3	Accelerom.	ax	ADC 6	9.0	0.0	-4.5	0.1 units/g	0.17 F.S.	+/-20 R	0.00108 v
4	Accelerom.	ay	ADC 7	0.0	-11.5	-4.5	0.1 units/g	0.17 F.S.	+/-20 R	0.00066 v
5	Accelerom.	az	ADC 8	-6.3	0.0	-4.5	0.1 units/g	0.17 F.S.	+/-20 R	0.00066 v
6	Accelerom.	mx	ADC 9	-1.3	0.0	-41.0	0.1 units R	0.17 F.S.	+/-20 R	0.00145 v
7	Accelerom.	my	ADC 10	0.0	-1.3	-41.0	0.1 units R	0.17 F.S.	+/-20 R	0.00065 v
8	Accelerom.	mz	ADC 11	-1.3	0.0	-87.8	0.1 units R	0.17 F.S.	+/-20 R	0.00050 v
9	Accelerom.	rx	ADC 12	0.0	-1.3	-87.8	0.1 units R	0.17 F.S.	+/-20 R	0.00001 v
10	Accelerom.	ry	ADC 13	10.00	20.8	-129.3	0.1 units R	0.17 F.S.	+/-20 R	0.00077 v
11	Accelerom.	rz	ADC 14	12.00	19.8	-129.3	0.1 units R	0.17 F.S.	+/-20 R	0.00103 v
										0.00049 v

1 unit = 10 volt

s = shuttle
m1 = upper mast location
m2 = lower mast location
r = reflector
F.S. = full scale
ADC = Analog-to-digital converter channel

TABLE II. TYPICAL THRUSTER DATA

TABLE II. TYPICAL THRUSTER DATA FOR SIXTY PSI NOZZLE PRESSURE.

Peak Thrust	0.641 lb
Steady State Thrust	0.32 lb
Rise Time	0.032 seconds
Thrust Duration	24 seconds

TABLE III. ACTUATOR PARAMETERS FOR CONTROL SYSTEM DESIGN

Component No.	Type	Actuation Direction	Signal Source	X Coord. (inches)	Y Coord. (inches)	Z Coord. (inches)	Sensitivity	Noise (mV rms)	Range	Bias
12	CNC (for.)	• roll • pitch	tx5 tx5	35.3 "	0.0 "	4.8 0.3448 (units/ft-lb)	0.3448 (units/ft-lb) 0.3448 (units/ft-lb)	— —	+/- 1.5 ft-lb +/- 1.5 ft-lb	0 0
13	CNC (left)	• pitch • yaw	tx5 tx5	-32.9 "	0.0 "	8.8 0.3448 (units/ft-lb) 0.3448 (units/ft-lb)	0.3448 (units/ft-lb) 0.3448 (units/ft-lb)	— —	+/- 1.5 ft-lb +/- 1.5 ft-lb	0 0
14	Thrusters	rx -rx ry -ry	DISC 1 DISC 2 DISC 3 DISC 4	12.5 " " "	21.0 " " "	-124.3 " " "	.35 lbs on/off .35 lbs on/off .35 lbs on/off .35 lbs on/off	0.0252 lb rms 0.0252 lb rms 0.0252 lb rms 0.0252 lb rms	0.35 lb avg 0.35 lb avg 0.35 lb avg 0.35 lb avg	0 0 0 0
15	Reaction Wheel	rx ry rz	DAC 0 DAC 1 DAC 2	0.0 -6.0 -4.5	0.0 0.0 -4.5	-6.0 -125.8 -125.8	not available not available not available	— — —	not available not available not available	0 0 0
16	Reaction Wheel	mx	DAC 3	4.0	0.0	-41.0	0.05 units/oz-in	—	+20 oz-in	0
17	Reaction Wheel	my	DAC 4	0.0	4.0	-41.0	0.05 units/oz-in	—	+20 oz-in	0
18	Reaction Wheel	mx2	DAC 5	4.0	0.0	-87.8	0.05 units/oz-in	—	+20 oz-in	0
19	Reaction Wheel	my2	DAC 6	0.0	4.0	-87.8	0.05 units/oz-in	—	+20 oz-in	0

1 unit = 10 volt
a = shuttle

m1 = upper mast location
m2 = lower mast location

r = reflector

F.S. = full scale
DAC = Digital-to-analog converter channel
DISC = Discrete output channel

CRITICAL PAGE
OF POOR QUALITY

TABLE IV. SCOLE APPARATUS MASS PROPERTIES AND COMPONENT LOCATIONS

Component No.	Component Type	X Coord. (in.)	Y Coord. (in.)	Z Coord. (in.)	Weight (lb.)	Moment X (lb. inches)	Moment Y (lb. inches)	Moment YZ (slug * inches 2)	Moment XX (slug * inches 2)	Moment YY (slug * inches 2)	Moment YY (slug * inches 2)
	<u>Sensor</u>										
1	Rate Gyro θ_x	27.8	0.0	-5.3	1.69	46.9	0.0	-8.9	1.4	41.9	40.4
2	Rate Gyro τ	0.0	0.0	-129.3	1.69	0.0	0.0	-218.5	877.5	0.0	0.0
3	Accelerometer a_x	0.0	-4.5	0.17	1.5	0.0	-0.8	0.1	0.5	0.4	0.0
4	Accelerometer a_y	0.0	-11.5	-6.5	0.17	0.0	-0.2	-0.8	0.8	0.1	0.7
5	Accelerometer a_z	-6.1	0.0	-4.5	0.17	-1.1	0.0	-0.8	0.1	0.3	0.2
6	Accelerometer m_x	-1.1	0.0	-41.0	0.17	-0.7	0.0	-7.0	8.9	8.9	0.0
7	Accelerometer m_y	0.0	-1.3	-41.0	0.17	0.0	-0.2	-7.0	8.9	8.9	0.0
8	Accelerometer m_z	-1.1	0.0	-97.8	0.17	-0.2	0.0	-14.9	40.7	40.7	0.0
9	Accelerometer m_2y	0.0	-1.1	-87.8	0.17	0.0	-0.2	-14.9	40.7	40.7	0.0
10	Accelerometer r_x	10.0	20.8	-129.3	0.17	1.7	3.5	-22.0	90.5	88.8	2.8
11	Accelerometer r_y	12.0	18.8	-129.3	0.17	2.0	3.2	-22.0	90.1	89.0	2.6

TABLE IV. SCOLE APPARATUS MASS PROPERTIES AND COMPONENT LOCATIONS (CONT'D)

Component No.	Component Type	X Coord. (in.)	Y Coord. (in.)	Z Coord. (in.)	Weight (lb.)	Moment X (b. inches)	Moment Y (b. inches)	Moment Z (b. inches)	I XX (slug. * in. 2)	I YY (slug. * in. 2)	I ZZ (slug. * in. 2)	I XY (slug. * inches 2)	I XZ (slug. * inches 2)	I YZ (slug. * inches 2)
<u>Actuators</u>														
12	CMC (for.)	35.3	0.0	4.8	34.27	1208.0	0.0	162.8	24.0	1346.5	1322.4	0.0	-179.3	0.0
13	CMC (aft.)	-32.9	0.0	8.8	34.27	-1127.5	0.0	299.9	81.5	1233.5	1152.0	0.0	308.3	0.0
14	Thrusters	12.0	20.8	-124.3	1.00	12.0	20.8	-124.3	493.3	484.3	17.9	-7.8	46.6	80.8
15	Reaction Wheel X	0.0	-6.0	-125.8	4.28	0.0	-25.7	-538.4	2108.3	2103.5	4.8	0.0	0.0	-101.0
16	Reaction Wheel Y	6.0	0.0	-125.8	4.28	-25.7	0.0	-538.4	2103.5	2108.3	4.8	0.0	-101.0	0.0
17	Reaction Wheel Z	-4.5	-4.5	-125.8	4.28	-19.3	-19.3	-538.4	2106.2	2106.2	5.4	-2.7	-75.7	-75.7
18	Reaction Wheel IY	4.0	0.0	-41.0	1.45	5.8	0.0	-59.4	75.7	76.4	0.7	0.0	7.4	0.0
19	Reaction Wheel 2X	4.0	0.0	-87.8	1.45	5.8	0.0	-127.3	347.1	347.9	0.7	0.0	15.9	0.0
20	Reaction Wheel IY	0.0	4.0	-41.0	1.45	0.0	5.8	-59.4	76.4	75.7	0.7	0.0	7.4	0.0
21	Reaction Wheel 2Y	0.0	4.0	-87.8	1.45	0.0	5.8	-127.3	347.9	347.1	0.7	0.0	0.0	15.9
22	Solenoid	4.0	7.0	-123.8	5.50	22.0	38.5	-680.9	2626.2	2620.6	11.1	-4.8	85.1	148.9
<u>Power Supplies</u>														
23	Lambda 1	-9.5	-10.1	0.0	26.00	-247.0	-267.8	0.0	65.7	72.9	158.5	-79.5	0.0	0.0
24	Lambda 2	-9.5	10.1	0.0	26.00	-247.0	-267.8	0.0	85.7	72.9	158.5	79.5	0.0	0.0
25	Lambda 3	-9.5	-10.1	5.5	26.00	-247.0	-267.8	143.0	110.1	97.3	158.5	-79.5	42.5	46.0
26	Lambda 4	-9.5	10.1	5.5	26.00	-247.0	267.8	143.0	110.1	97.3	158.5	79.5	42.5	-46.0
27	78v	-12.3	-10.5	5.0	7.25	-89.2	-76.1	36.3	30.5	39.7	58.9	-29.1	13.9	11.9
28	Variable	-11.5	10.8	5.8	30.00	-345.0	322.5	172.5	138.5	154.0	230.9	115.9	62.0	-57.9

ORIGINAL PAGE IS
OF POOR QUALITY

TABLE IV. SCOLE APPARATUS MASS PROPERTIES AND COMPONENT LOCATIONS (CONT'D)

Component No.	Component Type	X Coord. (In.)	Y Coord. (In.)	Z Coord. (In.)	Weight (lb.)	Moment X (lb. inche ²)	Moment Y (lb. inche ²)	Moment YZ (lb. inche ²)	I XX (in. ²)	I YY (in. ²)	I ZZ (in. ²)	I XY (inches ²)	I XZ (inches ²)	I YZ (inches ²)
29	5 +/- 15v	-8.5	-5.6	0.4	2.5	-19.5	-12.9	0.9	2.3	5.2	7.4	-3.4	0.2	0.2
30	6 +3v	-5.3	-10.0	10.8	4.00	-21.0	-40.0	43.2	26.9	17.9	15.8	-6.6	7.1	13.5
31	-5v	-2.3	-10.0	10.8	4.00	-9.2	-40.0	43.2	26.9	15.1	13.1	-2.9	1.5	13.5
<u>Counter Balance</u>														
32	wing +	-10.0	18.5	10.8	79.75	-791.5	1475.4	1724.6	2005.9	1405.9	1095.3	461.1	538.9	997.0
33	wing -	-10.0	-18.5	11.8	79.75	791.5	-1475.4	1724.6	2005.9	1405.9	1095.3	-461.1	538.9	997.0
34	nose	46.0	0.0	0.0	10.00	460.0	0.0	0.0	657.1	657.1	0.0	0.0	0.0	0.0
35	air tank	15.5	0.0	10.0	15.25	546.4	0.0	322.5	109.5	322.5	263.0	0.0	-170.7	0.0
36	power mount	-10.1	0.0	-2.6	19.13	-196.1	0.0	-50.3	4.1	66.5	62.4	0.0	-16.1	0.0
37	regulator	4.0	-9.1	0.1	4.00	16.0	-37.0	1.0	10.6	2.0	12.6	4.6	-0.1	0.1
38	bracket (affl.)	-26.8	0.0	6.5	13.00	-348.4	0.0	84.5	17.1	307.0	290.0	0.0	70.8	0.0
39	power amplifier	-15.5	0.0	7.5	5.98	-92.7	0.0	44.9	10.4	55.1	44.6	0.0	21.7	0.0
40	manifold bottom	0.0	0.0	-124.5	1.68	0.0	0.0	-209.2	808.7	0.0	0.0	0.0	0.0	0.0
41	manifold top	0.0	0.0	-4.3	3.19	0.0	0.0	-13.6	1.8	0.0	0.0	0.0	0.0	0.0
42	misc. 1	-7.5	-22.5	-2.5	5.00	-37.5	-112.5	-12.5	79.6	9.7	87.3	-26.4	-2.9	-8.8
43	misc. 2	42.5	0.0	-2.5	0.30	12.8	0.0	-0.8	0.1	16.9	16.8	0.0	1.0	0.0
<u>Structure</u>														
44	shuttle	4.9	0.0	-3.4	501.73	2458.5	0.0	-1693.3	1902.8	6967.7	8510.2	0.0	259.1	0.0

TABLE IV. SCOLE APPARATUS MASS PROPERTIES AND COMPONENT LOCATIONS (CONT'D)

Component No.	Component Type	X Coord. (In.)	Y Coord. (In.)	Z Coord. (In.)	Weight (lb.)	Moment X (lb. inches)	Moment Y (lb. inches)	Moment Z (slug * in. 2)	I XX (slug * in. 2)	I YY (slug * in. 2)	I ZZ (slug * in. 2)	I XY (slug * in. 2)	I YZ (slug * in. 2)	I ZX (slug * in. 2)
45	seat	0.0	0.0	-64.8	4.48	0.0	0.0	-290.1	747.7	747.7	0.0	0.0	0.0	0.0
46	reflector	12.0	20.8	-125.8	4.76	57.1	99.0	-598.6	2428.2	2385.3	134.9	-384.3	-223.0	36.9
	Total				1019.0	-82.3	133.3	-790.9	22407.3	29957.2	15817.8	-349.9	1398.3	69.1

ORIGINAL PAGE IS
OF POOR QUALITY

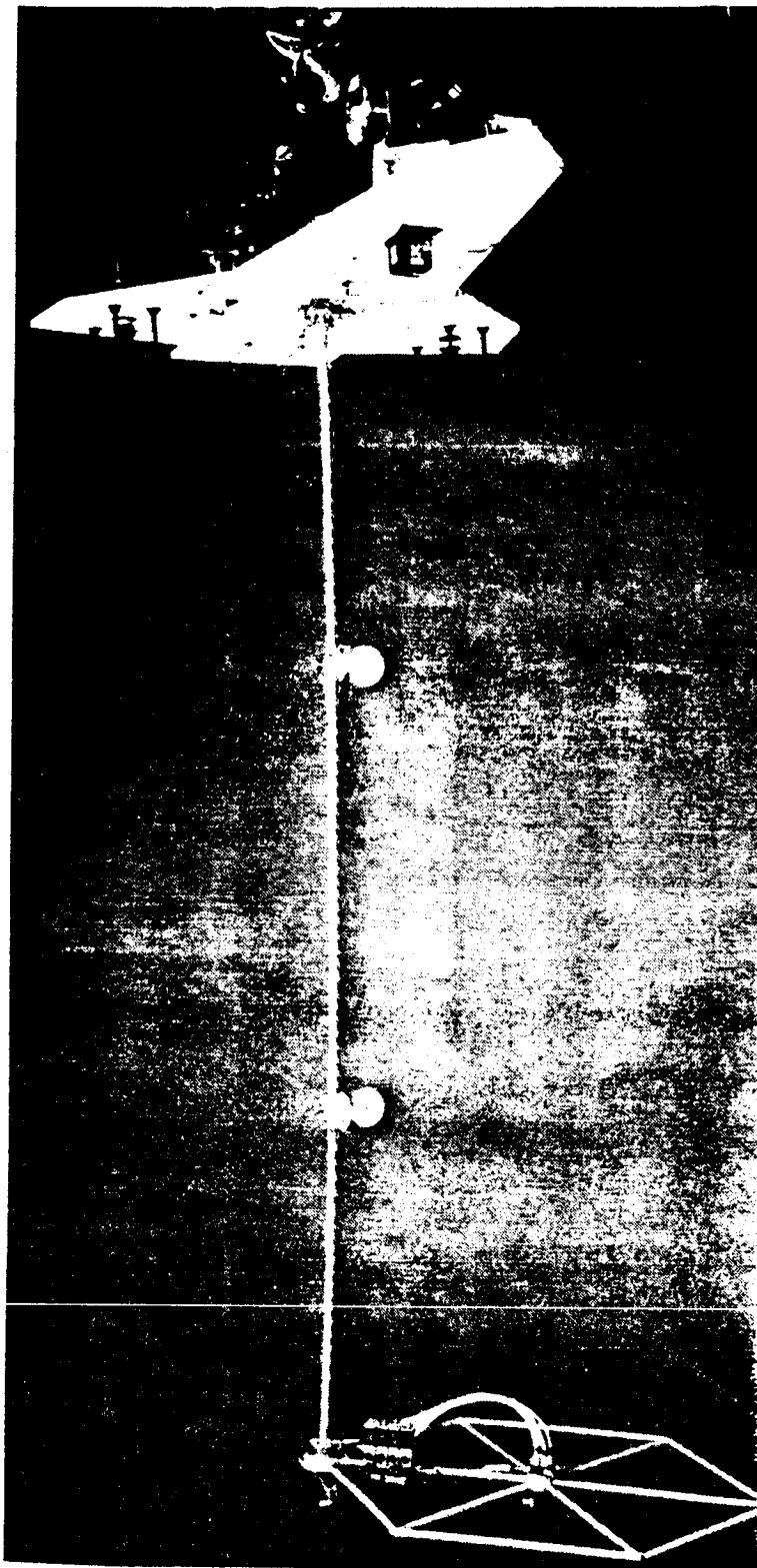


Figure 1. The SCOLE experiment apparatus.

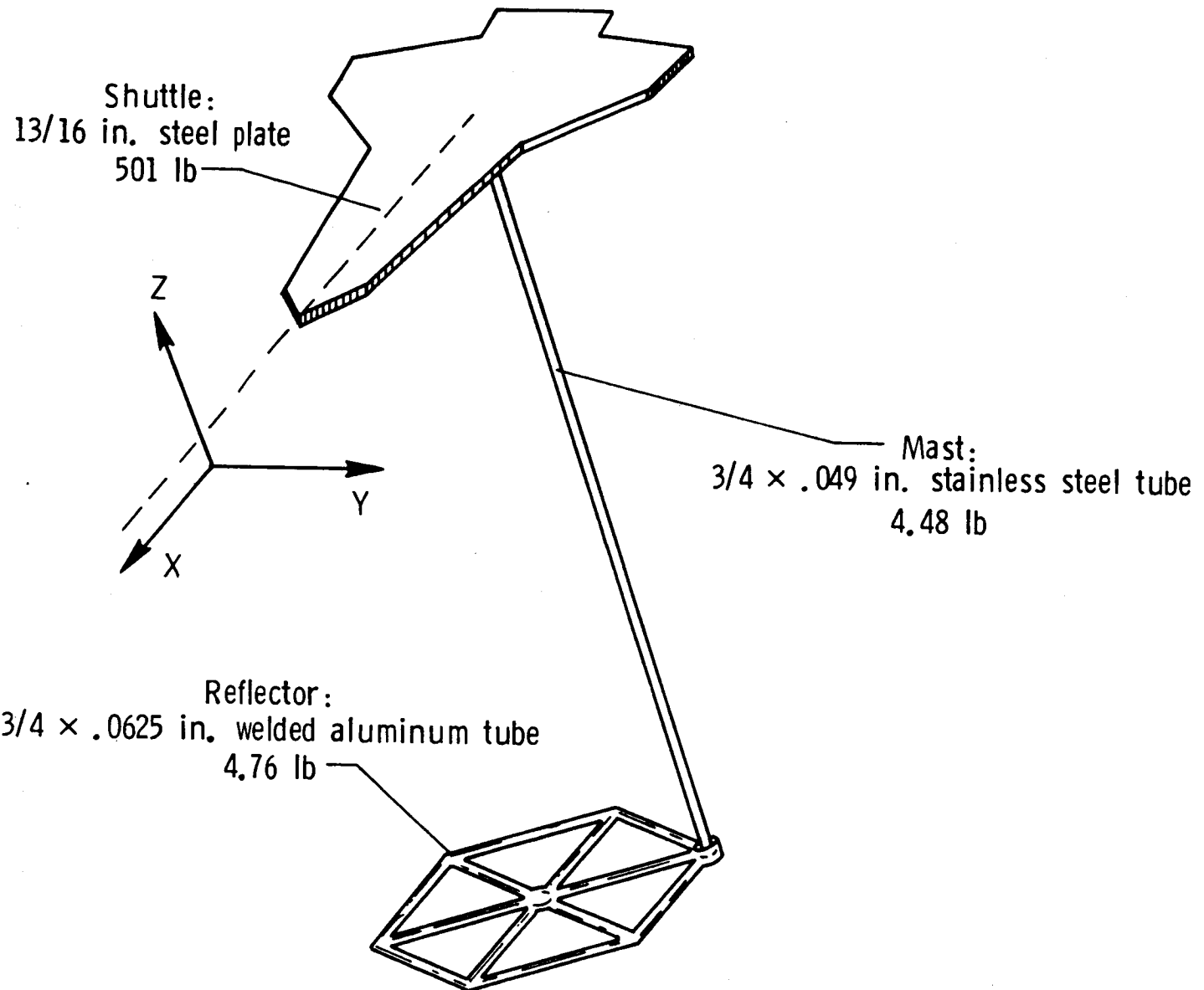


Figure 2. Basic SCOLE structural assembly.

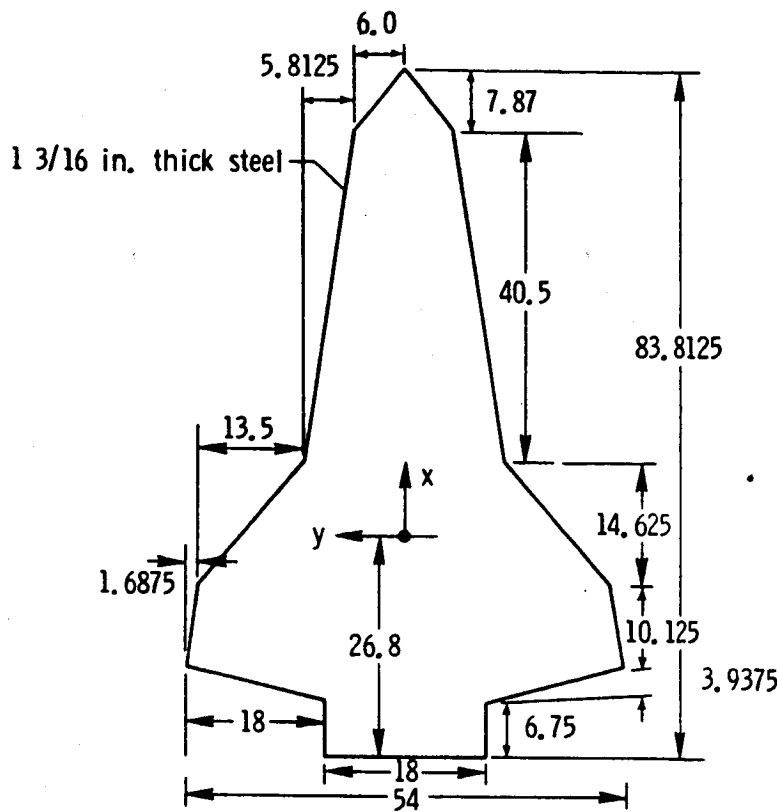


Figure 3. Shuttle planform.

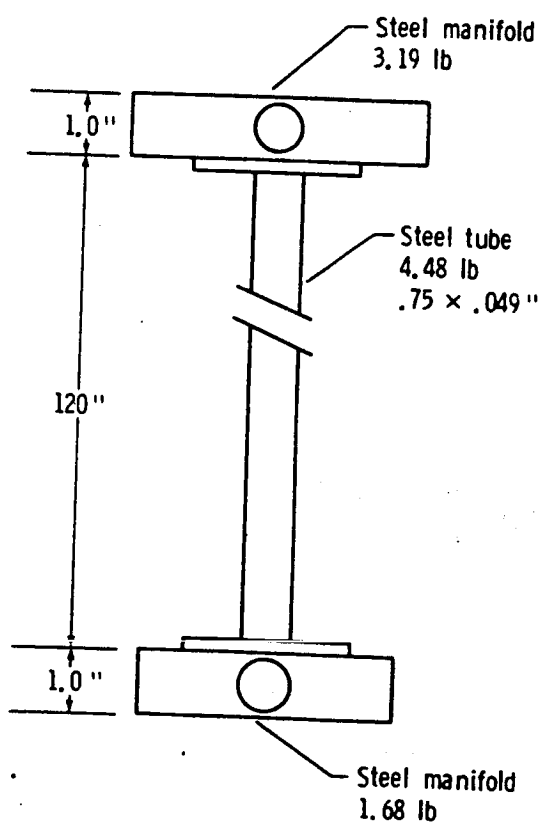
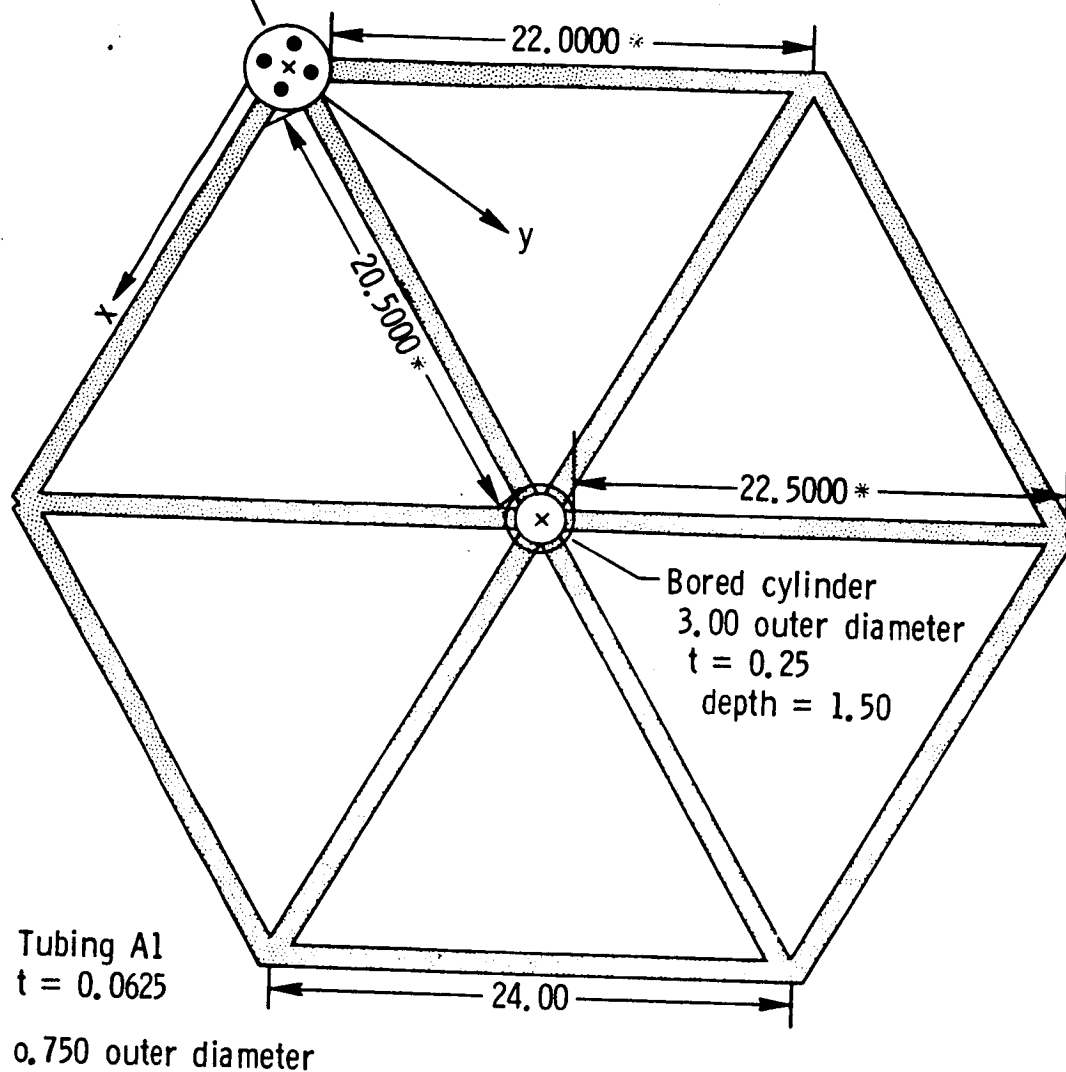


Figure 4. Mast and manifold assembly.

Bored cylinder
4.00 outer diameter
 $t = 0.25$, depth = 1.50
Top surface $t = 0.25$

Antenna
Weight 4.76 lb



All units are in inches
*Length does not include length of insert.

Figure 5. Reflector assembly.

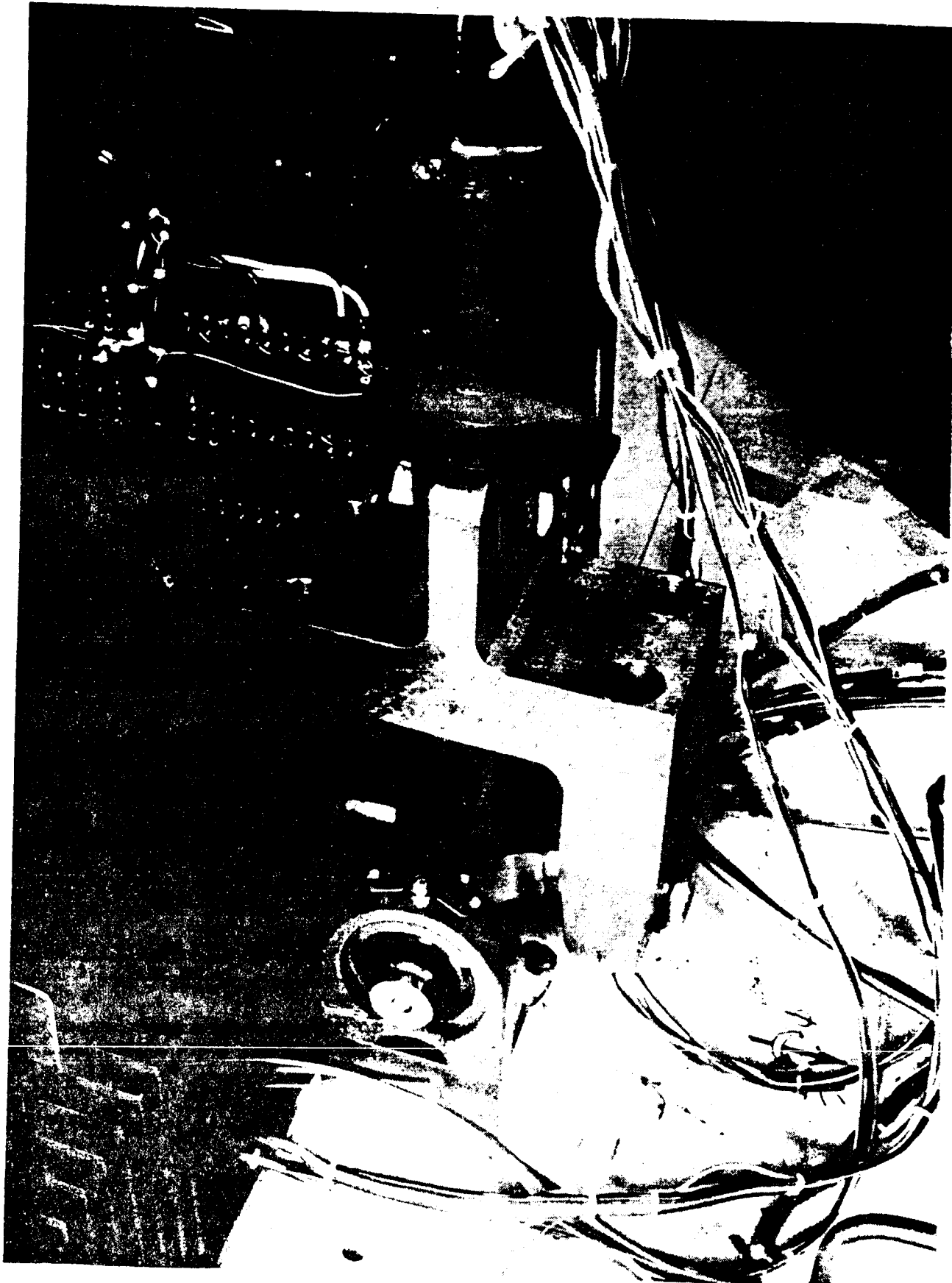


Figure 6. Universal joint suspension point.

447

ORIGINAL PAGE IS
OF POOR QUALITY

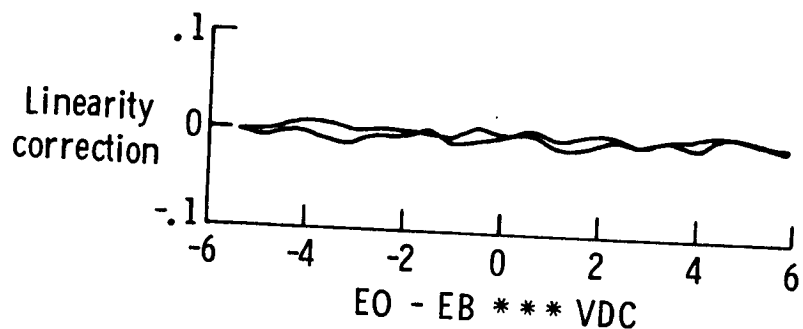
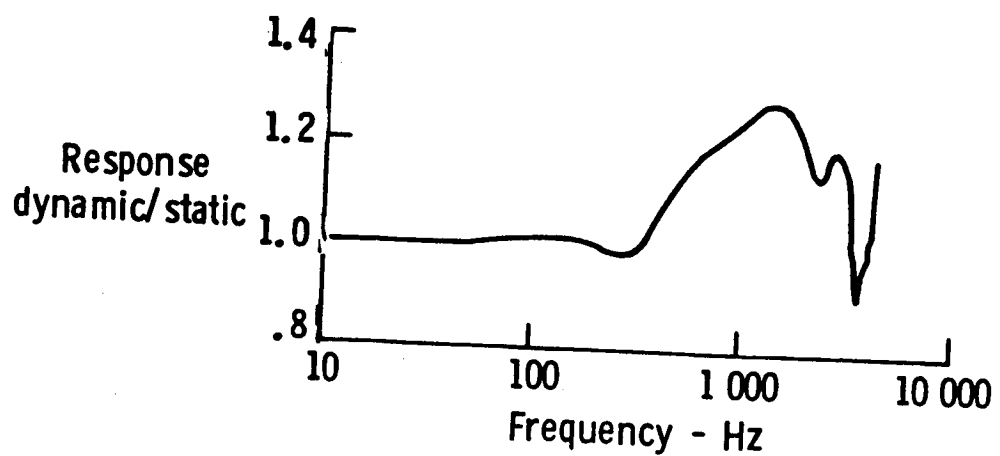


Figure 7. Typical accelerometer calibration.

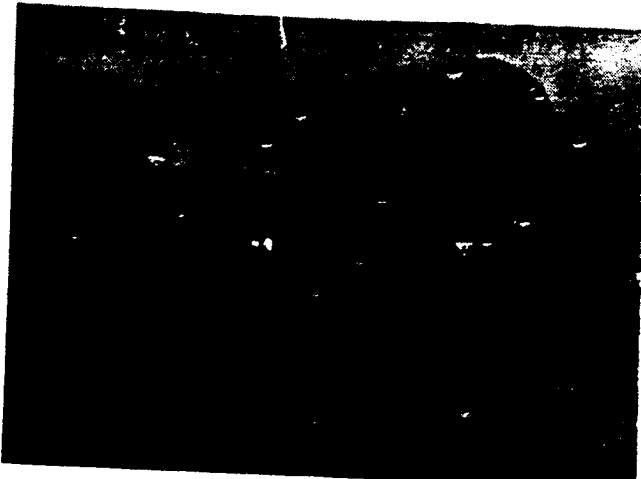


Figure 8a. Shuttle-mounted accelerometers.

ORIGINAL PAGE IS
OF POOR QUALITY

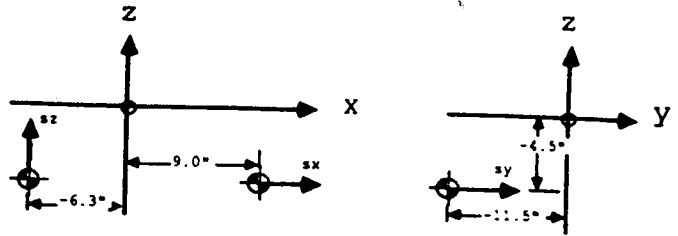


Figure 8b. Coordinates and sensing axis of
shuttle-mounted accelerometers.

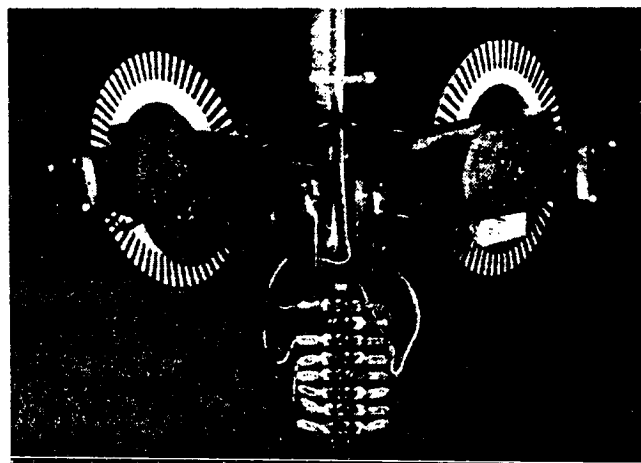


Figure 9a. Mast-mounted accelerometers.

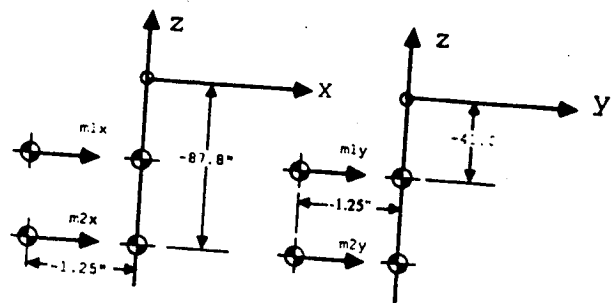


Figure 9b. Coordinates and sensing axis
of mast-mounted accelerometers.

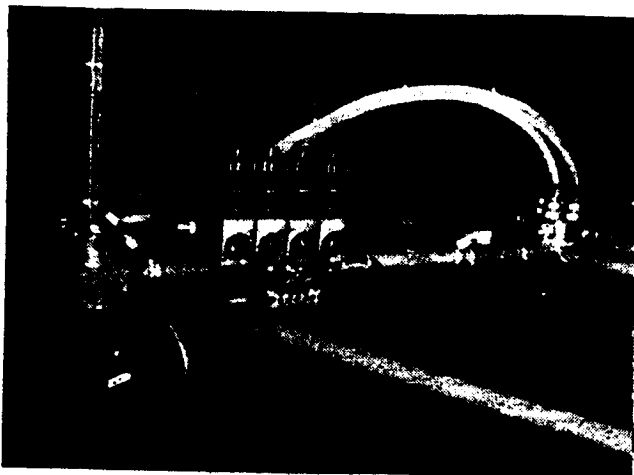


Figure 10a. Reflector-mounted accelerometers.

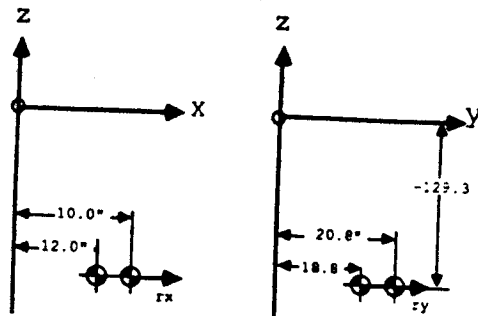


Figure 10b. Coordinates and sensing axis of reflector mounted accelerometers.

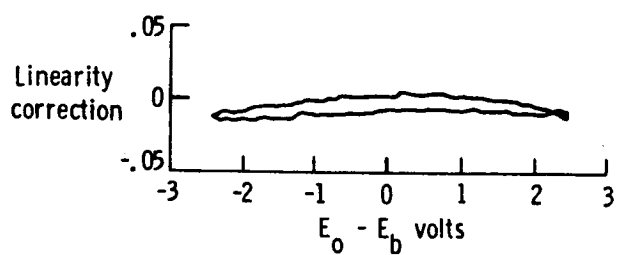
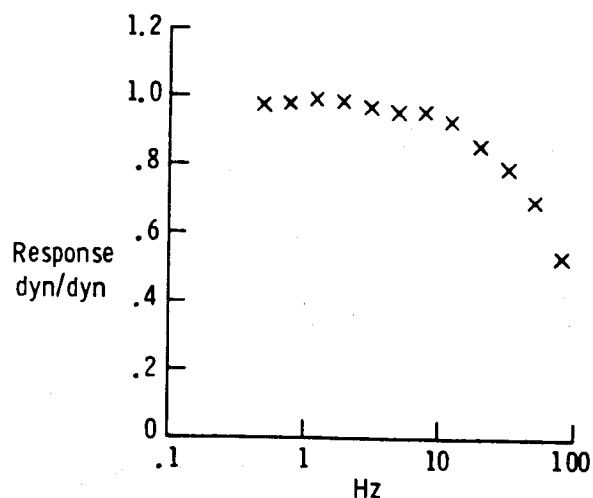


Figure 11. Typical rate sensor calibration.

450

ORIGINAL PAGE IS
OF POOR QUALITY

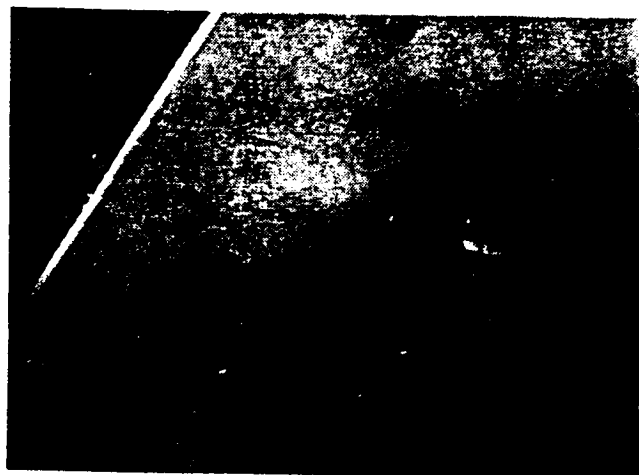


Figure 12a. Shuttle-mounted, three-axis
rate sensor.

ORIGINAL PAGE IS
OF POOR QUALITY

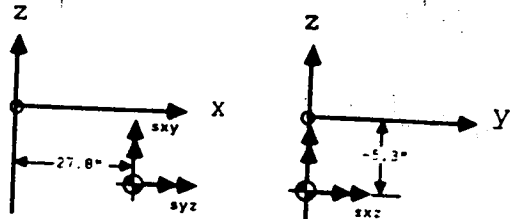


Figure 12b. Coordinates and sensing axis of
shuttle-mounted rate sensor.

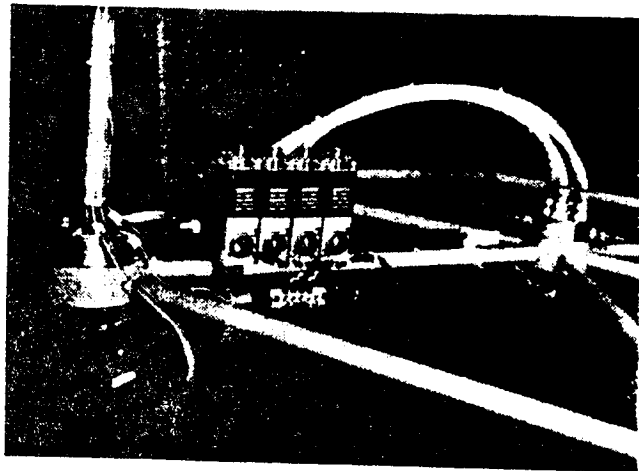


Figure 13a. Mast-end-mounted, three-axis
rate sensor.

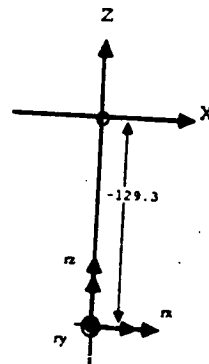


Figure 13b. Coordinates and sensing axis of
mast-end-mounted rate sensor.

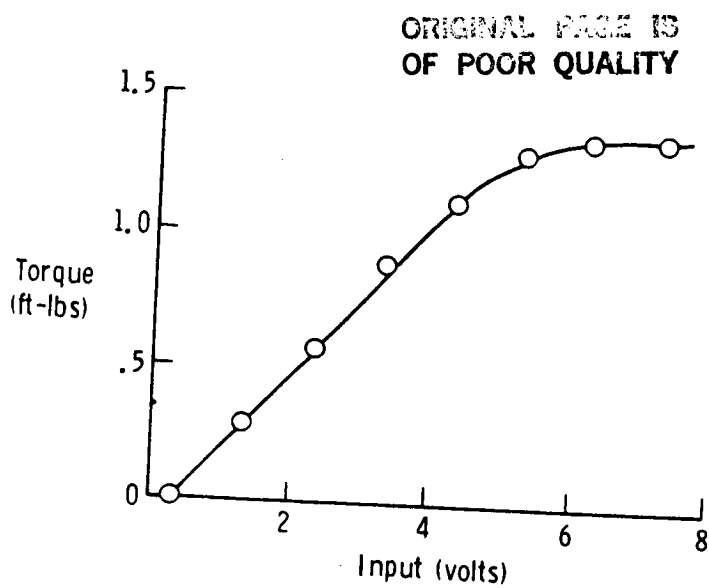


Figure 14. Typical CMG gimbal torque sensitivity curve.

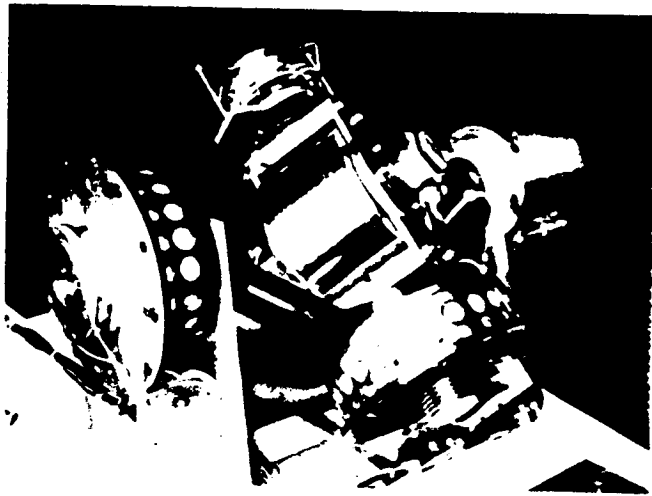


Figure 15a. Shuttle mounted forward CMG.

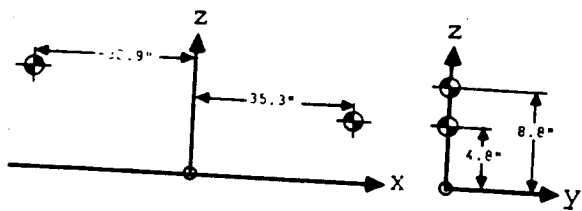


Figure 15b. Coordinates and actuation axis
of shuttle-mounted CMG's.

ORIGINAL PAGE IS
OF POOR QUALITY

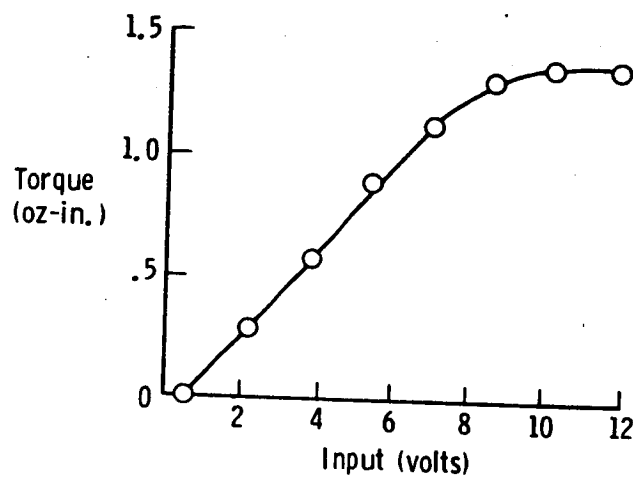


Figure 16. Typical reaction wheel torque sensitivity curve.

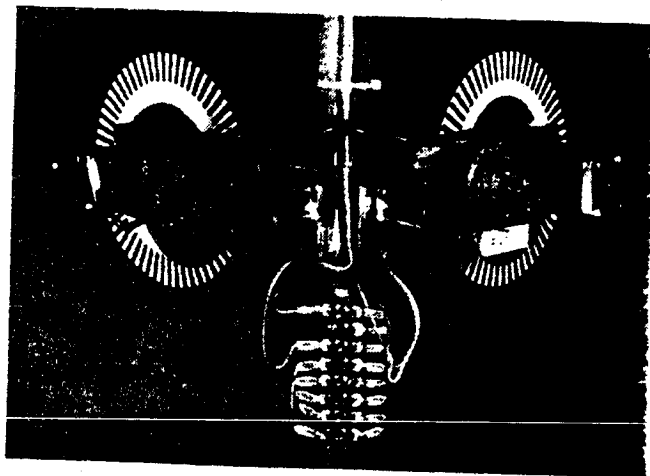


Figure 17a. Mast-mounted reaction wheels.

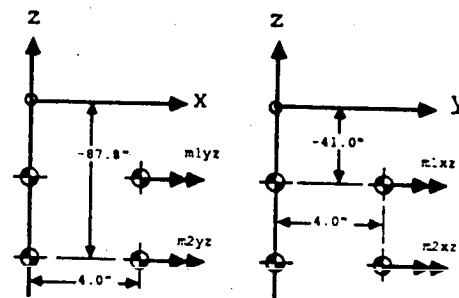


Figure 17b. Coordinates of mast-mounted
reaction wheels.

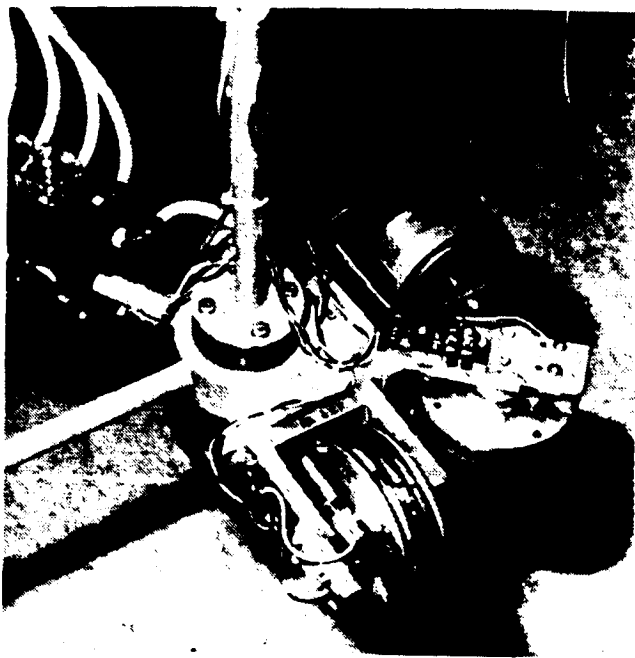


Figure 18a. Mast-end mounted reaction wheels.

ORIGINAL FILE IS
OF POOR QUALITY

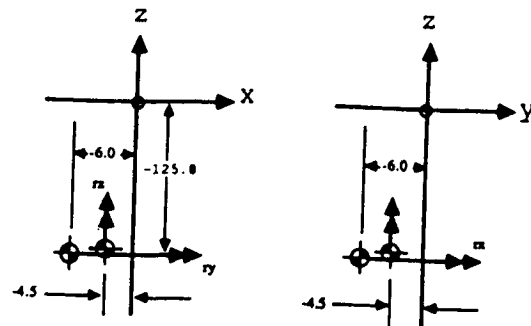


Figure 18b. Coordinate and axis of actuation
for mast-end mounted reaction
wheels.

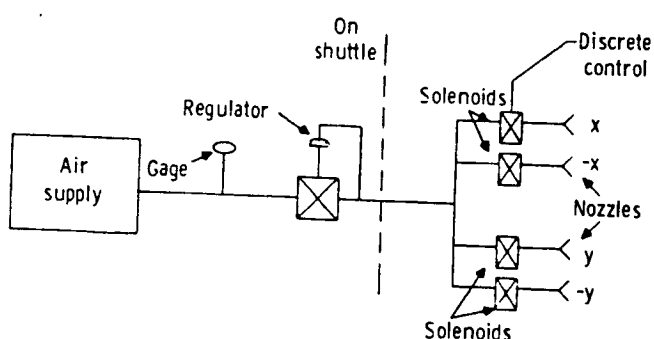


Figure 19. Thruster air supply schematic.

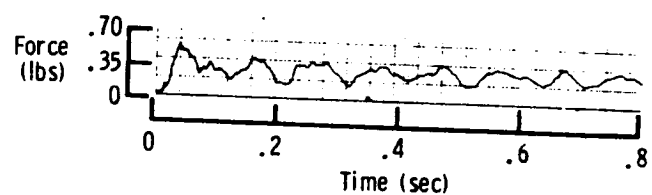


Figure 20. Thruster startup and transients.

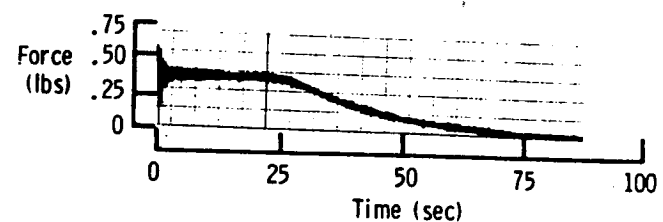


Figure 21. Thrust magnitude and duration.

ORIGINAL PAGE IS
OF POOR QUALITY

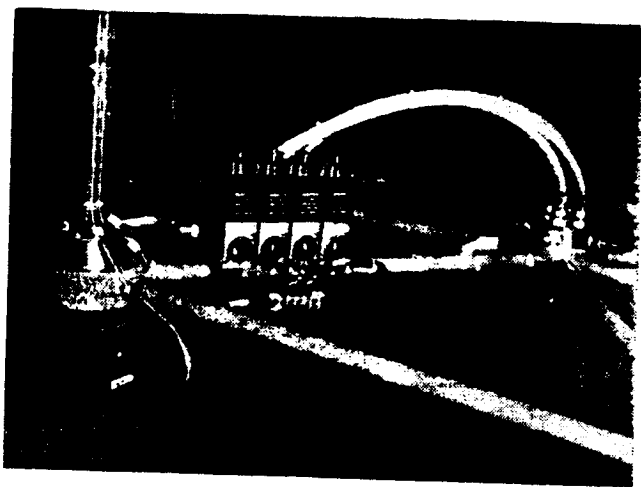


Figure 22a. Reflector-mounted thrusters.

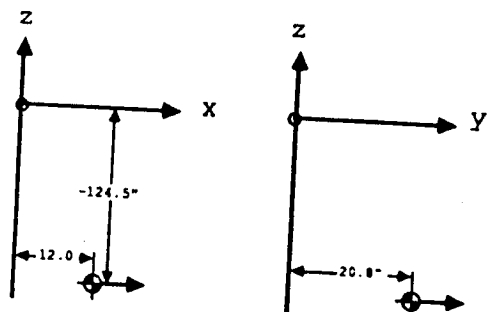


Figure 22b. Coordinates of reflector-mounted thrusters.

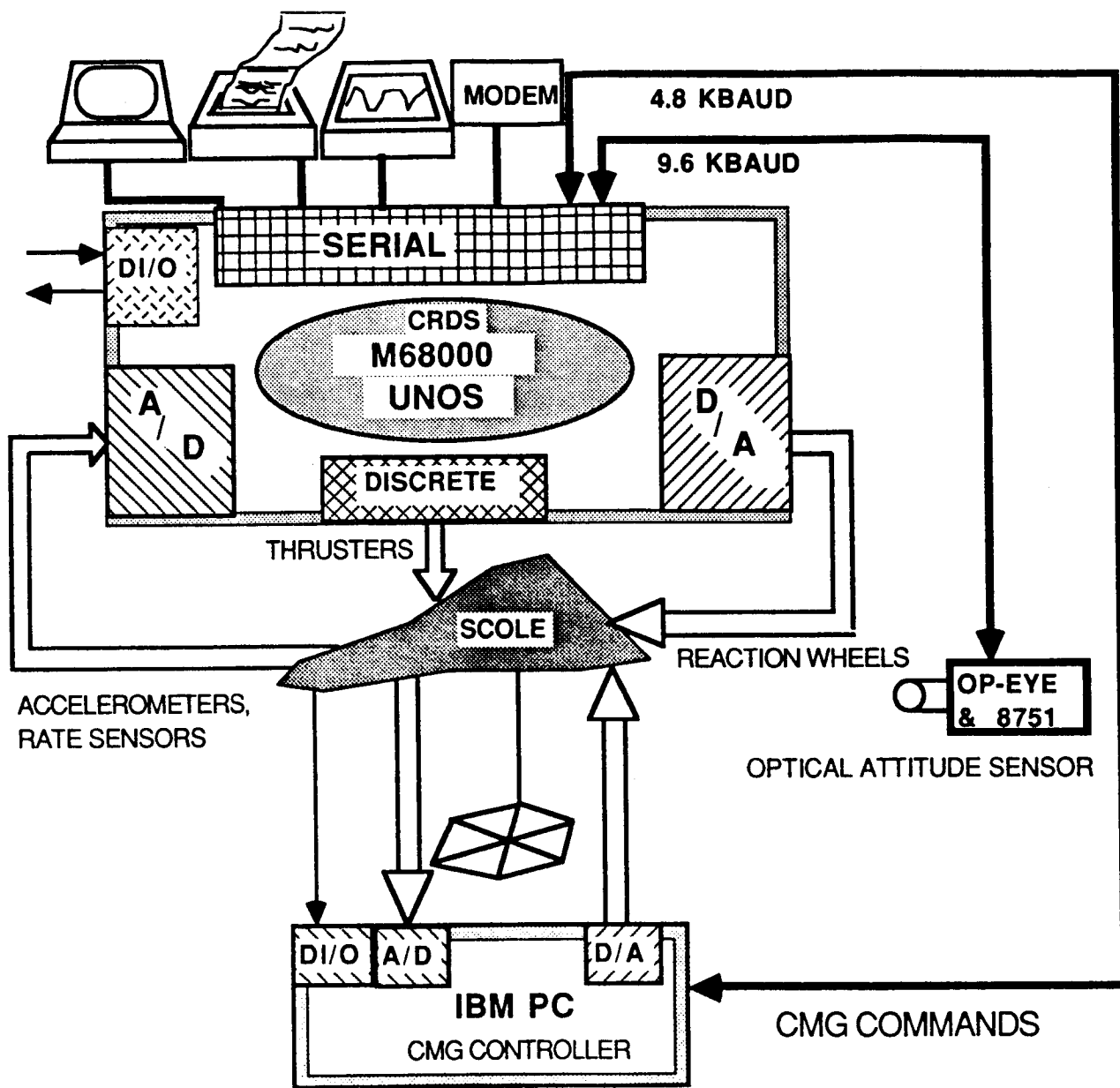


Figure 23. SCOLE computer interfaces

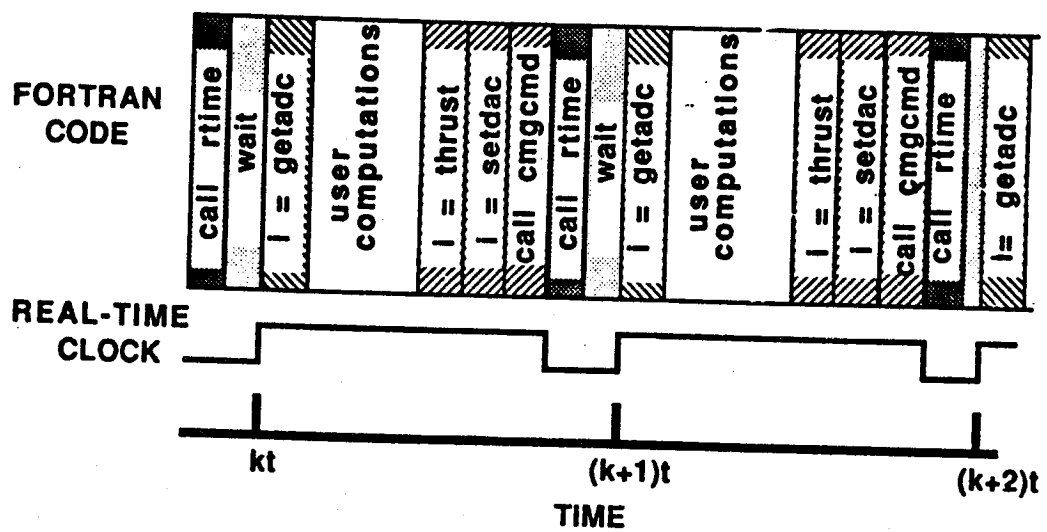


Figure 24. Real-time sample interval.

458

ATTENDEES

Dean Sparks	LaRC
Robert Skelton	Purdue
L. Meirovitch	VPI&SU
S. Yurkovitch	OSU
U. Ozguner	OSU
R. Miller	USC
Ted Baker	UC Berkeley
A. Musalem	RPI
Y. Harn	UC Berkeley
Gene Lin	CRC
Emmanuel Collins	Purdue
Brantley Hanks	LaRC
F. Li	HU
Ajit Choudhury	HU
Terry Leary	GWU
Eric Stewart	GWU
David Ghosh	LARC
William Grantham	LaRC
Shyh Wang	JPL
Mike Stieber	Dept of Communications
Mukhopadhyay	LaRC
N. Levan	UCLA
A.V. Balakrishnan	UCLA
Larry Taylor	LaRC
Jeffrey Williams	LaRC
Ernest Armstrong	LaRC
Peter Bainum	HU
A.S.S.R. Reddy	HU
Raymond Montgomery	LaRC
Suresh Joshi	LaRC
Jernan Juang	LaRC
Yogendra Kakad	UNNC
Shalom Fisher	NRL
Howard Kaufman	RPI
Michael Barrett	Honeywell
Anthony Calise	GA Tech

459

Willard Anderson	LaRC
Daniel Moerder	LaRC
Douglas Price	LaRC
Dave Oikawski	AFRPI
Alok Das	AFRPI
Roger Harding	GE
Robert Hughes	GE
Wayne Yuen	WPWFB
Irving Hirsch	Boeing

"AWARDS"

A. V. Balakrishnan was awarded full membership into the ORDER of the INFINITE ORDER SYSTEMS.

Bob Skelton was awarded full membership into the ORDER of the FINITE ORDER SYSTEMS.

R. K. Miller was presented and award for SMOOTHING by BANG-BANG Control.

Peter Bainum was presented an award for studying the SIGNIFICANCE of nearly INSIGNIFICANT effects.

Gene Lin was presented an award for the SLEWING of MONSTROUS structures.

Suresh Joshi was presented an award for LOOKING at the LINE-of-SIGHT.

Howard Kaufman was presented an award for being a MODAL MODEL FOLLOWER.

Mike Fisher was awarded membership into the order of the MYSTERIOUS, for his studies into the MYSTERIES of actuator placement.

462

Summary of Panel Discussions

1. The mathematical problem statement is incomplete in the sense that "rigidization" of the equations of motion does not yield the rigid body equations. Larry Taylor and Yogi Kakad intend to derive the missing kinematic terms in the partial differential equations of the flexible beam.
2. An accurate "proof model" of the SCOLE is needed for comparing approximate model responses and to evaluate the various control laws. Larry Taylor will see that such a model is made available as soon as a suitable model exists. The modeling difficulties have been more troublesome than expected.
3. The use of the term "modes" has been used loosely to include the admissible functions which are often modes under condition of no damping and no control. Also, the full model is nonlinear and consequently does not exhibit modes but mode-like characteristics.
4. It will be necessary to employ relatively low-order models for control synthesis, state estimation and on-line control. One must use caution, however, lest the designer forgets that the full model or the actual experimental apparatus is nonlinear and has infinite order.
5. Caution is called for in employing Kalman filter techniques for time-varying, nonlinear dynamics of infinite order, such as the SCOLE problem.

1. Report No. NASA TM- 89075 89075	2. Government Accession No.	3. Recipient's Catalog No.	
4. Title and Subtitle Proceedings of the 3rd Annual SCOLE Workshop		5. Report Date January 1987	
7. Author(s) Lawrence W. Taylor, Jr. (Compiler)		6. Performing Organization Code 506-46-11-01	
9. Performing Organization Name and Address NASA Langley Research Center Hampton, VA 23665		8. Performing Organization Report No.	
12. Sponsoring Agency Name and Address National Aeronautics and Space Administration Washington, DC 20546		10. Work Unit No.	
15. Supplementary Notes		11. Contract or Grant No.	
16. Abstract Proceedings of the Third Annual Spacecraft Control Laboratory Experiment (SCOLE) Workshop held at the NASA Langley Research Center, Hampton, VA November 17-18, 1986.		13. Type of Report and Period Covered Technical Memorandum	
17. Key Words (Suggested by Author(s)) Large Flexible Spacecraft, Control, Structural Dynamics		18. Distribution Statement Unclassified-Unlimited Subject Category-18	
19. Security Classif. (of this report) Unclassified	20. Security Classif. (of this page) Unclassified	21. No. of Pages 468	22. Price A20